New Transition Metal-Catalyzed Methodologies to Synthesize Ketones

Dissertation

der Mathematisch-Naturwissenschaftlichen Fakultät

der Eberhard Karls Universität Tübingen

zur Erlangung des Grades eines

Doktors der Naturwissenschaften

(Dr. rer. nat.)

vorgelegt von

Anne Haupt

aus Augsburg

Tübingen

2024

Gedruckt mit Genehmigung der Mathematisch-Naturwissenschaftlichen Fakultät der Eberhard Karls Universität Tübingen.

Tag der mündlichen Qualifikation:	12.06.2024
Dekan:	Prof. Dr. Thilo Stehle
1. Berichterstatterin:	Prof. Dr. Ivana Fleischer
2. Berichterstatter:	Prof. Dr. Martin E. Maier

Our greatest weakness lies in giving up.
The most certain way to succeed is always to try just one more time.

Thomas Edison

Table of Contents

1 Introduction

1.1 General Introduction

1.1.1 Ketones as Fundamental Building Blocks in Organic Chemistry

Ketones represent a widespread and essential compound class in organic chemistry. Besides being frequently found in agrochemicals and pharmaceuticals (Scheme 1-1A), they are also versatile synthetic building blocks for compounds inspired by natural products undergoing classic organic reactions, for instance Wittig-/ Horner–Wadsworth–Emmons-, Aldol- or Grignard reactions as well as Michael additions, Beckmann rearrangements or Bayer–Villiger oxidations.[1]

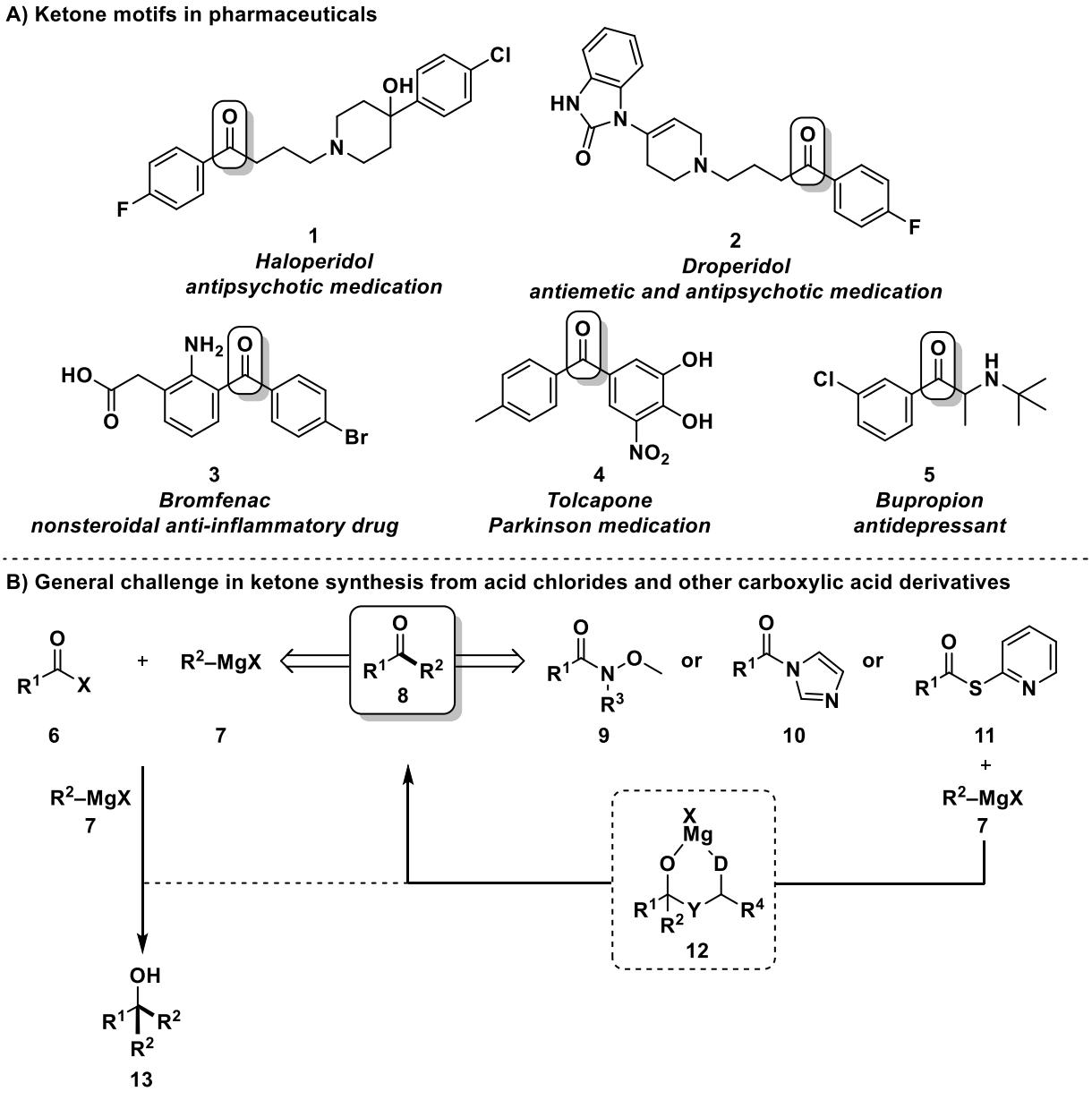

Scheme 1-1: A) Drugs containing the ketone structure.[2] B) General challenge in ketone synthesis using acid chlorides[3] and solutions to avoid over-addition; Y = Heteroatom, D = electron-donating atom.[4]

A wide range of transformations can introduce the ketone motif, from non-catalytic to catalytic methods. Traditional non-catalytic ways include the oxidation of secondary alcohols, Friedel–Crafts acylations and the reaction of carboxylic acid derivatives with organometallic reagents.[5] Although acid chlorides are cheap and industrially attractive acylation agents, they are unsuitable substrates in the reaction with Grignard reagents. Their implementation is usually disrupted by several side reactions, in particular an excess of Grignard reagent leads to an increased amount of tertiary alcohol and an unsatisfactory ketone yield (Scheme 1-1B).[3] Another disadvantage associated with acid chlorides is the use of thionyl chloride, phosgene or phosphorus trichloride as unpleasant and moisture-sensitive reagents for their synthesis.[6] Therefore, derivatization of carboxylic acids is usually needed, enabling a selective reaction with organometallic reagents by a stabilized chelate intermediate **12**. Examples of such acyl donors are the mostly used Weinreb amides **9**,[4a] Staab–Jost imidazolides **10**,[4b] or *S*-2-pyridyl thioesters **11** (Scheme 1-1B).[4c,d]

In recent decades, the focus of academic and industrial research has moved to the development of efficient reactions with high selectivity and product yield, ideally starting from bio-sourced substrates and using cost-effective, environmentally friendly reagents with high atom economy. From this point of view, transition metal-catalyzed cross couplings are another important, constantly growing pillar in the field of ketone syntheses alongside traditional transformations.[7]

1.1.2 Traditional Cross Couplings

In general, cross coupling chemistry refers to transformations between an electrophilic coupling partner and various types of nucleophilic organometallic compounds catalyzed by a transition metal, for instance palladium, nickel, iron, or cobalt.

The first observations attributed to this field were mentioned by Ullmann more than 120 years ago in 1901,[8] but it was only decades later, in the 1970s, that this chemistry was established by Negishi,[9] Heck[10] and Suzuki,[11] among others. The pioneering work was honored with the 2010 Nobel Prize in Chemistry ‘for palladium-catalyzed cross couplings in organic synthesis’.[12] The scope of organometallic coupling partners has been extended over the years, leading to a variety of reaction types. For instance, organoboron (Suzuki–Miyaura coupling),[11] organotin (Sille coupling),[13] organosilane (Hiyama–Denmark coupling),[14] organozinc (Negishi coupling),[9] or organomagnesium reagents (Kumada coupling)[15] as well as alkenes (Mizoroki–Heck reaction)[10,16] and alkynes (Cassar–Heck–Sonogashira coupling)[17] can be coupled with various electrophiles (Scheme 1-2). Furthermore, transformations forging new C–heteroatom bonds are also known, such as C–N (Buchwald–Hartwig)[18] or C–S couplings (Migita).[19]

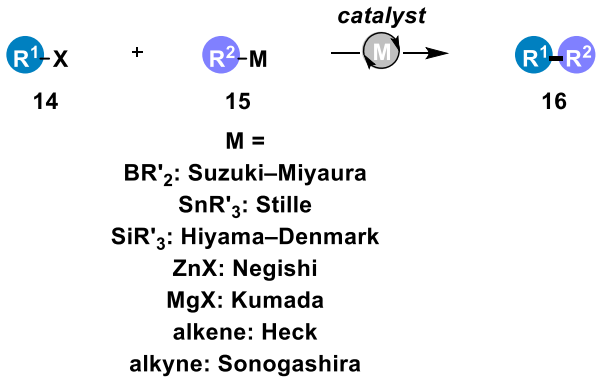

Scheme 1-2: Types of cross coupling reactions.

Cross couplings are widely used in various fields, from synthesis of bioactive pharmaceuticals and agrochemicals to material science and electronics.[20] Palladium catalysis dominates large-scale settings in pharmaceutical industry,[21] but also the use of nickel is gaining traction. Nickel has a favorable toxicological profile for orally administered drugs compared to palladium, as the presence of elemental impurities is regulated with an oral daily dose of palladium at 100 µg/day and nickel at 500 µg/day.[22] Nevertheless, the toxicity of a metal depends on its valence state, particle size and coordination sphere, all of which influence its solubility and choice of cellular transporters carrying it into the cell.[23] From this point, $NiCl_2$ is the most toxic compound compared to other transition metal chlorides that may be relevant for catalysis.[23] As exposure to highly nickel-contaminated environments can cause a variety of pathological effects in humans, ranging from contact dermatitis to lung fibrosis, cardiovascular, kidney diseases and even cancer, the removal or recovery of nickel from industrial waste is important from an economic and environmental perspective.[24] However, this can be challenging due to the often high water solubility of nickel salts, in contrast to the respective palladium salts,[23] but the following example demonstrates that nickel can outperform palladium when it comes to removal of residues in pharmaceuticals.

A nickel-catalyzed Suzuki–Miyaura coupling enabled access to a precursor of the PI3K inhibitor **20**, a drug to treat cancer, on a 55 kg scale (Scheme 1-3).[25] Both palladium and nickel catalysts were tested and suitable, but palladium required the use of expensive scavengers, for instance Florisil and Thio-Silica, and large amounts of solvents. Contrariwise, the nickel catalyst residues could be easily removed from the crude product by washing with aqueous ammonia followed by crystallization. After deprotection, the final active pharmaceutical ingredient **20** was obtained, in which nickel residues of only < 20 ppm were detected by ICP-MS (Scheme 1-3).[25]

Aside from these large-scale technical aspects, this example raises the question of what differentiates the two transition metals from a chemical perspective, as both are catalytically active, and why palladium dominates in the field of cross couplings.

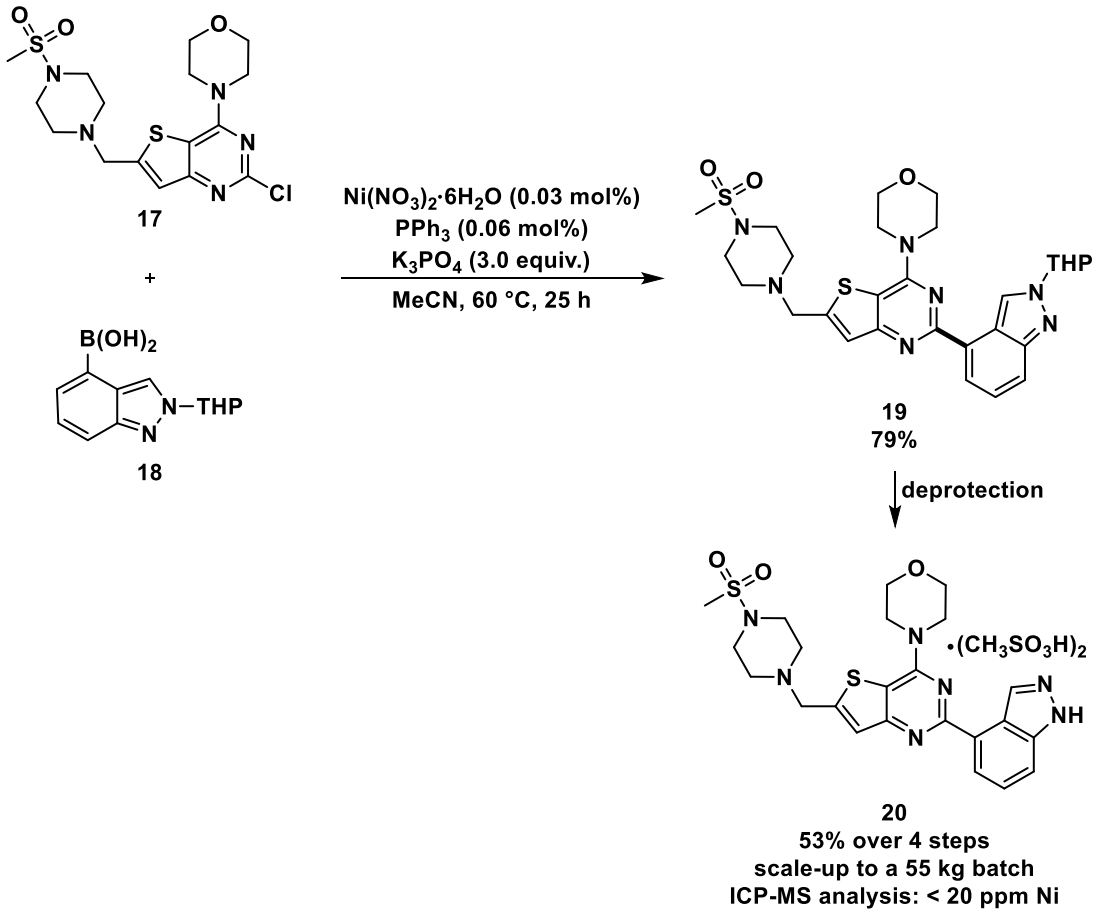

Scheme 1-3: Example of a nickel-catalyzed Suzuki–Miyaura cross coupling for the synthesis of pharmaceuticals.[25]

1.1.3 Choice of Metal Catalyst

Palladium is the means to an end in catalysts for cross couplings as its main advantages lie in its magnificent versatility and activity in two-electron redox processes, leading to high yields and selectivity for a broad substrate scope. Additionally, palladium-catalyzed transformations have been greatly optimized in recent years. High turnover numbers at mild reaction conditions, e.g. room temperature, and short reaction times can be achieved at low catalyst loadings from ppm to a few mol% with a wide range of ligands that are effective in the catalytic transformations.[26] Furthermore, the couplings are based on well-studied mechanisms involving the predictable oxidation states of palladium(0) and palladium(II) and the three critical steps of oxidative addition, transmetalation and reductive elimination.[12]

However, due to the low availability (distribution in the Earth's crust: 6×10^{-4} ppm for palladium *vs*. 80 ppm for nickel)[23] and high cost of palladium, the focus changed to the search for similarly efficient, cheaper catalysts. Nickel is still the most important alternative and differs from palladium not only in its price, but also in its properties.[27]

As a first-row transition metal, nickel exhibits a lower electronegativity (1.9 *vs*. 2.2), a smaller atomic radius (1.245 Å *vs*. 1.375 Å), and a lower reduction potential (-0.257 V *vs.*

+0.951 V) than the precious metal palladium.[27e] For this reason, nickel(0) species are generally less stable than palladium(0) under similar conditions, as they are more susceptible to oxidation, and substrate reduction reactions like oxidative addition are facilitated (Scheme 1-4). Therefore, nickel(0) compounds are usually more efficient at activating inert C–C, C(sp^3)–halogen and C–X (X = O, N, F, etc.) bonds compared to the respective palladium(0). In addition, nickel(II) activation often needs reductants, in contrast to palladium(II) that is more easily reduced to the active palladium(0), e.g. by an excess of a phosphine ligand. Moreover, intermediate nickel-alkyl complexes are less prone to β-hydride elimination, making nickel a particularly suitable catalyst for C(sp^3)–C(sp^n) couplings (Scheme 1-4).[27e] Additionally, nickel is characterized by accessible odd-electron oxidation states nickel(I) and nickel(III), which have a higher stability of open-shell electronic configurations, compared to the corresponding palladium species, allowing both single-electron and two-electron steps (Scheme 1-4). On the one hand, this is advantageous as variable oxidations states open the door to more mechanistic scenarios and a larger substrate pool, including inactive substrates like *O*-electrophiles. On the other hand, this can lead to complex mechanisms that are difficult to study, as there are a variety of possible oxidation states and off-cycle species resulting from dis- or comproportionation, making it difficult to control the favored reaction pathway in nickel catalysis.[27e]

In summary, the overview illustrates that both transition metals have their own advantages and drawbacks, and that the choice between the two depends on the specific chemical objective at hand.

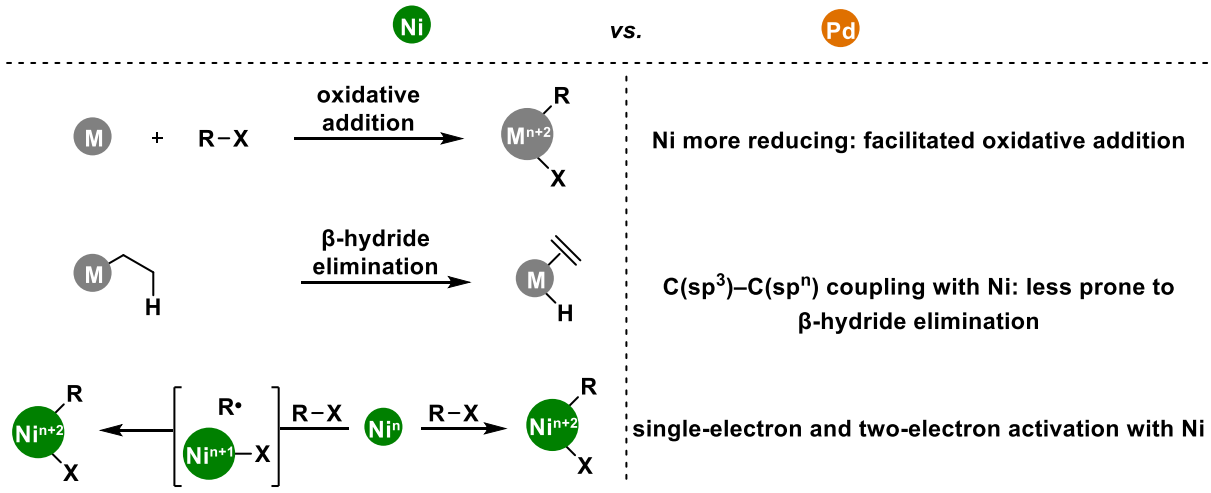

Scheme 1-4: Comparison of nickel and palladium in cross couplings.[27e]

1.2 References

[1] a) D. J. Foley, H. Waldmann, *Chem. Soc. Rev.* **2022**, *51*, 4094–4120; b) I. Karakaya, K. Rizwan, S. Munir, *ChemistrySelect* **2023**, *8*, e202204005.
[2] a) G. Rovere, F. M. Nadal-Nicolás, P. Sobrado-Calvo, D. Garcia-Bernal, M. P. Villegas-Pérez, M. Vidal-Sanz, M. Agudo-Barriuso, *Invest. Ophthalmol. Visual Sci.* **2016**, *57*, 6098–6106; b) M. A. Schuckit, *Engl. J. Med.* **2015**, *372*, 580–581; c) S. J. Peroutka, S. Synder, *Am. J. Psychiatry* **1980**, *137*, 1518–1522; d) A. Antonini, G. Abbruzzese, P. Barone, U. Bonuccelli, L. Lopiano, M. Onofrj, M. Zappia, A. Quattrone, *Neuropsychiatr. Dis. Treat.* **2008**, *4*, 1–9.
[3] X.-j. Wang, L. Zhang, X. Sun, Y. Xu, D. Krishnamurthy, C. H. Senanayake, *Org. Lett.* **2005**, *7*, 5593–5595.
[4] a) S. Nahm, S. M. Weinreb, *Tetrahedron Lett.* **1981**, *22*, 3815–3818; b) H. A. Staab, E. Jost, *Liebigs Ann. Chem.* **1962**, *655*, 90–94; c) T. Mukaiyama, M. Araki, H. Takei, *J. Am. Chem. Soc.* **1973**, *95*, 4763–4765; d) M. Araki, S. Sakata, H. Takei, T. Mukaiyama, *Bull. Chem. Soc. Jpn.* **1974**, *47*, 1777–1780.
[5] R. K. Dieter, *Tetrahedron* **1999**, *55*, 4177–4236.
[6] J. A. Greenberg, T. Sammakia, *J. Org. Chem.* **2017**, *82*, 3245–3251.
[7] I. Karakaya, K. Rizwan, S. Munir, *ChemistrySelect* **2023**, *8*, e202204005.
[8] F. Ullmann, J. Bielecki, *Ber. Dtsch. Chem. Ges.* **1901**, *34*, 2174–2185.
[9] E. Negishi, A. O. King, N. Okukado, *J. Org. Chem.* **1977**, *42*, 1821–1823.
[10] R. F. Heck, J. Nolley Jr, *J. Org. Chem.* **1972**, *37*, 2320–2322.
[11] N. Miyaura, K. Yamada, A. Suzuki, *Tetrahedron Lett.* **1979**, *20*, 3437–3440.
[12] C. C. C. Johansson-Seechurn, M. O. Kitching, T. J. Colacot, V. Snieckus, *Angew. Chem. Int. Ed.* **2012**, *51*, 5062–5085.
[13] a) D. Milstein, J. Stille, *J. Am. Chem. Soc.* **1978**, *100*, 3636–3638; b) J. K. Stille, *Angew. Chem. Int. Ed.* **1986**, *25*, 508–524.
[14] Y. Hatanaka, T. Hiyama, *J. Org. Chem.* **1988**, *53*, 918–920.
[15] a) K. Tamao, K. Sumitani, M. Kumada, *J. Am. Chem. Soc.* **1972**, *94*, 4374–4376; b) R. Corriu, J. Masse, *J. Chem. Soc., Chem. Commun.* **1972**, 144a-144a.
[16] T. Mizoroki, K. Mori, A. Ozaki, *Bull. Chem. Soc. Jpn.* **1971**, *44*, 581–581.
[17] a) K. Sonogashira, Y. Tohda, N. Hagihara, *Tetrahedron Lett.* **1975**, *16*, 4467–4470; b) L. Cassar, *J. Organomet. Chem.* **1975**, *93*, 253–257; c) a. H. Dieck, F. Heck, *J. Organomet. Chem.* **1975**, *93*, 259–263.
[18] a) J. Louie, J. F. Hartwig, *Tetrahedron Lett.* **1995**, *36*, 3609–3612; b) A. S. Guram, R. A. Rennels, S. L. Buchwald, *Angew. Chem. Int. Ed.* **1995**, *34*, 1348–1350.
[19] T. Migita, T. Shimizu, Y. Asami, J.-i. Shiobara, Y. Kato, M. Kosugi, *Bull. Chem. Soc. Jpn.* **1980**, *53*, 1385–1389.
[20] a) M. J. Buskes, M.-J. Blanco, *Molecules* **2020**, *25*, 3493; b) S. Xu, E. H. Kim, A. Wei, E.-i. Negishi, *Sci. Technol. Adv. Mater.* **2014**, *15*, 044201; c) P. Devendar, R.-Y. Qu, W.-M. Kang, B. He, G.-F. Yang, *J. Agric. Food Chem.* **2018**, *66*, 8914–8934; d) P. Ruiz-Castillo, S. L. Buchwald, *Chem. Rev.* **2016**, *116*, 12564–12649.
[21] a) Ó. López, J. M. Padrón, *Catalysts* **2022**, *12*, 164; b) C. Torborg, M. Beller, *Adv. Synth. Catal.* **2009**, *351*, 3027–3043.
[22] U. S. P. C. E. I.-. Limits in *United States Pharmacopeial Convention. <232> Elemental Impurities - Limits*, *Vol.* **2013**, pp. 1–3.
[23] K. S. Egorova, V. P. Ananikov, *Angew. Chem. Int. Ed.* **2016**, *55*, 12150–12162.
[24] V. Coman, B. Robotin, P. Ilea, *Resour. Conserv. Recycl.* **2013**, *73*, 229–238.

[25] Q. Tian, Z. Cheng, H. M. Yajima, S. J. Savage, K. L. Green, T. Humphries, M. E. Reynolds, S. Babu, F. Gosselin, D. Askin, I. Kurimoto, N. Hirata, M. Iwasaki, Y. Shimasaki, T. Miki, *Org. Process Res. Dev.* **2013**, *17*, 97–107.
[26] J. D. Hayler, D. K. Leahy, E. M. Simmons, *Organometallics* **2019**, *38*, 36–46.
[27] a) B. M. Rosen, K. W. Quasdorf, D. A. Wilson, N. Zhang, A.-M. Resmerita, N. K. Garg, V. Percec, *Chem. Rev.* **2011**, *111*, 1346–1416; b) S. Z. Tasker, E. A. Standley, T. F. Jamison, *Nature* **2014**, *509*, 299–309; c) V. P. Ananikov, *ACS Catal.* **2015**, *5*, 1964–1971; d) F. Buono, T. Nguyen, B. Qu, H. Wu, N. Haddad, *Org. Process Res. Dev.* **2021**; e) V. M. Chernyshev, V. P. Ananikov, *ACS Catal.* **2022**, *12*, 1180–1200.

2 Aims of This Work

Ketones constitute an important structural motif in organic chemistry and the search for new methods to synthesize them is still in high demand. Cross couplings represent a valuable alternative to traditional synthetic methods, since functionalized and green substrates as well as low-cost and environmentally friendly reagents can be used with high atom-economy. The overall aim of this work is the development of new approaches for the introduction of the ketone scaffold with thioesters as acyl donors and central substrates under nickel catalysis.

The first part of this work is targeted on ketone synthesis by the so-called Liebeskind–Srogl coupling, in which thioesters and organoboron compounds are reacted under palladium catalysis and stoichiometric amounts of a copper(I) reagent. To date, Liebeskind–Srogl couplings are limited to palladium catalysis, and the high cost of palladium has prompted an intensive search for efficient, but less expensive alternatives. Therefore, preliminary studies on a nickel-catalyzed Liebeskind–Srogl coupling are performed (Figure 2-1, left).

In the second part of the thesis, the focus shifts from traditional cross couplings to cross-electrophile couplings (Figure 2-1, right). In this methodology, benzylic alcohols as a desirable, easily accessible substrate class are coupled with thioesters under Lewis acid assistance and nickel catalysis, yielding ketones instead of the expected transesterification products.

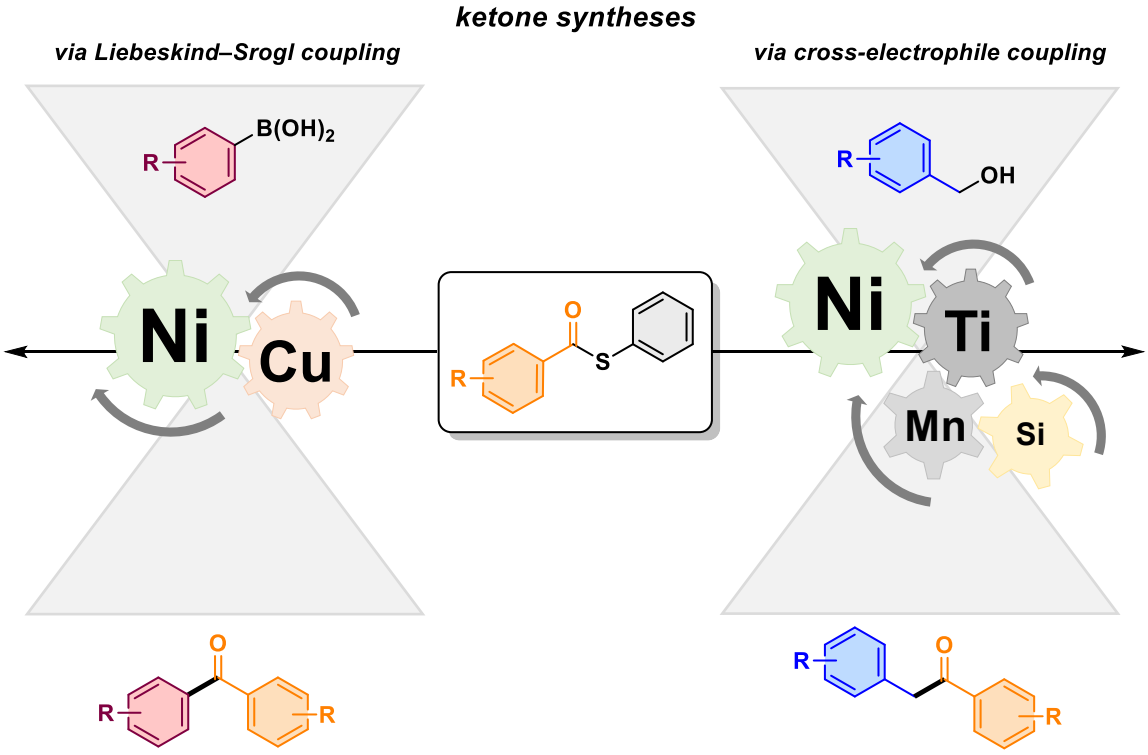

Figure 2-1: Overview of investigated transformations in this thesis: thioesters as acylation agents in ketone synthesis *via* nickel-catalyzed Liebeskind–Srogl coupling (left), and *via* nickel-catalyzed and Lewis acid-assisted cross-electrophile coupling (right).

3 Nickel-Catalyzed Liebeskind–Srogl Coupling

Author contribution:

The initial reaction design and preliminary optimization studies were conducted by the author of this thesis.

3.1 Introduction

The development of methods for ketone synthesis by traditional cross couplings is an intensively researched topic, and by now, a plethora of electrophiles have been shown to be suitable as acyl sources for reactions with various types of nucleophilic organometallic compounds. The next sections provide an overview of the current literature on nickel-catalyzed ketone syntheses, sorted according to the individual class of substrate.

3.1.1 Functionalization of α-Halocarbonyl Compounds

α-Haloketones are versatile compounds for the functionalization of the ketone framework under metal-catalyzed cross couplings with organometallic reagents. Especially the asymmetric coupling received considerable attention.

An enantioconvergent Kumada reaction of racemic α-bromoketones was developed using a chiral nickel/bis(oxazoline) complex (Scheme 3-1).[1] Dialkyl ketones required a slightly modified ligand. Detailed mechanistic investigations supported a radical-chain mechanism with a nickel(I) complex acting as the chain-carrying radical and an organonickel(II) complex as the resting state of the catalyst.[2]

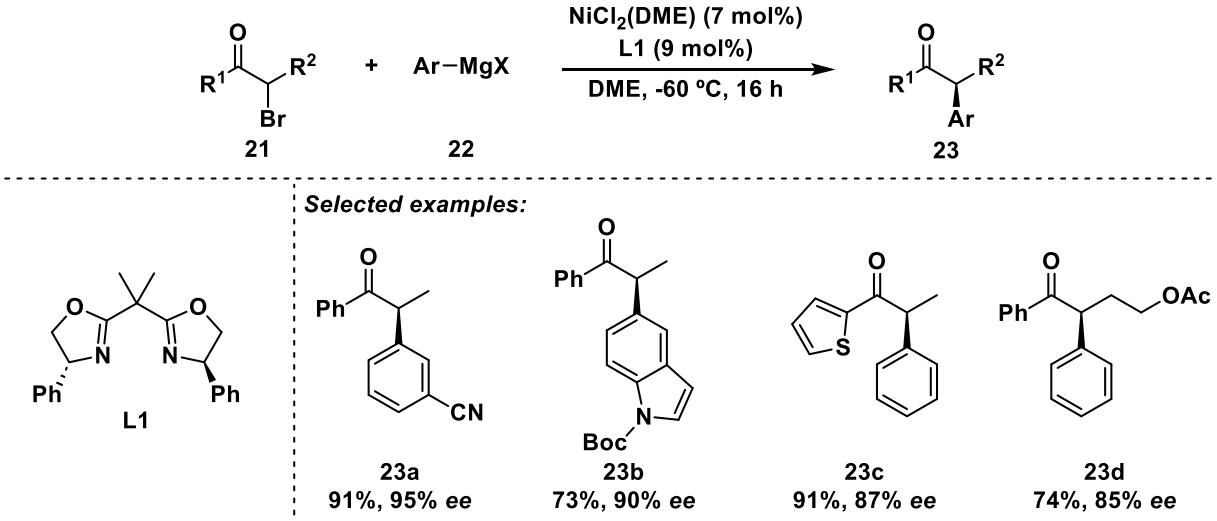

Scheme 3-1: Nickel-catalyzed asymmetric Kumada coupling between aryl Grignard reagents and α-bromoketones.[1]

3.1.2 Carboxylic Acid Derivatives

A promising substrate class for ketone synthesis by nickel-catalyzed cross couplings are carboxylic acid derivatives due to their wide-ranging reactivity and stability. Depending on the electrophilicity of the carbonyl C-atom and the favorability of the leaving group X, carboxylic acid derivatives are classified corresponding to their reactivity as follows: acyl chlorides > anhydrides > thioesters > carboxylic acid esters > carboxylic acids > amides > carboxylates (Figure 3-1).[3]

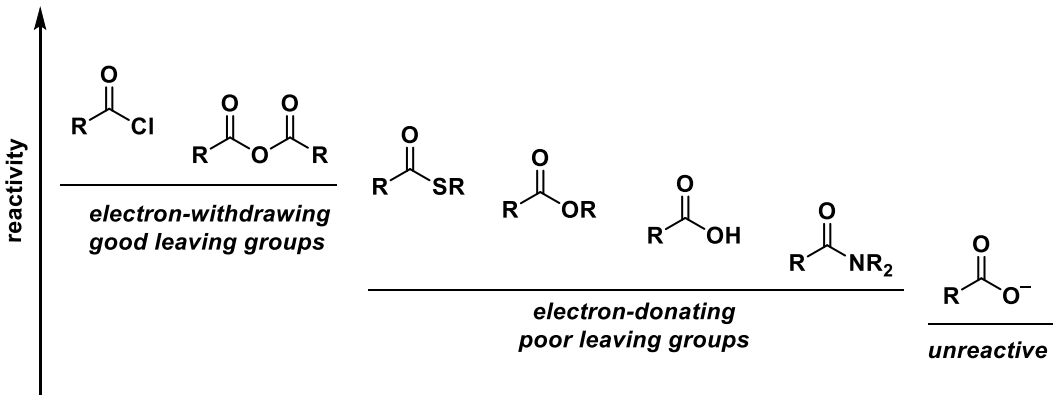

Figure 3-1: Classification of carboxylic acid derivatives by their carbonyl reactivity.[3]

In presence of a catalyst, they could serve as two different carbon-based building blocks for nucleophilic coupling partners. They can act either as a R–C(O) source *via* acyl coupling or as a R source *via* decarbonylative coupling. The well-accepted mechanism for the acyl coupling of various carboxylic acids includes the oxidative addition of the C(O)–X bond to the transition metal catalyst, followed by the transmetalation with the organometallic reagent and product formation after reductive elimination (Scheme 3-2).[4]

In the subsequent sections, an overview of acyl cross couplings using thermal nickel catalysis is given, sorted by different acylating agents and starting with acyl halides.

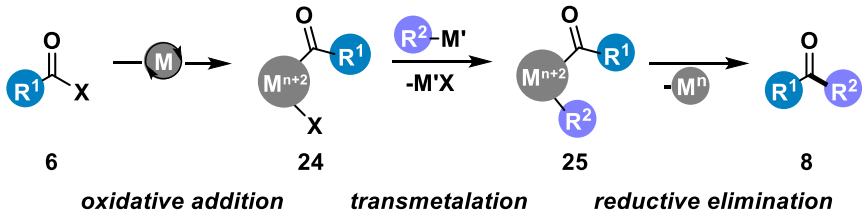

Scheme 3-2: Transition metal-catalyzed acyl cross coupling.[4]

3.1.2.1 Acyl Halides

Palladium catalysis dominates the coupling of acyl halides,[4,5] and only a few nickel-catalyzed reports are known.

In an early protocol from 1995, the reaction of acyl halides with Grignard reagents using $NiCl_2$(dppe) as a catalyst was described, furnishing dialkyl, diaryl and alkyl aryl ketones.[6] 1,2-Diketones or 2-acyldithianes were also synthesized under the same conditions.

Rovis described the rapid coupling of Ph_2Zn and several alkyl zinc reagents with carboxylic acid fluorides, chlorides, anhydrides, and thioesters using 10 mol% $Ni(cod)_2$ or 1 mol% $Ni(acac)_2$ in some cases, 12 mol% 2-[2-(diphenylphosphanyl)ethyl]pyridine (pyphos) and 20 mol% 4-fluorostyrene (Scheme 3-3).[7] Usually, the reaction time was quite short, e.g. 10–30 min, and no heating was necessary. Additionally, only 0.55 equivalents of the diorganozinc reagent were required, indicating that both organic moieties participate as nucleophilic fragments. Furthermore, the reaction could be conducted without loss of stereochemical integrity.

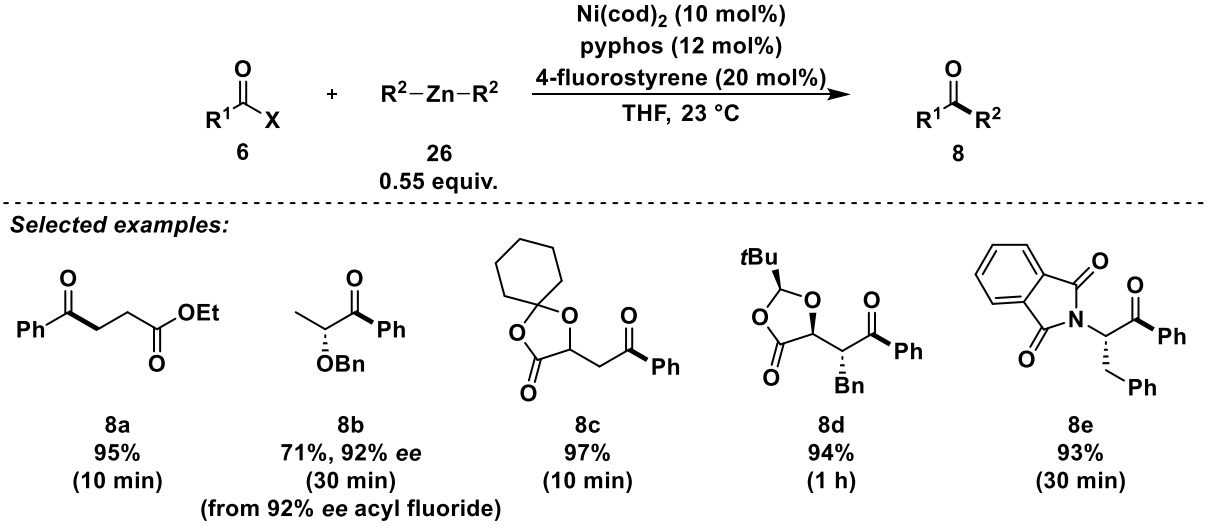

Scheme 3-3: Nickel-catalyzed coupling of different carboxylic acid derivatives with organozinc reagents. The shown examples were synthesized from the corresponding acyl fluorides.[7]

3.1.2.2 Amides

Nickel catalysis is very attractive for C(O)–N bonds of activated amides and thus makes another acyl source accessible.[8] Suzuki–Miyaura and Negishi couplings are most commonly performed with these substrates, and various amide electrophiles have been shown to be suitable.

Aryl ketones were synthesized from *N*-Bn-*N*-Boc amide derivatives **27** and organoboron reagents with a $Ni(cod)_2$/1,3-bis(2,6-diisopropylphenyl)imidazolidine (SIPr) catalyst system and K_3PO_4 as base (Scheme 3-4A).[9] Since inconsistencies in yields with organoboron coupling partners were attributed to variations in the water content,[10] it was found that the

addition of water (2 equiv.) led to a quantitative yield of ketone. Besides a broad substrate scope including substituents with different electronic motifs, ketones, esters, and heterocycles, the utility of the method was demonstrated by synthetic applications, for instance in a multistep synthesis with a controlled amide activation sequence. The substrate scope was extended to aliphatic amides by changing the *N*-heterocyclic carbene (NHC) ligand.[11]

Aliphatic amides could also be converted *in situ* to chiral alcohols by one-pot Suzuki–Miyaura cross coupling with boronates, followed by transfer-hydrogenation using 1-(4-(dimethylamino)phenyl)ethanol (DMPE) as reducing agent.[12] $Ni(cod)_2$ and a NHC ligand were suitable to catalyze the reaction.

Stanley described the nickel-catalyzed alkene carboacylation with *o*-allylbenzamides **32** and arylboronic esters to generate indanone derivatives **34** (Scheme 3-4B).[13] Mechanistically, the catalytic cycle is initiated by coordination of the NHC–Ni^0 complex to the amide and the oxidative addition of the C(O)–N bond to nickel(0), generating complex **35**. Then, the mechanism of the carboacylation could diverge depending on the sequence of transmetalation and migratory insertion events. Several observations have shown that the transmetalation of boronic ester initially leads to the formation of complex **36**, which subsequently undergoes a migratory insertion, resulting in species **37**. After reductive elimination, the product **34a** is obtained (Scheme 3-4B).

Moreover, the combination of $Ni(cod)_2$ and bis-dentate NHC ligand as well as K_2CO_3 and water as additives were used for the reaction of *N*-acylpyrroles and Ar–B(nep), affording diaryl ketones.[14]

N-Me-*N*-Ts amides were alkylated and benzylated with organozinc reagents under nickel catalysis and mild reaction conditions (Scheme 3-4C).[15] A combination of $Ni(cod)_2$ and NHC ligand was employed as the catalyst system, yielding the desired aryl alkyl ketones in yields of 62–87% and showing good tolerance towards various functional groups.

A selective $NiCl_2(PPh_3)_2$-catalyzed C(O)–N bond cleavage was achieved with distorted amides, and diaryl ketones were generated by implementation with arylzinc reagents.[16] With Et_2O as solvent, a considerable improvement of yield was observed, possibly due to stabilization effects on the intermediate. The reaction profile indicated that the coupling was completed in less than 10 min at room temperature. The developed system was widely applied to various substrates, in particular aryl amide electrophiles with indolyl and dimethylamino substituents, *ortho*-methoxy substituted aryl zinc nucleophiles and substrates bearing heterocycles, such as thiophene, furane and dioxolane.

Another protocol showed the nickel-catalyzed reaction of benzamides with bicyclic alkenes, in which both the C–H bond in the *ortho*-position of the benzene ring and the C(O)–N bond were cleaved to yield methanofluoren-9-one and 1,4-epoxyfluoren-9-one derivatives.[17]

A $Ni(OTf)_2$/BINAP catalyst system and AgOAc as an additive were chosen for the coupling, however harsh reaction conditions (140 °C, 60 h) were mandatory to turnover the reaction.

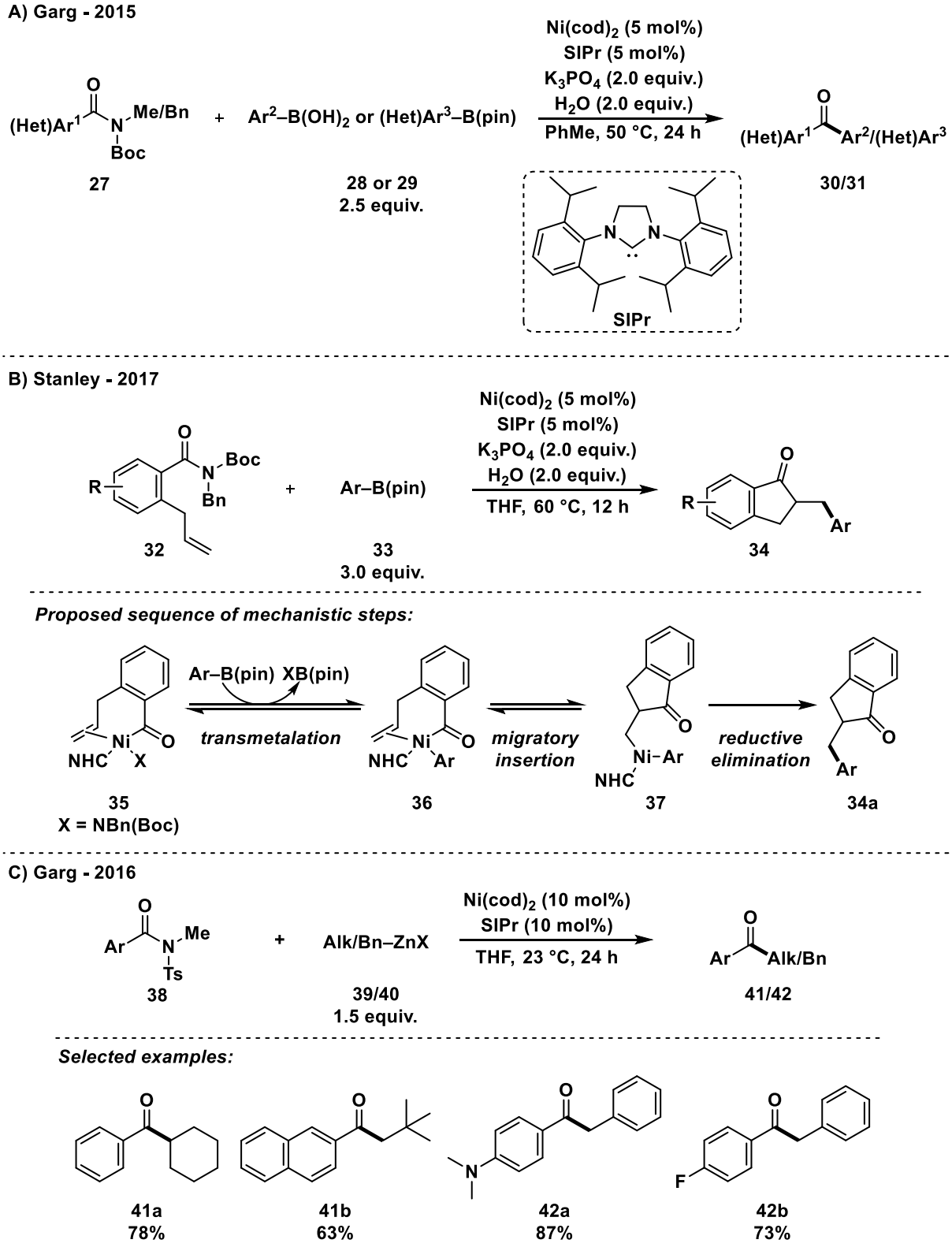

Scheme 3-4: Nickel-catalyzed arylation, carboacylation and alkylation of amide derivatives.[9,13,15]

3.1.2.3 Carboxylic Acids, Anhydrides and Esters

Carboxylic acids, anhydrides and esters are auspicious functionalities as they are abundant in nature and suitable for various catalytic transformations. For instance in relation to carboxylic acids, the possible reactions can include the extrusion of CO_2, reaction *via* metal carboxylates or (de)carbonylation through an acyl metal species.[8e,18] Nevertheless, nickel-catalyzed methodologies for ketone synthesis with these substrates are underdeveloped compared to palladium-catalyzed applications.

Regarding the direct use of carboxylic acids as substrates, an early report by Marchese in 1983 showed the selective formation of ketones over alcohols from the reaction of carboxylic acids and alkyl or aryl Grignard reagents using $NiCl_2$(dppe) as a catalyst.[19] In the absence of catalyst, tertiary alcohols were generated as main products in most cases.

Anhydrides were used much more frequently as substrates than carboxylic acids. Nickel-catalyzed Suzuki–Miyaura acylations with aromatic carboxylic acid anhydrides and arylboronic acids were carried out using 5 mol% $NiCl(PPh_3)_2$(1-naphthyl) as catalyst, 10 mol% PCy_3 as ligand and K_3PO_4 as base.[20] Interestingly, the yields of the desired diaryl ketones showed a dependency on the reactivity of anhydrides, decreasing in the order electron-rich > electron-neutral > electron-poor anhydrides. A competitive hydrolysis side-reaction of the anhydrides was proposed, which was more suppressed with electron-rich anhydrides. Mechanistically, oxidative addition of the anhydride to nickel(0) generates a RC(O)–Ni^{II}–OC(O)R complex, followed by transmetalation of the arylboronic acid. The desired ketone is delivered after reductive elimination from a RC(O)–Ni^{II}–Ar complex.[20]

Furthermore, a series of reports have been published on the nickel-catalyzed opening of cyclic anhydrides with alkylzinc reagents furnishing γ- or δ-keto acids (Scheme 3-5).[21]

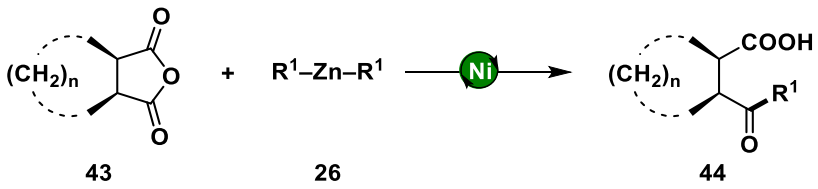

Scheme 3-5: Nickel-catalyzed opening of anhydrides with organozinc reagents.[21]

Compounds related to carboxylic acid anhydrides are also suitable as substrates, as shown by the use of thiophthalic anhydrides in nickel-catalyzed cycloaddition with alkynes.[22] Selectivity was controlled by the reaction conditions, i.e. ligand, Lewis acid additive and solvent, so that either thioisocoumarins, benzothiophenes or thiochromones were formed as products. In addition, isatoic anhydrides reacted with norbornenes[23] or alkynes[24] under nickel catalysis to form quinolones.

Although they are less reactive than anhydrides, carboxylic acid esters have nevertheless been used for nickel-catalyzed cross couplings. Alkylborane reagents were efficiently coupled with *O*-phenyl esters in the presence of a nickel(0) catalyst and a monodentate phosphine, either P*n*Bu$_3$ or PCy$_3$ (Scheme 3-6).[25] Additionally, the substrates reacted in a decarbonylative coupling after changing to a bidentate 1,2-bis(dicyclohexylphosphino)ethane (dcype) ligand and CsF as additive. For the acyl cross coupling, various phenyl-based esters were tolerated by the system, for instance with different electronic and steric demands as well as diverse substituents, including a benzyl-based ester, an amine, a ketone, or heterocyclic moieties. The reaction was performed with both primary B-alkyl-9-BBN (9-borabicyclo(3.3.1)nonane) and trialkyl boranes.

A modified catalyst system containing Ni(cod)$_2$ and a NHC-based ligand allowed the extension of the substrate scope to methyl esters,[26] the latter also being suitable as electrophiles for a nickel-catalyzed domino Heck/Suzuki–Miyaura coupling with organoboron compounds or in a Heck/reduction with a hydride source.[27]

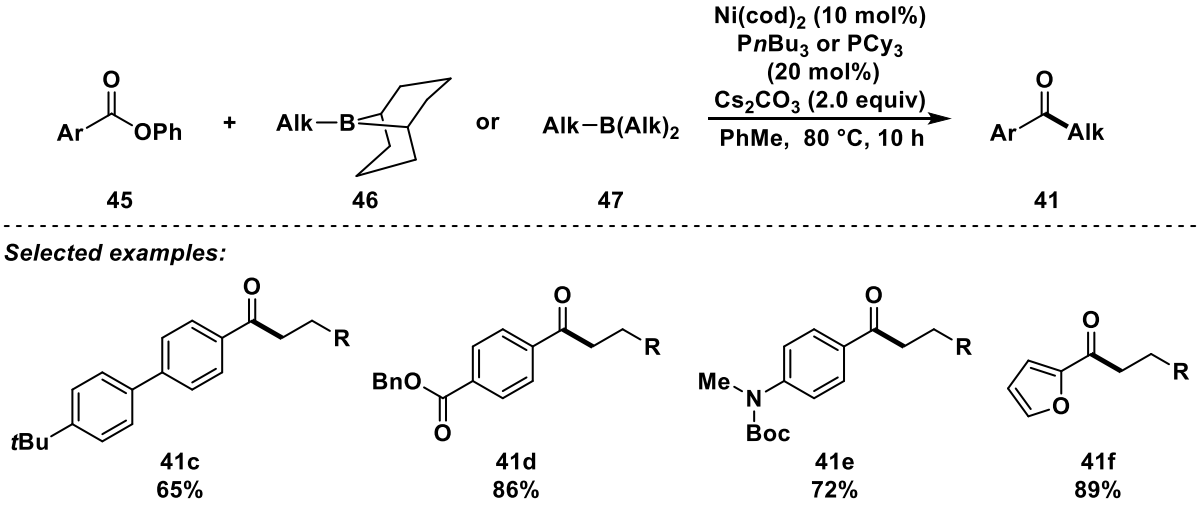

Scheme 3-6: Nickel-catalyzed coupling of alkyl boranes with esters, R = CH$_2$PMP (PMP = *p*-methoxyphenyl).[25]

In a study on the nickel-catalyzed conversion of aryl 2-pyridyl esters into secondary benzylic alcohols using organozinc reagents, Chen *et al.* also reported two aryl alkyl or aryl benzyl ketone syntheses.[28] In addition, the group demonstrated a single example of *S*-(pyridine-2-yl) benzothioate as a convenient acyl donor, yielding the aryl alkyl ketone in 77%.[28]

The example implies the possibility of employing thioesters as alternatives to carboxylic acid esters as electrophiles for cross couplings. In the following section, the focus is shifted from *O*-derived carboxylic acid derivatives to sulfurous building blocks, which are presented as another possible acyl source for ketone synthesis.

3.1.2.4 Organosulfur Building Blocks

Sulfur exhibits both oxidizability and reducibility due to its unique electron configuration [Ne] $3s^2$ $3p^4$. It can be oxidized to different valence states by losing two, four or six electrons. In contrast, sulfur is reduced by obtaining two electrons, reaching the noble gas electronic configuration of argon.[29] Due to its various valence states, sulfur has diverse chemical properties and sulfur-containing compounds are not only widely found in natural products,[30] pharmaceuticals,[31] and agrochemicals,[32] but the metal-thiolate interactions occur frequently in the biochemistry of life-sustaining processes.[33] Nature has evolved important metalloenzymatic processes that control key interactions of sulfur-containing functionalities with metals such as nickel, cobalt, copper and iron, thus overcoming the stability of the bond between a mercaptide ligand and redox-active metals.[33]

In the next section, selected organosulfur classes are reviewed, namely thiocarbamates, thiocarbonates and thioesters (Figure 3-2), outlining their properties and applications in cross coupling chemistry.

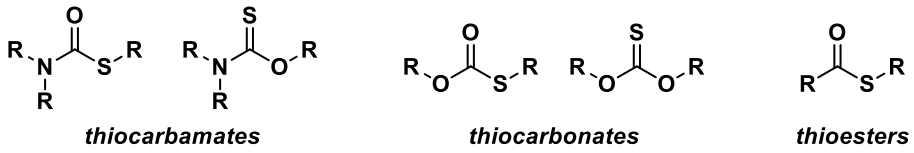

Figure 3-2: Organosulfur compounds covered by this thesis.

3.1.2.4.1 Thiocarbamates

Thiocarbamates, also known as thiourethanes, exhibit the $R_2N–C(S)–OR$ (*O*-thiocarbamates) or the $R_2N–C(O)–SR$ (*S*-thiocarbamates) framework. *O*-Aryl thiocarbamates can be isomerized to *S*-aryl thiocarbamates by the Newman–Kwart rearrangement.[34]

O-Thiocarbamates possess reduction potentials of roughly $E^0_{red(average)}$ = -1.55 V *vs.* SCE,[35] and are used as auxiliaries in radical reactions.[36] A protocol developed by Rousseaux showed that cyclopropanes can be arylated with organozinc reagents if they carry a redox-active *O*-thiocarbamate leaving group that activates the cyclopropane to form radicals.[37] In another contribution of the group, thiocarbonyl imidazolides were arylated by organozinc reagents in a nickel-catalyzed Negishi cross coupling.[38]

Huang reported a C–N bond cleavage event in the palladium-catalyzed intramolecular C–H bond sulfuration of aryl *O*-thiocarbamates **48** (Scheme 3-7). Multiply substituted benzo[*d*][1,3]oxathiol-2-ones **49** were formed in yields of 20–94%.[39]

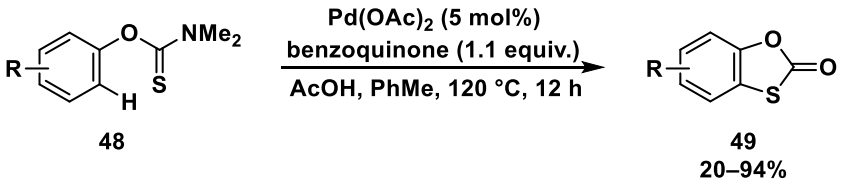

Scheme 3-7: Intramolecular oxidative C–H sulfuration of aryl thiocarbamates under palladium catalysis.[39]

Another approach demonstrated the application of cyclic *O*-thiocarbamates in a desulfurative Sonogashira cross coupling with alkynes.[40] Two synergistic copper(I) species, CuI and CuTC, activated the substrates for the coupling.

Moreover, the reaction of *S*-thiocarbamates and internal alkynes yielded tetrasubstituted vinyl sulfides as the *syn* isomer, using a $Ni(cod)_2$/P*i*Pr_3 catalyst system and harsh reaction conditions of 130 °C for 24 h.[41] It was proposed that the reaction mechanism includes the oxidative addition of the thiocarbamate to nickel(0), followed by the insertion of the alkyne and product supply after reductive elimination.

3.1.2.4.2 Thiocarbonates

Monothiocarbonates contain the CO_2S^{2-} framework, which includes thioncarbonates RO–C(S)–OR and thiolcarbonates RO–C(O)–SR, so that two different C–heteroatom bonds, for instance RO–C(O) and C(O)–SR of thiolcarbonates, can be activated. The spectrum of synthetic approaches towards monothiocarbonates is broad and ranges from the biosynthetic formation from a thioester by a monooxygenase-catalyzed Baeyer–Villiger oxidation[42] to the Schönberg rearrangement of thioncarbonates to thiolcarbonates at high temperature (280 °C).[43] There are also dithiocarbonates, of which xanthates, *O*-esters of dithiocarbonates, are derivatives, and trithiocarbonates, but only monothiocarbonates are considered in the following description of applications.

Monothiocarbonates have great potential as substrates for thermally induced cross couplings, as one of the two C–heteroatom bonds can be selectively cleaved depending on the catalyst and reaction conditions. The C–O bonds of thiocarbonates are known to have a higher BDE (100 kcal/mol) compared to C–S bonds (76 kcal/mol).[44]

A C(O)–SR bond cleavage of thiocarbonates was achieved through a Catellani strategy using a palladium/norbornene/copper co-catalyzed approach for the coupling with aryl iodides, yielding *ortho*-thiolated aryl esters.[45]

A protocol for the chemoselective cleavage of the RO–C(O) bond is also known. A nickel-catalyzed cross-electrophile coupling of aryl triflates with *O*-*t*Bu *S*-alkyl thiocarbonates gave benzoic acid thioesters (Scheme 3-8).[44] Both electron-poor and -rich triflates were coupled, however electron-rich substrates needed a change in the additive and an elevated temperature of 80°C.

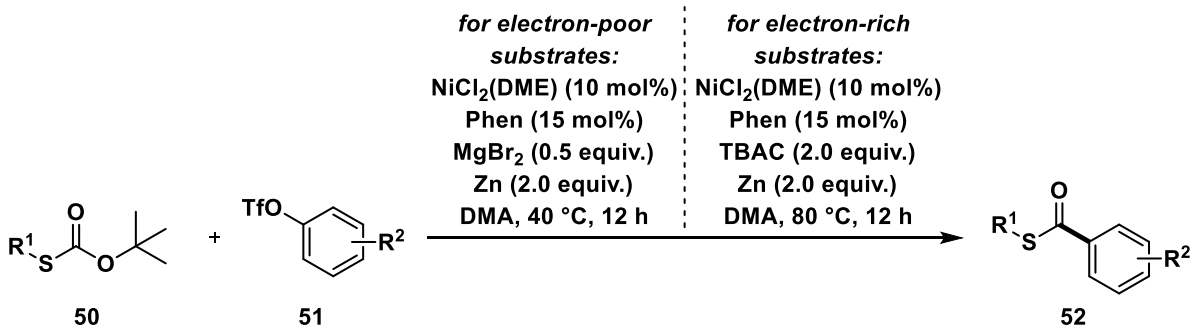

Scheme 3-8: Nickel-catalyzed cross-electrophile coupling of thiocarbonates and aryl triflates.[44] TBAC = tetrabutylammonium chloride.

Additionally, thiocarbonates were used as substrates in light-driven couplings. In 2021, Cook and co-workers published a Barton–McCombie-type reaction that allowed the copper-mediated light-induced deoxygenative trifluoromethylation of *O*-alkyl thiocarbonates.[46]

Finally, the presented substrate class can also be decarboxylated under catalytic conditions, for instance in the ruthenium-catalyzed synthesis of allyl(aryl)sulfide derivatives.[47]

3.1.2.4.3 Thioesters

3.1.2.4.3.1 Characteristic Properties

Thioesters are a highly desirable compound class, e.g. for thiocarbonylations, decarbonylations, allylic substitutions, dual photoredox/metal catalysis and cross couplings,[48] as they are bio-sourced substrates and frequently found in biochemical processes, with the most prominent example being acetyl coenzyme A as provider of the acetyl group for the citric acid cycle.[49]

The unique properties of thioesters are best illustrated by a comparison with amides and carboxylic acid esters. A change from the pnictogens to the chalcogens and the substitution of oxygen by sulfur as a higher homolog have electronic consequences that lead to different reactivities of *N*-, *O*- and *S*-containing compounds and can be explained by the orbital model (Figure 3-3A). In a C(O)–N bond, the n-π*-orbital overlap is excellent and the strong resonance results in a high thermodynamic stability, an enhanced rotation barrier and high bond dissociation energies, for instance in the range of 90–101 kcal/mol for amides (Figure 3-3B).[29,50]

Thioesters are activated esters, which reactivity towards nucleophiles is comparable to that of acid chlorides and anhydrides. The difference in reactivity compared to oxoesters is due to the lone pairs on the sulfur atom in 3p orbitals instead of 2p orbitals. These orbitals are too large to overlap efficiently with the 2p orbital on the carbon atom of the carbonyl group, which is why thioesters have less conjugation than oxoesters (Figure 3-3A).[48] The consequence is a lower π-character of the C–S bond and decreased bond strengths with BDEs in the range of 74–78 kcal/mol compared to the BDEs of the C–O ester bond (80–100 kcal/mol,

Figure 3-3B).[29] Contrariwise to the alkoxide, the thiolate exhibits a more pronounced leaving group ability, which is classified by the acid strength of the conjugated acid, meaning that a strong acid has a conjugated weak base with an excellent leaving group ability. Thiols are stronger acids than alcohols (pK_a = 6.6 for PhSH *vs.* pK_a = 10.0 for PhOH),[51] and thiolates are significantly more nucleophilic than alkoxides (N = 22.6 for RCH_2S^- *vs.* N = 16.0 for RCH_2O^-).[52]

In conclusion, a trend can be established with C(O)–N being the thermodynamically most stable, followed by C(O)–O, and then by C(O)–S compounds, which are the most reactive, resulting in an easier activation by transition metal catalysis (Figure 3-3B).[29]

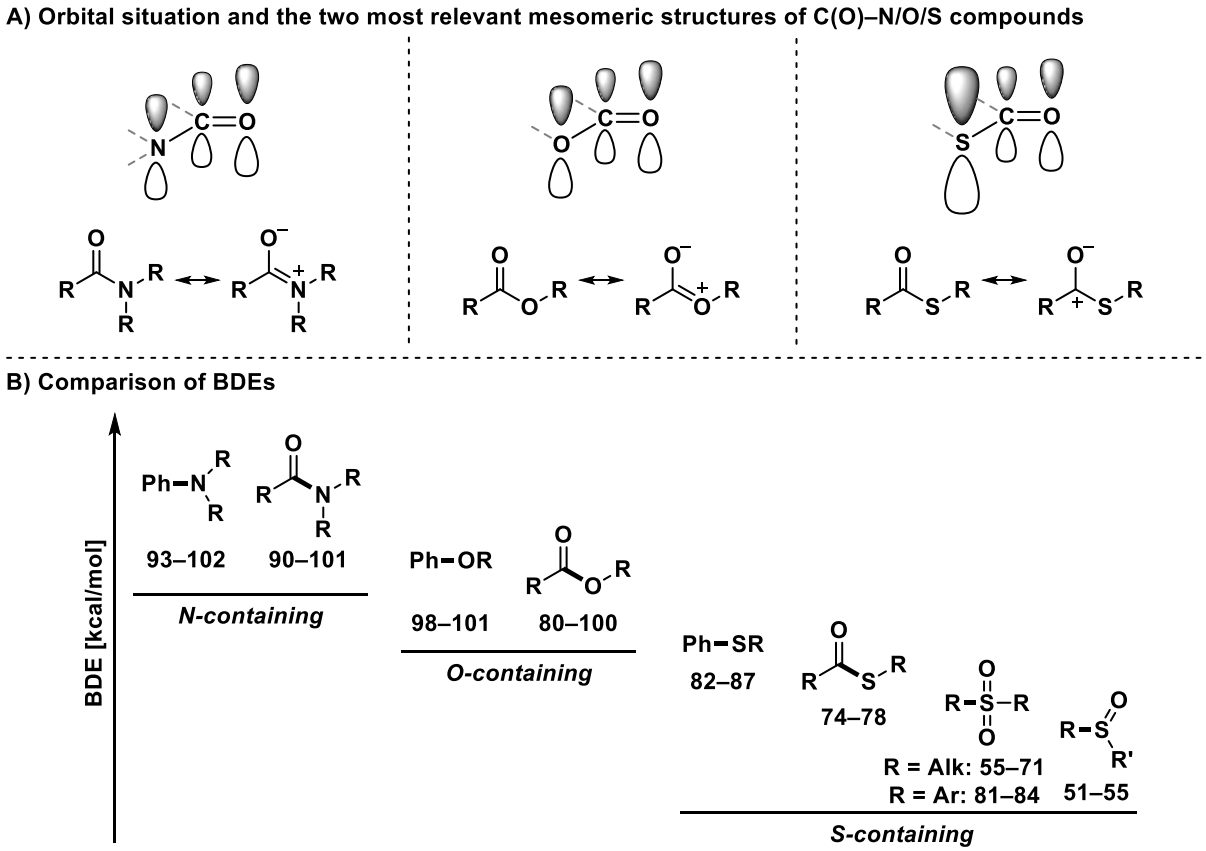

Figure 3-3: Comparison of the orbital situation and BDEs of *N*-, *O*- and *S*-containing compounds in kcal/mol.[29,48,50,53]

The reactivity of thioesters can be influenced by the thiol moiety, with *S*-(2-pyridyl) thioesters being the most reactive (Figure 3-4).[54] Therefore, they can be manipulated for synthetic purposes, e.g. by C(O)–S activation in transition metal-catalyzed acylations. In addition, *S*-aryl and *S*-(2-pyridyl) thioesters offer the possibility of fine-tuning the reactivity using substituents on the aromatic ring system with different electronic properties. The same applies to an Ar–C(O) moiety, for instance thioesters with an electron-withdrawing CF_3 substituent on the Ar–C(O) scaffold undergo a nickel-catalyzed thioacylation transfer reaction with a C–C bond cleavage to sp^2-hybridized electrophiles.[55]

Moreover, 2-pyridyl thioesters exhibit very low reduction potentials, e.g. for 2-pyridyl benzothioate E^0_{red} = -2.8 V *vs.* Fc/Fc$^+$,[56] and the advantage of chelation, as shown by the reaction with Grignard reagents for the synthesis of ketones.[57] However, a general problem of thioesters is the released thiolate, which impairs productive catalysis due to the competitive formation of thioethers and potentially reducing ketone yields (*vide postea*, section 4.3.1).[58] Deactivation of the catalytically active species is especially a problem for nickel catalysts, as they exhibit a high thiophilicity.[59]

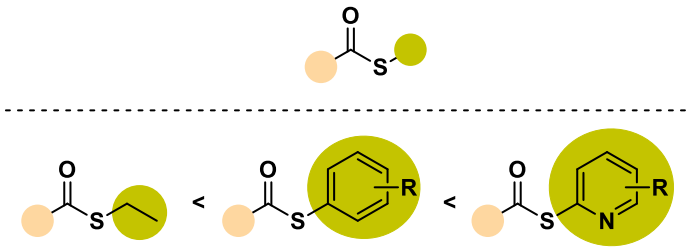

Figure 3-4: Order of reactivity towards C–S activation and fine-tuning by substituents R of thiol moieties in thioesters.[54]

Research on one-electron chemistry of thioesters, for instance as acyl radical sources for ketone synthesis by catalytic transformations, is underdeveloped. Gryko showed a light-driven, cobalt-catalyzed method for the generation of acyl radicals from 2-pyridyl thioesters, which were captured by activated olefins.[60] Acyl radicals were postulated as short-lived intermediates in a nickel-catalyzed variant of the Fukuyama cross coupling demonstrated by Fleischer *et al.*, using *S*-alkyl thioesters and arylzinc reagents as substrates together with an air and moisture stable nickel precatalyst.[61] Lee proposed the involvement of acyl radicals generated from thioesters during the reduction with $TiCl_4$/Zn, but this approach was not of a catalytic nature.[62]

Completing the overview of thioester properties, their advantageous stability towards decomposition is worth mentioning and it enables a prolonged storage. Additionally, they can be readily synthesized from acyl chlorides or by Steglich esterification,[63] and progress has also been made in developing new strategies to access the thioester motif.[48,64]

3.1.2.4.3.2 Application of Thioesters in Metal-Catalyzed Ketone Synthesis

To demonstrate the broad spectrum of applications, the following section describes various metal-catalyzed ketone syntheses starting from thioesters as substrates.

An early report by Marchese showed the formation of ketones by a sequential nickel- and iron-catalyzed coupling of Grignard reagents with *S*-phenyl carbonochloridothioate, from which the corresponding thioesters were formed as intermediate substrates.[65]

The use of thioesters in cross couplings was fully established by Fukuyama, who developed palladium-catalyzed conversions of thioesters either into ketones with organozinc reagents (Fukuyama cross coupling) or into aldehydes with silanes as reducing agents (Fukuyama reduction).[66] In the seminal reports on ketone synthesis, ethanethiol esters were coupled with alkyl and arylzinc reagents (1.5 equiv.) using 5–10 mol% $PdCl_2(PPh_3)_2$.[66a,b] The ketones were obtained in high yields (29 examples, 50–99%) at room temperature in very short reaction times of up to five minutes.

An advancement of the reaction was the phosphine-free synthesis of diaryl ketones with 1 mol% Pd_2dba_3.[67] The first enantioconvergent Fukuyama coupling of racemic benzylic organozinc reagents was developed in 2016, with enantioselectivity achieved by a $Pd(OAc)_2$/TADDOL phosphoramidite catalyst system.[68] A novel development synthesized a precursor of the natural product isoprekinamycin, using a bench-stable palladium precatalyst.[69]

Although the Fukuyama cross coupling was already very attractive with mild reaction conditions, short reaction times and a broad functional group tolerance (i.e. esters, aldehydes, or olefins), a disadvantage was the use of palladium as an expensive precious metal catalyst. However, progress on this topic has made it possible to replace palladium by other catalysts. A remarkable improvement of the reaction was done by Seki, who published the first nickel-catalyzed Fukuyama coupling (Scheme 3-9).[70] Contrary to the palladium-catalyzed variants, a significant excess of four equivalents organozinc reagents and a long reaction time (20 h) were necessary.

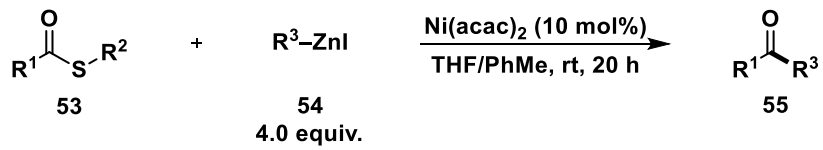

Scheme 3-9: First nickel-catalyzed Fukuyama coupling.[70]

A ketone yield of 95% within 10 minutes was achieved after the reaction of *S*-(2-pyridyl) thioester and 0.55 equivalents of Ph_2Zn with a $Ni(cod)_2$/pyphos catalyst system and 4-fluorostyrene as an additive (see Scheme 3-3).[7] A less reactive *S*-ethyl thioester required twice the amount of nucleophilic coupling partner (1.1 equiv.) and a longer reaction time (2 h),

but then furnished the ketone in 92% yield.[7] For the sake of completeness, reference should also be made once again to the nickel-catalyzed Fukuyama coupling developed by Fleischer *et al.* (see section 3.1.2.4.3.1).[61]

In addition, a cobalt-catalyzed variant was reported with (hetero)arylzinc pivalates and *S*-(2-pyridyl) thioesters as substrates.[71] The reaction enabled the acylation of α-chiral thiopyridyl esters with very high stereoretention, leading to optically enriched α-chiral ketones. Moreover, a $Fe(acac)_3$-precatalyst was used for the Fukuyama-type cross coupling of thioesters and aliphatic organomanganese reagents.[72]

The scope of the Fukuyama reaction was extended by the application of organoboron compounds as nucleophiles, the so-called Liebeskind–Srogl cross coupling, representing another method for the synthesis of ketones.

3.1.3 Liebeskind–Srogl Cross Coupling

3.1.3.1 Historical Development

Ketone synthesis by coupling organosulfur compounds with boronic acids is a research field of great interest, as both reaction partners are readily accessible, inexpensive, bench-stable and of low toxicity.

However, already in the pioneering work of Fukuyama in 1998, low yield of ketone was reported for the palladium-catalyzed reaction of thioester and boronic acid as nucleophile instead of an organozinc reagent.[66b] Two years later, Terfort mentioned sulfur-assisted acylation of boronic acids with thioesters as acylation agents only as side reaction in a primarily investigated coupling under Suzuki conditions.[73]

The examples are intended to illustrate the challenges posed by direct thioester-boronic acid cross coupling. The key step in such reactions is the transmetalation of the boronic acid to the metal thiolate intermediate **57** and the consequential replacement of the thiolate ligand (Scheme 3-10).[74] The ligand exchange is impeded by the usually strong metal-thiolate bond, which renders the elimination of the thiolate unfavored. This is exacerbated by the low thiophilicity combined with the less pronounced nucleophilic reactivity of organoboron compound, which must be overcome to achieve satisfactory yields of the desired products.[74]

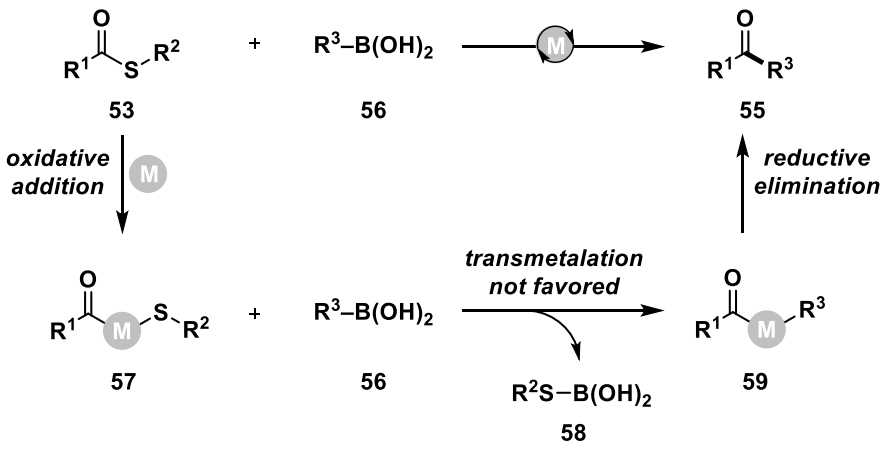

Scheme 3-10: Thioester-boronic acid cross coupling.[74]

The use of tetrahydrothiophene-based sulfonium salts as coupling partners in nickel- and palladium-catalyzed reactions with organoboron reagents solved the problems listed above, as tetrahydrothiophene does not interfere with the catalyst.[75] Liebeskind introduced the term of 'alkylative activation', which refers to the transformation of the strong palladium-thiolate bond **62** into a labile palladium-thioether bond **63**. In the absence of catalytic NaI, only trace amounts of ketone were obtained, and control reactions showed that the salt probably converts the alkyl bromide to alkyl iodide, facilitating the postulated intramolecular activation. The desired ketones were efficiently generated in good to excellent yields (Scheme 3-11).[76]

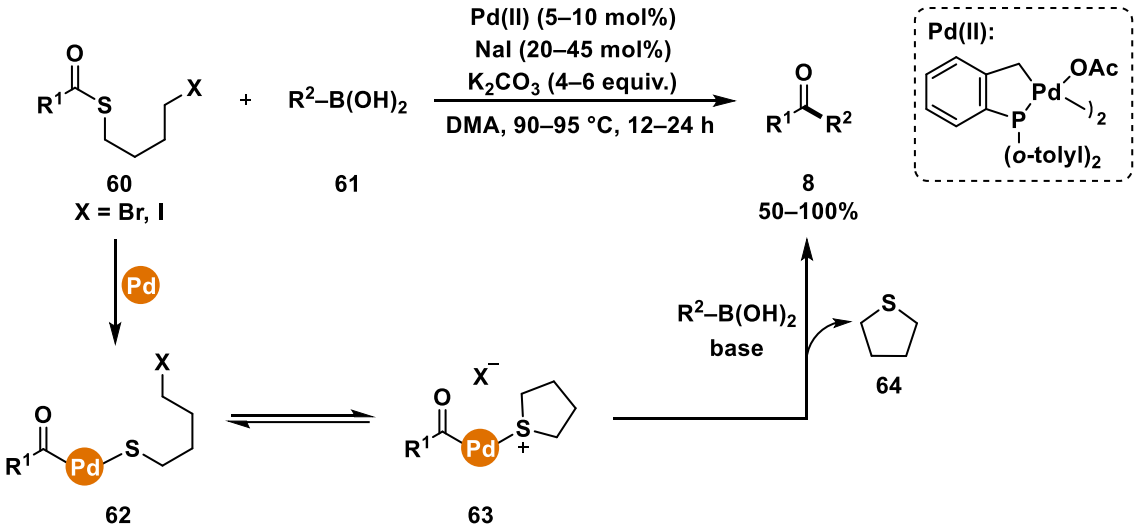

Scheme 3-11: Alkylative activation of the palladium-thiolate intermediate.[76]

Liebeskind and Srogl achieved a milestone in the development of couplings between thioesters and boronic acids.[77] In the so-called first generation of the Liebeskind–Srogl coupling (LSC), Pd_2dba_3/tri(2-furyl)phosphine (TFP) was used as the catalyst system and the dual thiophilic/borophilic activation was accomplished with stoichiometric amounts of copper(I) thiophene-2-carboxylate (CuTC) as additive (Scheme 3-12).[78] The substrate scope concerning thioesters and boronic acids was broad, tolerating a variety of substituents with

different electronic and steric properties, for instance free OH, NO_2 and CF_3 groups, heterocycles or sterically demanding naphthyl- or adamantyl scaffolds. The thiol moiety was not a limiting factor, as both *S*-aryl and alkyl thioesters could be converted without affecting the yields. Additionally, several aryl and vinylboronic acids were coupled, but heteroaromatic and alkylboron reagents proved to be unsuitable.[78]

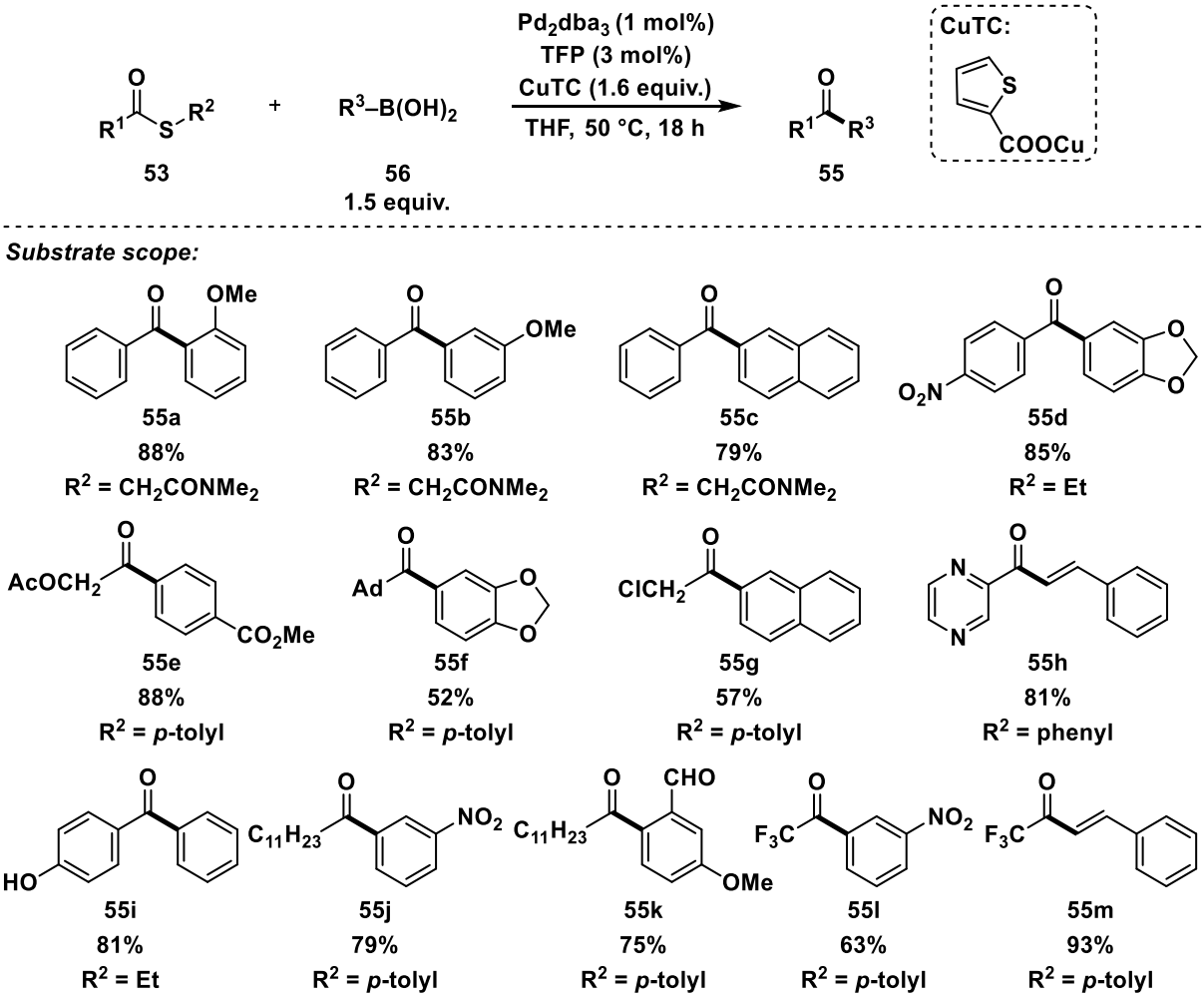

Scheme 3-12: CuTC-mediated cross coupling of thioesters and boronic acids.[78]

The corresponding mechanism is illustrated in Scheme 3-13.[78,79] The copper additive is the pivotal compound, as it coordinates to the sulfur center, thus polarizing and weakening the Pd–S bond. It also provides a carboxylate that facilitates the transmetalation from boron to palladium by coordinating to the boron center with simultaneous hydrogen bonding in a chair transition state **66** (Scheme 3-13).[80] In addition, copper thermodynamically favors the transmetalation and facilitates reductive elimination by forming a strong Cu–S bond (45–55 kcal/mol).[79b] In-depth DFT computations showed that the carboxylate also supports the phosphine ligand dissociation from the palladium center.[79b] Thereby, a less hindered and more electrophilic palladium-monophosphine intermediate is generated that promotes the transmetalation step.[79b]

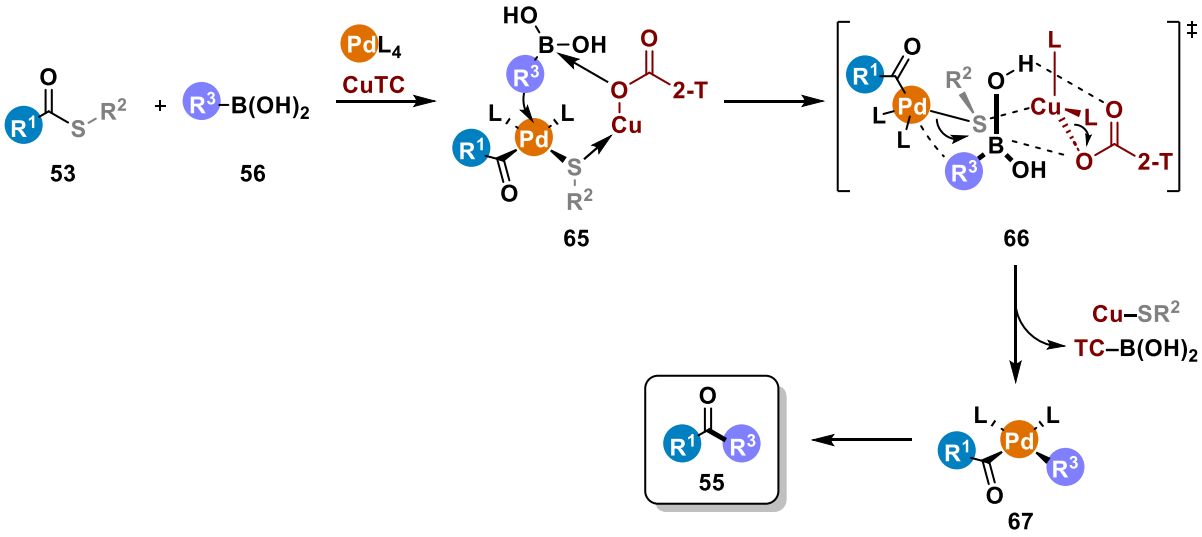

Scheme 3-13: Mechanistic considerations of the Liebeskind–Srogl coupling.[77b]

Contrariwise to the traditional Suzuki–Miyaura cross couplings, in which an oxygen atom containing base is essential for the success of the reaction,[81] bases have a detrimental effect in the Liebeskind–Srogl coupling between boronic acids and thioorganics.[78] An exception are 9-BBN-based alkylboronates as substrates. With these coupling partners, bases such as Cs_2CO_3, K_2CO_3 and K_3PO_4 improved the yields, as the formation of ternary complexes and activation by copper(I) is restricted with aliphatic boron reagents.[80b] Furthermore, organostannane,[82] organoindium[83] and organosilicium[82g,84] reagents can be employed as coupling partners under Liebeskind–Srogl conditions. Interestingly, the carboxylate anion of the copper species is not always decisive. For instance, Guillaumet and co-workers disclosed the palladium-catalyzed reaction of 2-thiouracil derivatives with organostannanes, which is only successful with CuBr instead of CuTC.[82h] In case of organoindium compounds, no sacrificial copper(I) reagent and no base were required to activate the organoindium reagents for alkyl transfer, in contrast to the reactions with alkylboronates.[83]

Based on the conditions of the first generation, which began with thioesters, the scope of sulfur-containing substrates was subsequently extended by Liebeskind himself and others (Figure 3-5). Functionalization of alkynes was realized by the coupling of thioalkyne derivatives and boronic acids under Liebeskind–Srogl conditions, achieving yields ranging from 39–91%.[80a] Neumann introduced a coupling of trimethylsilylethoxymethyl- (SEM) protected thiopseudourea compounds with boronic acids to generate fully protected benzamidines.[85] The *S*-coupling partner was easily accessible after deprotonation of a commercially available guanidylation reagent and subsequent treatment with SEM chloride. The synthesis of nitriles by a LSC was achieved with thiocyanates as substrates.[86] Furthermore, the assistance of microwaves supported the generation of more complex ketones from pyrimidine thioesters.[87] *N*-protected peptidyl ketones were generated in good to excellent yields and in high enantiopurity by the LSC of α-amino acid thioesters with aryl, electron-rich heteroaryl or

alkenyl boronic acids.[88] Moreover, several couplings of boronic acids and sulfur compounds containing various heteroaromatics, e.g. thioethers,[79a,82c,89] thiones[90] or thioamides,[91] have been published over the years.

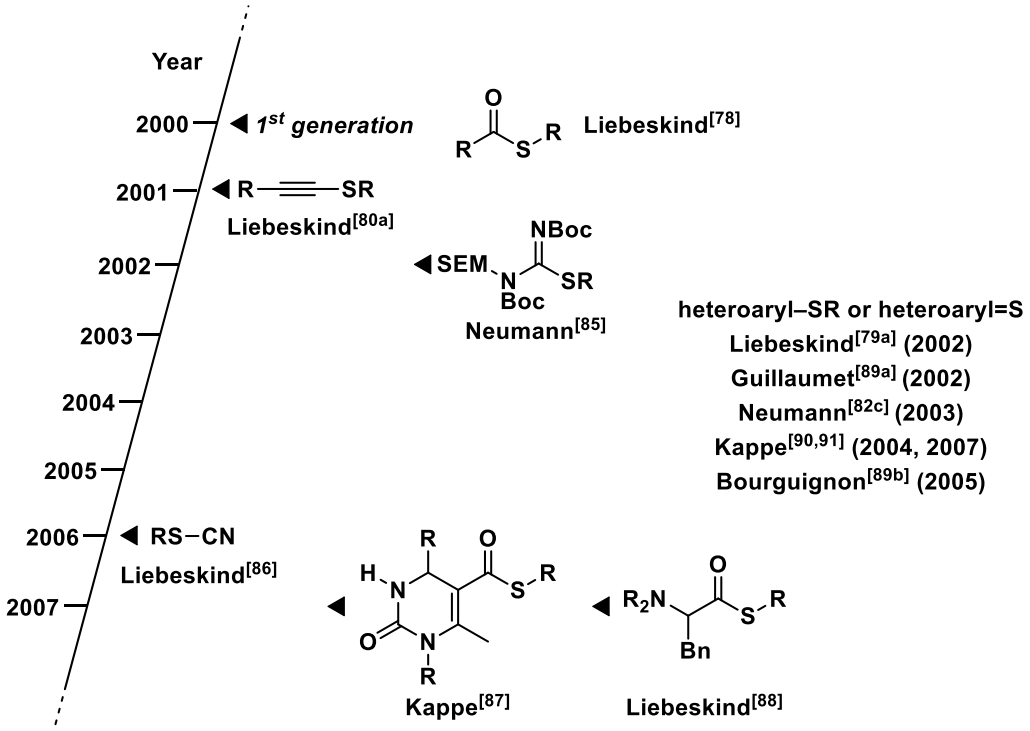

Figure 3-5: Chronological development of suitable sulfurous substrates for the first generation of LSC.[78,79,80a,82c,85-91]

In 2007, Liebeskind and co-workers introduced the second generation of LSC. In this system, *S*-acyl-NH*t*Bu thiosalicylamides and an excess (2.5 equiv.) of boronic acids reacted without a palladium catalyst, but with 5 mol% of copper(I) 3-methylsalicylate (CuMeSal) under aerobic conditions to form the desired ketones and thioethers (Scheme 3-14).[92] A mechanism has been proposed in which aerobic activation of copper(I) coordinated with the thioester occurs, resulting in an oxidized copper(II/III) intermediate **71** (Scheme 3-14, step I). This species can interact with the organoboron counterpart to form the ketone and a higher oxidized copper(II/III) thiolate **73** (steps II and III). The second equivalent of the boronic acid completes the catalytic cycle by regenerating copper(I) and removing the thiolate from the system by forming the corresponding thioether **69** (step IV).[92]

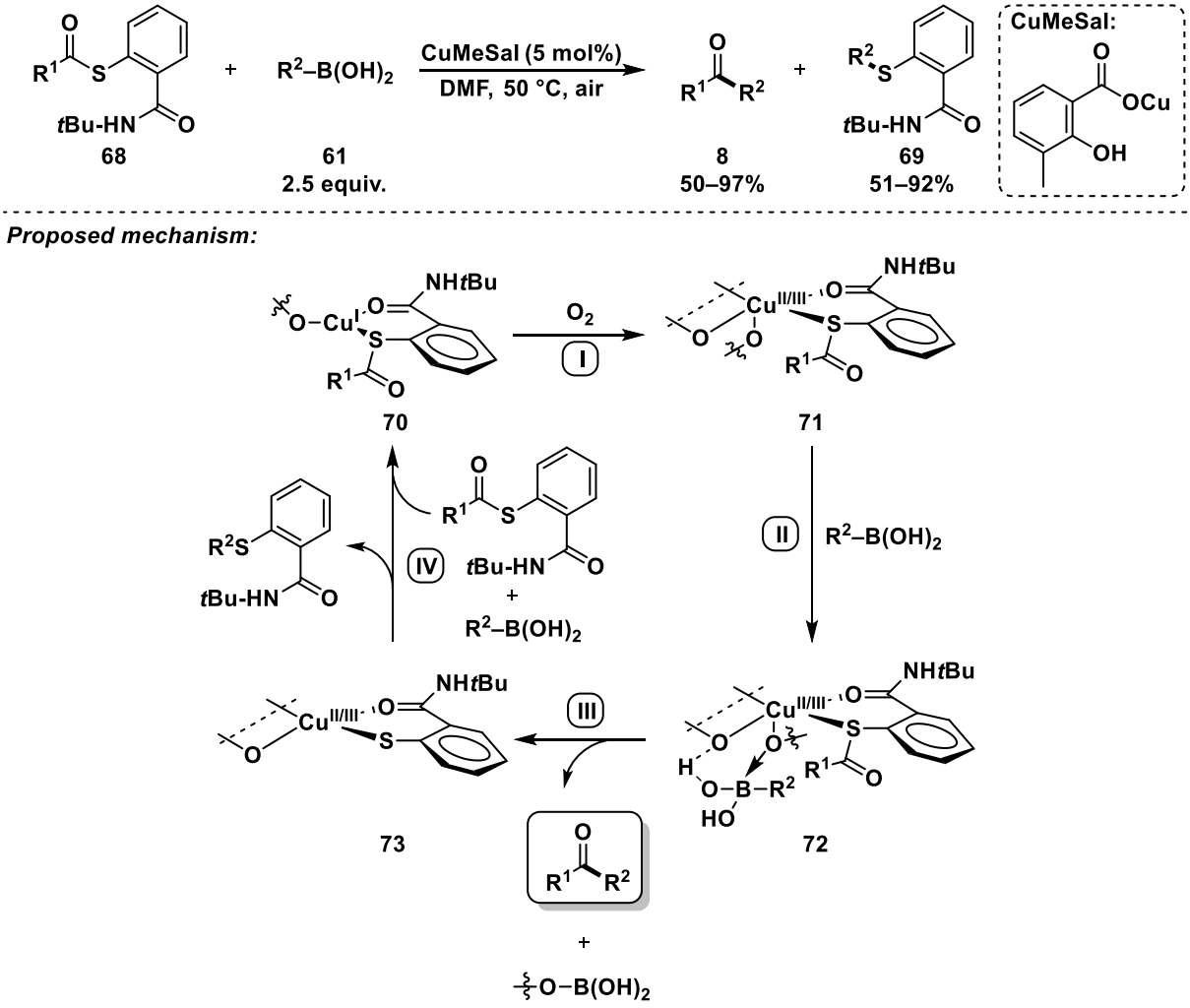

Scheme 3-14: Aerobic Liebeskind–Srogl coupling and the proposed mechanism.[92]

One example using aerobic Liebeskind–Srogl conditions yielded highly enantiopure peptidyl ketones from peptidic *S*-acylthiosalicylamides and boronic acids as substrates.[93] The products retained the stereochemistry of the thioesters with high fidelity, and neither racemization of monopeptidyl ketones nor epimerization of a dipeptidyl ketone was observed.

The main disadvantages of the previous Liebeskind–Srogl generations, the stoichiometric amount of CuTC (first generation) and the extra equivalent of boronic acid (second generation) were solved in 2011 with the third generation of LSC.[94]

In this work, Liebeskind was inspired by Nature's metallothioneins, a family of cysteine-rich, small proteins, and their biomolecular mechanisms that release catalytically important thiophilic metals such as copper from sulfur-containing binding sites.[94] In metallothionein, a metal-bound thiolate ligand attacks an exogenous disulfide **75**, which is thereby converted into a weakly binding disulfide ligand **77**, and the metal is liberated from the protein by an *S*-centered oxidation (Scheme 3-15A).[94] The basic concept of the third LSC was an analog of the metallothionein system, in which the S–S reactant of the biological system was replaced by a N–O unit (Scheme 3-15B). The oxime N–O bond is required for the *S*-centered oxidation

of copper(I) thiolate, which converts the strongly binding thiolate into a weak S–N bond of benzoisothioazole **79** (Scheme 3-15B). In the laboratory, the concept was realized by coupling thioesters with an *O*-methyl oxime moiety **80** and boronic acids or organotin reagents as nucleophiles using 20 mol% of CuMeSal and microwave irradiation (Scheme 3-15C).[94]

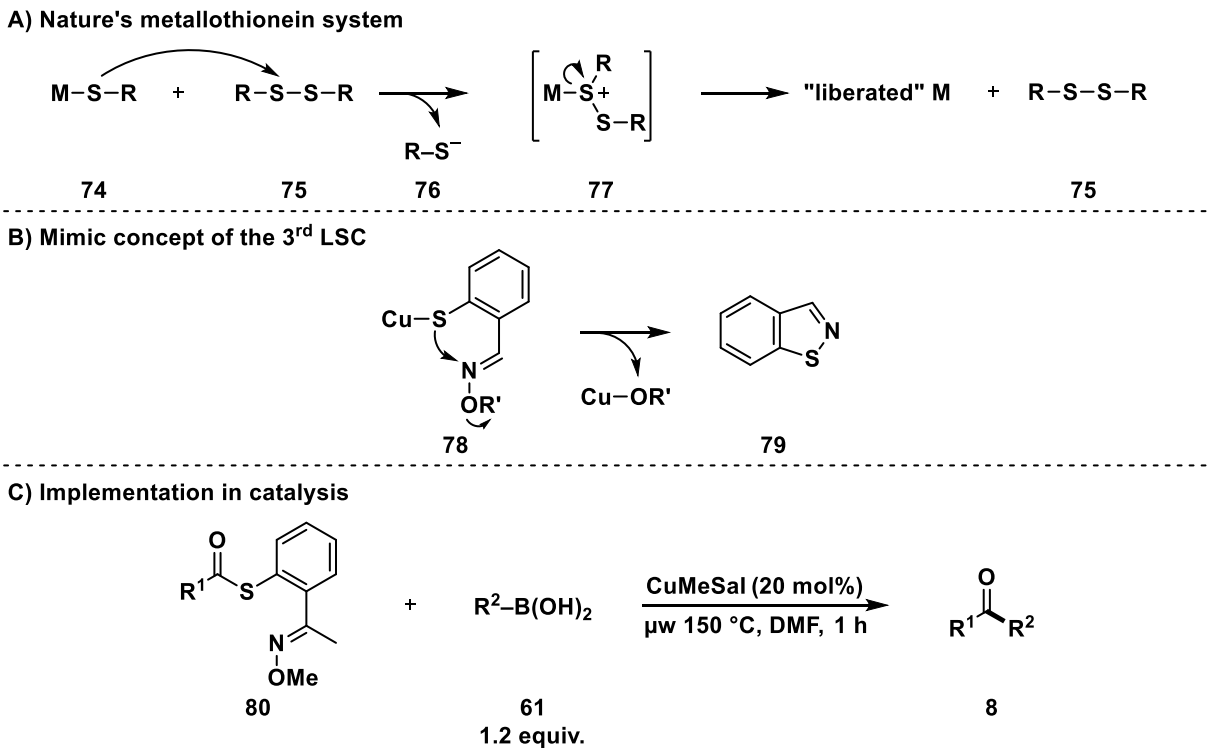

Scheme 3-15: Nature *vs.* biomimetic concept for LSC.[94]

3.1.3.2 Novel Developments

Even today, the number of publications in which Liebeskind's initial conditions are used is not decreasing, and the applications have been further expanded in recent years. In 2011, Nakada and co-workers introduced a one-pot hydroboration of ω-alkenyl thioesters with 9-BBN, followed by an intramolecular LSC for the synthesis of saturated 8–10 membered carbocyclic ketones.[95]

Another intramolecular protocol was applied to the synthesis of *exo*-methylene cycloalkanones **82** from unsaturated thioesters using $Pd(OAc)_2$ as catalyst and $P(OMe)_3$, CuTC and $Zn(O_2CH)_2$ as additives (Scheme 3-16A).[96] The total amount of CuTC was reduced from the original 3.2 equivalents to 1.6 equivalents by changing the ligand from tri(2-furyl)phosphine (TFP) to $P(OMe)_3$, without any loss in product formation. It was suggested that $P(OMe)_3$ facilitates the dissolution of CuTC in THF and/or creates a more beneficial coordination environment. A significant improvement in yield from 30% to 80% was achieved with $Zn(O_2CH)_2$ as additive, probably retarding the rate of palladium aggregate and/or palladium black formation. The reaction of thioesters with an alkyne motif and phenyl boronic acids was also possible under the developed reaction conditions.[96]

A cascade reaction demonstrated the synthesis of ketones from thioesters and boronic acids under traditional Liebeskind–Srogl conditions with a subsequent enantioselective enzymatic reduction or transamination of the ketone to chiral alcohols and amines.[97] The reactions were conducted in a reactor with two chambers, one for the coupling and one for the biocatalytic transformation, connected by a lipophilic polydimethylsiloxane membrane capable of capturing enzyme-deactivating components.

Furthermore, a chiral ketone **85** was obtained in 55% yield and with 92% *ee* by incurring the stereochemistry of the thioester substrate **83** under classical Liebeskind–Srogl conditions (Scheme 3-16B).[98]

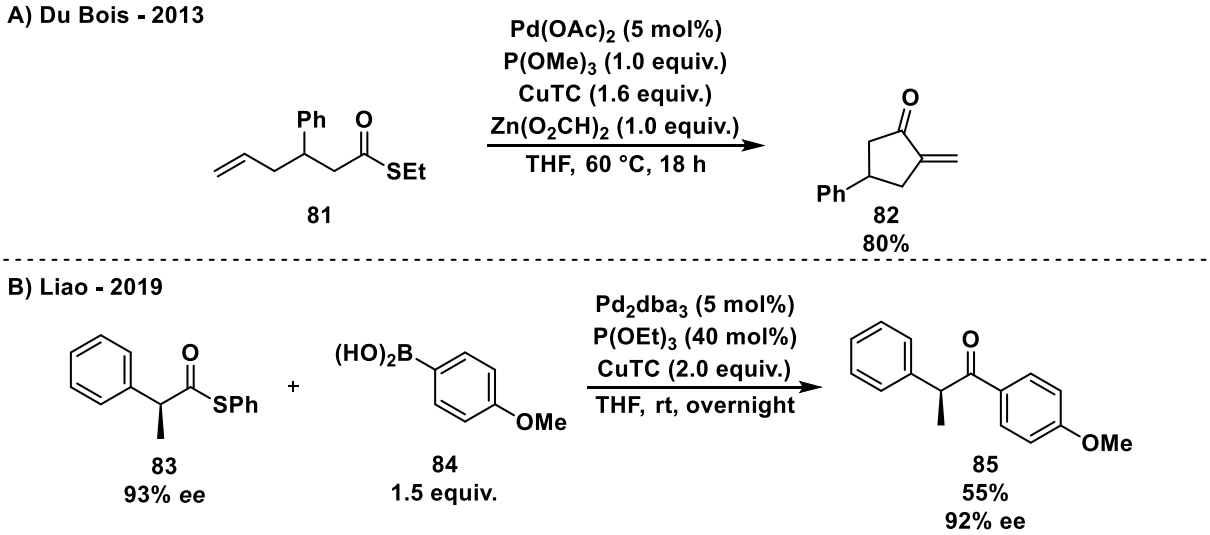

Scheme 3-16: Intramolecular carbocyclization of an unsaturated thioester and synthesis of a chiral ketone under LSC conditions.[96,98]

A recent publication from 2023 showed the discovery of a divergent Liebeskind–Srogl coupling under palladium/NHC catalysis (Scheme 3-17).[99] Two different copper cofactors directed the reaction pathway, leading either to an acyl cross coupling or to a decarbonylative reaction. Under palladium/NHC catalysis with CuI as additive, the acylation pathway was facilitated. The system was compatible with many functional groups, for instance a nitro group, a free hydroxy group, an *N*-heterocycle, and an aldehyde. Particularly noteworthy are the successful syntheses of 13 drug derivatives, including Oxaprozin **89**, Ciprofibrate **90** or Repaglinide **91**. In contrast, a very mild Suzuki coupling could be performed when the additive was changed from CuI to $Cu(OTf)_2$ (Scheme 3-17).[99] The proposed mechanisms of the different pathways are depicted in Scheme 3-17. Both catalytic cycles begin with the oxidative addition of thioester to NHC-ligated palladium(0) (step A). The carbonylative pathway follows the typically proposed mechanistic steps for LSC (left catalytic cycle, steps B–D). The decarbonylative pathway continues with a TfO ligand exchange, resulting in the removal of the thiolate from the catalytic cycle and the formation of a highly electrophilic palladium(II) species **96**, which undergoes CO deinsertion (right catalytic cycle, steps B, E). Subsequently,

the base adds to the CO ligand, generating species **98**, which is suitable for the decarbonylative transmetalation with the boronic acid (step F). The product is delivered after reductive elimination (step D).[99]

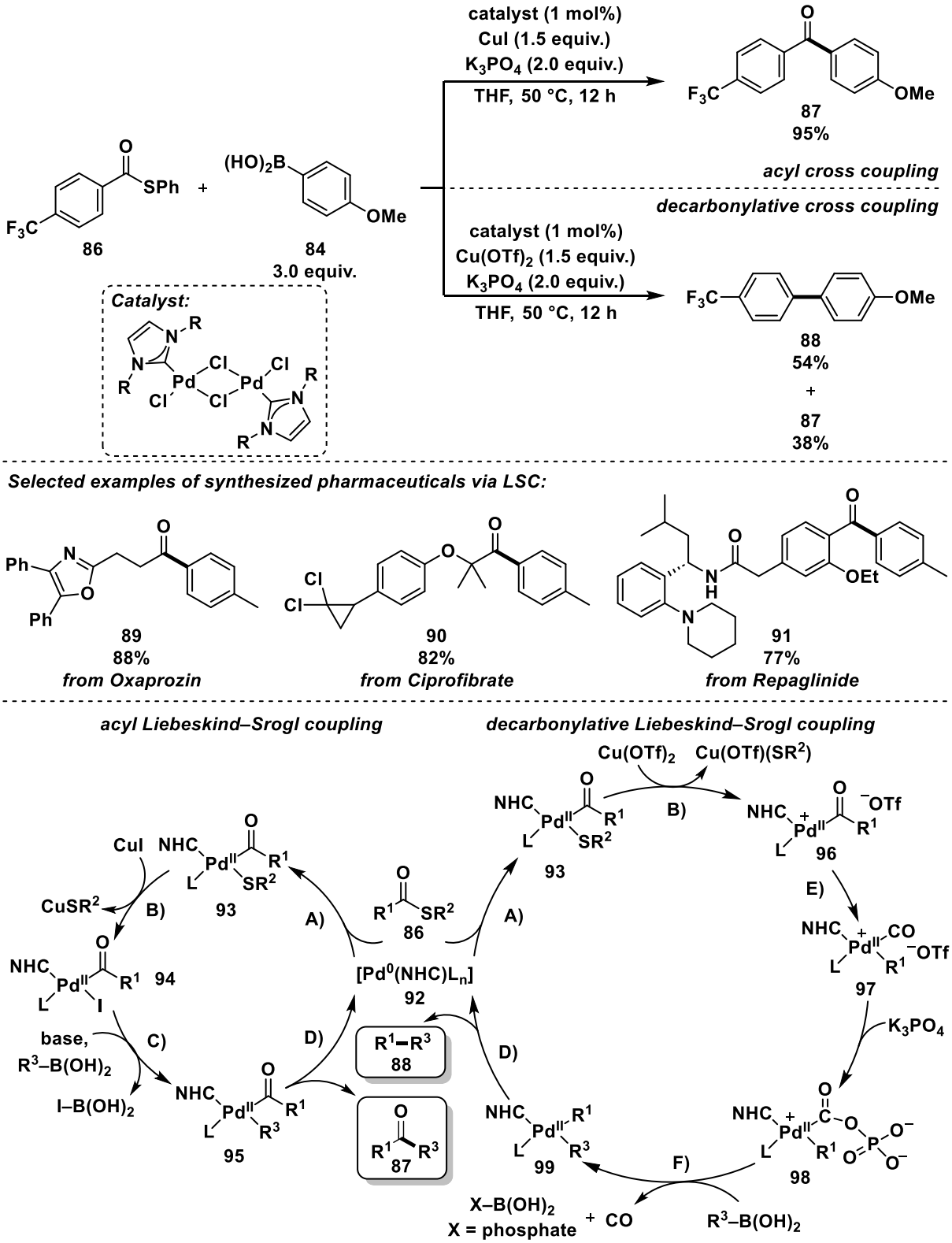

Scheme 3-17: Divergent acyl and decarbonylative Liebeskind–Srogl coupling and the proposed mechanisms with the steps A) oxidative addition, B) desulfitation, C) transmetalation, D) reductive elimination, E) CO deinsertion and F) decarbonylative transmetalation.[99] R^1 = 4-CF_3Ph, R^2 = Ph, R^3 = 4-MeOPh.

The 1,2-diketone structural motif is present in various biologically active compounds.[100] α-Ketothioesters can act as 1,2-dicarbonyl-forming reagents,[101] and boroxines were dicarbonylated under Liebeskind–Srogl conditions (Scheme 3-18).[102] Unusually for conventional LSCs, the substrates were reacted in a 1:1 ratio and a nitrogen-based ligand as well as K_2CO_3 and Na_2SO_4 as additives were used. Aryl boroxines with substituents of different electronic nature and fused rings were tolerated, and an alkyl borate was also a suitable coupling partner.

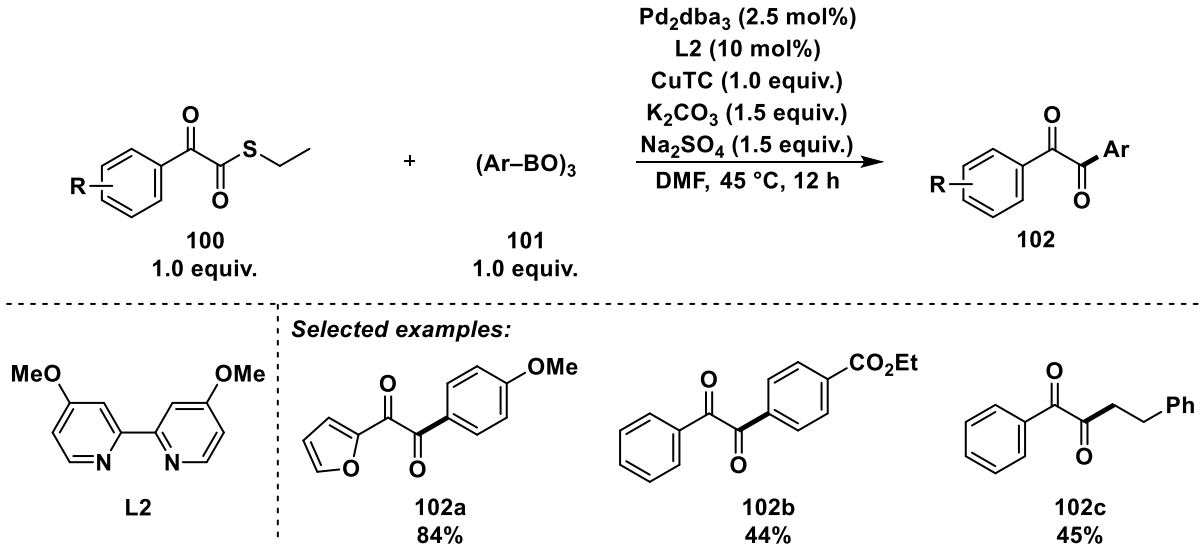

Scheme 3-18: α-Ketothioesters as 1,2-dicarbonyl-forming reagents in a Liebeskind–Srogl cross coupling.[102]

Furthermore, substrates other than thioesters and reaction conditions related to the traditional Liebeskind–Srogl coupling were also presented in several literature contributions. *O*-Methyl *S*-aryl thiocarbonates **103** are suitable substrates under Liebeskind–Srogl conditions, and a palladium-catalyzed and copper(I)-promoted methoxycarbonylation of arylboronic acids was developed (Scheme 3-19A).[103] The optimized reaction conditions comprised 5 mol% Pd_2dba_3, 20 mol% TFP as ligand and an excess of CuTC (1.6 equiv.). The utility of the method was demonstrated by the late-stage esterification of several drugs and bioactive molecules, including Estrone **105a**, Clofibrate **105b** and Epiandrosterone **105c** derivatives (Scheme 3-19A).[103]

A copper(I)-free synthesis of diaryl ketones was accomplished in the reaction of *N*-thiohydroxy succinimide esters **106** (NTSEs) with arylboronic acids using a $Pd(OAc)_2/PCy_3HBF_4$ catalyst system and KOH as an additive (Scheme 3-19B).[104] The tentatively proposed mechanism begins with the insertion of palladium into the C–S bond of NTSE. It was suggested that the succinimide has the dual role of polarizing the Pd–S bond and activating the trivalent boronic acid through O–B coordination. The sequence continues

with the transmetalation from boron to palladium, which is facilitated by the succinimidyl anion after sulfur removal, and reductive elimination to obtain the desired ketone.[104]

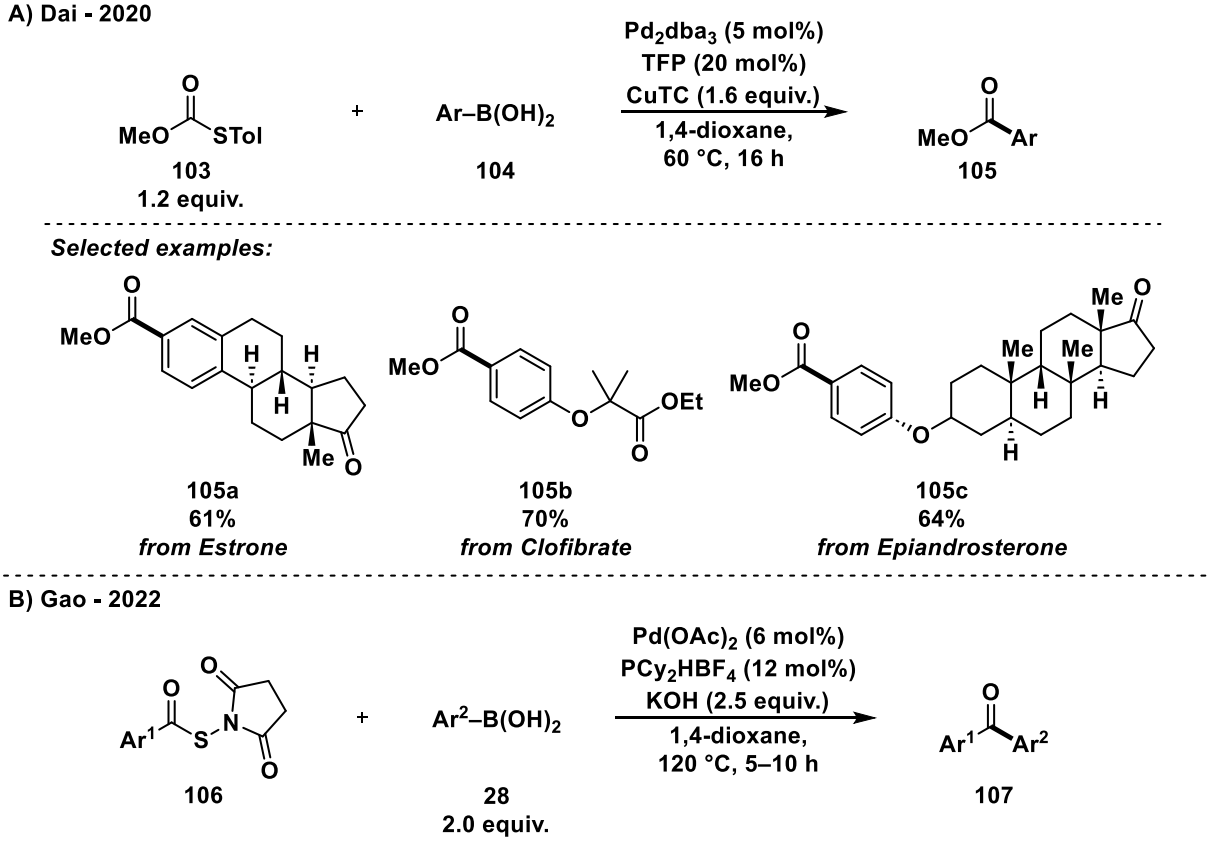

Scheme 3-19: Extension of substrates suitable for LSC conditions.[103,104]

Moreover, *meso*-substituted boron-dipyrromethenes (BODIPYs), highly fluorescent compounds that represent a valuable class of agents for photodynamic therapy, were coupled with boronic acids under traditional LSC conditions,[105] and mechanochemical activation with a minimal amount (0.2 mL) of THF under anaerobic conditions was also possible.[106]

Another example is the palladium-catalyzed arylation of 3-thioalkyl-6-methyltetrazines with boronic acids by a silver-mediated Liebeskind–Srogl coupling.[107] A considerable improvement in yield was observed when substituting CuMeSal or CuTC with Ag_2O. Nevertheless, a high $PdCl_2$(dppf) catalyst loading of 15 mol% was required for this arylation.

3.1.3.3 Application in Natural Product Synthesis

The usefulness of the Liebeskind–Srogl conditions have been demonstrated by a variety of synthetic applications,[77c] and selected examples are described in this section.

Sphingosines are the core structure for sphingolipids, which are important messengers for controlling the growth, maturation, survival, and death of cells.[108] Therefore, they are promising candidates for combating cancer and other proliferative diseases.

Liebeskind himself used the palladium-catalyzed and copper(I)-mediated LSC conditions in the 6-step synthesis of highly enantiomerically pure (-)-$_D$-*erythro*-sphingosine **111** starting from *N*-Boc-$_L$-serine (Scheme 3-20).[108] The high yielding, racemization-free LSC occurred between thiophenyl ester of *N*-Boc-*O*-TBS $_L$-serine **108** with *E*-1-pentadecenyl boronic acid **109**.

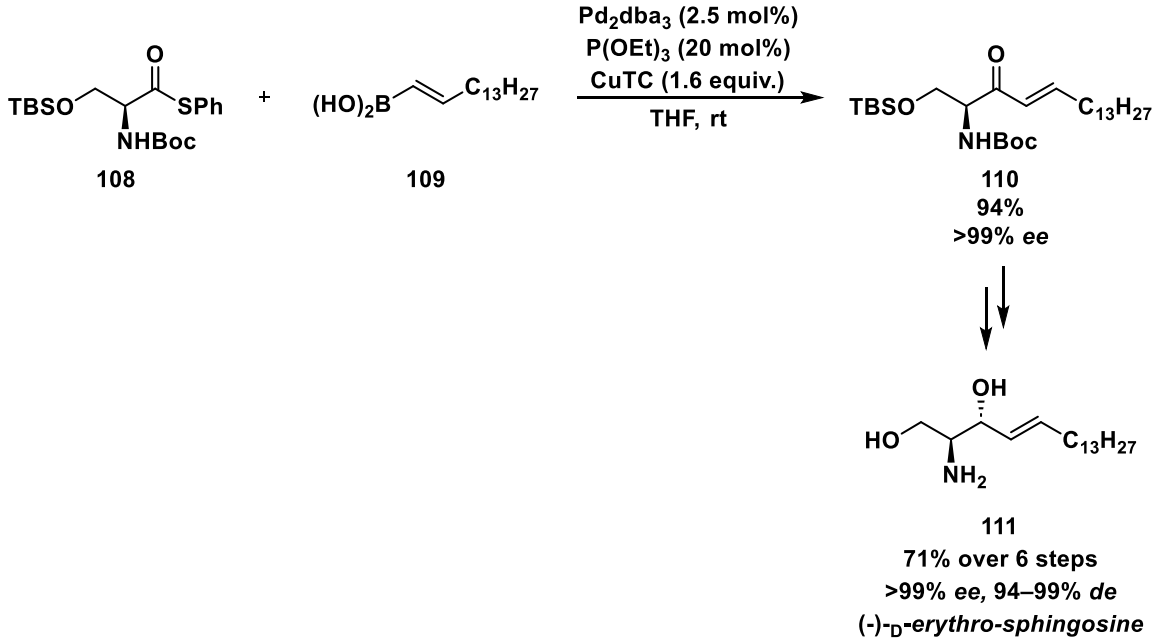

Scheme 3-20: Synthesis of (-)-$_D$-*erythro*-sphingosine **111** with a LSC step.[108]

A complete synthetic pathway has been found for the marine macrolide amphidinolide F **115**, an amphidinolide derivative belonging to a compound class known for their significant cytotoxic activities against some cancer cell lines.[109] In the protocol, a side chain was inserted by a Liebeskind–Srogl coupling reaction (Scheme 3-21). Initially, the reaction was carried out with the corresponding boronic acid derivative in the presence of CuTC and Pd_2dba_3/$P(OMe)_3$. However, under these conditions, non-reproducible results and yields in a range of 15–61% were obtained due to the instability of the boron reagent. The reproducibility issue was solved by using the more stable stannane **113** in combination with copper(I) diphenylphosphinate (CuDPP) and Pd_2dba_3/TFP.

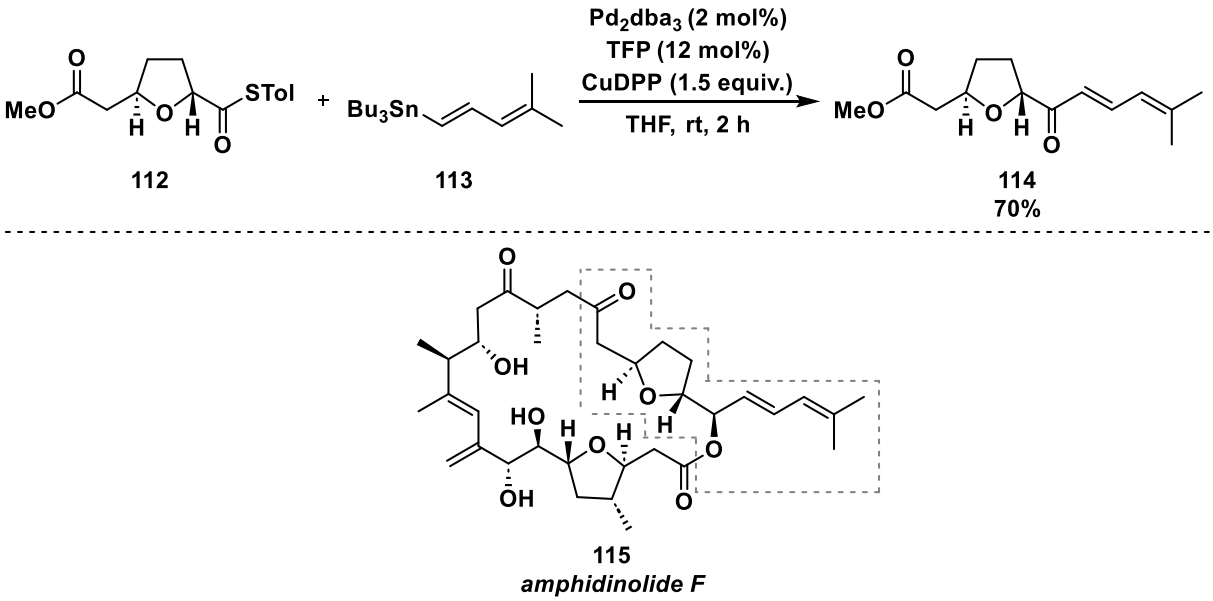

Scheme 3-21: Synthesis of a side chain of amphidinolide F *via* LSC.[109]

The synthesis of flueggeacosine B **118**, a dimeric securinega alkaloid isolated from the roots of *Flueggea suffruticosa*, was accomplished in a total of seven steps with a Liebeskind–Srogl cross coupling as the final one, using thioester **116** and organostannane **117** as functionalized fragments (Scheme 3-22).[110] Unusually, $AsPh_3$ was applied as ligand together with Pd_2dba_3 as catalyst and CuDPP as additive.

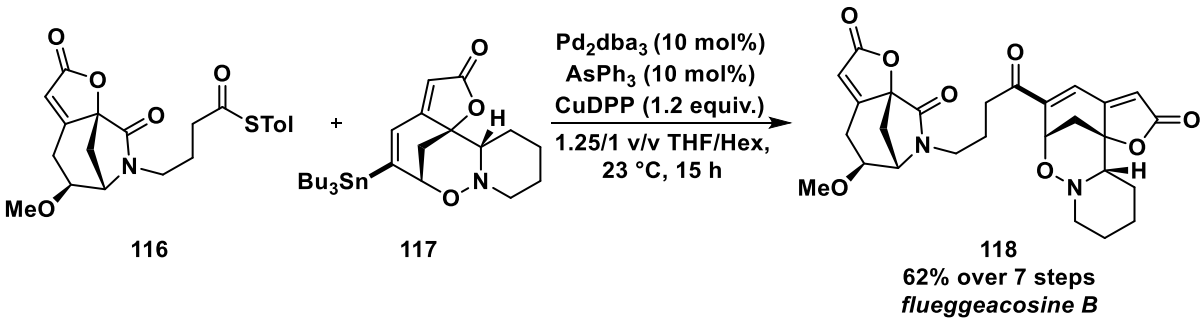

Scheme 3-22: LSC as the last step in the synthesis of dimeric securinega alkaloid flueggeacosine B.[110]

3.1.3.4 Related Cross-Electrophile Couplings

Besides the traditional cross coupling between an electrophilic and a nucleophilic species, related Liebeskind–Srogl couplings of two different electrophiles are known. The *ortho* C–H acylation and *ipso* thiolation of iodoarenes was enabled by combining the Catellani conditions of palladium/norbornene (NBE) with copper catalysis.[111] A catalyst system consisting of 10 mol% $PdCl_2$, 25 mol% TFP and 20 mol% CuI as well as NBE and Cs_2CO_3 as additives coupled iodoarenes and thioesters at elevated temperature (120 °C) with a definitive regioselectivity. The mechanism was not investigated in depth, but it was hypothesized that a palladacycle is involved and that the copper(I) salt could activate the thioester. The substrate scope was extended to thiocarbonates (*vide supra*, section 3.1.2.4.2).[45]

Another approach showed the palladium-catalyzed intramolecular C–H acylation of thioester-containing indoles under $Pd(PPh_3)_3$/1,5-bis(diphenylphosphino)pentane (dpppe) catalysis and additional CuTC (30 mol%).[112] The mechanism was proposed to include the oxidative addition of palladium(0) into the C(O)–S bond of thioester, resulting in a palladium(II) complex. Under the aid of CuTC, the electrophilicity of palladium(II) is enhanced, followed by intramolecular C–H activation of indole at the C2-position, generating a six-membered cyclopalladium species. Reductive elimination delivers the acylated product.

3.1.3.5 Nickel-catalyzed Liebeskind–Srogl Applications

The use of nickel in Liebeskind–Srogl couplings is rarely accessible due to the high thiophilicity of nickel, which leads to a strong Ni–S bond that deactivates the catalyst.[59] Two nickel-catalyzed protocols can be found in the literature, which are reminiscent to the traditional Liebeskind–Srogl coupling.

Gong introduced the copper-catalyzed and nickel-promoted trifluoromethylation of alkyl iodides with Togni's reagent II **120** (1-trifluoromethyl-1,2-benziodoxol-3(1*H*)-one), using $B_2(nep)_2$/LiOMe as reducing system (Scheme 3-23A).[113] The reaction was unsuccessful in absence of copper catalyst or diboron reagent. Without nickel catalyst, a considerable decrease in yield from 79% to 44% was observed. Several primary as well as cyclic and acyclic secondary alkyl iodides with different functional groups were trifluoromethylated under the developed conditions, whereby the primary substrates performed less efficiently. Of note is the tolerance of free amine and bromo groups with primary alkyl iodides. A mechanism has been proposed in which X–Cu^{I}–L **122** is converted to (nep)B–Cu^{I}–L **123** in the presence of diboron and base, followed by the oxidative addition of Alk–I (Scheme 3-23A). After iodine abstraction and combination with an alkyl radical, a copper(III) complex **125** is generated, from which (nep)B–I is reductively eliminated, forming Alk–Cu^{I}–L **126**. This copper intermediate reacts with Togni's reagent to give the product and X–Cu^{I}–L **122**, thereby completing the catalytic cycle. Experiments with radical scavenger revealed that this step could also involve a CF_3 radical. Furthermore, control reactions showed that nickel inhibits the reductive elimination of an Alk–B(nep) species **127** from copper(III) complex **125**, which explains the observed selectivity (Scheme 3-23A).[113]

Another approach showed the alkylation of heteroaromatic thiomethyl ethers **128** and alkyl bromides **129** (Scheme 3-23B).[114] To achieve high yields, a $NiBr_2$(diglyme)/dppf catalyst system as well as molecular sieves, K_2HPO_4 and zinc as additives were mandatory. In particular, the electronic and steric aspects of the ligand had a strong influence on the reaction, which occurred at 100 °C, a relatively untypically high temperature for cross-electrophile couplings. Regarding the substrate scope, the coupling was successful for several functionalized benzothiazoles, including a fluoride and ethers, benzoxazole thioethers and

other heterocycles such as pyridines, quinolines and pyridazines. The alkyl bromide scope even contained an open-chain secondary alkyl bromide, but primary alkyl bromides decreased the yield and tertiary alkyl bromides were unsuitable substrates.[114] Mechanistically, the involvement of an organozinc halide intermediate was discarded. Instead, nickel seems to be responsible for the radical formation from the bromide. After radical capture, a fast reductive elimination from a higher nickel oxidation state probably occurs, since no isomerization with open-chain secondary alkyl bromides was observed.[114]

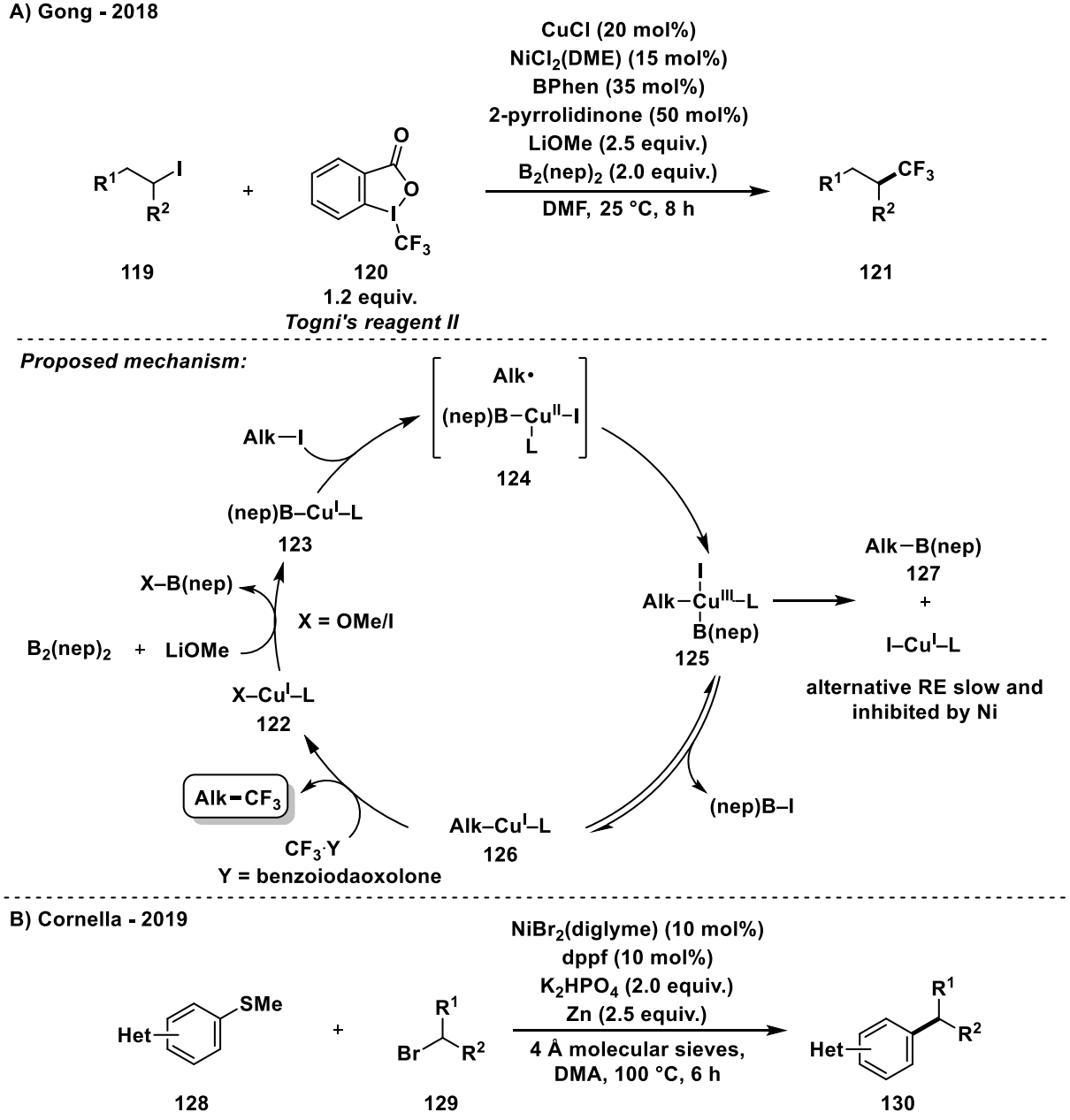

Scheme 3-23: Nickel-catalyzed related Liebeskind–Srogl couplings.[113,114] nep = neopentyl glycolato, RE = reductive elimination.

Finally, a $NiCl_2$(DME)/iridium dual photocatalytic Liebeskind–Srogl coupling enabled the reaction of benzylsulfonium salts with proline, which served as a radical source after decarboxylation, yielding 2-benzylpyrrolidines.[115]

3.2 Aims of This Chapter

The Liebeskind–Srogl cross coupling represents a remarkable strategy for the synthesis of ketones starting from readily accessible, low-cost and stable reaction partners, namely thioesters and organoboron compounds.

The copper additive is the linchpin of the system, allowing the simultaneous activation of both substrates and elegantly bypassing the deactivation of the catalyst by capturing the thiolate. Nevertheless, the reaction would be even more sustainable and attractive if the expensive palladium catalyst could be replaced by a similarly efficient but cheaper one. Nickel is still the most important alternative, but its application makes a successful reaction difficult due to the high thiophilicity of nickel. For this reason, there are still no traditional LSCs catalyzed by the first-row transition metal.

We intended to overcome the limitation and develop a method for a nickel-catalyzed Liebeskind–Srogl coupling (Figure 3-6, left). To this end, preliminary studies were carried out to investigate the copper-mediated reaction of thioesters and boronic acids under nickel catalysis, which are presented in the following chapter.

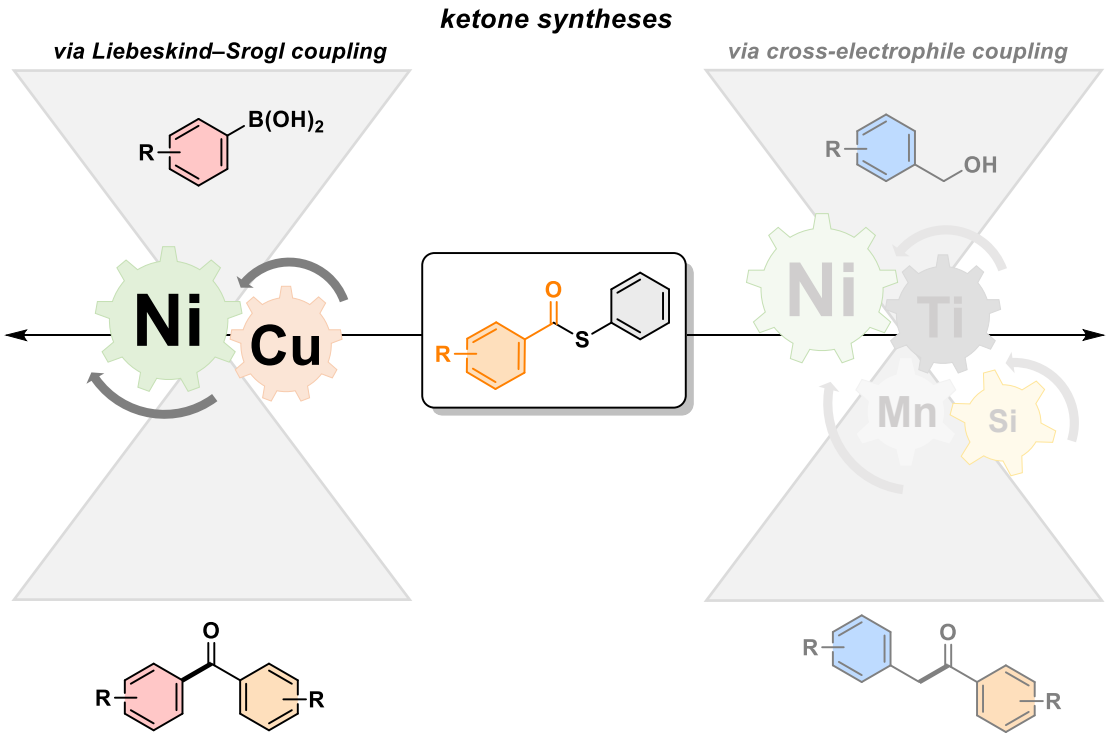

Figure 3-6: Overview of the investigated transformation in the subsequent chapter: thioesters as acylation agents in ketone synthesis *via* nickel-catalyzed Liebeskind–Srogl coupling.

3.3 Results and Discussion
3.3.1 Preliminary Studies and Optimization of Reaction Conditions

Liebeskind's original report enabled ketone syntheses by coupling thioesters and boronic acids using Pd_2dba_3 (1 mol%), tri(2-furyl)phosphine (TFP, 3 mol%) and CuTC (1.6 equiv.) under mild reaction conditions (50 °C, see Scheme 3-12).[78]

Initially, the reproducibility of the published conditions was investigated. For the organoboron compound, phenylboronic acid (**131**) was chosen as substrate. ^{1}H-NMR analysis revealed that the employed phenylboronic acid (**131**) was dehydrated over time and was mainly present as triphenyl boroxine **132-A** (boroxine:boronic acid 10:2.6, Figure 3-7). In addition to the boronic acid, water was visible in the ^{1}H-NMR spectrum (boroxine:water 1:0.6).

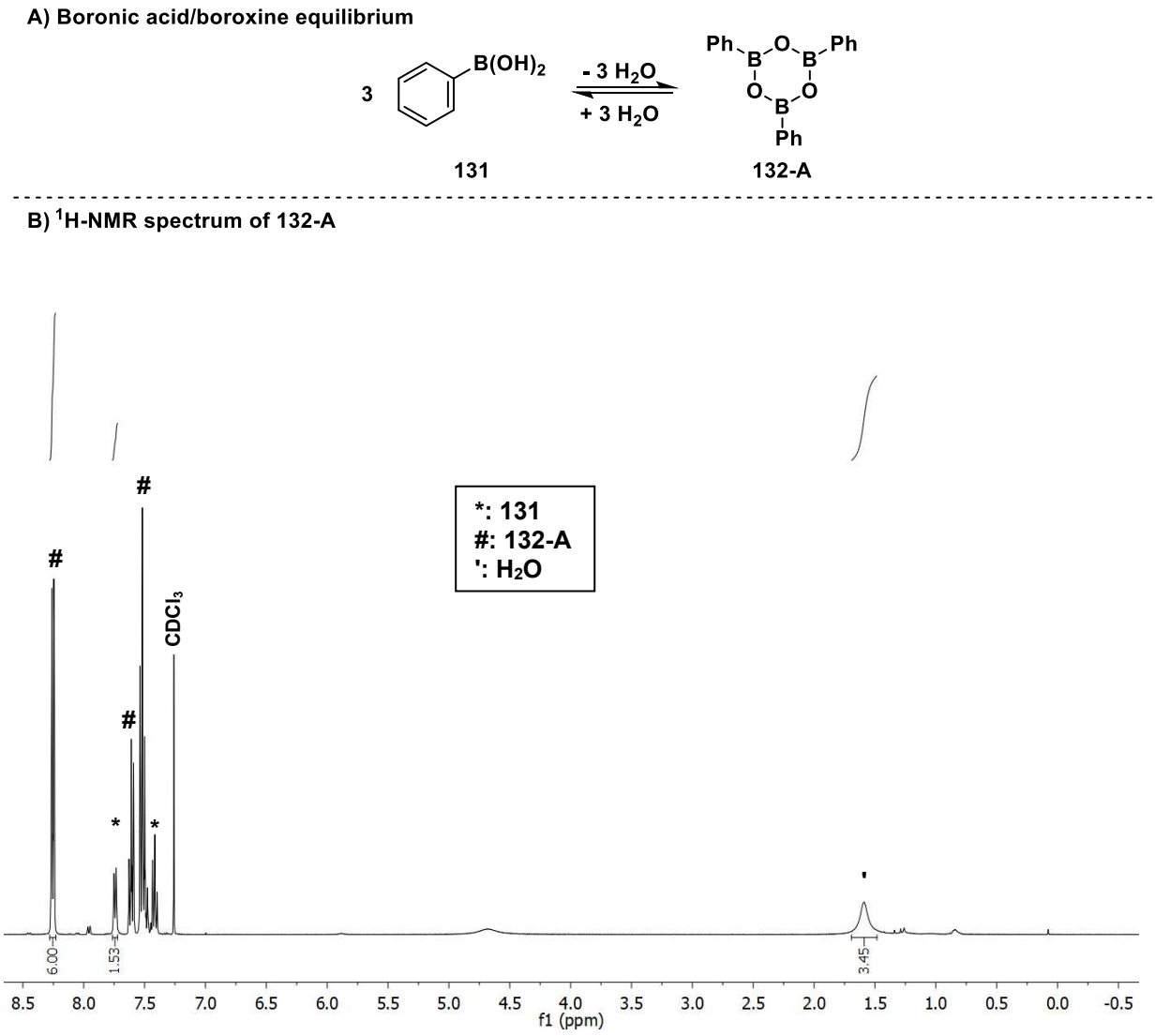

Figure 3-7: A) Entropically favorable dehydration of boronic acid **131** to form boroxine **132-A**. B) ^{1}H-NMR spectrum of **132-A** in $CDCl_3$ with selected integrated peaks of **132-A**, **131** and water to determine the respective ratios.

Setting the correct stoichiometry for boronic acids is therefore a general problem, as establishing the degree of dehydration is not straightforward in the equilibrium of boronic acid, boroxine and water, and it is common practice to add an excess of the reagent.[116] In this work, the required quantities for the subsequent preliminary studies were calculated on the assumption of 100% boroxine. A more precise procedure should be defined for future investigations on the reaction system to avoid reproducibility problems. One possibility would be the complete dehydration of boronic acids to reduce the boronic acid/water content, e.g. by azeotropic distillation or Kugelrohr apparatus, with subsequent determination of the boroxine/boronic acid and boroxine/water content by ^{1}H-NMR immediately before use.[117] Analogous to Snieckus' report, a ratio in the range of 1:0.06–1:0.10 boroxine:boronic acid and 1:0.08–1:0.11 boroxine:water is deemed suitable for cross couplings.[117b]

Additionally, boronic acids present a host of difficulties regarding their analysis and isolation. The boronic acid itself cannot be chromatographed, but dehydration to the corresponding boroxine allows the separation on silica gel.[118] Furthermore, the determination of boroxine conversions by quantitative GC-FID with an internal standard is an inept method and is not listed in this section.

In a first experiment, 0.6 equivalents of boroxine **132-A** and *S*-phenyl benzothioate (**133**) as acyl donor were selected for the traditional LSC. Benzophenone (**134**) was obtained in 96% yield, demonstrating the suitability of these substrates for the palladium-catalyzed reaction (Scheme 3-24). Biphenyl (**135**) was produced as the only byproduct in 7% yield. A control reaction showed that the coupling was unsuccessful in the absence of the copper(I) compound. After verification of the published conditions, a nickel-catalyzed Liebeskind–Srogl coupling with **132-A** and **133** as coupling partners was endeavored.

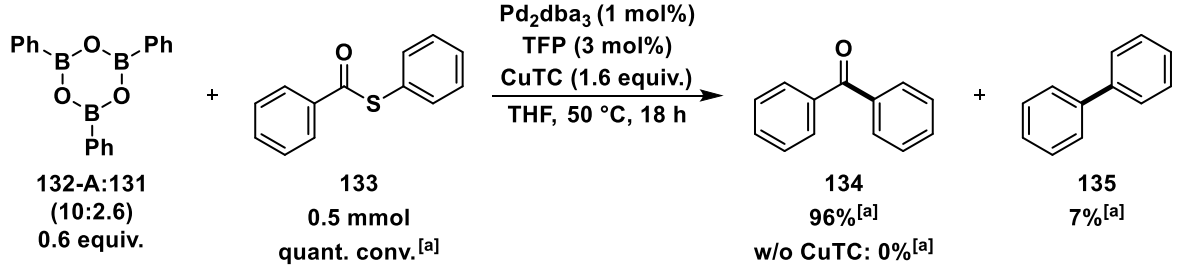

Scheme 3-24: Choice of standard substrates to reproduce the published conditions.[78] The number in parentheses indicates the molar fraction of triphenyl boroxine **132-A** in relation to free phenylboronic acid **131**, and was determined by ^{1}H-NMR spectroscopy. [a]: Determined by GC-FID using *n*-pentadecane as internal standard.

Due to their good availability, Ni(cod)$_2$ (5 mol%) and 1,10-phenanthroline (Phen, 10 mol%) were first chosen to enable a nickel-catalyzed LSC (Table 3-1). It was found that a successful coupling strongly depended on the used triphenyl boroxine, either **132-A** or **132-B**, and the proportion of contained phenylboronic acid **131** and water. With boroxine **132-A** as substrate and the Ni(cod)$_2$/Phen catalyst system, thioester **133** remained mainly unreacted and product

formation was suppressed (entry 1). Apparently, this detrimental effect only occurred in the presence of the nickel catalyst, but not in the previous palladium-catalyzed reaction (see Scheme 3-24), indicating that the nickel catalyst and/or the copper(I) additive were not able to activate the thioester under given reaction conditions. Contrariwise, a moderate conversion of thioester **133** (41%) to ketone **134** (34%) was achieved with the organoboron compound **132-B**, which had a higher ratio of triphenyl boroxine compared to boronic acid (boroxine:boronic acid 10:0.7) and a lower amount of water (boroxine:water 1:0.1) (entry 2). Biphenyl (**135**) was generated in 12% yield as the main byproduct, while the proportion of diphenyl sulfide (**136**) was low (4%, entry 2).

Table 3-1: Dependence of nickel-catalyzed LSC on the used boroxine and further control reactions.

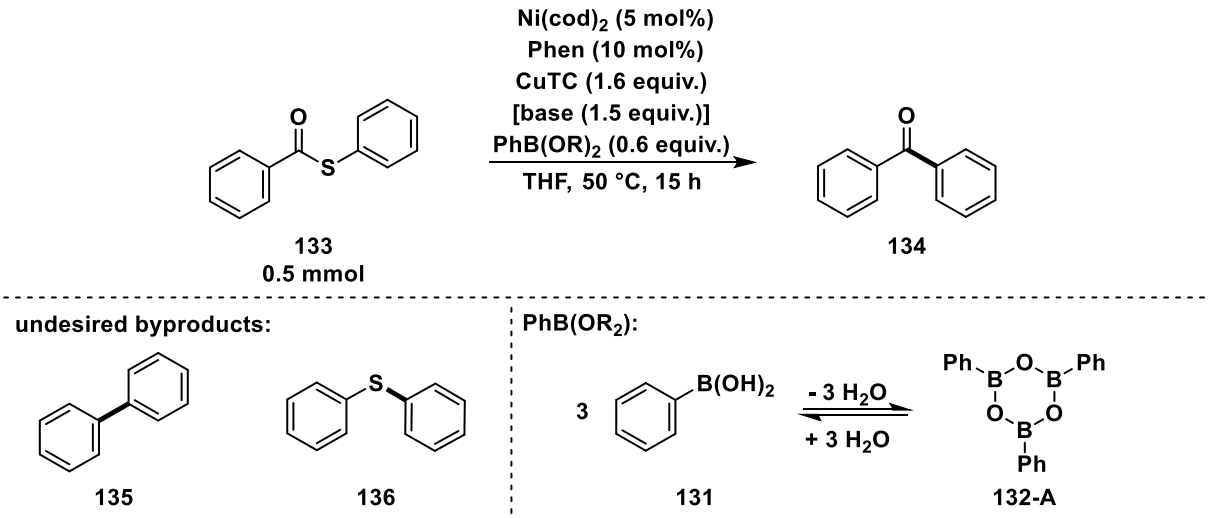

Entry	$PhB(OR)_2$, [base]	Ratio 132-A/B/C:131[a]	Conv. of 133 [%][b]	Yield of 134 [%][b]	Yield of 135 [%][b]	Yield of 136 [%][b]
1	132-A:131	10:2.6	11	4	traces	traces
2	132-B:131	10:0.7	41	34	12	4
3	132-C:131	10:0.5	45	45	8	traces
4[c]	132-B:131 [K_2CO_3]	10:0.7	41	12	traces	traces
5[d]	132-B:131	10:0.7	49	44	12	4

Reaction Conditions: $Ni(cod)_2$ (6.9 mg, 25 µmol, 5.0 mol%), 1,10-phenanthroline (9.0 mg, 50 µmol, 10 mol%), CuTC (153 mg, 800 µmol, 1.6 equiv.), **133** (107 mg, 500 µmol, 1.0 equiv.), [K_2CO_3 (104 mg, 750 µmol, 1.5 equiv.)], **132-A/B/C** (calculated on the assumption of 100% boroxine: 93.5 mg, 300 µmol, 0.6 equiv.), THF (2 mL), 50 °C, 15 h. [a]: Determined by ^{1}H-NMR spectroscopy; [b]: Determined by GC-FID using *n*-pentadecane as internal standard; [c]: K_2CO_3 was not dried before use; [d]: CuTC was not supplied under inert conditions.

The strong dependence of ketone formation on the employed organoboron compound **132-A** or **132-B** could be explained by the hydrolytic equilibrium between free boronic acid and boroxine. The released water could play a dual role. On the one hand, strictly anhydrous conditions could have an adverse effect on the reaction rate and a small amount of water is proposed to be responsible for the formation of the catalytically active boron species.

For instance, arylpotassium trifluoroborates[119] or pinacolatoboronates[9] only couple efficiently in the presence of water. Additionally, the reactivity of boroxines can be promoted by the addition of water, releasing the more reactive boronic acids.[10a,b,117b,120]

On the other hand, variations in water content could also lead to inconsistencies and reproducibility issues, which were already reported with boroxines/boronic acids as substrates in nickel-catalyzed Suzuki–Miyaura couplings.[9,10,117b] In addition, a large excess of water could increase the energy barrier of the transmetalation through coordination to the nickel catalyst or inhibit catalytic activity completely, for example by forming inactive metal hydroxides/oxides.[10a,117b,121] While palladium is known to catalyze Suzuki–Miyaura cross couplings even in aqueous media,[122] nickel catalysts, such as chlorides, are prone to hydrolysis and can be incompatible with aqueous conditions.[121,123] Therefore, the hydrolysis equilibrium between the free boronic acid and the less reactive boroxine must be controlled and the optimum balance between boroxine, boronic acid and water must be found.

To investigate the necessity of water in the reaction, boroxine **132-B** was subjected to azeotropic distillation,[124] and the proportion of boronic acid was decreased (boroxine:boronic acid 10:0.5). The boroxine **132-C** was then used as a substrate in the LSC, and a slightly higher yield (45%) of ketone **134** was obtained compared to the reaction without prior dehydration (34%, Table 3-1, entries 2 *vs.* 3).

Analogous to previous reports,[78] an oxygen atom containing base had an unfavorable effect on product yield (12%, Table 3-1, entry 4). Although the thioester conversion was moderate (41%), no byproducts were detected except for traces of biphenyl (**135**) and diphenyl sulfide (**136**). K_2CO_3 was not dried before use, as protocols showed that a water-containing base can lead to higher product yields in nickel-catalyzed Suzuki–Miyaura couplings.[10d,120] In addition, a theoretical study proposed that in the presence of an appropriate base and water, organoboronic acid exists in equilibrium with the $ArB(OH)_3^-$ anion, which is the actual species entering transmetalation of nickel-catalyzed cross couplings.[125] Nevertheless, the water-containing base could also be a reason for the low ketone yield and a systematic screening of water-free and water-containing bases should be conducted.

In contrast to the sensitivity of the used organoboron compound, the reaction was nearly independent on the applied copper(I) species (Table 3-1, entries 2 *vs.* 5). CuTC is described as air-stable in the absence of a solvent,[91a] which could be confirmed by the application of two different batches of CuTC, one of which was provided under inert atmosphere and the other under non-inert conditions. A moderate yield of ketone **134** (44%) was obtained with the CuTC supplied under non-inert conditions, similar to the reaction with CuTC delivered under inert atmosphere (34%, entries 2 *vs.* 5).

Subsequently, the amount of triphenyl boroxine (**132-B**) was optimized, but deviations from the original 0.6 equivalents led to a decrease in the conversion of thioester **133** and the yield of ketone **134** (Figure 3-8A). In general, biphenyl **135** was formed in low proportions (3–14%), and diphenyl sulfide (**136**) was only detected in trace amounts (3–6%, not depicted).

Furthermore, the conversion of thioester **133** and ketone formation were completely inhibited after boroxine **132-B** was replaced by boronic acids with altered steric and electronic properties or by a boronic ester (Figure 3-8B).

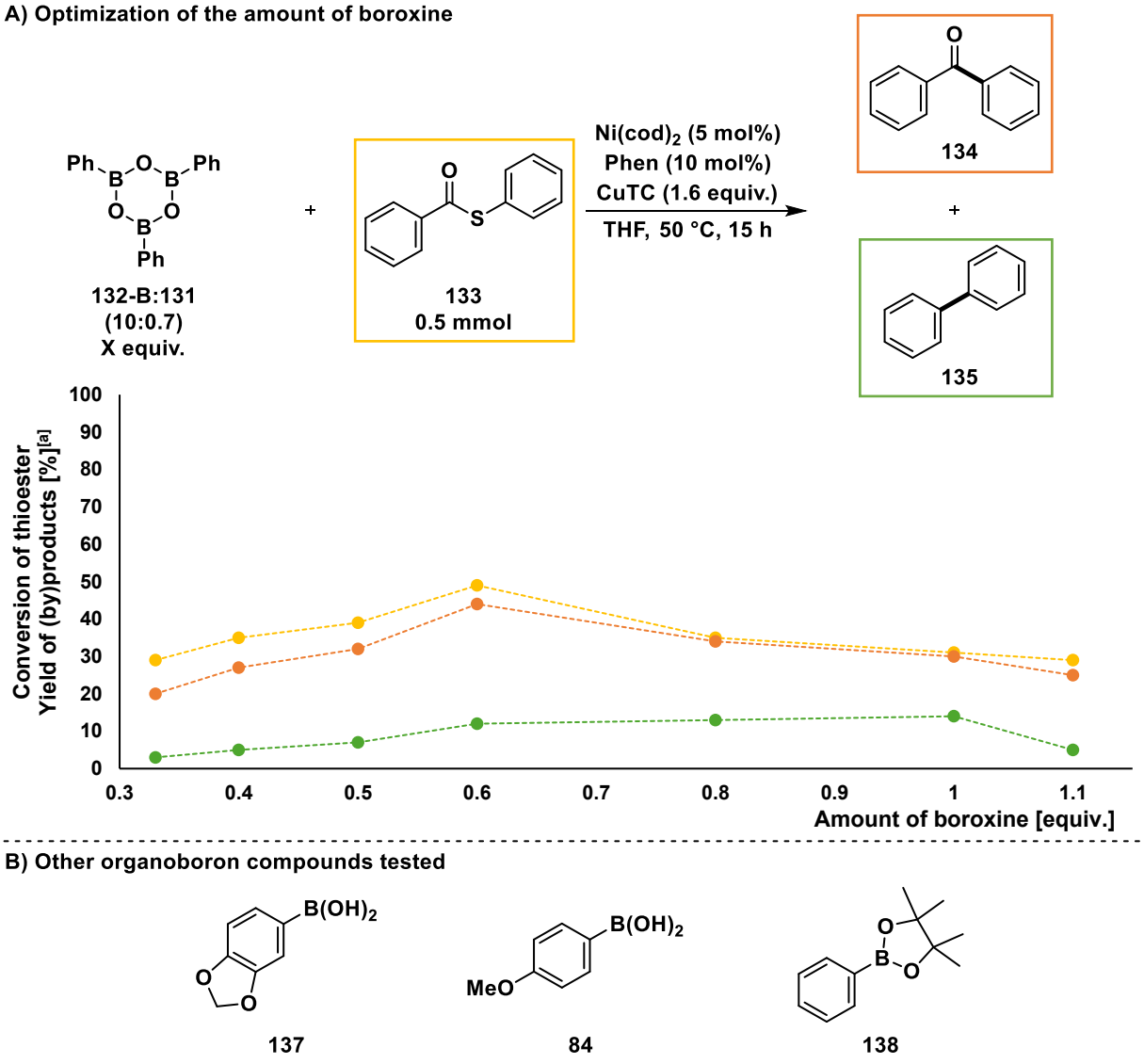

Figure 3-8: Optimization experiments for the organoboron coupling partner. [a]: Determined by GC-FID using *n*-pentadecane as internal standard.

In summary, the studies on the organoboron compounds have shown the dependence of the reaction on the hydrolytic equilibrium between free boronic acid and boroxine. The highest yield of ketone **134** (45%) was achieved with 0.6 equivalents triphenyl boroxine **132-C**, which had a ratio of 10:0.5 boroxine:phenylboronic acid. The addition of a base decreased the ketone yield, and the air stability of CuTC was confirmed.

Subsequently, the focus was shifted from boroxine to the thioester substrate. Initially, it was investigated whether the yield of ketone **134** could be influenced by a substituent on the thiol moiety of thioester (Figure 3-9). The lowest yield of ketone **134** (22%) and a slightly higher yield of biphenyl (**135**) (19%) were determined with an electron-donating OMe in *para* position. Additionally, a bromine substituent in *para* position reduced the yield of the desired ketone **134** to 33%. The highest yield of ketone **134** (44%) was obtained with previously used *S*-phenyl benzothioate (**133**).

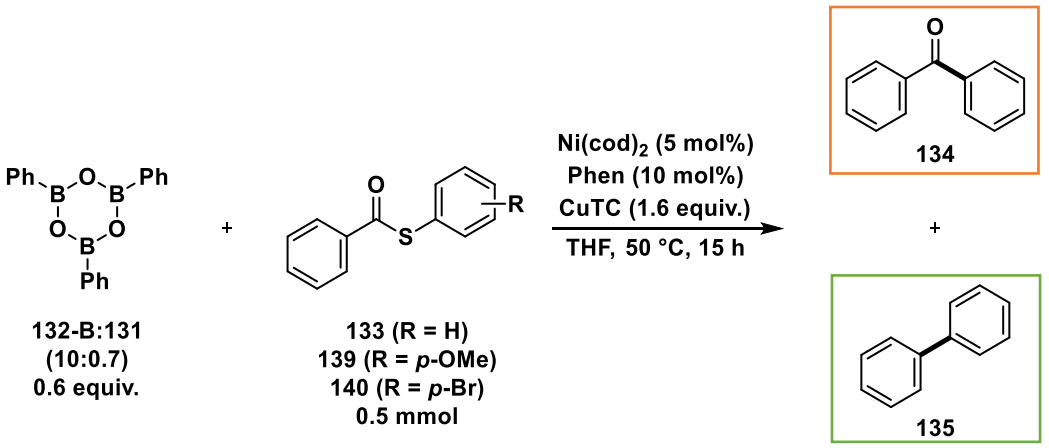

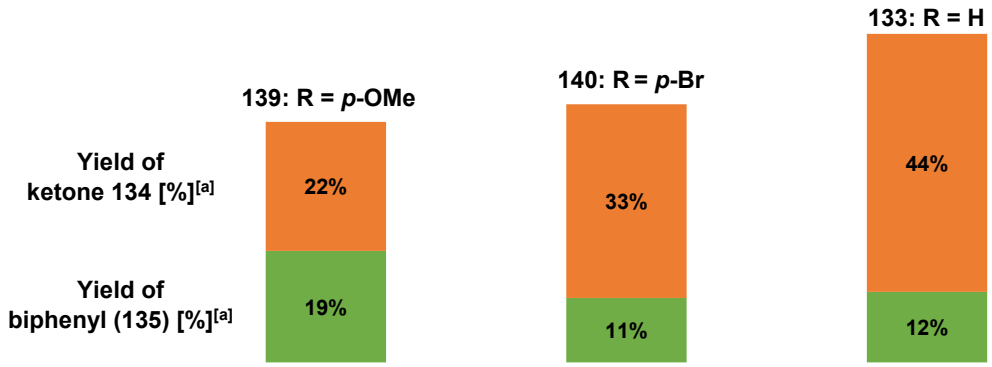

Figure 3-9: Influence of substituents on the yield of (by)products. [a]: Determined by GC-FID using *n*-pentadecane as internal standard.

The investigations on the substrates were followed by preliminary studies on the reaction conditions, which could possibly increase the ketone yield. With boroxines as substrates, high reaction temperatures are usually required to overcome the lower reactivity compared to boronic acids,[126] which is why the first step was to optimize the reaction temperature.

Figure 3-10 shows that an elevated temperature was required for the coupling, but temperatures higher than 50 °C had no major influence on the reaction. A reduced yield of 19% was determined at room temperature, while yields of 39–46% were achieved in the temperature range of 50–100 °C.

Concluding from these results, the LSC was further conducted at 50 °C, yielding 44% of the ketone **134**. However, with boronic acids and boroxines as substrates, it has been shown

that the optimal temperature depends on the used solvent,[126a,127] therefore the temperature screening should be repeated after determining the optimal reaction medium.

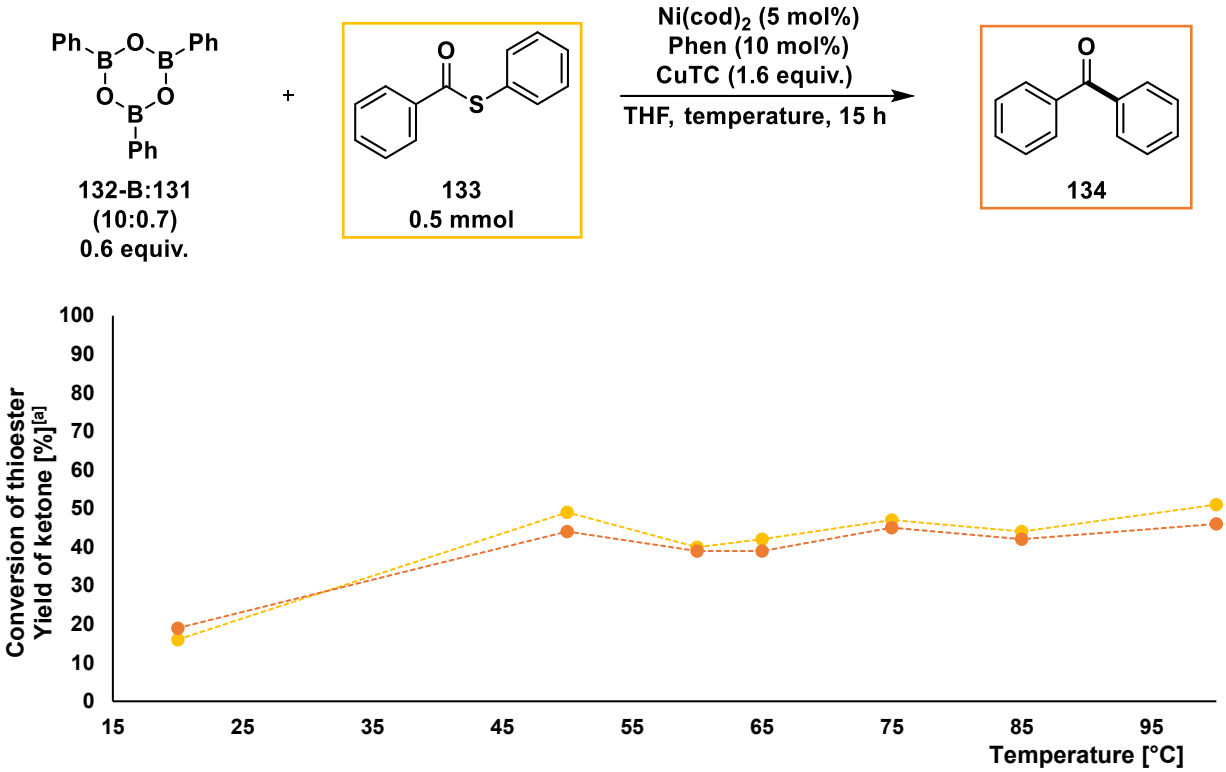

Figure 3-10: Temperature influence on LSC. [a]: Determined by GC-FID using *n*-pentadecane as internal standard.

It was continued with several control reactions regarding the copper additive and the nickel catalyst (Table 3-2). The copper(I) reagent was necessary for the reaction, and neither thioester conversion nor (by)product formation was observed in the absence of CuTC (entry 2). Since the early days of Liebeskind–Srogl couplings, phosphine ligands were generally employed,[78] which is why the *N*-ligand phenanthroline was substituted by tri(2-furyl)phosphine (TFP), resulting in a decreased yield of ketone **134** (30%) accompanied by a higher yield of diphenyl sulfide (**136**) (13%, entry 3). Then, it was tested whether a higher nickel catalyst loading (10 mol%) leads to a higher yield of ketone **134**, but contrary to expectations, a decrease in yield from 44% to 33% was observed (entry 4). Therefore, the reaction was studied in the absence of the nickel catalyst, and indeed 41% of the ketone **134** was obtained, indicating that the copper(I) species was the mediator of the reaction rather than the nickel catalyst (entry 5). However, the copper-assisted reaction was also found to be dependent on the used organoboron species, as ketone formation was again inhibited when boroxine **132-A** was used as a substrate (entry 6).

Table 3-2: Control reactions on the copper(I) additive and nickel catalyst.

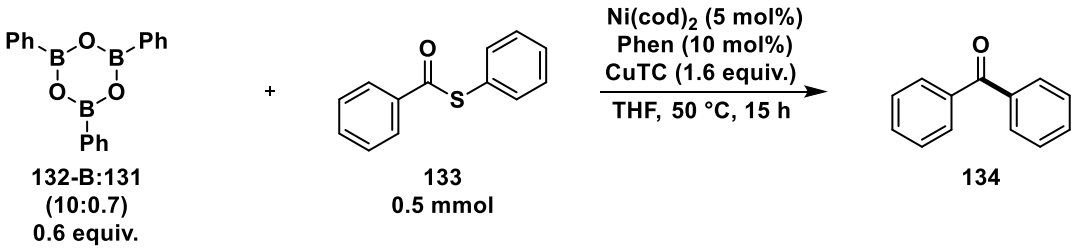

undesired byproducts:

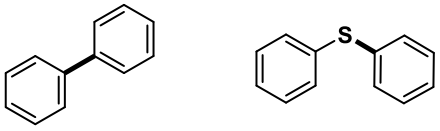

135 **136**

Entry	Deviations from standard conditions	Conv. of 133 [%][a]	Yield of 134 [%][a]	Yield of 135 [%][a]	Yield of 136 [%][a]
1	none	49	44	12	4
2	w/o CuTC	✘	✘	✘	✘
3	TFP as ligand	39	30	6	13
4	10 mol% $Ni(cod)_2$	50	33	5	6
5	w/o $Ni(cod)_2$	37	41	8	traces
6[b]	w/o $Ni(cod)_2$, 132-A instead of 132-B	5	✘	✘	✘

Standard Reaction Conditions: $Ni(cod)_2$ (6.9 mg or 13.8 mg, 25 µmol or 50 µmol, 5.0 or 10 mol%), 1,10-phenanthroline (9.0 mg, 50 µmol, 10 mol%) or TFP (12 mg, 50 µmol, 10 mol%), CuTC (153 mg, 800 µmol, 1.6 equiv.), **133** (107 mg, 500 µmol, 1.0 equiv.), **132-A/B** (calculated on the assumption of 100% boroxine: 93.5 mg, 300 µmol, 0.6 equiv.), THF (2 mL), 50 °C, 15 h. [a]: Determined by GC-FID using *n*-pentadecane as internal standard; [b]: **132-A** had a ratio of 10:2.6 boroxine:boronic acid.

In the last step of the reaction development, the amount of CuTC was varied in the presence or absence of phenanthroline as a ligand (Figure 3-11A *vs.* B). With stoichiometric amounts of CuTC and in the presence of phenanthroline, the selectivity for ketone formation and the overall yield of **134** were higher than in the reactions without ligand, but in general the yields decreased with lowering the amount of CuTC. Interestingly, ketone formation was only successful with a catalytic amount of CuTC in the absence of the ligand, albeit with a low yield of 7%. In contrast, the reaction was completely inhibited with 10 mol% CuTC and ligand. The experiments showed that the ligand has a considerable influence on (by)product formation, which is why an extensive screening could lead to a high ketone yield.

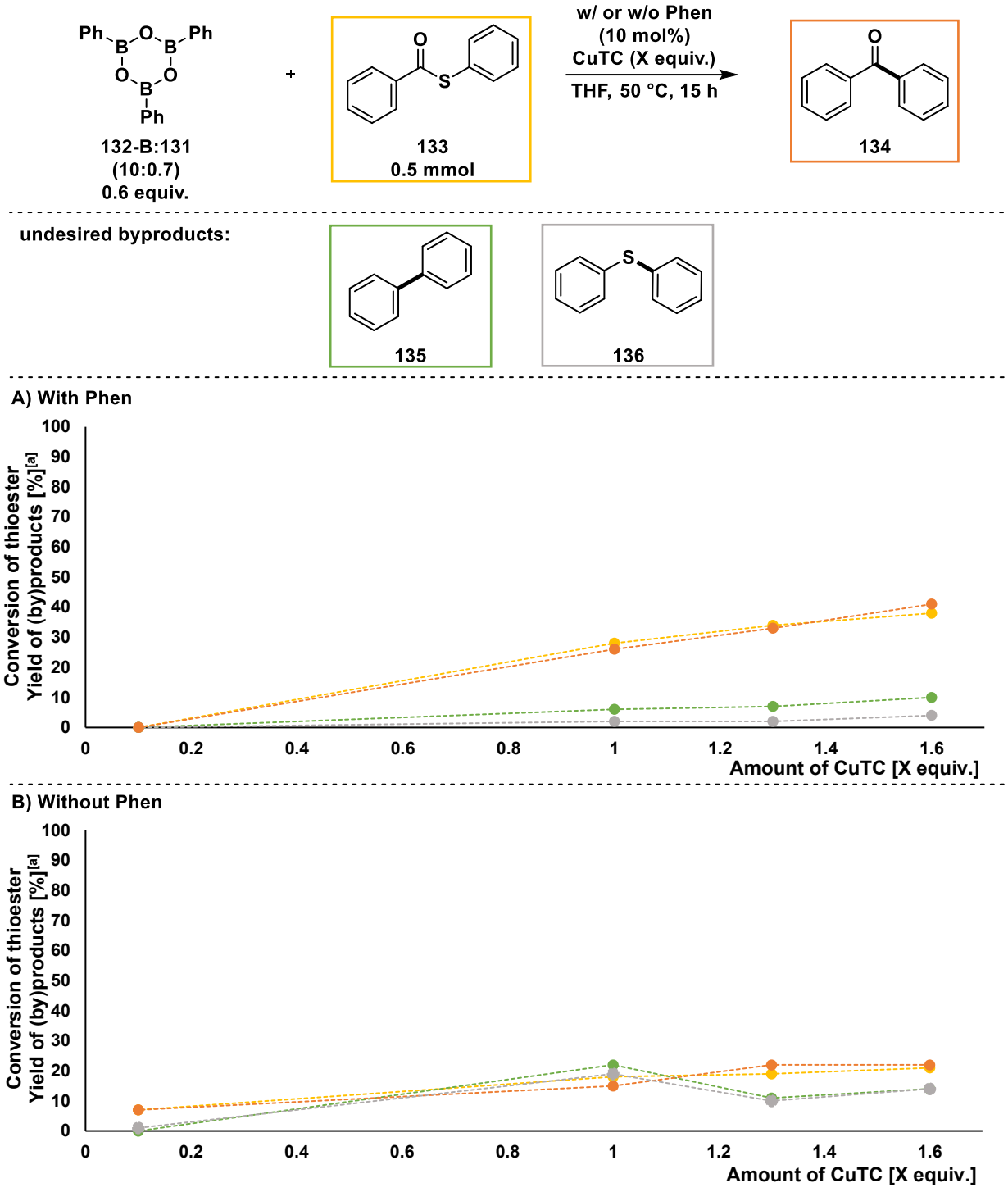

Figure 3-11: Dependence of the copper-mediated reaction between thioester **133** and boroxine **132-B** on the ligand. [a]: Determined by GC-FID using *n*-pentadecane as internal standard.

3.3.2 Possible Mechanistic Aspects and Literature Context

Although mechanistic studies of the copper-mediated or -catalyzed coupling have not yet been conducted, several mechanistic aspects of nucleophilic organocopper reactions are briefly described. Regardless of stoichiometric or catalytic processes, three elementary steps are postulated (Scheme 3-25A).[128] Both scenarios begin with the transmetalation between the copper(I) salt and the organometallic reagent to give either a mono- **141** or a diorganocuprate **142**, depending on the type of the organometallic coupling partner, the amount of copper(I) compound, and the presence of additives and ligands. The next steps are reliant on the nature of electrophile. For aryl (pseudo)halides, an oxidative addition step is followed including the nucleophilic attack of the d-orbital of the copper(I) atom on an electrophilic species R^1–X to generate organocopper(III) intermediates **143** or **144**. The subsequent reductive elimination furnishes the product and a neutral copper(I) species, which can take part in a possible next catalytic step. The transmetalation and the Cu^{I}/Cu^{III} redox sequences are the key processes in both stoichiometric and catalytic organocopper reactions.[128b,c] For primary and secondary aliphatic electrophiles, an S_N2-mechanism was suggested (Scheme 3-25A, grey pathway).[129]

Additionally, the substitution of an acyl electrophile with an organocuprate depends on the nature of the leaving group. For instance, a thiolate anion exhibits a high affinity to copper,[59] therefore the reaction of a thioester involves insertion of the copper atom into the C–S bond. In contrast, an acid chloride reacts *via* an eliminative pathway, as the chloride favors electrostatic interaction with the counterion.

In general, copper-mediated or -catalyzed reactions are mostly limited to more reactive organometallic compounds, such as organolithium, -magnesium, or -zinc reagents, but also reactions with organoboron compounds are known.[128c]

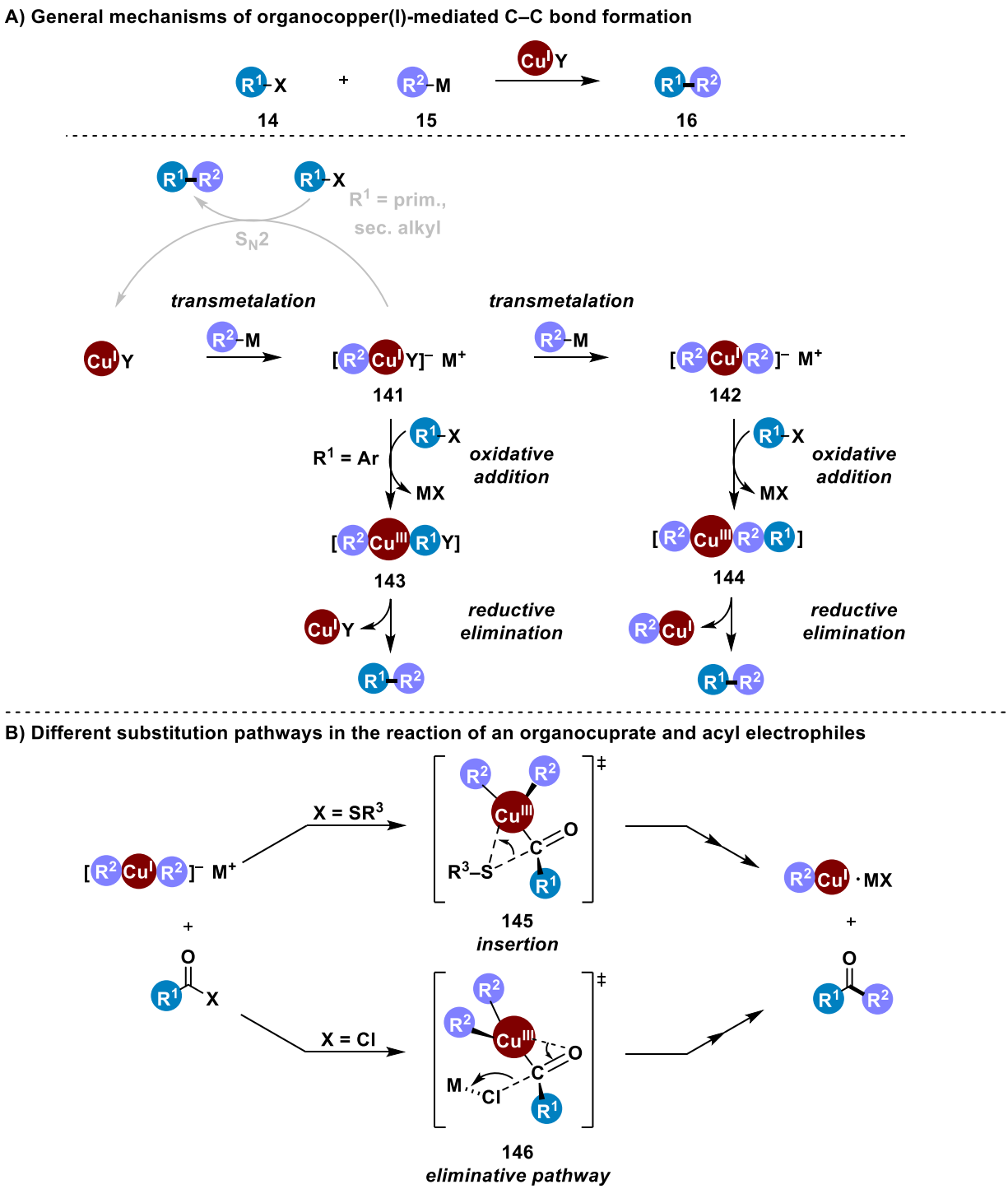

Scheme 3-25: A) General mechanisms for copper(I)-mediated or -catalyzed reactions, and B) substitution pathways in the reaction of an organocuprate with a thioester or an acid chloride.[128b,c]

The direct coupling of organocopper(I) compounds or copper-mediated couplings of organometallic reagents with carboxylic acid derivatives is an important method for the synthesis of ketones, exhibiting a broad applicability and functional group compatibility.[130] Thioesters were introduced as suitable substrates already in 1974 by Rosenblum, who developed a general method for ketone synthesis by reacting organocopper reagents with *S*-alkyl and *S*-aryl thioesters.[130c] A recent protocol from 2022 generated diarylcuprates(I)

in situ from CuTC and aryl Grignard reagents (1:1.3–1.5 ratio), which were then coupled with thioesters, yielding various multifunctionalized ketones in good to high yields (Scheme 3-26).[130i] Based on control experiments and DFT computations, a mechanism was proposed, which starts with the *in situ* generation of $[Cu^{I}Ph_2]^-$ **148** from the copper(I) salt and Grignard reagent **147**. The organocuprate is reactive towards thioester, forming an anionic copper(III) species **150** by oxidative addition of the C–S bond. Subsequent reductive elimination gives the corresponding ketone together with $[Ph–Cu^{I}–S^{n}Bu]^-$ **151**. Transmetalation between the latter thiolate species and $[CuPh]_4$ regenerates the organocuprate $[Cu^{I}Ph_2]^-$ **148** along with copper(I) thiolate *via* μ^2-phenyldicopper species **152**. The reaction byproduct, copper(I) thiolate, forms insoluble thiolate-bridged copper(I) clusters **153** (Scheme 3-26).[130i]

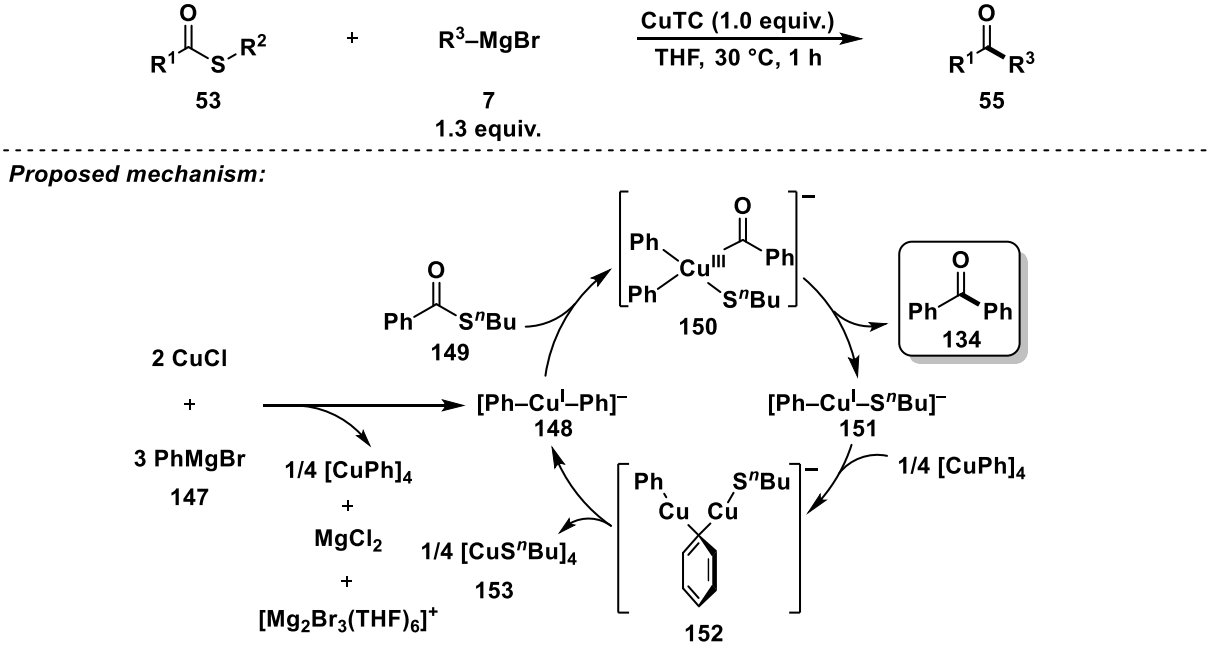

Scheme 3-26: Copper-mediated ketone synthesis from thioesters and Grignard reagents and proposed mechanism with R^1 = Ph, R^2 = ^{n}Bu, R^3 = Ph.[130i]

Nevertheless, copper-catalyzed methods are underexplored.[131] Only one of these few examples used thioesters and boronic acids as substrates, and a palladium-free Liebeskind–Srogl coupling was achieved with 20 mol% CuI and 5 mol% Ag_2CO_3 at elevated temperature (120 °C, Scheme 3-27).[131f] Diaryl ketones were obtained in moderate to good yields (48–85%). The mechanism was not studied in detail, but it was postulated that the C(O)–S bond could be weakened by coordination of the silver(I) salt to the thiol moiety, with subsequent elimination of the thiolate from the catalytic cycle by formation of disulfide **159**. As in the Chan–Lam coupling with O_2 as oxidant, the generated copper(II) complex **160** might undergo transmetalation with subsequent oxidation to form a copper(III) species **161**, from which the desired diaryl ketone could be reductively eliminated (Scheme 3-27).[131f]

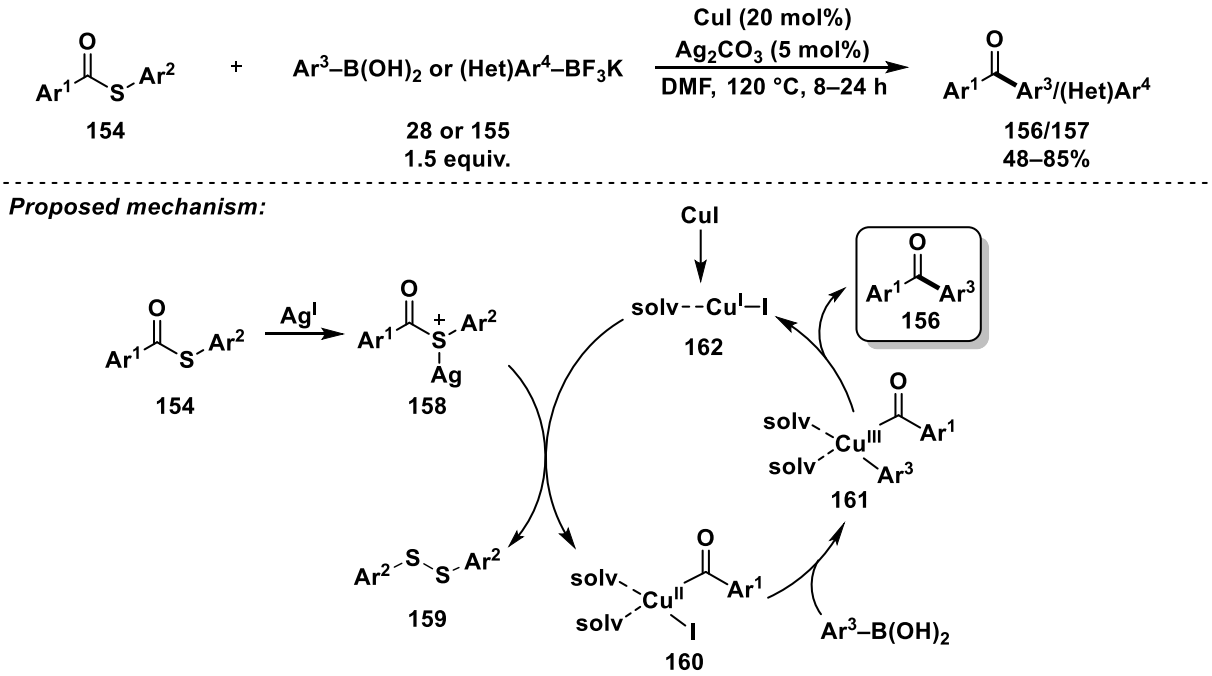

Scheme 3-27: Palladium-free and copper-catalyzed ketone synthesis from thioesters and boronic acids.[131f] solv = solvent.

Finally, based on the general mechanistic aspects for copper(I)-mediated or -catalyzed reactions,[128,130i] first drafts of a possible mechanistic scenario for the presented work are drawn. Transmetalation between the copper(I) salt and the boroxine/boronic acid could lead to an organocuprate to which thioester could be oxidatively added, resulting in a copper(III) intermediate. Subsequent reductive elimination could furnish the ketone and an inactive Cu–SPh species that renders the catalytic reaction unfeasible.

A classification in the context of known literature revealed that there is no example to date in which a stoichiometric amount of CuTC was used for the ketone synthesis from thioesters and boroxines in the absence of a palladium catalyst. Furthermore, only one example is given, where a catalytic amount of copper(I) was employed (Scheme 3-27).[131f] However, the protocol requires a relatively high catalyst loading, a high reaction temperature and long reaction times, and the yields could be optimized. Therefore, there is still great potential for the development and improvement of copper-mediated or copper-catalyzed ketone syntheses from thioesters and boroxines.

3.3.3 Conclusion and Outlook

Initially, the work began with investigations on the nickel-catalyzed and copper(I)-mediated coupling of *S*-phenyl benzothioate (**133**) and triphenyl boroxine as substrates for the formation of benzophenone (**134**).

First studies on the organoboron coupling partner indicated that the reaction appears to be sensitive to the ratio between boroxine and boronic acid as well as to the water content. The reaction was unsuccessful when the proportion of boronic acid was too high. At a ratio of

10:0.5 boroxine/boronic acid, the highest yield of ketone **134** was achieved (45%). The product yield could be improved by further optimizing the ratio of boroxine to boronic acid, for instance by azeotropic distillation or treatment in a Kugelrohr apparatus. Furthermore, water as additive may influence the boroxine/boronic acid equilibrium. To generate a higher yield of ketone, organoboron reagents with a different reactivity than the less reactive boroxine could be tested, for example other electronically and sterically modified boronic acids and boroxines, potassium trifluoroborates, neopentylglycolboronate or pinacol boronates. Although it is known that oxygen bases normally reduce the yields in LSC, they could have an unexpected positive effect on this system in their hydrous or anhydrous form and should be included in future optimizations.

In respect to the thioester, the highest yield of benzophenone (**134**) was obtained with *S*-phenyl benzothioate (**133**), and substituents on the thiol scaffold negatively affected the product yield. The reactivity could be further modulated by 2-pyridyl or alkyl moieties on the thiolate, which could presumably lead to a change in the thioester conversion. In addition, the application of thioesters with an *O*-methyl oxime moiety, which have been already used in the third generation of the Liebeskind–Srogl coupling,[94] could be interesting.

First studies on the reaction conditions have shown that the ketone yield almost stagnates at a temperature above 50 °C. Other conditions, such as reaction time and solvent, still need to be investigated.

A control reaction showed that ketone formation was successful even in the absence of the nickel catalyst, indicating that copper(I) is the active species in the coupling, and therefore the amount of CuTC was varied depending on the ligand. Stoichiometric amounts of CuTC generally gave higher yields of ketone **134** in the presence of a ligand. This was reversed when a catalytic amount of CuTC was used. Employing 10 mol% CuTC without ligand, ketone **134** was detected in 7% yield, while the reaction of thioester **133** and boroxine **132-B** was completely inhibited in the presence of a ligand. Potentially, with further optimization studies, including the application of other copper(I) sources such as CuMeSal or CuX and an extensive ligand screening, higher yields of the desired ketone **134** could be achieved. Additionally, the optimization studies should be performed in the presence and absence of different nickel sources, e.g. $Ni(^{4\text{-}t\text{Bu}}stb)_3$ (stb = *trans*-stilbene) instead of $Ni(cod)_2$,[132] to investigate whether a nickel-catalyzed method is possible depending on the choice of ligand and catalyst.

Following from the short literature overview on copper-mediated and copper-catalyzed ketone syntheses, the presented work could expand the horizon of established methods and may be another promising copper(I)-assisted or -catalyzed possibility to enable the formation of benzophenones starting from thioesters and boroxines as readily available and bench-stable substrates.

3.4 Experimental Part
3.4.1 General Information
3.4.1.1 Chemicals

Boroxine/phenylboronic acid was purchased from either Sigma-Aldrich (≥97%, stored under Ar during delivery, **132-A**), BLDpharm (98%, **132-B**/**C**) or Acros (98%, **132-D**). Copper(I) thiophene-2-carboxylate was supplied by either TCI, Sigma-Aldrich (both stored under Ar during delivery) or BLDpharm (not stored under Ar during delivery). Tris(2-furyl)phosphine (99%) and $Ni(cod)_2$ were purchased from Sigma-Aldrich. Pd_2dba_3 (Pd 21.5% min) and anhydrous 1,10-phenanthroline (99%) were supplied from Alfa Aesar. Phenylboronic acid pinacol ester (99.5%) and benzo[*d*][1,3]dioxol-5-ylboronic acid (98%) were supplied from BLDpharm. The following chemicals were stored and weighed in an Ar-filled glovebox from Glovebox Systemtechnik: Phenylboronic acid (Sigma-Aldrich), the different CuTCs, Pd_2dba_3, $Ni(cod)_2$ (additionally in a freezer), 1,10-phenanthroline and benzo[*d*][1,3]dioxol-5-ylboronic acid. K_2CO_3 was provided by the central chemical storage of the University of Tübingen and used as received. THF and DCM were either HPLC grade or technical grade and in this case were distilled before use.

3.4.1.2 General Techniques
3.4.1.2.1 Reaction Set-up

Air-sensitive syntheses were carried out under an Ar atmosphere. The glassware used for these reactions was flame-dried by heating with a propane torch under vacuum and subsequent cooling under dry Ar. The cycles were repeated three times. Anhydrous THF was prepared as follows: HPLC grade THF was distilled and stored over KOH flakes for at least three days. It was then filtered through a column of activated basic Al_2O_3 and stored under Ar over 3 Å molecular sieves for at least three days before use. Molecular sieves were activated by heating in a microwave (3 × 1 min) prior to use. THF was degassed by purging with Ar.

3.4.1.2.2 Analytical Techniques

Nuclear Magnetic Resonance Spectroscopy (NMR)

NMR spectra were recorded with a Bruker Avance 400 instrument. All measurements were performed at ambient temperature. Chemical shifts δ are given in parts per million [ppm] relative to the solvent signal as internal standard ($CDCl_3$: ^1H: δ = 7.26 ppm).[133]

Gas Chromatography (GC-MS or GC-FID)

Preparation of Samples for GC-FID and GC-MS Analysis

The catalytic reactions were quenched by adding Lewatit® TP 207 (Sigma-Aldrich). An internal standard (*n*-pentadecane, ≥99%, Sigma-Aldrich, 25 µL) was added to the reaction mixture, which was stirred for further 5 min. A sample of 0.1 mL was taken and filtered through a pad

of Celite® 545, activated basic Al_2O_3 and anhydrous $MgSO_4$ in a Pasteur pipette with DCM as eluent.

Gas Chromatography (GC)

GC-FID (flame ionization detection) analysis was carried out on an Agilent 7820A GC system with a 19091J-431 column (30 m × 320 µm × 0.25 µm) and dry hydrogen as carrier gas. The temperature program includes heating from 50 °C to 280 °C within 15 min. The internal standard method for quantitative GC-FID was used to determine yields and conversions. For this purpose, calibration was conducted by varying the mass ratio of substrate and standard with the subsequent analysis of the different samples by GC-FID (Equation 2).

$$\frac{A_X}{A_{Std.}} = R \cdot \frac{m_X}{m_{Std.}} \quad (2)$$

A_X: Peak area compound x

$A_{Std.}$: Peak area standard (*n*-pentadecane)

m_X: Mass compound x

m_{Std}: Mass standard (*n*-pentadecane)

R: Response factor

Mass Spectrometry (MS)

Low resolution GC-MS was performed on an Agilent 7820A GC system with a 190915-433UI column (30 m × 250 µm × 0.25 µm) and a 5977B MSD (EI) using dry hydrogen as carrier gas. The temperature program includes heating from 50 °C to 280 °C within 15 min.

3.4.2 Preparation of Substrates

3.4.2.1 Synthesis of Thioesters

General Procedure (GP):

A solution of the respective thiol (1.0 equiv.–1.2 equiv.) in DCM or THF (40 mL) was cooled to 0 °C. At this temperature, triethylamine (1.0 equiv.–1.2 equiv.) and the corresponding acyl chloride (1.0 equiv.) were added dropwise. After stirring at 0 °C for 30 min, the reaction mixture was warmed to rt. The suspension was stirred at rt until no more starting material was observed (TLC control) and then quenched by adding water (10 mL). The aqueous phase was extracted with EtOAc (2 × 15 mL). The combined organic layers were washed with HCl (1 M, 3 × 10 mL), aq. saturated $NaHCO_3$ (3 × 10 mL), and aq. saturated NaCl (2 × 10 mL). The combined organic layers were dried over anhydrous $MgSO_4$, filtered and concentrated under reduced pressure. Possible purification methods are mentioned detailed in the individual experiments.

3.4.2.2 Experimental Procedure and Analytical Data of Thioesters

S-phenyl benzothioate (133)

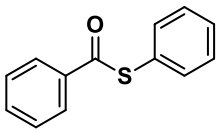

133

According to GP, *S*-phenyl benzothioate (**133**) was synthesized using benzoyl chloride (1.7 mL, 15 mmol, 1.0 equiv.), thiophenol (1.8 mL, 18 mmol, 1.2 equiv.), triethylamine (2.5 mL, 18 mmol, 1.2 equiv.) and DCM (20 mL) as solvent. The crude product was purified by column chromatography (*n*Hex/EtOAC 95:5) to yield the product **133** (1.83 g, 8.54 mmol, 57%) as a colorless solid. The analytical data are in good agreement with the literature.[134]

$C_{13}H_{10}OS$: 214.28 $\frac{\mathrm{g}}{\mathrm{mol}}$

R_f: 0.51 (Silica gel, *n*Hex/EtOAc 95:5, UV).

Melting point: 56.0–56.5 °C (*n*Hex/EtOAc).

^{1}H-NMR (400 MHz, $CDCl_3$): δ [ppm] = 8.04–8.01 (m, 2H), 7.64–7.58 (m, 1H), 7.53–7.44 (m, 7H).

^{13}C-NMR (101 MHz, $CDCl_3$): δ [ppm] = 190.3, 136.8, 136.2, 133.8, 129.7, 129.4, 128.9, 127.6, 127.5.

GC-MS (EI): t_R = 21.54 min, *m/z* (Int. %) = 214 (4) $[M]^{+\bullet}$, 105 (100) $[M]^{+\bullet}$-$[C_6H_5S]^{\bullet}$, 77 (37) $[M]^{+\bullet}$-$[C_7H_5OS]^{\bullet}$.

S-(4-methoxyphenyl) benzothioate (139)

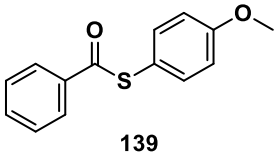

139

According to GP, *S*-(4-methoxyphenyl) benzothioate (**139**) was synthesized using benzoyl chloride (0.60 mL, 5.0 mmol, 1.0 equiv.), 4-methoxythiophenol (0.60 mL, 5.0 mmol, 1.0 equiv.), triethylamine (0.80 mL, 6.0 mmol, 1.2 equiv.) and THF (10 mL) as solvent. The crude product was purified by column chromatography (*n*Hex/EtOAc 95:5) to yield the product **139** (1.11 g, 4.54 mmol, 91%) as a colorless solid. The analytical data are in good agreement with the literature.[135]

$C_{14}H_{12}O_2S$: 244.31 $\frac{g}{mol}$

R_f: 0.24 (Silica gel, *n*Hex/EtOAc 95:5, UV).

Melting point: 98.8–99.4 °C (*n*Hex/EtOAc).

^{1}H-NMR (400 MHz, $CDCl_3$): δ [ppm] = 8.03–8.00 (m, 2H), 7.61 (t, *J* = 7.4 Hz, 1H), 7.48 (t, *J* = 8.0 Hz, 2H), 7.42 (d, *J* = 8.2 Hz, 2H), 6.99 (d, *J* = 8.2 Hz, 2H), 3.85 (s, 3H).

^{13}C-NMR (101 MHz, $CDCl_3$): δ [ppm] = 191.2, 180.9, 136.8, 133.7, 128.9, 127.6, 118.0, 115.1, 55.5.

GC-MS (EI): t_R = 24.48 min, *m/z* (Int. %) = 244 (13) $[M]^{+\bullet}$, 105 (100) $[M]^{+\bullet}$-$[C_7H_7OS]^{\bullet}$, 77 (32) $[M]^{+\bullet}$-$[C_8H_7O_2S]^{\bullet}$.

S-(4-bromophenyl) benzothioate (140)

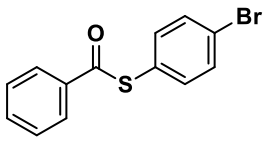

140

According to GP, *S*-(4-bromophenyl) benzothioate (**140**) was synthesized using benzoyl chloride (0.60 mL, 5.0 mmol, 1.0 equiv.), 4-bromothiophenol (945 mg, 5.00 mmol, 1.00 equiv.), triethylamine (0.70 mL, 5.0 mmol, 1.0 equiv.) and DCM (15 mL) as solvent. The crude product was purified by column chromatography (*n*Hex/EtOAC 95:5) to yield the product **140** (0.82 g, 2.8 mmol, 56%) as a colorless solid. The analytical data are in good agreement with the literature.[136]

$C_{13}H_9BrOS$: 293.18 $\frac{g}{mol}$

R_f: 0.50 (Silica gel, *n*Hex/EtOAc 95:5, UV).

Melting point: 81.3–83.5 °C (*n*Hex/EtOAc).

^{1}H-NMR (400 MHz, $CDCl_3$): δ [ppm] = 8.04–8.00 (m, 2H), 7.65–7.56 (m, 3H), 7.51–7.47 (m, 2H), 7.40–7.36 (m, 2H).

^{13}C-NMR (101 MHz, $CDCl_3$): δ [ppm] = 189.7, 136.7, 136.5, 134.0, 132.6, 129.0, 127.7, 126.6, 134.4.

GC-MS (EI): t_R = 24.66 min, *m/z* (Int. %) = 293 (2) $[M]^{+\bullet}$, 105 (100) $[M]^{+\bullet}$-$[C_6H_4BrS]^{\bullet}$, 77 (32) $[M]^{+\bullet}$-$[C_7H_4BrOS]^{\bullet}$.

3.4.2.3 Boronic Acid Study

The ratio of boroxine to phenylboronic acid or water was determined by ^{1}H-NMR analysis, comparing the respective integrated peaks.[117b]

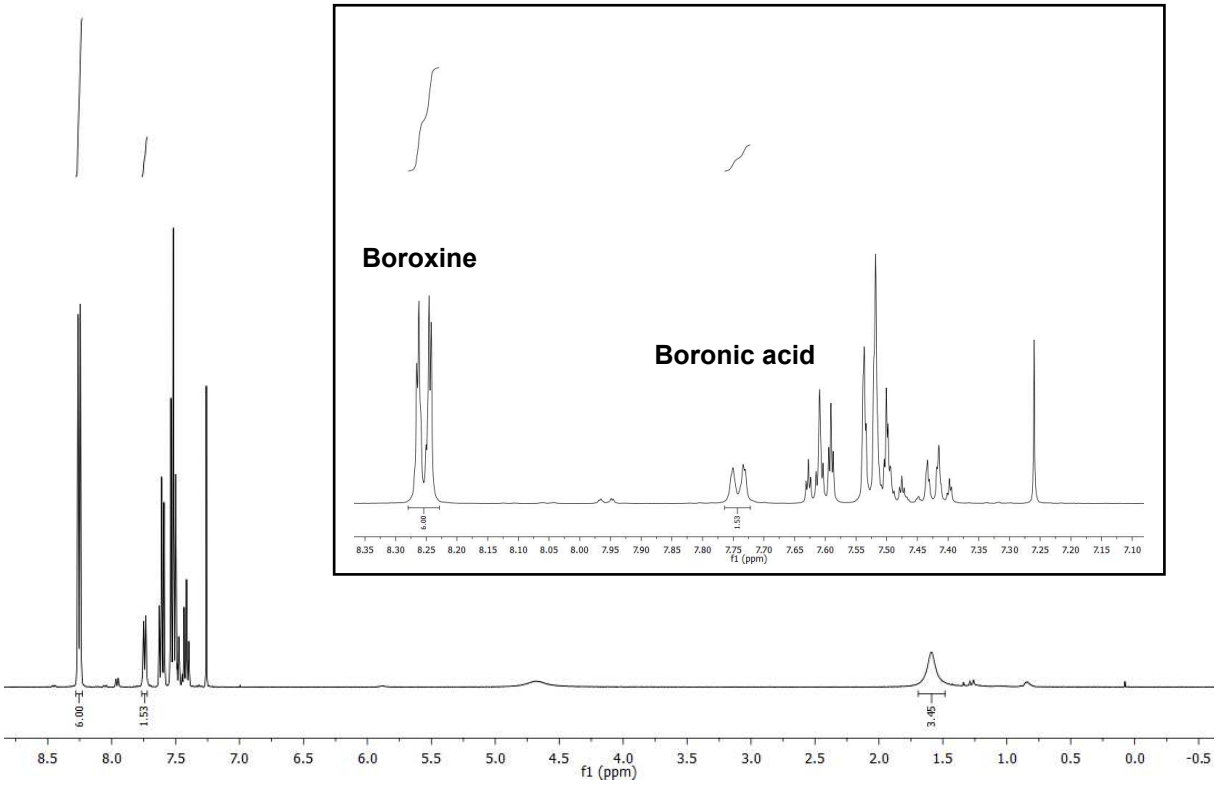

Figure 3-12: ^{1}H-NMR spectrum of **132-A**.

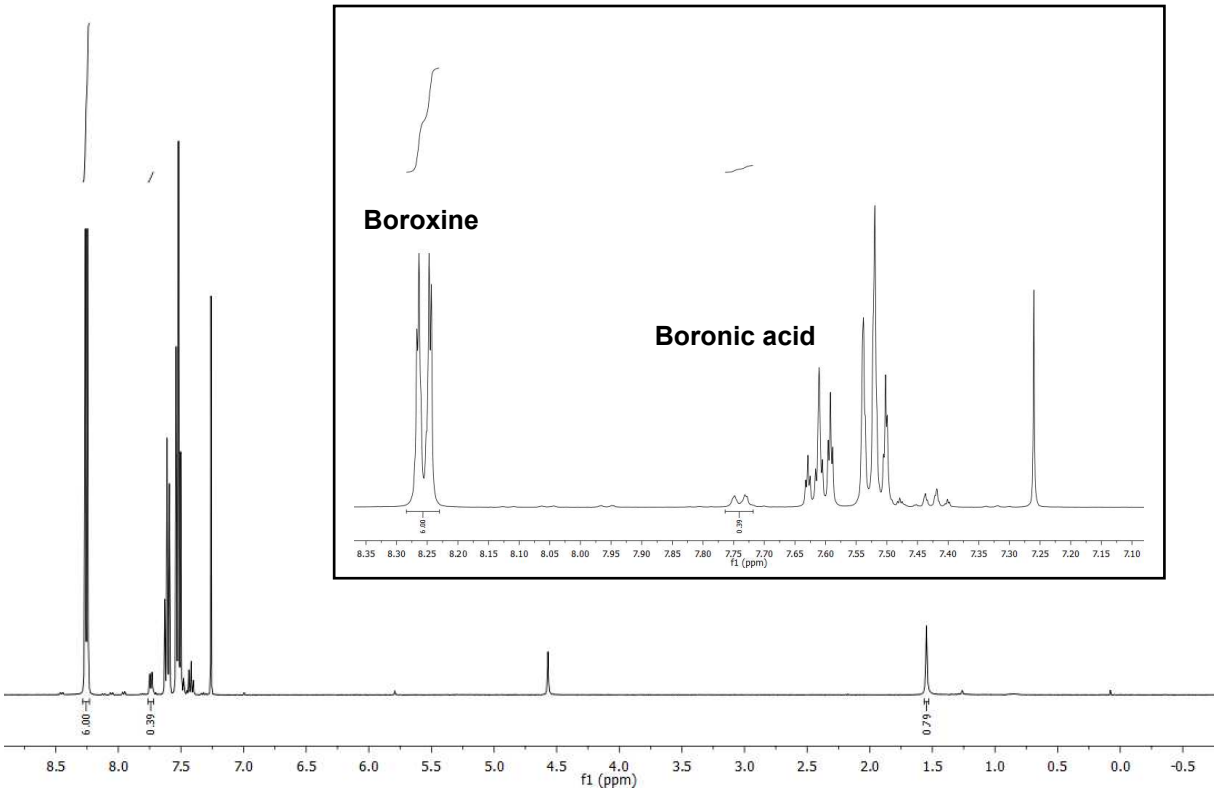

Figure 3-13: ^{1}H-NMR spectrum of **132-B**.

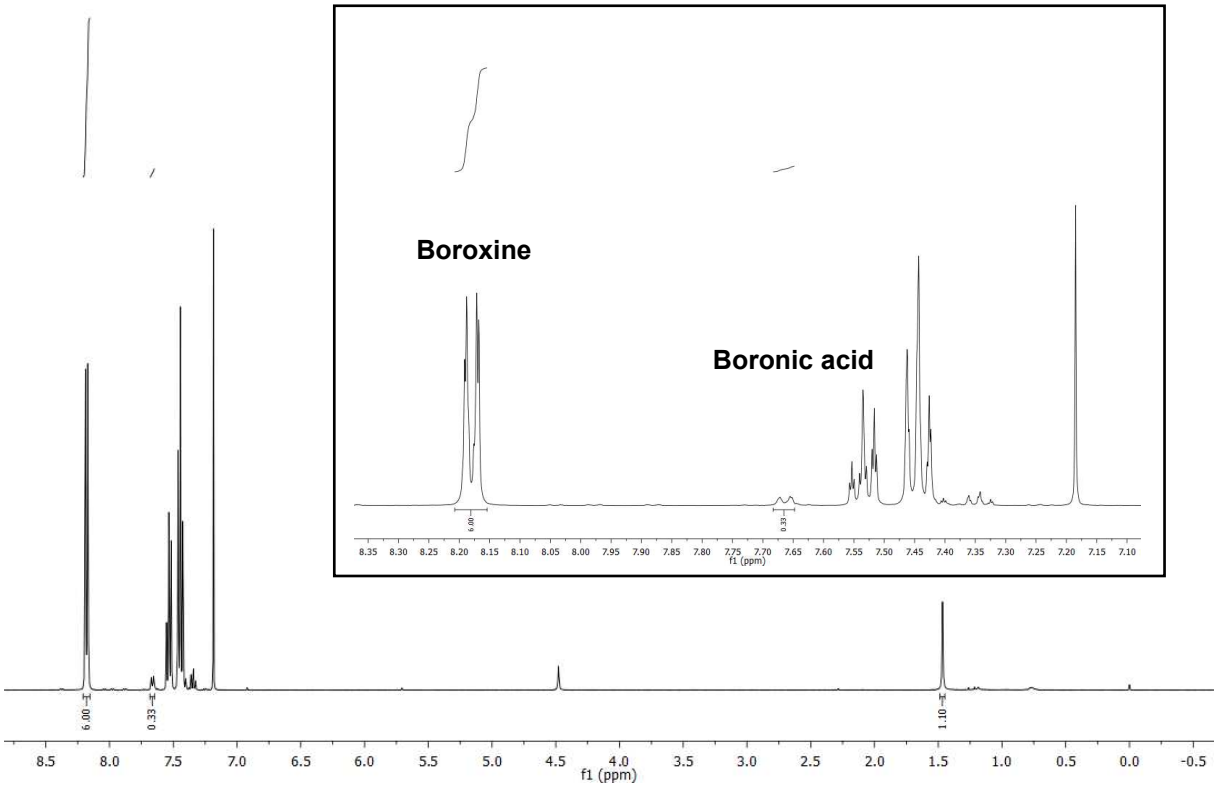

Figure 3-14: ^{1}H-NMR spectrum of **132-C**.

The experiments mentioned in section 3.3.1 were conducted with **132-B/C** purchased from BLDpharm. However, the cross coupling is also possible with phenylboronic acid **132-D** supplied by Acros. The ratios of boroxine:boronic acid (10:0.7) and boroxine:water (1:0.2) were determined by ^{1}H-NMR.

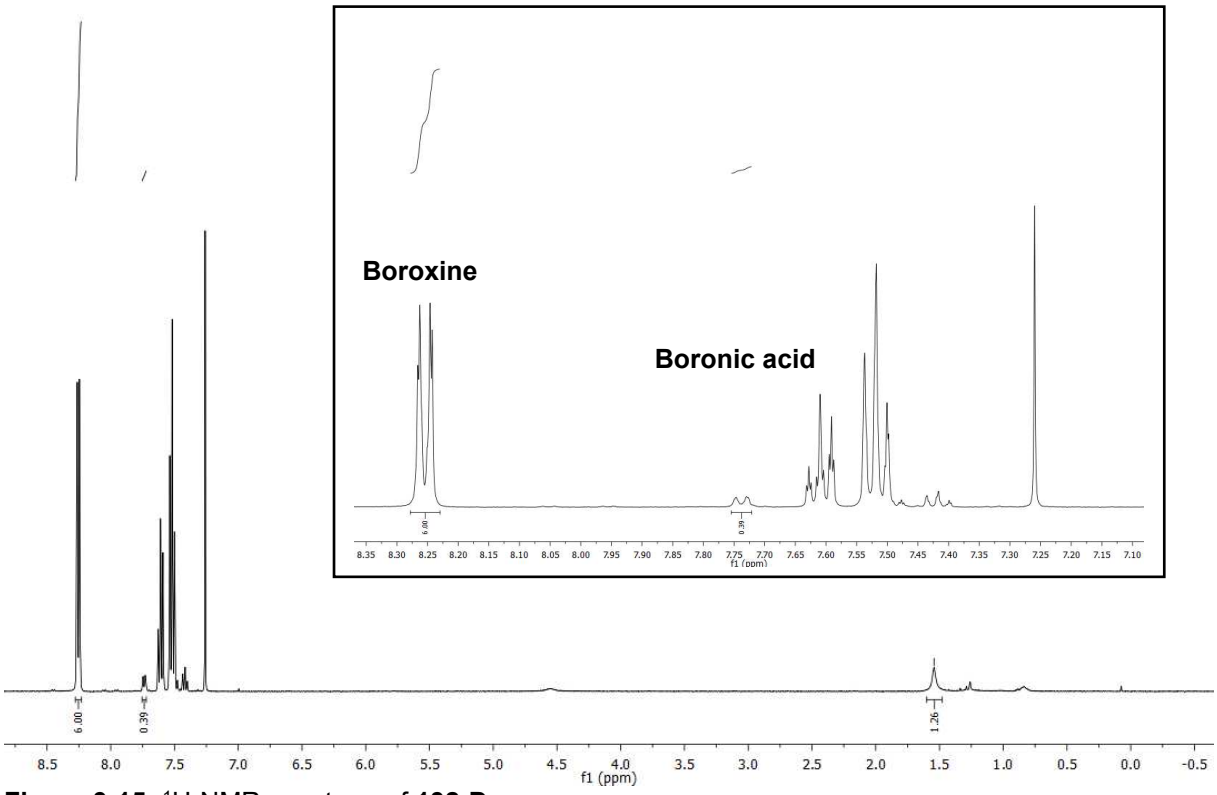

Figure 3-15: ^{1}H-NMR spectrum of **132-D**.

3.4.3 Catalytic Procedure

In a glovebox, a flame-dried Schlenk tube was charged with $Ni(cod)_2$ (6.9 mg, 25 µmol, 5.0 mol%), 1,10-phenanthroline (9.0 mg, 50 µmol, 10 mol%) and CuTC (153 mg, 800 µmol, 1.6 equiv.). After removal from the glovebox, *S*-phenyl benzothioate (**133**) (107 mg, 500 µmol, 1.0 equiv.), boroxine **132** (93.5 mg, 300 µmol, 0.6 equiv.) and THF (2 mL) were added successively. The reaction was stirred at 50 °C for further 15 h. After general sample preparation, the yields were determined by quantitative GC-FID analysis (see section 3.4.1.2.2).

3.4.4 Calibration Data for GC-FID
S-phenyl benzothioate (133)

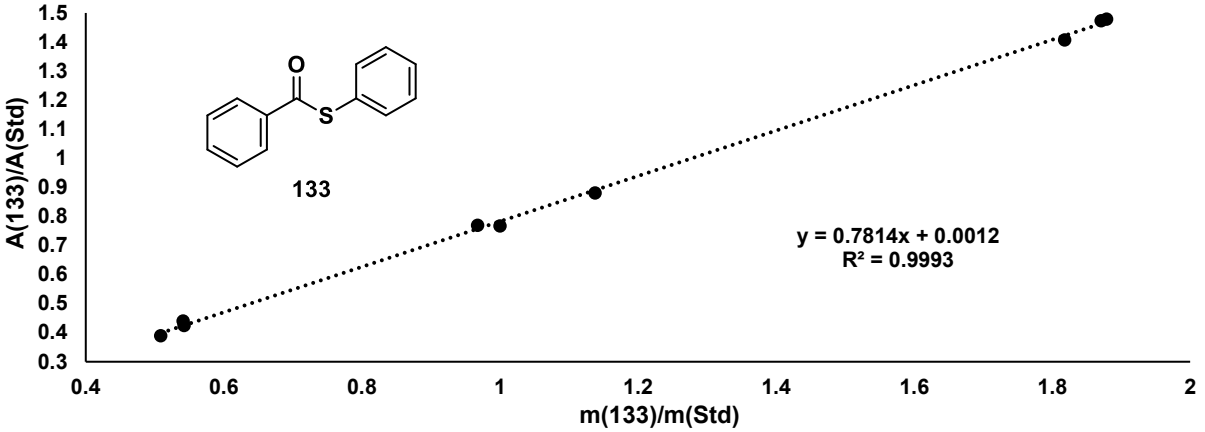

Mass ratio [mg(133)/mg(Std)]	A(133)	A(Std)	Area ratio [A(133)/A(Std)]
1.1	6921.8	7856.8	0.8809
1.0	6360.2	8269.7	0.7691
1.0	6199.4	8077.2	0.7675
1.9	12248	8311.2	1.4737
1.9	13064	8835.0	1.4786
1.8	12259	8715.1	1.4067
0.5	6648.8	15641	0.4250
0.5	7139.5	16206	0.4405
0.5	6207.7	15921	0.3899

S-(4-methoxyphenyl) benzothioate (139)

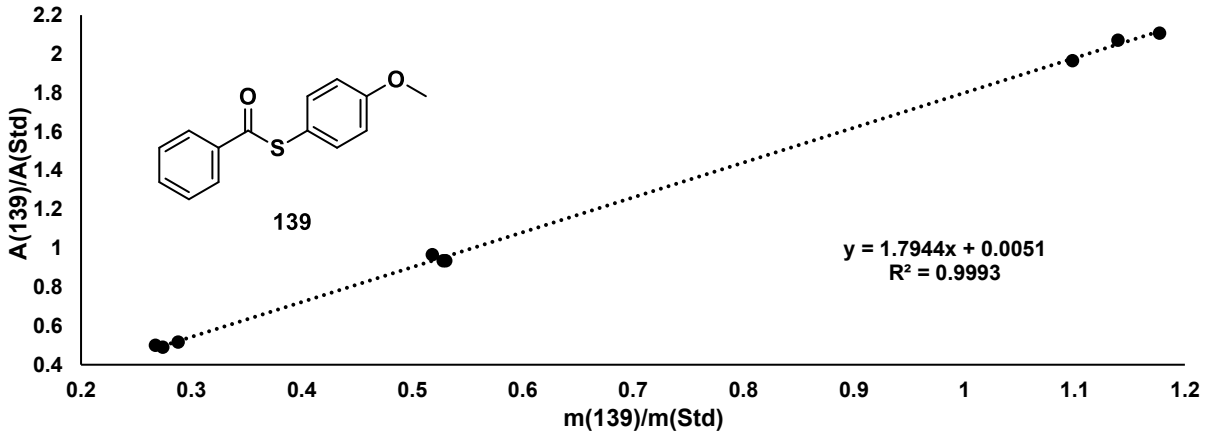

Mass ratio [mg(139)/mg(Std)]	A(139)	A(Std)	Area ratio [A(139)/A(Std)]
0.9	5626.0	8250.2	0.5282
1.0	5693.9	7212.5	0.5183
0.9	5633.9	8052.6	0.5306
0.5	5306.4	16593	0.2674
0.5	5681.6	17107	0.2882
0.5	5602.9	15522	0.2743
2.1	11317	7794.1	1.1771
2.1	10634	7782.2	1.1394
2.0	11049	7917.2	1.0983

S-(4-bromophenyl) benzothioate (140)

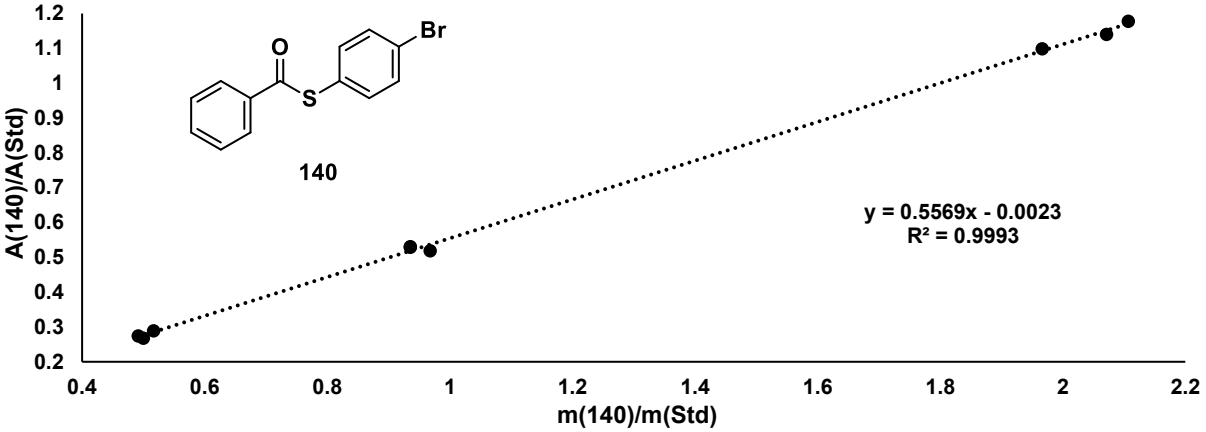

Mass ratio [mg(140)/mg(Std)]	A(140)	A(Std)	Area ratio [A(140)/A(Std)]
0.9	4448.3	8420.9	0.5282
1.0	4314.6	8324.9	0.5183
0.9	4364.8	8226.1	0.5306
0.5	4599.7	17199	0.2674
0.5	4658.2	16164	0.2882
0.5	4403.9	16057	0.2743
2.1	8603.8	7309.2	1.1771
2.1	8774.2	7700.4	1.1394
2.0	8843.7	8052.3	1.0983

benzophenone (134)

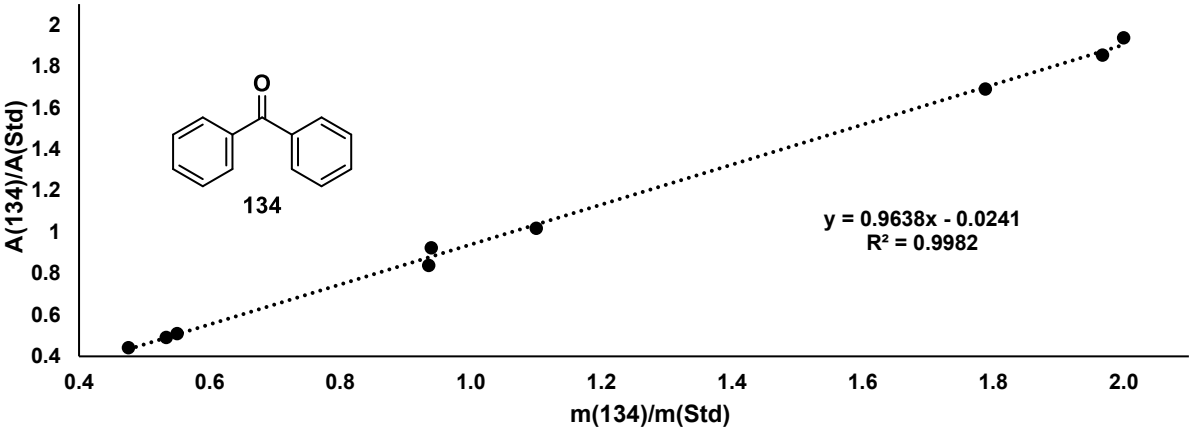

Mass ratio [mg(134)/mg(Std)]	A(134)	A(Std)	Area ratio [A(134)/A(Std)]
1.1	8373.9	8234.8	1.0168
0.9	7213.1	8605.4	0.8382
0.9	8127.5	8801.4	0.9234
1.9	15498	8360.9	1.8536
2.0	16226	8380.7	1.9361
1.8	15225	9008.1	1.6901
0.6	8368	16420	0.5096
0.5	8196	16708	0.4905
0.5	7322.7	16601	0.4411

biphenyl (135)

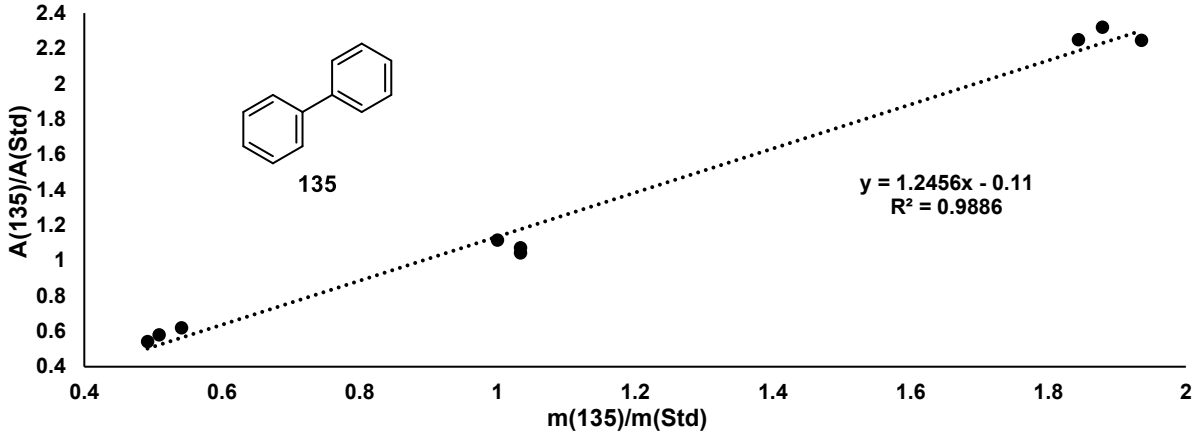

Mass ratio [mg(135)/mg(Std)]	A(135)	A(Std)	Area ratio [A(135)/A(Std)]
1.0	8915.7	7978.7	1.1174
1.0	9878.8	9204.2	1.0733
1.0	8138.5	7788.2	1.0449
1.9	18606.6	8015.7	2.3213
1.8	17169.5	7632.2	2.2496
1.9	17578.6	7824.9	2.2465
0.5	10578.2	17049.3	0.6204
0.5	9387.1	16146.4	0.5814
0.5	9083.8	16752.3	0.5422

diphenyl sulfide (136)

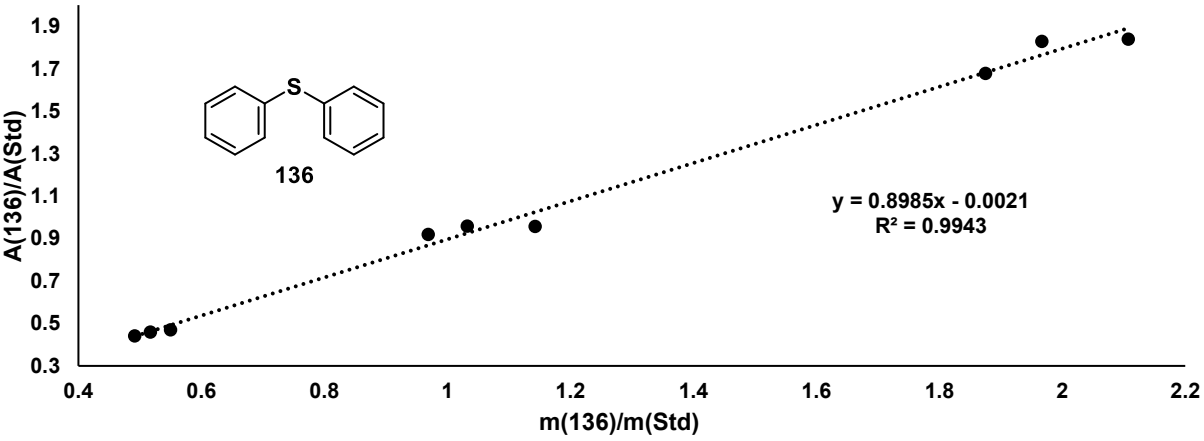

Mass ratio [mg(136)/mg(Std)]	A(136)	A(Std)	Area ratio [A(136)/A(Std)]
1.1	7610.4	7950.1	0.9573
0.9	7708.8	8390.2	0.9188
1.0	7702.0	8036.5	0.9584
2.1	14339	7794.3	1.8397
2.0	14185	7756.7	1.8287
1.9	14076	8391.1	1.6775
0.6	7920.8	16846	0.4702
0.5	7191.3	15639	0.4598
0.5	7076.2	16023	0.4416

3.5 References

[1] S. Lou, G. C. Fu, *J. Am. Chem. Soc.* **2010**, *132*, 1264–1266.
[2] H. Yin, G. C. Fu, *J. Am. Chem. Soc.* **2019**, *141*, 15433–15440.
[3] C. Schmuck in *Basisbuch Organische Chemie*, Pearson, **2018**, p. 323.
[4] Y. Ogiwara, N. Sakai, *Angew. Chem. Int. Ed.* **2020**, *59*, 574–594.
[5] J. Buchspies, M. Szostak, *Catalysts* **2019**, *9*, 53.
[6] C. Malanga, L. A. Aronica, L. Lardicci, *Tetrahedron Lett.* **1995**, *36*, 9185–9188.
[7] Y. Zhang, T. Rovis, *J. Am. Chem. Soc.* **2004**, *126*, 15964–15965.
[8] a) K. Ouyang, W. Hao, W.-X. Zhang, Z. Xi, *Chem. Rev.* **2015**, *115*, 12045–12090; b) G. Meng, S. Shi, M. Szostak, *Synlett* **2016**, *27*, 2530–2540; c) Q. Wang, Y. Su, L. Li, H. Huang, *Chem. Soc. Rev.* **2016**, *45*, 1257–1272; d) J. E. Dander, N. K. Garg, *ACS Catal.* **2017**, *7*, 1413–1423; e) R. Takise, K. Muto, J. Yamaguchi, *Chem. Soc. Rev.* **2017**, *46*, 5864–5888.
[9] N. A. Weires, E. L. Baker, N. K. Garg, *Nat. Chem.* **2016**, *8*, 75–79.
[10] a) K. W. Quasdorf, A. Antoft-Finch, P. Liu, A. L. Silberstein, A. Komaromi, T. Blackburn, S. D. Ramgren, K. N. Houk, V. Snieckus, N. K. Garg, *J. Am. Chem. Soc.* **2011**, *133*, 6352–6363; b) B.-T. Guan, Y. Wang, B.-J. Li, D.-G. Yu, Z.-J. Shi, *J. Am. Chem. Soc.* **2008**, *130*, 14468–14470; c) A. Antoft-Finch, T. Blackburn, V. Snieckus, *J. Am. Chem. Soc.* **2009**, *131*, 17750–17752; d) R. L. Jezorek, N. Zhang, P. Leowanawat, M. H. Bunner, N. Gutsche, A. K. Pesti, J. T. Olsen, V. Percec, *Org. Lett.* **2014**, *16*, 6326–6329.
[11] a) T. B. Boit, N. A. Weires, J. Kim, N. K. Garg, *ACS Catal.* **2018**, *8*, 1003–1008; b) M. M. Mehta, T. B. Boit, J. E. Dander, N. K. Garg, *Org. Lett.* **2019**, *22*, 1–5.
[12] T. B. Boit, M. M. Mehta, J. Kim, E. L. Baker, N. K. Garg, *Angew. Chem. Int. Ed.* **2021**, *60*, 2472–2477.
[13] J. A. Walker, Jr., K. L. Vickerman, J. N. Humke, L. M. Stanley, *J. Am. Chem. Soc.* **2017**, *139*, 10228–10231.
[14] P.-Q. Huang, H. Chen, *Chem. Commun.* **2017**, *53*, 12584–12587.
[15] B. J. Simmons, N. A. Weires, J. E. Dander, N. K. Garg, *ACS Catal.* **2016**, *6*, 3176–3179.
[16] S. Shi, M. Szostak, *Chem. Eur. J.* **2016**, *22*, 10420–10424.
[17] A. Skhiri, N. Chatani, *Org. Lett.* **2019**, *21*, 1774–1778.
[18] a) L. J. Gooßen, N. Rodríguez, K. Gooßen, *Angew. Chem. Int. Ed.* **2008**, *47*, 3100–3120; b) L. J. Gooßen, K. Gooßen, N. Rodríguez, M. Blanchot, C. Linder, B. Zimmermann, *Pure Appl. Chem.* **2008**, *80*, 1725–1733; c) J. B. Johnson, T. Rovis, *Acc. Chem. Res.* **2008**, *41*, 327–338.
[19] V. Fiandanese, G. Marchese, L. Ronzini, *Tetrahedron Lett.* **1983**, *24*, 3677–3680.
[20] Q. Chen, X.-H. Fan, L.-P. Zhang, L.-M. Yang, *RSC Adv.* **2014**, *4*, 53885–53890.
[21] a) E. A. Bercot, T. Rovis, *J. Am. Chem. Soc.* **2002**, *124*, 174–175; b) E. A. Bercot, T. Rovis, *J. Am. Chem. Soc.* **2005**, *127*, 247–254; c) J. B. Johnson, E. A. Bercot, J. M. Rowley, G. W. Coates, T. Rovis, *J. Am. Chem. Soc.* **2007**, *129*, 2718–2725; d) J. B. Johnson, R. T. Yu, P. Fink, E. A. Bercot, T. Rovis, *Org. Lett.* **2006**, *8*, 4307–4310; e) S. Kozuch, S. E. Lee, S. Shaik, *Organometallics* **2009**, *28*, 1303–1308; f) R. L. Rogers, J. L. Moore, T. Rovis, *Angew. Chem. Int. Ed.* **2007**, *46*, 9301–9304.
[22] T. Inami, Y. Baba, T. Kurahashi, S. Matsubara, *Org. Lett.* **2011**, *13*, 1912–1915.
[23] M. Sun, Y.-N. Ma, Y.-M. Li, Q.-P. Tian, S.-D. Yang, *Tetrahedron Lett.* **2013**, *54*, 5091–5095.
[24] Y. Yoshino, T. Kurahashi, S. Matsubara, *J. Am. Chem. Soc* **2009**, *131*, 7494–7495.
[25] A. Chatupheeraphat, H.-H. Liao, W. Srimontree, L. Guo, Y. Minenkov, A. Poater, L. Cavallo, M. Rueping, *J. Am. Chem. Soc.* **2018**, *140*, 3724–3735.

[26] Y.-L. Zheng, P.-P. Xie, O. Daneshfar, K. N. Houk, X. Hong, S. G. Newman, *Angew. Chem. Int. Ed.* **2021**, *60*, 13476–13483.
[27] Y. L. Zheng, S. G. Newman, *Angew. Chem. Int. Ed.* **2019**, *58*, 18159–18164.
[28] X. Wu, X. Li, W. Huang, Y. Wang, H. Xu, L. Cai, J. Qu, Y. Chen, *Org. Lett.* **2019**, *21*, 2453–2458.
[29] S. Huang, M. Wang, X. Jiang, *Chem. Soc. Rev.* **2022**, *51*, 8351–8377.
[30] C. Christophersen, U. Anthoni, *Sulfur Rep.* **1986**, *4*, 365–442.
[31] M. Feng, B. Tang, S. H Liang, X. Jiang, *Curr. Top. Med. Chem.* **2016**, *16*, 1200–1216.
[32] P. Devendar, G.-F. Yang in *Sulfur-containing agrochemicals*, (Ed. X. Jiang), Springer, **2019**, pp. 35–78.
[33] R. J. Huxtable, *Biochemistry of sulfur*, Springer Science & Business Media, **2013**.
[34] G. C. Lloyd-Jones, J. D. Moseley, J. S. Renny, *Synthesis* **2008**, *2008*, 661–689.
[35] B. A. Vara, N. R. Patel, G. A. Molander, *ACS Catal.* **2017**, *7*, 3955–3959.
[36] J. J. Monteith, S. A. L. Rousseaux, *Acc. Chem. Res.* **2023**, *56*, 3581–3594.
[37] L. R. Mills, J. J. Monteith, G. dos Passos Gomes, A. Aspuru-Guzik, S. A. L. Rousseaux, *J. Am. Chem. Soc.* **2020**, *142*, 13246–13254.
[38] J. J. Monteith, S. A. L. Rousseaux, *Org. Lett.* **2021**, *23*, 9485–9489.
[39] Y. Zhao, Y. Xie, C. Xia, H. Huang, *Adv. Synth. Catal.* **2014**, *356*, 2471–2476.
[40] S. Silva, B. Sylla, F. Suzenet, A. Tatibouët, A. P. Rauter, P. Rollin, *Org. Lett.* **2008**, *10*, 853–856.
[41] T. Inami, T. Kurahashi, S. Matsubara, *Chem. Commun.* **2015**, *51*, 1285–1288.
[42] M.-C. Tang, H.-Y. He, F. Zhang, G.-L. Tang, *ACS Catal.* **2013**, *3*, 444–447.
[43] A. Schönberg, L. v. Vargha, *Chem. Ber.* **1930**, *63*, 178–180.
[44] Z. Zhu, Y. Gong, W. Tong, W. Xue, H. Gong, *Org. Lett.* **2021**, *23*, 2158–2163.
[45] G. Du, P. Zhu, J. Wang, X. Li, D.-P. Zhang, C.-Z. Wang, F.-G. Sun, *Eur. J. Org. Chem.* **2023**, *26*, e202201382.
[46] Z.-Y. Liu, S. P. Cook, *Org. Lett.* **2021**, *23*, 808–813.
[47] R.-H. Zheng, H.-C. Guo, T.-T. Chen, Q. Huang, G.-B. Huang, H.-J. Jiang, *RSC Adv.* **2018**, *8*, 25123–25126.
[48] V. Hirschbeck, P. H. Gehrtz, I. Fleischer, *Chem. Eur. J.* **2018**, *24*, 7092–7107.
[49] L. Shi, B. P. Tu, *Curr. Opin. Cell Biol.* **2015**, *33*, 125–131.
[50] V. Pace, W. Holzer, B. Olofsson, *Adv. Synth. Catal.* **2014**, *356*, 3686–3686.
[51] I. Ugur, A. Marion, S. Parant, J. H. Jensen, G. Monard, *Chem.Inf. Model.* **2014**, *54*, 2200–2213.
[52] T. B. Phan, M. Breugst, H. Mayr, *Angew. Chem. Int. Ed.* **2006**, *45*, 3869–3874.
[53] G. McDowell, A. Philpott, *Int. J. Biochem. Cell Biol.* **2013**, *45*, 1833–1842.
[54] Y. Tian, L. Wang, H.-Z. Yu, *RSC Adv.* **2016**, *6*, 61996–62004.
[55] X. Wu, J. Li, S. Xia, C. Zhu, J. Xie, *J. Org. Chem.* **2022**, *87*, 10003–10017.
[56] J. Wang, B. P. Cary, P. D. Beyer, S. H. Gellman, D. J. Weix, *Angew. Chem. Int. Ed.* **2019**, *58*, 12081–12085.
[57] T. Mukaiyama, M. Araki, H. Takei, *J. Am. Chem. Soc.* **1973**, *95*, 4763–4765.
[58] a) A. C. Wotal, D. J. Weix, *Org. Lett.* **2012**, *14*, 1476–1479; b) Y. Ai, N. Ye, Q. Wang, K. Yahata, Y. Kishi, *Angew. Chem. Int. Ed.* **2017**, *56*, 10791–10795.
[59] K. P. Kepp, *Inorg. Chem.* **2016**, *55*, 9461–9470.
[60] M. Ociepa, O. Baka, J. Narodowiec, D. Gryko, *Adv. Synth. Catal.* **2017**, *359*, 3560–3565.
[61] P. H. Gehrtz, P. Kathe, I. Fleischer, *Chem. Eur. J.* **2018**, *24*, 8774–8778.
[62] C. K. Jin, H. J. Jeong, M. K. Kim, J. Y. Kim, Y.-J. Yoon, S.-G. Lee, *Synlett* **2001**, *2001*, 1956–1958.

[63] B. Neises, W. Steglich, *Angew. Chem. Int. Ed. Eng.* **1978**, *17*, 522–524.
[64] X. Wang, Z. B. Dong, *Eur. J. Org. Chem.* **2022**, *2022*, 119–137.
[65] C. Cardellicchio, V. Fiandanese, G. Marchese, L. Ronzini, *Tetrahedron Lett.* **1985**, *26*, 3595–3598.
[66] a) H. Tokuyama, S. Yokoshima, T. Yamashita, L. Shao-Cheng, L. Leping, T. Fukuyama, *J. Braz. Chem. Soc.* **1998**, *9*, 381–387; b) H. Tokuyama, S. Yokoshima, T. Yamashita, T. Fukuyama, *Tetrahedron Lett.* **1998**, *39*, 3189–3192; c) H. Tokuyama, S. Yokoshima, S.-C. Lin, L. Li, T. Fukuyama, *Synthesis* **2002**, *2002*, 1121–1123.
[67] K. Kunchithapatham, C. C. Eichman, J. P. Stambuli, *Chem. Commun.* **2011**, *47*, 12679–12681.
[68] R. Oost, A. Misale, N. Maulide, *Angew. Chem. Int. Ed.* **2016**, *55*, 4587–4590.
[69] S.-Q. Tang, J. Bricard, M. Schmitt, F. Bihel, *Org. Lett.* **2019**, *21*, 844–848.
[70] T. Shimizu, M. Seki, *Tetrahedron Lett.* **2002**, *43*, 1039–1042.
[71] F. H. Lutter, L. Grokenberger, M. S. Hofmayer, P. Knochel, *Chem. Sci.* **2019**, *10*, 8241–8245.
[72] V. J. Geiger, G. Lefèvre, I. Fleischer, *Chem. Eur. J.* **2022**, *28*, e202202212.
[73] B. Zeysing, C. Gosch, A. Terfort, *Org. Lett.* **2000**, *2*, 1843–1845.
[74] L. S. Liebeskind, J. Srogl, C. Savarin, C. Polanco, *Pure Appl. Chem.* **2002**, *74*, 115–122.
[75] a) J. Srogl, G. D. Allred, L. S. Liebeskind, *J. Am. Chem. Soc.* **1997**, *119*, 12376–12377; b) S. Zhang, D. Marshall, L. S. Liebeskind, *J. Org. Chem.* **1999**, *64*, 2796–2804.
[76] C. Savarin, J. Srogl, L. S. Liebeskind, *Org. Lett.* **2000**, *2*, 3229–3231.
[77] a) H. Prokopcová, C. O. Kappe, *Angew. Chem. Int. Ed.* **2008**, *47*, 3674–3676; b) H. Prokopcova, C. O. Kappe, *Angew. Chem. Int. Ed.* **2009**, *48*, 2276–2286; c) H.-G. Cheng, H. Chen, Y. Liu, Q. Zhou, *Asian J. Org. Chem.* **2018**, *7*, 490–508.
[78] L. S. Liebeskind, J. Srogl, *J. Am. Chem. Soc.* **2000**, *122*, 11260–11261.
[79] a) L. S. Liebeskind, J. Srogl, *Org. Lett.* **2002**, *4*, 979–981; b) D. G. Musaev, L. S. Liebeskind, *Organometallics* **2009**, *28*, 4639–4642.
[80] a) C. Savarin, J. Srogl, L. S. Liebeskind, *Org. Lett.* **2001**, *3*, 91–93; b) Y. Yu, L. S. Liebeskind, *J. Org. Chem.* **2004**, *69*, 3554–3557.
[81] N. Miyaura, A. Suzuki, *Chem. Rev.* **1995**, *95*, 2457–2483.
[82] a) F.-A. Alphonse, F. Suzenet, A. Keromnes, B. Lebret, G. Guillaumet, *Org. Lett.* **2003**, *5*, 803–805; b) M. Egi, L. S. Liebeskind, *Org. Lett.* **2003**, *5*, 801–802; c) C. Kusturin, L. S. Liebeskind, H. Rahman, K. Sample, B. Schweitzer, J. Srogl, W. L. Neumann, *Org. Lett.* **2003**, *5*, 4349–4352; d) R. Wittenberg, J. Srogl, M. Egi, L. S. Liebeskind, *Org. Lett.* **2003**, *5*, 3033–3035; e) A. Morita, S. Kuwahara, *Org. Lett.* **2006**, *8*, 1613–1616; f) H. Li, H. Yang, L. S. Liebeskind, *Org. Lett.* **2008**, *10*, 4375–4378; g) N. Arshad, J. Hashim, C. O. Kappe, *J. Org. Chem.* **2009**, *74*, 5118–5121; h) Q. Sun, F. Suzenet, G. Guillaumet, *J. Org. Chem.* **2010**, *75*, 3473–3476; i) M. Klečka, R. Pohl, J. Čejka, M. Hocek, *Org. Biomol. Chem.* **2013**, *11*, 5189–5193; j) H. Li, A. He, J. R. Falck, L. S. Liebeskind, *Org. Lett.* **2011**, *13*, 3682–3685; k) A. Aguilar-Aguilar, L. S. Liebeskind, E. Peña-Cabrera, *J. Org. Chem.* **2007**, *72*, 8539–8542; l) H. Kobayashi, J. A. Eickhoff, A. Zakarian, *J. Org. Chem.* **2015**, *80*, 9989–9999.
[83] B. W. Fausett, L. S. Liebeskind, *J. Org. Chem.* **2005**, *70*, 4851–4853.
[84] V. P. Mehta, A. Sharma, E. Van der Eycken, *Adv. Synth. Catal.* **2008**, *350*, 2174–2178.
[85] C. L. Kusturin, L. S. Liebeskind, W. L. Neumann, *Org. Lett.* **2002**, *4*, 983–985.
[86] Z. Zhang, L. S. Liebeskind, *Org. Lett.* **2006**, *8*, 4331–4333.
[87] H. Prokopcová, L. Pisani, C. O. Kappe, *Synlett* **2007**, *2007*, 0043-0046.
[88] H. Yang, H. Li, R. Wittenberg, M. Egi, W. Huang, L. S. Liebeskind, *J. Am. Chem. Soc.* **2007**, *129*, 1132–1140.

[89] a) F.-A. Alphonse, F. Suzenet, A. Keromnes, B. Lebret, G. Guillaumet, *Synlett* **2002**, *2002*, 0447-0450; b) S. Oumouch, M. Bourotte, M. Schmitt, J.-J. Bourguignon, *Synthesis* **2005**, *2005*, 25–27.
[90] A. Lengar, C. O. Kappe, *Org. Lett.* **2004**, *6*, 771–774.
[91] a) H. Prokopcová, C. O. Kappe, *Adv. Synth. Catal.* **2007**, *349*, 448–452; b) H. Prokopcová, C. O. Kappe, *J. Org. Chem.* **2007**, *72*, 4440–4448.
[92] J. M. Villalobos, J. Srogl, L. S. Liebeskind, *J. Am. Chem. Soc.* **2007**, *129*, 15734–15735.
[93] L. S. Liebeskind, H. Yang, H. Li, *Angew. Chem.* **2009**, *121*, 1445–1449.
[94] Z. Zhang, M. G. Lindale, L. S. Liebeskind, *J. Am. Chem. Soc.* **2011**, *133*, 6403–6410.
[95] K. Tsuna, N. Noguchi, M. Nakada, *Tetrahedron Lett.* **2011**, *52*, 7202–7205.
[96] A. P. Thottumkara, T. Kurokawa, J. Du Bois, *Chem. Sci.* **2013**, *4*, 2686–2689.
[97] P. Schaaf, T. Bayer, M. Koley, M. Schnürch, U. T. Bornscheuer, F. Rudroff, M. D. Mihovilovic, *Chem. Commun.* **2018**, *54*, 12978–12981.
[98] X. Wang, B. Wang, X. Yin, W. Yu, Y. Liao, J. Ye, M. Wang, L. Hu, J. Liao, *Angew. Chem. Int. Ed.* **2019**, *58*, 12264–12270.
[99] S. Yang, X. Yu, M. Szostak, *ACS Catal.* **2023**, *13*, 1848–1855.
[100] dik
[101] S. Naskar, K. Mal, R. Maity, I. Das, *Adv. Synth. Catal.* **2021**, *363*, 1160–1184.
[102] M. Wang, Z. Dai, X. Jiang, *Nat. Commun.* **2019**, *10*, 2661.
[103] Y.-F. Cao, L.-J. Li, M. Liu, H. Xu, H.-X. Dai, *J. Org. Chem.* **2020**, *85*, 4475–4481.
[104] Y.-F. Li, Y.-F. Wei, J. Tian, J. Zhang, H.-H. Chang, W.-C. Gao, *Org. Lett.* **2022**, *24*, 5736–5740.
[105] a) E. Peña-Cabrera, A. Aguilar-Aguilar, M. González-Domínguez, E. Lager, R. Zamudio-Vázquez, J. Godoy-Vargas, F. Villanueva-García, *Org. Lett.* **2007**, *9*, 3985–3988; b) L. Betancourt-Mendiola, I. Valois-Escamilla, T. Arbeloa, J. Banuelos, I. Lopez Arbeloa, J. O. Flores-Rizo, R. Hu, E. Lager, C. F. Gomez-Duran, J. L. Belmonte-Vazquez, *J. Org. Chem.* **2015**, *80*, 5771–5782.
[106] M. Pérez-Venegas, M. N. Villanueva-Hernández, E. Peña-Cabrera, E. Juaristi, *Organometallics* **2020**, *39*, 2561–2564.
[107] W. D. Lambert, Y. Fang, S. Mahapatra, Z. Huang, C. W. Am Ende, J. M. Fox, *J. Am. Chem. Soc.* **2019**, *141*, 17068–17074.
[108] H. Yang, L. S. Liebeskind, *Org. Lett.* **2007**, *9*, 2993–2995.
[109] L. Ferrié, J. Fenneteau, B. Figadère, *Org. Lett.* **2018**, *20*, 3192–3196.
[110] G. Kang, S. Han, *J. Am. Chem. Soc.* **2022**, *144*, 8932–8937.
[111] F. Sun, M. Li, C. He, B. Wang, B. Li, X. Sui, Z. Gu, *J. Am. Chem. Soc.* **2016**, *138*, 7456–7459.
[112] M. Liu, Y.-W. Liu, H. Xu, H.-X. Dai, *Tetrahedron Lett.* **2019**, *60*, 151061.
[113] Y. Chen, G. Ma, H. Gong, *Org. Lett.* **2018**, *20*, 4677–4680.
[114] Y. Ma, J. Cammarata, J. Cornella, *J. Am. Chem. Soc.* **2019**, *141*, 1918–1922.
[115] B. Varga, Z. Gonda, B. L. Tóth, A. Kotschy, Z. Novák, *Eur. J. Org. Chem.* **2020**, *2020*, 1466–1471.
[116] A. J. Lennox, G. C. Lloyd-Jones, *Chem. Soc. Rev.* **2014**, *43*, 412–443.
[117] a) Y. Tokunaga, H. Ueno, Y. Shimomura, *Heterocycles* **2002**, *57*, 787–790; b) A. Antoft-Finch, T. Blackburn, V. Snieckus, *J. Am. Chem. Soc.* **2009**, *131*, 17750–17752.
[118] N. Miyaura, *Cross-Coupling Reactions: A Practical Guide* **2002**, 11–59.
[119] N. Zhang, D. J. Hoffman, N. Gutsche, J. Gupta, V. Percec, *J. Org. Chem.* **2012**, *77*, 5956–5964.

[120] L. Xu, B.-J. Li, Z.-H. Wu, X.-Y. Lu, B.-T. Guan, B.-Q. Wang, K.-Q. Zhao, Z.-J. Shi, *Org. Lett.* **2010**, *12*, 884–887.
[121] K. Inada, N. Miyaura, *Tetrahedron Lett.* **2000**, *56*, 8657–8660.
[122] a) V. Polshettiwar, A. Decottignies, C. Len, A. Fihri, *ChemSusChem* **2010**, *3*, 502–522; b) A. Chatterjee, T. R. Ward, *Catal. Lett.* **2016**, *146*, 820–840.
[123] a) J.-C. Galland, M. Savignac, J.-P. Genêt, *Tetrahedron Lett.* **1999**, *40*, 2323–2326; b) F.-S. Han, *Chem. Soc. Rev.* **2013**, *42*, 5270–5298.
[124] S.-L. Zhang, Y. Lu, Y.-H. Li, K.-Y. Wang, J.-H. Chen, Z. Yang, *Org. Lett.* **2017**, *19*, 3986–3989.
[125] Z. Li, S.-L. Zhang, Y. Fu, Q.-X. Guo, L. Liu, *J. Am. Chem. Soc.* **2009**, *131*, 8815–8823.
[126] a) M. Gray, I. P. Andrews, D. F. Hook, J. Kitteringham, M. Voyle, *Tetrahedron Lett.* **2000**, *41*, 6237–6240; b) L. Gooßen, J. Paetzold, *Adv. Synth. Catal.* **2004**, *346*, 1665–1668.
[127] R. Kakino, S. Yasumi, I. Shimizu, A. Yamamoto, *Bull. Chem. Soc. Jpn.* **2002**, *75*, 137–148.
[128] a) S. Mori, E. Nakamura, K. Morokuma, *J. Am. Chem. Soc.* **2000**, *122*, 7294–7307; b) N. Yoshikai, E. Nakamura, *Chem. Rev.* **2012**, *112*, 2339–2372; c) S. Thapa, B. Shrestha, S. K. Gurung, R. Giri, *Org. Biomol. Chem.* **2015**, *13*, 4816–4827.
[129] a) J. Terao, H. Todo, S. A. Begum, H. Kuniyasu, N. Kambe, *Angew. Chem. Int. Ed.* **2007**, *46*, 2086–2089; b) C.-T. Yang, Z.-Q. Zhang, J. Liang, J.-H. Liu, X.-Y. Lu, H.-H. Chen, L. Liu, *J. Am. Chem. Soc.* **2012**, *134*, 11124–11127.
[130] a) G. Posner, C. Whitten, *Tetrahedron Lett.* **1970**, *11*, 4647–4650; b) G. H. Posner, C. E. Whitten, P. McFarland, *J. Am. Chem. Soc.* **1972**, *94*, 5106–5108; c) R. Anderson, C. Henrick, L. Rosenblum, *J. Am. Chem. Soc.* **1974**, *96*, 3654–3655; d) P. Knochel, M. C. P. Yeh, S. C. Berk, J. Talbert, *J. Org. Chem.* **1988**, *53*, 2390–2392; e) R. K. Dieter, R. R. Sharma, W. Ryan, *Tetrahedron Lett.* **1997**, *38*, 783–786; f) A. Metzger, M. A. Schade, G. Manolikakes, P. Knochel, *Chem. Asian J.* **2008**, *3*, 1678–1691; g) Y. Huang, X. He, H. Li, Z. Weng, *Eur. J. Org. Chem.* **2014**, *2014*, 7324–7328; h) X. Ispizua-Rodriguez, S. B. Munoz, V. Krishnamurti, T. Mathew, G. Prakash, *Chem. Eur. J.* **2021**, *27*, 15908–15913; i) D. Kato, T. Murase, J. Talode, H. Nagae, H. Tsurugi, M. Seki, K. Mashima, *Chem. Eur. J.* **2022**, *28*, e202200474.
[131] a) S. Fumie, K. Hiroyuki, T. Yasuji, S. Masao, *Chem. Lett.* **1979**, *8*, 623–626; b) L. J. Gooßen, F. Rudolphi, C. Oppel, N. Rodríguez, *Angew. Chem. Int. Ed.* **2008**, *47*, 3043–3045; c) C. He, S. Guo, L. Huang, A. Lei, *J. Am. Chem. Soc.* **2010**, *132*, 8273–8275; d) L. Gu, C. Jin, H. Zhang, L. Zhang, *J. Org. Chem.* **2014**, *79*, 8453–8456; e) H.-S. Jung, S.-H. Kim, *Synlett* **2015**, *26*, 666–670; f) P. Ghosh, B. Ganguly, E. Perl, S. Das, *Tetrahedron Lett.* **2017**, *58*, 2751–2756; g) A. Sagadevan, V. P. Charpe, A. Ragupathi, K. C. Hwang, *J. Am. Chem. Soc.* **2017**, *139*, 2896–2899; h) M. Bouquin, F. Jaroschik, M. Taillefer, *Tetrahedron Lett.* **2021**, *75*, 153208; i) G. Danoun, A. Tlili, F. Monnier, M. Taillefer, *Angew. Chem. Int. Ed.* **2012**, *51*, 12815–12819; j) Y. Huang, X. He, X. Lin, M. Rong, Z. Weng, *Org. Lett.* **2014**, *16*, 3284–3287; k) L. J. Goossen, C. Linder, N. Rodríguez, P. P. Lange, *Chem. Eur. J.* **2009**, *15*, 9336–9349; l) S. Grosso, M. Mlynczak, G. Evano, O. Riant, *Eur. J. Org. Chem.* **2023**, *26*, e202300938.
[132] L. Nattmann, J. Cornella, *Organometallics* **2020**, *39*, 3295–3300.
[133] G. R. Fulmer, A. J. Miller, N. H. Sherden, H. E. Gottlieb, A. Nudelman, B. M. Stoltz, J. E. Bercaw, K. I. Goldberg, *Organometallics* **2010**, *29*, 2176–2179.
[134] M. N. Burhardt, R. H. Taaning, T. Skrydstrup, *Org. Lett.* **2013**, *15*, 948–951.
[135] M. M. Rahman, G. Li, M. Szostak, *Synthesis* **2020**, *52*, 1060–1066.
[136] P. Singh, R. K. Peddinti, *Tetrahedron Lett.* **2017**, *58*, 1875–1878.

4 Nickel-Catalyzed and Lewis Acid-Assisted Cross-Electrophile Coupling of Benzylic Alcohols and Thioesters

Author contribution:

The initial reaction design and preliminary optimization studies were conducted in the author's Master Thesis.[1] In the presented thesis, the author completed the optimization studies, performed the syntheses of starting materials and the substrate screening, and collected data for the mechanistic inquiry.

The HR-MS analysis and parts of the GC-MS measurements were performed by the MS department of the University of Tübingen. The EPR measurements were acquired with the aid of the NMR department of the University of Tübingen. R. Richter from the working group of I. Fleischer, University of Tübingen, provided the thiocarbamates **393** and **394** as well as nickel(I) complex $[Ni(cod)_2][Al(OC(CF_3)_3)_4]$ and acquired ^{19}F-NMR spectra on the Bruker Avance III HDX 700 instrument.

4.1 Introduction

4.1.1 The Terminology of Cross-Electrophile Coupling

C–C bond formation methods are not limited to classical cross couplings between electrophiles and various types of organometallic compounds, but modern chemical research is also focused on establishing new areas such as cross-nucleophile couplings,[2] dehydrogenative cross couplings[3] and cross-electrophile couplings (XEC). The latter transformation is defined as a catalytic method that selectively couples two different carbon electrophiles under reductive conditions (Scheme 4-1).

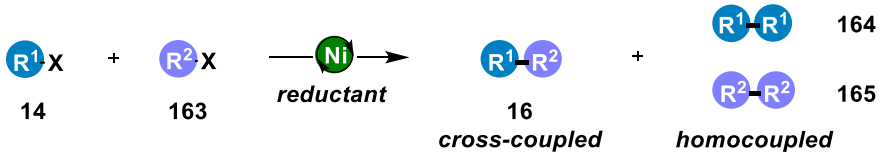

Scheme 4-1: General scheme for nickel-catalyzed cross-electrophile couplings.

In 2010, Weix and his research group pioneered this field and demonstrated that nickel is capable of catalyzing cross-electrophile couplings, which have gained increasing interest in recent decades due to nickel's advantageous properties in terms of reactivity, cost and sustainability, thus bypassing palladium (see section 1.1.3).[4]

Additionally, cross-electrophile couplings compensate for the disadvantages associated with conventional cross couplings.[5] A key attraction of this approach is the avoidance of a nucleophilic reaction partner, such as boronic acids, organozinc- and Grignard reagents. These compounds can cause selectivity problems, reduce functional group tolerance, e.g. for acidic protons or (un)protected amines and alcohols, and they often require point-of-use preparation to avoid decomposition and are commercially limited.

Nevertheless, XEC processes have their own drawbacks, such as the difficulty in differentiating between substrates with similar reactivity and selectively forming the desired cross-coupled instead of homocoupled product, or the necessity to use a reducing agent, usually zinc or manganese powder, leading to heterogenous reaction mixtures and often long reaction times.[5]

In addition to thermal catalysis using reducing agents, reductive couplings have also been achieved by combining nickel catalysis with photo-,[6] electro-,[6a,7] and mechanochemistry.[8] Due to the wide range of possibilities, cross-electrophile coupling has become an increasingly used tool for the formation of C–C bonds in medicinal chemistry[9] and total synthesis[10] in recent years.

An impressive example from 2021 showed the total synthesis of (-)-berkelic acid, a compound with selectivity against the human ovarian cancer cell line OVCAR-3, where the penultimate step was a late-stage nickel-catalyzed reductive coupling compatible with a -COOMe and free -OH substituent (Scheme 4-2).[10e] The final (-)-berkelic acid was

accessed by the selective saponification of the (-)-berkelic acid methyl ester **168** in the presence of $(Bu_3Sn)_2O$ (34% yield over eight steps).[10e]

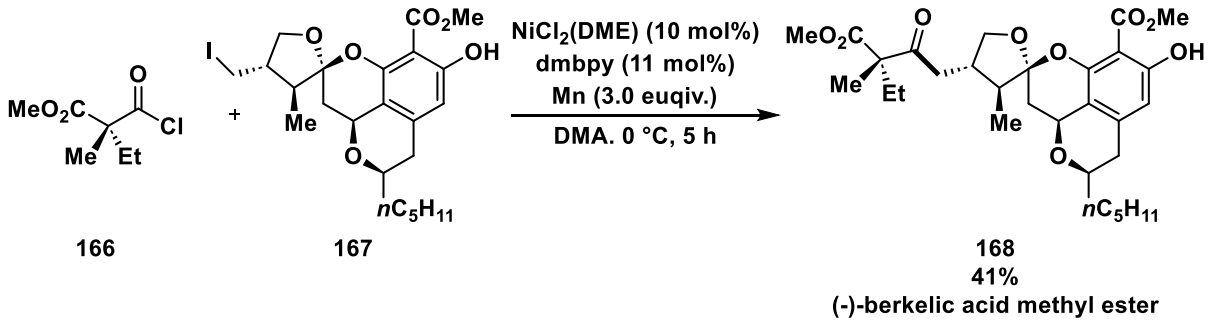

Scheme 4-2: Late-stage nickel-catalyzed reductive coupling in the total synthesis of (-)-berkelic acid.[10e]

4.1.2 Historical Development

Historically, the origins of XEC date back over 100 years to the Wurtz–Fittig coupling of aryl halides with alkyl halides mediated by sodium metal.[11] In this coupling, stoichiometric amount of metal was used as both reducing agent and mediator, but the disadvantages were high temperatures and poor functional group compatibility. Decades later, the nickel-mediated Ullman homocoupling of aryl halides led to milder conditions and the first use of zinc to reduce the metal mediator.[12]

Semmelhack performed early investigations on nickel-mediated reductive couplings in the 1970 and 1980s.[13] Stoichiometric nickel(0) complexes were employed in the homocoupling of reactive aryl halides, exhibiting a functional group tolerance not seen with traditional couplings using organometallic coupling partners (Scheme 4-3A).[13c] Based on these reports, Kumada developed a homocoupling of aryl halides catalyzed by nickel in presence of zinc powder (Scheme 4-3B).[14] Even in this early work, an additive effect was observed, as a significant rate enhancement and higher yield were achieved at room temperature, employing an equimolar amount of potassium iodide. In 1981, Mukaiyama *et al.* introduced the cross-electrophile coupling of a *S*-2-pyridyl thioester with an alkyl iodide using $NiCl_2$ and zinc dust, yielding the corresponding ketone in 46% yield (Scheme 4-3C).[15]

Périchon made his mark on the field of electrochemically enabled cross-electrophile couplings, which began in 1986 with first observations of cross-coupled products after the reaction of aryl bromides under electro-reductive conditions.[16] However, a statistical distribution of cross- and homo-coupled products was observed (Scheme 4-3D). The selectivity problem was tackled by coupling an *ortho*-substituted aryl halide with an aryl halide counterpart with different steric and electronic properties.[17] Shortly after the initial report, the scope of suitable electrophiles was extended to α-bromoesters, which gave high yields of α-arylated products when reacted with aryl halides.[18] In a nickel-catalyzed electrochemical

synthesis of ketones from acid chlorides and alkyl as well as aryl halides, the selectivity of cross-coupled *vs.* homo-coupled products was controlled by different reaction rates of electrophiles in the oxidative addition step to nickel(0).[19]

These early findings laid the foundation for the field of cross-electrophile couplings. However, traditional cross couplings dominated the literature in the 1990s and 2000s, and reductive couplings did not experience a renaissance until the early 2010s. The seminal report of Weix showed the coupling of aryl halides with alkyl halides under a dual-ligand nickel catalyst system and drew new attention to the field of cross-electrophile couplings (Scheme 4-3E).[4] From then on, XEC gradually found a revival that continues to this day.

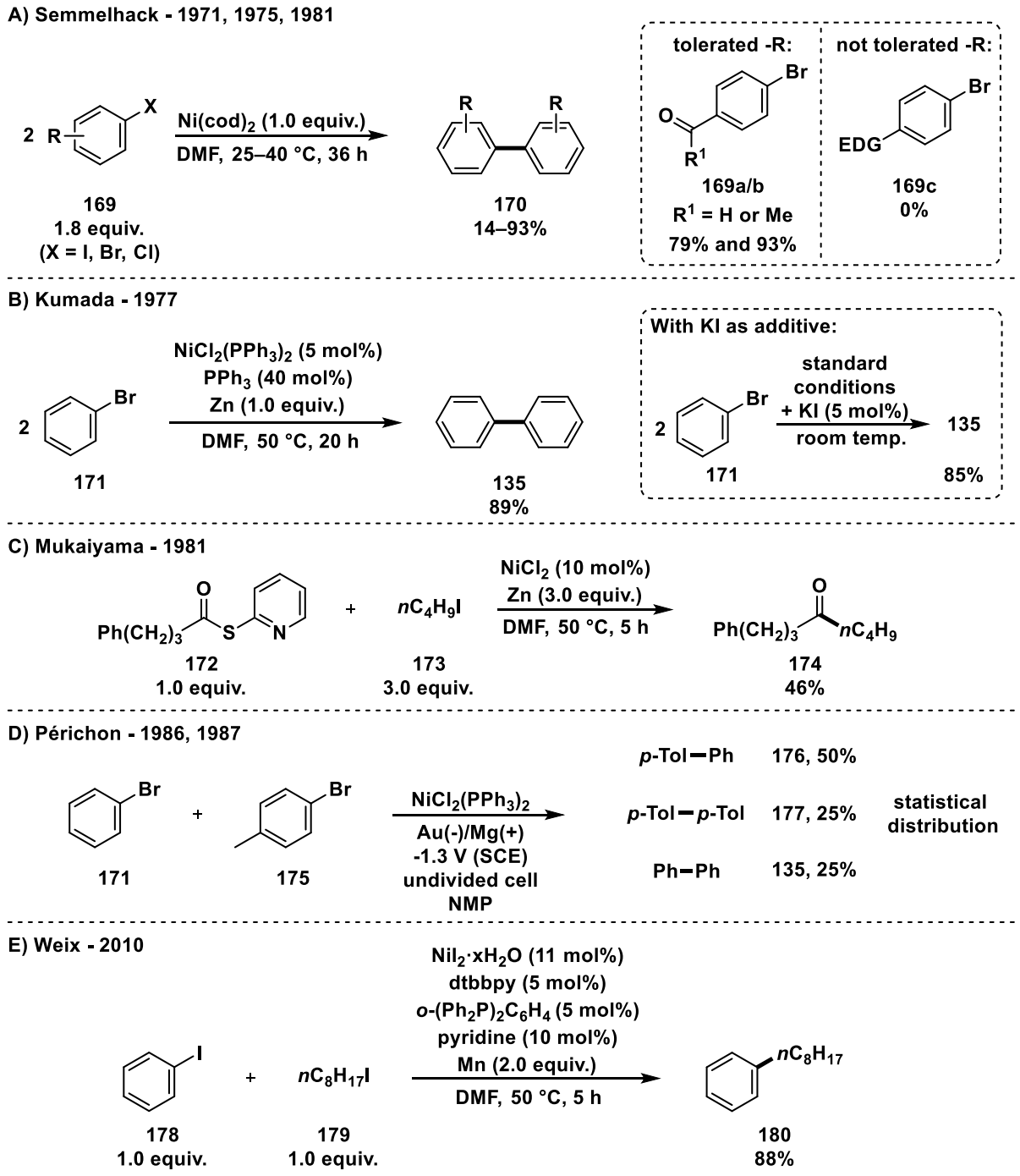

Scheme 4-3: Milestones in the establishment of cross-electrophile couplings.[4,13-16]

4.1.3 Mechanistic Considerations

Although investigations are rather difficult and less studied with nickel compared to palladium, several mechanistic frameworks for nickel-catalyzed cross-electrophile couplings have been established that explain the observed reactivity of different substrates during reaction development. Two general categories encompass possible mechanisms in nickel-catalyzed XEC: A) sequential activation, which includes a double oxidative addition (or sequential reduction) and B) parallel activation, which implies radical-chain mechanisms. In practice, extensive mechanistic studies are required to distinguish between the two models, and further nuances within each mechanism must be considered, as in both cases several oxidation states are possible for nickel, for instance nickel(I/II/III) or nickel(0/II/III) catalytic cycles.

In scenarios with a double oxidative addition (Scheme 4-4A), a low-valent nickel center, for instance nickel(0), is generated, which can activate the more reactive electrophile R^1–X *via* oxidative addition. Subsequently, the generated X–Ni^{II}–R^1 species **183** is reduced to Ni^{I}–R^1 **184** by the reductant, enabling a second oxidative addition of R^2–X. A formal nickel(III) species **186** is formed after an in-cage radical/nickel rebound process, which can undergo reductive elimination to furnish the cross-coupled product. The reduction of the generated nickel(I) complex closes the catalytic cycle.[5j,20]

The selectivity-determining steps of this catalytic process are dependent on the activation sequence of the electrophiles (Scheme 4-4B). A faster initial oxidative addition of R^1–X and the faster subsequent oxidative addition of R^2–X outcompetes pathways leading to homocoupled products. This preference in reaction rates is attributed to differences of electronic properties originating from functional groups or substituents and steric matching between substrates and catalyst. Additionally, the involved oxidation states of nickel effect selectivity.[5j,21]

A double oxidative addition pathway was mechanistically investigated in the nickel-catalyzed 1,2-dicarbofunctionalization of alkyl bromides incorporating a pendant terminal olefin unit with aryl bromides.[20a] It was shown that zinc is only sufficient to reduce the nickel(II) precatalyst to a nickel(I) species, which selectively activates the aryl bromide by oxidative addition, thus excluding the involvement of nickel(0). Alkyl bromides undergo single-electron activation to afford radicals.

These remarkable investigations broadened the view of possible nickel oxidation states in cross-electrophile couplings and paved the way for further studies on nickel(I/II/III) catalytic cycles, which complemented the nickel(0/II/III) catalytic cycles frequently proposed in this field until then.

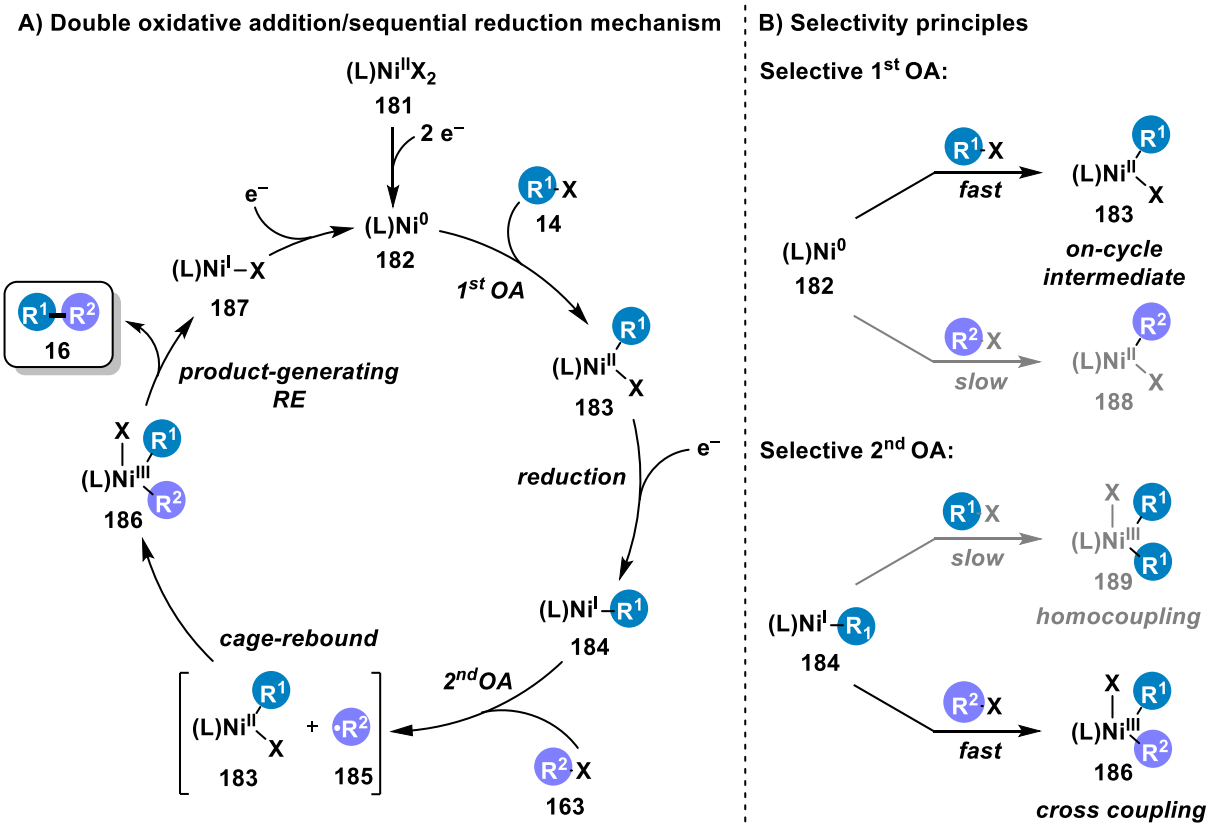

Scheme 4-4: A) Example of a nickel(0/I/II/III) double oxidative addition sequence and B) selectivity-determining principles.[5j] OA = oxidative addition, RE = reductive elimination.

In a radical-chain mechanism, parallel activation of both substrates occurs (Scheme 4-5A). Initially, the precatalyst is activated by reduction with the reducing agent. After the subsequent two-electron oxidative addition to nickel(0), a nickel(II) complex **183** is formed. Meanwhile, a radical species **185** is generated from the other electrophile by reduction/halide abstraction by nickel(I) **187**, followed by its diffusion into the bulk solution. The nickel(II) complex **183** then intercepts the radical species of the other electrophile by one-electron oxidative addition, forging a second Ni–C bond and generating a nickel(III) intermediate **186**. The cross-coupled product is released after reductive elimination from nickel(III) **186**, simultaneously forming the nickel(I) complex **187** required for the radical generation. The catalytic cycle is closed after the reduction of the generated nickel(II) intermediate to nickel(0).[21]

For the initiation of the catalytic cycle, different possibilities have been proposed in the literature (Scheme 4-5B).[21,22] Besides the reductant, which can initiate radical formation, self-initiation at low radical concentration could also originate from the nickel(II) complex **183** by halogen atom abstraction of the R^2–X electrophile. The resulting nickel(III) complex **190** could extrude R^1–X to form Ni^I–X **187** as a proposed on-cycle intermediate.[21] Another possibility could be the direct disproportionation of two molecules X–Ni^{II}–R^1 to nickel(III) **189** and nickel(I) **187**, thereby initiating the radical formation.[22,23]

In this postulate of mechanism, selectivity can be explained by the similar reaction rates that correspond to the activation of both electrophiles, while the homocoupling proceeds relatively slowly (Scheme 4-5C).[5j] The lifetime of the radical species involved, which either reacts *via* a radical rebound process in the solvent cage (double oxidative addition) or is long-lived and escapes the cage (radical-chain mechanism), is key to distinguish between the two mechanistic models.[5k,24] The framework of radical-chain mechanism therefore includes the terminologies of persistent radical effect[25] and persistent metal effect in multimetallic reactions and is dependent on bond dissociation energies and radical stability (Scheme 4-5C).[5j,26] Furthermore, both nickel(0/II/III) and nickel(I/II/III) radical-chain mechanisms are proposed in the literature.[27]

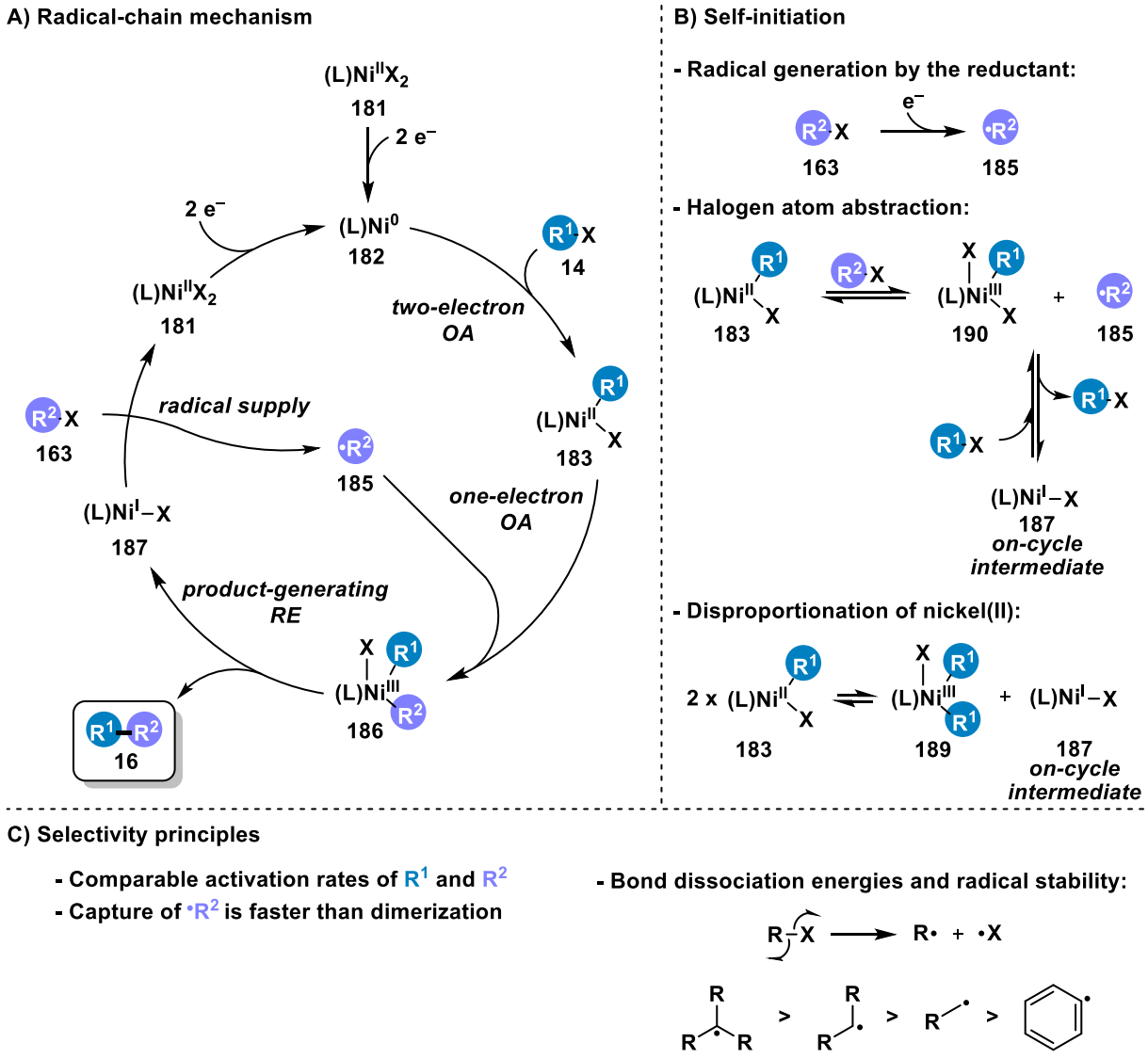

Scheme 4-5: A) Example of a nickel(0/II/III) radical-chain mechanism, B) possibilities of self-initiation[21,22] and C) selectivity-determining principles.[21]

In such mechanisms, the crucial steps are the radical supply from interaction of nickel(I) with the electrophile, radical capture by nickel(II) and reductive elimination from nickel(III).[28]

Several pathways have been postulated for the nickel(I)-mediated radical formation from the electrophile, either by single-electron transfer (SET) and halide dissociation, by oxidative addition and the subsequent radical ejection, or by a concerted halogen atom dissociation pathway. An electroanalytical study by Diao supports the latter pathway as the most likely one (Scheme 4-6A).[29]

With regard to the radical capture by nickel(II), it has been shown that the rate-determining steps (RDS) can vary, depending on the aryl or alkyl substituents of the nickel(II) oxidative addition product (Scheme 4-6B).[30] For Ar–Ni complexes, radical trapping of nickel(II) is the rate-determining step, leading to the accumulation of the radical species, while the subsequent reductive elimination occurs rapidly. For Alk–Ni complexes, the radical capture is fast, compared to the subsequent reductive elimination, which is the rate-determining step. In both cases of the study, a benzyl radical species was generated.[30]

The subsequent reductive elimination step can be promoted by kinetic driving forces caused by ligand association or dissociation and by thermodynamic effects. For instance, the incorporation of electron-deficient or bulky ligands or oxidation of the metal center can increase the driving force by destabilization of the starting material and stabilization of the resulting low-valent metal species.[28]

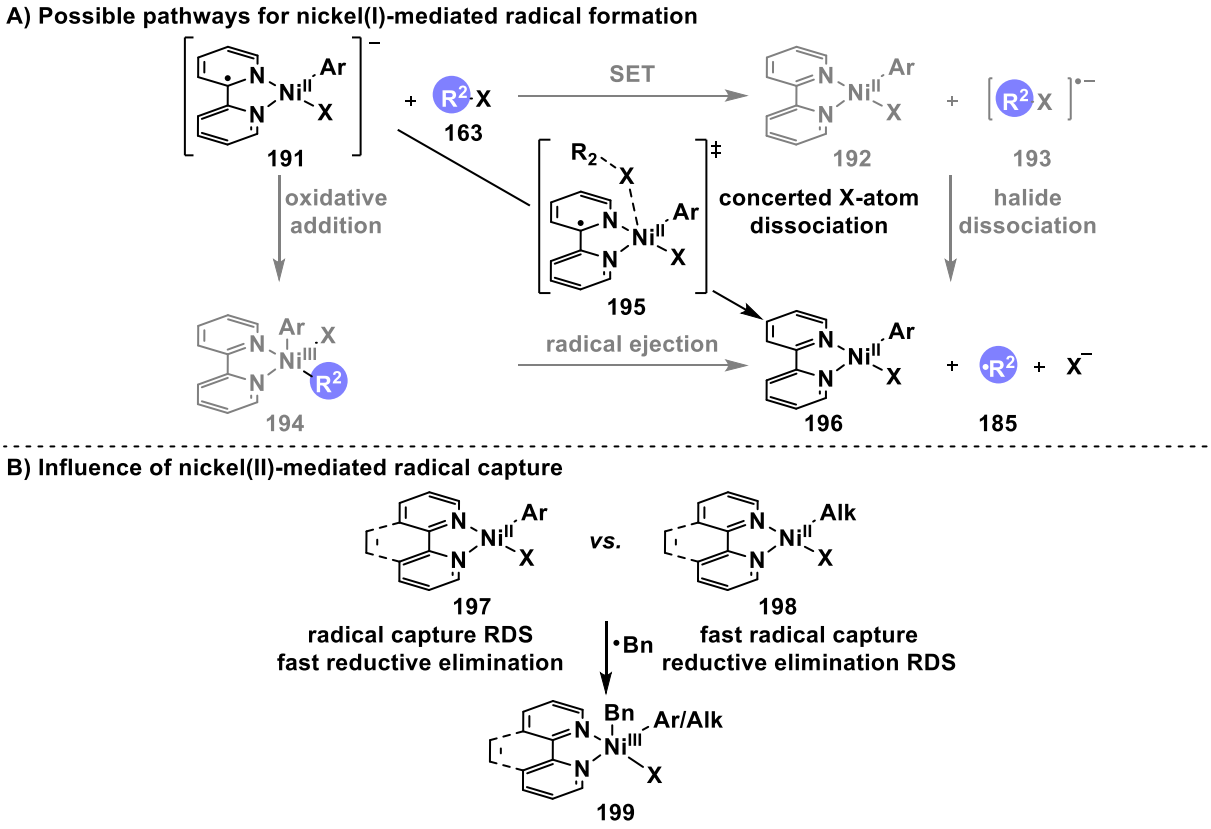

Scheme 4-6: A) Possible pathways for nickel(I)-mediated radical formation,[28] and B) influence of nickel(II)-mediated radical capture.[28]

4.1.4 Selectivity Modulation

A wide array of other strategies have been employed to achieve selectivity in nickel-catalyzed cross-electrophile couplings after Weix' initial report in 2014.[5b]

One example is the use of a large excess of the less reactive coupling partner (Scheme 4-7A). Although this strategy is often successful in generating high yields of cross-coupled product, it is not effective with regards to cost and waste, and usually reinforces the formation of undesired homocoupled products, which can make purification of the product more difficult.

Another, more sustainable strategy that is directly applicable in the laboratory, is the fine-tuning of substrates. As aforementioned, the control of electronic and steric properties affects the rates of oxidative addition and reductive elimination (Scheme 4-7B), although this can result in restricted substrate scopes. Another approach is the controlled *in situ* generation of the active electrophile from a less reactive precursor. Moreover, additives such as salts or Lewis acids can influence the activation of substrates, potentially leading to a higher yield of the cross-coupled product. However, the role of salt additives in cross-electrophile couplings is less understood and they are often attributed to the activation of the reductant surface.[31]

Furthermore, the nickel catalyst and the corresponding ligand can influence the substrate activation and thereby the selectivity (Scheme 4-7C). The ligands, commonly redox-active 2,2'-bipyridine (bpy) and 1,10-phenanthroline (Phen) motifs, play a crucial role, and their redox activity depends on the geometry and coordination number of the low-valent organonickel radical complexes. This may favor radical pathways or lead to notable changes in the mechanism, and an extensive ligand design could be required to control a reaction.[32] A more convenient approach than modulating the ligand is to influence the activation rates of the electrophile by using a co-catalyst in addition to the nickel catalyst. For instance, dual nickel catalyst systems,[4,33] nickel/palladium,[31a,34] nickel/cobalt,[35] and nickel/titanium co-catalyzed systems have been developed. An overview of dual nickel/titanium activation is given in section 4.1.5.2.10.3.3.

Another important component, which can be modified, are the reducing agents as electron donors (Scheme 4-7D). Heterogenous reductants, such as manganese, zinc, and magnesium, are generally employed in cross-electrophile couplings due to their well-defined reduction potentials, low cost, and air stability. Contrary, the generation of heterogenous mixtures can be detrimental, due to irreproducible kinetics that arise from mass-transfer limitations. Furthermore, polar amide-based solvents and activation of the reductant surface are often necessary. Additionally, it is not possible to modify the reducing agent and thus adapt to the redox potential of a catalyst or substrate, and the reaction rates of the redox processes are difficult to control due to the large number of parameters that affect the electron transfer from

a heterogenous reductant to a species in solution.[36] To overcome these disadvantages, other electron sources, such as electrochemistry, photocatalysis and homogeneous reductants are employed. In recent years, organic electron donors such as tetraaminoethylenes and 4-dimethylaminopyridine (DMAP) derivatives found increased attention after Weix' initial report, in which tetrakis(dimethylamino)ethylene (TDAE) was used as reducing agent.[4] Tetraaminoethylenes exhibit a reduction potential in the range of E^0_{red} = -0.5– -0.9 V *vs.* SCE, illustrating the advantageous fine-tuning by modifying their framework and thus the reduction potential.[36,37] Additionally, the range of organic reductants has been expanded in recent years by employing diboron reagents.[38] Gong's seminal report applied B_2pin_2 (pin = pinacolato) and LiOMe as the reductive system in nickel-catalyzed cross-electrophile couplings.[39] Organoboron reductants require bases that facilitate the transmetalation of the boron reagents with the transition metal and possibly stabilize the reactive low-valent metal species.[38]

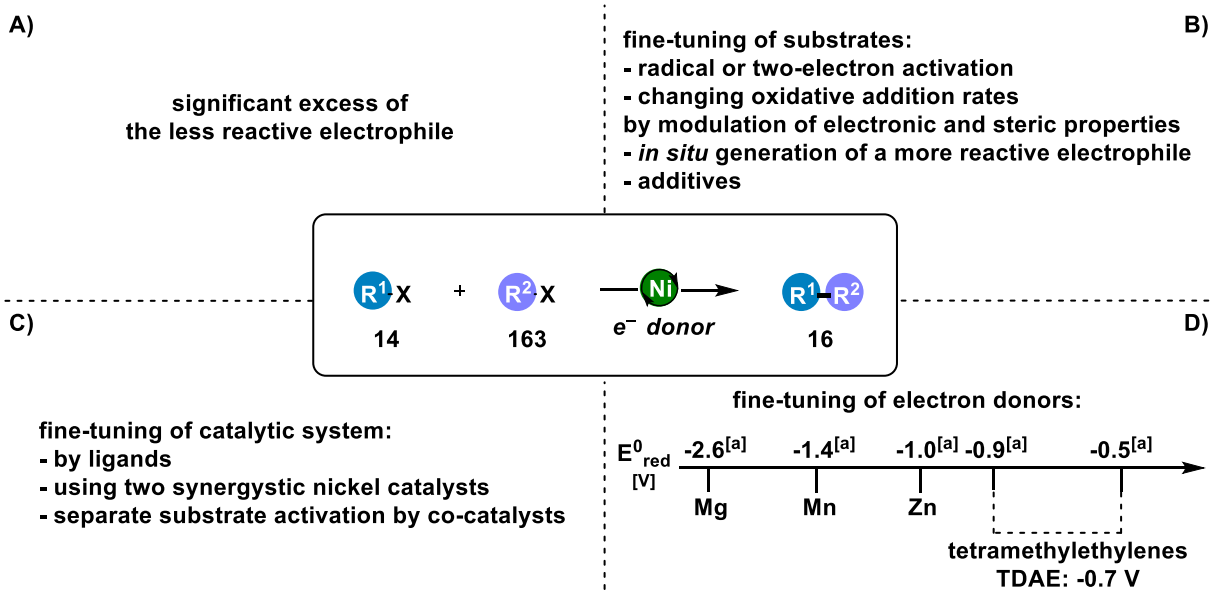

Scheme 4-7: Strategies for cross-selective XEC reactions. Potentials are adapted from cited references and should serve as a rough comparison.[5a,36] [a]: *vs.* SCE, reduction potentials originally reported *vs.* Fc/Fc^+ were converted to V *vs.* SCE using $E^0_{red}(Fc/Fc^+)$ = +0.400 V *vs.* SCE.[40]

4.1.5 Choice of Substrates

During the initial stages of cross-electrophile couplings, the focus was mainly on the reactions of organic halides and pseudo halides. Recent studies have widened the range of electrophiles, including fragments that can be easily derived from naturally occurring scaffolds, such as alcohols, ketones, amines, and acids. Thereby, the scope of suitable electrophiles was considerably broadened and rendered cross-electrophile couplings more practical, versatile and sustainable. The next section highlights ketone syntheses by nickel-catalyzed cross-electrophile couplings using various acylation agents such as acyl chlorides, carboxylic acids, anhydrides, (thio)esters, and other common acyl and carbonyl sources. This is followed by an overview of recent results concerning readily available, low-cost, and stable, but unreactive *O*-electrophiles, such as sulfonates, oxalates, formates, activated esters, acetates, ethers, acetals and free alcohols.

4.1.5.1 Acylation Agents in XEC

Carboxylic acids and their derivatives are characterized by the difference in reactivities (see section 3.1.2) and serve as acylating agents in cross-electrophile couplings. An overview of metal-catalyzed reductive couplings of organic halides with carbonyl-type compounds was provided by Martin *et al.* and it covers publications up to 2014 and includes reductive carbonylation and carboxylation reactions as well as palladium and cobalt catalysis.[5c] Additionally, several nickel/photoredox dual catalyzed acyl cross couplings were reported.[6e,41] In the next sections, recent progress in acylation chemistry using thermal nickel catalysis is presented, sorted by different acylating agent and starting with acyl chlorides.

4.1.5.1.1 Acyl Chlorides

The high reactivity of acid chlorides makes them ideal coupling partners in reductive couplings, compared to other less reactive carbonyl compounds, which often require activation.

Since the historical development of acid chlorides as acyl sources in XEC began with electrochemical protocols, these are described briefly. The first report using electrochemical techniques dates back to the late 1970s and it showed the halogen abstraction from acyl halides and alkyl or aryl halides by an anodic cadmium metal, yielding unsymmetrical ketones.[42] One of the key work on nickel-catalyzed cross-electrophile couplings was provided by Périchon, who showed the electrochemical synthesis of ketones from acid chlorides and alkyl as well as aryl halides.[19,43]

The early beginnings of acyl species in thermal catalysis began in 1975 by an initial attempt of Favero, who detected diethyl and diphenyl ketones in very poor yields after the decomposition of acyl nickel complexes.[44] Rieke *et al.* used NiX_2 (X = Cl, Br, I) and lithium

metal for the *in situ* generation of metallic nickel over naphthalene, which was reacted with acid chlorides and various halides to provide unsymmetrical ketones in high yields.[45] The mechanism was proposed to follow a nickel(0/II) catalytic cycle with oxidative addition of both reactants by the nickel metal, metathesis, and reductive elimination.

Thermally induced, nickel-catalyzed cross-electrophile couplings were fully established in 2012, by both Weix and Gong. In Weix' work, unsymmetrical dialkyl ketones were generated after the coupling of carboxylic acid chlorides with alkyl iodides or benzylic chlorides using 5 mol% of $NiCl_2$(DME) and dtbbpy as ligand (Scheme 4-8A).[46] Due to competing dimerization, benzylic chlorides provided lower yields than alkyl iodides. The system was also suitable for 2-pyridyl thioesters as substrates, showed a remarkable functional group tolerance and even sterically hindered ketones could be obtained in high yields. The oxidative addition of the alkyl iodide and a subsequent disproportionation of the nickel(II) complex **183** were proposed as key mechanistic steps, enabling the formation of the ketone and closure of the catalytic cycle (Scheme 4-8A).

Gong and co-workers used a $Ni(acac)_2$/bathophenanthroline/Zn catalyst system for the XEC of aryl acyl chlorides with alkyl halides and found that the addition of $MgCl_2$ had a beneficial effect on the ketone yields. Additionally, an upscaling experiment was possible under these conditions.[47] Mechanistically, they suggested a kinetically favored oxidative addition of PhCOCl over the alkyl iodide to form PhC(O)–Ni^{II}–Cl, which was reduced to PhC(O)–Ni^{I}, followed by a second oxidative addition of the alkyl iodide, generating a formal nickel(III) complex, from which the product is released after reductive elimination.[48]

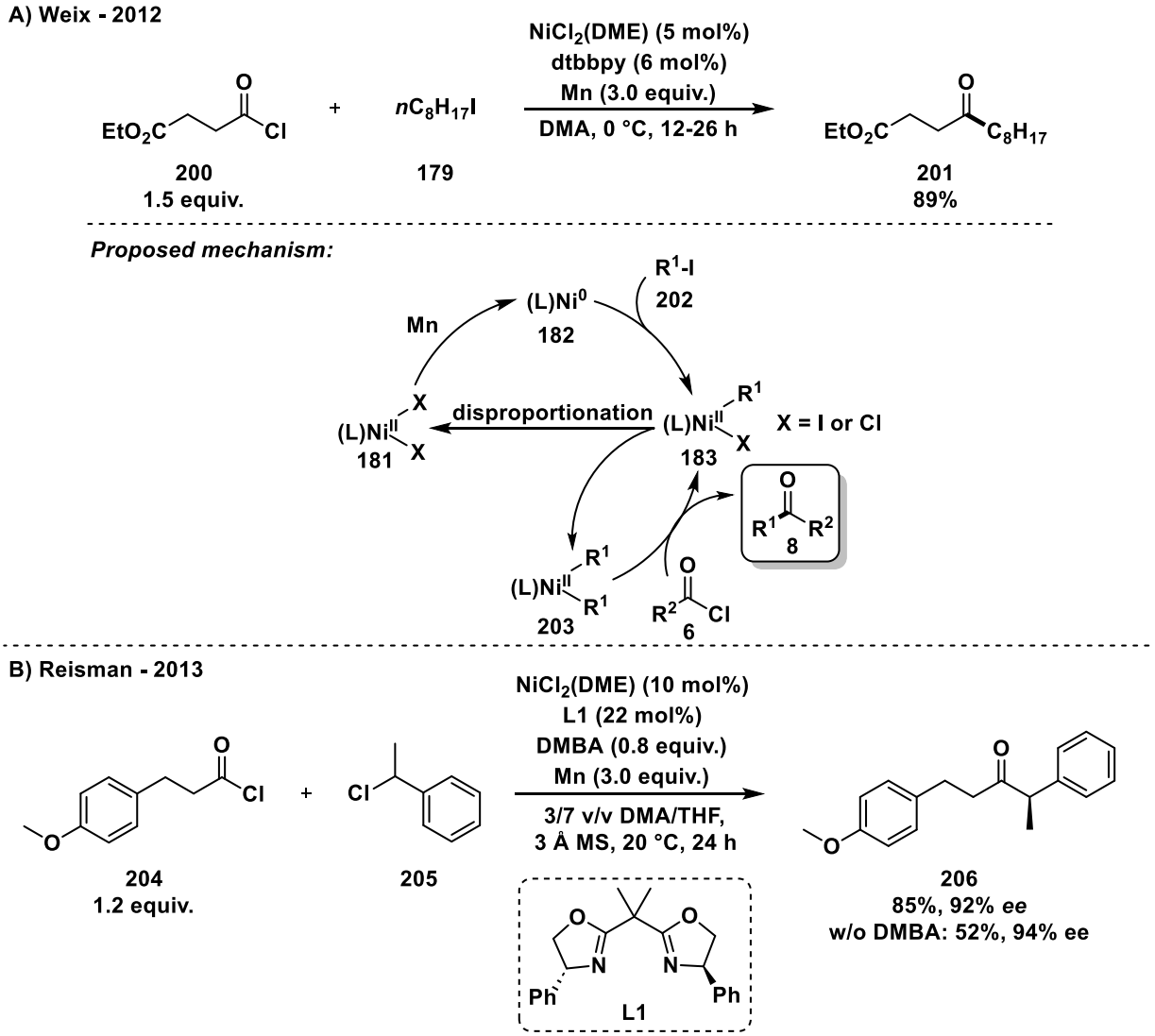

Scheme 4-8: A) Weix' pioneer work, which introduced acyl chlorides as substrates in XEC, and B) first enantioselective coupling of acyl chlorides with secondary alkyl halides.[46,49] MS = molecular sieves.

The first enantioselective nickel-catalyzed reductive cross coupling between acid chlorides and secondary alkyl halides was published by Reisman in 2013 (Scheme 4-8B).[49] Interestingly, the addition of 2,6-dimethylbenzoic acid (DMBA) resulted in a significant improvement in yield. Moreover, the desired ketone was formed in 44% and 92% *ee* after the reaction of the alkyl halide with the mixed anhydride, which could be generated *in situ* from the reaction of acyl chloride and DMBA. Therefore, it could not be completely ruled out that an anhydride was the active intermediate in the reaction, although the formation of an anhydride was not observed under standard conditions. A double oxidative addition pathway was suggested as the mechanism.[49]

Another enantioselective coupling was recently published, showing an asymmetric acyloin synthesis starting from acid chlorides and α-bromobenzoates (Scheme 4-9).[50] For these substrates, $NiCl_2$(DME) was used in combination with a chiral bis(oxazoline) ligand for the enantioselective control. The desired products were also obtained from *in situ* generated

α-bromobenzoates using the corresponding aldehydes, 20 mol% $ZnCl_2$ and benzyl bromide in DCM (Scheme 4-9).[50] The method showed a wide substrate scope, including electron-poor and -rich, *ortho*-methylated, naphthyl, thienyl and alkyl acid chlorides. Furthermore, various aliphatic aldehydes with different chain sizes, sterically demanded, branched aldehydes and different substituents such as (thio)esters, ethers, and heterocyclic rings were tolerated. The approach showed a preference for aroyl chlorides bearing potentially reactive functional groups such as chloride and bromide, generating the desired chiral α-oxygenated ketones with complete chemoselectivity. Mechanistically, a radical-chain mechanism was proposed with a ketyl radical formed from α-bromobenzoates.[50]

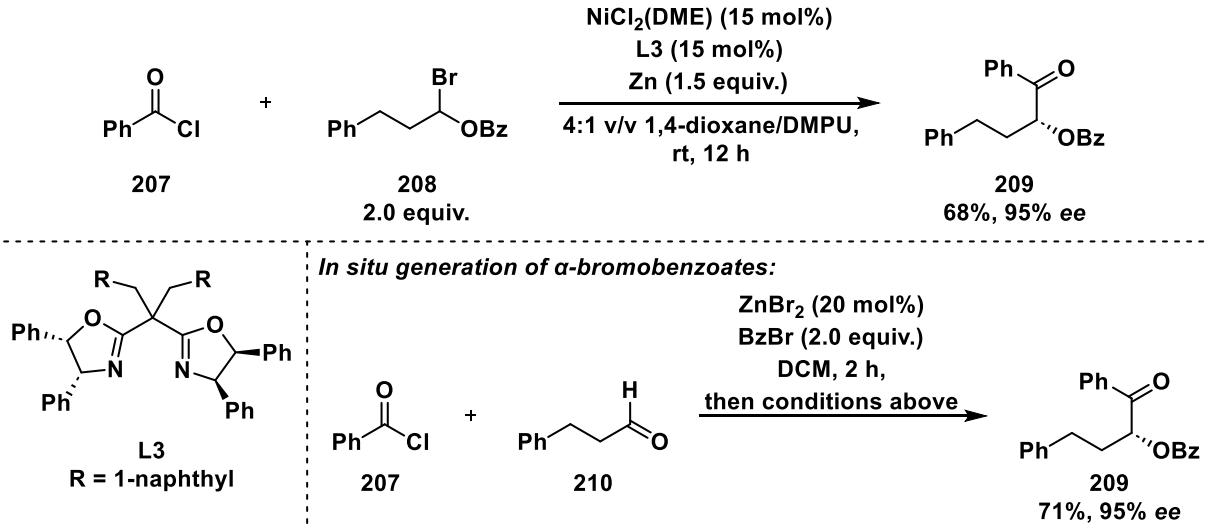

Scheme 4-9: An asymmetric acyloin synthesis from acid chlorides and α-bromobenzoates.[50]

Zhang and co-workers demonstrated the nickel-catalyzed coupling of acyl chlorides with racemic α-trifluoromethyl bromides, yielding chiral α-trifluoromethyl ketones. As ligand, a sterically hindered bisoxazoline ligand was found to be the most effective.[51]

In 2014, the Weix group directly synthesized PhC(O)–Ni^{II}–Cl complexes from acyl chlorides, and investigated the selectivity in the reaction with alkyl halides.[52] In the same year, methyl tosylates were employed for the methylation of alkyl halides and acid chlorides under nickel catalysis, which is one of the first examples with B_2pin_2 and LiOMe as reducing system instead of heterogenous manganese or zinc.[53] A double oxidative addition was proposed as the mechanism. Additionally, it was suggested that methyl tosylates are slowly converted to Me–X by a sulfonate halogen exchange. Moreover, Weix showed the nickel-catalyzed generation of ethyl 4-oxododecanoate from an alkyl halide and an acid chloride as well as a single example for the nickel-catalyzed ketone synthesis from an acid chloride and a redox-active NHP (*N*-hydroxyphthalimide) ester.[54,55]

Enones were formed from the nickel-catalyzed reaction of acid fluorides with vinyl triflates.[56] Besides acid fluorides, a 2-pyridyl thioester, a symmetric anhydride and Boc-protected benzoic acid proved to be convenient acyl sources, although the latter gave

only a moderate yield of the desired product. The method found application in the late-stage modification of several biologically active carboxylic acid compounds.

It has been demonstrated that pyridinium salts are also suitable coupling partners with acid chlorides. A mechanistic study of the nickel-mediated cross-electrophile coupling between acid chlorides and Katritzky salts revealed a nickel(I/II/III) radical-chain mechanism (Scheme 4-10A). $NiBr_2$(Phen) precatalyst is reduced by manganese to nickel(I) and not to the commonly proposed nickel(0) species, which could only be generated after a longer reduction time. In addition, a synergistic reduction of pyridinium salts by nickel(I) and manganese was disclosed.[27] A recent example generates ketones from the nickel-catalyzed coupling of carboxylic acid chlorides and alkyl pyridinium salts *via* C–N bond cleavage.[57]

A variety of cyanoketones, e.g. **215**, under cyanide-free conditions were synthesized by the combination of cross-electrophile coupling and C–C bond cleavage (Scheme 4-10B).[58] Cycloketone oxime esters such as **214** underwent a ring-opening and then reacted with aromatic acid chlorides, whereby the method required a relatively atypically low temperature of -55 °C. Furthermore, oxime esters incorporating a pendant terminal olefin unit were successfully implemented with acid chlorides or anhydrides to generate diverse pyrrolines in moderate to excellent yields.[59] A $NiCl_2$(DME)/biquinoline catalyst system and zinc as reducing agent proved to be most suitable for the reaction.

A three-component reaction gave access to diversified β-fluoroalkyl ketones by functionalizing alkenes with acid chlorides and alkyl halides under a $NiCl_2$/dtbbpy catalyst system.[60] It was proposed that the mechanism follows a radical relay strategy.

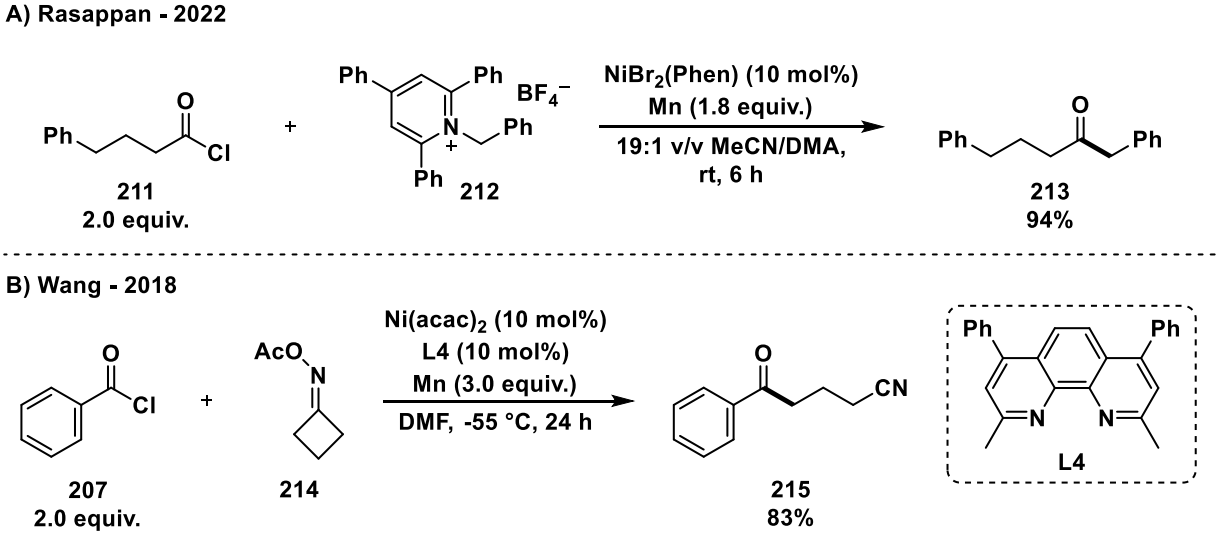

Scheme 4-10: Examples for *N*-containing substrates in the coupling with acid chlorides.[27,58]

In conclusion, acyl halides were frequently used as substrates for nickel-catalyzed acylation by cross-electrophile couplings. However, due to the high instability of acyl halides to moisture, anhydrous reaction conditions and an excess are often necessary, as shown in the examples

of Scheme 4-10. Another drawback of acyl halides is their synthesis with aggressive reagents, such as $SOCl_2$ and PCl_3. Therefore, the spectrum of acyl sources was extended to include carboxylic acids and their anhydrides.

4.1.5.1.2 Carboxylic Acids and Their Anhydrides

Carboxylic acids are another promising class of substrates, being commercially available, inexpensive and naturally abundant.[61] They are less reactive than carboxylic acid chlorides or anhydrides, thus they are usually activated *in situ* by forming the corresponding anhydrides.

The first reports on XEC of coupling anhydrides and halides were again based on electrochemical methods.[62] Later, Gong presented the direct coupling of alkyl halides mainly with aryl acid anhydrides and the *in situ* activation of aryl acids in the presence of Boc_2O with subsequent cross-electrophile coupling. The highest yield of alkyl aryl ketones was achieved with 10 mol% $Ni(cod)_2$, bathophenanthroline (BPhen), $MgCl_2$ as additive and zinc as reducing agent.[63]

The group further improved the system,[64] amongst others enabling the coupling of *in situ* generated anhydrides and inactivated tertiary alkyl and glycosyl halides under a $Ni(acac)_2$/bpy catalyst system, $MgCl_2$ as additive and zinc as reductant (Scheme 4-11A).[64a] Several mechanistic experiments indicated that a radical-chain mechanism is favored. Experiments with $MgCl_2$ showed that the additive is possibly responsible for anion exchange on nickel(II).[64a]

Another remarkable contribution was reported by the Baran group, who introduced the nickel-catalyzed decarboxylative coupling of NHP esters and carboxylic acids, which are activated *in situ* by $(PhCO)_2O$ (Scheme 4-11B).[22] A wide scope of suitable substrates (50 examples) was presented, including gram-scale synthesis, drugs, and natural products. Mechanistically, a radical-chain mechanism was proposed, which starts with the oxidative addition of the *in situ* formed mixed anhydride to nickel(0), forming nickel(II) complex **222** (Scheme 4-11B). Then, ligand exchange occurs, replacing the carboxylate for the chloride. Complex **223** captures a radical derived from NHP ester, forming nickel(III) complex **224**. The ketone **8** and nickel(I) complex **225** responsible for radical generation are delivered after reductive elimination. It was proposed that the reaction can be initiated from nickel(II) complexes **222** or **223** by disproportionation.[22]

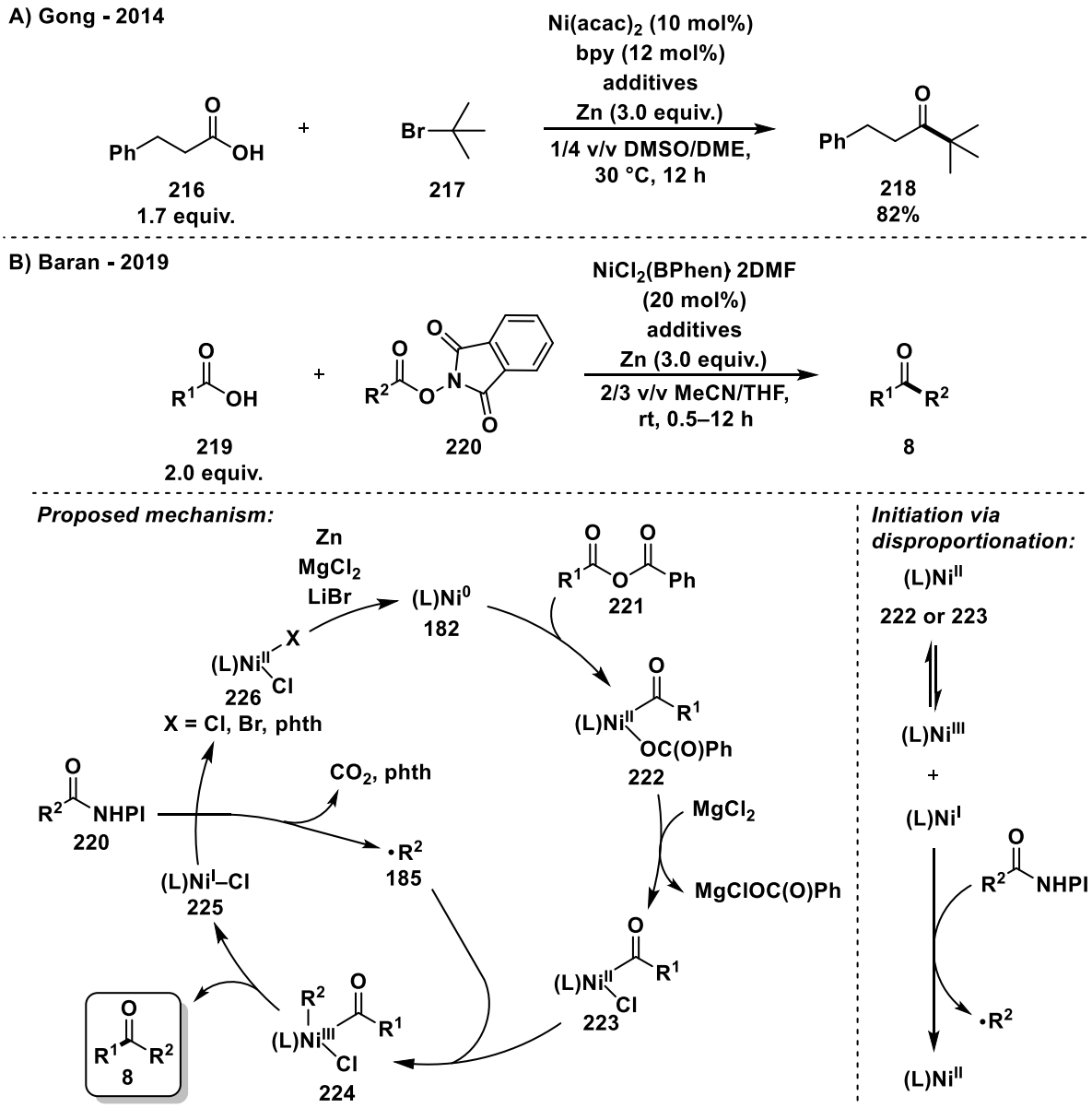

Scheme 4-11: Nickel-catalyzed reductive couplings of carboxylic acids with A) tertiary halides or B) NHP esters.[22,64a] Additives: A) *i*Pr$_2$NEt (0.9 equiv.), $MgCl_2$ (1.0 equiv.), Boc_2O (2.0 equiv.),[64a] B) LiBr(1.0 equiv.), $MgCl_2$ (1.5 equiv.), $(PhCO)_2O$ (2.2 equiv.).[22] phth = phthalimide.

A migratory reductive acylation between alkyl halides or alkenes and alkyl carboxylic acids was enabled with 10 mol% $NiBr_2 \cdot 3H_2O$, 6,6'-dimethyl-bpy as ligand, Boc_2O to activate the carboxylic acid, zinc as reducing agent and $MgCl_2$ as well as NaI as additives.[65] The benzylic sp^3 C–H bond of the alkyl halide or alkene was directly acylated with high yield as a single regioisomer.

Carboxylic acids were also coupled with pyridinium salts after the *in situ* activation by Boc_2O to form the corresponding anhydride,[57] and an electrochemical approach with this activation method is also known.[66]

A nickel-catalyzed desymmetrizing reaction between cyclic *meso*-anhydrides with aryl triflates afforded γ-keto acids.[67] For that, a high catalyst and ligand loading of

20 mol% $Ni(cod)_2$ and 30 mol% bpy as well as TMSCl and ZnI_2 as additives were required. Interestingly, when changing the substrates from aryl triflates to alkyl bromides, the γ-keto acid was not observed, but the carboxylic acid was generated.[68] Mechanistic experiments revealed the participation of a nickel homoenolate, which is generated after oxidative addition of the anhydride by the loss of carbon monoxide. The mechanism continues with a single-electron transfer process and the acid coupling product is delivered from a zinc carboxylate.[68]

Another activation of carboxylic acids was shown by Weix *et al.*, who used fluoro-*N*,*N*,*N'*,*N'*-bis(tetramethylene)formamidinium hexafluorophosphate **231** (TFFH) and 1,8-bis(dimethylamino)naphthylene **232** as base for the *in situ* generation of acyl fluorides from the respective acids (Scheme 4-12).[69] This enabled the coupling with pyridinium salts using 10 mol% $NiCl_2$(DME). Depending on the ligand, primary and secondary pyridinium salts and primary, secondary, and tertiary carboxylic acids were coupled and a single example for an aryl carboxylic acid was also given.

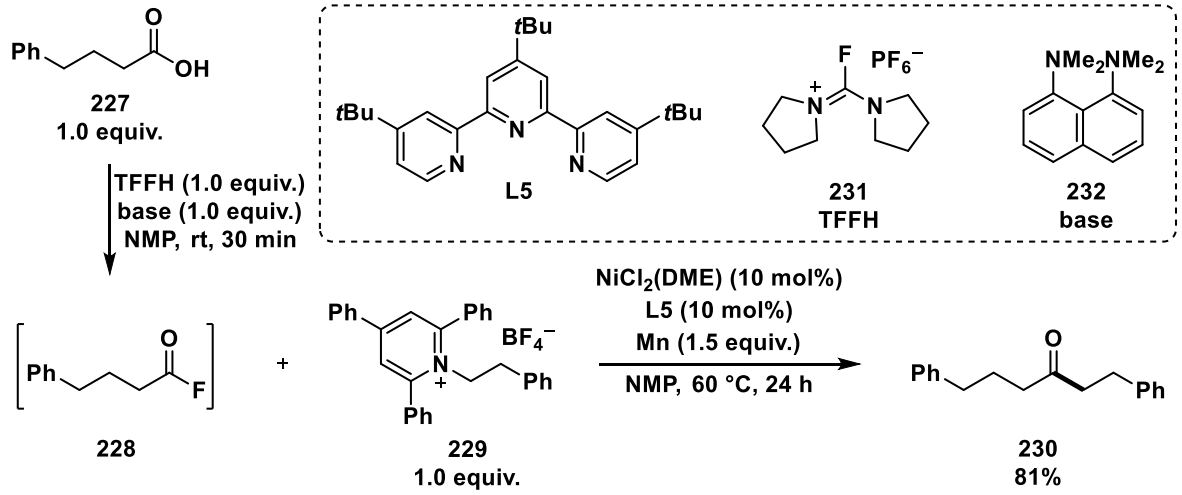

Scheme 4-12: Synthesis of dialkyl ketones from activated carboxylic acids and *N*-alkyl pyridinium salts.[69]

The literature overview on carboxylic acids as substrates has shown that they cannot be used directly as acyl sources in cross-electrophile couplings due to their low reactivity and that OH protection and activation are required. On the one hand, they can be activated by the *in situ* formation of more reactive anhydrides, usually using Boc_2O or similar reagents, or by the direct use of cyclic *meso*-anhydrides that can be ring-opened and thus serve as acyl sources. On the other hand, approaches were developed in which carboxylic acids were activated by the *in situ* formation of acyl fluorides.

In addition to acyl halides and anhydrides, cross-electrophile couplings with carboxylic acid esters are also literature known, as illustrated in the subsequent section.

4.1.5.1.3 Carboxylic Acid Esters

The oxidative addition of carboxylic acid esters and the C–O bond cleavage by nickel(0) was initially investigated by Yamamoto in 1976.[70] Depending on the type of esters, nickel catalyst and ligands, the cleavage could occur at the RC(O)–OR or the RC(O)O–R bond. For instance, *O*-aryl esters favored a RC(O)–OR bond cleavage, while *O*-alkyl esters preferably underwent a RC(O)O–R bond cleavage. With regard to cross-electrophile couplings, carboxylic acid esters are usually activated by 2-pyridyl substituents, which serve both as a good leaving group and as a directing group, resulting in a higher reactivity.[41o]

The first nickel-catalyzed cross-electrophile coupling of 2-pyridyl carboxylates with alkyl iodides was described by Mukaiyama *et al.* in 1981, who employed 10 mol% of $NiCl_2$ and zinc dust, affording alkyl ketones in a range of 35–87% yields.[15]

In a recent publication, the nickel-catalyzed reductive coupling of arylcarboxylic acid 2-pyridyl esters and alkyl methanesulfonates was demonstrated, yielding alkyl aryl ketones.[71] Tetrabutylammonium bromide was used for the *in situ* activation of mesylates by bromide formation. A 2-pyridyl thioester substrate was also compatible with the system.[71]

A directing group (DG) strategy, in which the cleavage of the C–O ester bond was enabled by a neighboring coordinating group, was realized using the hydroxyl or sulfonamide moiety (Scheme 4-13). These esters were applied to the nickel-catalyzed coupling with alkyl halides, yielding aryl alkyl ketones.[72] The method was extended to arylmethyl trimethylammonium triflates as electrophilic coupling partners instead of halides.[73] A nickel(I/II/III) radical-chain mechanism involving interaction of the hydroxyl- or sulfonamide substituents with the active nickel intermediates **236**, **237** and **238** was proposed (Scheme 4-13).

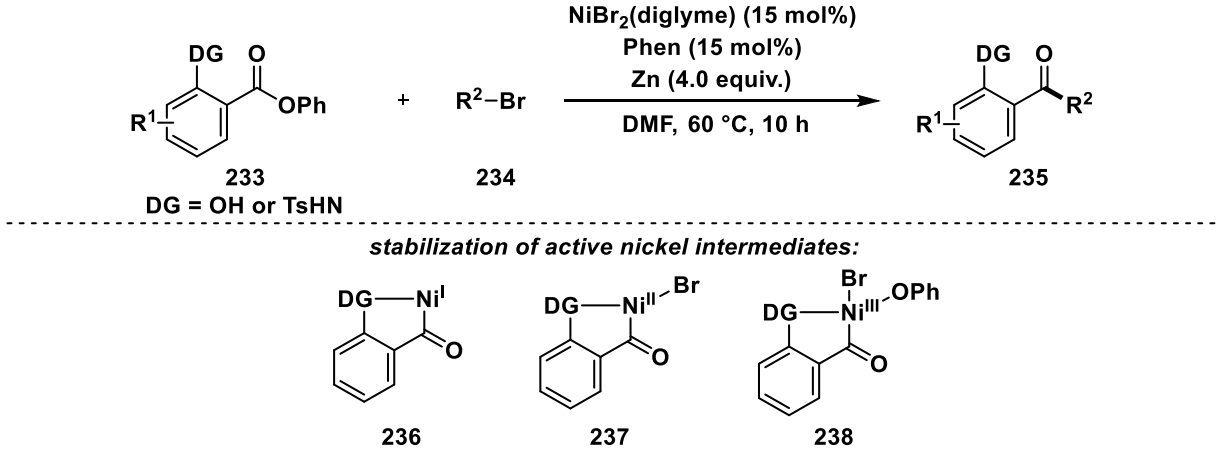

Scheme 4-13: Directing group strategy to couple carboxylic acid esters.[72]

In summary, protocols using carboxylic acid esters as substrates focus either on reactive 2-pyridyl esters or on a directing group strategy with coordinating groups near the carboxylate moiety.

The use of thioesters as alternative acyl sources, which are more reactive than carboxylic acid esters (see section 3.1.2.4.3.1), has been increasingly used in cross-electrophile couplings in recent years, as will be shown in the next section.

4.1.5.1.4 Thioesters

The initial work with this substrate class was done by Mukaiyama *et al.*, who introduced the synthesis of symmetrical aromatic ketones by the homocoupling of 2-pyridyl thioesters under the treatment with $Ni(cod)_2$.[74] In the aforementioned report from 1981, the Mukaiyama group also described the first example of a nickel-catalyzed cross-electrophile coupling using a *S*-(2-pyridyl) thioester as substrate, yielding 46% of the aryl alkyl ketone (*vide supra*, Scheme 4-3C).[15]

Wotal and Weix significantly improved the system using a $NiCl_2$(DME)/dtbbpy catalyst system and zinc as reductant.[46] An increase in ketone yield and a decrease in thioether yield was achieved by changing the reducing agent from manganese to zinc and stirring the precatalyst with zinc for one hour before adding the thioester.[46]

Another contribution of Weix was the decarboxylative nickel-catalyzed coupling of 2-pyridyl thioesters with NHP esters (Scheme 4-14A).[75] In this system, the choice of ligand influenced the ratio of desired ketone to thioether. With **L6**, ketone **241** was formed as main product, while formation of thioether **242** was suppressed. The conditions found application in the synthesis of ketones with strained rings or α-heteroatoms and in the coupling of a complex peptide fragment.

Kishi established a novel coupling method using alkyl iodides and 2-pyridyl thioesters as substrates, 10 mol% of $NiBr_2$(dtbbpy), zinc as reducing agent and a stoichiometric amount of Cp_2ZrCl_2, whereby the thiolate was captured (Scheme 4-14B).[76] The mechanism was proposed to involve both a nickel and a zirconium catalytic cycle connected by a transmetalation step. The proposed mechanism starts with the reduction of the nickel(II) precatalyst to the active nickel(0), followed by its oxidative addition to 2-pyridyl thioester. On the one hand, Cp_2ZrCl_2 and/or a low-valent zirconium species could accelerate the oxidative addition step. On the other hand, a second catalytic cycle occurs involving a low-valent zirconium species **248**, which activates the alkyl iodide and forms a metal-centered radical species **250**. The nickel and zirconium cycles are coupled *via* transmetalation generating a nickel(II) complex **252**, from which the desired ketone could be reductively eliminated (Scheme 4-14B).[76] The system was improved by using a mixture of nickel(I) and nickel(II) catalysts with a low catalyst loading of 1 mol%. Thereby, a 1:1 molar mixture of the coupling partners was sufficient for ketone synthesis.[33]

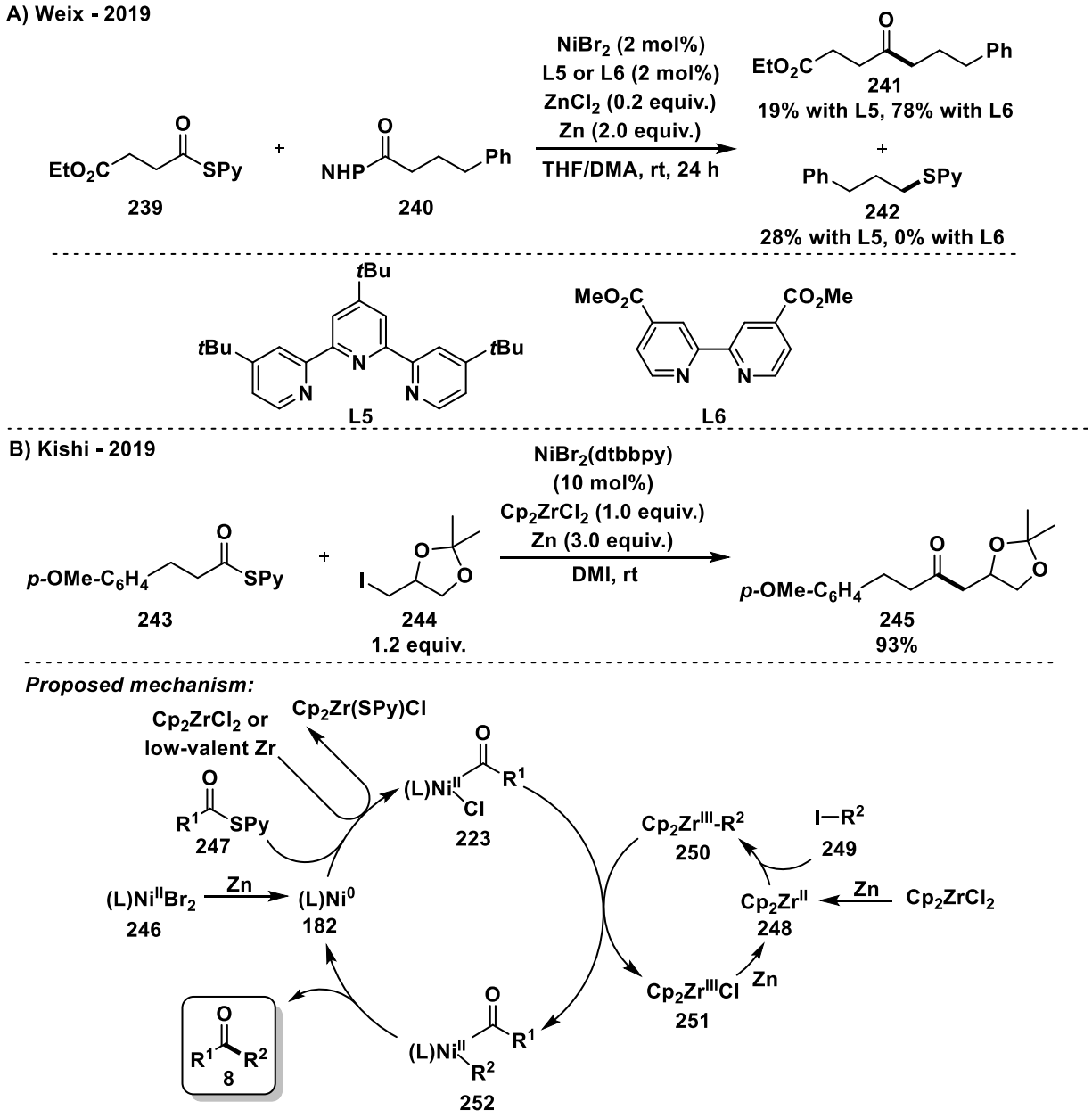

Scheme 4-14: Thioesters as acyl sources in ketone synthesis by cross-electrophile couplings.[75,76]

Furthermore, a nickel-catalyzed deaminative cross coupling of alkylpyridinium salts with thiopyridine esters was reported using a $Ni(cod)_2$/dtbbpy catalyst system, manganese as reductant and $MgCl_2$ as additive.[77] A radical-chain mechanism was proposed in which the role of $MgCl_2$ as Cl-donor for ligand exchange on a nickel(II) species was suggested, thereby removing the thiolate from the catalytic cycle.

It can be summarized from the literature overview that the focus typically lies on reactive thiopyridine esters and protocols with less reactive thiol moieties like alkyl or aryl are not known. Despite their favorable reactivity, a detrimental problem of thioesters is the liberated thiolate, which interferes with a productive nickel catalyst and forms thioethers as undesired byproducts.[46,76]

4.1.5.1.5 Other Acyl and Carbonyl Sources

Several other acyl and carbonyl sources proved to be suitable for cross-electrophile couplings (Table 4-1).

An early report from 2002 showed the $NiBr_2$(dppe)-catalyzed coupling of aryl iodides and benzaldehydes at high temperature (110 °C), generating aromatic ketones (entry 1).[78] The generality of the reaction was demonstrated by the application of heterocyclic and aliphatic aldehydes.

Furthermore, it was reported that diphenyl oxalate as a CO source enables the nickel-catalyzed reductive carbonylation of two equivalents of alkyl electrophile giving symmetric dialkyl ketones (entry 2).[79]

In a three-component acylation, high chemoselectivity was achieved with a 1:1:1 ratio of aryl iodide to alkyl iodide to oxalyl chloride as the CO surrogate (entry 3).[80] The reaction consisted of a $NiCl_2$(DME)/bpy catalyst system and was characterized by a wide substrate scope. Mechanistic studies showed that the reaction of zinc and oxalyl chloride at 40 °C in a THF/DMF mixture can slowly release CO and CO_2.[80]

Chloroformates are another suitable CO surrogate for nickel-catalyzed reductive couplings. Hereby, alkyl esters were formed after the coupling of alkyl halides with alkyl chloroformates.[81] The three-component coupling of alkyl halides and ethyl chloroformate delivered symmetric and unsymmetrical dialkyl ketones (entry 4).[82] Interestingly, the reaction favors the carbonylative cross coupling of two different alkyl halides over the carbonylative homocoupling even whilst utilizing equimolar stoichiometry. It was proposed that the selectivity arises from two different activation processes of the alkyl halides, which are influenced by their steric and thermodynamic properties.[82]

Another nickel-catalyzed three-component protocol coupled ethyl chloroformate as CO source, aryl iodides and alkyl halides, yielding the corresponding aryl alkyl ketones (entry 5).[83] DFT computations and mechanistic investigations showed that the sequence of oxidative additions starts with the aryl halide, followed by ethyl chloroformate, and closes with the alkyl halide.

Moreover, ethyl chloroformate was used as CO source in the nickel-catalyzed multicomponent reaction of inactivated alkenes with racemic secondary benzyl chlorides or NHP esters of protected α-amino acids as the alkylation agent (entry 6).[84] The regio- and enantioselective coupling *via* sequential hydroformylation and carbonylation was achieved with NiI_2, a chiral bisoxazoline ligand, KF as additive and a silane as reducing agent, yielding α-chiral ketones. The method impresses with a wide substrate scope and the late-stage functionalization of complex molecules.

Table 4-1: Acyl and carbonyl sources in nickel-catalyzed cross-electrophile couplings.

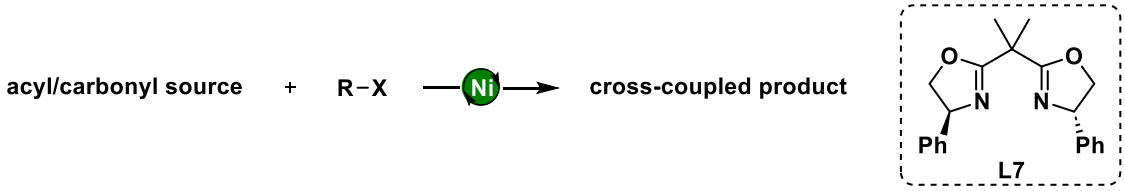

Entry	Acyl/carbonyl source	R–X	Ni catalyst (mol%)	Ligand (mol%)	Cross-coupled product	Ref.
1	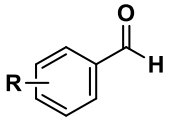 253	Ar–I	$NiBr_2$(dppe) (10)	–	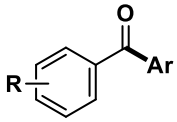 254	[78]
2	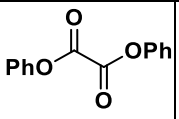 255	2 × Alk–Br/OTs	$NiBr_2$ (10)	dtbbpy (20)	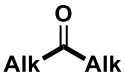 256a	[79]
3	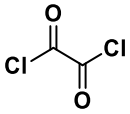 257	Alk–I + Ar–I	$NiCl_2$(DME) (10)	bpy (10)	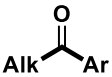 42	[80]
4	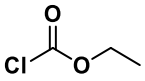 258	2 × Alk/Alk'–I/Cl	$NiBr_2$ (diglyme) (10)	bpy (15)	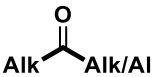 256a/b	[82]
5	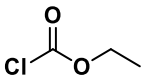 258	Alk–Br + Ar–I	NiI_2 (10)	Phen (15)	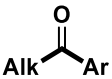 42	[83]
6	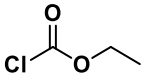 258	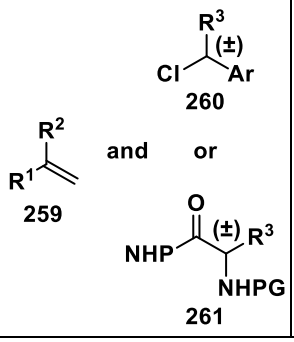 259 and 260 or 261	NiI_2 (10)	L7 (12)	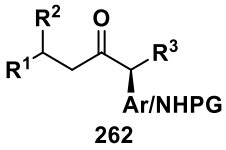 262	[84]

For the sake of completeness, two indirect methods are also presented, which converted an existing ketone framework or α-hydroxycarbonyl compounds modified with oxalyl groups.

A nickel-catalyzed regioselective reductive ring opening of aryl cyclopropyl ketones with alkyl bromides was presented by Wang and co-workers.[85] The method was applied to a wide range of substrates, obtaining the alkylated ketones. Mechanistic experiments revealed that the cyclopropylketone oxidatively adds to nickel(0), resulting in a six-membered oxa-nickelacyle. The latter is reduced to nickel(I), which stays in an equilibrium with an enolate

via tautomerization. Alkyl bromide undergoes two-electron oxidative addition to nickel(I) complex, and the product is delivered after reductive elimination from the nickel(III) complex.

The substitution of functional groups in the α-position of a carbonyl group is not only a way in traditional cross couplings (see section 3.1.1), but also in cross-electrophile couplings. A nickel-catalyzed C–O bond functionalization of oxalates derived from α-hydroxy esters with aryl and vinyl (pseudo)halides was developed, yielding mainly esters and one single example of a ketone **264** (Scheme 4-15).[86] $MgCl_2$ was required as an additive in the reaction, which is probably due to the activation of the oxalate and the stabilization of a radical anion intermediate formed from the oxalate by a chelation effect. In addition, an excess of pyridine led to a drastically increased yield.

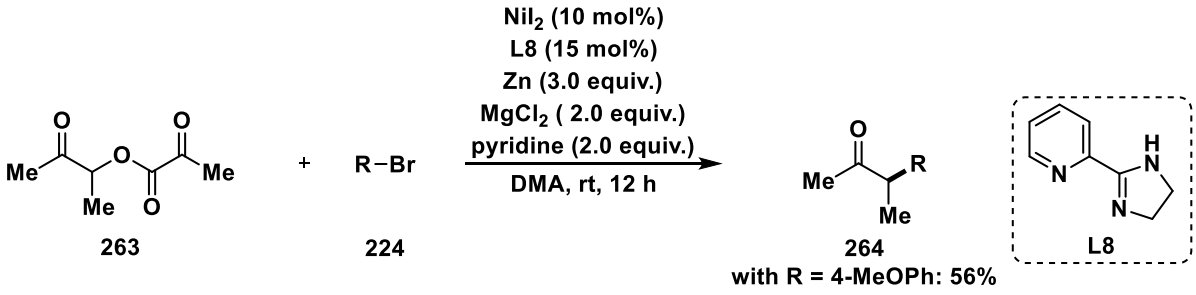

Scheme 4-15: Nickel-catalyzed reductive C–O bond arylation of an oxalate.[86]

Furthermore, several approaches were developed, in which nitrogen-containing substrates serve as acyl sources, for instance nitriles can be hydrolyzed and thus used to introduce acyl units.

In one protocol, the intermolecular insertion of aryl iodides to nitriles was demonstrated under nickel catalysis and reductive conditions, although a high temperature of 100 °C was required.[87]

A dual catalytic approach with $NiCl_2$(DME) and Cp_2TiCl_2 under reductive conditions couples aryl or alkyl nitriles and bromides (Scheme 4-16A).[88] It was found that TMSCl was mandatory to turn over the titanium catalyst. The mechanism has not been fully deciphered, but a radical intermediate, for instance an imidoyl radical **267** may be involved (Scheme 4-16A).[88] A recent publication showed the visible light-induced and nickel-catalyzed cross-electrophile coupling of aryl bromides with nitriles.[89]

A C–N activation was demonstrated in the nickel-catalyzed cross-electrophile coupling between amides and aryl iodides using NiI_2, terpy as ligand, KF as additive and zinc as reducing agent (Scheme 4-16B). For this system, a radical-chain mechanism was proposed.[90] A mechanochemical cross-electrophile coupling of twisted amides with alkyl halides, enabled by ball-milling, was published by Browne.[8d] The acylated products were obtained with 10 mol% $NiCl_2 \cdot 6H_2O$, Phen as ligand, sodium chloride as additive, manganese as reducing agent and after mixing in a mill at 30 Hz for two hours. It is noteworthy that in

addition to the acylated products, several heteroarylated products were also synthesized, including compounds bearing hydroxyl and amine substituents. The mechanism has not yet been fully elucidated and either a radical-chain mechanism or a Negishi-type pathway could be operative.[8d] With regard to amides, an electrochemical protocol is also known, in which aliphatic amides were coupled with alkyl halides.[91] A nickel-catalyzed reductive deaminative cross-electrophile coupling of aromatic amides and Katritzky salts yielded the aromatic ketones in moderate to high yields. The mechanism was proposed to follow a radical-chain pathway.[92]

Acylimidazoles are another acyl source, which can be easily prepared from carboxylic acids and *N*,*N'*-carbonyldiimidazole (CDI), and were used in a nickel-catalyzed cross-electrophile coupling with aryl or alkyl bromides (Scheme 4-16C).[93] The substrate scope was remarkably broad, including electron-rich and -deficient substituents, heterocycles, natural product derivatives such as **273a**–**c** as well as alkyl imidazolides and bromides. For the mechanism, two different scenarios were proposed, depending on the steric of the acylimidazole. For spatially accessible acylimidazoles, a single-electron transfer with an acyl radical **274** and a CO-extrusion-recombination phenomenon was suggested. For sterically hindered acylimidazoles, a concerted oxidative addition was drawn.[93]

Finally, a cooperative nickel and photoredox-catalyzed approach was also developed using *N*-acyl-imides and inactivated alkyl bromides as substrates.[41k]

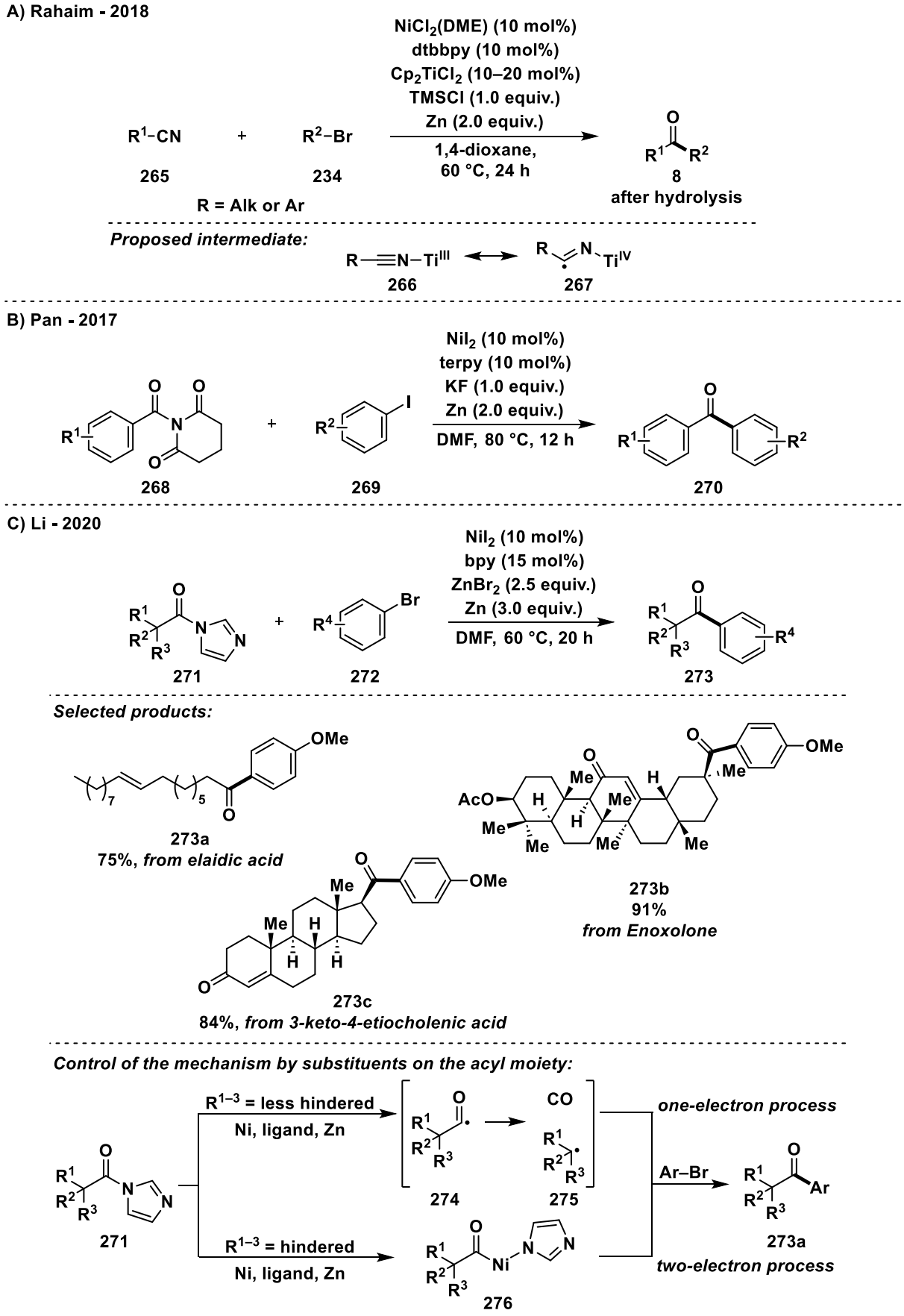

Scheme 4-16: *N*-Containing electrophiles as acyl sources in cross-electrophile couplings.[90,93,94]

The examples in this section showed that various other acyl sources were used in nickel-catalyzed cross-electrophile couplings. These are aldehydes and CO sources such as diphenyl oxalate, oxalyl chloride and ethyl chloroformate. Indirect methods by ring-opening aryl cyclopropyl ketones or the application of oxalates derived from α-hydroxy esters are also known. Furthermore, *N*-containing compounds like nitriles, amides and acylimidazoles are suitable acyl sources under reductive conditions.

4.1.5.2 *O*-Electrophiles

The general drawbacks, which are associated with organic halides as substrates are the formation of halogenated waste and the low accessibility of functionalized aryl halides, especially for aryl iodides and bromides.[95] Therefore, a general mission of modern research is to expand the molecular diversity for cross couplings, which set aside these disadvantages. *O*-Electrophiles dominate the ten most common functional groups in natural products, with the alcoholic hydroxy group on alkyl moieties being the most frequent, accounting for 61% of the molecules examined (Figure 4-1A).[96] Therefore, a highly desirable class of substrates for cross-electrophile couplings are *O*-electrophiles such as sulfonates, carbamates, esters, ethers, and alcohols.[97] All of these classes have their own advantages and detriments. In general, the reactivity, moisture instability and cost of these substrates decreases from sulfonates over carbamates and carbonates to esters, ethers and alcohols, accompanied by an increase in the accessibility (Figure 4-1B).[95] In recent years, the use of *O*-electrophiles as substrates for cross-electrophile couplings has attracted increasing attention.[98] Therefore, the different classes and their applications in XEC are illustrated in the next sections, starting with sulfonates and ending with alcohols.

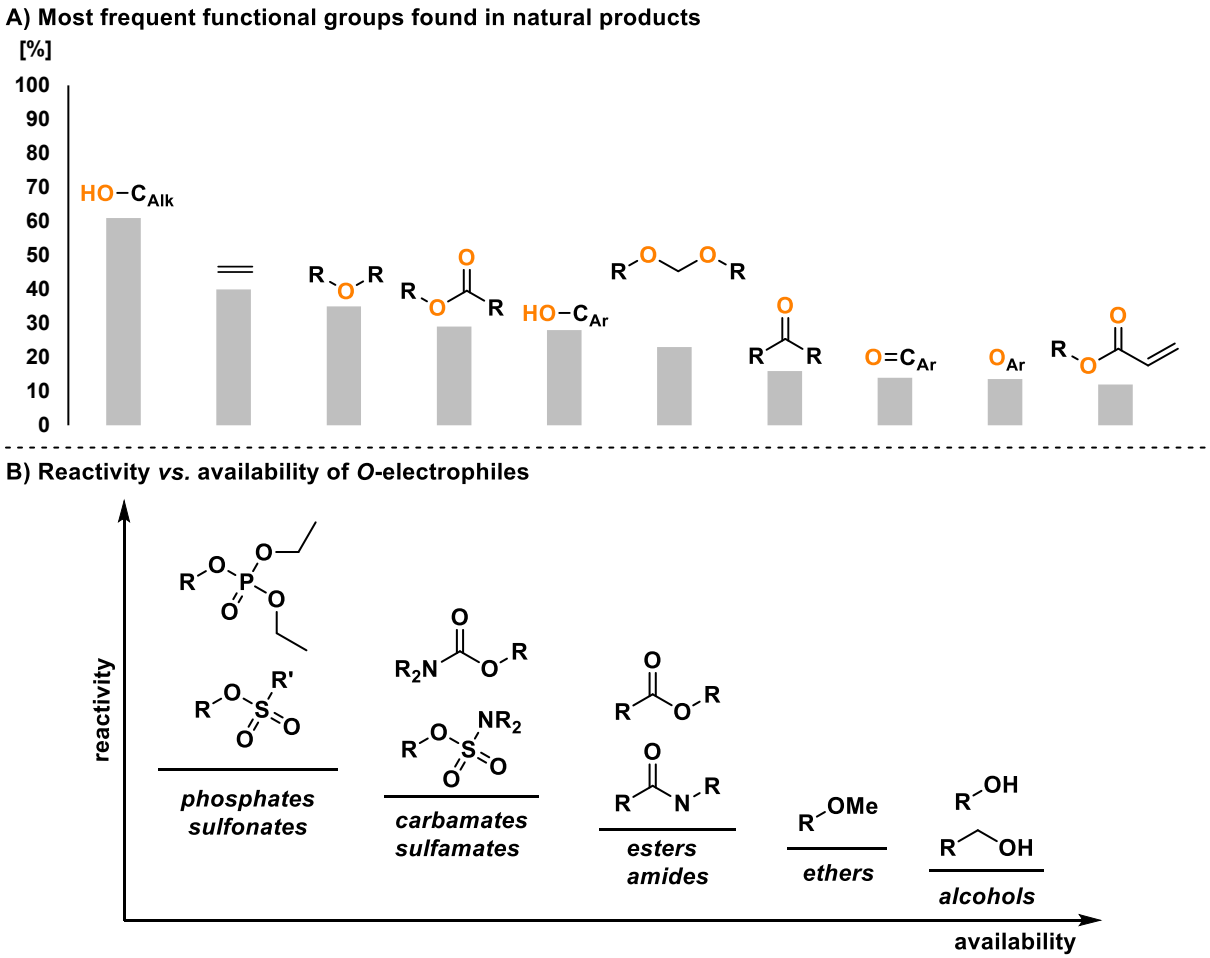

Figure 4-1: A) Most frequent functional groups found in natural products. The numbers were adapted from a cited reference[96] and indicate the percentage of molecules having this group found in 'The Dictionary of Natural Products', which contains over 186 000 molecules.[83] B) Comparison of *O*-electrophiles as substrates in metal-catalyzed cross couplings, with R = alkyl or aryl and R' = CF_3, Me, *p*-MeC_6H_4.[95,99]

4.1.5.2.1 Sulfonates

The class of sulfonates, which includes mesylates, tosylates and triflates, is the most reactive one with a high leaving group ability of the sulfonyloxy group. In addition, they exhibit a low activation barrier for the C–O bond cleavage and the oxidative addition is facilitated. Contrary, their high prices and moisture instability may limit the applications.[95,99] Protection of the hydroxyl group as mesylates, tosylates and triflates has been widely used as strategy in cross-electrophile couplings and an overview of these approaches is given below.

4.1.5.2.2 Mesylates

Jarvo established the synthesis of alkylcyclopropanes by the intramolecular nickel-catalyzed dialkyl cross coupling of 1,3-dimesylates.[100] The required reagents for a successful reaction are 5 mol% $Ni(cod)_2$, 5 mol% *rac*-BINAP and MeMgI, which has been shown to convert the mesylate *in situ* to a 1,3-diiodide, the proposed active intermediate. Then, radical formation proceeds at the 2° alkyl iodide center of the diiodide.[101] The approach of

intramolecular cyclization of mesylates was extended to a conjunctive method, which enables the synthesis of 3,5-vicinal carbocyclic rings and the late-stage functionalization of natural products and medicinal agents.[102]

4.1.5.2.3 Tosylates

(Hetero)aryl bromides were alkylated with heterocyclic alkyl tosylates under nickel catalysis, reductive conditions and potassium iodide as additive.[103] The mechanism of the reaction has not been investigated, but it was postulated that the alkyl tosylate is activated *in situ* with potassium iodide, forming the alkyl iodide.

Additionally, a reductive nickel-catalyzed cross coupling of aryl halides with alkyl tosylates was described, in which the tosylates were activated with a vitamin B_{12} (VB_{12} = cyanocobalamin) catalyst.[104] Potassium iodide as additive was beneficial, but not mandatory for the reaction, while the choice of ligand was crucial, with 2,2'-bipyridine being the best. Mechanistically, two catalytic cycles are included. Both are initiated with the generation of the active nickel(0) and cobalt(I) complexes from the initial nickel(II) and VB_{12} by the reduction with manganese. Aryl halide oxidatively adds to nickel(0) and a sequential reduction with manganese preferentially produces an $Ar–Ni^{I}$ species. In a second catalytic cycle, highly nucleophilic cobalt(I) undergoes substitution with alkyl tosylates, generating a $Alk–Co^{III}$ species. A high-valent $Ar–Ni^{III}–Alk$ complex forms by an alkyl radical transfer, and the product is delivered after reductive elimination from the nickel(III) intermediate.[104]

Gong described the direct nickel-catalyzed methylation of aryl halides and tosylates with methyl tosylate.[105] In addition, Cantillo and co-workers developed an electrochemically enabled, nickel-catalyzed $C(sp^3)–C(sp^3)$ coupling of alkyl halides with alkyl tosylates.[106] In this approach, sodium bromide was mandatory as supporting additive, whereby small amount of the more reactive bromide is gradually generated from the tosylate.

4.1.5.2.4 Triflates

Especially for the substrate class of triflates, several approaches have been demonstrated to modulate the activation rates of electrophiles by synergistic catalysts, combining nickel and palladium (Table 4-2).

Selectivity was achieved in the cross-electrophile coupling of aryl triflates and aryl bromides by the cooperation of $NiBr_2$(bpy) and $PdCl_2$(dppp) as catalysts (entry 1). Palladium preferentially reacts with aryl triflates to afford a persistent intermediate, while nickel prefers to react with aryl bromides to form a transient species.[34a]

Another example, in which multimetallic catalyst systems similar to those mentioned above were used, activated aryl triflates and aryl chlorides separately (entry 2).[31a] It was found that LiCl as salt additive was essential for the system by accelerating the reduction of nickel(II) to

nickel(0) and counteracting the inhibition of the reduction at zinc(0) by formed zinc(II) salts. Furthermore, the nickel and palladium multimetallic cross-electrophile coupling of aryl triflates with aryl tosylates was demonstrated (entry 3).[34d] The reaction was characterized by a very low catalyst loading, 1 mol% for both nickel and palladium catalysts. In this system, nickel reacts preferentially with aryl tosylates, while palladium prefers the aryl triflate. Both catalytic cycles are linked by a transmetalation step with zinc salts.[34d]

Additionally, the cross-electrophile coupling between aryl and vinyl triflates with vinyl tosylates for the synthesis of *gem*-difluoroalkenes was enabled by nickel and palladium cooperative catalysis (entry 4).[34e]

The multimetallic cross-electrophile coupling of heteroaryl triflates and heteroaryl halides delivered a wide range of biheteroaryls (entry 5).[34b] A cooperative catalyst system consisting of $NiBr_2$(DME) and $PdCl_2$ directed the selectivity.

Table 4-2: Coupling of triflates in nickel/palladium-catalyzed cross-electrophile couplings.

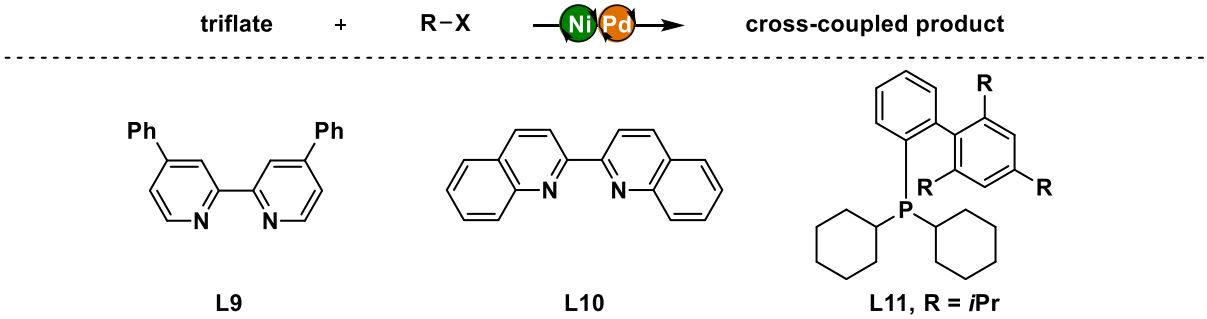

Entry	Triflate	R–X	Ni catalyst (mol%) ligand (mol%)	Pd catalyst (mol%) ligand (mol%)	Cross-coupled product	Ref.
1	Ar–OTf	Ar–Br	$NiBr_2$(bpy) (5)	$PdCl_2$ (5)	Ar–Ar	[34a]
2	Ar–OTf	Ar–Cl	$NiCl_2$(DME) (10) dtbbpy (5)	$PdCl_2$ (5) dppb (5)	Ar–Ar	[31a]
3	Ar–OTf	Ar–OTs	$NiCl_2$(DME) (1) L9 (1)	$PdCl_2$ (1) dppb (1)	Ar–Ar	[34d]
4	Ar/Vinyl –OTf	Vinyl –OTs	Ni(acac) (5) L10 (5)	PdI_2 (5) L11 (10)	Ar/Vinyl–Vinyl	[34e]
5	Ar_{Het}–OTf	Ar_{Het}–Br	$NiBr_2$(DME) (5) dtbbpy (6)	$PdCl_2$ (5) dppp (6)	Ar_{Het}–Ar_{Het}	[34b]

gem-Difluoroalkenes were applied as substrates in the defluorinative $C(sp^2)$–$C(sp^2)$ cross-electrophile coupling with several alkenyl electrophiles, including triflates, tosylates and halides.[107] Several additives were required for this approach ($MgCl_2$, $YbCl_3$, TMSCl and 4 Å molecular sieves).

Alkenyl triflates coupled with alkyl mesylates using a simple NiI_2/tpy catalyst system at elevated temperature (100 °C).[108] The suitability of this method for late-stage functionalization was demonstrated, amongst others, by the selective introduction of alkyl groups into

substrates derived from lithocholic acid **277** and epiandrosterone **278**, two biologically active compounds (Scheme 4-17).

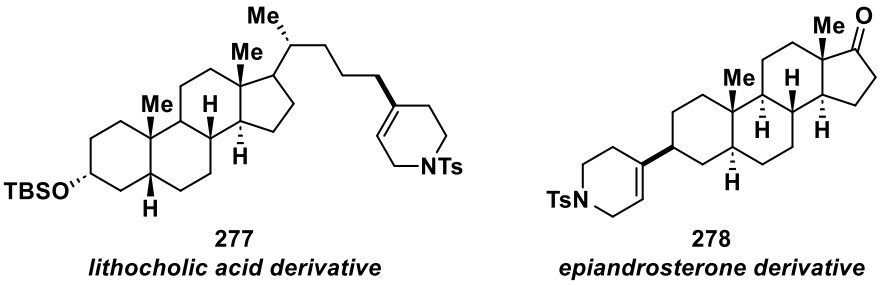

Scheme 4-17: Natural products derivatized by cross-electrophile coupling.[108]

4.1.5.2.5 Oxalates and Formates

Oxalates and chloroformates as *O*-derivatives are used not only as CO surrogates, but also as radical sources in cross-electrophile couplings.

Shu chose benzyl oxalates,[109] while Gong applied tertiary alkyl oxalates for the formation of alkylated and arylated quaternary carbon centers.[110]

In the latter system, oxalates were coupled with alkenes as radical acceptors (Scheme 4-18).[110] Control reactions showed that the reaction was still successful in the absence of nickel catalyst, but at the expense of the yield, which dropped from 83% to 32%. In contrast, $MgCl_2$, 2-(2-pyridyl)benzimidazole (PBI) and Zn were crucial for the reaction. It was hypothesized that the reduction of dialkyl oxalate by zinc leads to the formation of a radical anionic oxalate intermediate **284** (Scheme 4-18). Additionally, $MgCl_2$ or the $Mg(PBI)Cl_2$ complex activates zinc by removing surface impurities.

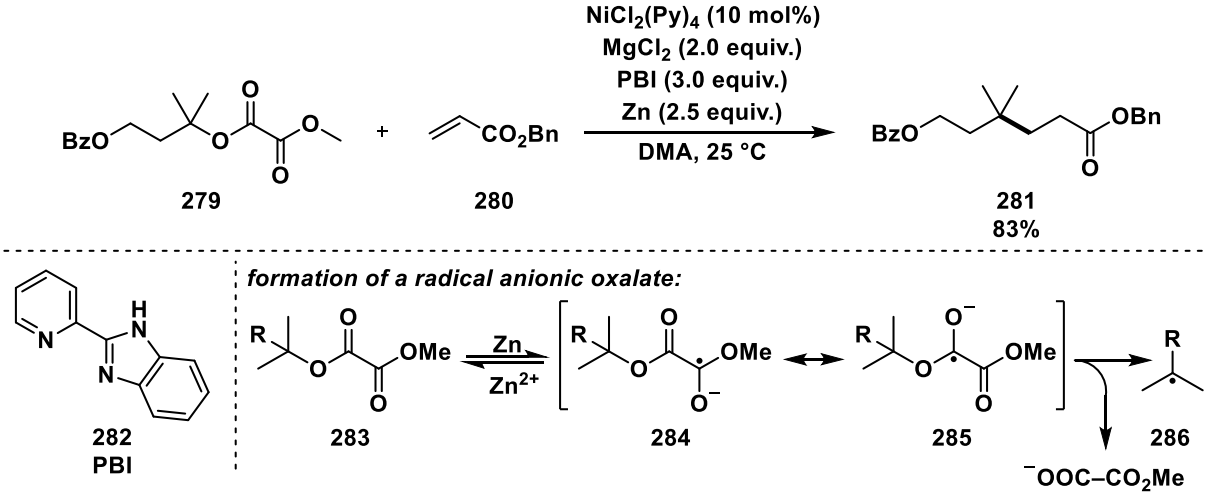

Scheme 4-18: Zinc-mediated fragmentation of tertiary oxalates and coupling with activated alkenes.[110]

Furthermore, a nickel-catalyzed and zinc-mediated reductive addition of isocyanides with inactivated tertiary alkyl oxalates was described in the literature, yielding 6-alkylated phenanthridines as products.[111]

Gong developed a protocol with benzyl chloroformates as substrates, which underwent a C–O bond radical fragmentation and subsequent coupling with aryl iodides under nickel catalysis, forming diaryl methane products.[112]

4.1.5.2.6 Activated Esters

Under the terminology of activated esters, several examples of pivalates and redox-active NHP esters are presented as substrates in cross-electrophile couplings.

Naphthyl and *O*-benzylic pivalates were carboxylated with CO_2 under nickel catalysis.[113] An $NiBr_2$(DME)-mediated intra- and intermolecular coupling of benzylic pivalates with aryl halides was described by Jarvo.[114] In the intramolecular protocol, cyclic products were formed, including naphthylic esters, benzofuran and benzothiophene moieties as well as *N*-heterocyclic substrates. Additionally, a stereospecific cyclization of a secondary benzylic ester was demonstrated.[114]

Access to α-vinyl and aryl amino acids was given by the nickel-catalyzed cross-electrophile coupling of *N*-carbonyl-protected α-pivaloyloxy glycine with vinyl or aryl halides and triflates (Scheme 4-19A).[115] $NiBr_2$/dtbbpy as catalyst system as well as $MgCl_2$, tetrabutylammonium iodide (TBAI) and zinc as additives were used. Pivaloyloxy glycine was found to be activated *in situ* with TBAI to form an α-iodoglycine **292** or an imino/iminium ester **293** (Scheme 4-19A). In the presence of zinc, the activated species forms a glycine α-carbon radical **294** (Gly), which oxidatively adds to nickel(0), forming a Gly–Ni^{I} intermediate. DFT computations showed that the auxiliary chelation of the *N*-carbonyl oxygen to the nickel center appears to be crucial for the stabilization of the Gly–Ni^{I} intermediate. Subsequent oxidative addition of an aryl halide to Gly–Ni^{I} would give a Gly–Ni^{III}–Ar intermediate, from which the product is reductively eliminated.[115]

Redox-active NHP esters serve as radical sources and are popular alternatives to classic *O*-esters in cross-electrophile couplings. In 2016, Weix demonstrated the decarboxylation of NHP esters and subsequent coupling with aryl iodides using a simple $NiBr_2$(dtbbpy)/Zn system (Scheme 4-19B).[55] In addition, a $NiBr_2$(DME)/dtbbpy/Mn catalyst system enabled the reductive decarboxylative alkynylation of NHP esters with bromoalkynes.[116] Stoichiometric amounts of LiBr as additive improved the yield of alkynylated product.

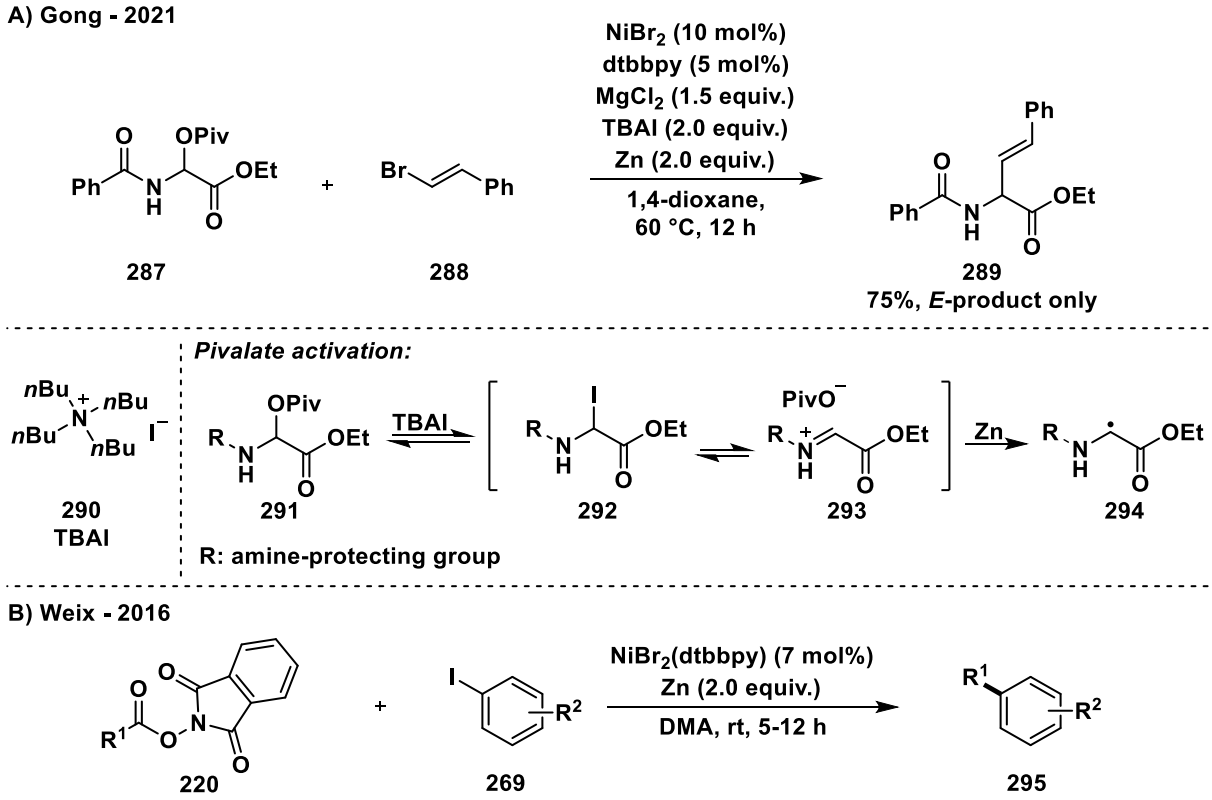

Scheme 4-19: A) Vinylation of α-amino acids,[115] and B) Weix' approach for the coupling of NHP esters.[55]

Secondary α-aryl amides were synthesized by a nickel-catalyzed reductive arylation of redox-active NHP esters of malonic acid half amides with aryl iodides.[117] The NHP esters were easily prepared from Meldrum's acid. Interestingly, homocoupling of aryl iodide was suppressed by optimizing the reducing system, i.e. four equivalent each of manganese and zinc, and with $PhMeSiCl_2$ as an additive.

In a nickel-catalyzed one-pot method for $C(sp^3)$–$C(sp^3)$ bond formation based on cross-electrophile coupling, the NHP esters were generated *in situ* with *N*,*N'*-diisopropylcarbodiimide (DIC) and then reacted with inactivated alkyl bromides. Probably, both substrates are converted to alkyl radicals during the reaction.[118]

Activated NHP esters and Katritzky salts were used as substrates in the nickel-catalyzed decarboxylative respective deaminative glycosylation with iodo-glycals.[119] The scope of substrates was found to be quite broad and late-stage functionalization of different natural products was possible. With regards to the decarboxylative glycosylation reaction of redox-active esters, derivatives of probenecid, dehydrocholic acid, pregabalin and indomethacin were successfully glycosylated. A double oxidative addition pathway was proposed as the mechanism.

4.1.5.2.7 Acetates

A seminal report from 2012 showed the coupling of aryl bromides and an allylic acetate, using 10 mol% NiI_2, dtbbpy as ligand, pyridine, tetrabutylammonium bromide and $MgCl_2$ as additives and zinc as reducing agent.[120] The additives may play a role in the activation of zinc by removing salts from the surface. The reaction showed limitations regarding the substituents of aryl bromides, with electron-withdrawing groups achieving the highest product yields.

Furthermore, alkenyl acetates were coupled with alkyl bromides under a $NiBr_2$(diglyme)/4,4'-dmbpy catalyst system (Scheme 4-20).[121] A wide scope was demonstrated, including heteroaryl-substituted as well as nonactivated cyclic alkenes and five- to seven-membered cyclic enones. Additionally, a gram-scale synthesis of (±)-Curcumene ether and several syntheses of natural products and biologically active molecules were accessible with this system. A nickel(I/II/III) radical-chain mechanism was tentatively proposed.[121]

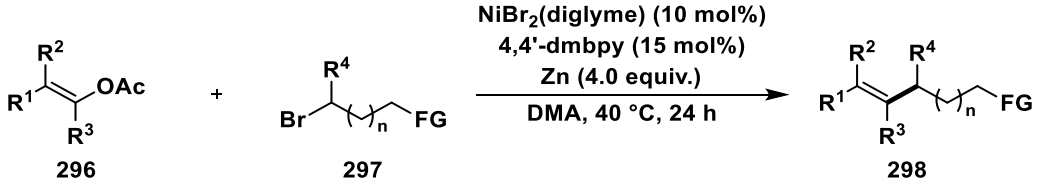

Scheme 4-20: Reductive coupling of alkenyl acetates with alkyl bromides.[121]

Li reported a nickel-catalyzed cross-electrophile coupling to prepare *C*-aryl-nucleoside analogues from furanosyl acetates and aryl iodides.[122] Besides nickel catalyst, ligand and zinc as reducing agent, an excess of TMSBr was crucial for a successful reaction. Electron-rich, electron-neutral, and electron-poor aryl iodides were coupled, and products with heterocyclic backbones and a compound bearing the same aromatic rings as dapagliflozin, a drug used to treat type 2 diabetes, were synthesized. First mechanistic experiments showed that an anomeric radical is involved in the process, which could be generated directly from the reduction of furanosyl acetate by zinc in the presence of TMSBr.[122]

Vinylation of (hetero)aryl bromides was achieved with vinyl acetate and $NiCl_2$(dppp) as catalyst in dimethyl isosorbide as an unusual solvent for XEC.[123]

A nickel-catalyzed cross-electrophile coupling of allylic acetates and *gem*-difluorovinyl tosylates afforded a variety of allylic *gem*-difluorovinyl arenes in moderate to good yields. Control experiments revealed that the reaction comprises two different Ni^0/Ni^{II} catalytic cycles with a difluorovinyl zinc reagent and a transmetalation step as a link between both.[124]

4.1.5.2.8 Ethers

Shi reported the nickel-catalyzed cross-electrophile coupling of aryl methyl ethers and aryl bromides with 5 mol% of $Ni(cod)_2$, 1,3-di-*tert*-butylimidazol-2-ylidene (I^tBu) as ligand and magnesium as reducing agent.[125] Besides aryl methyl ethers, the coupling was possible with an aryl isopropyl ether, a carboxylate and a carbamate, but a phenol was unsuitable. A Kumada-type mechanism with an *in situ* formed Grignard species was proposed as less likely.

Jarvo introduced several approaches for the functionalization of ethereal scaffolds. Photocatalytic oxydifluoromethylation of an olefin with a subsequent nickel-catalyzed intramolecular cross-electrophile coupling between a difluoromethyl moiety and a benzylic ether yielded fluorinated cyclopropanes.[126] Another protocol showed the stereospecific ring contraction of 2-aryl-4-chlorotetrahydropyrans to afford substituted cyclopropanes, using 5 mol% each of $Ni(cod)_2$ and *rac*-BINAP as the catalyst system and MeMgI as reducing agent.[127] It turned out that the reaction was not stereoconvergent, but highly stereospecific with respect to the alkyl halide. This outcome is not consistent with an initial oxidative addition of the alkyl halide moiety. Unfortunately, no in-depth mechanistic study has been conducted so far.

Another approach coupled a redox active ether **299** and iodoarenes under nickel catalysis in the presence of TMSCl, zinc as reducing agent and DMA as reaction medium (Scheme 4-21).[128] Computationally, it was found that a zinc(II) Lewis acidic interaction is responsible for activating and promoting the N–O bond cleavage of the phthalimide framework, generating an oxygen-centered alkoxy radical **302**. The pivotal mechanistic step is the DMA-assisted 1,2-hydrogen atom transfer (HAT) process **303** of the oxygen-centered radical to generate a nucleophilic α-hydroxy-α-trifluoromethyl *C*-centered radical **304**, which subsequently participates in the nickel-mediated cross-electrophile coupling.

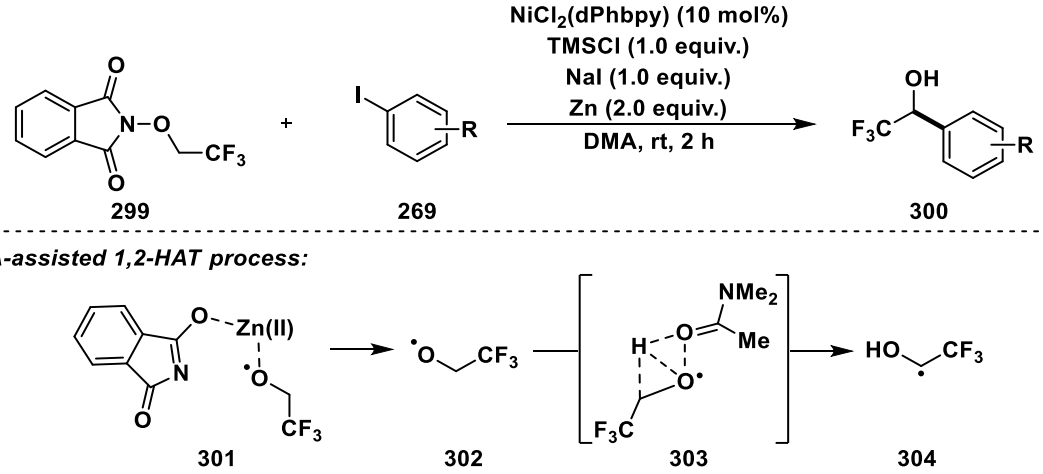

Scheme 4-21: Nickel-catalyzed synthesis of α-aryl-α-triflurомethyl alcohols from *N*-trifluoroethoxyphthalimides.[128]

4.1.5.2.9 Acetals

The Doyle group introduced the nickel-catalyzed cross-electrophile coupling of benzyl acetals and aryl iodides, affording dialkyl ethers.[129] TMSCl was used for the activation of the formal C(sp^3)–O bond in benzylic acetals, from which an α-oxy radical **307** is generated with TMSCl and zinc (Scheme 4-22).

Another contribution of the group used data science techniques to guide the analysis of the aryl bromide substrate scope in a nickel- and photoredox-catalyzed cross coupling with acetals as alcohol-derived radical sources.[130]

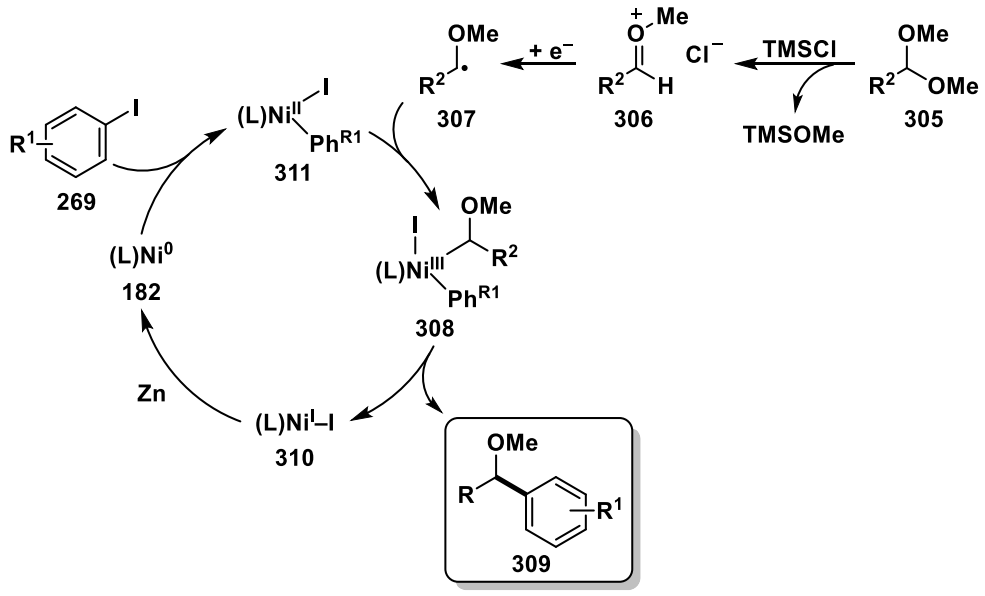

Scheme 4-22: Mechanism of dialkyl ether formation by coupling of acetals and aryl iodides.[129]

4.1.5.2.10 Alcohols in XEC

Alcohols are ubiquitous organic motifs, commonly found as feedstock for chemicals and as sources in naturally occurring products and synthetic molecules (Figure 4-2A). The number of commercially available primary, secondary and tertiary alcohols is distinctly higher than the number of organic halides, indicating the easy accessibility as substrates and low prices (Figure 4-2B).[131] If not commercially available, alcohols can be synthesized from carbonyl compounds in a simple and environmentally friendly way. Further characteristics of the OH functional group, which can also be disadvantageous, are the good coordination ability, easy oxidation by β-H elimination and its protic nature.

Additionally, the lower reactivity, which is due to the higher bond dissociation energies and consequential higher C–O bond strengths compared to the C–halogen bond, is unfavorable (Figure 4-2C).[98d,132] Therefore, the activation of the C–O bond usually requires the protection of the hydroxyl group, which also circumvents the poor leaving group ability of the latter.[133]

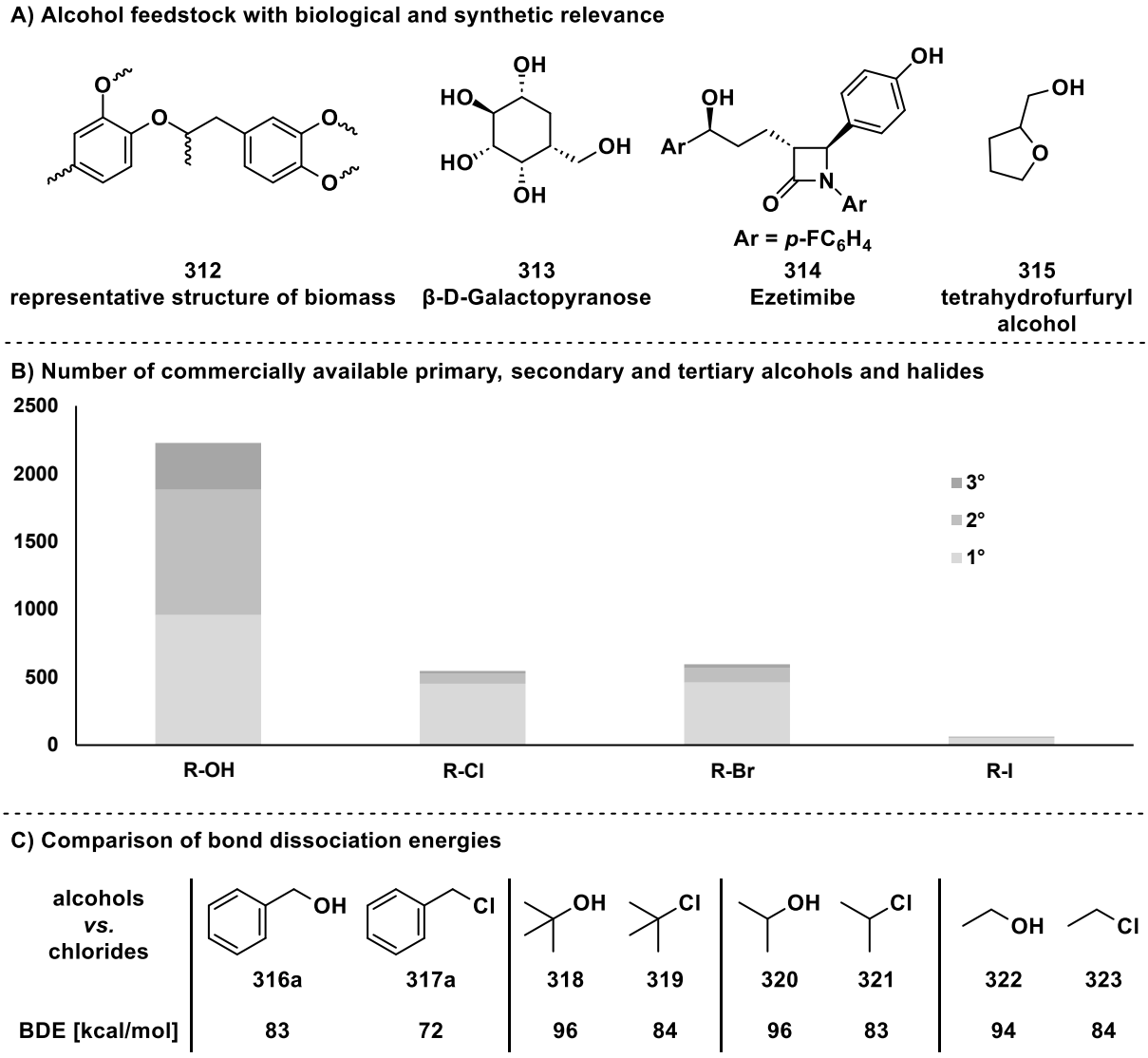

Figure 4-2: A) Selected alcohol feedstock with biological and synthetic relevance, B) number of commercially available primary, secondary and tertiary compounds and C) BDEs of selected alcohols and chlorides.[98b,131,134]

In the last years, the direct functionalization of alcohols has been achieved with the aid of nucleophilic reaction partners, for instance in Friedel–Crafts alkylation catalyzed by Lewis acidic metals,[135] in the hydrogen autotransfer process for the alkylation of different nucleophilic agents,[136] and in traditional cross couplings of activated alcohols and organometallic compounds.[133,137]

Due to the advantages of cross-electrophile couplings (see section 4.1.1), the manipulation of inert C–O bonds in alcohols, which allows for the coupling with other electrophiles, represents the current state of the art in the field of reductive couplings, but still remains a challenge.[98b,c]

4.1.5.2.10.1 *In situ* Generation of a More Reactive Species Using Electro- and Photochemistry

One way to achieve the direct coupling of alcohols is the combination of electro- or photoredox chemistry with nickel catalysis.

Li and co-workers demonstrated an electrochemical dehydroxylative arylation using an undivided cell with a graphite anode, a nickel foam cathode with $NiBr_2$/dtbbpy as the catalyst, a distinct excess (3 or 7 equiv.) of PPh_3, *N*,*N*-diisopropylethylamine (DIPEA) as base and LiBr as additive (Scheme 4-23A).[138] A range of primary and secondary alkyl alcohols as well as allylic and benzylic alcohols were coupled under the developed conditions. Additionally, late-stage arylation of several natural products and pharmaceuticals demonstrated the utility of the method. Mechanistically, LiBr is anodically oxidized to Br_2, which reacts with PPh_3 to PPh_3Br_2. This brominating agent activates the alcohol *in situ* by the Appel reaction, generating the alkyl bromide **327**, which could undergo single-electron reduction to produce an alkyl radical **328**. The nickel catalytic cycle follows a radical-chain mechanism, in which the alkyl radical is intercepted by nickel(II) complex **329**. The formed nickel(III) complex **330** delivers the product after reductive elimination (Scheme 4-23A).[138]

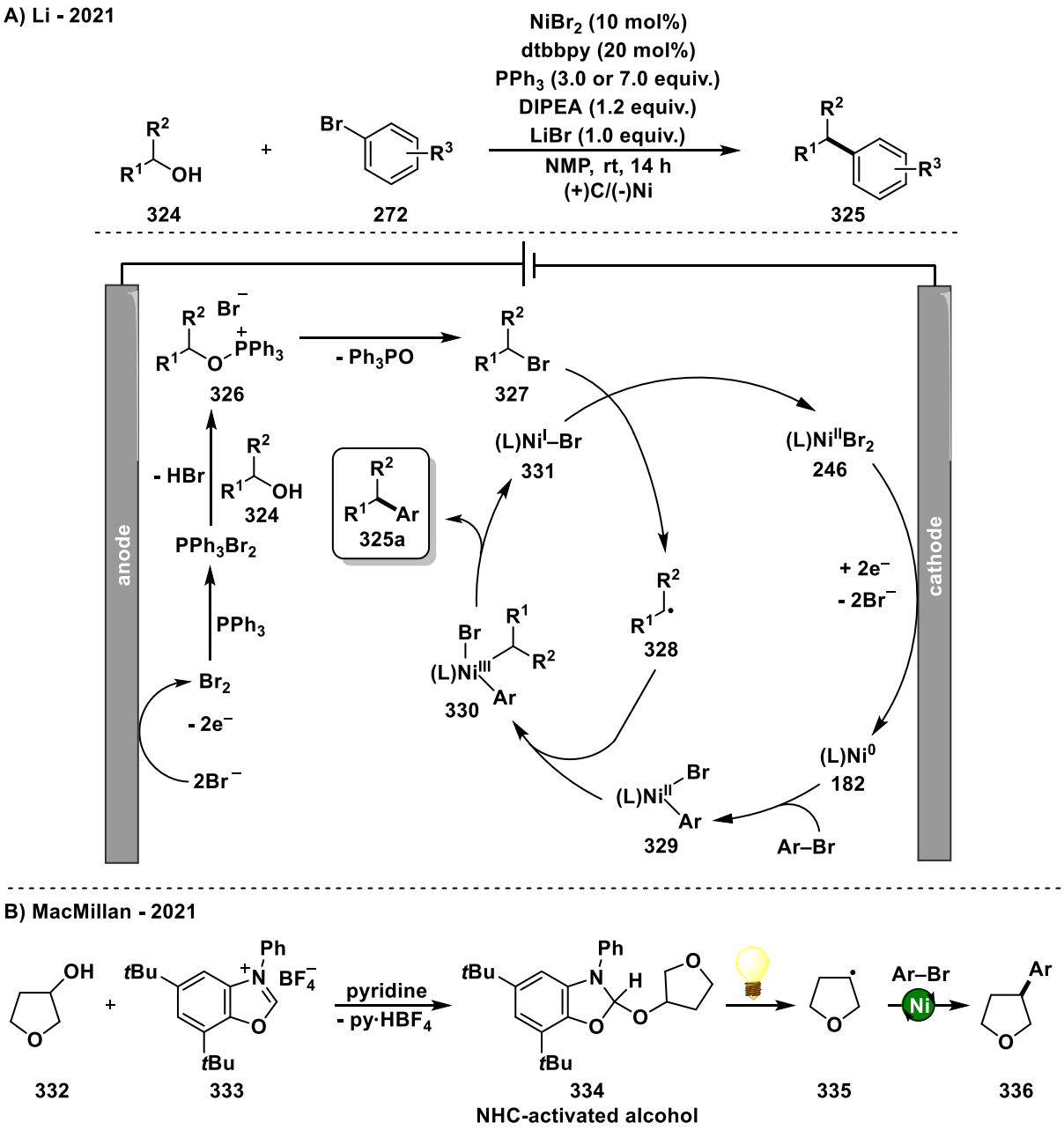

Scheme 4-23: A) Electrochemical and B) NHC-mediated alcohol activation.[138,139]

MacMillan and co-workers have made substantial progress in the field of coupling *O*-electrophiles under photoredox catalysis. In an early report and in collaboration with the Doyle group, MacMillan introduced the synergistic photoredox and nickel-catalyzed decarboxylative coupling of amino acids with aryl bromides.[140] In addition, a deoxygenative coupling of alcohols was developed in which these are activated *in situ* with *N*-heterocyclic carbene (NHC) salts, resulting in NHC-activated alcohols, e.g. species **334**, which can be coupled under photoredox and nickel catalysis with aryl bromides (Scheme 4-23B).[139] Further developments showed that the NHC-activated alcohols can be also reacted under iron catalysis [141] and the activation method is suitable for the coupling of alcohols and carboxylic acids under visible light photoredox and nickel catalysis.[142] In this protocol, radical formation

occurs from alcohols *via N*-heterocyclic carbene-mediated deoxygenation and from carboxylic acids *via* hypervalent iodine-mediated decarboxylation. The selectivity is controlled by radical sorting based on differences in the relative stabilities (more stable tertiary alkyl radical from the carboxylic acid), Ni–C bond strength (stronger Ni–C bond from primary alkyl radical derived from the alcohol) and the reversibility of radical capture for hindered alkyl radicals.[142] NHC-mediated radical generation of alcohols under irradiation in the absence of a nickel catalyst was further used for the conjugated alkylation of Michael acceptors[143] and alkenes.[144]

Besides NHC activation, other strategies for the activation of strong C–O bonds under photoredox catalysis have been demonstrated. Radicals are generated from alcohols or carboxylic acids when implementing them with a phosphine-centered radical cation, accessible under photoredox-catalyzed SET with PPh_3. Polar nucleophilic reaction to the cation with the C–O compound (alcohol or carboxylic acid) would generate a phosphoranyl radical, which can undergo β-scission, delivering the corresponding radicals and triphenylphosphine oxide.[145]

Additionally, C(sp^3)–OH bond cleavage can be achieved by the activation of free alcohols with a neutral diphenyl boryl radical generated from sodium tetraphenylborate under visible light conditions.[146]

4.1.5.2.10.2 *In situ* Generation of a More Reactive Species Using Thermal Activation

Bypassing the low reactivity of alcohols by generating a more reactive species *in situ* is a common approach not only in electro- and photochemistry, but also in thermal catalysis. The high reduction potentials of alcohols are circumvented by C–O bond activation resulting in easier one-electron reduction to generate carbon radicals, which can participate in nickel-catalyzed cross-electrophile couplings (Scheme 4-24).

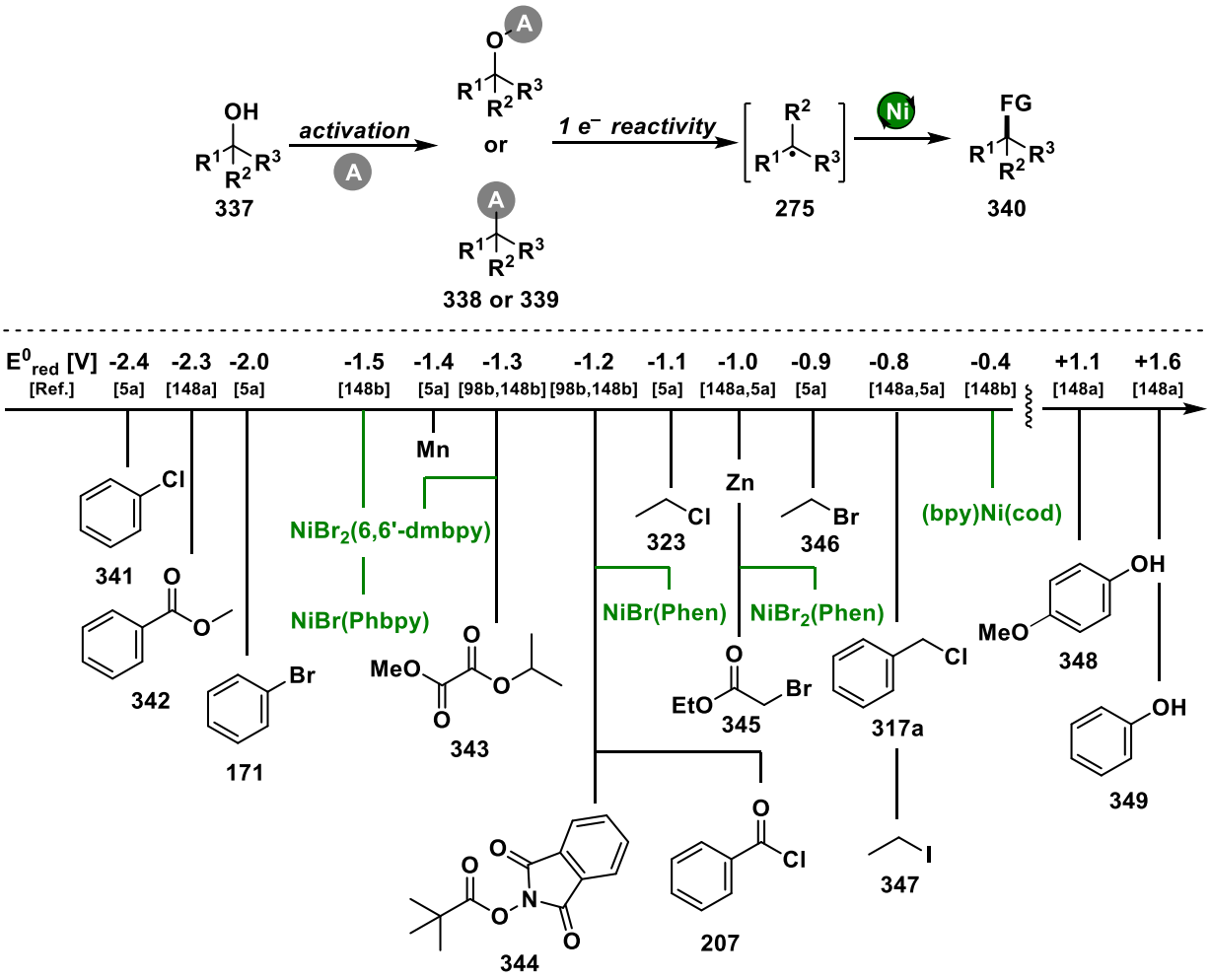

Scheme 4-24: Radical deoxyfunctionalization strategy,[147] and rough comparison of reduction potentials of XEC-relevant species.[5a,98b,148] Nickel(II/I) potentials are shown. Reduction potentials are listed as E^0_{red} *vs.* SCE, and the values originally reported *vs.* Fc/Fc^+ were converted to V *vs.* SCE using $E^0_{red}(Fc/Fc^+)$ = +0.400 V *vs.* SCE.[40]

In 2015, Weix and co-workers showed the nickel-catalyzed cross-electrophile coupling of benzylic alcohols and aryl halides.[35a] Here, the active species of the alcohol coupling partner was an *in situ* generated mesylate **351**, from which radical formation with cobalt phthalocyanine (Co(Pc)) as a co-catalyst can occur more easily (Scheme 4-25A). After oxidative addition of the aryl halide to nickel(0), the generated nickel(II) complex intercepts the

benzyl radical, which thereby selectively reacts with the aryl halide to form the cross-coupled product after reductive elimination.

A dynamic kinetic cross-electrophile coupling was reported by Shu and co-workers, who demonstrated the direct functionalization of benzyl alcohols by (hetero)aryl electrophiles under nickel catalysis.[149] The pivotal step of the reaction is the nickel/manganese-catalyzed *in situ* transesterification of benzylic alcohols by dimethyl oxalate (DMO) as activator. It was proposed that the transesterification is initiated by the single-electron reduction of DMO with Ni^0/Mn to afford a radical anion intermediate. A proton exchange with the benzyl alcohol **350** gives an alcohol anion Bn–O^-, which can participate in the base-catalyzed transesterification of DMO, generating oxalate **354**. The latter serves as a radical source and is thus involved in the catalytic cycle (Scheme 4-25B). The approach was extended to alkenyl triflates as coupling partners.[150]

Almost simultaneously, two different approaches for the *in situ* bromination of alcohols were published (Scheme 4-25C). Gong used the combination of CEBO and TBAB,[151] while Weix solved the activation of alcohols by bromination using Hendrickson's POP reagent, TBAB and Barton's base.[152] With the combination of CEBO and TBAB, primary and secondary alcohols were brominated prior to the subsequent nickel-catalyzed reductive coupling with aryl halides. In short-chained diols, the bromination showed excellent mono-selectivity due to an intrinsic inductive effect upon formation of an OEBO intermediate **359** containing an iminium cation (Scheme 4-25C). For longer chained diols, the mono-selectivity was considerably enhanced by a slow addition of CEBO and TBAB *via* syringe pump.[151]

In Weix' system, inactivated 1° and 2° alcohols were brominated with POP/TBAB within one minute before being combined with aryl halide, $NiBr_2$(DME) as catalyst and two different ligands. The potential of the method in parallel synthesis applications was demonstrated by successfully coupling all combinations of alcohols with 12 aryl halides on a 96-well plate.[152]

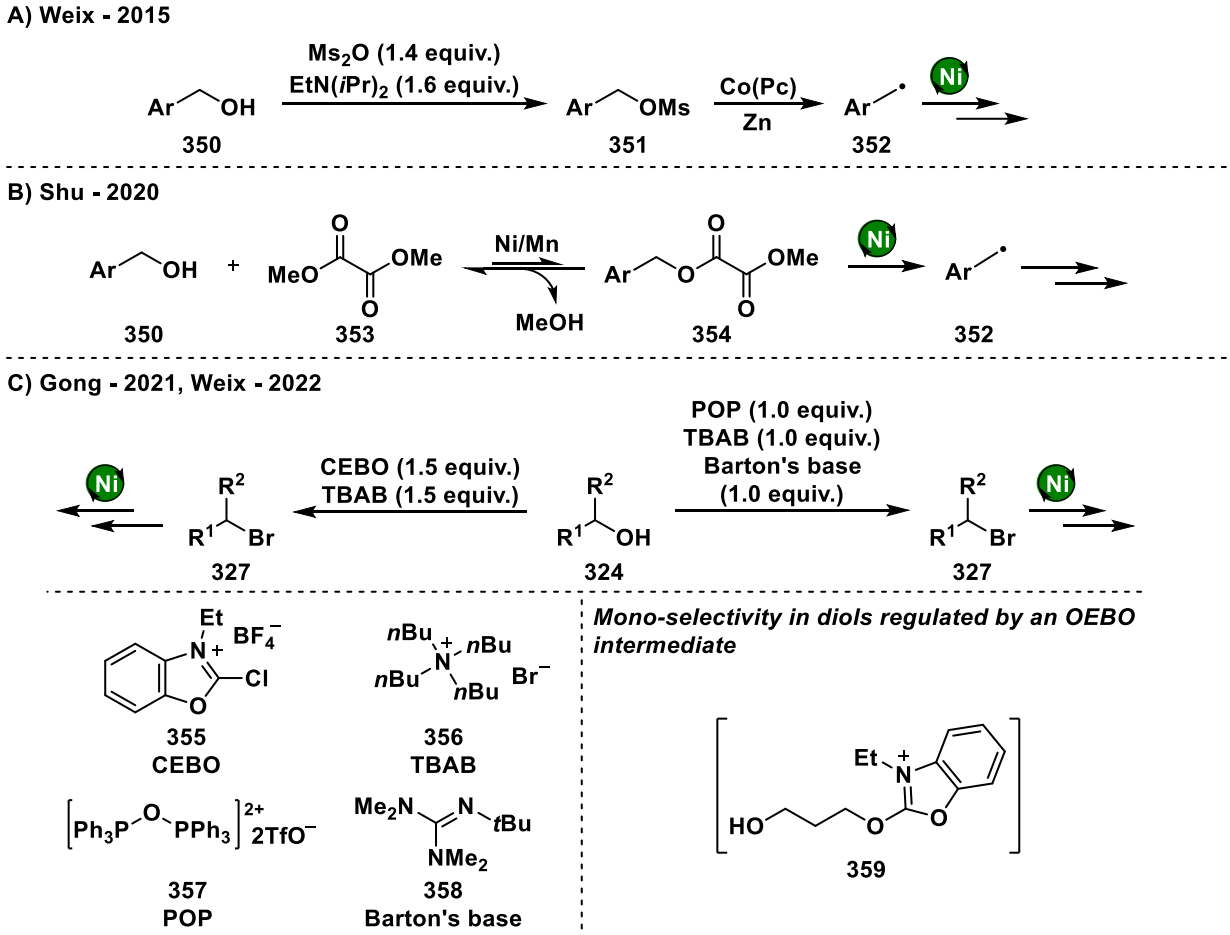

Scheme 4-25: Different approaches for the *in situ* activation of alcohols under thermal catalysis.[35a,149,151,152]

4.1.5.2.10.3 Lewis Acid Activation

Facilitating reactions by Lewis acid activation is a common tool in organic synthesis that has been used for years.[153] Pearson's HSAB (hard and soft acids and bases) concept serves as a theoretical framework, delineating in thermodynamic and kinetic terms that hard acids prefer to associate with hard bases, and soft acids prefer to associate with soft bases.[154] Under transition metal catalysis, Lewis acids normally do not change their oxidation states and are usually considered to activate unsaturated C–heteroatom bonds through σ-coordination or *via* formation of adducts.[155] The beneficial effects of Lewis acids in transition metal-catalyzed reactions lie in the promotion of reactivity, the increase of selectivity or even in the change of the reaction direction.[134] Exploiting this, several cooperative metal and Lewis acid-promoted approaches are shown in the literature.[156]

In the next sections, characteristic properties of the Lewis acids Cp_2TiCl_2 and Cp_2TiCl are outlined, and a literature overview is given regarding titanium-catalyzed dehydroxylative functionalization of alcohols. The interaction of titanium-based Lewis acids in cooperative systems with nickel is also demonstrated. The section is closed with applications of other Lewis acids in cross-electrophile couplings.

4.1.5.2.10.3.1 Characteristics of Cp_2TiCl_2 and Cp_2TiCl Lewis Acids

Titanium, the 9th most abundant element (0.63%) in the Earth's crust, is one of the cheapest and nontoxic transition metals. With the electron configuration of [Ar] $4s^2$ $3d^2$, the metal has empty orbitals in the valence shell for coordination.[157]

Titanocene chlorides are attractive titanium derivatives due to their stability, simple synthesis, and the associated low prices. In 1954, Wilkinson and Birmingham described the first synthesis of Cp_2TiCl_2 by the reaction of cyclopentadienylsodium with $TiCl_4$.[158] The reduction of titanocene dichloride with a metal reductant, for instance Mg, Zn or Mn, gives the low-valent Cp_2TiCl,[159] a 15-electron d^1 Ti^{III}–Cl species with one unpaired electron, exhibiting a reduction potential of E^0_{red} = -0.8 V *vs.* Fc/Fc^+.[160]

Another characteristic of Cp_2TiCl is the presence of additional empty valence shell orbitals, which leads to its Lewis acidity and enables the coordination of electron-pair donors, demonstrated in several literature applications.[161] Thereby, the acid strength of the titanium species depends on the nature and electronegativity of the substituents. Electron-withdrawing groups such as -F or -Cl increase the acid strength, while electron-donating substituents like alkoxy reduce the acid strength of the titanium atom. Besides electronic effects, the activity of a Lewis acid also depends on the steric hindrance to coordination.[153]

Additionally, the high oxophilicity of titanium should be mentioned,[162] which can be explained with the hard Lewis acidic nature of titanium matching the hard Lewis basicity of oxygen, resulting in strong Ti–O bonds (e.g. $E_{Ti\text{-}O}$ = 112 kcal/mol in $Ti(O\textit{i}Pr)_4$)[163] and making Cp_2TiCl_2 and Cp_2TiCl unique catalysts for single-electron activation of C–O bonds.

In the 1980s, Nugent and RajanBabu laid the groundwork on Cp_2TiCl in synthetic chemistry, with the titanium(III)-induced cyclization of epoxy olefins and the radical ring-opening reactions of epoxides.[164] Therefore, Cp_2TiCl is also known as the Nugent reagent. In these seminal reports, a stoichiometric amount of Cp_2TiCl_2 was required. Gansäuer's pioneer work enabled the catalytic application of Cp_2TiCl_2 using chloride additives such as R_3NHCl and TMSCl for regeneration of the titanium catalyst.[165] Furthermore, Cp_2TiCl and its derivatives found application as single-electron transfer catalysts in free radical reactions,[166] and natural product synthesis.[167]

4.1.5.2.10.3.2 Titanium in Reductive Dehydroxylative Functionalization of Alcohols

The preliminary work on the radical dehydroxylation of alcohols was already reported in 1965 by Schwartz, who showed that the reaction of alkoxides with $TiCl_4$ yielded dichlorotitanium(IV) dialkoxide, which can be reduced with potassium to titanium(II) dialkoxide.[168] After the thermal decomposition of the latter titanium(II) species, homocoupling occurs, leading to alkyl dimers.

In 2010, Barrero demonstrated the dehydroxylation of various allylic and benzylic alcohols by the combination of stoichiometric amount of Cp_2TiCl_2 and manganese.[169] The catalytic approach with 30 mol% Cp_2TiCl_2 was established in the presence of TMSCl (4 equiv.). Supported by DFT computations, coordination of alcohol to $Cp_2Ti^{III}Cl$ occurs, forming complex **361**, which undergoes C–O bond homolysis to generate a carbon radical **185**. The latter recombines with another $Cp_2Ti^{III}Cl$, generating species **363**, and after protonation by an acidic quench, the dehydroxylated product is delivered (Scheme 4-26).[169]

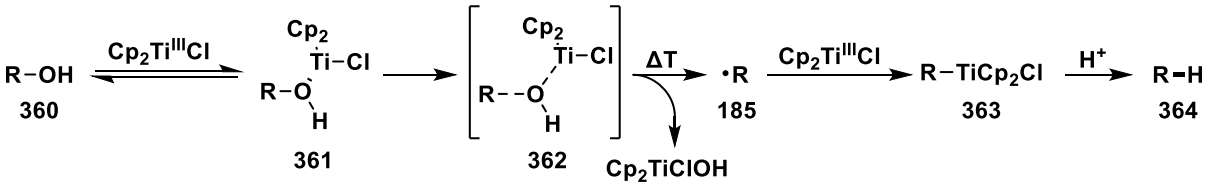

Scheme 4-26: Proposed mechanism for the titanium(III)-mediated alcohol deoxygenation.[169]

Besides homocoupling or protonation, the formed carbon radicals from alcohols can also react with alkenes. Zheng and Huang reported a dehydroxylative radical coupling of hemiaminals with activated alkenes using a Cp_2TiCl_2/Mg/TMSCl catalyst system.[170] The system is widely applicable, including esters, Weinreb amides, nitriles and ketones, and has been applied in the total synthesis of (±)-9,10-diepi-stemoamide. Mechanistically, they proposed the *in situ* chlorination of the hemiaminal with TMSCl to form chlorolactam, from which a radical is formed by Cp_2TiCl.[170]

In 2018, Ukaji reported the low-valent titanium-mediated radical conjugate addition using benzyl alcohols as radical source and electron-deficient alkenes.[171] The combination of $TiCl_4$(col) (col = 2,4,6-collidine) and manganese generates a low-valent titanium species, which can react with benzyl alcohols to a titanate. After thermal decomposition, a benzyl radical is delivered and Giese-type radical addition of the latter to alkenes follows.

Analogously to this report, the group developed more similar Ti/Mn systems and extended the substrate scope. For instance, the $TiCl_4$(col)/Mn system can be also used for the coupling of benzyl alcohols and 2-carboxyallyl acetates.[172]

A change to $TiCl_4$(TMEDA)/Mn (TMEDA = tetramethylethylenediamine) enables the generation of an α-alkoxy radical species from acetals.[173] With $TiCl_2$(cat)/Zn

(cat = catecholate), inactivated primary, secondary and tertiary alcohols can be coupled with alkenes, yielding the deoxy-alkylated products **365** (Scheme 4-27).[131] However, high reaction temperatures are partly required for the reaction: 120 °C for secondary and tertiary alcohols, even 140 °C for primary substrates and only 70 °C for benzylic alcohols. Several mechanistic experiments demonstrated that the 1:2 complex **367** of alcohol and Ti(IV) is reduced by three-electron reduction to a Ti(III)-alkoxide **368** and H_2. The rate-determining step is the cleavage of the C–O bond, resulting in formation of radical **185**. A pathway containing a C–Cl species **369** was excluded. The radical species reacts with the alkene, and the product is delivered either after a metalation *via* species **371** and subsequent protonation or by a titanium-promoted HAT **372** from DMA as solvent (Scheme 4-27).[131]

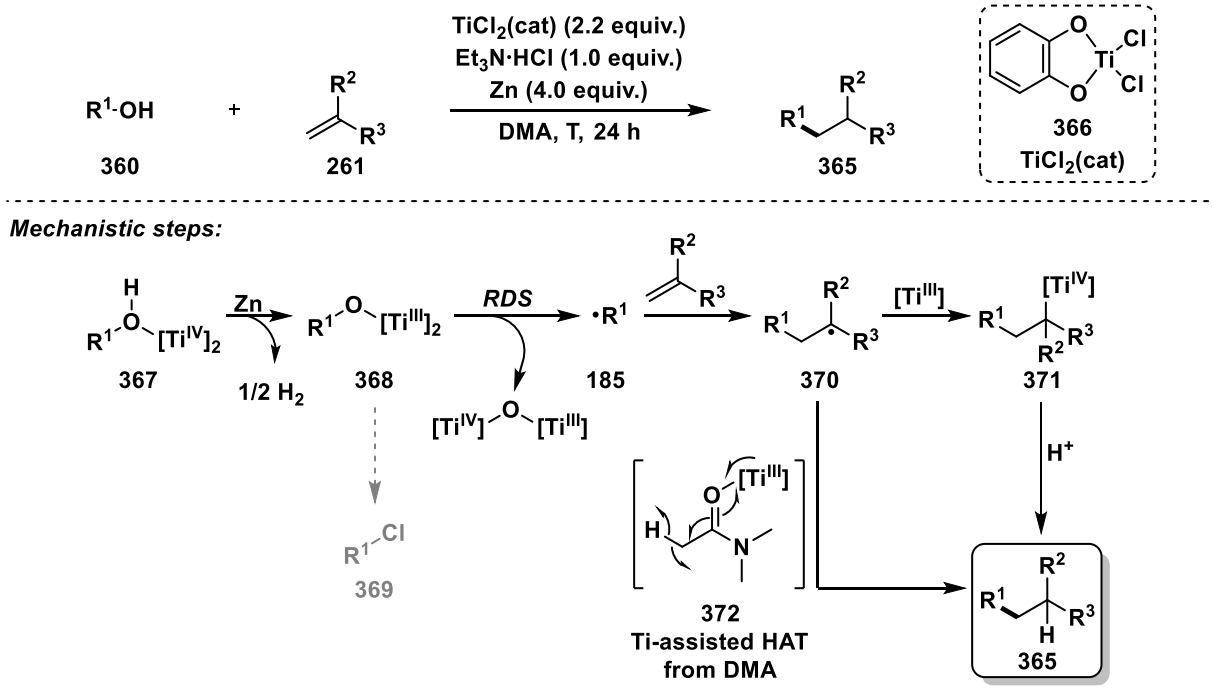

Scheme 4-27: Titanium-mediated carbon radical formation from aliphatic alcohols.[131]

A milder reaction temperature (60 °C) is sufficient for the coupling of tertiary alkyl alcohols with electron-poor alkenes using 10 mol% Cp*$TiCl_3$, zinc as reductant and TESCl as regenerating agent for titanium(IV).[174] Various cyclic and acyclic alcohols were coupled and all-carbon quaternary centers were generated in biologically active compounds such as (+)-Cedrol and Gomisin A. The substrate scope was extended to alkenyl halides, which afforded preferentially the *E*-products after the reaction with tertiary alcohols.[175] It was suggested that steric effects drive the *E*/*Z* transformation, favoring the *E*-conformation. Additionally, the direct dehydroxylation of tertiary aliphatic alcohols was achieved with the Cp*$TiCl_3$/Zn/TESCl system using $PhSiH_3$ as hydrogen source.[176] Besides a metal reductant, isopropyl alcohol can be used as reducing agent for the titanium-catalyzed dehydroxylative dimerization of benzylic alcohols under photoirradiation.[177]

4.1.5.2.10.3.3 Dual Nickel/Titanium Cooperative Reactions

For the selective coupling of two relatively unreactive electrophilic substrates, cooperative reactions, in which each substrate is activated separately in a catalytic or stoichiometric manner by different metals, are one possible way to achieve this goal. The combination of nickel and titanium is highly suitable for this, as titanium has been demonstrated to generate carbon-centered radicals that can be scavenged from nickel by its versatile oxidation states.

As aforementioned in section 4.1.5.1.5, Cp_2TiCl_2 was used to activate nitriles enabling the nickel-catalyzed coupling with organobromides, yielding symmetric ketones.[88] In this system, zinc and TMSCl were applied as additives.

Cuerva used nickel/titanium-based systems for allylation reactions. Amongst others, with allylic carbonates, intramolecular Oppolzer-type cyclization and allylation occurs with 20 mol% $NiCl_2(PPh_3)_2$ and an excess of Cp_2TiCl_2.[178] Furthermore, they applied 10 mol% $NiCl_2(PPh_3)_2$, 40 mol% Cp_2TiCl_2 and the combination of TMSCl, 2,4,6-collidine and manganese as regenerating agents in the nickel(0)/titanium(III)-catalyzed allylation of aldehydes and ketones.[179] Allyl carbonate was used as allylating reagent, while crotyl and prenyl derivatives were unreactive.

In another nickel/titanium bimetallic protocol, two different reactions can occur, namely a Heck- or a reductive cyclization of alkyl iodides, while the chemoselectivity is controlled by the absence or presence of water.[180]

Another protocol described the nickel/titanium-mediated inter- and intramolecular conjugate addition of aryl or alkenyl halides and triflates to α,β-unsaturated carbonyls.[181] The intermolecular reaction requires a considerable excess of acrylate (10 equiv.) as well as 20 mol% $NiCl_2$, 0.7 equiv. Cp_2TiCl_2, PPh_3 as ligand, manganese and TMSCl. Mechanistically, the catalytic cycle of the intermolecular addition of aryl halide to methyl acrylate could be initiated by the oxidative addition of aryl halide to nickel(0) and the coordination of acrylate, generating a nickel(II) complex. Subsequently, 1,2-insertion into the α,β-unsaturated carbonyl could occur, generating a nickel(II) enolate. Instead of a β-hydride elimination process, a transmetalation follows, producing a titanium(III) enolate and recovering the initial nickel(II) catalyst. Cp_2TiCl would play a dual role in the mechanism by favoring the more efficient reduction of the nickel(II) species to the catalytically capable nickel(0) through a Lewis acidic interaction on the one hand, and by acting as an efficient Lewis acid that activates the α,β-unsaturated carbonyl for the insertion reaction on the other hand.[181]

In the nickel-catalyzed opening of epoxides and coupling with aryl halides, the regioselectivity was controlled by co-catalysis.[182] With an iodide co-catalyst, an opening at the less hindered position occurs *via* an iodohydrin intermediate, and a terminal addition follows. Titanocene dichloride co-catalysis results in the opening at the more hindered

position, probably by coordination of the titanium(III) species to the oxygen, resulting in C–O bond homolysis and formation of a secondary radical.[182]

In a subsequent protocol, *meso*-epoxides were coupled enantioselectively with aryl bromides using a chiral titanocene catalyst, yielding *trans*-β-arylcycloalkanols through a chiral titanium-alkoxide radical intermediate.[183] The chiral ring-opened products were obtained in good yields and in diastereo- and enantiomeric excess.

Another cross-electrophile coupling of epoxides and (hetero)aryl iodides was enabled by the combination of $NiBr_2$(diglyme), Cp_2TiCl_2, and photoredox catalysis, yielding ring-opened products in high regioselectivity.[184] The substrate scope could be extended by the modification of the nitrogen-based ligand for nickel.

Suga and Ukaji accomplished the direct coupling of benzyl alcohols and aryl iodides using $NiCl_2(Me_4Phen)\cdot 2H_2O$ as catalyst and a low-valent titanium reagent generated from $TiCl_4$(lutidine) (lutidine = 2,6-lutidine) and manganese (Scheme 4-28).[185] The substrate scope could be extended to alkenyl halides[186] and triflates.[187] Mechanistically, oxidative addition of aryl iodide to nickel(0) initiates the catalytic cycle. Then, one-electron oxidative addition of a benzyl radical presumably results in a nickel(III) complex **376**. After reductive elimination, diaryl methane is delivered. The benzyl radical is supplied to the main catalytic cycle *via* species **374** and a low-valent titanium-mediated homolytic C–O bond cleavage (Scheme 4-28).[185]

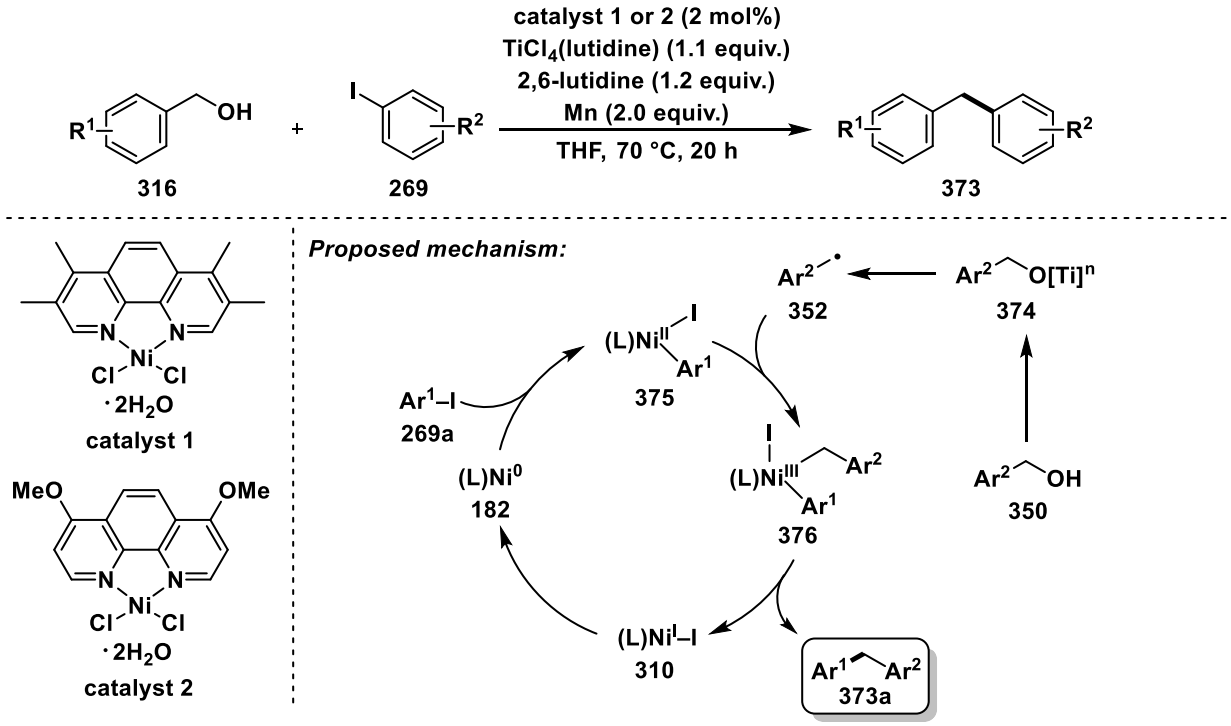

Scheme 4-28: Direct nickel-catalyzed cross-electrophile coupling of benzylic alcohols and aryl halides.[185]

4.1.5.2.10.3.4 Other Lewis Acid Activation of Alcohols in XEC

In addition to titanium-based Lewis acids, further examples of acids are given, which activate *O*-electrophiles in cross-electrophile couplings.

For instance, $ZrCl_4$[188] or $MgCl_2$[189] are suitable for the coupling of allylic alcohols. In 2018, the Shu group reported the cross-electrophile coupling of aryl halides with allylic alcohols using 10 mol% $NiCl_2$(dppp), 20 mol% bpy, 10 mol% $ZrCl_4$ and manganese as reducing agent.[188] Mechanistic studies revealed that probably a double oxidative addition pathway is operative, in which the second oxidative addition is facilitated by Lewis acid activation of the allylic alcohol.[188] In a nickel-catalyzed coupling of aryl chlorides and allylic alcohols, a stoichiometric amount of $MgCl_2$ was required for activation, which presumably occurs through the coordination of Mg^{2+} to oxygen of the alcohol.[189]

Rahaim and co-workers showed an elegant way to directly couple benzylic alcohols and aryl bromides under nickel catalysis using TMSCl as additive (Scheme 4-29).[190] Cp_2TiCl_2 as co-catalyst was not needed, but TMSCl was necessary to enable the reaction. Diarylmethanes or 1,3-diarylpropenes were generated in moderate to high yields. The reaction strongly depended on the presence and position of electron-donating substituents on the benzyl alcohols. The electron-rich *para*-methoxy benzyl alcohol was the most effective benzyl alcohol, while switching -OMe to the *ortho*- or *meta*-position led to decreased yields. Additionally, more active benzyl allyl alcohols were suitable substrates. Benzyl alcohols with electron-withdrawing groups were completely unreactive.

Several mechanistic experiments showed that a silyl ether is not the active species in the developed coupling. Furthermore, full conversion of electron-rich, electron-neutral, and electron-poor benzyl alcohols to benzyl chlorides was observed with TMSCl in DMA. Therefore, the *in situ* formation of a chloride from the respective alcohol was investigated. Electron-rich, electron-neutral and electron-poor benzyl chlorides were subjected to the reaction conditions, but the desired products were yielded for electron-rich and electron-neutral substrates. In contrast, only electron-rich benzylic alcohols enabled product formation, wherefore an *in situ* formation of a chloride was excluded in the presence of the nickel catalyst and manganese. Radical scavenging experiments with TEMPO probably indicated the occurrence of radical intermediates.[190]

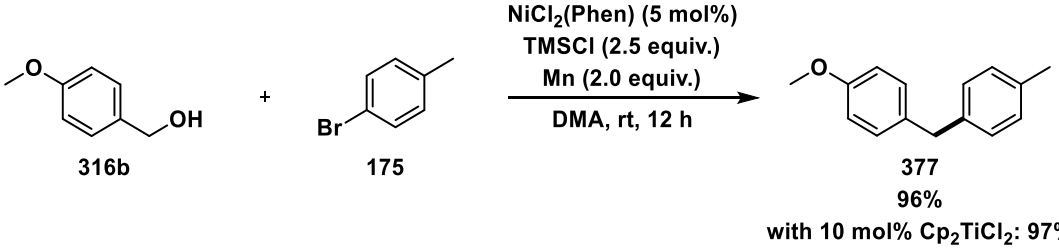

Scheme 4-29: TMSCl-assisted and nickel-catalyzed deoxygenative coupling of benzylic alcohols and aryl bromides.[190]

4.2 Aims of This Chapter

The field of cross-electrophile couplings using sustainable, but difficult-to-couple substrates is a constantly growing area of current research. Despite the potential of thioesters as acyl sources, they have not yet been sufficiently explored in ketone synthesis *via* cross-electrophile couplings, and it is required to expand the scope of electrophiles to include these substrates. In addition, although they are characterized by beneficial properties, the direct deoxygenative participation of free alcohols in ketone syntheses *via* nickel-catalyzed cross-electrophile couplings is unknown, as this substrate class poses several challenges (*vide supra*). Therefore, there is a strong incentive to advance the direct homolytic activation of strong C–O bonds and thereby enable coupling with acyl sources.

We envisioned to overcome the limitations of the direct nickel-catalyzed cross-electrophile coupling of benzylic alcohols and thioesters by Lewis acid promotion, selectively activating these sustainable and highly desirable substrate classes. To this end, we sought to utilize a cooperative titanium and silicon Lewis acid strategy originally developed by Rahaim and co-workers [190] and substitute aryl bromides with thioesters to gain access to the ketone motif (Figure 4-3, right). Studies on the system were performed to optimize the reaction conditions, followed by exploration of the thioester and benzyl alcohol substrate scope and scrutinizing potential intermediates to gain insight into the mechanism of the nickel-catalyzed and Lewis acid-assisted cross-electrophile coupling of benzylic alcohols and thioesters.

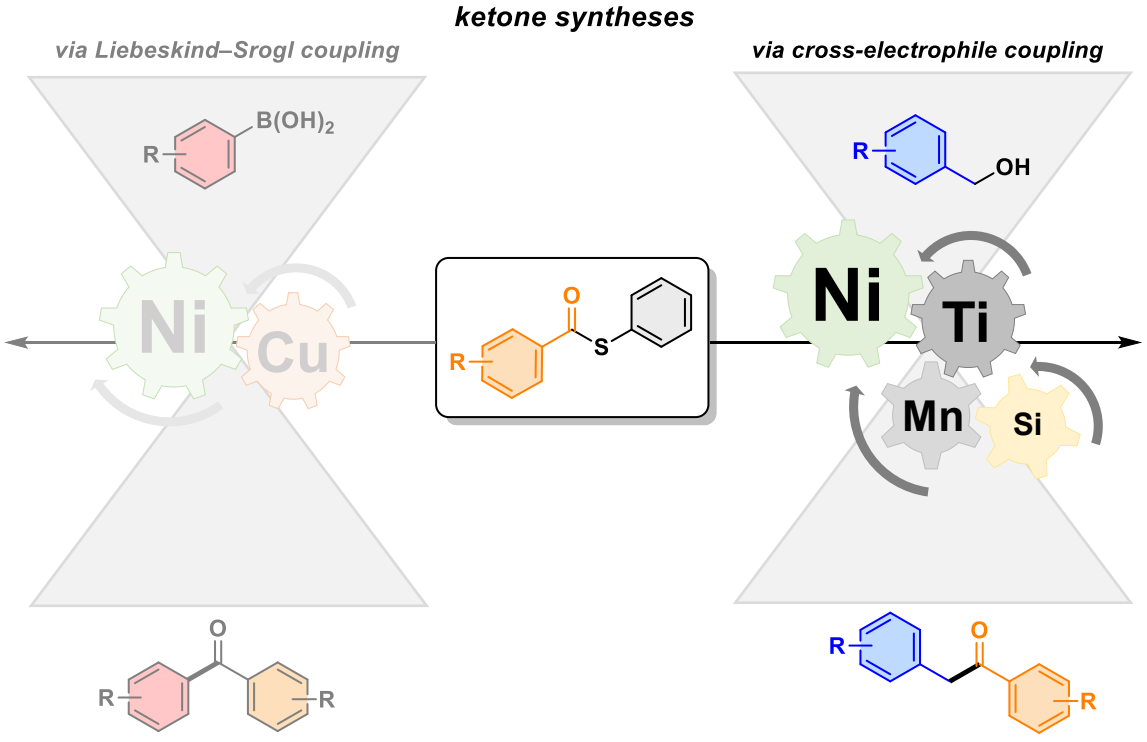

Figure 4-3: Overview of the investigated transformation in the subsequent chapter: thioesters as acylation agents in ketone synthesis *via* nickel-catalyzed and Lewis acid-assisted cross-electrophile coupling.

4.3 Results and Discussion
4.3.1 Optimization of Reaction Conditions
4.3.1.1 Overview of Standard Reaction

The general objective of the author's Master Thesis was to achieve ketone synthesis by the nickel-catalyzed cross-electrophile coupling of sustainable but challenging substrates such as alcohols and thioesters.[1]

Rahaim and co-workers published the nickel-catalyzed deoxygenative cross-electrophile coupling of benzylic alcohols and aryl bromides under the assistance of trimethylsilyl chloride (TMSCl) and reductive conditions affording diarylmethanes (*vide supra*, Scheme 4-29).[190]

Upon slight adjustment of the reaction conditions, it was found that these published reaction conditions enabled the coupling of benzylic alcohols and thioesters, obtaining the desired ketones as products.[1] The reaction of a significant excess (3 equiv.) of 4-methoxybenzyl alcohol (**316b**) and *S*-phenyl benzothioate (**133**) gave ketone **378a** in 63% yield using manganese as reductant, a dual catalyst system consisting of $NiCl_2$(Phen) and Cp_2TiCl_2 as well as TMSCl as additive (Scheme 4-30). Moreover, thioether **379a** was generated in 84% and dimeric oxoether **380** in 21% yield. In addition to these (by)products, the formation of 4-methoxybenzyl chloride (**317b**) and homocoupled product **381** was observed. The theoretically expected transesterification product **382** and disulfide **383a** were not detected under standard conditions (Scheme 4-30). Control reactions showed that the reaction is fully inhibited in the absence of nickel catalyst, TMSCl or manganese.[1]

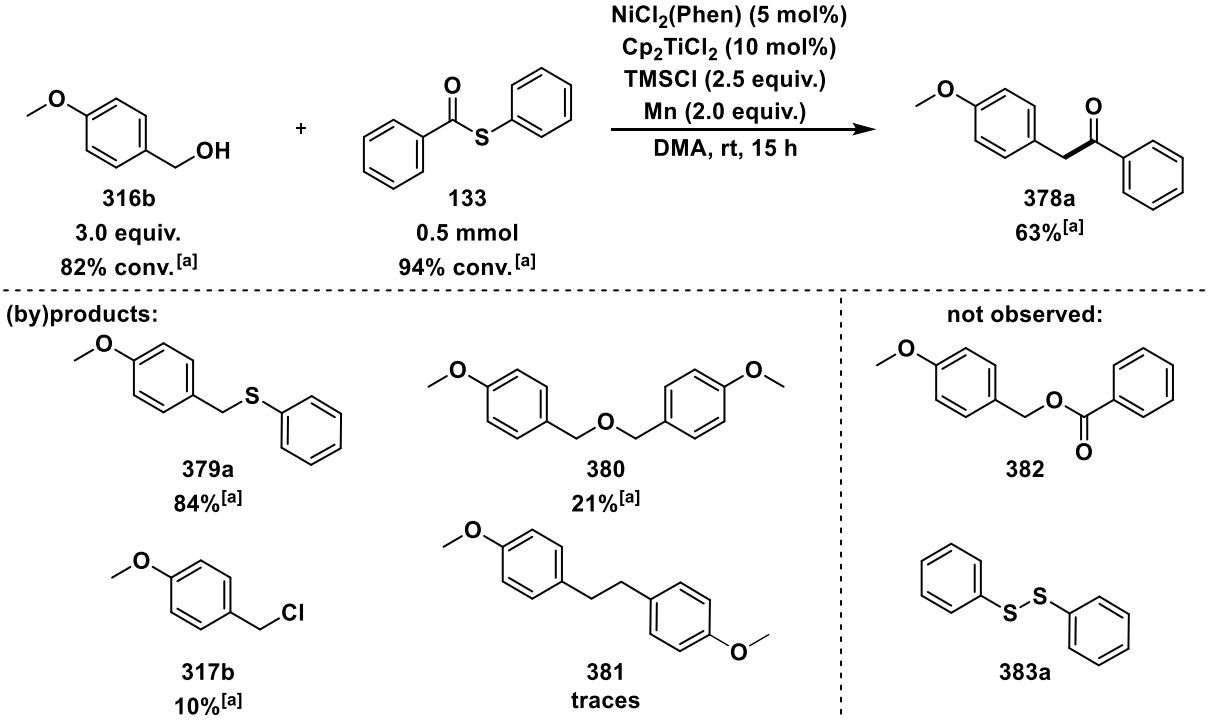

Scheme 4-30: Initial reaction conditions and overview of (by)products for the cross-electrophile coupling of benzylic alcohol and thioester.[1] [a]: Determined by GC-FID using *n*-pentadecane as internal standard.

4.3.1.2 Preliminary Optimization Studies

Selected optimization experiments from the author's Master Thesis are briefly presented (Table 4-3).[1] The initial optimization of the reaction started from 1.5 equivalents of benzylic alcohol **316b**. The variation of the reaction temperature disclosed a detrimental effect on the ketone yield at lower or higher temperature than room temperature (Table 4-3A). Additionally, the solvent influence was strong, and DMA could not be substituted. All tested solvents resulted in yields lower than 10%, with exception of *N*,*N*'-dimethylpropyleneurea (DMPU), which promoted the generation of the ketone in 29% (Table 4-3B). The amount of alcohol **316b** is the limiting factor for ketone formation, as the yield of the desired product is restricted by the competing formation of several (by)products, including thioether **379a** from the released thiolate and oxoether **380**, which reduces the availability of alcohol **316b** for the product-forming reaction step. This consideration was consistent with the experimental results, as doubling the amount of alcohol from 1.5 equivalents to three equivalents also led to a doubling of the ketone yield (Table 4-3C).[1]

Table 4-3: Preliminary optimization studies.[1]

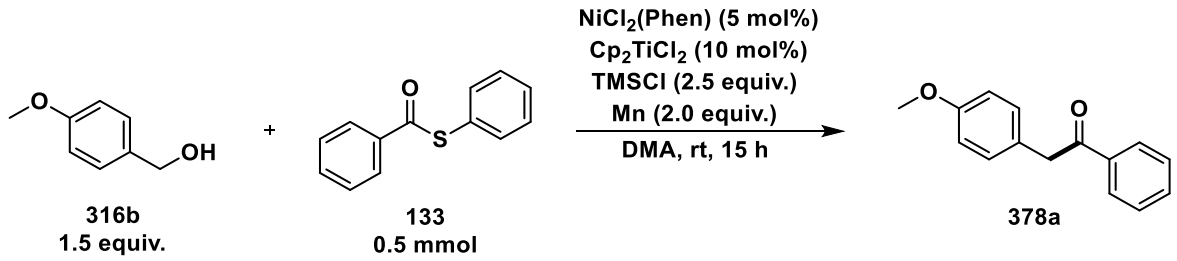

A) Optimization of reaction temperature

Entry	Temperature [°C]	Yield of 378a [%][a]
1	0	✘
2	rt	43
3	30	33
4	40	11
5	80	11

B) Optimization of solvent

Entry	Solvent	Yield of 378a [%][a,b]
1	MeCN	(<5)
2	DMF	(10)
3	DMA	43 (28)
4	NMP	(<5)
5	DMPU	29
6	THF	(<5)
7	PhMe	✘

C) Optimization of alcohol amount

Entry	Amount of 316b [equiv.]	Yield of 378a [%][a]
1	1.5	43
2	2.0	58
3	2.5	73
4	3.0	85

Reaction Conditions: Mn (54.9 mg, 1.00 mmol, 2.0 equiv.), Cp_2TiCl_2 (12.5 mg, 50.0 µmol, 10 mol%), $NiCl_2$(Phen) (7.8 mg, 25 µmol, 5.0 mol%), **133** (107 mg, 500 µmol, 1.0 equiv.), **316b** (93.4 µL, 750 µmol, 1.5 equiv.), TMSCl (159 µL, 1.25 mmol, 2.5 equiv.), rt, 5 min; then abs. DMA (2 mL), rt, 15 h. [a]: Determined by GC-FID using *n*-pentadecane as internal standard; [b]: The number in parentheses indicates the yields determined by ^{1}H-NMR spectroscopy using 1,3,5-trimethoxybenzene as internal standard.

In this thesis, the reaction conditions of the system were further optimized, starting with investigations on the reproducibility of the previous results in relation to the equivalents of alcohol **316b**. Then, it was continued with investigations on the influence of temperature, DMA as solvent, manganese as reductant, the nickel/titanium catalyst system, and the impact of TMSCl and other additives. In addition, the suppression of thioether **379a** and dimeric oxoether **380** was thoroughly examined, ensuring a chemoselective formation of ketone **378a**. Subsequently, the optimized reaction conditions were applied to several thioesters and benzylic alcohols to test the scope of the catalytic reaction. Additionally, a variety of substrates like benzyl chlorides, thiocarbonates and thiocarbamates were subjected to standard conditions. Finally, mechanistic studies were performed to elucidate the nature of intermediates in the dual catalytic cross-electrophile coupling.

4.3.1.3 Variation of Substrate Equivalents

The first step of the optimization process consisted of varying the substrate equivalents. In previous studies shown in Table 4-3, it was found that three equivalents of alcohol result in the highest ketone yield.[1] Due to reproducibility problems of this result, the variation of the alcohol equivalents was repeated (Figure 4-4). The screening revealed the highest ketone yield of 77% with 2.7 equivalents alcohol **316b**. Thioether **379a** and dimeric oxoether **380** were formed in 79% and 22% yield, respectively.

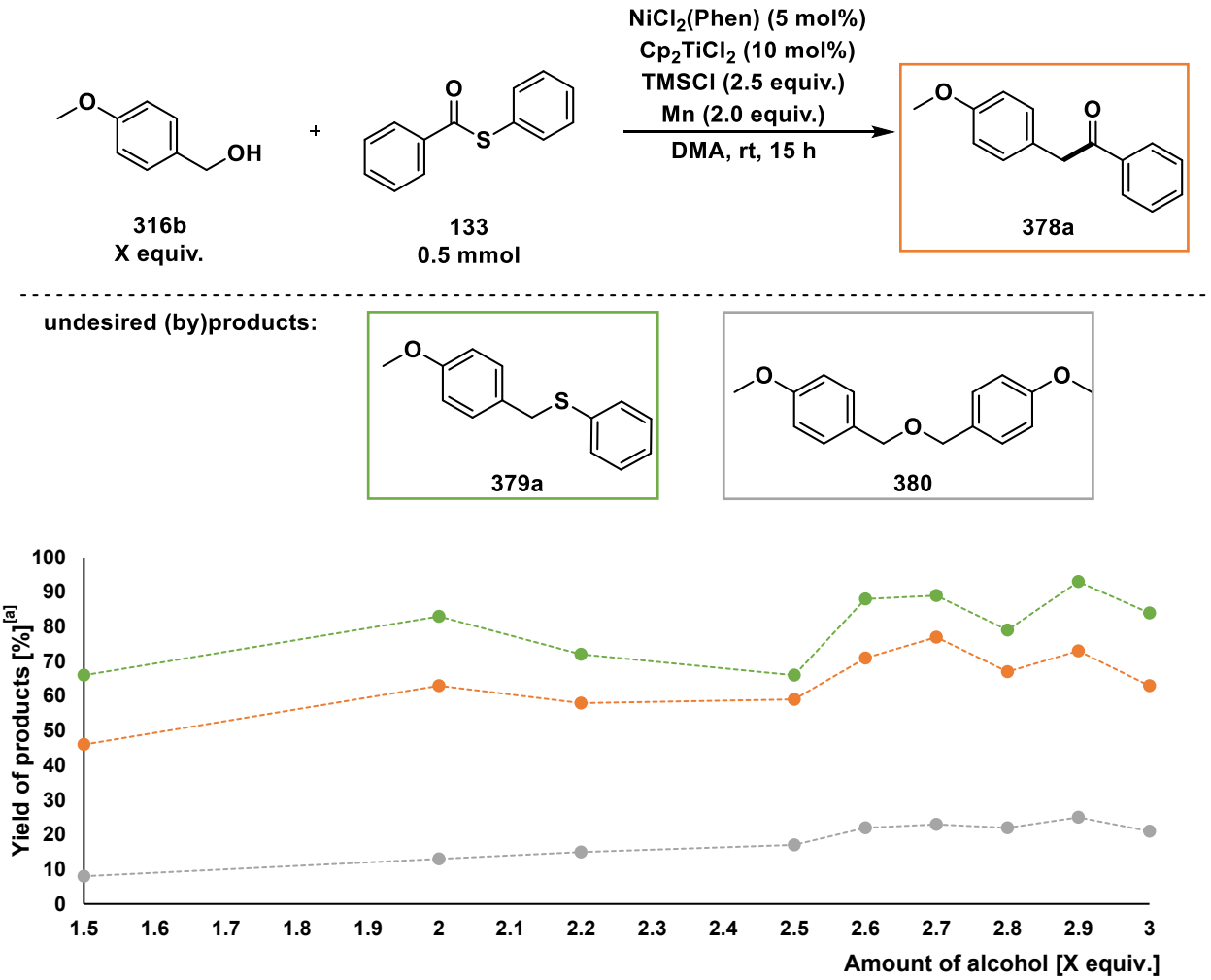

Figure 4-4: Influence of the alcohol amount on (by)product formation. [a]: Determined by GC-FID using *n*-pentadecane as internal standard.

4.3.1.4 Temperature Influence

Subsequently, the temperature influence on the reaction was investigated again (Figure 4-5). At low temperatures of -20 °C and 0 °C, conversion of substrates and formation of products were strongly decreased compared to the reaction at room temperature. With elevated temperatures from 40–80 °C, the yields of thioether **379a** and especially ketone **378a** were reduced despite high conversions of substrates **133** and **316b**. Instead, benzylic dimer **381**, oxoester **382** and disulfide **383a** were formed. The formation of dimeric oxoether **380** was temperature-independent. Due to the unfavorable effects of lower and higher temperatures, the reaction was still conducted at room temperature.

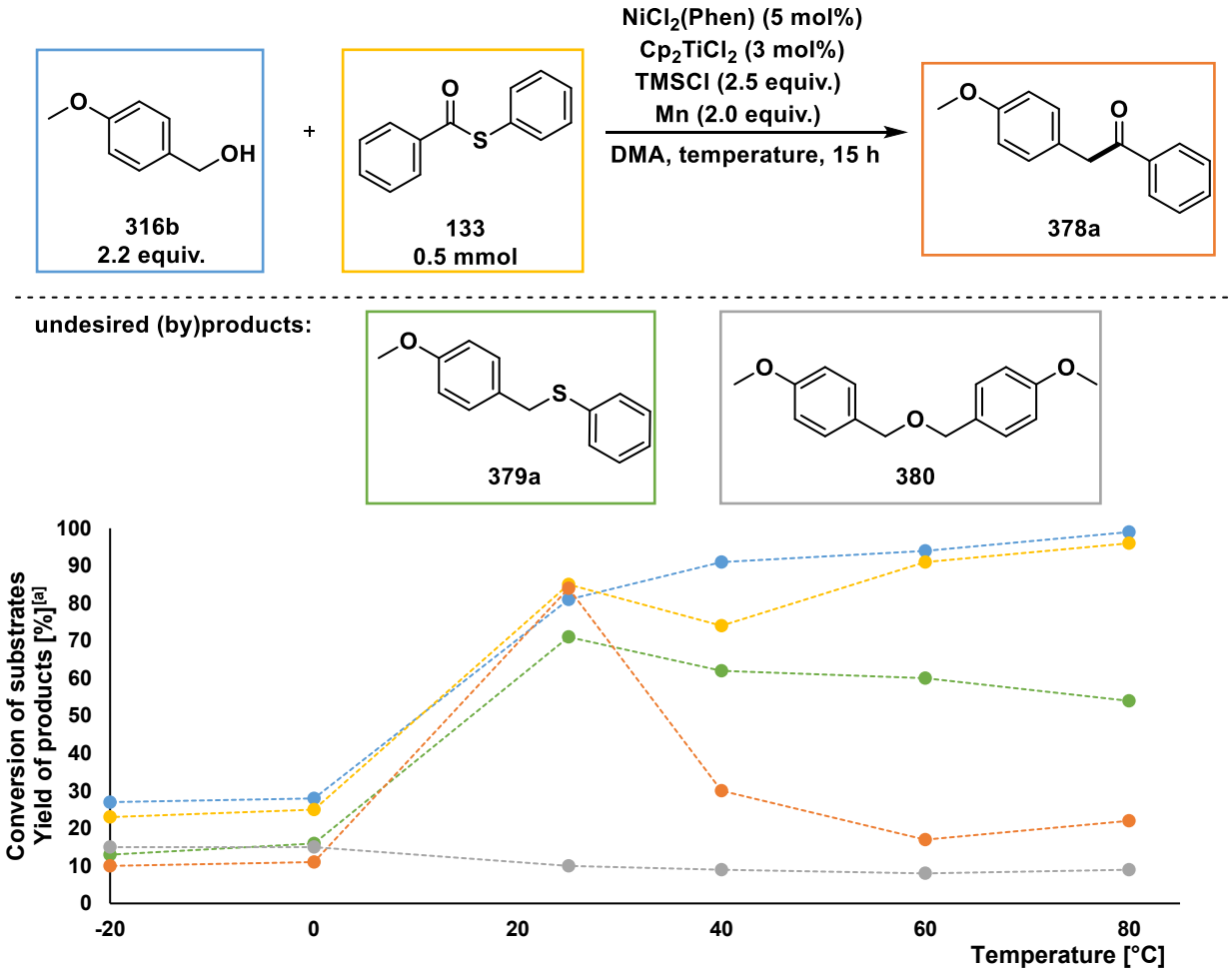

Figure 4-5: Temperature influence on (by)product formation using 2.2 equiv. of **316b** and 3 mol% of Cp_2TiCl_2. [a]: Determined by GC-FID using *n*-pentadecane as internal standard.

4.3.1.5 DMA as Solvent

In continuation of the optimization process, a solvent screening was completed, which had been initiated during the author's Master Thesis.[1] In this previous screening, only 1.5 equiv. of alcohol was applied, evaluating acetonitrile, DMF, NMP, DMPU and toluene as solvents resulting in a diminished yield of ketone **378a** (see Table 4-3).[1] Herein, THF, DME and ethyl acetate were additionally tested (Table 4-4). In THF, a solvent commonly employed in titanium(III) chemistry,[164a,b,191] ketone was detected only in traces (entry 2). The product formation was completely inhibited in DME and ethyl acetate (entries 3, 4). In general, the conversion of thioester **133** was stronger affected and decelerated by the solvent change than the conversion of alcohol **316b**. The formation of dimeric oxoether **380** was again independent of the change in conditions. From this screening it can be deduced that the reaction is strongly dependent on DMA as a solvent.

Table 4-4: Completion of solvent screening.

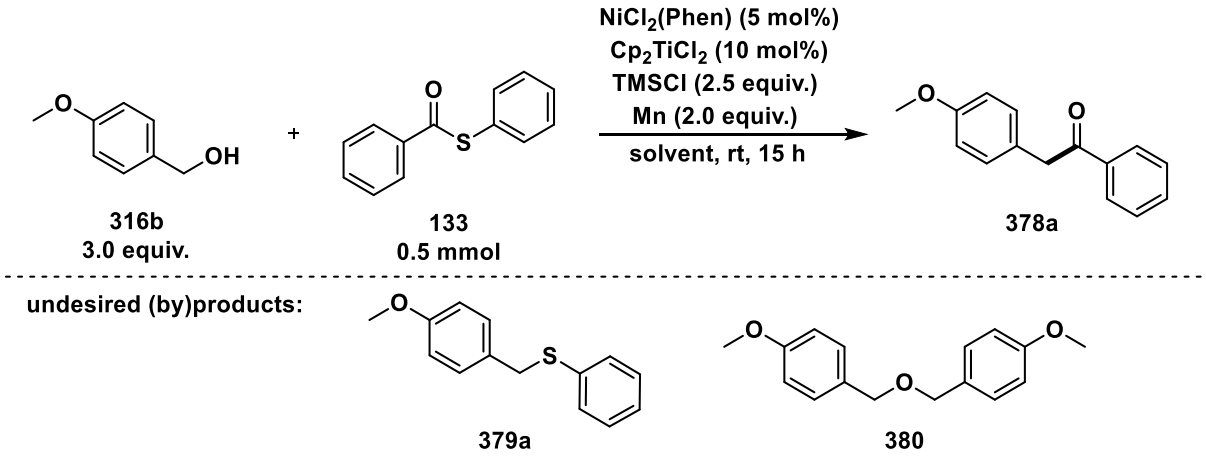

Entry	Solvent	Conv. of 316b [%][a]	Conv. of 133 [%][a]	Yield of 378a [%][a]	Yield of 379a [%][a]	Yield of 380 [%][a]
1	DMA	82	94	84	84	21
2	THF	46	10	5	5	23
3	DME	93	traces	✘	✘	23
4	EtOAc	94	23	✘	✘	20

Reaction Conditions: Mn (54.9 mg, 1.00 mmol, 2.0 equiv.), Cp_2TiCl_2 (12.5 mg, 50.0 µmol, 10 mol%), $NiCl_2$(Phen) (7.8 mg, 25 µmol, 5.0 mol%), **133** (107 mg, 500 µmol, 1.0 equiv.), **316b** (186 µL, 1.50 mmol, 3.0 equiv.), TMSCl (159 µL, 1.25 mmol, 2.5 equiv.), rt, 5 min; then abs. solvent (2 mL), rt, 15 h. [a]: Determined by GC-FID using *n*-pentadecane as internal standard.

In addition to the type of solvent, the sequence of addition was found to be crucial for the reaction and changes in the order of addition resulted in complete inhibition of ketone formation (Scheme 4-31A, B). Therefore, it was continued to add DMA at last, as already done under standard conditions (Scheme 4-31C). Especially the conversion of alcohol **316b** was strongly reduced if the sequence of addition was deviated, while the conversion of thioester **133** was less affected.

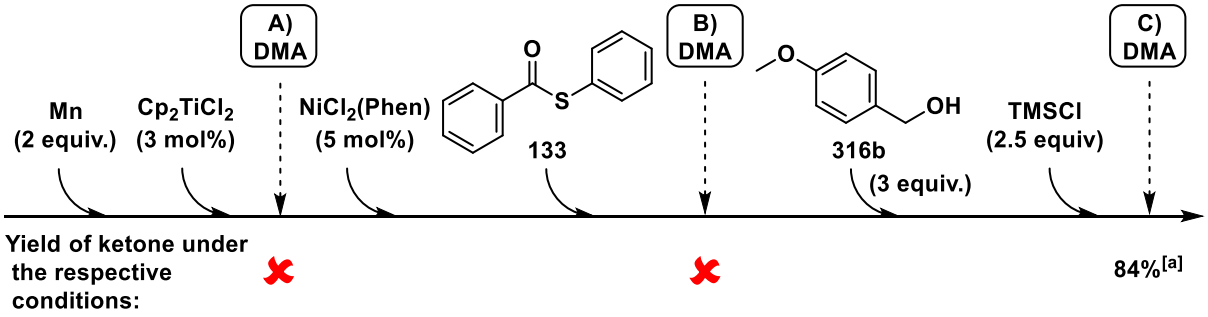

Scheme 4-31: Influence of the order of DMA addition. [a]: Determined by GC-FID using *n*-pentadecane as internal standard.

Finally, increasing the concentration of the reaction mixture by reducing the amount of DMA resulted in low conversions of substrates and proportions of ketone **378a** and thioether **379a** as qualitatively observed by GC-MS analysis.

4.3.1.6 Optimization of Reductant

Following the solvent screening, the influence of amount and type of reducing agent was investigated (Figure 4-6). The reaction was completely inhibited in the absence of an electron donor and the yield was halved when only one equivalent of manganese was employed (Figure 4-6A). Increasing the amount of manganese from two equivalents as under standard conditions to three equivalents led to nearly the same yield of ketone **378a** (71% and 70%, Figure 4-6A).

Additionally, other reductants were applied to the system (Figure 4-6B). It is known in literature that organic electron donors such as tetrakis(dimethylamino)ethylene (TDAE) can be used in cross-electrophile couplings (see section 4.1.4).[36,37] However, TDAE was not suitable for the studied system, as a complete inhibition of substrate conversion and thus product formation was observed in its presence (Figure 4-6B). With zinc, which is less powerful than manganese ($E^0(Zn^{II}/Zn^0)$ = -1.02 V *vs.* SCE compared to $E^0(Mn^{II}/Mn^{0)}$ = -1.44 V *vs.* SCE),[5h] a significant drop in yield of ketone **378a** was determined (9%, Figure 4-6B). Interestingly, the ketone formation was completely inhibited with zinc as reducing agent when replacing thioester **133** with bromine-substituted thioester **140**. The experiments showed that the amount and type of reductant already used was the most appropriate for the developed system.

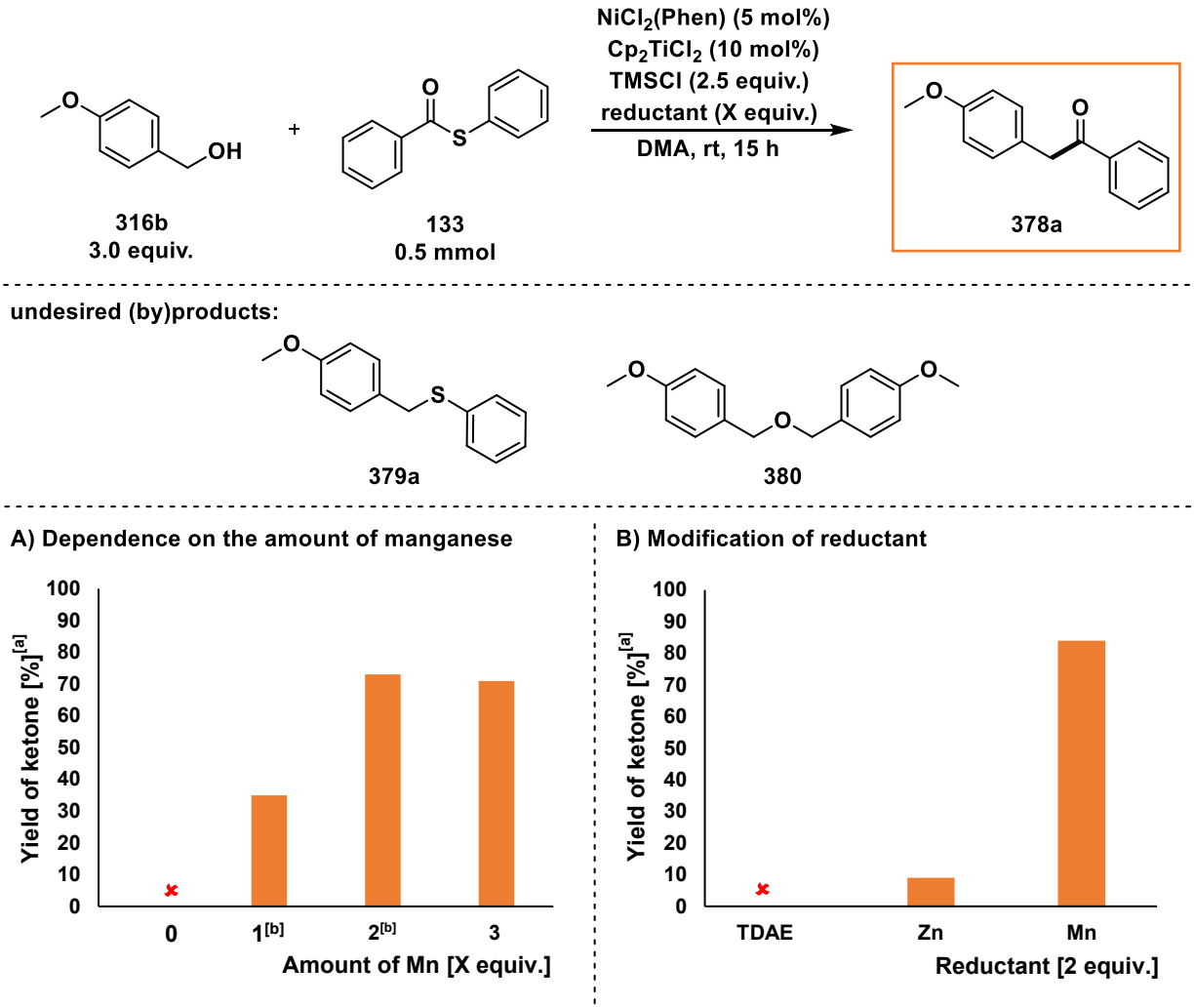

Figure 4-6: A) Dependence of the reaction on the amount of manganese and B) modification of reductant. [a]: Determined by GC-FID using *n*-pentadecane as internal standard; [b]: Thioester **140** instead of **133**, 2.2 equiv. of **316b** and 3 mol% of Cp_2TiCl_2 were used.

4.3.1.7 Optimization of Titanium Catalyst

Next, the titanium catalyst was optimized. In addition to Cp_2TiCl_2, 10 mol% of the Lewis acid base complex $TiCl_4$(lutidine), which is known to generate carbon-centered radicals from benzylic alcohols (*vide supra*, Scheme 4-28),[185] can catalyze the reaction, albeit in reduced yield compared to standard conditions (Table 4-5, entries 1 *vs.* 2).

Table 4-5: Modification of titanium(IV) source.

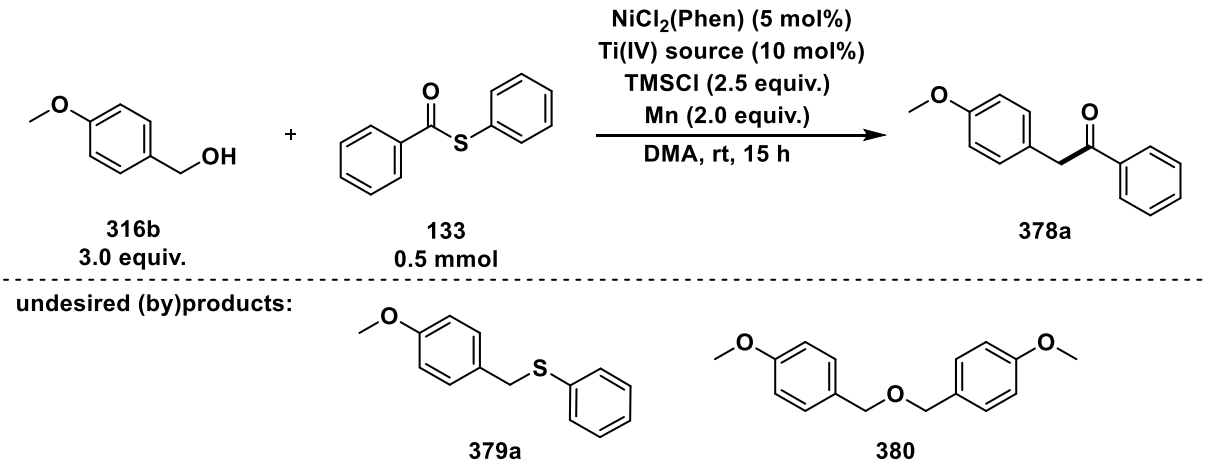

Entry	Ti(IV) source	Conv. of 316b [%][a]	Conv. of 133 [%][a]	Yield of 378a [%][a]	Yield of 379a [%][a]	Yield of 380 [%][a]
1	Cp_2TiCl_2	82	94	84	84	21
2	$TiCl_4$(lutidine)	91	99	64	75	23

***Reaction Conditions*:** Mn (54.9 mg, 1.00 mmol, 2.0 equiv.), Ti(IV) source (50 µmol, 10 mol%), $NiCl_2$(Phen) (7.8 mg, 25 µmol, 5.0 mol%), **133** (107 mg, 500 µmol, 1.0 equiv.), **316b** (186 µL, 1.50 mmol, 3.0 equiv.), TMSCl (159 µL, 1.25 mmol, 2.5 equiv.), rt, 5 min; then DMA (2 mL), rt, 15 h. [a]: Determined by GC-FID using *n*-pentadecane as internal standard.

A control reaction indicated that the developed cross-electrophile coupling between benzylic alcohol **316b** and thioester **133** was successful even in the absence of titanium catalyst, however with significantly lower yield of ketone (31%, Figure 4-7). The result led to the assumption that Cp_2TiCl_2 could act as a co-catalyst by activating the substrates. To determine the interaction of titanium catalyst with each substrate, the respective conversions were monitored in relation to the Cp_2TiCl_2 loading. Hence, a dependence of thioester conversion on the amount of titanium catalyst was observed, whereas the alcohol conversion appeared independent from the titanium catalyst loading (Figure 4-7). In the presence of stoichiometric amount of Cp_2TiCl_2, alcohol **316b** reacted to the benzyl dimer **381** and conversion of thioester **133** was decelerated. With 3 mol% of Cp_2TiCl_2, a high conversion of **133** (94%) and the highest yield of ketone **378a** (83%) were achieved. These experiments showed that the titanium catalyst could be responsible for thioester activation. Further investigations on the role of Cp_2TiCl_2 are presented in section 4.3.3.7.

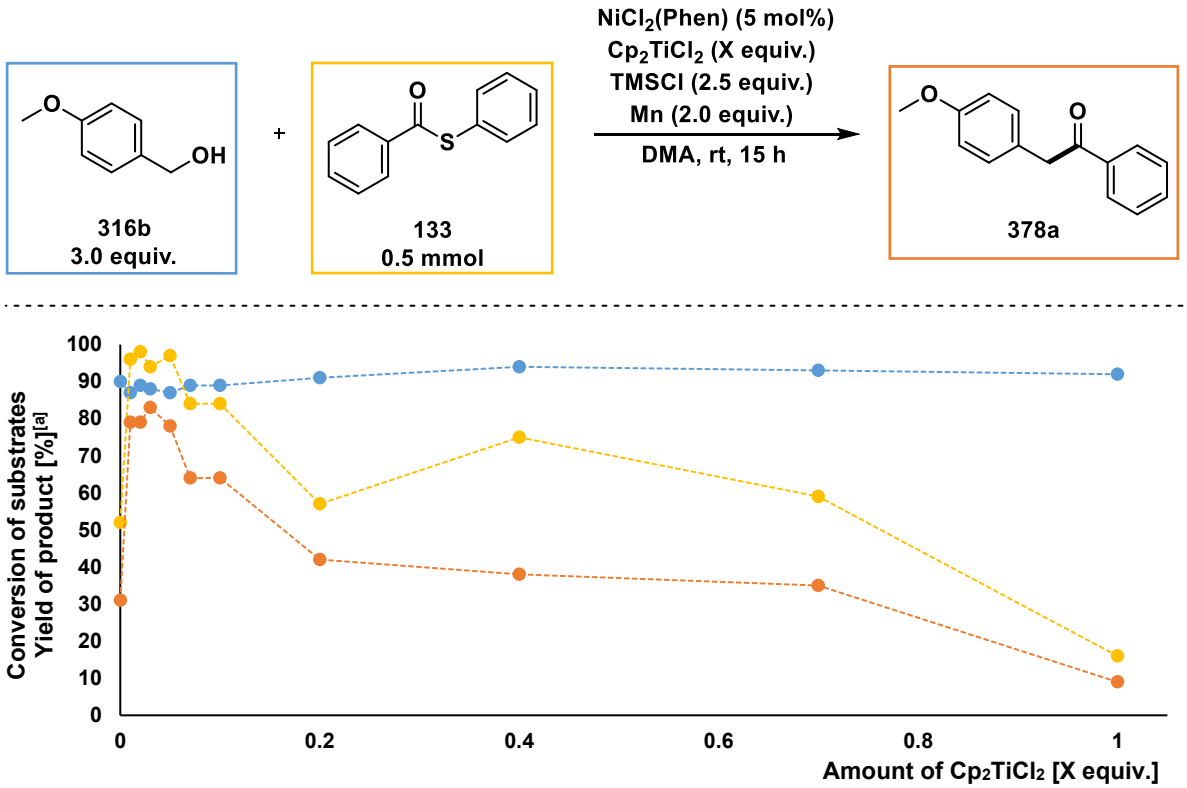

Figure 4-7: Dependence of thioester conversion on titanocene dichloride amount. [a]: Determined by GC-FID using *n*-pentadecane as internal standard.

The optimized titanium catalyst loading of 3 mol% was then applied in standard reaction together with the previously optimized amount of alcohol (2.7 equiv., *vide supra*, Figure 4-4). Under these conditions, ketone **378a** was generated in a yield of 74%, but thioether **379a** and dimeric oxoether **380** were also obtained in high yields of 67% and 24%, respectively.

4.3.1.8 Investigations on Ni(II) Source

Subsequently, investigations were carried out on the nickel catalyst, whereby other nickel(II) precatalysts were tested first (Table 4-6). With 5 mol% $NiCl_2$(Phen), as used in the standard reaction, 76% of ketone **378a** was determined (entry 1). For the screening, 10 mol% of the respective precatalyst and 15 mol% of 1,10-phenanthroline were applied to the reaction. Similar yields to the standard reaction were achieved with other nickel(II) sources (entries 1 *vs.* 2–6), with the exception of $Ni(CH_3O_2)_2{\cdot}4H_2O$, where a decrease in yield to 41% was determined, probably due to the water present (entry 7). A significantly higher yield of dimeric oxoether **380** was observed in all experiments which could be assigned to the slow addition of TMSCl in this screening (*vide postea*, Table 4-10). Since no other nickel(II) source led to an improvement in yield of ketone **378a** and a higher loading of the nickel catalyst can be avoided (5 mol% *vs.* 10 mol%, entry 1 *vs.* entries 2–7), the screening was continued with the original $NiCl_2$(Phen).

Table 4-6: Screening of different nickel(II) sources.

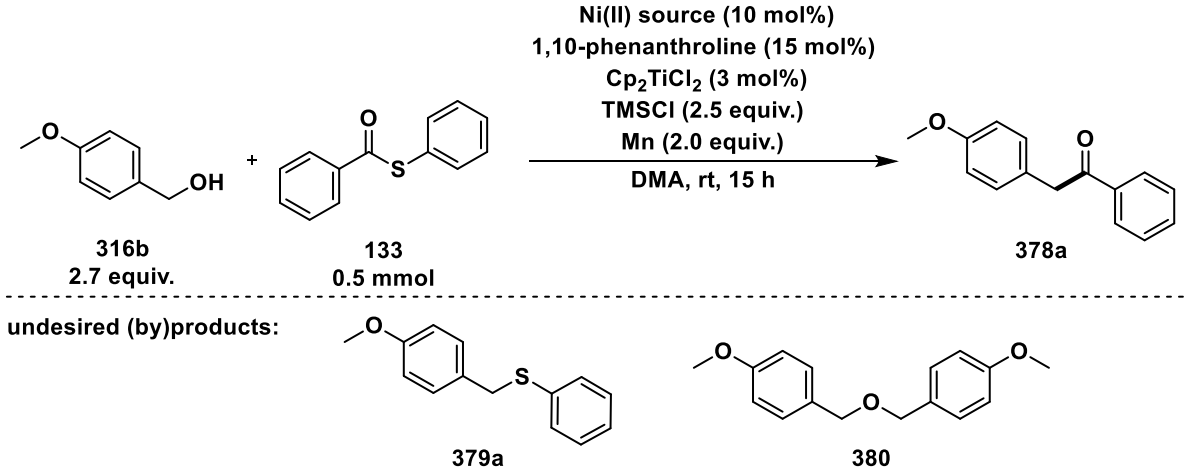

Entry	Ni(II) Source	Conv. of 316b [%][a]	Conv. of 133 [%][a]	Yield of 378a [%][a]	Yield of 379a [%][a]	Yield of 380 [%][a]
1	$NiCl_2$(Phen) (5 mol%)	97	93	76	71	34
2	$NiCl_2$(DME)	96	88	70	74	31
3	$NiBr_2$(DME)	99	87	76	75	31
4	$Ni(acac)_2$	94	90	74	76	33
5	$NiCl_2{\cdot}6H_2O$	98	85	74	76	30
6	$NiCl_2$	91	77	70	71	35
7	$Ni(CH_3CO_2)_2{\cdot}4H_2O$	63	65	41	57	29

***Reaction Conditions*:** Mn (54.9 mg, 1.00 mmol, 2.0 equiv.), Cp_2TiCl_2 (3.7 mg, 15 µmol, 3.0 mol%), Ni(II) source (25 µmol or 50 µmol, 5.0 mol% or 10 mol%), 1,10-phenanthroline (13.5 mg, 75.0 µmol, 15 mol%), **133** (107 mg, 500 µmol, 1.0 equiv.), **316b** (168 µL, 1.35 mmol, 2.7 equiv.), TMSCl (159 µL, 1.25 mmol, 2.5 equiv.) *via* syringe pump over a time range of 5 min, rt, 5 min; then abs. DMA (2 mL), rt, 15 h. [a]: Determined by GC-FID using *n*-pentadecane as internal standard.

The nickel(II) catalyst studies were followed by a ligand screening (Scheme 4-32). Chelating nitrogen-based ligands, such as phenanthrolines and bipyridines, were shown to be especially active with nickel(II) precursors and in reactions involving radicals.[5a,32,192] A redox activity has been observed for phenanthroline,[20a,193] bipyridine[194] and terpyridine[195] complexes, resulting in the transfer of electrons from the metal to the π* orbital of the ligand.[192,196]

In general, steric and electronic nature of the ligands and coordination power of nickel have played an important role in stabilizing the intermediates, e.g. electron-rich ligands were found to provide extra electronic support to the nickel atom, thus reinforcing the stability of acyl-nickel complexes.[197] Phosphine-based ligands do not perform as well as those based on nitrogen in nickel-catalyzed cross-electrophile couplings, but notable successes were reported especially for cobalt-catalyzed couplings.[198] Additionally, it is also known that synergistic effects of nitrogen- and phosphine-based ligands can improve selectivity for the product formation and suppress the proportion of byproduct.[4]

Initially, the developed cross-electrophile coupling was investigated in the absence of a ligand. Only $NiCl_2$(DME) as a precatalyst promoted mainly the conversion of alcohol **316b** to benzylic chloride **317b**, benzyl dimer **381** and dimeric oxoether **380**, while the conversion of thioester **133** remained low (23%). Thioether **379a** was generated in 15% yield, with only traces of ketone **378a** formed.

For the ligand screening, 15 mol% of the respective ligand were applied and $NiCl_2$(DME) (10 mol%) was chosen as precatalyst due to its good accessibility and similar yield compared to the reaction with $NiCl_2$(Phen) (*vide supra*, Table 4-6, entry 1 *vs.* entry 2). For the sake of clarity, only the yields of ketone **378a** are given in Scheme 4-32. The experiments showed that the influence of the ligand is much stronger than that of the nickel(II) source. It was started testing several phenanthroline-based ligands (Scheme 4-32A). With 1,10-phenanthroline **L12** as ligand, ketone **378a** was detected in 68% yield. Other ligands with the phenanthroline backbone **L13**–**L16** gave significant decreases in yields ranging from 21–39%. Moreover, several bipyridines were also screened (Scheme 4-32B). With 2,2'-bipyridine **L17**, ketone was formed in a moderate yield of 49%, while bipyridines **L18**–**L20** bearing OMe, Me or *t*Bu substituents reduced the yields to around 29%. Employing an electron-poor bipyridine ligand **L21**, ketone was generated in 53% yield. Monodentate, tridentate or phosphine ligands were all unsuitable for the developed cross-electrophile coupling, resulting in very low yields of ketone **378a** (Scheme 4-32C, D, **L22**–**L25**).

To sum up the ligand screening, 1,10-phenanthroline was the best ligand in combination with $NiCl_2$(DME), but the highest ketone yield was achieved with the previously used nickel(II) precatalyst $NiCl_2$(Phen).

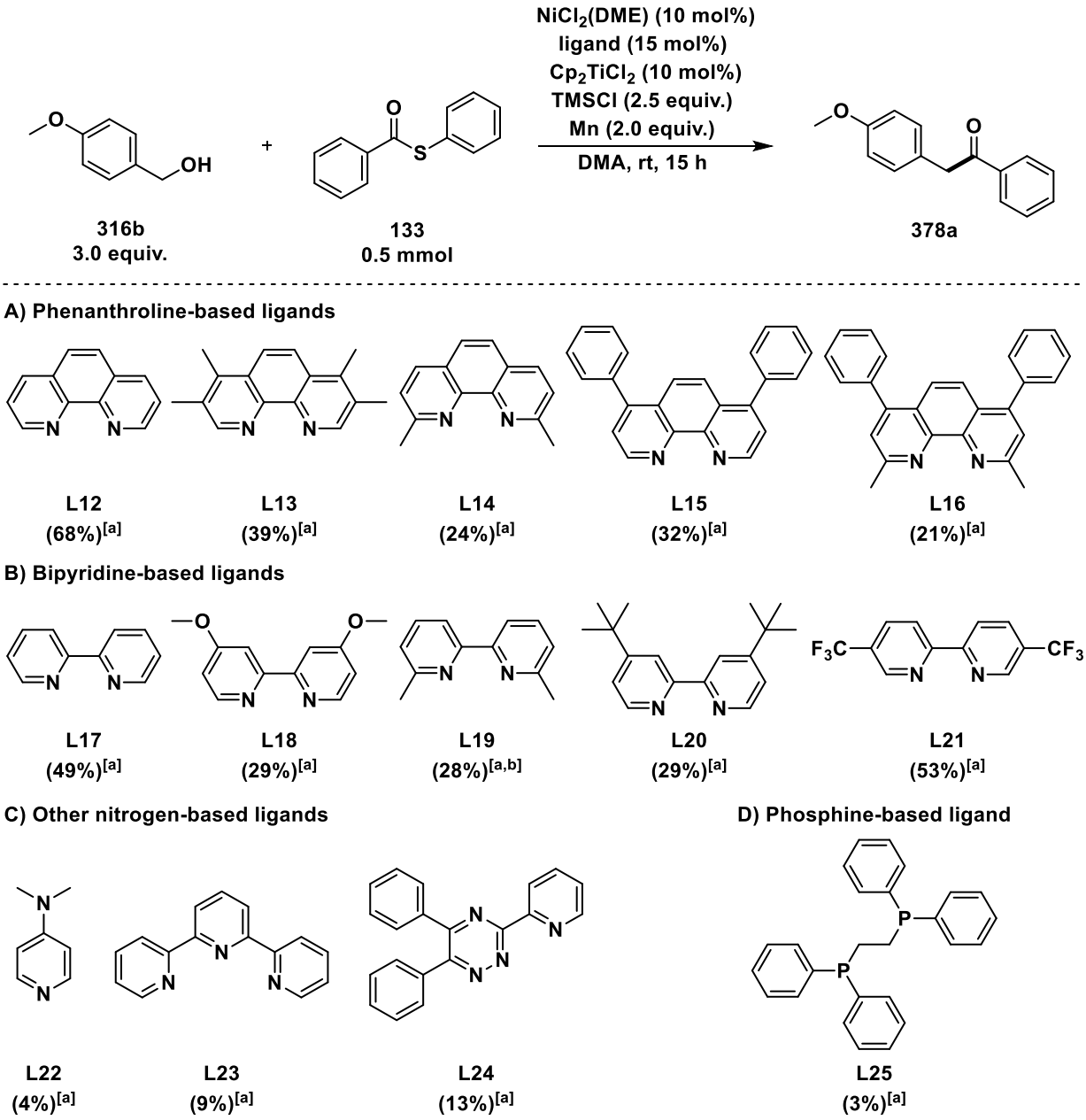

Scheme 4-32: Ligand screening. [a]: Ketone yields are given in parentheses and were determined by GC-FID using *n*-pentadecane as internal standard; [b]: 12 mol% ligand was used.

With the optimal catalyst system in hand, it was investigated whether a decreased or an increased nickel precatalyst loading had a beneficial effect on the product yield (Table 4-7). However, it could be shown that 5 mol% of $NiCl_2$(Phen) as used under standard conditions was optimal for the reaction system and deviations led to lower yields of the desired ketone **378a** (entries 2 *vs.* 1, 3, 4)

Table 4-7: Optimization of nickel precatalyst loading.

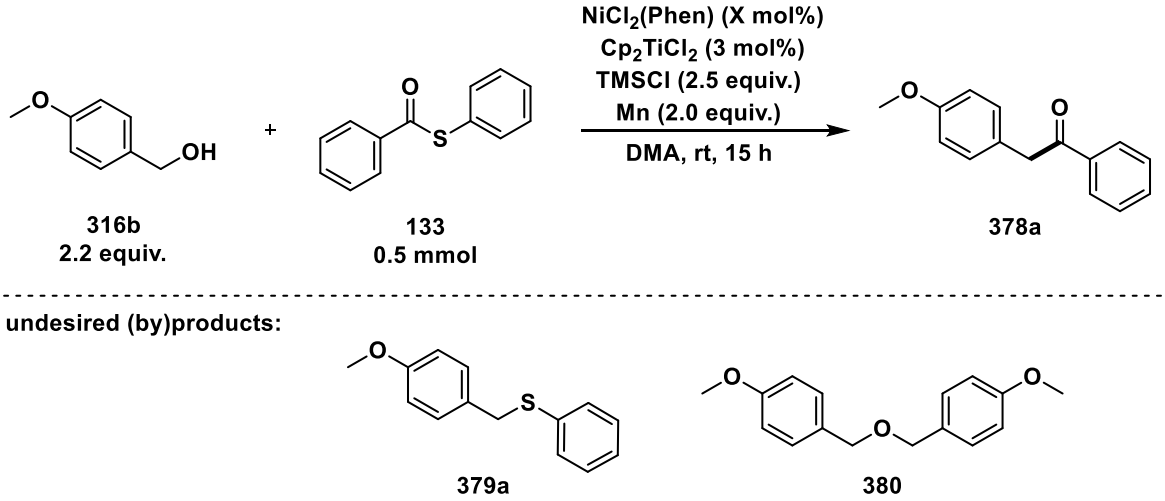

Entry	Amount of $NiCl_2$(Phen) (X mol%)	Conv. of 316b [%][a]	Conv. of 133 [%][a]	Yield of 378a [%][a]	Yield of 379a [%][a]	Yield of 380 [%][a]
1	3	85	88	69	61	11
2	5	89	88	77	66	10
3	7	75	82	56	59	10
4	10	77	80	70	69	10

Reaction Conditions: Mn (54.9 mg, 1.00 mmol, 2.0 equiv.), Cp_2TiCl_2 (3.7 mg, 15 µmol, 3.0 mol%), $NiCl_2$(Phen) (15–50 µmol, 3.0–10 mol%), **133** (107 mg, 500 µmol, 1.0 equiv.), TMSCl (159 µL, 1.25 mmol, 2.5 equiv.), **316b** (137 µL, 1.10 mmol, 2.2 equiv.) *via* syringe pump (SP) over 5 min, rt, 5 min; then abs. DMA (2 mL) *via* SP over 5 min, rt, 15 h. [a]: Determined by GC-FID using *n*-pentadecane as internal standard.

4.3.1.9 TMSCl as Additive

The optimization process was continued with studies on TMSCl as additive (Figure 4-8). In its absence, the conversion of substrates was significantly lowered to 25% and 56% for alcohol **316b** and thioester **133**, respectively, and the formation of products and byproduct was completely inhibited. Instead of product formation, transesterification product **382** and disulfide **383a** were detected. As the amount of TMSCl increased, the conversion of substrates and yields of (by)products also grew. The maximum yield of ketone **378a** was obtained with 2.5 equivalents TMSCl, as employed under standard conditions.

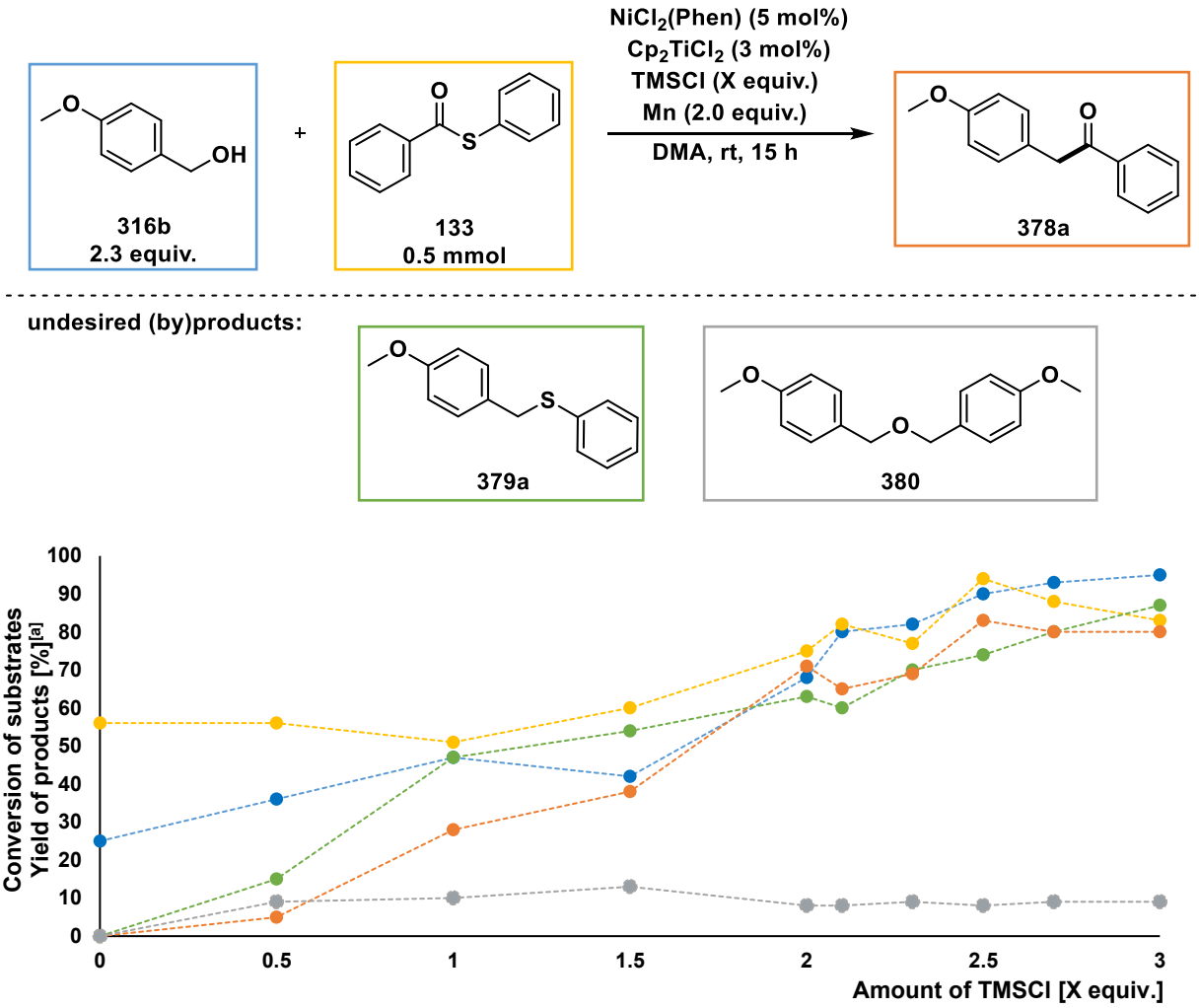

Figure 4-8: Variation of TMSCl amount. [a]: Determined by GC-FID using *n*-pentadecane as internal standard.

Additionally, the substitution of TMSCl by other chlorosilanes was investigated (Table 4-8) With dimethyldichlorosilane and *t*-butyldimethylchlorosilane (TBSCl), a decrease in yield to 57% and 11%, respectively, was observed (entries 2, 3). With TBSCl, only silyl-protected alcohol was generated as main product. Similar to TMSCl, triethylchlorosilane (TESCl) gave a high yield of ketone **378a** (84% *vs.* 80%, entries 1 *vs.* 4). However, TMSCl was not replaced by TESCl for economic reasons (TMSCl 0.84 €/mL *vs.* TESCl 3.08 €/mL).[199] $TiCl_4$ was also tested as additive, with which the formation of 4-methoxybenzyl chloride (**317b**) from alcohol **316b** was observed, but the formation of ketone **378a** was completely prevented (entry 5).

In addition to chlorosilanes, trimethylbromosilane (TMSBr) was applied as an additive. After reaction completion, qualitative GC-MS analysis showed unreacted thioester **133** and the conversion of alcohol **316b** to benzyl dimer **381** as main product. Traces of ketone **378a**, thioether **379a** and oxoether **380** were generated, however bromination of alcohol **316b** by TMSBr could not be observed.

Table 4-8: Substitution of TMSCl.

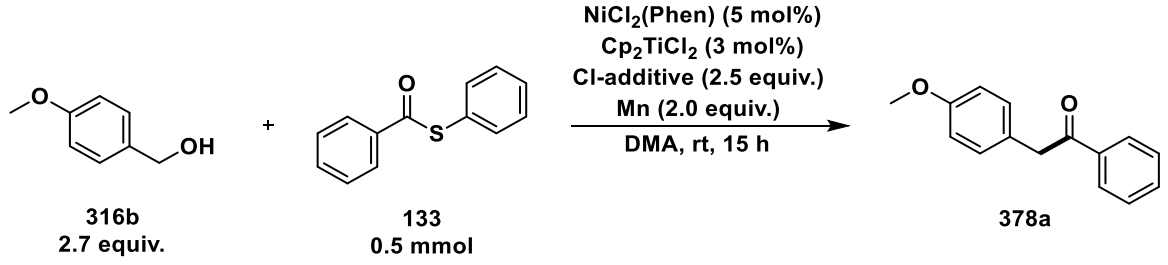

undesired (by)products:

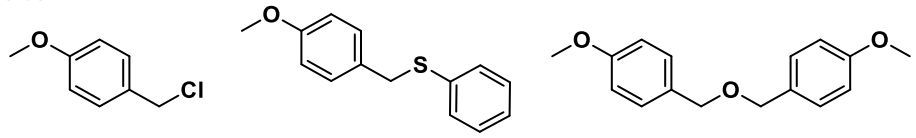

317b 379a 380

Entry	Cl-additive	Conv. of 316b [%][a]	Conv. of 133 [%][a]	Yield of 378a [%][a]	Yield of 379a [%][a]	Yield of 380 [%][a]
1	$(CH_3)_3SiCl$	96	93	84	77	34
2	$(CH_3)_2SiCl_2$	60	48	57	62	traces
3	(*t*-Bu)$(CH_3)_2SiCl$	91	41	11	33	20
4	$(CH_3CH_2)_3SiCl$	96	92	80	77	26
5[b]	$TiCl_4$	77	46	✘	13	6

Reaction Conditions: Mn (54.9 mg, 1.00 mmol, 2.0 equiv.), Cp_2TiCl_2 (3.7 mg, 15 µmol, 3.0 mol%), $NiCl_2$(Phen) (7.8 mg, 25 µmol, 5.0 mol%), **133** (107 mg, 500 µmol, 1.0 equiv.), **316b** (168 µL, 1.35 mmol, 2.7 equiv.), Cl-additive (1.25 mmol, 2.5 equiv.), if liquid, *via* syringe pump over 5 min, rt, 5 min; then abs. DMA (2 mL), rt, 15 h. [a]: Determined by GC-FID using *n*-pentadecane as internal standard; [b]: 3.0 equiv. **316b** and 10 mol% Cp_2TiCl_2 were used.

4.3.1.10 Other Additives

It is well established that salt additives can increase the reaction efficiency in nickel-catalyzed cross-electrophile couplings, but often their effects are not well-understood. The following is a brief literature overview of common salt additives in XEC.

For instance, LiCl facilitates the reduction of the nickel precatalyst at the zinc surface and counteracts the inhibition of the reduction process at the zinc surface caused by *in situ* formed zinc(II) salts.[31a] Blum *et al.* disclosed by fluorescence microscopy that the LiCl additive enhances the solubility of otherwise persistent organometallic intermediates from the surface of zinc.[200] Several more examples demonstrated the advantageous impact of LiCl.[201]

In addition to LiCl, $MgCl_2$ is also known for a positive effect on product yields. In the coupling of electron-rich aryl iodides and tertiary alkyl halides, the combination of $MgCl_2$ and LiCl supports the catalytic transformation efficiency and the activation of zinc as reducing agent.[201c] Moreover, $MgCl_2$ was found to have the additional role of generating more soluble nickel species and enabling the reduction of a $(DMAP)_2Ni(acac)_2$ precatalyst. More examples were reported, which use $MgCl_2$ as beneficial additive in cross-electrophile

coupling.[22,64a,112,151,202] Other known salt additives are NaI,[203] LiBr,[22,34d,116,204] K_3PO_4,[205] and KF.[34a] Additionally, $Et_3N{\cdot}HCl$ is used as regenerating agent in titanium(III) chemistry,[206] whereas PPh_3 is known as Lewis base additive for a low-valent titanium reagent in the presence of TMSCl and Mg.[207] Suga and Ukaji introduced the Lewis acid-base adduct $TiCl_4$(lutidine) for generation of a carbon radical from benzyl alcohols (*vide supra*, Scheme 4-28),[185] while Shu and co-workers used dimethyl oxalate (DMO), nickel catalysis and manganese for the *in situ* transesterification of benzylic alcohols, enabling radical formation and participation in the catalytic cycle (*vide supra*, Scheme 4-25B).[149,204b]

Based on these literature reports, an extensive (salt) additive screening was conducted (Table 4-9). When using KCl as additive, only 58% of ketone **378a** and 53% of thioether **379a** were obtained despite the high conversion of thioester **133** (80%, entry 2). Alkali, alkaline earth, and transition metal chlorides were then applied (entries 3–8). While NaCl and KCl gave similar yields to the standard conditions, LiCl and $MgCl_2$ were unfavorable and reduced the ketone yields to 48% and 59%, respectively (entries 3–6). With $MnCl_2$, high conversion of substrates was observed, and ketone **378a** was furnished in a slightly higher yield of 85%. However, a higher yield of dimeric oxoether **380** (16%) and a higher proportion of a not characterized byproduct were also observed with this additive (entry 7). In contrast, $ZnCl_2$ as additive significantly suppressed ketone formation (entry 8). Subsequently, alkali bromides and iodides were investigated. LiBr and NaBr decreased the conversion of thioester **133** resulting in lower yields of ketone **378a** and thioether **379a** (entries 9, 10). With KBr, similar yield to the standard reaction was obtained (76%, entry 11). The addition of NaI resulted in a lower yield of ketone (45%) and for KI, complete product inhibition was observed (entries 12, 13).

The use of different carbonates reduced the yields of ketone (entries 14–16). Additionally, it seems that ammonium cations are not suitable for the reaction. All applied ammonium salts led to a significant decrease in yield of ketone **378a**, while the yield of thioether **379a** was less affected (entries 16–19). In addition, various acetates gave diminished yields of the desired product **378a** (entries 18–23).

With $Et_3N{\cdot}HCl$ and PPh_3, lower conversions of substrates were observed resulting in a decreased yield of ketone **378a** (49% and 13%, entries 24, 25). In entry 25, conversion of thioester **133** was relatively high in contrast to the yields of products **378a** and **379a**. This could be explained by GC-MS analysis, which showed the formation of disulfide **383a** and oxoester **385**. A detrimental effect on substrate conversion was observed with $TiCl_4$(lutidine) as additive, as ketone **378a** was formed only in 41% (entry 26). To remove traces of liberated water, molecular sieves were added, however no improvement in yield of ketone **378a** was observed (entries 27).

The application of DMO in the presented system resulted only in the formation of trace amounts of ketone **378a** and thioether **379a** (entry 28). To ensure the *in situ* transesterification of alcohol **316b** with DMO analogous to the report of Shu and co-workers (*vide supra*, Scheme 4-25B),[149] and to guarantee that alcohol is not converted to benzylic chloride **317b** instead, the reaction was conducted in the absence of TMSCl.

In summary, the screening showed that a higher conversion of substrates and a slightly higher yield of ketone **378a** was achieved with $MnCl_2$ as additive, however the yield of undesired dimeric oxoether **380** also increased. Nevertheless, the amount of $MnCl_2$ was further optimized (Table 4-9, entries 29–31), but a dependence of ketone yield on the amount of $MnCl_2$ could not be correlated. With 1.6 equivalents, a high yield of ketone **378a** (80%) was obtained in combination with a low yield of dimeric oxoether **380** (11%) (entry 31). However, this result could not be reproduced.

Due to the only slightly higher yield of ketone **378a** and the associated higher yield of dimeric oxoether **380**, reproducibility problems and the avoidance of an additional reagent in this already complex system, $MnCl_2$ was not further used as additive in standard reactions.

Table 4-9: (Salt) additive screening.

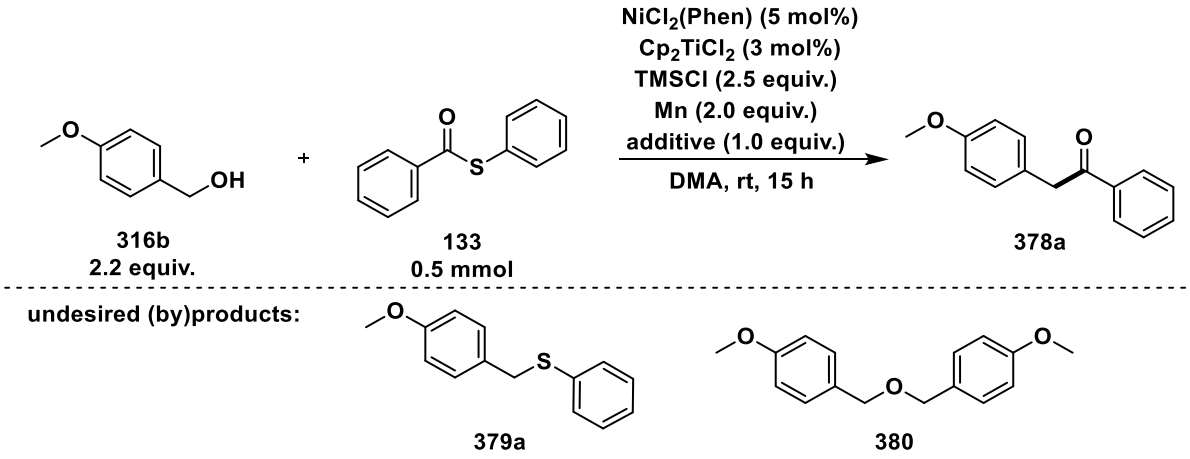

Entry	Additive[a]	Conv. of 316b [%][b]	Conv. of 133 [%][b]	Yield of 378a [%][b]	Yield of 379a [%][b]	Yield of 380 [%][b]
1	w/o	81	85	74	60	9
2	KF	66	80	58	53	9
3	LiCl	94	72	48	52	15
4	NaCl	73	62	73	71	12
5	KCl	92	74	74	67	8
6	$MgCl_2$	94	85	59	60	18
7	$MnCl_2$	93	93	85	70	16
8	$ZnCl_2$	99	33	38	8	traces
9	LiBr	94	46	54	52	14
10	NaBr	76	48	44	50	10
11	KBr	77	69	76	76	11
12	NaI	82	67	45	21	traces
13	KI	83	15	✘	9	13
14	Na_2CO_3	45	54	44	37	8
15	K_2CO_3	70	68	52	44	12
16[c]	$(NH_4)_2CO_3$	traces	41	11	68	15
17[d]	NH_4PF_6	78	64	36	87	✘
18	NH_4OAc	68	74	5	63	18
19	$(t\text{Bu})_4NOAc$	52	46	6	25	traces
20	NaOAc	77	76	50	57	16
21	KOAc	59	46	9	26	12
22	CuOAc	24	15	traces	traces	✘
23	AgOAc	74	54	24	22	17
24	$Et_3N{\cdot}HCl$	69	79	49	66	11
25[e]	PPh_3	76	65	13	9	✘
26	$TiCl_4$(lutidine) (0.5 equiv.)	56	66	41	64	6
27[f]	molecular sieves	100	13	traces	traces	15
28[g]	DMO (2.2 equiv.)	46	24	6	traces	✘
29	$MnCl_2$ (1.2 equiv.)	97	86	75	68	20
30	$MnCl_2$ (1.4 equiv.)	87	74	65	67	24
31	$MnCl_2$ (1.6 equiv.)	91	92	80	94	11

Reaction Conditions: Mn (54.9 mg, 1.00 mmol, 2.0 equiv.), Cp_2TiCl_2 (3.7 mg, 15 µmol, 3.0 mol%), additive (500 µmol, 1.0 equiv.), $NiCl_2$(Phen) (7.8 mg, 25 µmol, 5.0 mol%), **133** (107 mg, 500 µmol, 1.0 equiv.), TMSCl (159 µL, 1.25 mmol, 2.5 equiv.), **316b** (137 µL, 1.10 mmol, 2.2 equiv.) *via* syringe pump (SP) over 5 min rt, 5 min; then abs. DMA (2 mL) *via* SP over 5 min rt, 15 h. [a]: Hygroscopic additives were dried before use; [b]: Determined by GC-FID using *n*-pentadecane as internal standard; [c]: Area of internal standard was too low; [d]: 3 equiv. **316b**, 10 mol% Cp_2TiCl_2 and 1.2 equiv. additive were used; [e]:The yield of **380** could not be determined due to peak overlap with PPh_3; [f]: 32 mol% molecular sieves were used; [g]: In the absence of TMSCl.

4.3.1.11 Suppression of Oxoether Formation
4.3.1.11.1 Investigations on Reaction Time

In continuation of the salt additive screening, the formation of dimeric oxoether **380** was investigated in depth. To achieve the best atom economy, it is required to design a reaction, in which the highest amount of ketone **378a** and the smallest possible amount of byproduct **380** are generated with a sufficiently low amount of unreacted starting material **316b**. Another reason for the necessity of reducing the amount of oxoether **380** is that TLC of the crude product mixture showed almost the same retardation factor R_F of the desired ketone **378a** and dimeric oxoether **380**, which led to difficulties during purification. Therefore, another part of the optimization process included the reduction of the formation of oxoether **380** as byproduct. To this end, kinetic experiments were performed to see if the formation of oxoether **380** could be affected by the reaction time (Figure 4-9). Unfortunately, this was not the case, as the dimeric oxoether **380** formed during the initial reaction period and then remained at constant yield (Figure 4-9). Consequently, the reaction time was maintained at 15 hours.

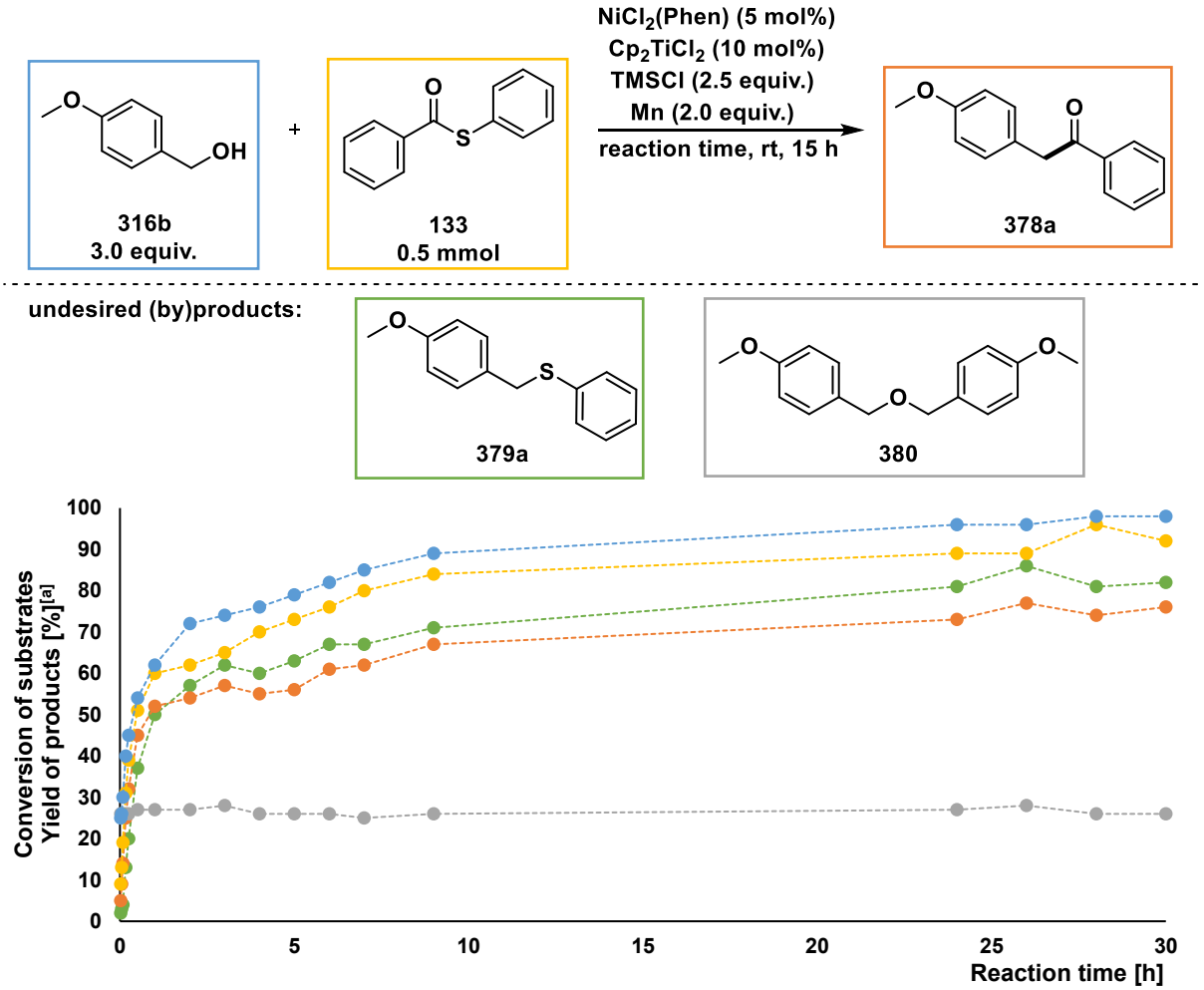

Figure 4-9: Investigations on time dependence of oxoether formation. [a]: Determined by GC-FID using *n*-pentadecane as internal standard.

4.3.1.11.2 Separate Generation of Benzyl Chloride from Alcohol

Since the formation of benzylic chloride **317b** from alcohol **316b** was observed under standard conditions (*vide supra*, Scheme 4-30), it was proposed that **316b** could be activated *in situ* by the formation of chloride **317b** and thereby allowing cross-electrophile coupling. As dimeric oxoether **380** is formed from the reaction of benzylic alcohol **316b** and benzylic chloride **317b**, it was assumed that the formation of oxoether **380** could be suppressed after complete conversion of alcohol **316b** to chloride **317b**.

To examine this, **316b** was added to TMSCl in a separate Schlenk tube (Schlenk tube 1, Scheme 4-33) and after stirring for 5 min, DMA was added to the mixture. The solution was stirred for further 30 min, and then added to a second Schlenk tube loaded with nickel and titanium catalyst, thioester **133**, and manganese (Schlenk tube 2, Scheme 4-33). After completion of the reaction, GC-FID analysis showed benzyl chloride **317b** in 14%, ketone **378a** in 91% and thioether **379a** in 48% yield. Nevertheless, oxoether **380** was also generated in 6% yield. Subsequently, the formation of benzyl chloride **317b** was evaluated conducting kinetics experiments.

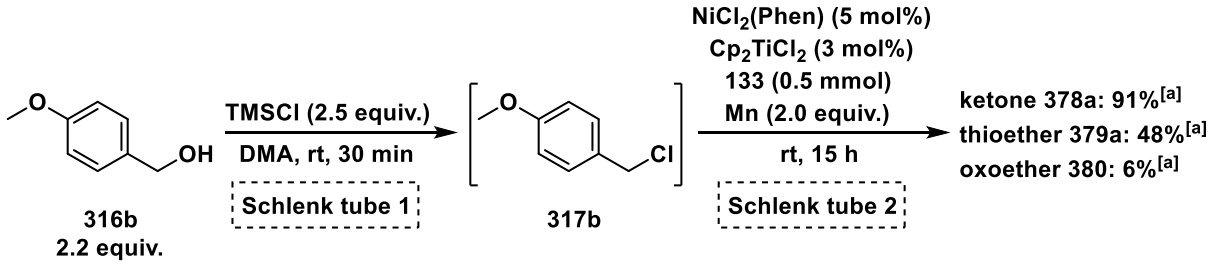

Scheme 4-33: Separate generation of benzyl chloride **317b** and application in cross-electrophile coupling. [a]: Determined by GC-FID using *n*-pentadecane as internal standard.

4.3.1.11.3 Time Dependence of Chloride and Oxoether Formation

It was found that the reaction of solely benzylic alcohol **316b** and TMSCl without DMA under solvent-free reaction conditions (SFRC) gave full conversion of alcohol to benzyl chloride **317b** and only traces of oxoether **380** were generated. Kinetic experiments of the reaction between alcohol **316b** and TMSCl in DMA showed full conversion of **316b** to benzyl chloride **317b** and dimeric oxoether **380** from the first minute of reaction (Figure 4-10), and when the reaction progressed, no further changes in yields of chloride **317b** and oxoether **380** were observed. The experiments indicated that the combination of TMSCl and DMA are responsible for formation of oxoether **380**, which thus cannot be avoided under standard conditions.

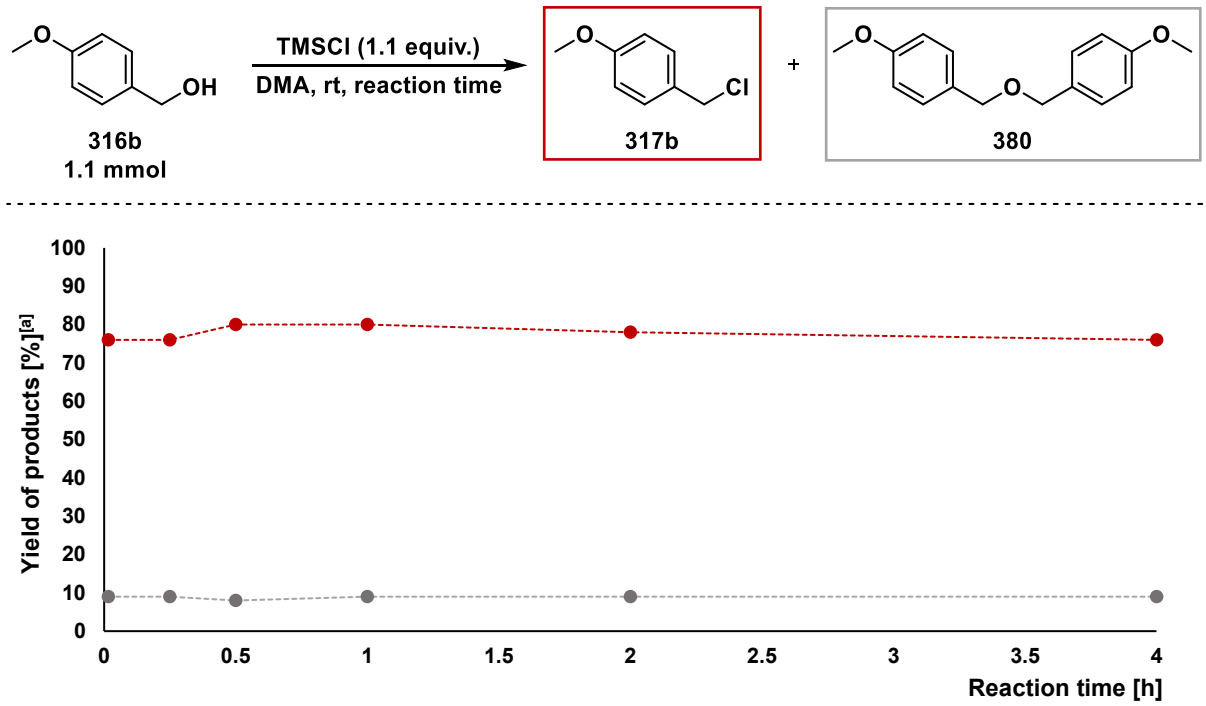

Figure 4-10: Time dependence of byproducts formation from benzylic alcohol **316b**, TMSCl and DMA. [a]: Determined by GC-FID using *n*-pentadecane as internal standard.

4.3.1.11.4 Investigations on Sequence and Rate of Addition

After kinetic investigations, the influence of sequence and rate of substrate and reagent addition on the formation of dimeric oxoether **380** was examined (Table 4-10).

In entry 1, which illustrates the standard reaction, manganese, titanocene dichloride, nickel catalyst, thioester **133**, benzylic alcohol **316b** and TMSCl were sequentially added before the addition of DMA. The addition of alcohol **316b** and TMSCl before thioester **133** resulted in slightly lower yield of ketone **378a** (63%) and a slightly higher yield of oxoether **380** (29%, entry 2). A slow addition of TMSCl *via* syringe pump led to higher yields of ketone **378a** (84%) and thioether **379a** (77%), but also furnished a higher yield of dimeric oxoether **380** (34%, entry 3). Slow addition of alcohol **316b** and TMSCl at the same time *via* syringe pump gave similar results to the standard reaction (entries 1 *vs.* 4). A suppression of oxoether formation was achieved by changing the order of addition, adding TMSCl first and then alcohol **316b** slowly *via* syringe pump (entry 5). An even slower addition of alcohol **316b** had no significant effect on the yield of oxoether **380** (entry 6). Also adding DMA slowly in addition to alcohol **316b** did not have a strong effect on the (by)product yields (entry 7). However, the yields of ketone **378a** and oxoether **380** were further optimized by reducing the amount of alcohol and slowly adding alcohol **316b** and DMA *via* syringe pump (entries 8–10). The highest yield of ketone **378a** (88%) in combination with a low yield of dimeric oxoether **380** (10%) was achieved by inverting the sequence of addition of TMSCl and alcohol **316b**, and by the slow addition of 2.2 equiv. **316b** and DMA *via* syringe pump (entry 9).

Table 4-10: Investigations on sequence and rate of substrate and reagent addition.

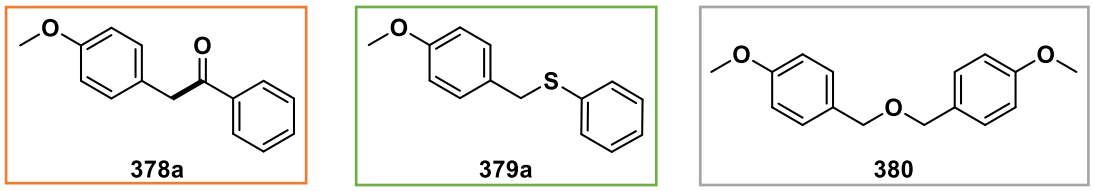

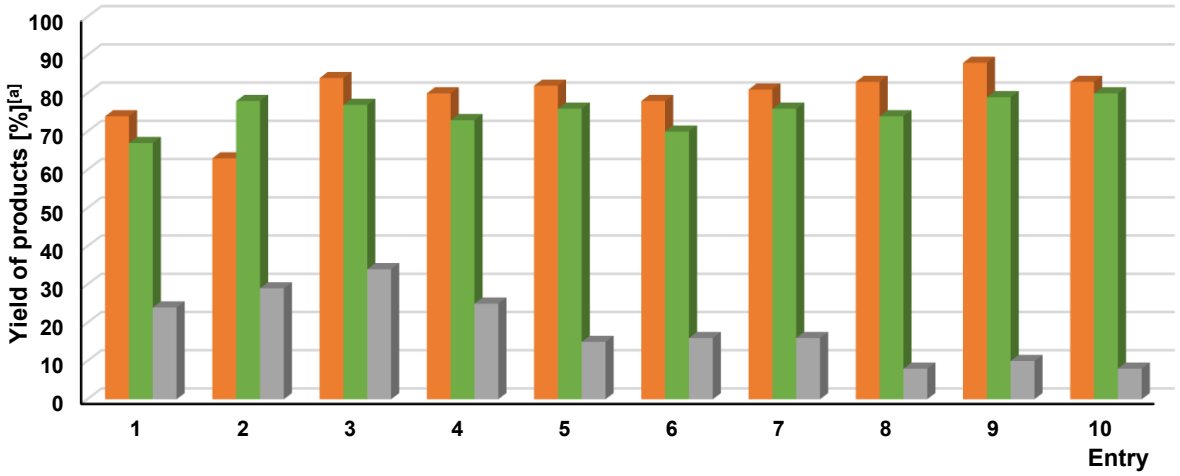

Entry	Reaction conditions
1	Mn (2.0 equiv.), Cp_2TiCl_2 (3 mol%), $NiCl_2$(Phen) (5 mol%), (2.7 equiv.), TMSCl (2.5 equiv.), stirring for 5 min, DMA
2[b]	Mn (2.0 equiv.), Cp_2TiCl_2 (10 mol%), $NiCl_2$(Phen) (5 mol%), (3 equiv.), TMSCl (2.5 equiv.), stirring for 5 min, DMA
3	Mn (2.0 equiv.), Cp_2TiCl_2 (3 mol%), $NiCl_2$(Phen) (5 mol%), (2.7 equiv.), TMSCl (2.5 equiv.) *via* SP over 5 min, stirring for 5 min, DMA
4	Mn (2.0 equiv.), Cp_2TiCl_2 (3 mol%), $NiCl_2$(Phen) (5 mol%), (2.7 equiv.), and TMSCl (2.5 equiv.) *via* SP over 5 min at the same time, stirring for 5 min, DMA
5	Mn (2.0 equiv.), Cp_2TiCl_2 (3 mol%), $NiCl_2$(Phen) (5 mol%), TMSCl (2.5 equiv.), *via* SP over 5 min (2.7 equiv.), stirring for 5 min, DMA
6	Mn (2.0 equiv.), Cp_2TiCl_2 (3 mol%), $NiCl_2$(Phen) (5 mol%), TMSCl (2.5 equiv.), *via* SP over 10 min (2.7 equiv.), stirring for 5 min, DMA
7	Mn (2.0 equiv.), Cp_2TiCl_2 (3 mol%), $NiCl_2$(Phen) (5 mol%), TMSCl (2.5 equiv.), *via* SP over 5 min (2.7 equiv.), stirring for 5 min, DMA *via* SP over 5 min

Continuation of Table 4-10: Investigations on sequence and rate of substrate and reagent addition.

Entry	Reaction conditions
8	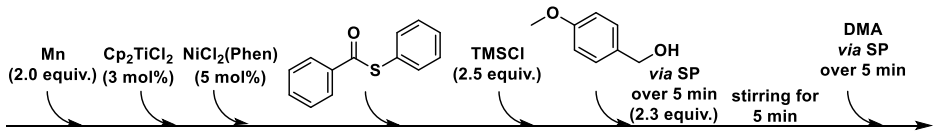
9	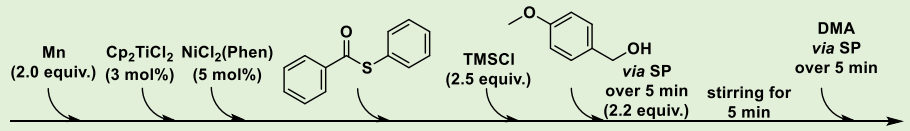
10	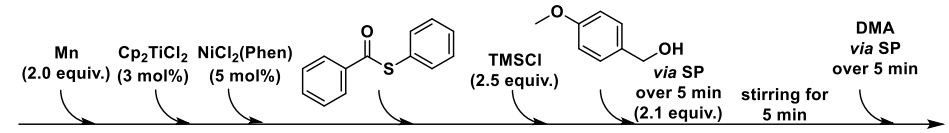

***Reaction Conditions*:** Mn (54.9 mg, 1.00 mmol, 2.0 equiv.), Cp_2TiCl_2 (3.7 mg, 15 µmol, 3.0 mol%), $NiCl_2$(Phen) (7.8 mg, 25 µmol, 5.0 mol%), **133** (107 mg, 500 µmol, 1.0 equiv.), **316b** (168 µL, 1.35 mmol, 2.7 equiv.), TMSCl (159 µL, 1.25 mmol, 2.5 equiv.), rt, 5 min; then abs. DMA (2 mL), rt, 15 h. [a]: Determined by GC-FID using *n*-pentadecane as internal standard; [b]: 3 equiv. **316b** and 10 mol% Cp_2TiCl_2 were used.

4.3.1.12 Suppression of Thioether Formation

Besides the undesirable formation of dimeric oxoether **380**, the generation of thioether **379a** as additional product unnecessarily consumes alcohol, which is thus not available for the product-forming reaction step. Since thioether is formed from the reaction of benzylic chloride **317b** and the released thiolate, it was assumed that the formation of thioether **379a** could be suppressed by scavenging the thiolate, and several attempts to this end are presented in the following sections.

4.3.1.12.1 Application of Michael Acceptors

Initially, it was tried to reduce the thioether formation by adding Michael acceptors, which could trap the liberated thiolate. The more electron-deficient the C=C double bond of the Michael acceptor is, the more sensitive it is to a Michael addition. Therefore, they can be assorted by their reactivity from maleimides with the highest reactivity over vinyl sulfones, acrylates and acrylamides to methacrylates with the lowest reactivity (Figure 4-11).[208]

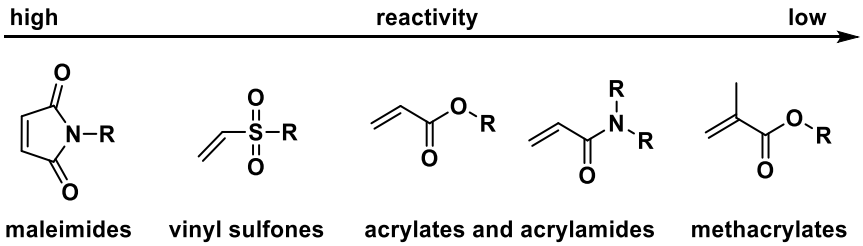

Figure 4-11: Comparison of reactivity of commonly used vinyl groups in thiol-Michael addition reactions.[208]

Michael acceptors with different reactivities were applied as additives in the developed cross-electrophile coupling, starting with the most reactive maleimide as additive, which led to low conversion of substrates and the complete inhibition of ketone formation (Table 4-11, entry 1). With divinyl sulfone, maleic anhydride and methyl acrylate, formation of ketone **378a** and thioether **379a** was enabled, but in significant lower yields compared to the standard reaction (entry 1 *vs.* 3–5). With these three Michael acceptors, the conversion of thioester **133** was more inhibited than the conversion of alcohol **316b**, and the latter was mostly transformed to benzyl chloride **317b** and bibenzyl **381**. A benzyl radical that appears to be involved in bibenzyl **381** formation was not scavenged with the Michael acceptors and no thiol-Michael adduct was observed *via* GC-MS analysis, probably demonstrating the unsuitable reactivity of Michael acceptors for the reaction pathway.

Table 4-11: Application of Michael acceptors.

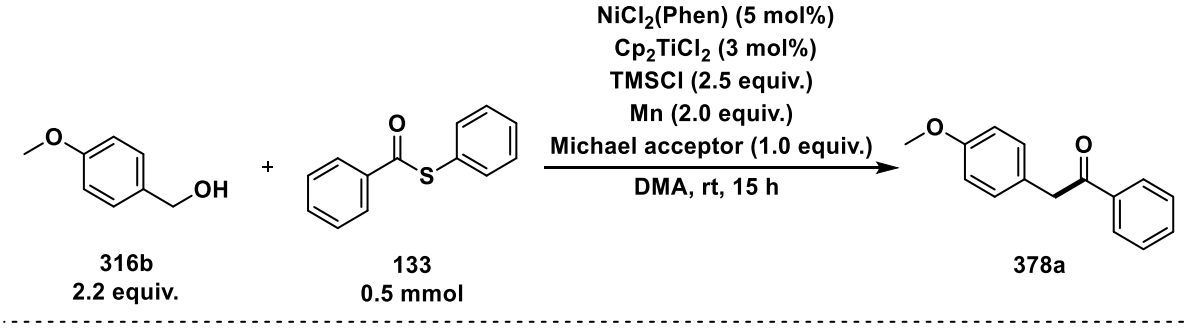

Entry	Michael acceptor	Conv. of 316b [%][a]	Conv. of 133 [%][a]	Yield of 378a [%][a]	Yield of 379a [%][a]	Yield of 380 [%][a]
1	w/o	88	91	88	79	10
2	maleimide	19	9	✘	✘	✘
3	divinyl sulfone	84	33	15	19	9
4	maleic anhydride	82	17	6	12	12
5	methyl acrylate	78	46	28	37	11

***Reaction Conditions*:** Mn (54.9 mg, 1.00 mmol, 2.0 equiv.), Cp_2TiCl_2 (3.7 mg, 15 µmol, 3.0 mol%), $NiCl_2$(Phen) (7.8 mg, 25 µmol, 5.0 mol%), **133** (107 mg, 500 µmol, 1.0 equiv.), Michael acceptor (500 µmol, 1.0 equiv.), TMSCl (159 µL, 1.25 mmol, 2.5 equiv.), **316b** (137 µL, 1.10 mmol, 2.2 equiv.) *via* syringe pump (SP) over 5 min, rt, 5 min; then abs. DMA (2 mL) *via* SP over 5 min, rt, 15 h. [a]: Determined by GC-FID using *n*-pentadecane as internal standard.

4.3.1.12.2 Application of Thiophilic Metals

Another attempt to avoid the formation of thioether **379a** as an additional product, was to scavenge the released thiolate from thioester **133** with thiophilic metals (Table 4-12).

For this purpose, zirconocene dichloride (Cp_2ZrCl_2) was applied instead of Cp_2TiCl_2, which has already been used to increase the coupling rate for ketone synthesis by inhibiting thioether formation.[33,76] With 3 mol% of Cp_2ZrCl_2, lower conversion of thioester **133** (78%) and lower yields of ketone **378a** and thioether **379a** (60% and 59%) were observed than in the reaction with Cp_2TiCl_2 (entry 1 *vs.* 2). A slight increase of Cp_2ZrCl_2 to 5 mol% led to significantly lower yields of ketone **378a** and thioether **379a** (entry 3, 23% and 37%). With stoichiometric amount of the zirconium reagent, the deceleration of thioester conversion was not affected as much as with Cp_2TiCl_2 (see Figure 4-7). Nevertheless, ketone **378a** and thioether **379a** were only formed in 37% and 46%, respectively.

Liebeskind and Srogl used stoichiometric amounts of copper(I) thiophene-2-carboxylate (CuTC) in the palladium-catalyzed reaction of thioesters and organoboron compounds to bind the liberated thiolate (*vide supra*, Scheme 3-12).[209] In analogy to this literature report, different copper(I) compounds were applied in the developed system. However, CuTC as additive had a detrimental effect resulting in a decreased yield of ketone **378a** and a similar yield of thioether **379a** (31% and 27%, entry 5). The negative effect was not as strong when CuCl was used, giving 70% of ketone **378a**, but also yielding thioether **379a** in 70% (entry 6).

Consequently, the released thiolate could not be scavenged by thiophilic metals, which led to high proportions of thioether **379a** in all experiments and in some cases to a negative influence on the yield of both products, ketone **378a** and thioether **379a**.

Table 4-12: Application of thiophilic metals.

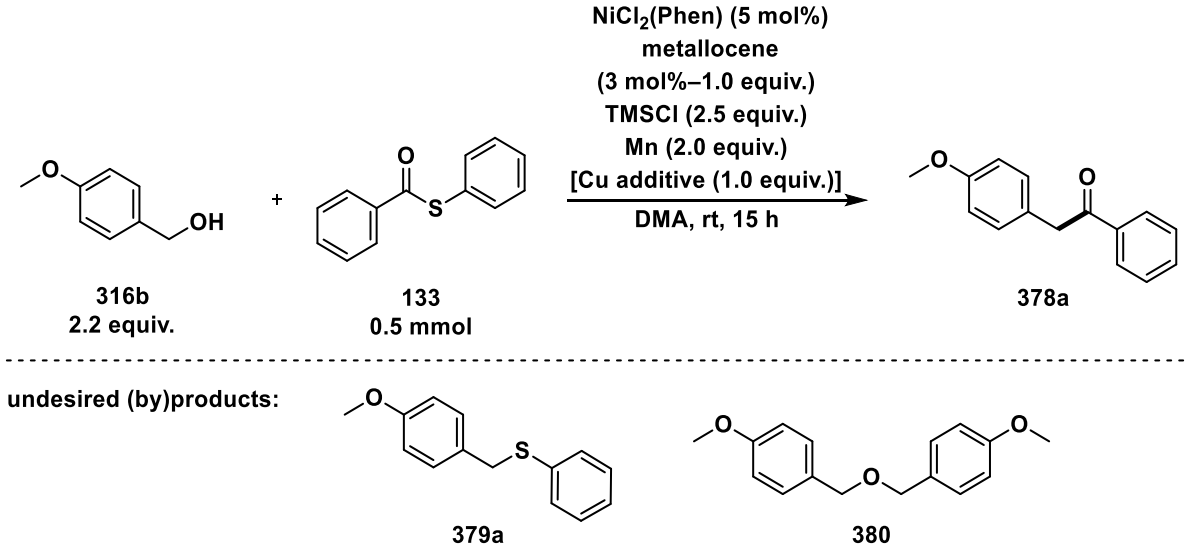

Entry	Metallocene [Cu additive]	Conv. of 316b [%][a]	Conv. of 133 [%][a]	Yield of 378a [%][a]	Yield of 379a [%][a]	Yield of 380 [%][a]
1	Cp_2TiCl_2 (3 mol%)	88	91	88	79	10
2	Cp_2ZrCl_2 (3 mol%)	81	78	60	59	11
3	Cp_2ZrCl_2 (5 mol%)	86	67	23	37	10
4	Cp_2ZrCl_2 (1 equiv.)	57	64	37	46	12
5	Cp_2TiCl_2 (3 mol%) [CuTC]	69	41	31	27	15
6	Cp_2TiCl_2 (3 mol%) [CuCl]	86	74	70	70	15

Reaction Conditions: Mn (54.9 mg, 1.00 mmol, 2.0 equiv.), metallocene (15 µmol–500 µmol, 3.0 mol%–1.0 equiv.), [Cu additive (500 µmol, 1.0 equiv.)], $NiCl_2$(Phen) (7.8 mg, 25 µmol, 5.0 mol%), **133** (107 mg, 500 µmol, 1.0 equiv.), TMSCl (159 µL, 1.25 mmol, 2.5 equiv.), **316b** (137 µL, 1.10 mmol, 2.2 equiv.) *via* syringe pump (SP) over 5 min, rt, 5 min; then abs. DMA (2 mL) *via* SP over 5 min, rt, 15 h. [a]: Determined by GC-FID using *n*-pentadecane as internal standard.

4.3.1.12.3 Variation of Thioester

Since the reactivity of thioesters can be controlled by the thiol scaffold (*vide supra*, section 3.1.2.4.3.1), it was continued to investigate whether the formation of thioether **379a** could be suppressed by modifying the thiol moiety of thioester while the yield of ketone **378a** is supposed to remain high. To this end, thioesters with ethyl-, phenyl- and 2-pyridyl thiol moieties were applied to the standard conditions (Figure 4-12A). With ethyl and 2-pyridyl thioesters, significantly lower yields of ketone **379a** were determined than in the reaction with *S*-phenyl benzothioate (**133**) as substrate, so that these were excluded as suitable substrates for the developed system (Figure 4-12A).

Subsequently, the reactivity of thioester **133** was fine-tuned by modifying the electronic properties of the *S*-phenyl moiety. With the aim of possibly reducing the thioether yield, this could also influence the oxidative addition of the thioesters to nickel catalyst. Stereoelectronic effects of the substrate itself on the oxidative addition are well studied for aryl electrophiles, with electron-deficient aryl electrophiles undergoing a faster oxidative addition than the corresponding electron-rich substrates.[210] Lautens demonstrated the selective coupling of aryl and heteroaryl chlorides, the latter with a more electron-deficient nature and thereby more activated towards the oxidative addition.[202b] Furthermore, Yamamoto showed that during the oxidative addition (OA) of phenyl propionate to nickel(0) and the accompanied cleavage of the acyl–O bond, the electronic properties of the *para* position of the phenyl ring are crucial, as an electron-withdrawing group enhances the OA, whereas an electron-donating group decreases the reactivity of the ester.[70b]

Following these literature contributions, various *S*-aryl thioesters were employed under the standard conditions and their performance in production of ketone **378a** was compared to that of *S*-phenyl (88% of **378a**, Figure 4-12B). With a bromine substituent in *para* position, a slightly lower ketone yield of 77% was determined, which decreased further with a chlorine in *para* or a bromine in *meta* position. The lowest yield of ketone **378a** was obtained with an electron-donating OMe substituent in *para* position (16%, Figure 4-12B). Pleasingly, in addition to the slight decrease in ketone **378a** yield, the undesired formation of thioether **379a** was hampered by the bromine substituent in *para* position compared to the reaction with *S*-phenyl thioester (79% **379a** *vs.* 13% **379b**, Figure 4-12C). Surprisingly, bromine was tolerated in the presence of the nickel catalyst and the competing oxidative addition of C–Br to nickel(0) did not occur with this substituent. One might also expect the suppression of thioether **379a** could occur with other substituents in *para* position, e.g. chlorine, but it was not observed (Figure 4-12D).

Since thioesters with a bromine substituent in *para* position provide a good compromise between high yield of ketone **378a** and low thioether yield, the subsequent substrate screening was carried out with these.

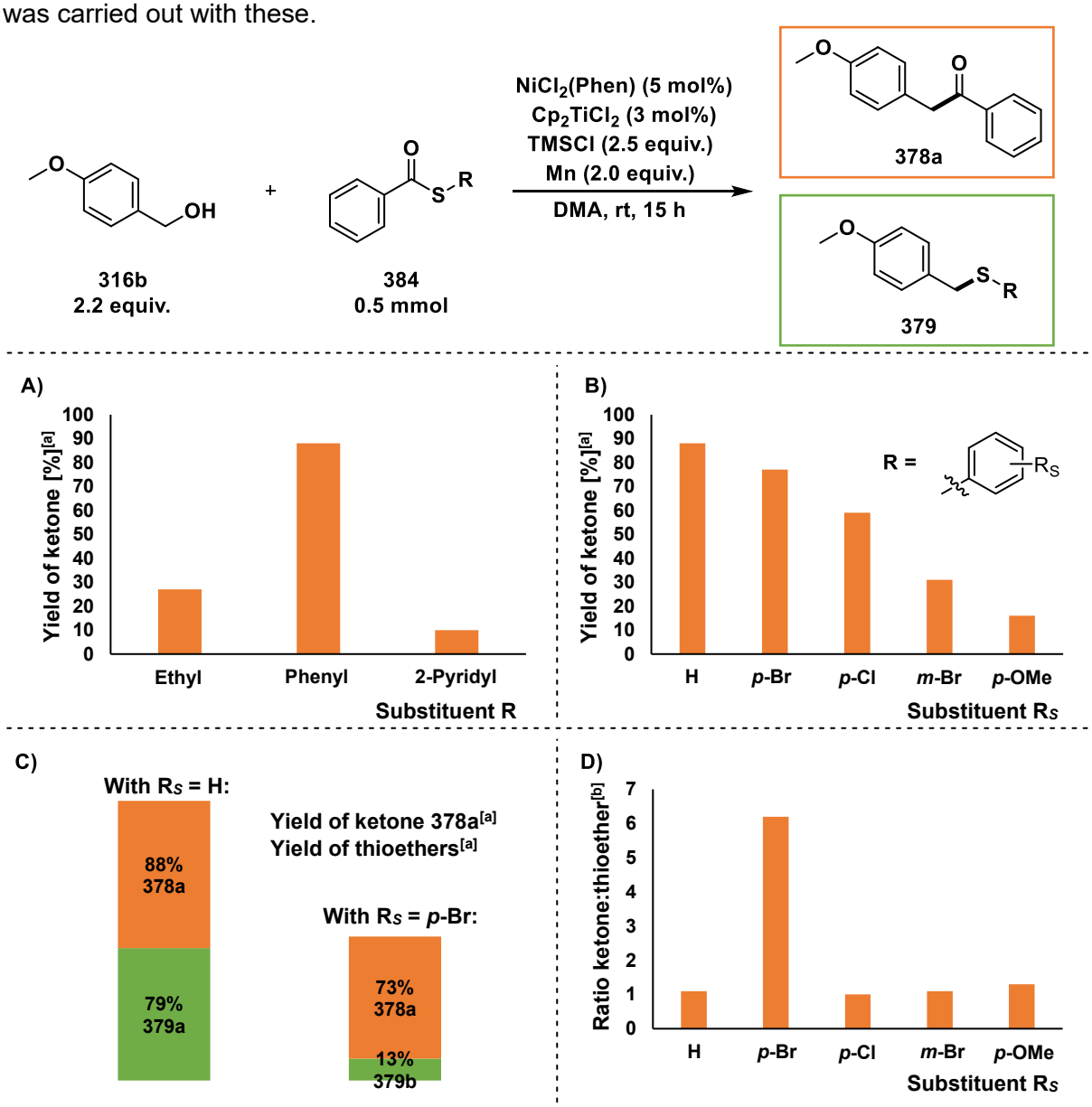

Figure 4-12: A) Modification of thiol moiety of thioester and B–D) influence of phenyl substituent on formation of thioether **379**. [a]: Determined by GC-FID using *n*-pentadecane as internal standard; [b]: The ratio of ketone:thioether was estimated by dividing the peak height of ketone **378a** by the peak height of the respective thioether **379**, both determined in the total ion chromatogram of the GC-MS measurements.

As a lower amount of thioether **379b** was generated with bromine-substituted thioester **140**, it was hypothesized that a lower amount of alcohol **316b** should be sufficient. This could lead to a lower amount of oxoether **380** and hence facilitate the purification of ketone **378a**. Therefore, different equivalents of benzylic alcohol **316b** were applied (Figure 4-13). However, the lower the equivalents of alcohol **316b**, the lower the yield of ketone **378a** and the higher the yield of thioether **379b** (Figure 4-13). Following from these experiments, the reaction set-up was continued with 2.2 equivalents of benzylic alcohol.

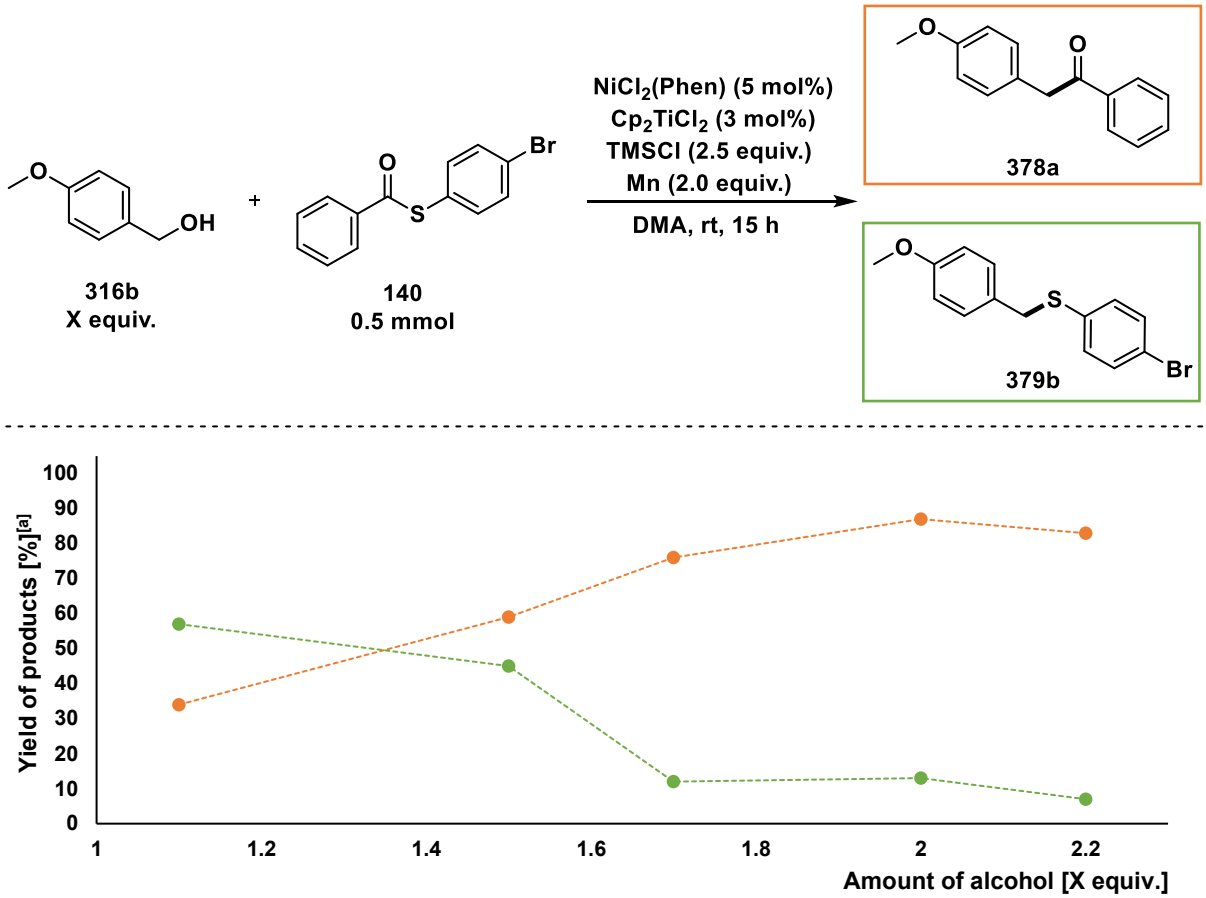

Figure 4-13: Re-optimization of alcohol **316b** amount using bromine-substituted thioester **140**. [a]: Determined by GC-FID using n-pentadecane as internal standard.

4.3.1.13 Summary of Optimization

Initially, the optimization was performed for the reaction of 3 equiv. 4-methoxybenzyl alcohol (**316b**) and *S*-phenyl benzothioate (**133**) using 5 mol% $NiCl_2$(Phen), 10 mol% Cp_2TiCl_2 and an excess of TMSCl (2.5 equiv.) and manganese (2 equiv.) (Table 4-13, entry 1). Control reactions indicated that the coupling was completely inhibited without nickel catalyst, TMSCl or manganese (entry 2).[1] In contrast, in the absence of the titanium catalyst, ketone formation was successful, albeit with a lower yield of 27% (entry 3). In addition, Zn and TDAE performed poorly as alternative reducing agents (entries 4, 5). A significant improvement of product yield was accomplished after reducing the titanium catalyst loading from 10 mol% to 3 mol% (entry 6). Moreover, the amount of alcohol **316b** was further optimized with a lower titanium catalyst loading (entry 7). The reaction was found to depend strongly on the sequence of addition (entries 8, 9), for instance if DMA was not added last, ketone formation did not occur. Additionally, DMA as solvent cannot be replaced. Extensive investigations on the sequence and rate of substrate and reagent addition revealed that a slow addition of alcohol **316b** and DMA coincided with the highest yield of ketone **378a** and the lowest yield of dimeric oxoether **380** (entry 9). The substantial formation of thioether **379** was suppressed by introducing a bromine substituent on the thiol moiety of thioester. With these optimized reaction conditions, ketone **378a** was formed in 72%, thioether **379b** only in 13% and oxoether **380** in 7% yield (entry 10).

Table 4-13: Summary of optimization.

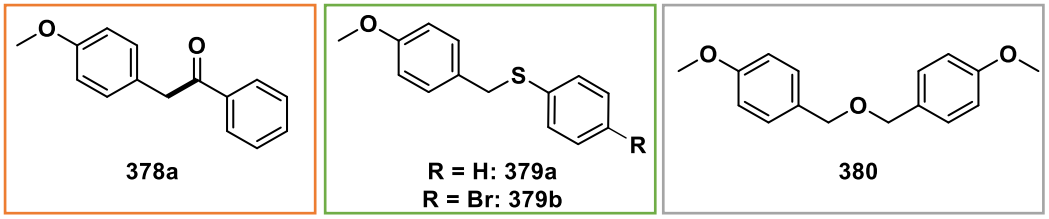

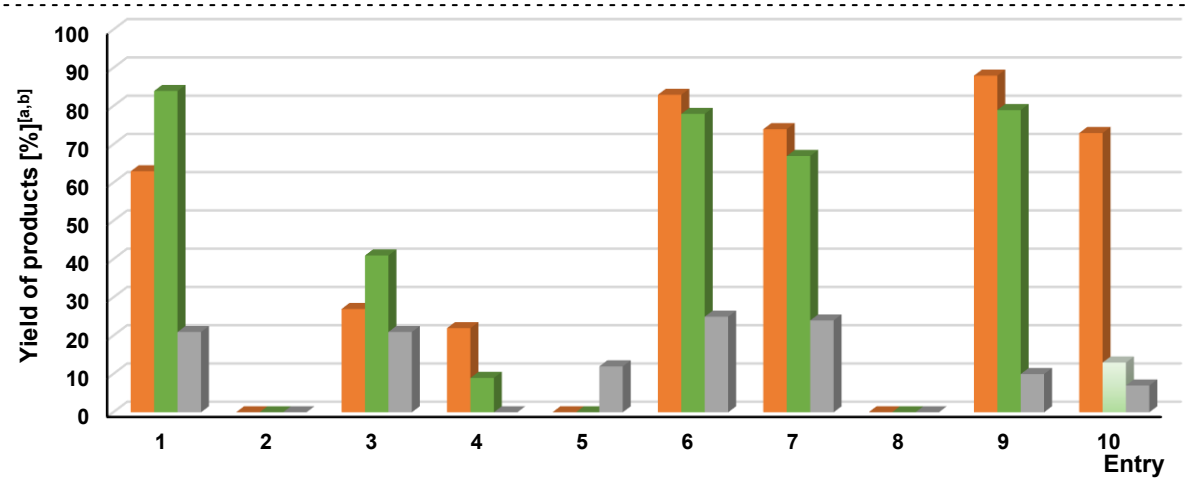

Entry	Reaction conditions
1	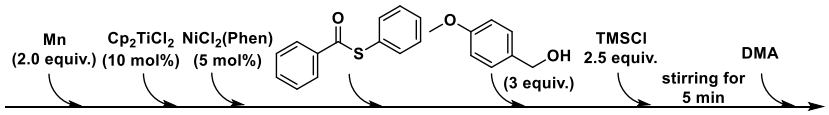
2 [1]	w/o Ni, TMSCl or Mn
3	w/o Cp_2TiCl_2
4 [c]	Zn instead of Mn
5 [c]	TDAE instead of Mn
6	3 mol% Cp_2TiCl_2 instead of 10 mol%
7	2.7 equiv. 316b + 3 mol% Cp_2TiCl_2
8	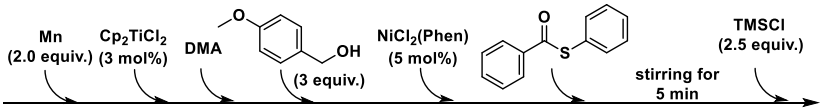
9 [c]	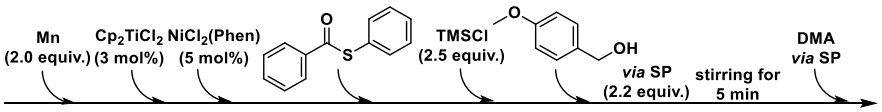
10 [c]	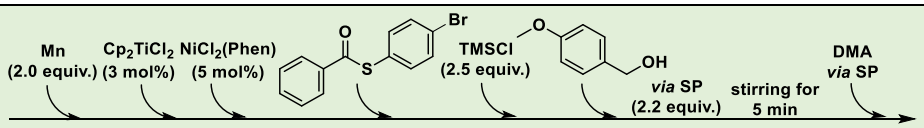

Optimized Reaction Conditions: Mn (54.9 mg, 1.00 mmol, 2.0 equiv.), Cp_2TiCl_2 (3.7 mg, 15 µmol, 3.0 mol%), $NiCl_2$(Phen) (7.8 mg, 25 µmol, 5.0 mol%), **140** (146 mg, 500 µmol, 1.0 equiv.), TMSCl (159 µL, 1.25 mmol, 2.5 equiv.), **316b** (137 µL, 1.10 mmol, 2.2 equiv.) *via* syringe pump (SP) over 5 min, rt, 5 min; then abs. DMA (2 mL) *via* SP over 5 min, rt, 15 h. [a]: Determined by GC-FID using *n*-pentadecane as internal standard; [b]: Dark green columns correspond to thioether **379a**, light green column corresponds to thioether **379b**; [c]: 2.2 equiv. **316b** and 3 mol% Cp_2TiCl_2 were used.

4.3.2 Evaluation of Substrate Scope

4.3.2.1 Separation of Ketone and Oxoether after Standard Reaction

With the optimized reaction conditions in hand, the attention was turned towards the isolation of coupling products and the investigation of the substrate scope. However, the separation of ketones from dimeric oxoether **380** generally proved difficult because the retardation factors were nearly identical. Different approaches were conducted to simplify the purification step after the standard reaction. Attempts to fully separate the mixture of ketone and dimeric oxoether by recrystallization and column chromatography remained unsuccessful. Reversed phase (RP) column chromatography revealed ketone **378a** in 52% yield, which was then contaminated by carbonylated byproduct **385** (Scheme 4-34A). Quantitative NMR analysis displayed a mass ratio of 82% ketone **378a** and 18% compound **385**. Therefore, the corrected yield of ketone **378a** was 43%.

To facilitate the isolation of pure ketone **378a**, subsequent functionalization of the carbonyl group was attempted (Scheme 4-34B).[211,212] For the protection of the carbonyl-group as hydrazone, two different procedures adapted from the literature were applied using phenylhydrazine hydrochloride, but the desired hydrazone **386** was not formed (Scheme 4-34B, I).[211] Another method showed the functionalization of 2-phenyl acetophenone as semicarbazone using semicarbazide hydrochloride in the presence of sodium acetate.[212a] However, the approach was not suitable for ketone **378a** and the expected semicarbazone **387** was not formed (Scheme 4-34B, II). Finally, protection of the desired ketone as an acetal **388** was also unsuccessful (Scheme 4-34B, III).[212b]

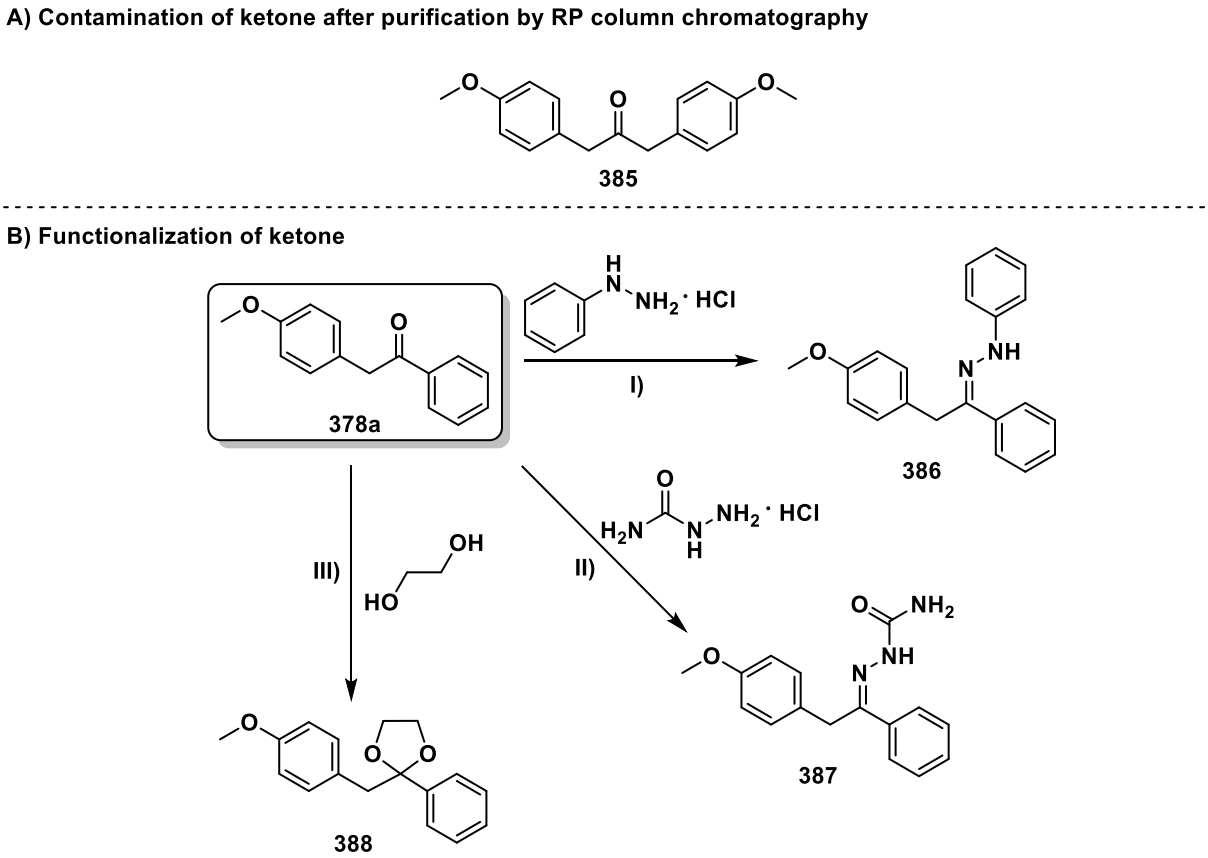

Scheme 4-34: A) Contamination of ketone **378a** after RP column chromatography. B) Different approaches for the functionalization of **378a**.[211,212] Reaction conditions: I) **378a** (62.5 µmol), phenylhydrazine hydrochloride (1.2 equiv.), NaOH (1.0 equiv.); II) **378a** (250 µmol), semicarbazide hydrochloride (1.0 equiv.), NaOAc (1.0 equiv.); III) **378a** (250 µmol), ethylene glycol (1.1 equiv.), *p*TsOH (3.0 mol%).

4.3.2.2 Scope of Thioesters

Subsequently, the scope of suitable thioesters was explored, also assuming that the purification step would be simplified by modifying the acyl groups of the thioesters and sufficient differences in the retardation factors were achieved (Scheme 4-35).

The coupling of thioesters with phenyl- and tolyl-moieties led to the corresponding ketones **378a** and **378b** in moderate yields. The system also tolerated a strong electron-withdrawing fluorine substituent, even though ketone **378c** was obtained in a reduced yield of 21%. Additionally, the coupling of a naphthyl-bearing substrate was possible resulting in 47% yield of ketone **378d**, and the above-mentioned compound **385** could also be synthesized in 63%. The reaction of other benzylic- and homobenzylic thioesters delivered products **378e**–**h** in modest to good yields, depending on the steric demand of thioesters. The bulkier the benzylic- and homobenzylic thioesters, the lower were the yields of respective ketones. With primary and secondary alkyl thioesters, a separation of ketones and dimeric oxoether **380** was facilitated and alkyl ketones **378i** and **378j** were obtained in moderate yields. Nevertheless, the synthesis of sterically challenging mesityl-ketone **378k** was unsuccessful.

This is the only example of thioester, which uniquely facilitated the coupling between alcohol **316b** and the bromine substituent of thiol moiety to give compound **390** in 54%. The desired ketone **378k** was also not formed after replacing the bromine substituent by a hydrogen atom.

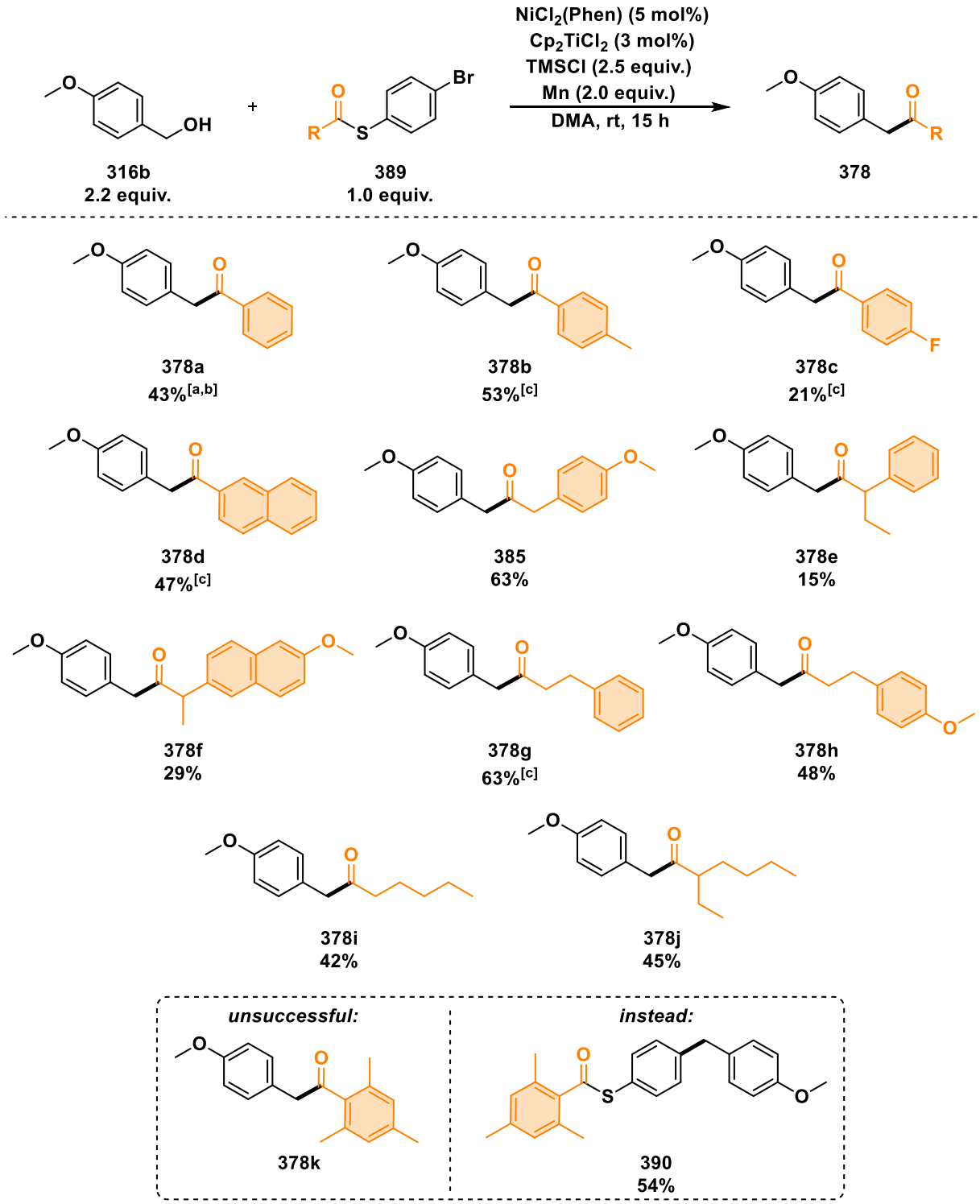

Scheme 4-35: Evaluation of the substrate scope with respect to thioester. [a]: Isolated as an inseparable mixture with carbonylated byproduct **385**, yield was determined by quantitative ^{1}H-NMR spectroscopy; [b]: Thioester **133** instead of **140**; [c]: Isolated as an inseparable mixture with dimeric oxoether **380**, yields were determined by quantitative ^{1}H-NMR spectroscopy.

4.3.2.3 Scope of Alcohols

Next, the scope of benzyl alcohols was investigated. It was found that the modification of alcohol **316b** was much more limited than that of thioester **140** (Scheme 4-36). Besides the model substrate **316b**, only alcohols with methoxy substituents in *ortho*- or in *para*- and *meta*-positions generated the desired ketones **378l** and **378m** in modest to moderate yields. The coupling is highly dependent on electron-donating substituents and their positions and omitting or replacing methoxy with other electron-donating groups proved difficult (**316a**–**f**, Scheme 4-36). Additionally, an electron-withdrawing CF_3-substituent on benzylic alcohol **316g** was found to completely inhibit product formation, similar to the findings of Rahaim.[190] Furthermore, secondary, tertiary and more reactive allyl alcohols were unsuitable substrates (**316h**–**n**, Scheme 4-36).

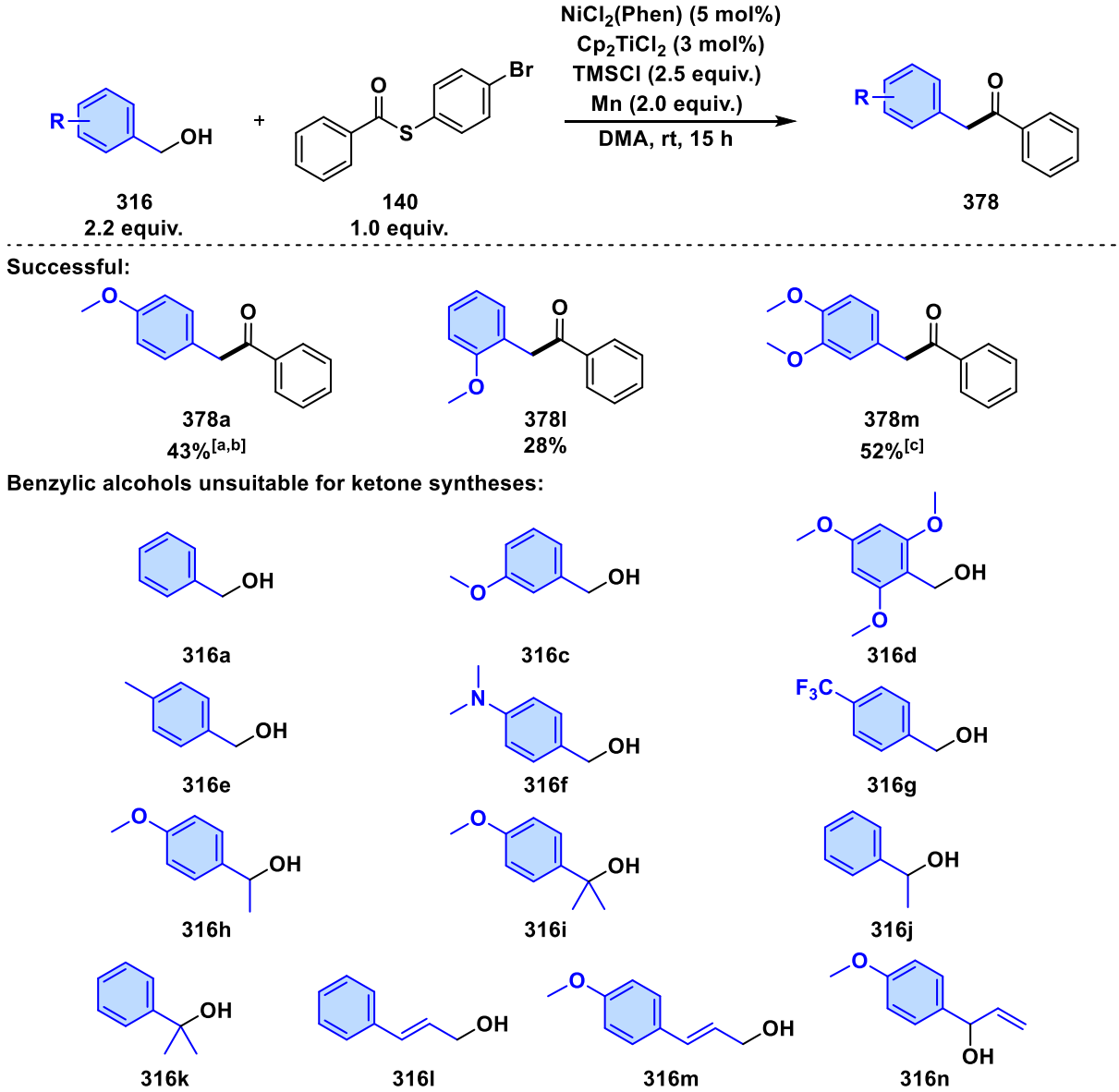

Scheme 4-36: Evaluation of the substrate scope with respect to alcohol. [a]: Isolated as an inseparable mixture with carbonylated byproduct **385**, yield was determined by quantitative ^{1}H-NMR spectroscopy; [b]: Thioester **133** instead of **140**; [c]: Isolated with impurities.

4.3.2.4 Other Substrates
4.3.2.4.1 Application of Benzyl Chlorides

In the optimization process, first hints were given that a formed chloride species from the alcohol could be the active intermediate in the reaction. This assumption was further investigated in various mechanistic experiments (*vide postea*, section 4.3.3.1), and several control reactions were conducted to investigate the direct use of benzyl chlorides in the present system and to determine the influence of the different reagents on the coupling (Table 4-14).

The reaction of thioester **140** with 4-methoxybenzyl chloride (**317b**) gave ketone **378a** in 83% yield under standard conditions (entry 1-A). The previously failed reaction of benzyl alcohol was successful with the direct use of benzyl chloride (**317a**) giving ketone **378n** in a moderate yield (44% and 41%, entry 1-B). In the absence of titanium catalyst, the reaction with 4-methoxybenzyl chloride (**317b**) was more impaired than the reaction with benzyl chloride (**317a**), as a decrease from 83% to 30% was observed in the first case and a similar yield to the standard reaction was obtained in the reaction with benzyl chloride (**317a**) (39%, entry 2-A *vs.* B). In entry 3, TMSCl was omitted and yield of ketone **378a** was comparable to the standard conditions in the reaction with OMe as substituent (entry 1 *vs.* 3-A). In contrast, yield of ketone **378n** was more than doubled in the absence of TMSCl (entry 1 *vs.* 3-B). The reaction of 4-methoxybenzyl chloride (**317b**) and thioester **140** was completely inhibited without titanium catalyst and TMSCl (entry 4-A), while the reaction of benzyl chloride (**317a**) and thioester **140** gave ketone **378n** in 73% (entry 4-B). These experiments strikingly showed the strong influence of substituents and Lewis acids on the reaction. Seemingly, it is necessary to activate electron-rich benzylic chlorides by Lewis acids, either by Cp_2TiCl_2 or by TMSCl. Entry 4 also illustrates the higher selectivity of nickel undergoing oxidative addition favorably into the C(O)–S bond rather than the C–Br bond of thioester **140**, although Rahaim and co-worker showed that the reaction of benzyl chloride **317a** and 4-bromotoluene **175** gives the cross-coupled product in 94% yield with a $NiCl_2$(Phen) precatalyst under reductive conditions.[190] Additionally, a comparison of entry 3-B and 4-B provided further evidence that Cp_2TiCl_2 could act as a co-catalyst and is probably responsible for the activation of substrates, resulting in a higher yield of ketone **378n** (96% *vs.* 73%, entries 3-B, 4-B). The role of titanium catalyst was examined in more detail in section 4.3.3.7.

Nevertheless, the approach showed that the developed cross-electrophile coupling and its scope of application could be extended in the future by the direct use of benzyl chlorides with a simpler reaction set-up compared to the alcohols.

Table 4-14: Control reactions for the coupling of benzyl chlorides and thioester **140**.

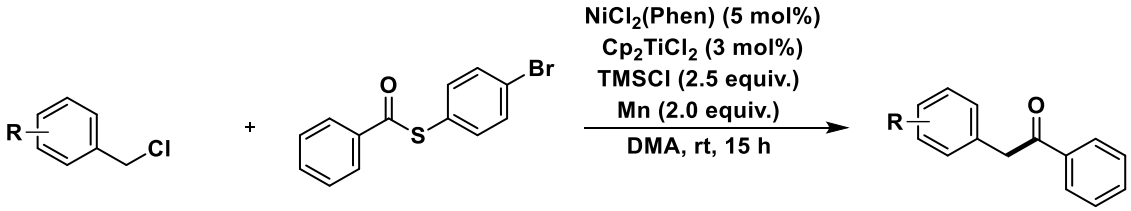

317b (R = 4-OMe)
317a (R = 4-H)
2.2 equiv.

140
0.5 mmol

378a (R = 4-OMe)
378n (R = 4-H)

Entry	Reaction conditions	A) Yield of 378a [%][a]	B) Yield of 378n [%][a]
1	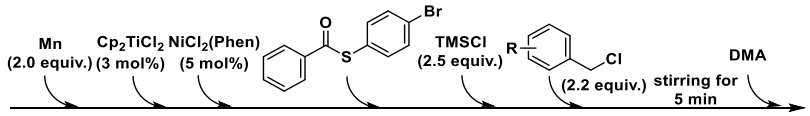	83	44 (41)[b]
2	w/o Cp_2TiCl_2	30	39
3	w/o TMSCl	73	96
4	w/o Cp_2TiCl_2, w/o TMSCl	✖	73

***Standard Reaction Conditions*:** Mn (54.9 mg, 1.00 mmol, 2.0 equiv.), Cp_2TiCl_2 (3.7 mg, 15 µmol, 3.0 mol%), $NiCl_2$(Phen) (8.0 mg, 25 µmol, 5.0 mol%), **140** (146 mg, 500 µmol, 1.0 equiv.), TMSCl (159 µL, 1.25 mmol, 2.5 equiv.), chloride **317a/b** *via* syringe pump over 5 min (1.1 mmol, 2.2 equiv.), rt, 5 min; then abs. DMA *via* syringe pump over 5 min (2 mL), rt, 15 h. [a]: Determined by GC-FID using *n*-pentadecane as internal standard; [b]: The number in parentheses indicates the isolated yield.

Subsequently, the scope of suitable chlorides under standard conditions was explored. 2-Phenylacetophenone (**378n**) was generated in a moderate yield of 41%, and the coupling of benzylic chlorides bearing OMe and Me substituents in *meta* and *para* positions gave similar yields of ketones **378o** and **378p** (33% and 44%, Scheme 4-37A). The re-optimized conditions with the absence of TMSCl were also applied to several chlorides (Scheme 4-37B). In addition to the formation of ketones **378a** and **378n** in yields of 43% and 42%, it was also possible to synthesize naphthyl-containing ketone **378q** and alkyl ketone **378r**, albeit in modest yields (14%, 23%, Scheme 4-37B). Additionally, ketone **378s**, which contains the Ibuprofen scaffold, was isolated in 28% yield (Scheme 4-37B). From this initial approach it could be followed that the reaction has a high potential for late-stage functionalization of pharmaceuticals and natural products, but further optimization is needed.

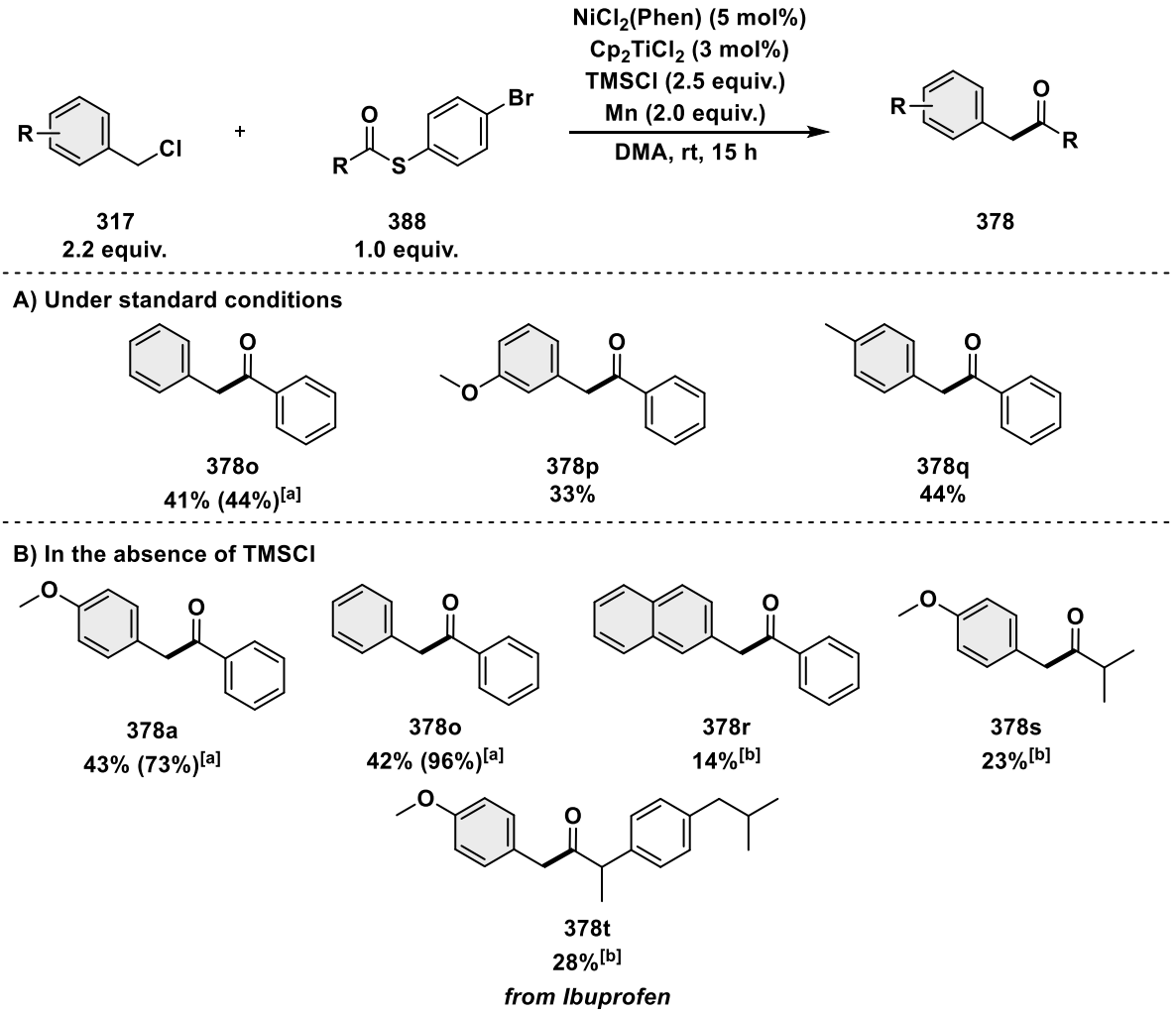

Scheme 4-37: Direct application of benzyl chlorides under nickel/titanium catalysis and reductive conditions. [a]: The number in parentheses indicates the yield determined by GC-FID using *n*-pentadecane as internal standard; [b]: 1.3 equiv. benzylic chloride was used.

4.3.2.4.2 Application of Other Carbonyl-Sulfur Building Blocks

Besides thioesters, thiocarbonates and thiocarbamates were investigated as possible substrates. In this preliminary work, thiocarbonates and thiocarbamates with alkyl and aryl substituents were applied in the catalytic reaction to see where the bond cleavage occurs.

In case of thiocarbonates, GC-MS analysis indicated a C–S bond cleavage and the formation of ester **395** and thioethers **379a** and **379c** (Scheme 4-38A, B). This finding corresponds to the theoretical considerations, which predict a comparatively poor π-overlap within the C–S bond (BDE = 76 kcal/mol) and a weaker σ-bonding compared to C–O (BDE = 100 kcal/mol).[213] Although ester **395** formed, its proportion was relatively low and most of the thiocarbonates were recovered. Apparently, the formation of ester **395** is independent from the choice of thiol moiety, since the same proportion of **395** was approximated with both thiocarbonates **391** and **392**. In contrast, the formation of thioethers **379a** and **379c** was influenced by the thiol moieties and a higher proportion of thioether was achieved with an *S*-phenyl moiety.

For aryl thiocarbamate **393**, the formed thioether **379a** revealed the cleavage of the C–S bond, while the other part of the thiocarbamate, which could be expected to form an amide together with alcohol **316b**, was not observed *via* GC-MS. Regarding alkyl thiocarbamate **394**, neither a formed amide nor thioether nor any other formed product indicated a C–S or C–N bond cleavage.

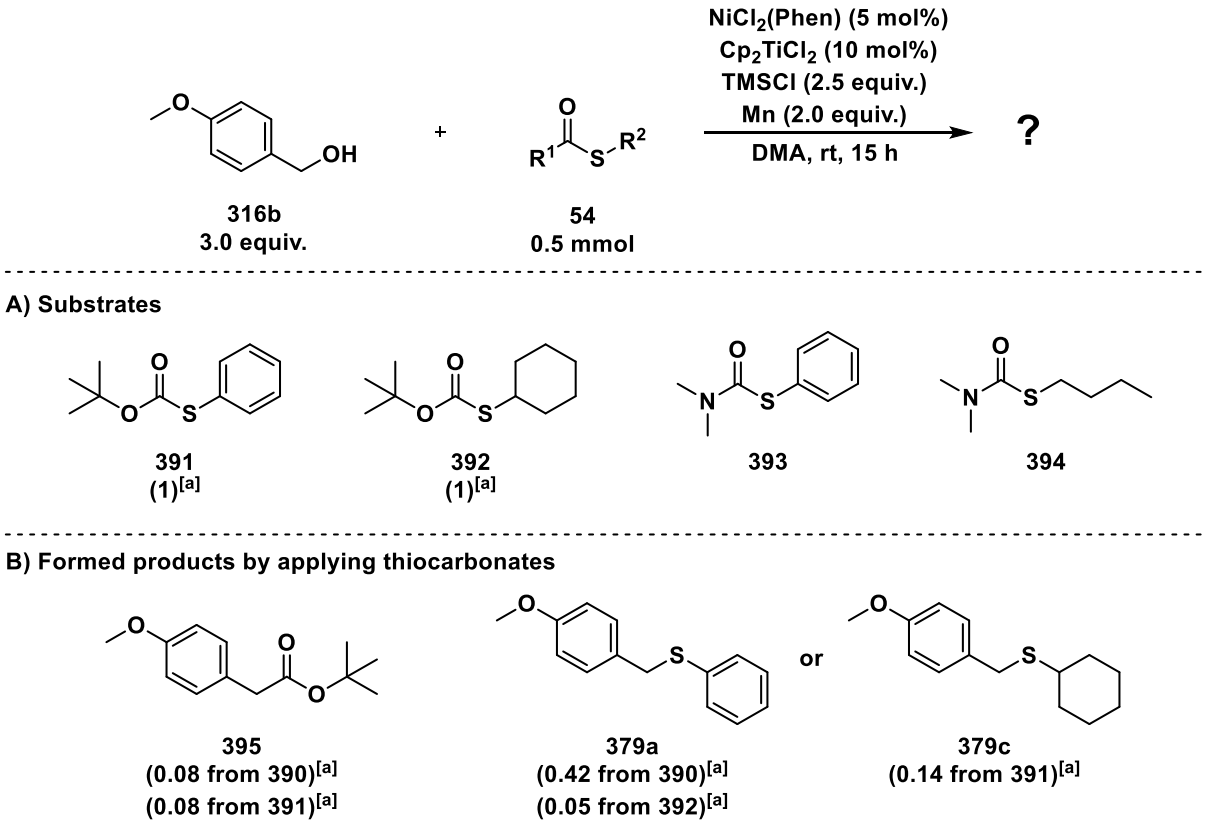

Scheme 4-38: Thiocarbonates and thiocarbamates as substrates in the presented cross-electrophile coupling. [a]: Product analysis was conducted *via* GC-MS. The peak ratios are given in parentheses and were approximated by integrating the highest peaks in the GC chromatogram and relating the areas to the largest peak area, which was set equal to 1.

4.3.3 Mechanistic Inquiry

To better understand the influence of the individual components of this rather complex catalytic system, thorough mechanistic studies were conducted. They are presented in the next sections, starting with the activation of alcohol and continuing with investigations on the role of manganese, the oxidation states of nickel catalyst and the influence of Cp_2TiCl_2.

4.3.3.1 Investigations on Alcohol Activation

Initially, the activation of alcohol **316b** under standard conditions was investigated by omitting thioester **140** (Scheme 4-39A). GC-MS analysis showed the formation of benzylic chloride **317b** even under solvent-free reaction conditions (SFRC) and analogously to the work of Ajvazi and Stavber,[214] only TMSCl is required for chloride generation (Scheme 4-39A, B). After the addition of DMA, homocoupling of chloride was observed, which led to the formation of benzyl dimer **381** (Scheme 4-39A). To further probe whether alcohol **316b** can also be activated by other chlorinating agents, TMSCl was substituted by thionyl chloride and tetrabutylammonium chloride in the standard reaction. However, the replacement of TMSCl proved to be difficult. A complete conversion of alcohol **316b** to benzyl chloride **317b** was observed with thionyl chloride, but the formation of ketone **378a** was suppressed. Neither benzyl chloride **317b**, nor product **378a** formation was observed with tetrabutylammonium chloride. Meanwhile, almost complete formation of benzylic bromide **396** from alcohol **316b** was observed with TMSBr under SFRC (Scheme 4-39B), whereas the employment of TMSBr instead of TMSCl in the standard reaction gave ketone **378a** only in 17% yield, besides a low conversion of thioester **140** (25%).

Recently, Reisman and co-workers classified different Lewis acids by the relative rates in respect to benzyl dimer formation from *N*-hydroxyphthalimide (NHP) esters.[215] They observed that the rate of radical generation from tetrakis(dimethylamino)ethylene (TDAE) reduction of NHP ester increases as the leaving group ability (I > OTf > Br > Cl) of different silyl TMS–X species improves. Following from that, a higher ketone yield would be expected with TMSBr as Lewis acid, contrasting the results from this work. It appears that TMSCl is important for another facet of the developed cross-electrophile coupling that cannot be mediated by TMSBr.

In addition to benzyl chlorides as possible activated intermediates from alcohols, it is known that nickel can undergo oxidative addition into benzyl ethers,[216] and silyl ether **397** could be the predominant electrophile in the developed reaction. To exclude the involvement of a silyl ether species, protected alcohol **397** was applied to standard conditions with and without additional TMSCl, resulting in complete inhibition of ketone formation in both cases (Scheme 4-39C). Moreover, silyl ether **397** was found to be stable under Lewis acidic and solvent-free reaction conditions, but surprisingly **397** was deprotected in solution with TMSCl and DMA, and alcohol **316b** was regenerated, which could be due to traces of water present in DMA.

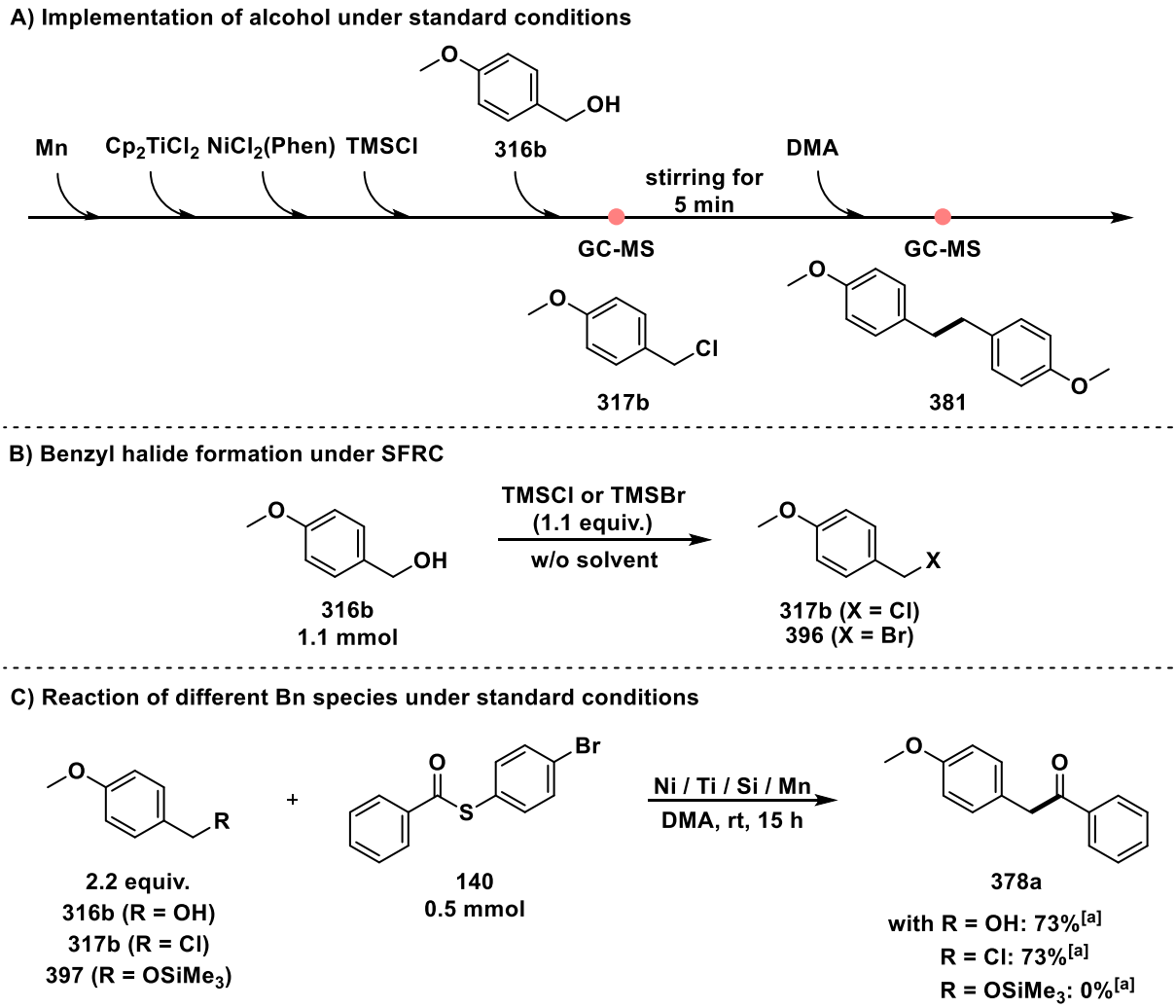

Scheme 4-39: Investigations on benzyl chloride and silyl ether formation under standard conditions. Reaction conditions for Ni / Ti / Si / Mn: $NiCl_2(Phen)$ (5 mol%), Cp_2TiCl_2 (3 mol%), TMSCl (2.5 equiv. for R^1, w/o for R^2, either 1.5 equiv. or w/o for R^3), Mn (2.0 equiv.). [a]: Determined by GC-FID using *n*-pentadecane as internal standard.

These experiments demonstrated that benzyl alcohol **316b** is activated through the *in situ* formation of benzyl chloride **317b**, and the corresponding reaction sequence was investigated in more detail.

Ajvazi and Stavber observed the direct halogenation of different alcohol types using TMSCl and solvent-free reaction conditions.[214] They obtained high yields of the corresponding chlorides with secondary and tertiary benzyl alcohols, but with a dependency on substituents, e.g. electron-rich 4-methoxybenzyl alcohol (**316b**) gave 98% of benzylic chloride **317b**. While tertiary alkyl alcohols could also be converted, chlorination by TMSCl was not observed with electron-poor benzylic alcohols, e.g. with *m*-NO_2 or *m*-CF_3 substituents, nor with primary and secondary alkyl alcohols. Additionally, 2-chloro-2-phenylmethanol was formed quantitatively and chemoselectively from 1-phenyl-1,2-ethanediol.[214] Based on their results, the authors argued that the reaction could occur *via* a S_N1-type nucleophilic substitution process.

The formation of carbeniumion intermediates can be explained by at least two mechanisms.[214] Either the hydrolysis of TMSX with a small amount of water present in the system generates HCl, followed by the protonation of alcohol, the formation of carbeniumion and the reaction with the released chloride ion. Or another possible explanation is related to catalysis caused by the 'halogen bonding' phenomenon.[214] This refers to the non-covalent interaction between a positive site of a covalently bonded halogen X in a molecule R–X with a negative site B, e.g. a lone pair of a Lewis base, resulting in R–X··B interactions.[217] The authors therefore assigned TMSCl a dual role, acting both as a 'halogen bonding' catalyst for the benzyl alcohol, accelerating the formation of carbeniumion intermediates, and as the halogen source.[214]

In the present work, one of the limitations causing a restricted scope of benzylic alcohols could be the insufficient formation of benzylic chlorides. Therefore, unsuccessfully coupled alcohols were reacted with TMSCl under SFRC to investigate which products were generated within the five minutes prior to DMA addition (Scheme 4-40). Benzyl alcohol (**316a**) was completely recovered, while silyl ether **398** was generated from 4-methylbenzyl alcohol (**316e**). Despite the formation of benzylic chloride **317c** from secondary alcohol **316h** under SFRC, the application of **316h** in the catalytic reaction only resulted in the homocoupling instead of ketone formation. Another hint for a cationic intermediate and a S_N1-type nucleophilic substitution pathway was provided by the reaction of 2-(4-methoxyphenyl)propan-2-ol (**316i**) and TMSCl, in which the elimination product **399** was formed as the main compound. According to these experiments, the success of the developed cross-electrophile coupling depends on the prior formation of the chloride species and is influenced by the stabilization of the cationic intermediate.

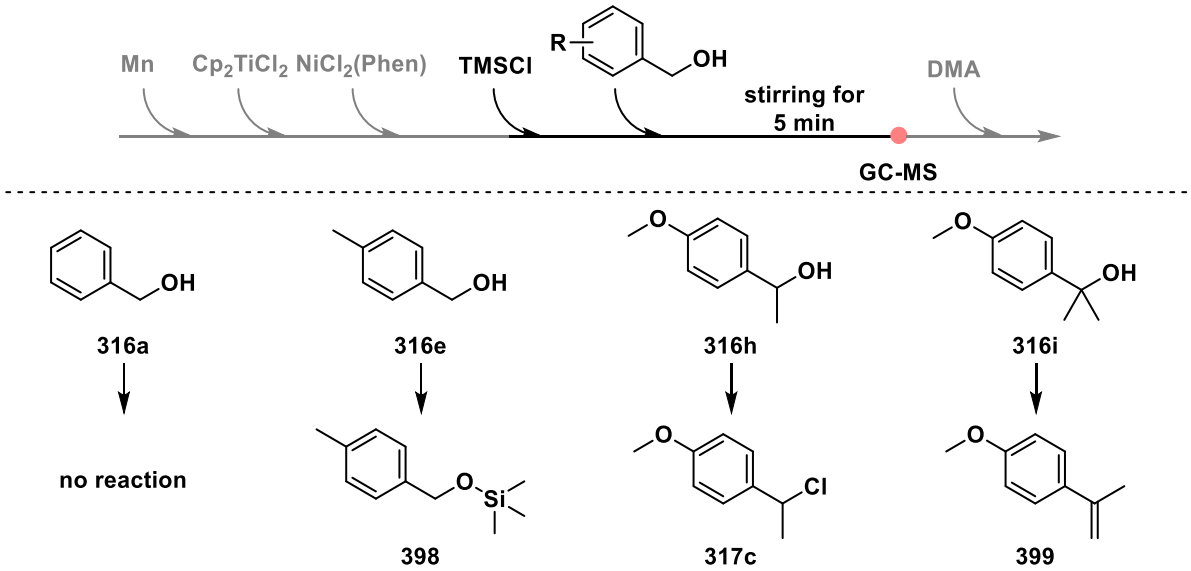

Scheme 4-40: Products after the reaction of benzylic alcohols and TMSCl under SFRC. Product analysis was conducted by GC-MS. The rest of the standard reaction is illustrated in gray to better classify the investigated sequence in the overall reaction. Reaction conditions: TMSCl (1.1 equiv.), respective alcohol (1.1 mmol).

For benzyl alcohol (**316a**) and 4-methylbenzyl alcohol (**316e**), chloride formation was enabled for both substrates at elevated temperature (75 °C) analogous to the conditions of Ajvazi and Stavber (Scheme 4-41A).[214] However, when the catalytic reaction with benzylic alcohol **316e** as substrate was carried out at a higher temperature to allow chloride formation before DMA addition, the formation of silyl ether **398** was again observed (Scheme 4-41B).

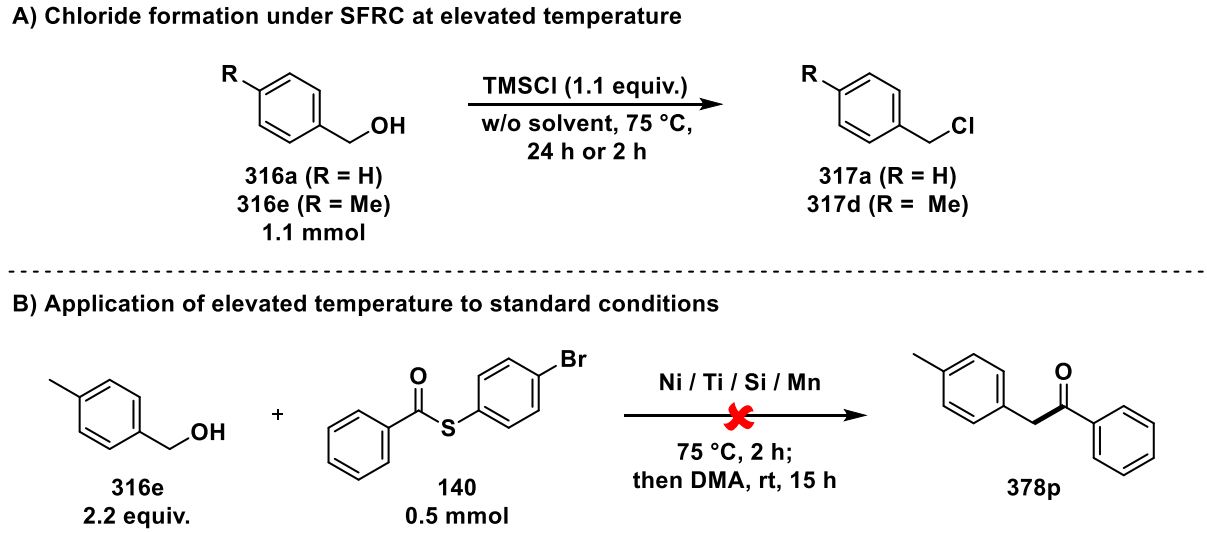

Scheme 4-41: Application of higher temperature from published reaction conditions to allow chloride formation.[214] Reaction conditions for Ni / Ti / Si / Mn: $NiCl_2$(Phen) (5 mol%), Cp_2TiCl_2 (3 mol%), TMSCl (2.5 equiv.), Mn (2.0 equiv.).

The collective experiments on the activation of alcohols showed that the pivotal point is the formation of benzyl chlorides under solvent-free reaction conditions. The inflexibility in the choice of benzylic alcohols under standard conditions can be explained by the restrictive step of chloride formation, e.g. only electron-rich benzylic alcohols probably stabilizing the cationic intermediate,[214] and by the strong dependence of the cross-electrophile coupling on the reaction conditions, e.g. room temperature, which does not allow the chloride formation from less activated alcohols. The involvement of a silyl ether species as the active intermediate could be excluded (Scheme 4-42).

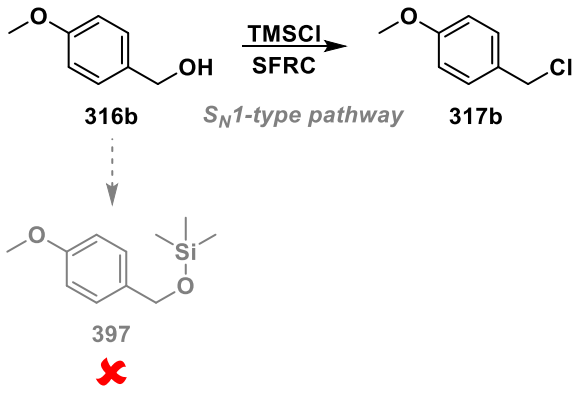

Scheme 4-42: Activation of alcohol **316b** by benzylic chloride **317b** formation.

4.3.3.2 Exclusion of a Classical Cross Coupling Mechanism

Since the chloride appears to be the important intermediate in the reaction, the question arose whether the reaction proceeds according to a classical cross coupling mechanism *via* a nucleophilic organomanganese compound **402** and the mechanistic steps of oxidative addition, transmetalation and reductive elimination (Scheme 4-43).

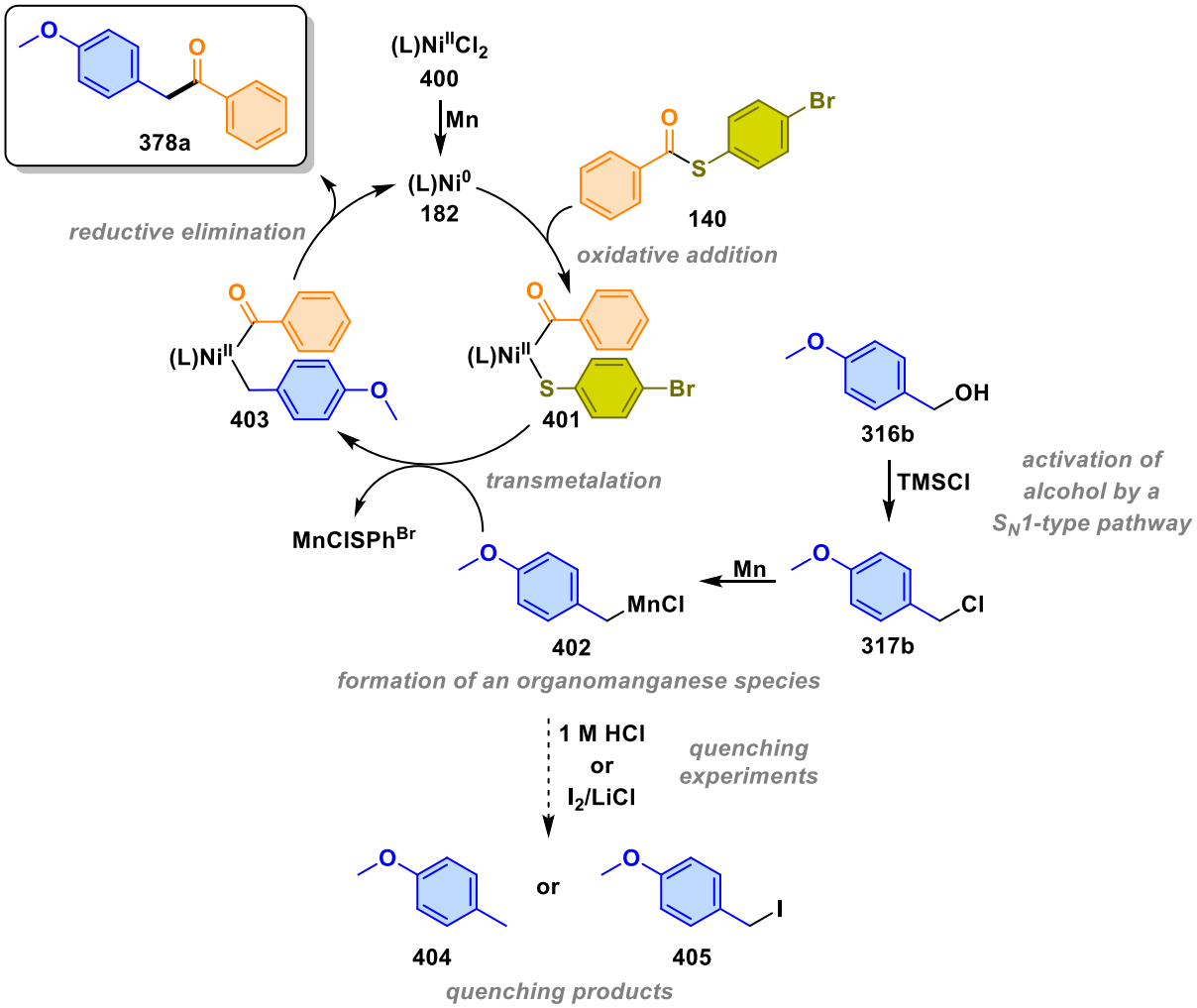

Scheme 4-43: Possible cross coupling mechanism and conducted quenching experiments.

To verify an organomanganese intermediate **402**, two different quenching experiments were conducted. Initially, the reaction was quenched with HCl, and the dechlorinated product **404** was detected in traces. The formation of **404** could result either from traces of R–MnX or from another reactive species, for instance a benzyl radical. However, the formation of **402** was ruled out by a second experiment using an I_2/LiCl solution as quenching agent,[218] since the expected 4-methoxybenzyl iodide (**405**) was not observed at all (Scheme 4-43).

Furthermore, the reaction of benzylic alcohol **316b**, TMSCl and manganese in DMA excluded a classical cross coupling mechanism (Scheme 4-44). If an organomanganese species had formed under these reaction conditions, the latter would have reacted with the *in situ* generated chloride **317b** to dimer **381**. However, dimer **381** was detected only in traces, probably due to radical formation mediated by manganese (*vide postea*, section 4.3.3.5), whereas chloride **317b** was generated as main product.

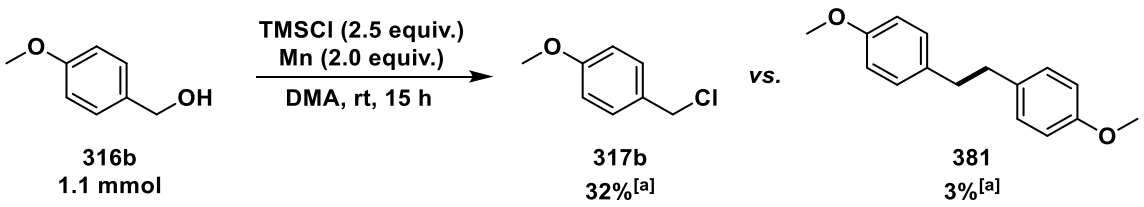

Scheme 4-44: Exclusion of an organomanganese compound after the reaction of alcohol **316b**, TMSCl and manganese in DMA. [a]: Determined by GC-FID using *n*-pentadecane as internal standard.

In summary, the formation of an organomanganese compound from benzyl chloride **317b** and thus a classical cross coupling mechanism was ruled out as a possible pathway for the presented system (Scheme 4-45).

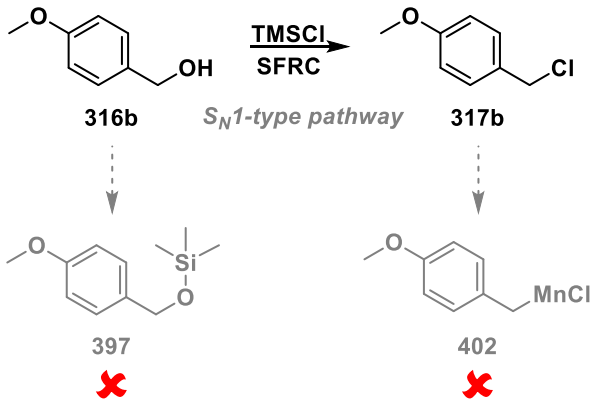

Scheme 4-45: Exclusion of an organomanganese compound **402** formed from benzyl chloride **317b**.

4.3.3.3 Evidence of a Radical Intermediate

In the light of the immediate formation of benzyl dimer **381** from the reaction of alcohol **316b** under standard conditions (*vide supra*, Scheme 4-39A), it was concluded that benzyl radicals could be involved in the mechanism. They are more readily generated from benzyl chlorides than from benzyl alcohols (BDEs: Bn–Cl 71 kcal/mol *vs.* Bn–OH 83 kcal/mol).[7a,134] To test this assumption, several reactions of alcohol **316b** were conducted under different conditions (Scheme 4-46). The conversion of alcohol under standard conditions, but in the absence of nickel precatalyst, resulted in the formation of benzyl chloride **317b**, and alcohol **316b** remained unreacted in the absence of TMSCl (Scheme 4-46A, B).

Another control reaction showed that nickel precatalyst, TMSCl and manganese as reducing agent were required for the formation of dimer **381** (Scheme 4-46C). Interestingly, TMSCl was also necessary for a successful homocoupling of benzylic chloride **317b** under nickel catalysis (Scheme 4-46C). In the absence of TMSCl, benzylic chloride **317b** was not converted, indicating that the Lewis acid additive could be responsible not only for chloride generation from alcohol, but also for activation of the manganese surface, which has been already proposed in literature.[203]

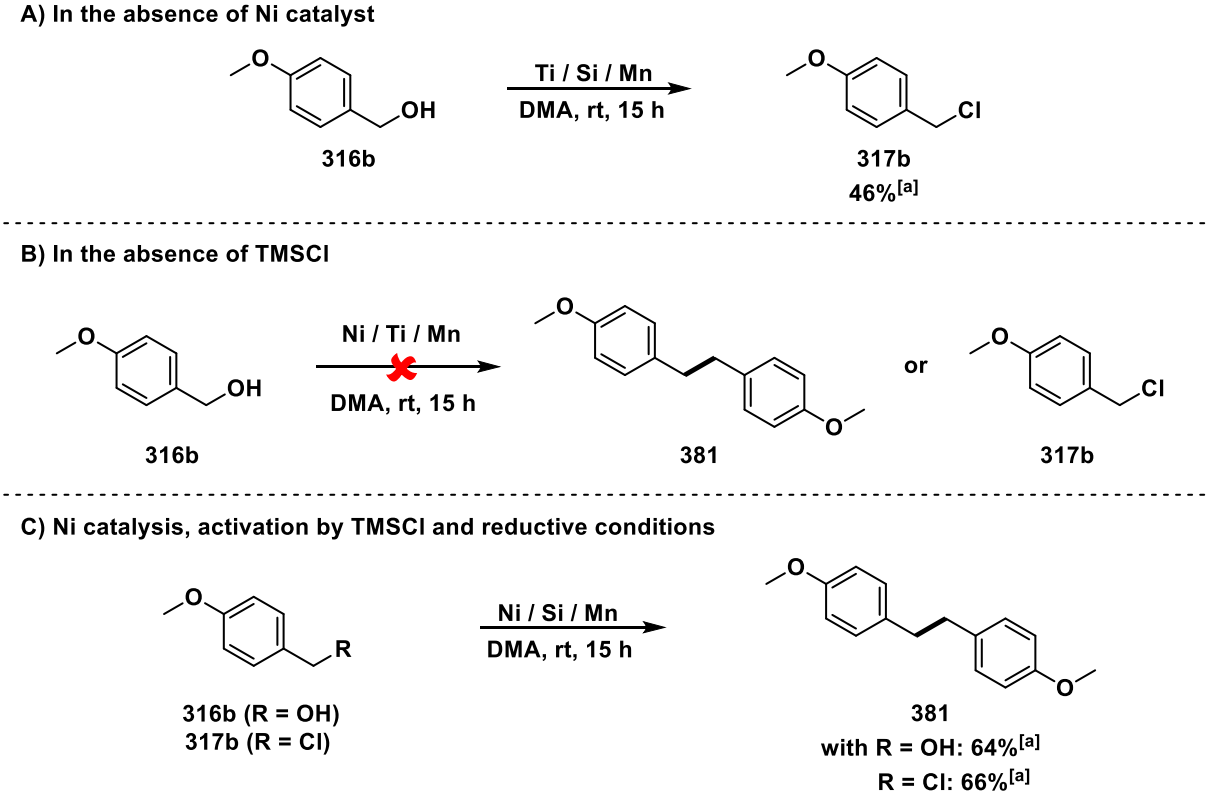

Scheme 4-46: Reaction of **316b** under different reaction conditions and product analysis *via* GC-MS. Reaction conditions for Ni / Ti / Si / Mn: $NiCl_2$(Phen) (5 mol%), Cp_2TiCl_2 (3 mol%), TMSCl (2.5 equiv.), Mn (2.0 equiv.). [a]: Determined by GC-FID using *n*-pentadecane as internal standard.

To exclude that dimer **381** is directly involved in the mechanism, it was applied in the reaction with thioester **140** under standard conditions, but no conversion of substrates was observed (Scheme 4-47).

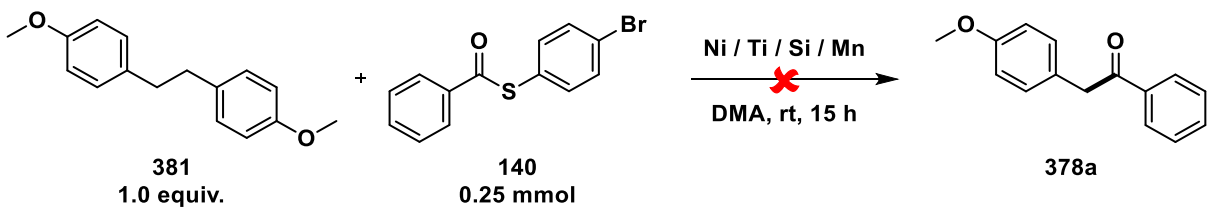

Scheme 4-47: Reaction of dimer **381** and thioester **140** under standard conditions. Reaction conditions for Ni / Ti / Si / Mn: $NiCl_2$(Phen) (5 mol%), Cp_2TiCl_2 (3 mol%), TMSCl (2.5 equiv.), Mn (2.0 equiv.).

Investigations on the involvement of a radical intermediate were pursued by conducting several experiments with radical scavengers (Table 4-15). The TEMPO and Galvinoxyl radicals completely suppressed the product formation, however they are also known to poison the nickel(0) species (entries 2, 3).[219] In contrast, the reactions with BHT, PBN, 9,10-DHA and diethyl HE allowed product formation, albeit in decreased yields (entries 4–7). In all cases, none of the expected radical adducts were detected.

Table 4-15: Radical scavenger screening.

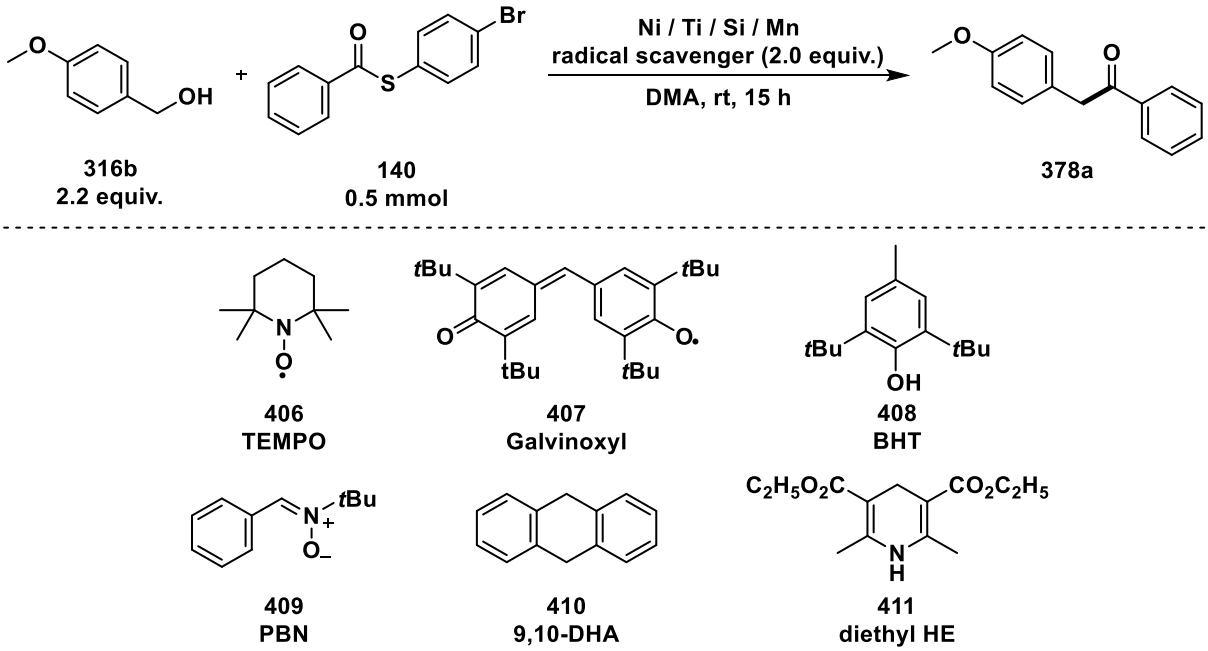

Entry	Radical scavenger	Yield of 378a [%][a]
1	w/o	73
2	TEMPO	✘
3	Galvinoxyl	✘
4	BHT	13
5	PBN	63
6	9,10-DHA	40
7	diethyl HE	40

Reaction Conditions: Mn (54.9 mg, 1.00 mmol, 2.0 equiv.), Cp_2TiCl_2 (3.7 mg, 15 µmol, 3.0 mol%), $NiCl_2$(Phen) (7.8 mg, 25 µmol, 5.0 mol%), **140** (146 mg, 500 µmol, 1.0 equiv.), TMSCl (159 µL, 1.25 mmol, 2.5 equiv.), **316b** *via* syringe pump (SP) over 5 min (137 µL, 1.10 mmol, 2.2 equiv.), rt, 5 min, radical scavenger (1.0 mmol, 2.0 equiv.); then abs. DMA *via* SP over 5 min (2 mL), rt, 15 h. [a]: Determined by GC-FID using *n*-pentadecane as internal standard.

A success in verifying a radical intermediate was achieved by reacting an excess of benzylic alcohol **316b** with both radical scavenger TEMPO and *tert*-butyl acrylate as radical acceptor under standard conditions, but in the absence of thioester **140** (Scheme 4-48). The TEMPO-adduct **412** was detected *via* HPLC-HR-MS, while the radical acceptor adduct **414** was isolated as an inseparable mixture with benzyl dimer **381**.

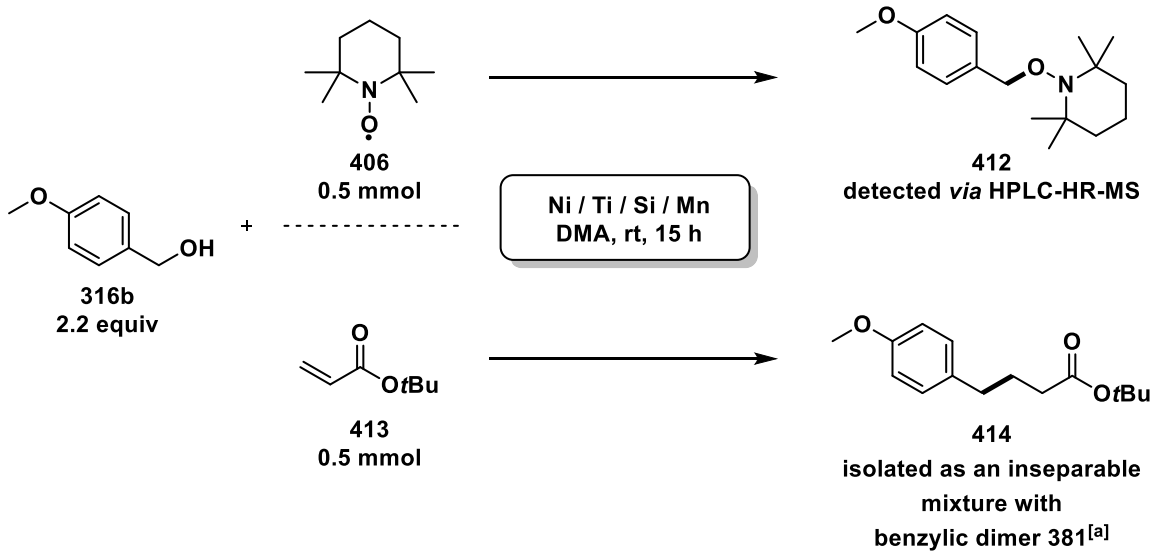

Scheme 4-48: Trapping the benzyl radical with TEMPO and *tert*-butyl acrylate. Reaction conditions for Ni / Ti / Si / Mn: $NiCl_2$(Phen) (5 mol%), Cp_2TiCl_2 (3 mol%), TMSCl (2.5 equiv.), Mn (2.0 equiv.). [a]: Mass ratio: dimer **381**: 97%, adduct **414**: 3%, determined by ^{1}H-NMR spectroscopy.

The benzyl radical was further evidenced by radical clock experiments. In contrast to expectations, the reaction of thioester **140** and cyclopropyl(4-methoxyphenyl)methanol (**316o**) did not give the ring-opened product **378t**. Instead, full conversion to the ring-opened chloride **317e** was detected besides unreacted thioester **140** (Scheme 4-49A, above). However, when using α-cyclopropylbenzyl alcohol (**316p**) as substrate, ketone **378u** was isolated in 22% yield (Scheme 4-49A, below). To gain further insight into possible intermediates of the radical clock reaction, α-cyclopropylbenzyl alcohol (**316p**) was reacted with TMSCl under SFRC, generating a mixture of chlorinated radical clock **317f**, ring-opened chloride **317g** and traces of not converted alcohol **316p**, with chlorinated radical clock **317f** as the main product with a molar fraction of 64% (Scheme 4-49B).

The experiments showed unusual reactivities and ring-openings of the alcohols in the presence of TMSCl, depending on the respective substituents. Further experiments are required to explain the favored ring-opening with electron-rich cyclopropyl(4-methoxyphenyl)methanol (**316o**). A related approach in the literature described the Lewis acidic transformation of substituted α-cyclopropylbenzyl alcohols into homoallylic halides with magnesium halides, whereby the substituents influence the formation and stabilization of an intermediate magnesium oxonium species.[220] However, the direct halogenation of α-cyclopropylbenzyl alcohols without ring-opening was not mentioned.

The application of ring-opened chloride **317g** in the coupling led to the recovery of substrates (Scheme 4-49C, above). In contrast, the mixture of chlorinated radical clock **317f** and ring-opened chloride **317g** gave the expected ketone **378u** under standard conditions (Scheme 4-49C, below). Chlorinated radical clock **317f** was fully consumed and the ring-opened chloride **317g** was still present, indicating that **317g** was not involved in the

formation of ketone **378u**. Seemingly, chlorinated radical clock **317f** was the active intermediate.

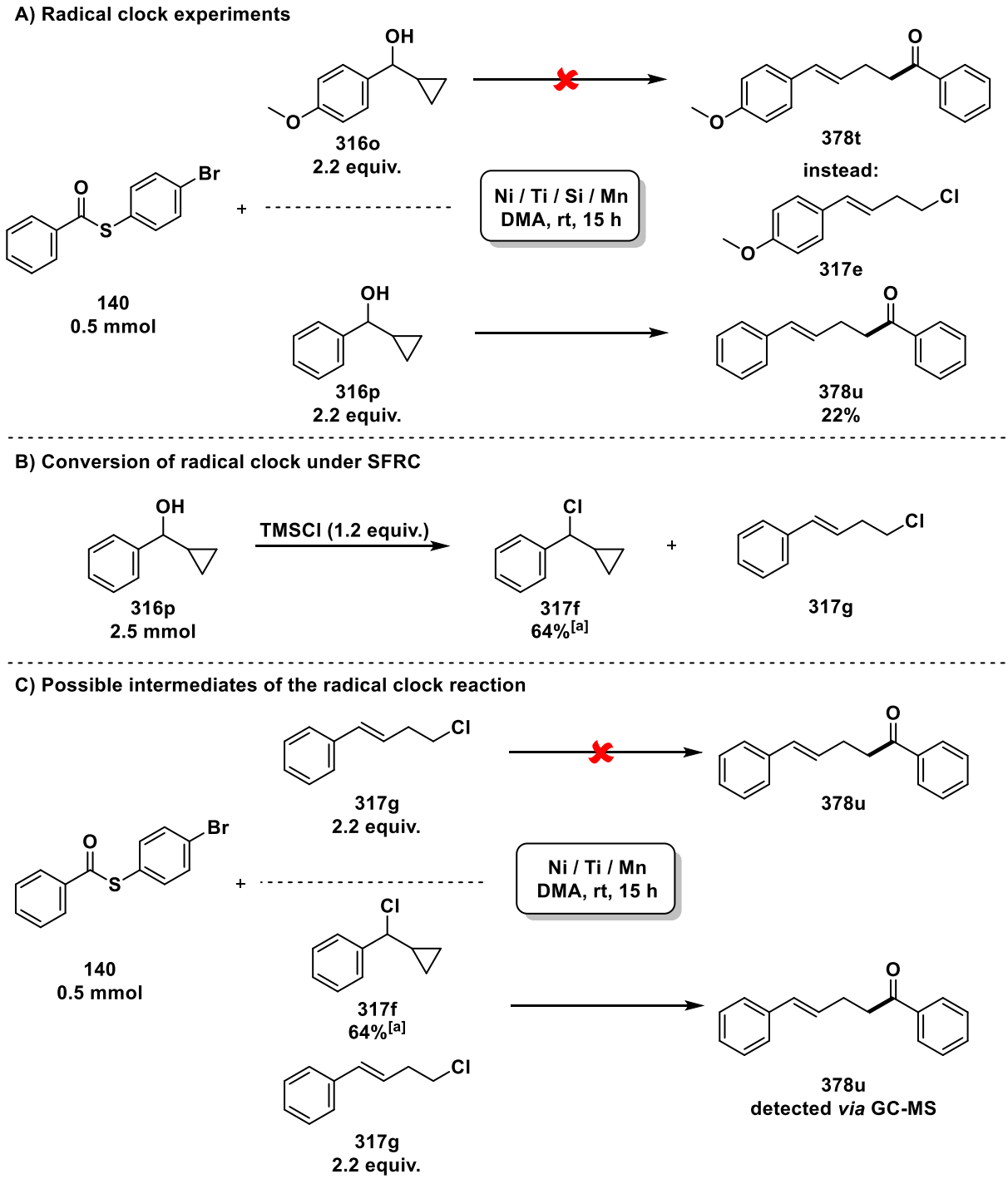

Scheme 4-49: Radical clock experiments. Reaction conditions for Ni / Ti / Si / Mn: $NiCl_2$(Phen) (5 mol%), Cp_2TiCl_2 (3 mol%), TMSCl (2.5 equiv.), Mn (2.0 equiv.). [a]: Determination of the molar fraction by ^{1}H-NMR spectroscopy.

With the verification of the benzyl radical **415**, which is generated from chloride **317b** under the aid of nickel, TMSCl and manganese, another part of the mechanism was disclosed (Scheme 4-50).

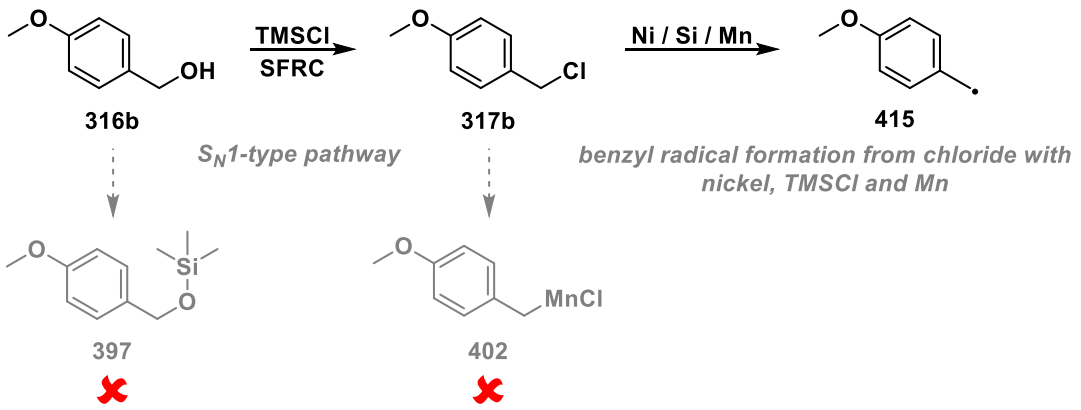

Scheme 4-50: Benzyl radical formation from benzyl chloride **317b** with nickel, TMSCl and manganese.

4.3.3.4 Possible Mechanisms in XEC

Several mechanistic frameworks have emerged from studies on nickel-catalyzed cross-electrophile couplings encompassing two general categories: A) radical-chain mechanisms and B) double oxidative additions (or sequential reductions) (*vide supra*, section 4.1.3).[20,21] There are two possible scenarios that can be considered for the presented system (Scheme 4-51).

In a radical-chain pathway, an active nickel(0) species could be generated by the reduction of the nickel(II) precatalyst with manganese allowing the subsequent oxidative addition of thioester and the generation of the nickel(II) oxidative addition product **401**. The alcohol could be activated *in situ* by chloride formation, generating the benzyl radical **415** through reduction/halide abstraction by nickel(I) complex **187**, a later intermediate of the catalytic cycle. The benzyl radical could undergo one-electron oxidative addition to nickel(II) complex **401**, furnishing a nickel(III) intermediate **416**. Nickel(I) complex **187**, which is responsible for radical generation, and the desired ketone **378a** are released after reductive elimination from nickel(III) species **416**. The catalytic cycle is closed by the reduction of nickel(II) **181** to nickel(0) **182** with manganese as electron donor.

Alternatively, a double oxidative addition could operate. It would start again with the generation of the active nickel(0) species **182** and the oxidative addition of thioester **140**. With another equivalent of manganese, nickel(I) intermediate **417** could be generated. A second oxidative addition of benzyl chloride to nickel(I) **417** gives a formal nickel(III) species **419**, from which the desired ketone **378a** could be reductively eliminated and a nickel(I) species **225** can be delivered. The reduction of the latter by manganese closes the catalytic cycle.

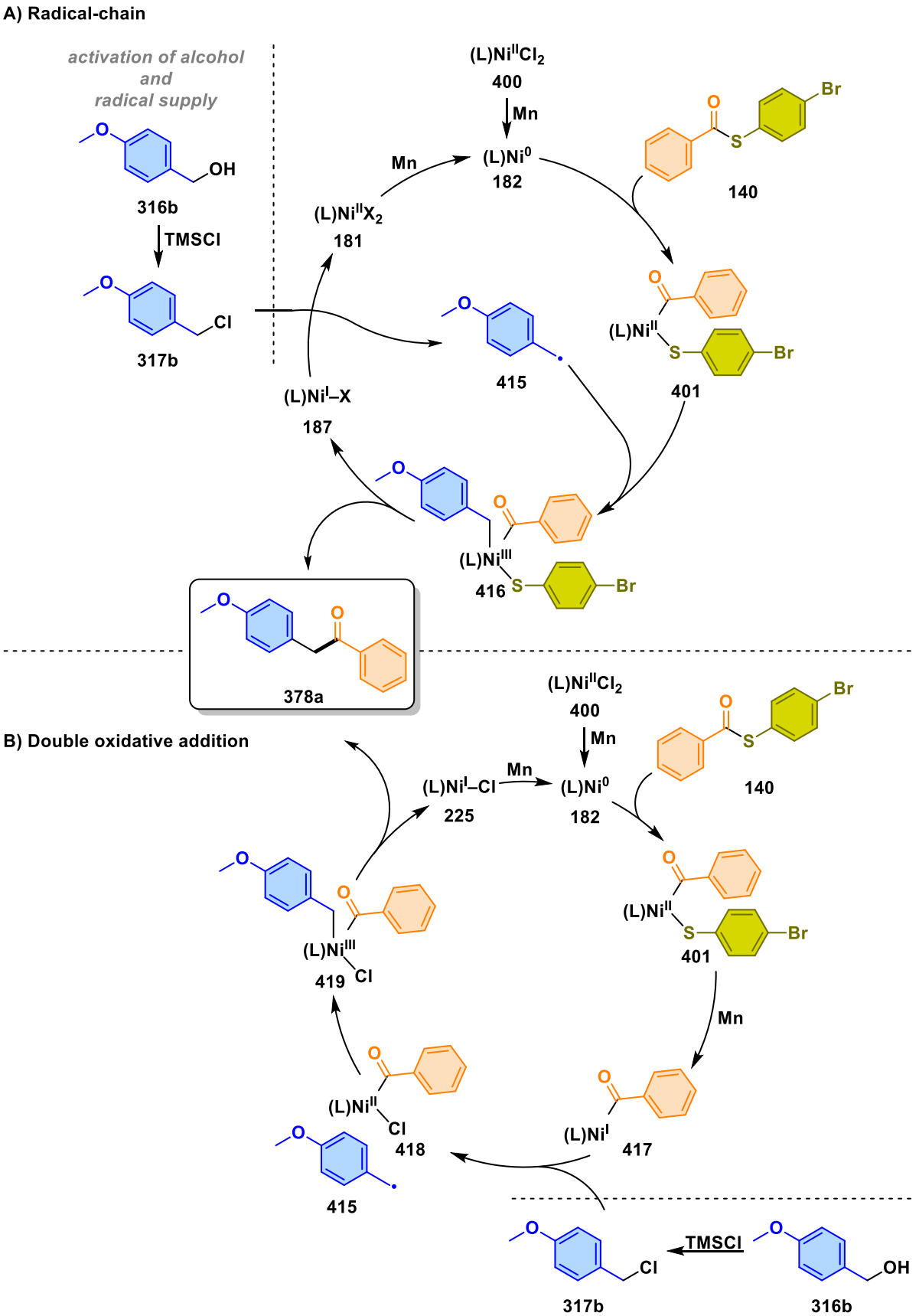

Scheme 4-51: Possible mechanisms for the developed cross-electrophile coupling. L = 1,10-phenanthroline, X = thiolate or Cl.

4.3.3.5 Role of Manganese

Subsequently, the use of manganese as reductant was investigated. As already shown in Figure 4-6, the reaction strongly depends on the equivalents of reducing agent. Increasing the amount of manganese from two equivalents as in standard reaction to three equivalents led to nearly the same ketone yield. In contrast, the yield was reduced by 50% when the amount of manganese was halved. Finally, the reaction was completely inhibited in the absence of reducing agent (*vide supra*, Figure 4-6).

Replacing nickel(II) precatalyst and manganese directly by 5 mol% $Ni(cod)_2$ and 1,10-phenanthroline (Phen) as ligand completely inhibited product formation (Scheme 4-52A, entry 1). Interestingly, the coupling was still not successful with stoichiometric amount of $Ni(cod)_2$ and Phen (Scheme 4-52A, entry 2). Instead, thioester **140** was recovered, and alcohol **316b** was transformed to chloride **317b**, indicating that a nickel(0)-initiated catalytic cycle is not possible without an intermediate reduction. Confirming the assumption, the reaction with $Ni(cod)_2$ was enabled by catalytic amount of ligand and two equivalents manganese, yielding ketone **378a** in 39% (Scheme 4-52A, entry 3). The results showed that $Ni(cod)_2$/Phen is a less effective catalyst system in contrast to $NiCl_2$(Phen), which could be due to inefficient ligand exchange and the detrimental inhibitory effect of cod ligand on oxidative addition.[210c,222] In addition, manganese is apparently involved in an indispensable reduction step of the catalytic cycle and does not only serve as an initial reducing agent for the precatalyst. The amount of Phen as ligand can negatively influence the ketone yield, as shown in entry 4 (Scheme 4-52A). The yield of ketone **378a** was lowered to 17% with catalytic amount of $Ni(cod)_2$, stoichiometric amount of ligand and the presence of manganese. A similar yield was observed with $Ni(^{4\text{-}t\text{Bu}}stb)_3$ (stb = *trans*-stilbene) as nickel(0) source,[223] stoichiometric amount of Phen and with manganese, forming ketone **378a** in 25% yield.

Furthermore, it is known that benzyl radicals can be generated from benzyl chlorides by zinc in DMA.[224] Therefore, it is possible that manganese could be involved in radical formation in addition to nickel(I). Thus, the generation of a benzylic radical by manganese was investigated in radical quenching experiments with TEMPO (Scheme 4-52B). Indeed, the reaction of TEMPO, an excess of benzylic alcohol **316b**, TMSCl and manganese in DMA yielded the expected TEMPO-adduct **412**, which was detected by HPLC-HR-MS. In contrast, **412** was not observed after the reaction of TEMPO, benzyl chloride **317b** and manganese in DMA. Nevertheless, the formation of adduct **412** was enabled after the addition of TMSCl to these conditions, emphasizing the role of TMSCl in the activation of the manganese surface. The radical trapping experiments revealed that a synergistic reduction of benzyl chloride by nickel(I) and manganese occurs in the developed cross-electrophile coupling.

A) Experiments with Ni(0)

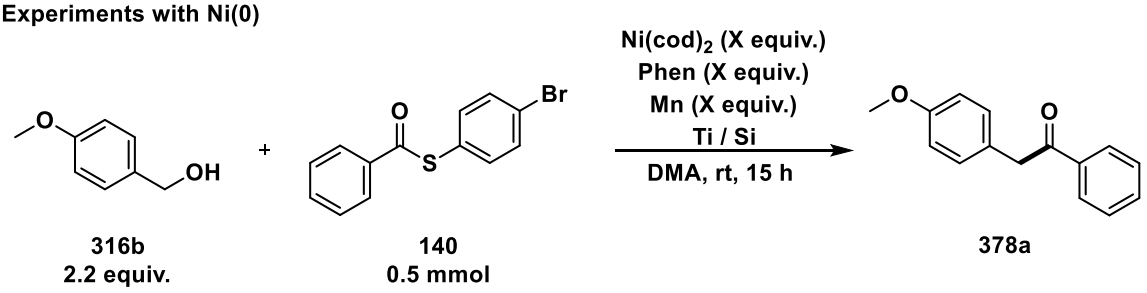

Entry	1	2	3	4
$Ni(cod)_2$ (X equiv.)	0.05	1.0	0.1	0.1
Phen (X equiv.)	0.1	1.1	0.1	1.1
Mn (X equiv.)	✘	✘	2.0	2.0
Yield of 378a [%][a]	✘	✘	39	17

B) Radical generation by Mn

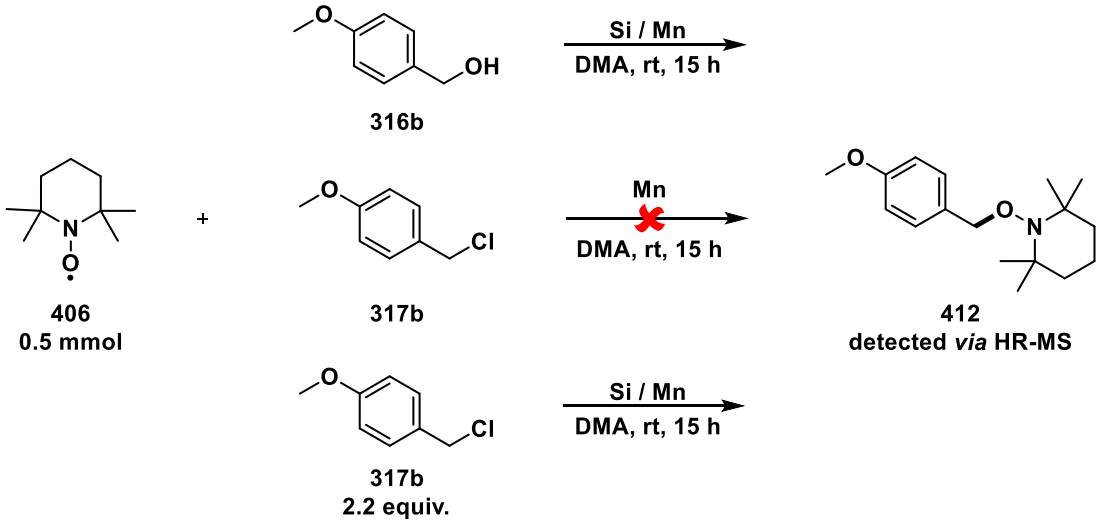

Scheme 4-52: Investigations on the role of manganese. Reaction conditions for Ti / Si / Mn: Cp_2TiCl_2 (3 mol%), TMSCl (2.5 equiv.), Mn (2.0 equiv.). [a]: Determined by GC-FID using *n*-pentadecane as internal standard.

In summary, it was already shown in the optimization process that the amount of manganese (2 equiv.) in the standard reaction could not be reduced. Furthermore, a nickel(0) catalyst requires additional manganese for ketone formation, demonstrating the role of manganese as a mediator in closing the catalytic cycle. Reactions with radical scavenger TEMPO indicated that manganese supports the radical formation. Finally, TMSCl not only forms the benzyl chloride **317b** from alcohol **316b**, but also activates the manganese surface (Scheme 4-53B).

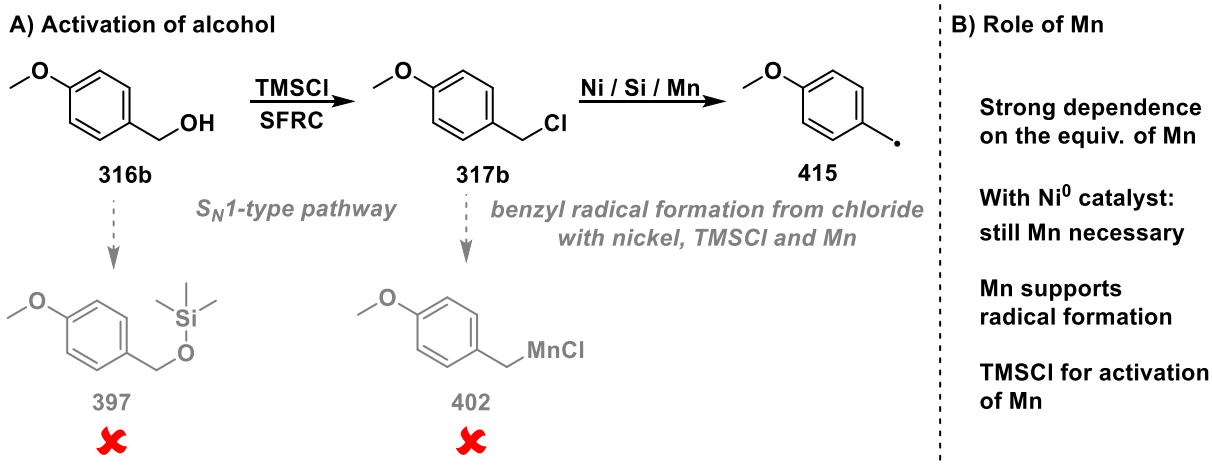

Scheme 4-53: Revealing the role of manganese.

4.3.3.6 Oxidation States of Nickel Catalyst

Subsequently, the mechanistic investigations focused on the nickel catalyst. It was hypothesized that nickel(II) precatalyst could be reduced by manganese to either nickel(0) or nickel(I), two general proposed oxidation states of nickel in cross-electrophile couplings.[5b,d,j,20a,21,27,221] The experiments on the role of manganese have shown that the nickel(0) oxidation state is most likely part of the mechanism and that manganese completes the catalytic cycle.

To obtain more information about the oxidation states involved, the initial reduction of $NiCl_2$(Phen) precatalyst with manganese in DMA was investigated by EPR analysis (Figure 4-14). The reaction resulted in a peak splitting that could be attributed to a paramagnetic nickel species involved, while $NiCl_2$(Phen) in DMA was EPR-silent. Interestingly, the formation of the expected $MnCl_2$ peak was suppressed (*vide postea*, experimental part 3.4, section 4.4.4.5.12). A comparison with related studies in the literature revealed that the EPR spectrum of $Ni^{I}Br$(Phen*) (Phen* = 2,9-di-*sec*-butyl-phenanthroline) in toluene at 10 K shows an axial signal without hyperfine splitting.[20a] A similar spectrum with an axial signal and lack of hyperfine splitting was observed for a mixture of $NiBr_2$(Phen) and zinc in DMA, which was therefore assigned to the formation of $Ni^{I}Br$(Phen).[20a] A rough comparison of these literature known spectra with the spectrum presented in Figure 4-14 does not support the formation of a nickel(I) species. However, since it has already been shown that the reduction of $NiBr_2$(Phen) with manganese instead of zinc also generates nickel(I) as an active catalyst and not the nickel(0) species usually proposed,[27] further investigations are required to completely exclude a nickel(I) species being involved in the initial reduction step. A generated nickel(I) would then react in a nickel(I/II/III) double oxidative addition or radical-chain pathway.[20a,27]

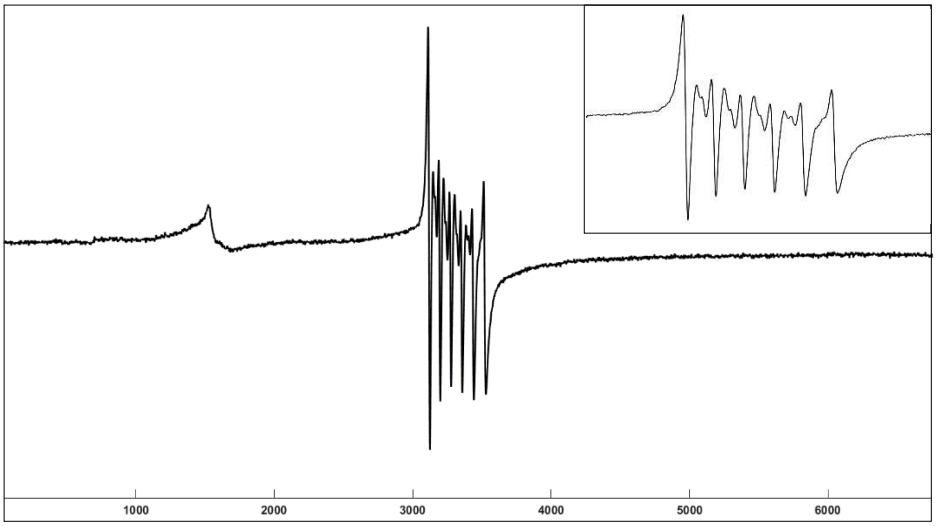

Figure 4-14: EPR spectra of $NiCl_2$(Phen) precatalyst and Mn in DMA (X-band, 9.299 GHz, DMA, 180 K).

Moreover, the used Lewis acids could also affect the nickel catalyst. Various examples show the use of cooperative nickel/titanium catalysts for cross-electrophile couplings (*vide supra*, section 4.1.5.2.10.3.3). Additionally, the distinct excess of TMSCl could influence the nickel catalyst. Experiments supplemented by DFT computations and described in the literature indicated that the Lewis acid additive $MgCl_2$ can act as Cl-ligand donor,[201c] or could be responsible for anion metathesis on the nickel catalyst.[22,64a,77] TMSCl could act in a similar way by providing Cl-ligands for the nickel catalyst and/or removing the thiolate by anion exchange as 4-BrPhS–$SiMe_3$, a compound already known in the literature,[225] but not observed under standard conditions *via* GC-MS.

The studies were then continued by investigations on the oxidative addition step. Initially, the coupling of fluorine-labeled thioester **420** and benzyl chloride **317b** was conducted with stoichiometric amounts of Ni(cod)(Phen) **421** and external ligand, followed by reaction monitoring over time through ^{19}F-NMR analysis (Figure 4-15A). The examination disclosed a fast coupling with the formation of ketone **378c** from the first minute. In addition, unreacted thioester **420** and an uncharacterized compound at -119.2 ppm were detected in the reaction mixture. GC-MS analysis revealed unreacted chloride **317b**, ketone **378c** and thioether **379b** (Figure 4-15B).

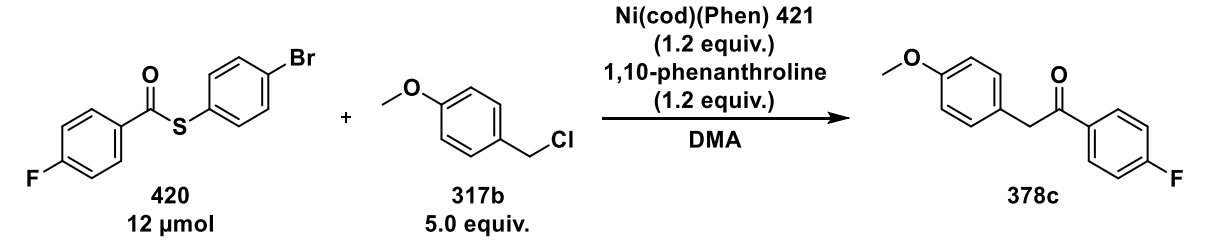

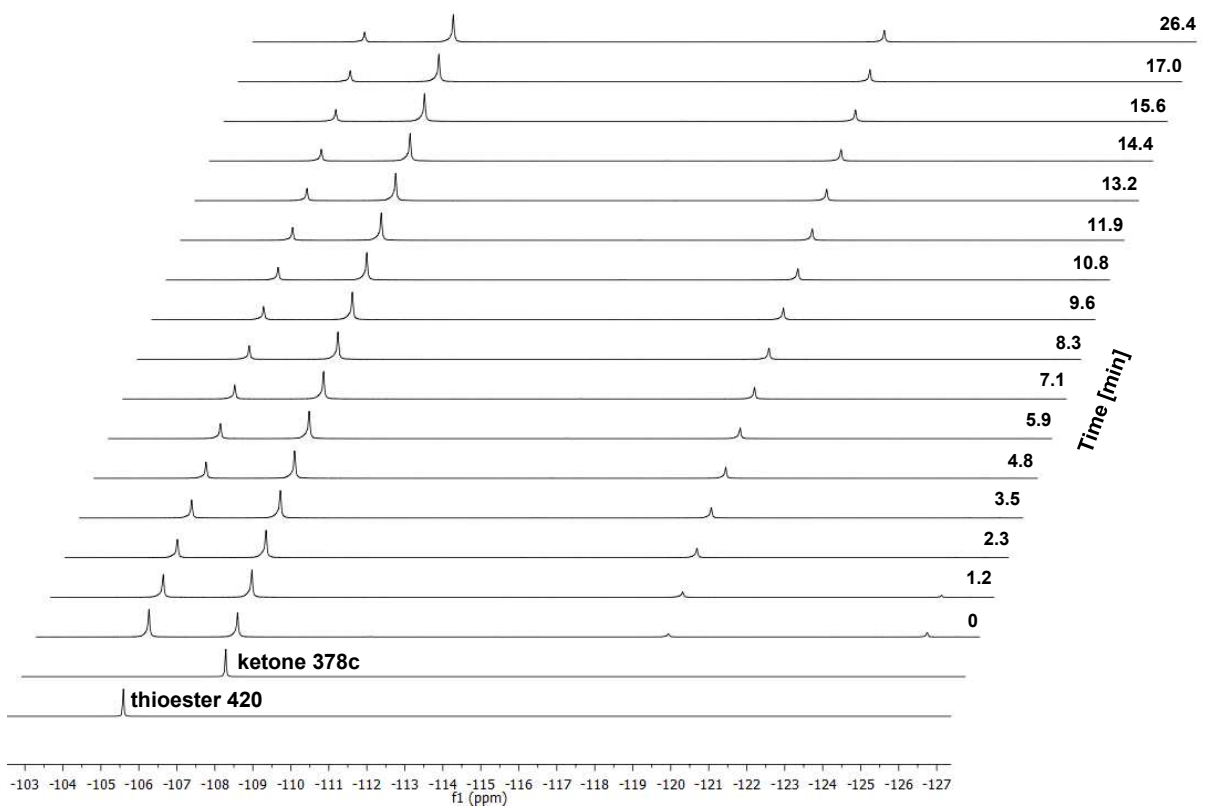

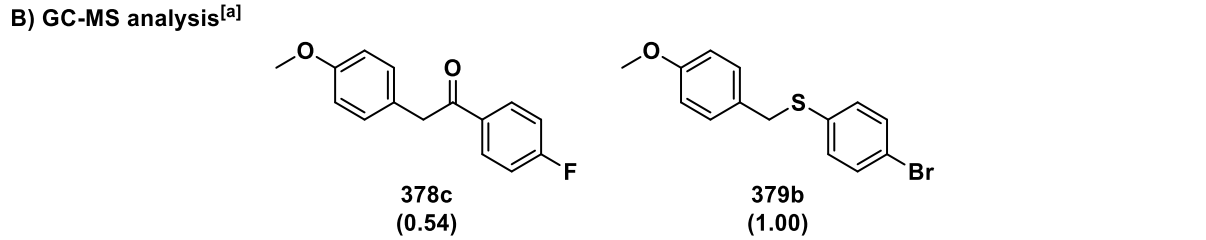

Figure 4-15: 19F-NMR and GC-MS analysis of the reaction between thioester **420** and benzyl chloride **317b** with stoichiometric amount of Ni(cod)(Phen) **421**. NMR spectra were recorded at 658.85 MHz and 298 K. [a]: The peak ratios are given in parentheses and were approximated by normalizing all given peaks to the highest product peak (thioether) in the GC chromatogram, which was set equal to 1.

Subsequently, the interaction between fluorine-labeled thioester **420** and Ni(cod)(Phen) **421** was monitored *via* ^{19}F-NMR in the absence of benzylic chloride **317b** and under lower temperature conditions (286 K). Within the first minute of the reaction, **420** underwent almost complete conversion, accompanied by the emergence of two additional peaks at -110.3 and -125.0 ppm. Notably, the relative intensity of these peaks varied over the course of reaction, as depicted in Figure 4-16.

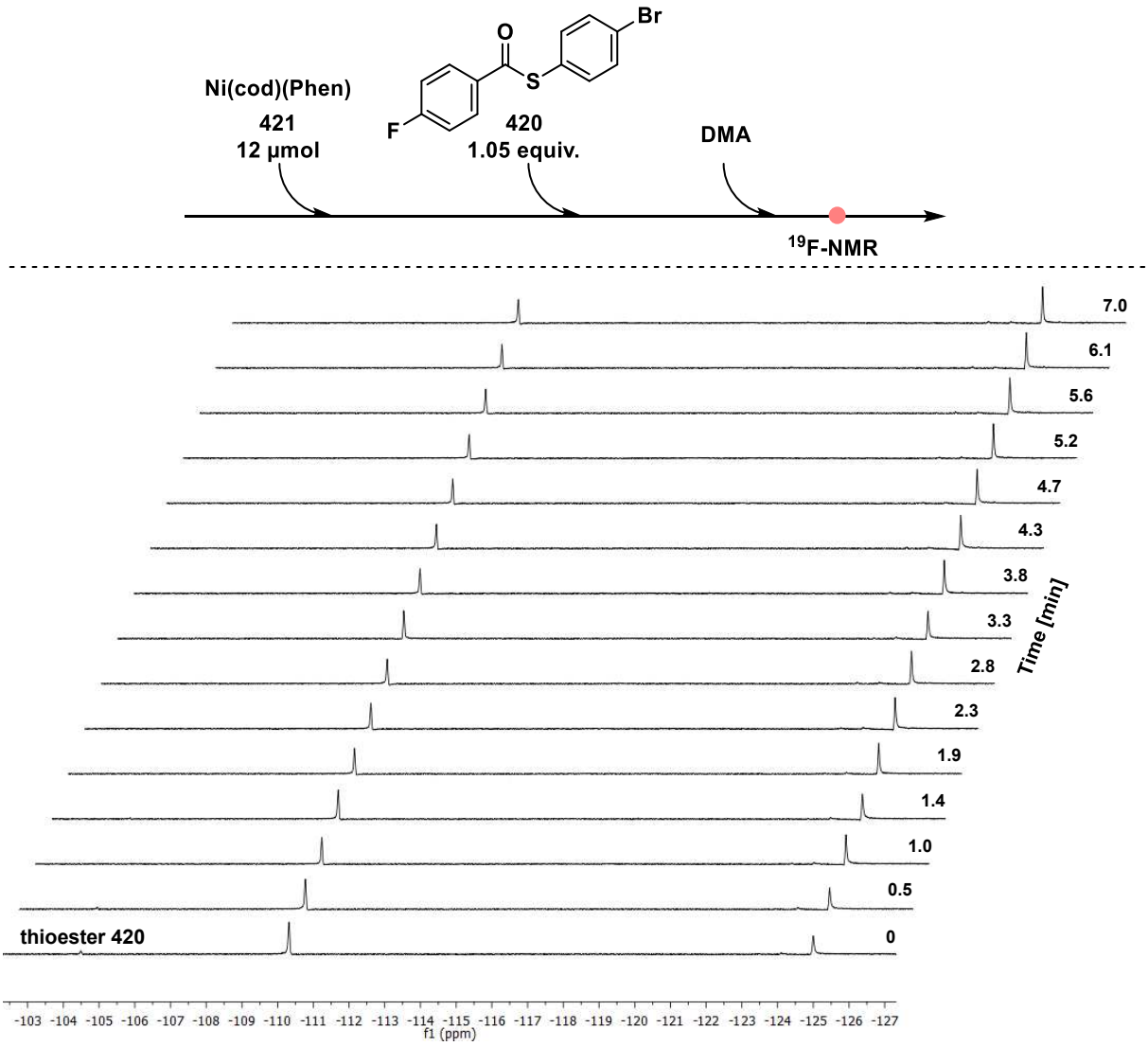

Figure 4-16: ^{19}F-NMR spectra over time of the reaction between thioester **420** and Ni(cod)(Phen) **421**. NMR spectra were recorded in DMA without deuterated solvent, at 658.93 MHz and 286 K in a time interval of 28 s over 7 min.

To assign the peaks to the active nickel species responsible for ketone formation, the fluorine-labeled nickel(II) complex **423-A**, which would form after the oxidative addition of thioester **420** to nickel(0), was synthesized by the reaction of Ni(cod)(Phen) **421** and thioester **420** (Scheme 4-54).

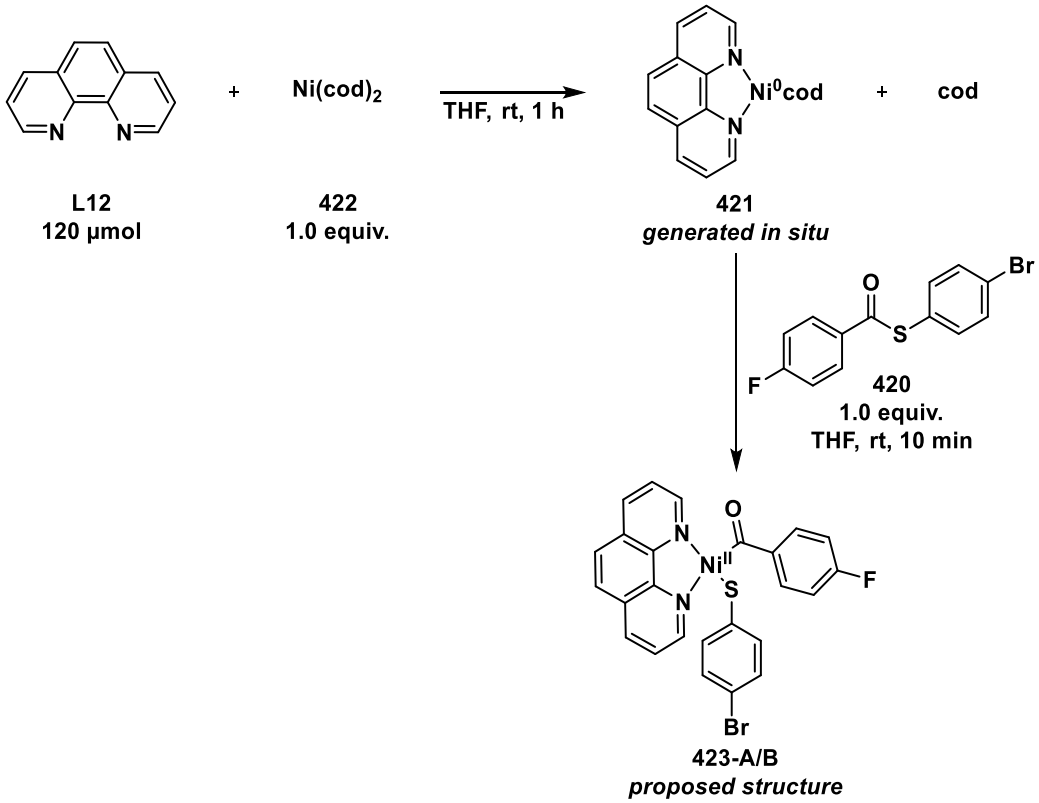

Scheme 4-54: Reaction sequence for the synthesis of the oxidative addition product **423-A/B**.

The ^{19}F-NMR spectrum of **423-A** in DMA showed two peaks similar to those in Figure 4-16 (Figure 4-17A). Nevertheless, slight changes in chemical shifts could be due to differences in spectrometer frequencies (300 MHz *vs.* 700 MHz) and temperatures (286 K *vs.* 296 K). Both peaks disappeared after the reaction of complex **423-A** and benzyl chloride **317b** in the presence of additional phenanthroline in DMA. Ketone **378c** was identified as the formed main product after a spike experiment (Figure 4-17A).

The reproducibility of the synthesis remained difficult, as shown by complex **423-B**, which was synthesized in a second approach. Its ^{19}F-NMR spectrum in DMA exhibited a main peak at -110.5 ppm as well as unconverted thioester **420** and only traces of the compound at -125.1 ppm (Figure 4-17B). It was surmised that the differences could originate from slight changes in the work-up process. Furthermore, it was observed in previous experiments that the nickel(II) complexes were not stable in the presence of residual THF, and the stability of the complexes in DMA has not yet been investigated in detail. The nickel(II) complex **423-B** exhibited an unremarkable EPR spectrum in DMA, probably emphasizing the nickel(II) oxidation state. Again, both peaks (-110.5 ppm and traces of -125.1 ppm) were completely

converted during the reaction of complex **423-B** with benzyl chloride **317b**, delivering ketone **378c** as the product (Figure 4-17B).

As both peaks resulted in product formation, it was hypothesized that the two observed signals could originate from a dynamic (conformational) equilibrium of nickel(II) complexes.[226] Gong *et al.* performed DFT computations to demonstrate that the conversion of the square planar conformer to the more stable tetrahedral $(Py)_2Ni^{II}(Ar)(Cl)$ complex by a Berry pseudorotation-type mechanism facilitates the uptake of a radical by a single-electron transfer in a radical-chain mechanism.[201c]

The experiments also illustrate the difficulties in the reproducibility of the synthesis and characterization of nickel complexes, which probably depend on the work-up process and reaction conditions, e.g. retention time in DMA. In addition, it was indicated that manganese is not required for product formation in the stoichiometric experiments shown in Figure 4-17.

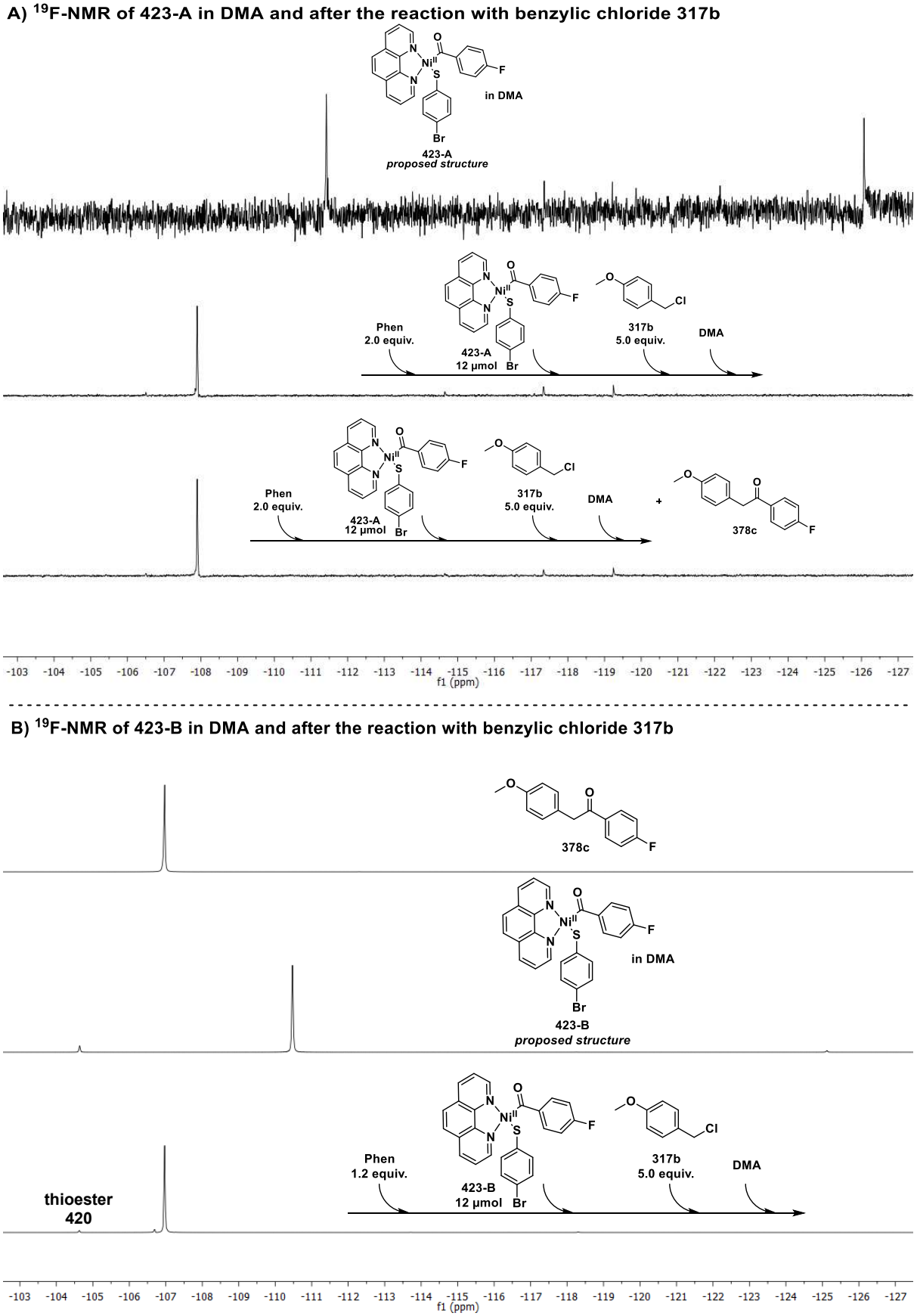

Figure 4-17: ^{19}F-NMR spectra of synthesized nickel(II) complexes **423-A/B** in DMA, and after the reaction with benzyl chloride **317b**. Product analysis in B) was conducted *via* GC-MS. NMR spectra were recorded in DMA without deuterated solvent and in A) at 282.40 MHz, 296 K, after 3 h, and in B) at 658.79 MHz, 296 K, after 1 h 38 min.

Subsequently, experiments in regard to nickel in the oxidation state +II were conducted based on the contributions of Weix and co-workers, who investigated the selectivity differences in reactions of acyl nickel(II) complexes with various halides.[52] They showed that a benzyl halide is selectively coupled to an acyl nickel(II) complex regardless of reducing agent, suggesting that an initial reduction of nickel(II) is not necessary.[52]

Nickel(II) complex **401**, which could be generated after the oxidative addition of thioester **140** to nickel(0), was synthesized by the reaction of Ni(cod)(Phen) **421** and thioester **140**. Then, the complex **401** reacted with an excess of benzyl chloride **317b**, in the absence and presence of additional phenanthroline and manganese (Table 4-16).

In the absence of reducing agent and ligand, ketone **378a**, thioether **379b** and decarbonylated product **424** were formed, indicating that an intermediate reduction of **401** is not required before it can react with benzyl chloride **317b** (Table 4-16, reaction A). In the presence of reducing agent, the selectivity for ketone formation was lowered and several coupling products were generated, amongst others de- and carbonylated products **424** and **385** (Table 4-16, reaction B).

The reaction of nickel(II) complex **401** with benzyl chloride **317b** in the absence of manganese but with additional ligand gave a higher selectivity for the formation of ketone and thioether. This was presumably due to the stabilization of the active nickel intermediate and the nickel complex formed after reductive elimination by the ligand (Table 4-16, reaction C).[227] High proportion of ketone **378a** and thioether **379b** and only traces of the decarbonylated product **424** were observed. The reaction reinforced the assumption that the nickel(II) oxidation state is directly involved and no initial reduction of nickel(II) complex **401** is required for ketone formation. In contrast, formation of ketone **378a** was significantly suppressed in the presence of both manganese and 1,10-phenanthroline (Table 4-16, reaction D). To gain insight into the initiation of reactions A and B, both were also analyzed by EPR, which revealed no signals.

Table 4-16: Reaction of nickel(II) complex **401** with benzylic chloride **317b**.

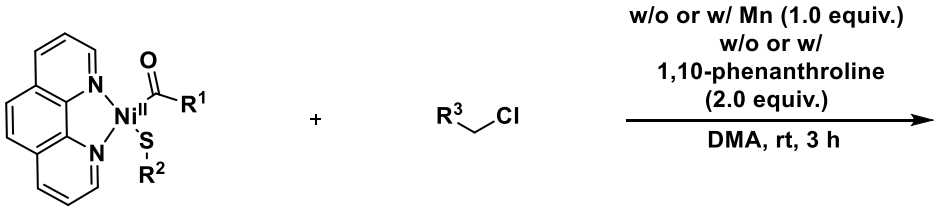

401
30 µmol
R^1 = Ph
R^2 = 4-BrPh

317b
5.0 equiv.
R^3 = 4-MeOPh

reaction A: w/o Mn, w/o 1,10-phenanthroline[a]	**reaction B:** w/ Mn, w/o 1,10-phenanthroline[a]
378a (0.47); **379b** (1.00); **424** (0.59)	**378a** (0.67); **379b** (1.00); **381** (0.68); **424** (0.64); **385** (0.14)
reaction C: w/o Mn, w/ 1,10-phenanthroline[a]	**reaction D:** w/ Mn, w/ 1,10-phenanthroline[a]
378a (0.39); **379b** (1.00); **424** (0.04)	**378a** (0.29); **379b** (1.00)

[a]: Product analysis was conducted *via* GC-MS. The peak ratios are given in parentheses and were approximated by normalizing all given peaks to the highest product peak (thioether) in the GC chromatogram, which was set equal to 1.

Since manganese is not essential for ketone formation from nickel(II) complex **401**, the latter could be an intermediate of a radical-chain mechanism, in which no immediate reduction of the nickel(II) complex **401** is required, before it can react with the benzyl chloride (Scheme 4-55).[21,64a] The absence of benzylic dimer **381** formed from benzylic chloride **317b** in reaction A and only small amount of the dimer **381** under standard conditions further support a radical-chain mechanism.[22] The *p*-methoxy substituted benzyl radical exhibits a large radical stabilization energy (RSE = -53.2 kJ/mol)[228] and is thermodynamically stabilized, but transient with respect to the kinetic stability. Therefore, it can be captured by the persistent metalloradical complex **401** analogous to the persistent radical effect,[25] instead of dimerizing itself (Scheme 4-55).[22]

The initiation of the reaction between nickel(II) complex **401** and benzyl chloride **317b** was not investigated further, but from the experiments shown in Table 4-16 and based on suggestions in the literature (*vide supra*, section 4.1.3), it was concluded that the self-initiation could begin either by halogen atom abstraction of nickel(II) complex **401** from benzyl chloride **317b** or by disproportionation of nickel(II) species **401**.[21,22]

Furthermore, manganese is necessary to close the catalytic cycle, as shown in the experiments in section 4.3.3.5, but also supports the formation of a low-valent nickel species, resulting in a loss of cross-selectivity and off-cycles (Table 4-16, reaction B). The formation of a low-valent nickel species by the reduction of nickel(II) complex **401** was investigated by EPR. The latter nickel(II) complex **401** in DMA was EPR-silent, but the reaction of **401**, external phenanthroline and manganese in DMA revealed an EPR signal of a paramagnetic species, which could be nickel(I) (Figure 4-18). The spectrum was clearly different from that shown in Figure 4-14.

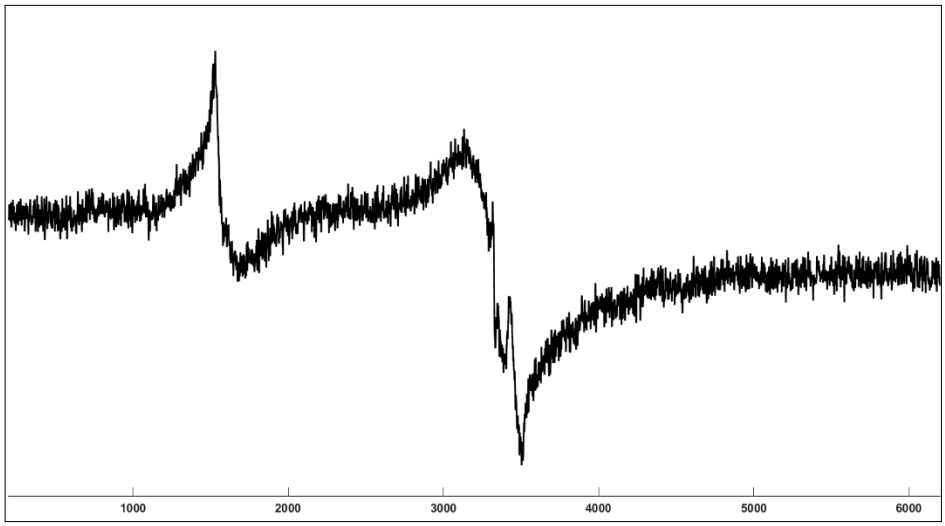

Figure 4-18: EPR spectrum of the reaction of nickel(II) complex **401** and Mn in DMA (X-band, 9.319 GHz, DMA, 180 K).

Based on these results, it was hypothesized that a double oxidative addition could occur simultaneously with the radical-chain mechanism as an off-cycle during the reaction. In such pathway, the reduction of nickel(II) complex **401** by manganese is required, which is an important difference from a radical-chain mechanism, and a nickel(I) species **417** could be generated (Scheme 4-55). A second oxidative addition of benzyl chloride to nickel(I) *via* nickel(II) complex **418** gives a formal nickel(III) species **419** from which the desired ketone could be reductively eliminated (Scheme 4-55). Although PhC(O)–Ni^{I} **417** is not yet known, it has been proposed in the literature to be produced by one-electron reduction of a PhC(O)–Ni^{II} intermediate with zinc.[48,49,63]

The assumption of two concurrent mechanisms has also been investigated in the literature, where it was found that the rate-determining step in a double oxidative addition is only 0.7 kcal/mol higher than the rate-limiting barrier in a radical-chain mechanism. Therefore, the two mechanisms compete with each other and one of them may become dominant depending on the reaction conditions, including the heterogeneous nature of the catalyst system, additives and the activation of the reducing agent.[201c]

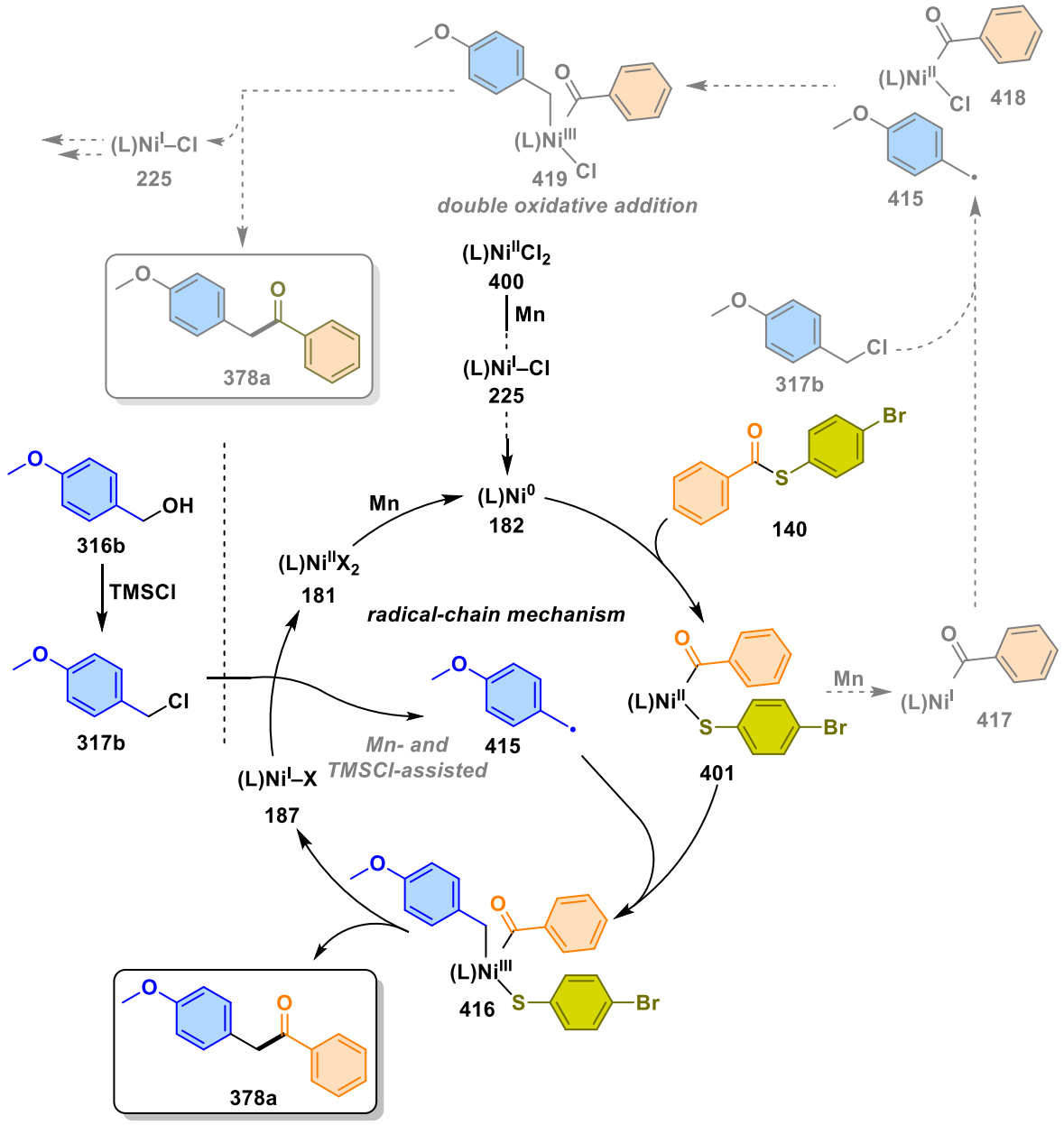

Scheme 4-55: Postulated radical-chain mechanism and a simultaneous double oxidative addition. L = 1,10-phenanthroline, X = thiolate or Cl.

The hypothesis of a parallel double oxidative addition was further investigated with Krossing's nickel(I) salt $[Ni(cod)_2][Al(OC(CF_3)_3)_4]$.[229] The reaction of benzylic alcohol **316b** and thioester **140** under standard conditions, but with 5 mol% of nickel(I) complex and 10 mol% 1,10-phenanthroline as catalyst system, yielded the ketone **378a** in 74% (Scheme 4-56).

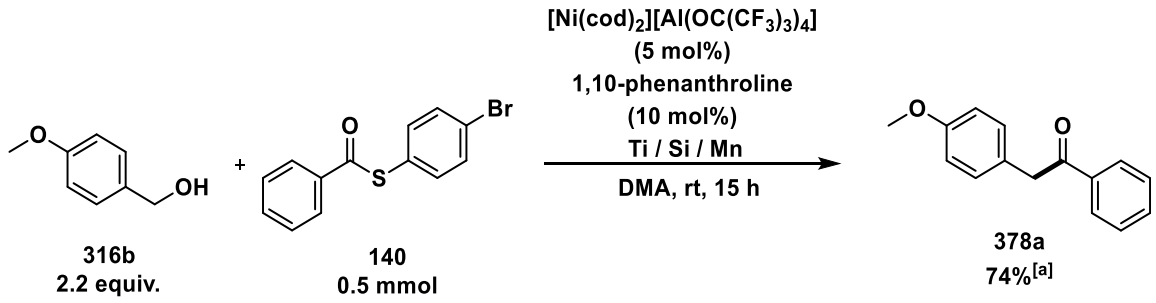

Scheme 4-56: Application of Krossing's nickel(I) salt under standard conditions.[229] Reaction conditions for Ti / Si / Mn: Cp_2TiCl_2 (3 mol%), TMSCl (2.5 equiv.), Mn (2.0 equiv.). [a]: Determined by GC-FID using *n*-pentadecane as internal standard.

Subsequently, a stoichiometric amount of the nickel(I) complex was used in the reactions with thioester **140**, an excess of chloride **317b**, external ligand, and without or with additional manganese (Table 4-17A *vs.* B). Strikingly, no substrate conversion was observed in the absence of the reducing agent, although at least the conversion of benzyl chloride **317b** to bibenzyl **381** would have been expected with the nickel(I) catalyst, which probably demonstrated the unsuitable reactivity of the complex (Table 4-17A). In the presence of manganese, thioester **140** was fully consumed after 3 h and only traces of chloride **317b** were still available (Table 4-17B). Additionally, ketone **378a**, thioether **379b** as well as de- and carbonylated products **424** and **385** were generated. Based on the importance of manganese to turn over the reaction, the generation of an active nickel(0) catalyst capable of performing the oxidative addition of thioester could be possible. Furthermore, the ligands of nickel(I) could play a role in inhibiting the reaction. As shown in earlier experiments and in the ligand screening, a significant influence of phenanthroline was observed. Therefore, the application of further nickel(I) compounds is necessary to exclude or verify it as a possible intermediate.

Table 4-17: Stoichiometric reactions of Krossing's nickel(I) salt with benzyl chloride **317a** and thioester **140**.[229]

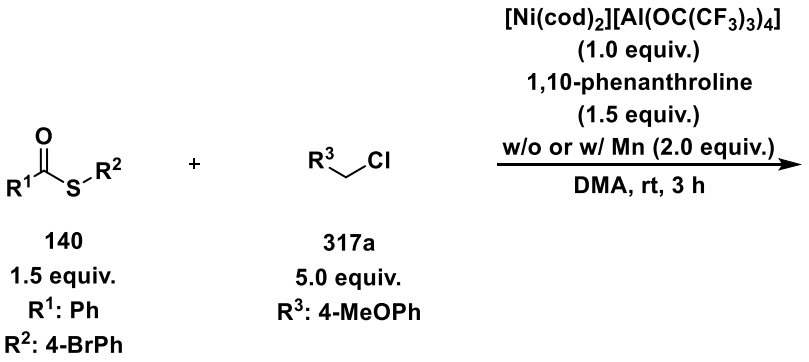

A) w/o Mn[a]	B) w/ Mn[a]
no substrate conversion	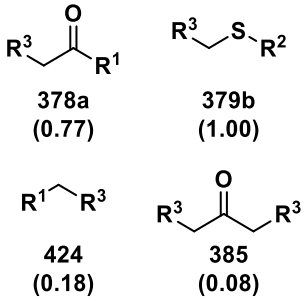 **378a (0.77)** **379b (1.00)** **424 (0.18)** **385 (0.08)**

[a]: Product analysis was conducted *via* GC-MS. The peak ratios are given in parentheses and were approximated by normalizing all given peaks to the highest product peak (thioether) in the GC chromatogram, which was set equal to 1.

As the presented cross-electrophile coupling showed a strong dependence on the solvent, the influence of DMA on different nickel species, such as (L)Ni^{I}X·(DMA)$_n$ or (L)Ni^{0}·(DMA)$_n$ should be considered. Hadt and co-workers published detailed electrochemical studies, which underline the coordination influence of amide-based solvents, especially DMA, on catalytically relevant nickel complexes and support a single-electron reduction event involving a (L)Ni^{I}X·DMA species generated from a nickel(II) precatalyst.[230]

Finally, nickel(II) complex **425**, which could be an intermediate in a double oxidative addition mechanism, was synthesized in analogy to a literature report,[231] and reacted with benzylic chloride **317b** in the absence or presence of manganese (Table 4-18A *vs.* B). As in previous results, ketone **378a** was already observed without manganese besides traces of the de- and carbonylated products **424** and **385** (Table 4-18A). In addition to these products, homocoupling of chloride to bibenzyl **381** was monitored in the presence of the reducing agent (Table 4-18B). Due to the similar behavior of nickel(II) complex **425** compared to nickel(II) species **401**, it was again assumed that both a radical-chain mechanism and a double oxidative addition could operate in the presence of manganese. Nevertheless, the experiment also shows that the presence of thiolate ligand is not decisive.

Table 4-18: Reaction of acyl nickel(II) complex **425** with benzyl chloride **317b**.

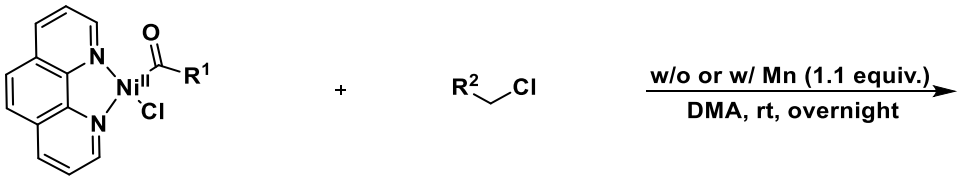

425
1.0 equiv.
R^1: 4-FPh

317b
5.0 equiv.
R^2: 4-MeOPh

reaction A: w/o Mn[a]	reaction B: w/ Mn[a]
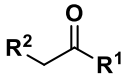 **378a** **(1.00)**  **424** **(0.16)**  **385** **(traces)**	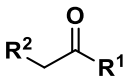 **378a** **(1.00)**  **424** **(1.86)** 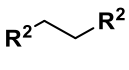 **381** **(2.00)** 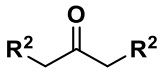 **385** **(1.42)**

[a]: Product analysis was conducted *via* GC-MS. The peak ratios are given in parentheses and were approximated by normalizing all given peaks to the highest product peak (ketone) in the GC chromatogram, which was set equal to 1.

In conclusion, the mechanistic experiments on the nickel catalyst illustrated that an array of possible oxidation states could be involved and that it is still difficult to provide definitive evidence about the actual mechanism (Scheme 4-57).

Several experiments supported the involvement of a nickel(0) species in the catalytic cycle. However, a contribution of a nickel(I) intermediate and thus a nickel(I/II/III) catalytic cycle cannot be completely excluded due to EPR signals observed after the reduction of $NiCl_2$(Phen) by manganese. Additionally, the oxidative addition product **401** is involved in the reaction and no initial reduction of the latter is required before it can react with the benzyl chloride **317b**. This observation mainly strengthens a radical-chain mechanism. The self-initiation could occur by halogen atom abstraction or by disproportionation of nickel(II) species **401**.[21,22] However, ketone **378a** is also formed after the reaction of oxidative addition product **401** and benzyl chloride in the presence of manganese, which would speak for a concurrent double oxidative addition mechanism. The reaction with nickel(II) complex **425** showed that the thiolate ligand plays a subordinate role (Scheme 4-57).

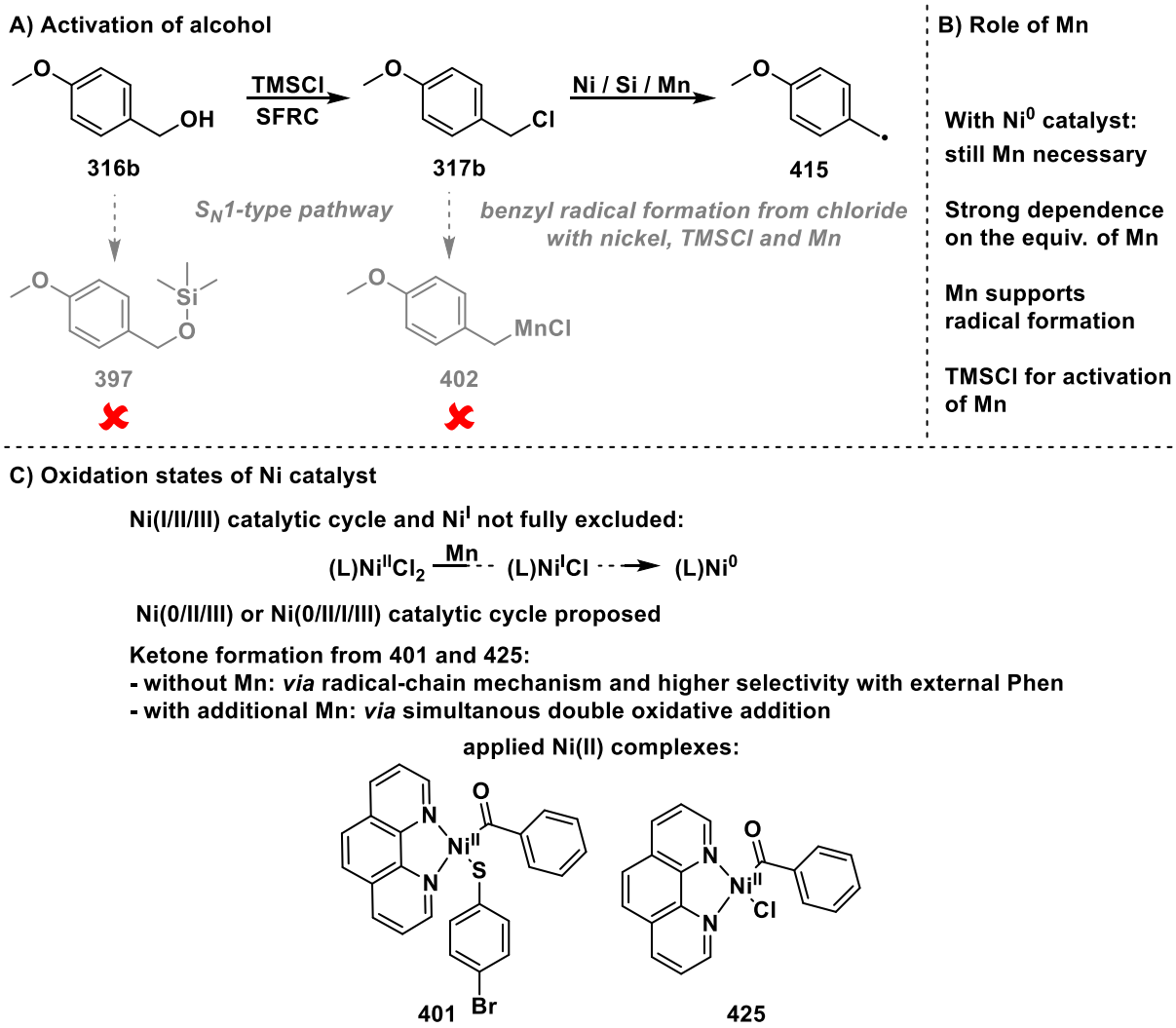

Scheme 4-57: Overview of all mechanistic results regarding the role of alcohol **316b**, manganese, and nickel catalyst.

4.3.3.7 Role of Titanium Catalyst

Finally, the influence of titanium catalyst on the system was elucidated. A control reaction indicated that the developed cross-electrophile coupling between benzylic alcohol **316b** and thioester **140** is successful even in the absence of titanium catalyst; but gave significantly lower yield (*vide supra*, section 4.3.1.7, Figure 4-7). The result led to the assumption that Cp_2TiCl_2 could act as a co-catalyst, probably by activating the substrates. The optimization of the titanium catalyst loading proved that Cp_2TiCl_2 is not involved in the activation of alcohol **316b**, as a dependence of the thioester conversion on the amount of Cp_2TiCl_2 was observed during the screening, while the conversion of alcohol **316b** remained the same (Figure 4-7).

Furthermore, it is known that the $Ti^{III/IV}$ redox couple formed from Cp_2TiCl_2 and manganese offers unique opportunities for accessing radical intermediates from benzylic alcohols,[232] which is not the case for the presented system, as the reaction of alcohol **316b**, Cp_2TiCl_2 and manganese in DMA only showed unreacted **316b** (Scheme 4-58, above).

In addition, homocoupling of chloride **317b** was not observed under titanium catalysis and in the presence of the reducing agent (Scheme 4-58, above). The reaction of thioester **140** under the mentioned reaction conditions led to an almost complete recovery of **140**, but disulfide **383b** was also detected in low proportion (Scheme 4-58, below).

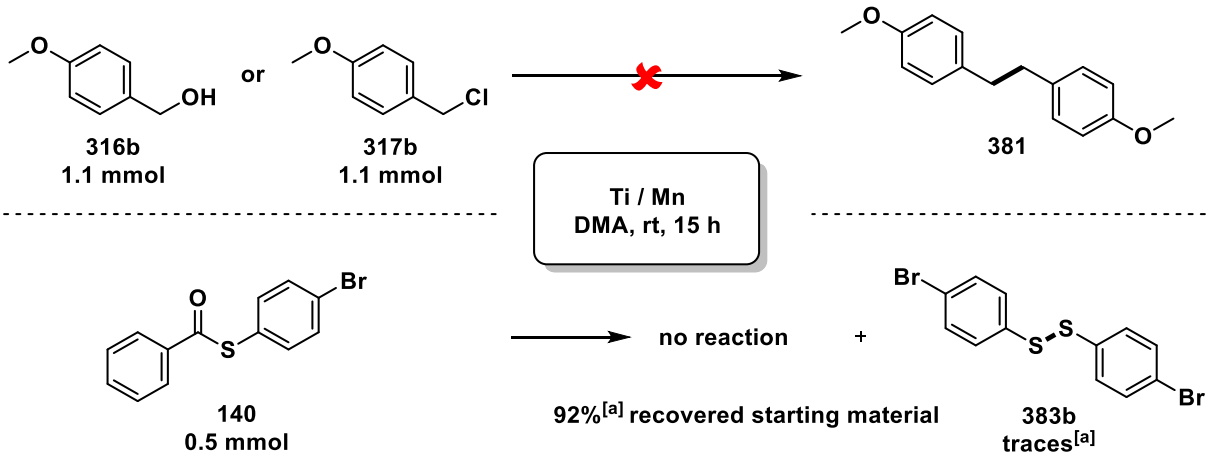

Scheme 4-58: Reaction of alcohol **316b**, chloride **317b** or thioester **140** under titanium catalysis and reductive conditions. Reaction conditions for Ti / Mn: Cp_2TiCl_2 (1 mol% for 1.1 mmol of substrate, 3 mol% for 0.5 mmol), Mn (0.9 equiv. for 1.1 mmol of substrate, 2.0 equiv. for 0.5 mmol). [a]: Determined by GC-FID using *n*-pentadecane as internal standard.

EPR analysis indicated a low-valent oxidation state of titanium during the reaction, as a catalytic amount of Cp_2TiCl_2 with a significant excess of manganese in DMA, analogous to the ratio under standard conditions, revealed the strong signal of manganese(II), while no signal was observed for manganese(0) in DMA (*vide postea*, section 4.4.4.5.12).

Another advantageous property of titanocenes is their Lewis acidic character, which makes them widely used as activators in organic synthesis.[233] The Lewis acid activation on the system was further investigated by replacing Cp_2TiCl_2 with other acids (Table 4-19). As already established during the optimization process, ketone **378a** was formed in the absence of Cp_2TiCl_2, albeit in a reduced yield of 31% (entry 1). Regardless of the Lewis acid applied, GC-MS analysis showed high conversion of alcohol **316b** in all experiments, although the exact value could not be determined due to peak overlap with the dominant peak of benzylic chloride **317b**. The conversion of thioester **140** depended on the screened Lewis acid, with the highest conversion being achieved with Cp_2TiCl_2, followed by Cp_2ZrCl_2 > $AlCl_3$ > $ZnCl_2$ > $MnCl_2$ > tris(pentafluorophenyl)borane (BCF) (Table 4-19).

Additionally, the highest yield of ketone **378a** was observed with Cp_2TiCl_2 (entry 2). With Cp_2ZrCl_2 and $AlCl_3$, a notably decreased yield of ketone **378a** was observed (38% and 23%, entries 3, 4). In the case of Cp_2ZrCl_2, a relatively low yield of ketone **378a** was formed despite the high conversion of thioester (92% conversion *vs.* 38% yield, entry 3). GC-MS analysis showed the formation of transesterification product **382** and disulfide **383b** in addition to the desired product **378a**, but no other acyl-containing products could be identified.

Moreover, ketone formation was completely inhibited with $ZnCl_2$ and $MnCl_2$ as Lewis acids (entries 5,6). However, it could be possible that they are disabled by ate complex formation with TMSCl. For instance, TMSCl can react directly with $AlCl_3$ or with traces of water to form HCl, which deactivates $AlCl_3$ (Scheme 4-59).[234] Water could be present in the system after the conversion of benzyl alcohol **316b** into benzyl chloride **317b** and oxoether **380**.

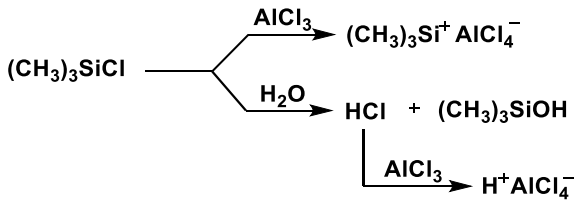

Scheme 4-59: Possible deactivation of $AlCl_3$.[234]

With BCF, an activation of thioester **140** was not observed, and the latter was fully recovered (entry 6). The experiments disclosed that highly oxophilic titanium(III), which is apparently present in the system, has the greatest positive effect on thioester conversion and product yield.[162]

Table 4-19: Influence of Lewis acids on the reaction.

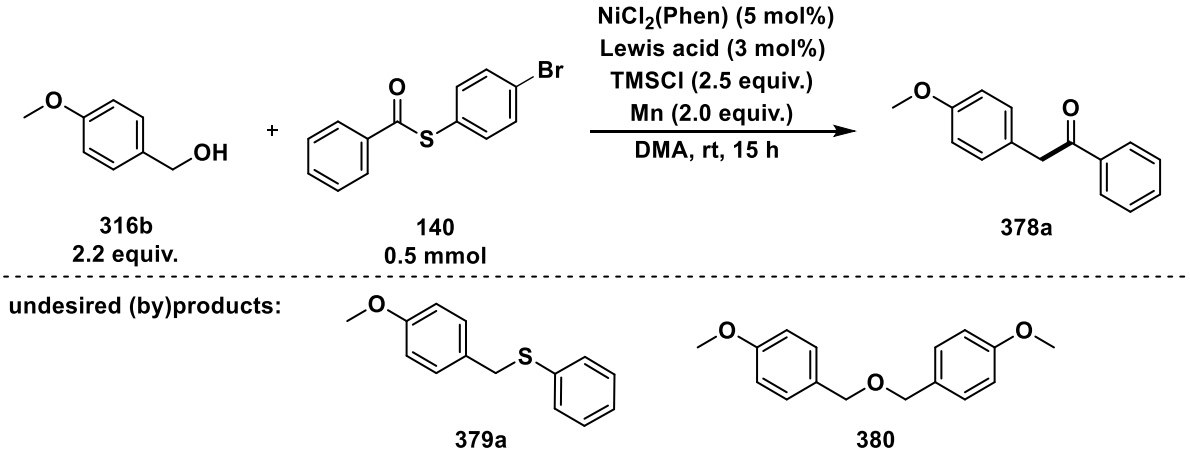

Entry	Lewis acid	Conv. of 140 [%][a]	Yield of 378a [%][a]	Yield of 379a [%][a]	Yield of 380 [%][a]
1[b]	w/o	52	31	44	21
2	Cp_2TiCl_2	100	73	13	7
3	Cp_2ZrCl_2	92	38	10	8
4	$AlCl_3$	49	23	24	9
5	$ZnCl_2$	20	✘	traces	21
6	$MnCl_2$	13	✘	traces	16
7	BCF	✘	✘	✘	✘

***Reaction Conditions*:** Mn (54.9 mg, 1.00 mmol, 2.0 equiv.), Lewis acid (15 µmol, 3.0 mol%), $NiCl_2$(Phen) (7.8 mg, 25 µmol, 5.0 mol%), **140** (146 mg, 500 µmol, 1.0 equiv.), TMSCl (159 µL, 1.25 mmol, 2.5 equiv.), **316b** (137 µL, 1.10 mmol, 2.2 equiv.) *via* syringe pump (SP) over 5 min, rt, 5 min; then abs. DMA (2 mL) *via* SP over 5 min, rt, 15 h. [a]: Determined by GC-FID using *n*-pentadecane as internal standard; [b]: *S*-phenyl benzothioate (**133**) (107 mg, 500 µmol, 1.0 equiv.) was used instead of **140**.

To further investigate the influence of Lewis acids on thioester **140**, the latter was implemented in the absence of benzyl alcohol **316b** under different reaction conditions (Scheme 4-60).

It was found that thioester **140** was almost completely recovered employing the nickel precatalyst and reductive conditions, but in the absence of Cp_2TiCl_2 and TMSCl (Scheme 4-60A). However, after the addition of 3 mol% Cp_2TiCl_2, the conversion of thioester **140** was facilitated, and the formation of benzophenone (**134**) in a very low yield of 5% and thioether **379d** were observed (Scheme 4-60B, above). In contrast to *S*-(4-bromophenyl) benzothioate (**140**), no conversion was observed when *S*-phenyl benzothioate (**133**) was used as a substrate, even in the presence of Cp_2TiCl_2, displaying the influence of bromine substituent on the reactivity of thioester **140**. Under nickel catalysis, reductive conditions and TMSCl as additive instead of catalytic amount of Cp_2TiCl_2, bromine-substituted thioester **140** was fully converted, amongst others to disulfide **383b** and benzophenone (**134**) (Scheme 4-60B, below). The experiments illustrated that nickel precatalyst, reductive conditions and either Cp_2TiCl_2 or TMSCl as Lewis acids are required for C(O)–S bond cleavage.

The formation of benzophenone (**134**) could be attributed to the involvement of an acyl radical generated from thioester **140**. This assumption was further supported by the reaction of thioester **140** with a stoichiometric amount of Cp_2TiCl_2 under nickel catalysis and reductive conditions. Thioester **140** was fully converted to several products, amongst others disulfide **383b**, thiol and benzil **426**, which was isolated in 20% yield (Scheme 4-60C, above). The experiment again demonstrated the influence of bromine substituent on the thioester reactivity. In the optimization process, the conversion of *S*-phenyl benzothioate (**133**) was reduced to 16% with stoichiometric amount of Cp_2TiCl_2, resulting in a low yield of ketone **378a** (9%, *vide supra*, section 4.3.1.7, Figure 4-7). Additionally, the acyl radical adduct **427** was detected by HR-MS after the reaction of thioester **140** with TEMPO under nickel catalysis and Cp_2TiCl_2 as additive (Scheme 4-60C, below).

Another experiment demonstrating the activation of thioester by Cp_2TiCl_2 was the initially unsuccessful reaction of benzyl chloride (**317a**) and *S*-phenyl benzothioate (**133**) under nickel catalysis and reductive conditions (Scheme 4-60D). After adding a catalytic amount of Cp_2TiCl_2 to the reaction conditions, the desired ketone was isolated in 23% yield (Scheme 4-60D). Hereby, thioether **379a** was generated as the main product, emphasizing the importance of the missing *para*-bromine substituent, suppressing thioether formation.

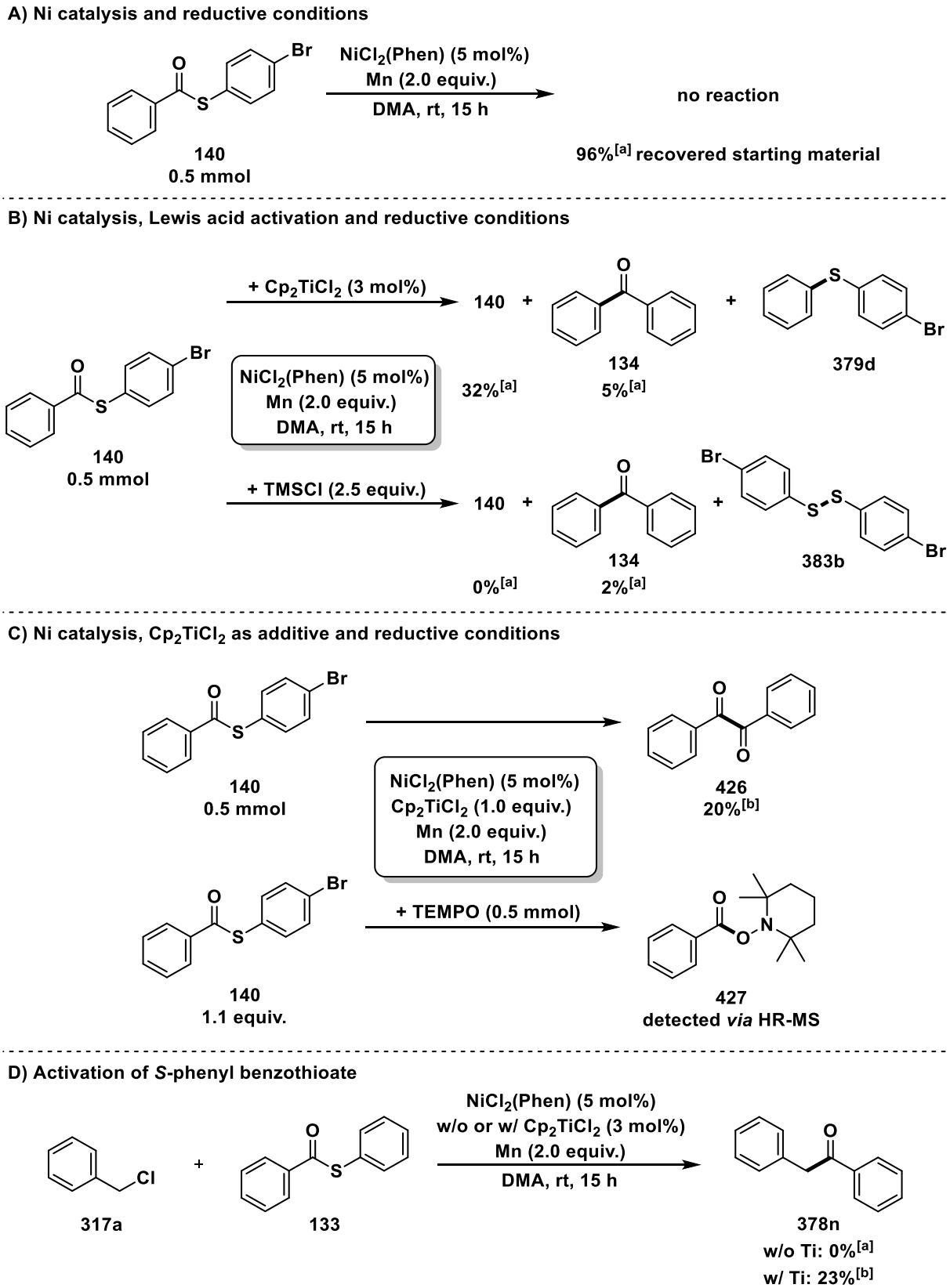

Scheme 4-60: Implementation of thioesters **133** and **140** under different reaction conditions. [a]: Determined by GC-FID using *n*-pentadecane as internal standard; [b]: Isolated yield.

From the conducted experiments on the role of titanium catalyst, the following results were concluded (Scheme 4-61). As the developed cross-electrophile coupling is successful in the absence of Cp_2TiCl_2 but shows a higher yield of ketone in its presence, it was followed that Cp_2TiCl_2 is mainly responsible for the Lewis acidic activation of thioester. After the reduction of titanium(IV) by manganese, the generated titanium(III) species, which is known for its ability to activate carbonyl groups,[161a] could be responsible for the activation of thioester by coordination to the carbonyl oxygen. Thus, the oxidative addition step can be facilitated by the altered reactivity of the thioester, leading to a higher turnover of the catalytic cycle and consequently to a higher yield of ketone **378a** (Scheme 4-61).

The trapping of the acyl radical **428** from thioester **140** demonstrated that the reaction of thioester with nickel(0) is probably not simply a concerted oxidative addition involving nickel(0/II) oxidation states (Scheme 4-61, I), but rather a stepwise oxidative addition *via* SET reactions (Scheme 4-61, II). Such a process has been previously postulated,[235] and could be initiated by the reduction of nickel precatalyst with manganese, which is probably activated by TMSCl. Under the aid of titanium(III), thioester **140** could undergo a single-electron transfer-type stepwise oxidative addition to the zero-valent nickel species to form an acyl radical **428** that recombines with the nickel(I) species **429** (Scheme 4-61, II).

This could explain the observed side-reactions, as the acyl radical could recombine to benzil **426** or decarbonylation could occur, which leads to the formation of benzophenone (**134**). A still open question is the reversibility of the oxidative addition, which has already been investigated and suggested for a nickel(0/II) pathway.[21]

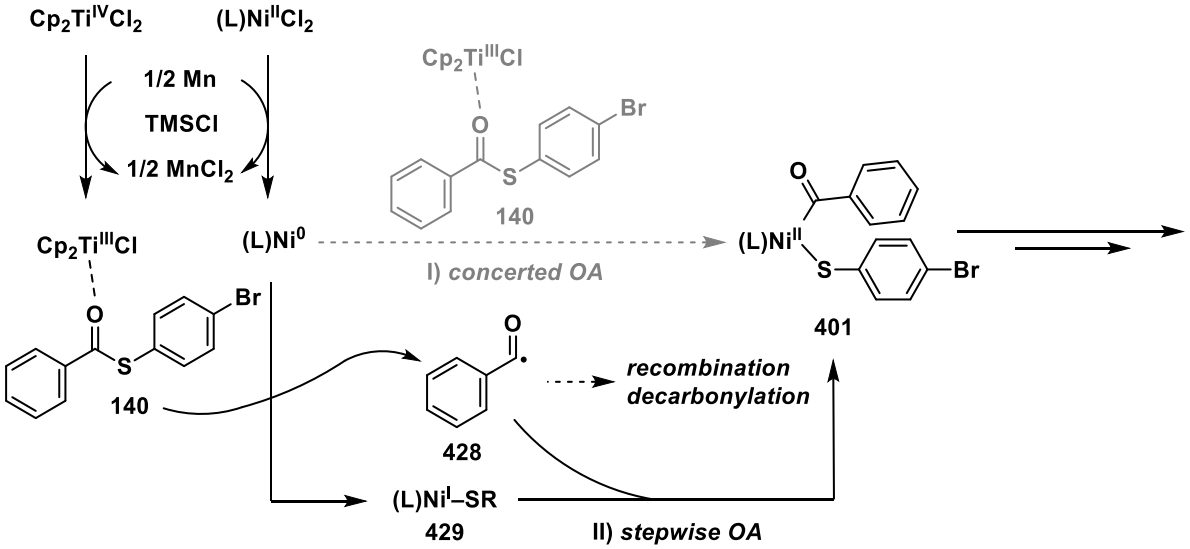

Scheme 4-61: Possible interaction of Lewis acid with thioester **140** and I) concerted *vs.* II) stepwise oxidative addition. L = 1,10-phenanthroline.

4.3.3.8 Proposed Mechanism

The collective mechanistic studies led to the following proposal of the mechanism (Scheme 4-62). The reduction of nickel(II) precatalyst by manganese may constitute the first step of the catalytic cycle, producing either nickel(I) or nickel(0) species **182**. Several experiments with nickel(0) led to the assumption that the latter is mainly the active intermediate. Simultaneously, titanium(IV) appears to be reduced to titanium(III), which facilitates the single-electron transfer-type stepwise oxidative addition of thioester **140** to the zero-valent nickel species to form an acyl radical **428** that recombines with the nickel(I) species **429**. The oxidative addition complex **401** may then react either in a radical-chain mechanism as the main catalytic cycle or in a concurrent double oxidative addition. In both catalytic cycles, the alcohol **316b** appears to be activated *in situ* by formation of chloride **317b** *via* a S_N1-type pathway, with subsequent generation of a benzyl radical **415** in a synergistic manner by nickel(I) and manganese. Thereby, TMSCl is required to activate the manganese surface.

In a radical-chain mechanism, the benzyl radical **415** could undergo one-electron oxidative addition to the nickel(II) complex **401**, furnishing a formal nickel(III) species **416**, from which the desired ketone **378a** and a nickel(I) species **187** can be released. The latter nickel(I) complex **187** could support the radical formation from benzyl chloride **317b** as an on-cycle intermediate.

A simultaneous double oxidative addition would again start with the formation of the active nickel(0) species and the oxidative addition of thioester, followed by the reduction of the oxidative addition product **401** to a nickel(I) species **417** with a further equivalent of manganese. This could initiate a double oxidative addition process, which starts with the benzyl radical formation by nickel(I) **417** and ends in a formal nickel(III) species **419**, from which the product could be reductively eliminated.

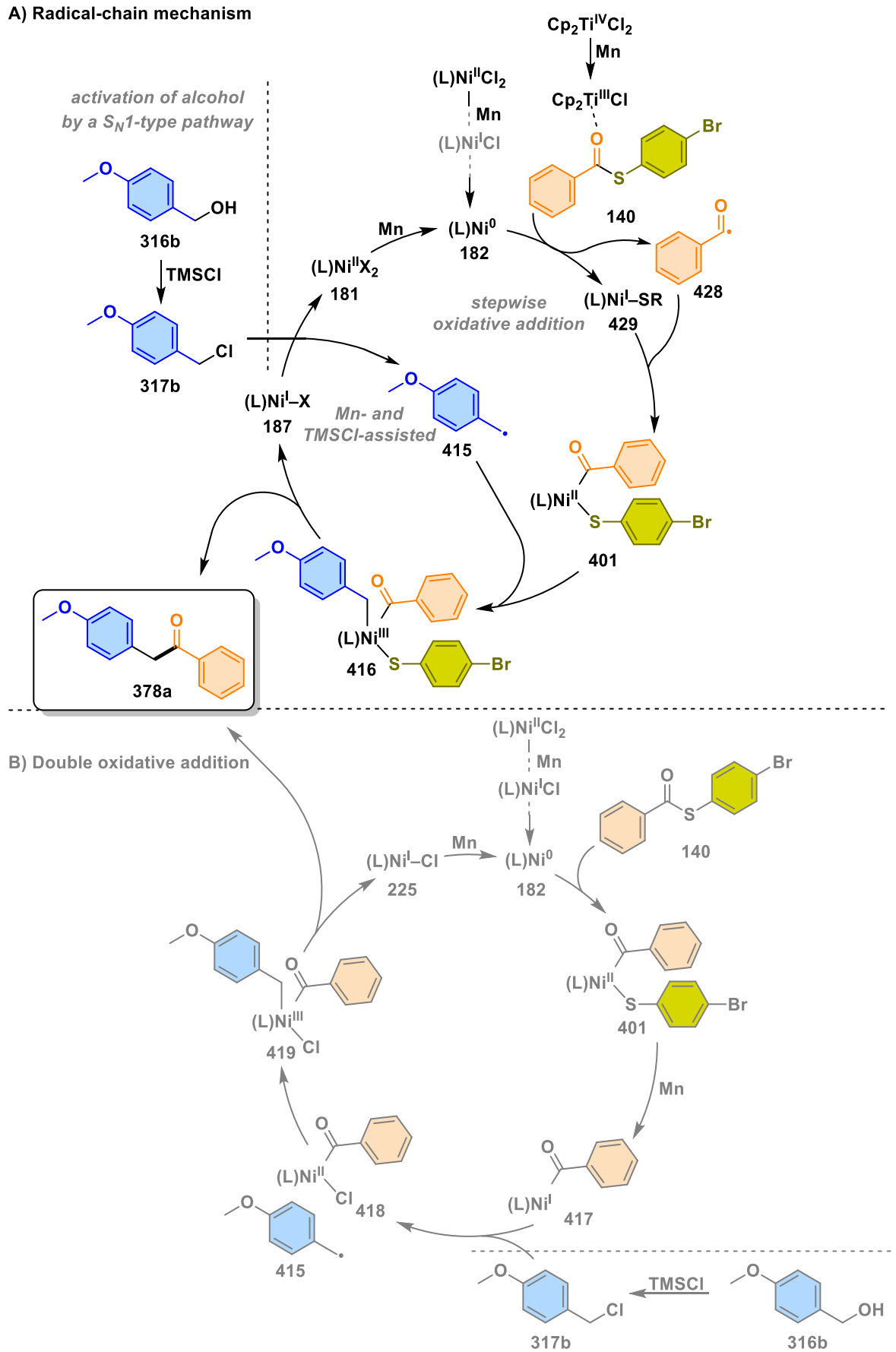

Scheme 4-62: Proposed mechanisms for the nickel-catalyzed and Lewis acid-assisted XEC of benzylic alcohols and thioesters. L = 1,10-phenanthroline, X = thiolate or Cl.

4.3.4 Conclusion and Outlook

In summary, a novel method for ketone synthesis was developed based on a nickel-catalyzed and Lewis acid-assisted cross-electrophile coupling of benzylic alcohols and thioesters.

The reaction strongly depends on substituents of both substrates, as on the one hand, the thioether formation is minimized with an electron-withdrawing substituent on the thiol moiety of the thioester. Thus, thioesters with different acyl moieties can be applied to give the desired ketones in modest to moderate yields. On the other hand, electron-rich benzylic alcohols bearing a methoxy substituent in *para*-position are required for ketone formation. In addition to benzylic alcohols, benzylic chlorides can also be coupled with thioesters, being more tolerant to changes in substituents.

Mechanistic experiments point out that the reaction does not operate *via* a silyl ether or an organomanganese species, but that the alcohol is transformed *in situ* to benzyl chloride by TMSCl resulting in an easier formation of a benzyl radical, which was evidenced by several radical scavenger and -clock experiments. The benzyl radical is probably formed in a synergistical way by both nickel(I) and manganese, the latter being activated by TMSCl. While a nickel(I/II/III) catalytic cycle is less likely, but cannot be fully ruled out, there is growing evidence that the catalytic cycle starts from a nickel(0) oxidation state. Thioester is presumably activated by Lewis acid interaction with $Cp_2Ti^{III}Cl$ and reacts with nickel(0) in a stepwise oxidative addition involving an acyl radical. Several experiments with nickel(II) oxidative addition products demonstrated that the radical-chain pathway could be the main catalytic cycle, but a double oxidative addition seems to be a off-cycle.

In conclusion, this work does not only introduce a new methodology to synthesize ketones, but it also expands the horizon of possibilities in cross-electrophile couplings giving insights into relevant mechanistic steps and should support further development of challenging reductive transformations. Additionally, the use of thioesters as acyl radical sources was established using nickel catalysis, reductive conditions and Lewis acid activation by Cp_2TiCl_2. The method could open access to a new method of synthesizing benzophenones or diketones from a single substrate.

4.4 Experimental Part
4.4.1 General Information
4.4.1.1 Chemicals

$NiCl_2$(Phen) was either synthesized from anhydrous $NiCl_2$ and anhydrous 1,10-phenanthroline or purchased from Sigma-Aldrich. Anhydrous $NiCl_2$ was obtained by drying $NiCl_2(H_2O)_6$ at 110°C under vacuum. $NiCl_2(H_2O)_6$ (p.A. grade) was provided by the central chemical storage of the University of Tübingen. Anhydrous 1,10-phenanthroline (99%) was supplied by Alfa Aesar and stored in an argon (Ar) -filled glovebox from Glovebox Systemtechnik. Anhydrous DMA (99.8%) was purchased from Alfa Aesar and transferred under Ar counterflow to a Schlenk round-bottom flask (RBF) filled with 3 Å molecular sieves, which were activated by heating in a microwave (3 × 1 min) prior to use. DMA was degassed by purging with Ar. 4-Methoxybenzyl alcohol **316b** (98%), TMSCl (≥ 98%) and titanocene dichloride (97%) were purchased from Sigma-Aldrich. 4-Methoxybenzyl alcohol **316b** was stored under inert gas in a Schlenk RBF filled with activated 3 Å molecular sieves. TMSCl was distilled over calcium hydride before use and stored under inert gas in a Schlenk RBF in the absence of light. 4-Methoxybenzyl chloride **317b** was purchased from TCI and stored under an Ar atmosphere in a refrigerator. Manganese (-325 mesh, 99.95%) was bought from Alfa Aesar. Titanocene dichloride and manganese were stored in a glovebox. The suppliers of all other chemicals were generally Sigma-Aldrich, TCI, BLDpharm, abcr, Acros and Fluorochem. Solvents for chromatography, thin-layer chromatography and reaction work-up were either HPLC grade or technical grade and in this case were distilled prior to use.

4.4.1.2 General Techniques
4.4.1.2.1 Reaction Set-up

Air-sensitive syntheses were performed under an Ar or nitrogen (N_2) atmosphere. The glassware used for these reactions was flame-dried by heating with a propane torch under vacuum and subsequent cooling under dry Ar or N_2. The cycles were repeated three times. A slow addition of liquids was carried out with a Chemyx syringe pump, model Fusion 100. Solvents were degassed by purging the respective liquid with Ar. Dry solvents were prepared according to standard procedures.

4.4.1.2.2 Column Chromatography

Normal phase column chromatography was performed using silica gel (0.04–0.063 mm) from Macherey-Nagel as stationary phase. Reversed phase (RP) column chromatography was conducted with LiChroprep RP-18 (40–63 µm, CAS: 108688-10-4) as stationary phase.
Thin-layer chromatography (TLC) was performed on aluminum plates, pre-coated with silica gel 60 F_{254} (ALUGRAM Xtra SIL G UV254, layer thickness: 0.2 mm) and analyzed under

ultraviolet (UV) light (λ = 254 nm). Alternatively, the plates were stained with an anisaldehyde TLC dipping solution and smoothly heated.

4.4.1.3 Analytical Techniques

4.4.1.3.1 Nuclear Magnetic Resonance Spectroscopy (NMR)

NMR spectra were recorded with a Bruker Avance 400, a Bruker Avance III HD 300 NanoBay or a Bruker Avance III HDX 700 instrument. Unless otherwise noted, all measurements were performed at ambient temperature. ^{13}C-NMR experiments were performed in a proton-decoupled mode. In experiments without a deuterated solvent, shimming was conducted without a lock signal. The corresponding method was introduced by the NMR department of the University of Tübingen. Chemical shifts δ are given in parts per million [ppm] relative to the solvent signal as internal standard ($CDCl_3$: ^{1}H: δ = 7.26 ppm; ^{13}C: δ = 77.1 ppm, CD_2Cl_2: ^{1}H: δ = 5.32 and ^{13}C: δ = 53.8, DMSO-d_6: ^{1}H: δ = 2.50 ppm; ^{13}C: δ = 39.5 ppm).[236] Coupling constants are given in *J* (Hz) with usual designations for splitting patterns (s = singlet, d = doublet, t = triplet, q = quartet, quin = quintet, sext = sextet, sept = septet, m = multiplet, br = broad). For quantitative NMR, integrals of selected peaks (one peak per compound) were determined, and the mass ratio of the respective compounds was calculated using Equation 1.

$$R_x = \frac{\frac{I_x}{k_x} \cdot M_x}{\sum_{i=1}^{n} \frac{I_i}{k_i} \cdot M_i} \cdot 100\% \quad (1)$$

R_x: Mass ratio of compound x in %

$I_{x,i}$: Integral height of the selected peak of compound x,i

$k_{x,i}$: Number of nuclei belonging to the selected peak of compound x,i

$M_{x,i}$: Molar mass of compound x,i

n: Number of compounds in the sample/reaction mixture

4.4.1.3.2 Electron Paramagnetic Resonance Spectroscopy (EPR)

EPR measurements were carried out by the NMR department of the Institute of Organic Chemistry, University of Tübingen, on a Bruker EMXmicro with PremiumX microwave-bridge. The general sample set-up is described in detail in section 4.4.4.5.12.

4.4.1.3.3 Gas Chromatography (GC-MS or GC-FID)

4.4.1.3.3.1 Preparation of Samples for GC-FID and GC-MS Analysis

The catalytic reactions were quenched by adding Lewatit® TP 207 (Sigma-Aldrich) and aq. saturated NaCl (0.1 mL). An internal standard (*n*-pentadecane, ≥99%, Sigma-Aldrich, 25 µL) was added to the reaction mixture, which was stirred for further 5 min. A sample of 0.1 mL was taken and filtered through a pad of Celite® 545, activated basic Al_2O_3 and anhydrous $MgSO_4$ in a Pasteur pipette with DCM as eluent.

4.4.1.3.3.2 Gas Chromatography (GC)

GC-FID (flame ionization detection) analysis was carried out on an Agilent 7820A GC system with a 19091J-431 column (30 m × 320 µm × 0.25 µm) and dry hydrogen as carrier gas. The temperature program includes heating from 50 °C to 280 °C within 15 min. The internal standard method for quantitative GC-FID was used to determine yields and conversions. For this purpose, calibration was conducted by varying the mass ratio of substrate and standard with the subsequent analysis of the different samples by GC-FID (Equation 2).

$$\frac{A_X}{A_{Std.}} = R \cdot \frac{m_X}{m_{Std.}} \quad (2)$$

A_X: Peak area compound x

$A_{Std.}$: Peak area standard (*n*-pentadecane)

m_X: Mass compound x

m_{Std}: Mass standard (*n*-pentadecane)

R: Response factor

4.4.1.3.3.3 Mass Spectrometry (MS)

Low resolution GC-MS was performed on an Agilent 7820A GC system with a 190915-433UI column (30 m × 250 µm × 0.25 µm) and a 5977B MSD (EI) using dry hydrogen as carrier gas. The temperature program includes heating from 50 °C to 280 °C within 15 min (method A).
In addition, samples were measured by the MS department of the University of Tübingen using an Agilent 8890A GC system with a 5977B MSD (EI) and helium as carrier gas. The temperature program began with a holding time of 3 min at 40 °C, was then heated to 320 °C within 32 min and held at this temperature for 10 min (method B).

4.4.1.3.3.4 High Resolution Mass Spectrometry (HR-MS)

HR-MS and HPLC-HR-MS measurements were carried out by the MS department of the University of Tübingen on a maXis 4G instrument from Bruker (ESI, APCI) coupled with HPLC (UltiMate 300, Thermo Scientific).

4.4.1.3.3.5 Infrared Spectroscopy (IR)

Infrared spectra were recorded on an Agilent Cary 630 FTIR spectrometer, equipped with an ATR (attenuated total reflection) module. Absorption bands are reported in wave numbers ($\tilde{\nu}$) in cm^{-1}.

4.4.1.3.3.6 Melting Point Determination

Melting points were determined with a Schorpp MPMHV3 instrument and are uncorrected (heating rate: 1 °C/min).

4.4.1.3.3.7 Elemental Analysis (EA)

Elemental analysis was conducted with a Euro EA Analyzer 3000 from HEKAtech.

4.4.2 Syntheses of Involved Components

4.4.2.1 Synthesis of Nickel Precatalyst

400

The nickel precatalyst was synthesized similar to a literature procedure.[185] A flame-dried 25 mL two-neck flask equipped with stirring bar and condenser was charged with finely ground nickel chloride (132 mg, 1.02 mmol, 1.02 equiv.) and dry ethanol (4 mL) was added. The suspension was stirred under argon until the powder dissolved completely. Subsequently, 1,10-phenanthroline (180 mg, 1.00 mmol, 1.00 equiv.) was added. After stirring at reflux temperature overnight, the precipitate was collected by filtration under air, washed with dry ethanol and dry *n*-hexane, and dried for 24 h under reduced pressure. The product (138 mg, 440 µmol, 43%) was isolated as a green, air-stable solid.

$C_{12}H_8Cl_2N_2Ni$: 309.80 $\frac{g}{mol}$

Anal. Calcd. for $C_{12}H_8Cl_2N_2Ni$: C 46.52, H 2.60, N 9.04, found: C 46.55, H 2.74, N 8.93.

HR-MS (ESI): *m/z* = $[M\text{-}2Cl+HCOO]^+$ calc. for $C_{13}H_9N_2NiO_2$ 283.00120, found 283.00066.

^{1}H-NMR (400 MHz, MeOH-d_4): δ [ppm] = 46.6 (s br, 2H), 23.8 (s br, 3H), 17.8 (s br, 3H).

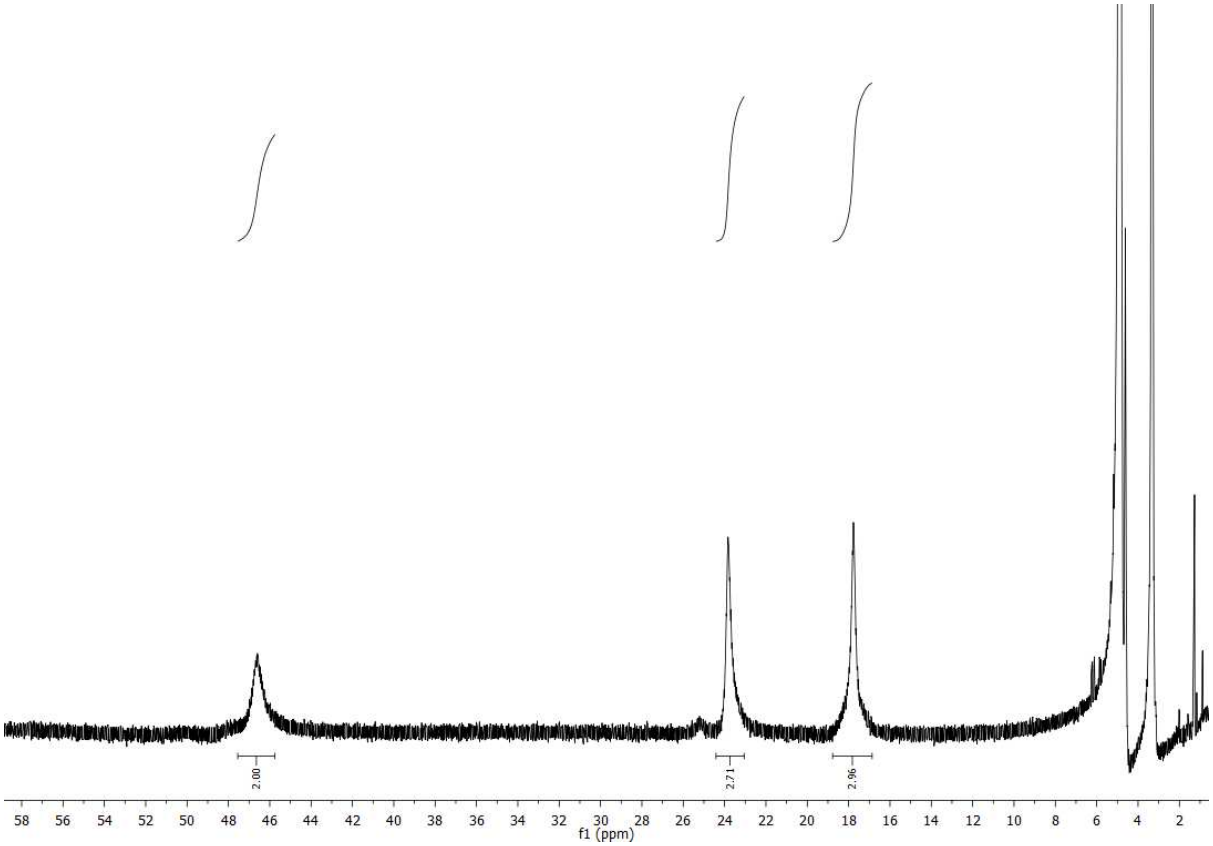

Figure 4-19: ^{1}H-NMR spectrum of nickel precatalyst in MeOH-d_4.

4.4.2.2 Synthesis of Alcohols

2-(4-methoxyphenyl)propan-2-ol (316i)

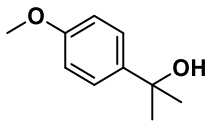

316i

The synthesis followed a literature procedure.[237] At 0 °C, methylmagnesium chloride (3.0 M in THF, 13.6 mL, 34.0 mmol, 3.4 equiv.) was added dropwise over one hour to a solution of 4′-methoxyacetophenone (1.50 g, 10.0 mmol, 1.0 equiv.) in THF (20 mL). After completion, the solution was stirred at room temperature overnight. Then, the reaction was quenched by the addition of H_2O (30 mL) and a colorless solid participated. After filtration, the organic layer was washed with aq. saturated NaCl (3 × 15 mL), dried over anhydrous Mg_2SO_4 and concentrated under reduced pressure. The crude product was purified by column chromatography (PE/EtOAc 8:2) to yield the product **316i** (640 mg, 3.85 mmol, 39%) as a light yellow oil. The analytical data are in good agreement with the literature.[238]

$C_{10}H_{14}O_2$: 166.22 $\frac{g}{mol}$

R_f: 0.28 (Silica gel, PE/EtOAc 4:1, UV).

Melting point: Ambient temperature (PE/EtOAc).

^{1}H-NMR (400 MHz, $CDCl_3$): δ [ppm] = 7.43–7.40 (m, 2H), 6.89–6.86 (m, 2H), 3.80 (s, 3H), 1.75 (s, 1H), 1.57 (s, 6H).

^{13}C-NMR (101 MHz, $CDCl_3$): δ [ppm] = 158.8, 141.5, 125.7, 113.6, 72.3, 55.4, 31.9.

GC-MS (EI): t_R = 5.24 min, *m/z* (Int. %) = 166 (17) $[M]^{+\bullet}$, 151 (100) $[M]^{+\bullet}$-$[C_9H_{11}O_2]^{\bullet}$.

E-3-(4-methoxyphenyl)prop-2-en-1-ol (316m)

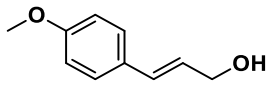

316m

The synthesis followed a literature procedure.[239] To a solution of 4-methoxycinnamaldehyde (1.62 g, 10.0 mmol, 1.0 equiv.) in EtOH/MeOH (35 mL, 2/1 v/v), sodium borohydride (380 mg, 10.0 mmol, 1.0 equiv.) was added in one portion at 0 °C. The reaction was first stirred at 0 °C for further 30 min and then at rt for 30 min. Subsequently, acetone (5 mL) was added to the mixture, which was stirred for further 5 min. Then, the reaction was quenched with aq. saturated NH_4Cl (10 mL) and the aqueous layer was extracted with MTBE (2 × 30 mL). The combined organic layers were dried over anhydrous $MgSO_4$ and concentrated under reduced pressure. To remove residual H_2O, the crude product was redissolved in MeOH (20 mL), the solution was dried again over anhydrous $MgSO_4$ and concentrated under reduced pressure. The product **316m** (1.23 g, 7.50 mmol, 75%) was obtained as colorless, crystalline solid and used without further purification steps. The analytical data are in good agreement with the literature.[239]

$C_{10}H_{12}O_2$: 164.2 $\frac{g}{mol}$

R_f: 0.31 (Silica gel, PE/EtOAc 95:5, UV).

Melting point: 74.2–76.1°C (EtOH).

^{1}H-NMR (400 MHz, $CDCl_3$): δ [ppm] = 7.27 (d, *J* = 8.7 Hz, 2H), 6.83 (d, *J* = 8.7 Hz, 2H), 6.52 (d, *J* = 15.9 Hz, 1H), 6.21 (dt, *J* = 15.9, 6.0 Hz, 1H), 4.25 (d, *J* = 6.0 Hz, 2H), 3.76 (s, 3H), 1.35 (s, 1H).

^{13}C-NMR (101 MHz, $CDCl_3$): δ [ppm] = 159.5, 131.1, 129.6, 127.8, 126.4, 114.2, 64.1, 55.4.

GC-MS (EI): t_R = 6.71 min, *m/z* (Int. %) = 164 (37) $[M]^{+\bullet}$, 121 (100) $[M]^{+\bullet}$-$[C_2H_4O]^{\bullet}$, 108 (46) $[M]^{+\bullet}$-$[C_3H_6O]^{\bullet}$.

1-(4-methoxyphenyl)prop-2-en-1-ol (316n)

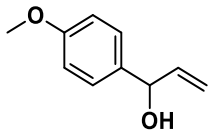

316n

The synthesis of 1-(4-methoxyphenyl)prop-2-en-1-ol (**316n**) followed a literature procedure.[240] Anisaldehyde (1.09 g, 8.00 mmol, 1.0 equiv.) was dissolved in dry THF (20 mL) and the solution was cooled to 0 °C. Vinyl magnesium bromide (0.6 M in THF, 26 mL, 16 mmol, 2.0 equiv.) was added dropwise over 45 min. The mixture was stirred at 0 °C for further 2 h and was then quenched by the addition of aq. saturated NH_4Cl (30 mL). The aqueous phase was extracted with EtOAc (3 × 30 mL). The combined organic layers were washed with aq. saturated NaCl (30 mL), dried over $MgSO_4$ and concentrated under reduced pressure. The product **316n** was obtained as a yellow oil (1.22 g, 7.43 mmol, 93%) and used without further purification steps. The analytical data are in good agreement with the literature.[240]

$C_{10}H_{12}O_2$: 164.2 $\frac{g}{mol}$

R_f: 0.16 (Silica gel, PE/EtOAc 9:1, UV).

Melting point: Ambient temperature (EtOAc).

^{1}H-NMR (400 MHz, $CDCl_3$): δ [ppm] = 7.30 (d, *J* = 8.7, 2H), 6.89 (d, *J* = 8.7, 2H), 6.05 (ddd, *J* = 16.4, 10.5, 6.1 Hz, 1H), 5.34 (d, *J* = 17.1, 1.4 Hz, 1H), 5.22–5.14 (m, 2H), 3.81 (s, 3H), 1.89 (s, 1H).

^{13}C-NMR (101 MHz, $CDCl_3$): δ [ppm] = 159.4, 140.5, 135.0, 127.8, 114.1, 113.9, 75.1, 55.4.

GC-MS (EI): t_R = 21.97 min, *m/z* (Int. %) = 164 (73) $[M]^{+\bullet}$, 137 (47) $[M]^{+\bullet}$-$[C_2H_3]^{\bullet}$.

4.4.2.3 Synthesis of Chloride

2-(chloromethyl)naphthalene (317h)

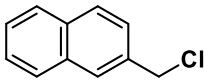

317h

The synthesis of 1-(4-methoxyphenyl)prop-2-en-1-ol (**317h**) followed a literature procedure.[214] A Schlenk tube was charged with 2-naphthalenemethanol (0.95 g, 6.0 mmol, 1.0 equiv.) and TMSCl (0.80 mL, 6.6 mmol, 1.1 equiv.). The mixture was stirred under solvent-free reaction conditions at 75 °C overnight and then quenched by adding water (5 mL). The suspension was diluted with EtOAc (5 mL) and the aqueous phase was extracted with EtOAc (3 × 5 mL). The combined organic layers were washed with NaCl (3 × 5 mL), dried over anhydrous $MgSO_4$, filtered, and concentrated under reduced pressure. The crude product was purified by column chromatography (PE/EtOAC 99:1) to yield the product **317h** (301 mg, 1.70 mmol, 28%) as a colorless solid. The analytical data are in good agreement with the literature.[214]

$C_{11}H_9Cl$: 176.64 $\frac{g}{mol}$

R_f: 0.39 (Silica gel, PE/EtOAc 99:1, UV).

Melting point: 47.4–47.7 °C (PE/EtOAc).

^{1}H-NMR (400 MHz, $CDCl_3$): δ [ppm] = 7.87–7.81 (m, 4H), 7.53–7.48 (m, 3H), 4.77 (s, 2H).

^{13}C-NMR (101 MHz, $CDCl_3$): δ [ppm] = 134.9, 133.30, 133.26, 128.9, 128.1, 127.9, 127.7, 126.64, 126.61, 126.4, 46.7.

GC-MS (EI): t_R = 6.70 min, *m/z* (Int. %) = 176 (16) $[M]^{+\bullet}$, 141 (100) $[M]^{+\bullet}$-$[Cl]^{\bullet}$.

4.4.2.4 Synthesis of Thioesters
4.4.2.4.1 Synthesis of *S*-(2-pyridyl) Thioester

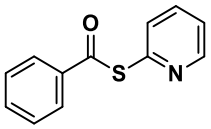

384a

The synthesis followed a literature procedure.[241] Benzoic acid (305 mg, 2.50 mmol, 1.0 equiv.), 2,2'-dipyridyl disulfide (605 mg, 2.80 mmol, 1.1 equiv.) and triphenylphosphine (721 mg, 2.80 mmol, 1.1 equiv.) were added to dry acetone (20 mL). The reaction mixture was stirred at rt, until the benzoic acid was completely consumed (TLC control, PE/EtOAc 8:2, UV). The solvent was removed under reduced pressure and the crude product was purified by column chromatography (PE/EtOAc 8:2). The product **384a** was obtained as a yellow oil (260 mg, 1.21 mmol, 48%). The analytic data are in good agreement with the literature.[241]

$C_{12}H_{16}OS$: 215.27 $\frac{g}{mol}$

R_f: 0.40 (Silica gel, PE/EtOAc 8:2, UV).

Melting point: 43.7–44.0 °C (PE/EtOAc).

^{1}H-NMR (400 MHz, $CDCl_3$): δ [ppm] = 8.73–8.71 (m, 1H), 8.04–8.01 (m, 2H), 7.85 (dt, *J* = 7.7 Hz, 1.9 Hz, 1H), 7.78–7.76 (m, 1H), 7.65–7.59 (m,1H), 7.50–7.48 (m, 2H), 7.41–7.37 (m, 1H).

^{13}C-NMR (101 MHz, $CDCl_3$): δ [ppm] = 189.6, 151.5, 150.8, 137.6, 136.8, 134.2, 131.2, 129.1, 127.9, 124.0.

GC-MS (EI): t_R = 22.56 min, *m/z* (Int. %) = 215 (0.03) $[M]^{+\bullet}$, 105 (100) $[M]^{+\bullet}$-$[C_6H_4NS]^{\bullet}$, 77 (43) $[M]^{+\bullet}$-$[C_6H_4NOS]^{\bullet}$.

4.4.2.4.2 General Procedures

General Procedure A (GP-A): Synthesis of Thioesters from Acid Chlorides

A solution of the respective thiol (1.0 equiv.–1.2 equiv.) in DCM or THF (40 mL) was cooled to 0 °C. At this temperature, triethylamine (1.0 equiv.–1.2 equiv.) and the corresponding acyl chloride (1.0 equiv.) were added dropwise. After stirring at 0 °C for 30 min, the reaction mixture was warmed to rt. The suspension was stirred at rt until no more starting material was observed (TLC control) and then quenched by adding water (10 mL). The aqueous phase was extracted with EtOAc (2 × 15 mL). The combined organic layers were washed with HCl (1 M, 3 × 10 mL), aq. saturated $NaHCO_3$ (3 × 10 mL), and aq. saturated NaCl (2 × 10 mL). The combined organic layers were dried over anhydrous $MgSO_4$, filtered and concentrated under reduced pressure. The purification methods are described detailed in the individual experiments.

General Procedure B (GP-B): Synthesis of Thioesters *via* Steglich Esterification

The reaction was conducted following a modified literature procedure.[242] The respective carboxylic acid (1.0 equiv.) was dissolved in DCM or THF (40 mL) and the corresponding thiol (1.0 equiv.–1.2 equiv.) was added dropwise. The solution was cooled to 0 °C and 4-dimethylaminopyridine (DMAP) (0.1 equiv.) as well as *N*,*N'*-dicyclohexylcarbodiimide (DCC) (1.1 equiv.) were added at the same temperature. The reaction was warmed to rt and stirred overnight. Then, the suspension was filtered through a short plug of silica gel using DCM as eluent. The filtrate was washed with HCl (6 M, 5 × 10 mL), aq. saturated $NaHCO_3$ (2 × 10 mL), and aq. saturated NaCl (2 × 10 mL). The combined organic layers were dried over anhydrous $MgSO_4$, filtered and concentrated under reduced pressure. The purification methods are described detailed in the individual experiments.

4.4.2.4.3 Experimental Procedure and Analytical Data of Thioesters Synthesized by GP-A

Thioesters **133**, **139** and **140** have already been synthesized in previous work and stored in a freezer before use. The detailed experimental procedure and analytical data are described in section 3.4.2.2.

S-phenyl 2,4,6-trimethylbenzothioate (154a)

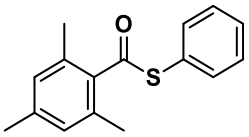

154a

According to GP-A, *S*-phenyl 2,4,6-trimethylbenzothioate (**154a**) was synthesized using 2,4,6-trimethylbenzoyl chloride (0.80 mL, 5.0 mmol, 1.0 equiv.), thiophenol (0.60 mL, 6.0 mmol, 1.2 equiv.), triethylamine (0.80 mL, 6.0 mmol, 1.2 equiv.) and DCM (30 mL) as solvent. Purification by column chromatography (PE/EtOAc 95:5) delivered the product **154a** (1.04 g, 4.06 mmol, 81%) as a colorless solid. The analytical data are in good agreement with the literature.[243]

$C_{16}H_{16}OS$: 256.36 $\frac{g}{mol}$

R_f: 0.29 (Silica gel, PE/EtOAc 98:2, UV).

Melting point: 54.8–55.6 °C (PE/EtOAc).

^{1}H-NMR (400 MHz, $CDCl_3$): δ [ppm] = 7.55–7.45 (m, 5H), 6.88 (s, 2H), 2.39 (s, 6H), 2.30 (s, 3H).

^{13}C-NMR (101 MHz, $CDCl_3$): δ [ppm] = 196.2, 139.7, 137.3, 134.5, 133.9, 129.7, 129.5, 128.6, 128.2, 21.3, 19.2.

GC-MS (EI): t_R = 23.32 min, *m/z* (Int. %) = Molecular peak is not detectable, 147 (100) $[M]^{+\bullet}$-$[C_6H_5S]^{\bullet}$, 119 (34) $[M]^{+\bullet}$-$[C_7H_5OS]^{\bullet}$.

S-phenyl 4-fluorobenzothioate (154b)

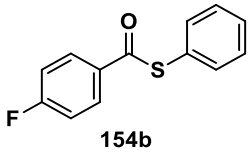

154b

According to GP-A, *S*-phenyl 4-fluorobenzothioate (**154b**) was synthesized using 4-fluorobenzoyl chloride (1.2 mL, 10 mmol, 1.0 equiv.), thiophenol (1.2 mL, 12 mmol, 1.2 equiv.), triethylamine (1.7 mL, 12 mmol, 1.2 equiv.) and DCM (25 mL) as solvent. The crude product was purified by column chromatography (PE/EtOAC 95:5) to yield the product **154b** (1.84 g, 8.58 mmol, 86%) as a colorless crystalline solid. The analytical data are in good agreement with the literature.[244]

$C_{13}H_9FOS$: 214.28 $\frac{g}{mol}$

R_f: 0.49 (Silica gel, PE/EtOAc 95:5, UV).

Melting point: 59.2–59.9 °C (PE/EtOAc).

^{1}H-NMR (400 MHz, $CDCl_3$): δ [ppm] = 8.09–8.04 (m, 2H), 7.54–7.44 (m, 5H), 7.20–7.14 (m, 2H).

^{13}C-NMR (101 MHz, $CDCl_3$): δ [ppm] = 188.8, 166.4 (d, *J* = 255.8 Hz), 135.2, 133.1 (d, *J* = 2.9 Hz), 130.2 (d, *J* = 9.5 Hz), 129.8, 129.4, 127.2, 116.1 (d, *J* = 22.0 Hz).

^{19}F-NMR (376 MHz, $CDCl_3$): δ [ppm] = -104.1 (m).

GC-MS (EI): t_R = 20.92 min, *m/z* (Int. %) = 232 (3) $[M]^{+\bullet}$, 123 (100) $[M]^{+\bullet}$-$[C_6H_5S]^{\bullet}$, 95 (29) $[M]^{+\bullet}$-$[C_7H_5OS]^{\bullet}$.

S-ethyl benzothioate (384b)

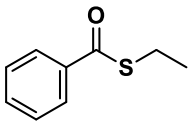

384b

According to GP-A, *S*-ethyl benzothioate (**384b**) was synthesized using benzoyl chloride (1.7 mL, 15 mmol, 1.0 equiv.), ethanethiol (1.3 mL, 18 mmol, 1.2 equiv.), triethylamine (2.0 mL, 15 mmol, 1.0 equiv.) and DCM (15 mL) as solvent. The product **384a** (2.42 g, 14.5 mmol, 97%) was obtained as a colorless oil and used without further purification. The analytical data are in good agreement with the literature.[245]

$C_9H_{11}OS$: 160.28 $\frac{g}{mol}$

R_f: 0.69 (Silica gel, PE/Et_2O 95:5, UV).

Melting point: Ambient temperature (PE/Et_2O).

^{1}H-NMR (400 MHz, $CDCl_3$): δ [ppm] = 7.98–7.95 (m, 2H), 7.59–7.54 (m, 1H*)*, 7.47–7.42 (m, 2H*)*, 3.09 (q, *J* = 7.4 Hz, 2H), 1.36 (t, *J* = 7.4 Hz, 3H).

^{13}C-NMR (101 MHz, $CDCl_3$): δ [ppm] = 192.1, 137.2, 133.2, 128.5, 127.1, 23.4, 14.8.

GC-MS (EI): t_R = 5.62 min, *m/z* (Int. %) = 166 (7) $[M]^{+\bullet}$, 105 (100) $[M]^{+\bullet}$-$[C_2H_5S]^{\bullet}$, 77 (48) $[M]^{+\bullet}$-$[C_3H_5OS]^{\bullet}$, 51 (15) $[M]^{+\bullet}$-$[C_{14}H_{11}O]^{\bullet}$.

S-(4-chlorophenyl) benzothioate (384c)

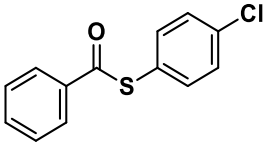

384c

According to GP-A, *S*-(4-chlorophenyl) benzothioate (**384c**) was synthesized using benzoyl chloride (1.7 mL, 15 mmol, 1.0 equiv.), 4-chlorothiophenol (2.17 g, 15.0 mmol, 1.00 equiv.), triethylamine (2.2 mL, 18 mmol, 1.2 equiv.) and DCM (30 mL) as solvent. Purification by column chromatography (*n*Hex/EtOAc 99:1) delivered the product **384c** (3.34 g, 13.4 mmol, 89%) as a colorless solid. The analytical data are in good agreement with the literature.[246]

$C_{13}H_9ClOS$: 248.72 $\frac{g}{mol}$

R_f: 0.65 (Silica gel, *n*Hex/EtOAc 99:1, UV).

Melting point: 73.8–74.9 °C (*n*Hex/EtOAc).

^{1}H-NMR (400 MHz, $CDCl_3$): δ [ppm] = 8.04–8.01 (m, 2H), 7.65–7.60 (m, 1H), 7.52–7.48 (m, 2H), 7.45–7.43 (m, 4H).

^{13}C-NMR (101 MHz, $CDCl_3$): δ [ppm] = 189.8, 136.4, 136.1, 134.0, 129.6, 128.9, 127.6, 126.0.

GC-MS (EI): t_R = 23.48 min, *m/z* (Int. %) = 248 (2) $[M]^{+\bullet}$, 105 (100) $[M]^{+\bullet}$-$[C_6H_4ClS]^{\bullet}$, 77 (33) $[M]^{+\bullet}$-$[C_7H_4ClOS]^{\bullet}$.

S-(3-bromophenyl) benzothioate (384d)

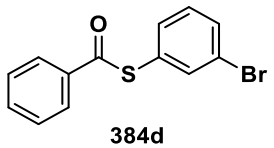

384d

According to GP-A, *S*-(3-bromophenyl) benzothioate (**384d**) was synthesized using benzoyl chloride (0.60 mL, 5.0 mmol, 1.0 equiv.), 3-bromothiophenol (0.60 mL, 5.0 mmol, 1.2 equiv.), triethylamine (0.80 mL, 6.0 mmol, 1.2 equiv.) and DCM (20 mL) as solvent. Purification by column chromatography (*n*Hex/EtOAC 92:8) delivered the product **384d** (1.21 g, 4.13 mmol, 83%) as colorless crystals.

$C_{13}H_9BrOS$: 293.18 $\frac{g}{mol}$

R_f: 0.51 (Silica gel, *n*Hex/EtOAc 92:8, UV).

Melting point: 85.6–86.8 °C (*n*Hex/EtOAc).

^{1}H-NMR (400 MHz, $CDCl_3$): δ [ppm] = 8.03–8.00 (m, 2H), 7.69 (t, *J* = 1.8 Hz, 1H), 7.65–7.61 (m, 1H), 7.60–7.57 (m, 1H), 7.52–7.50 (m, 2H), 7.49–7.45 (m, 1H), 7.34 (t, *J* = 7.8 Hz, 1H).

^{13}C-NMR (101 MHz, $CDCl_3$): δ [ppm] = 189.4, 137.7, 136.4, 134.1, 133.8, 132.8, 130.6, 129.5, 129.0, 127.7, 122.9.

GC-MS (EI): t_R = 24.54 min, *m/z* (Int. %) = Molecular peak is not detectable, 105 (100) $[M]^{+\bullet}$-$[C_6H_4BrS]^{\bullet}$, 77 (30) $[M]^{+\bullet}$-$[C_7H_4BrOS]^{\bullet}$.

HR-MS (ESI): *m/z* = $[M+Na]^+$ calc. for $C_{13}H_9BrOSNa$ 314.94497, found 314.94495.

IR (ATR): $\tilde{\nu}$ [cm^{-1}] = 1669.8 (s, sh), 1558.0 (m, sh), 1442.5 (m, sh), 1394.0 (m, sh), 890.8 (s, br), 767.8 (s, sh), 674.6 (s, sh).

S-(4-bromophenyl) 2,4,6-trimethylbenzothioate (389a)

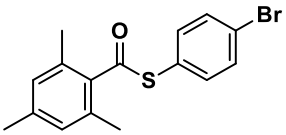

389a

According to GP-A, *S*-(4-bromophenyl) 2,4,6-trimethylbenzothioate (**389a**) was synthesized using 2,4,6-trimethylbenzoyl chloride (0.80 mL, 5.0 mmol, 1.0 equiv.), 4-bromothiophenol (945 mg, 5.00 mmol, 1.00 equiv.), triethylamine (0.70 mL, 5.0 mmol, 1.0 equiv.) and DCM (20 mL) as solvent. The crude product was purified by column chromatography (PE/EtOAC 98:2) to yield the product **389a** (0.99 g, 3.0 mmol, 59%) as a colorless solid.

$C_{16}H_{15}BrOS$: 335.26 $\frac{g}{mol}$

R_f: 0.38 (Silica gel, PE/EtOAc 98:2, UV).

Melting point: 58.7–59.6 °C (PE/EtOAc).

^{1}H-NMR (400 MHz, $CDCl_3$): δ [ppm] = 7.61–7.57 (m, 2H), 7.40–7.37 (m, 2H), 6.88 (s, 2H), 2.37 (s, 6H), 2.30 (s, 3H).

^{13}C-NMR (101 MHz, $CDCl_3$): δ [ppm] = 195.5, 140.0, 137.0, 135.9, 133.9, 132.7, 128.6, 127.3, 124.3, 21.3, 19.2.

GC-MS (EI): t_R = 25.86 min, *m/z* (Int. %) = Molecular peak is not detectable, 147 (100) $[M]^{+\bullet}$-$[C_6H_4BrS]^{\bullet}$, 119 (10) $[M]^{+\bullet}$-$[C_7H_4BrOS]^{\bullet}$.

HR-MS (ESI): *m/z* = $[M+Na]^+$ calc. for $C_{16}H_{15}BrOSNa$ 356.99192, found 356.99186.

IR (ATR): 3011.7 (w, br), 2922.2 (w, br), 2981.9 (w, br), 1677.3 (s, sh), 1472.3 (m, sh), 1203.9 (m, sh), 816.3 (s, sh).

S-(4-bromophenyl) 2-methylpropanethioate (389b)

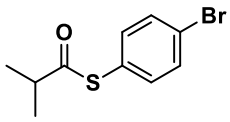

389b

According to GP-A, *S*-(4-bromophenyl) 2-methylpropanethioate (**389b**) was synthesized using isobutyryl chloride (0.70 mL, 7.0 mmol, 1.0 equiv.), 4-bromothiophenol (1.32 g, 7.00 mmol, 1.0 equiv.), triethylamine (1.2 mL, 8.4 mmol, 1.2 equiv.) and DCM (50 mL) as solvent. Purification by column chromatography (PE/EtOAc 95:5) delivered the product **389b** (1.11 g, 4.28 mmol, 61%) as a transparent oil. The analytical data are in good agreement with the literature.[247]

$C_{10}H_{11}BrOS$: 259.16 $\frac{g}{mol}$

R_f: 0.55 (Silica gel, PE/EtOAc 95:5, UV).

Melting point: Ambient temperature (PE/EtOAc).

^{1}H-NMR (400 MHz, $CDCl_3$): δ [ppm] = 7.54–7.48 (m, 2H), 7.27–7.23 (m, 2H), 2.84 (sept, *J* = 6.9 Hz, 1H), 1.25 (d, *J* = 6.9 Hz, 6H).

^{13}C-NMR (101 MHz, $CDCl_3$): δ [ppm] = 201.2, 136.1, 132.3, 127.0, 123.9, 43.1, 19.4.

GC-MS (EI): t_R = 7.19 min, *m/z* (Int. %) = Molecular peak is not detectable, 71 (100) $[M]^{+\bullet}$-$[C_6H_4BrS]^{\bullet}$.

S-(4-bromophenyl) 4-methylbenzothioate (389c)

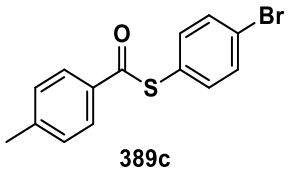

389c

According to GP-B, *S*-(4-bromophenyl) 4-methylbenzothioate (**389c**) was synthesized using 4-methylbenzoyl chloride (0.90 mL, 7.0 mmol, 1.0 equiv.), 4-bromothiophenol (1.30 g, 7.00 mmol, 1.0 equiv.), triethylamine (1.0 mL, 7.0 mmol, 1.0 equiv.) and THF (30 mL) as solvent. Purification by column chromatography (PE/EtOAc 95:5) delivered the product **389c** (1.63 g, 5.31 mmol, 76%) as a colorless solid. The analytical data is in good agreement with literature.[247]

$C_{14}H_{11}BrOS$: 307.21 $\frac{g}{mol}$

R_f: 0.30 (Silica gel, PE/EtOAc 95:5, UV).

Melting point: 126.5–127.5 °C (PE/EtOAc).

^{1}H-NMR (400 MHz, $CDCl_3$): δ [ppm] = 7.92–7.90 (m, 2H), 7.59–7.57 (m, 2H), 7.38–7.36 (m, 2H), 7.30–7.28 (m, 2H), 2.44 (s, 3H).

^{13}C-NMR (101 MHz, $CDCl_3$): δ [ppm] = 189.2, 145.0, 136.7, 133.9, 132.5, 129.6, 127.7, 126.8, 124.3, 21.9.

GC-MS (EI): t_R = 25.75 min, *m/z* (Int. %) = 307 (1) $[M]^{+\bullet}$, 119 (100) $[M]^{+\bullet}$-$[C_6H_4BrS]^{\bullet}$, 91 (33) $[M]^{+\bullet}$-$[C_7H_4BrOS]^{\bullet}$.

S-(4-bromophenyl) 4-fluorobenzothioate (420)

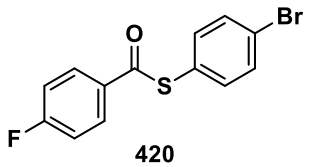

420

According to GP-A, *S*-(4-bromophenyl) 4-fluorobenzothioate (**420**) was synthesized using 4-fluorobenzoyl chloride (1.2 mL, 10 mmol, 1.0 equiv.), 4-bromothiophenol (1.89 g, 10.0 mmol, 1.00 equiv.), triethylamine (1.7 mL, 12 mmol, 1.2 equiv.) and DCM (25 mL) as solvent. The crude product was purified by column chromatography (PE/EtOAC 95:5) to yield the product **420** (2.56 g, 8.23 mmol, 82%) as a colorless solid.

$C_{13}H_8BrFOS$: 311.17 $\frac{g}{mol}$

R_f: 0.37 (Silica gel, PE/EtOAc 95:5, UV).

Melting point: 97.1–97.9 °C (PE/EtOAc).

^{1}H-NMR (400 MHz, $CDCl_3$): δ [ppm] = 8.00–7.94 (m, 2H), 7.54–7.50 (m, 2H), 7.32–7.28 (m, 4H), 7.13–7.07 (m, 2H).

^{13}C-NMR (101 MHz, $CDCl_3$): δ [ppm] = 188.2, 166.5 (d, *J* = 255.9 Hz), 136.7, 132.8 (d, *J* = 3.2 Hz), 132.7, 130.3 (d, *J* = 8.9 Hz), 126.3, 124.5, 116.2 (d, *J* = 22.5 Hz).

^{19}F-NMR (376 MHz, $CDCl_3$): δ [ppm] = -103.6 (m).

GC-MS (EI): t_R = 23.93 min, *m/z* (Int. %) = 310 (2) $[M]^{+\bullet}$, 123 (100) $[M]^{+\bullet}$-$[C_6H_4BrS]^{\bullet}$, 95 (24) $[M]^{+\bullet}$-$[C_7H_4BrOS]^{\bullet}$.

HR-MS (ESI): *m/z* = $[M+Na]^+$ calc. for $C_{13}H_8BrFOSNa$ 332.93555, found 332.93560.

IR (ATR): 3011.7 (w, br), 3075.1 (w, br), 1669.8 (s, sh), 1595.6 (m, sh), 1502.1 (m, sh), 1226.3 (m, sh), 1155.5 (s, sh), 909.5 (s, sh), 842.4 (s, sh), 808.8 (s, sh).

4.4.2.4.4 Experimental Procedure and Analytical Data of Thioesters Synthesized by GP-B

S-(4-bromophenyl) naphthalene-2-carbothioate (389d)

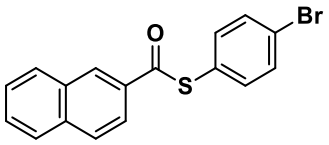

389d

According to GP-B, *S*-(4-bromophenyl) naphthalene-2-carbothioate (**389d**) was synthesized using 2-naphthoic acid (0.90 mL, 5.0 mmol, 1.0 equiv.), 4-bromothiophenol (1.13 g, 6.00 mmol, 1.2 equiv.), DMAP (61.0 mg, 500 µmol, 0.1 equiv.), DCC (1.03 g, 5.00 mmol, 1.0 equiv.) and a mixture of THF (5 mL) and DCM (20 mL) as solvent. Purification by column chromatography (PE/EtOAc 95:5) delivered the desired product **389d** (0.75 g, 2.2 mmol, 44%) as a colorless solid.

$C_{17}H_{11}BrOS$: 343.24 $\frac{g}{mol}$

R_f: 0.50 (Silica gel, PE/EtOAc 95:5, UV).

Melting point: 121.2–121.8 °C (PE/EtOAc).

^{1}H-NMR (400 MHz, $CDCl_3$): δ [ppm] = 8.60 (s, 1H), 8.04–7.98 (m, 2H), 7.96–7.87 (m, 2H), 7.69–7.55 (m, 4H), 7.47–7.38 (m, 2H).

^{13}C-NMR (101 MHz, $CDCl_3$): δ [ppm] = 189.5, 136.7, 136.1, 133.8, 132.64, 132.59, 129.8, 129.3, 128.94, 128.90, 128.0, 127.2, 126.7, 124.4, 123.3.

GC-MS (EI): t_R = 29.96 min, *m/z* (Int. %) = 343 (1) $[M]^{+\bullet}$, 155 (100) $[M]^{+\bullet}$-$[C_6H_4BrS]^{\bullet}$, 127 (53) $[M]^{+\bullet}$-$[C_7H_4BrOS]^{\bullet}$.

HR-MS (ESI): *m/z* = $[M+Na]^+$ calc. for $C_{17}H_{11}BrOSNa$ 364.96062, found 364.96055.

IR (ATR): 3056.4 (w, br), 1673.6 (s, sh), 1382.8 (w, br), 1349.3 (w, br), 1166.7 (m, sh), 902.0 (s, sh), 812.6 (s, sh), 745.5 (s, sh).

S-(4-bromophenyl) 2-(4-methoxyphenyl)ethanethioate (389e)

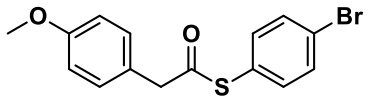

389e

According to GP-B, *S*-(4-bromophenyl) 2-(4-methoxyphenyl)ethanethioate (**389e**) was synthesized using 2-(4-methoxyphenyl)acetic acid (831 mg, 5.00 mmol, 1.0 equiv.), 4-bromothiophenol (1.04 g, 5.50 mmol, 1.1 equiv.), DMAP (61.0 mg, 500 µmol, 0.1 equiv.), DCC (1.13 g, 5.00 mmol, 1.1 equiv.) and THF (30 mL) as solvent. The crude product was purified by column chromatography (PE/EtOAc 95:5) to yield the product **389e** (0.88 g, 2.6 mmol, 52%) as a colorless solid.

$C_{15}H_{13}BrO_2S$: 337.23 $\frac{g}{mol}$

R_f: 0.36 (Silica gel, PE/EtOAc 95:5, UV).

Melting point: 54.4–54.9 °C (PE/EtOAc).

^{1}H-NMR (400 MHz, $CDCl_3$): δ [ppm] = 7.53–7.49 (m, 2H), 7.26–7.21 (m, 4H), 6.91–6.89 (m,2H), 3.85 (s, 2H), 3.82 (s, 3H).

^{13}C-NMR (101 MHz, $CDCl_3$): δ [ppm] = 195.4, 159.3, 136.0, 132.5, 131.0, 127.1, 125.1, 124.1, 114.3, 55.4, 49.5.

GC-MS (EI): t_R = 27.24 min, *m/z* (Int. %) = 336 (2) $[M]^{+\bullet}$, 121 (100) $[M]^{+\bullet}$-$[C_7H_4BrOS]^{\bullet}$.

HR-MS (ESI): *m/z* = $[M+Na]^+$ calc. for $C_{15}H_{13}BrO_2SNa$ 358.97118, found 358.97123.

IR (ATR): 3011.7 (w, br), 2903.6 (w, br), 2832.8 (w, br), 1684.8 (s, sh), 1509.6 (m, sh), 1464.8 (m, sh), 1248.7 (s, sh), 1028.7 (s, sh), 1006.4 (s, sh), 812.6 (s, sh).

S-(4-bromophenyl) 2-phenylbutanethioate (389f)

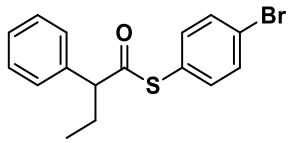

389f

According to GP-B, *S*-(4-bromophenyl) 2-phenylbutanethioate (**389f**) was synthesized using 2-phenylbutanoic acid (821 mg, 5.00 mmol, 1.0 equiv.), 4-bromothiophenol (1.04 g, 5.50 mmol, 1.1 equiv.), DMAP (61.0 mg, 500 µmol, 0.1 equiv.), DCC (1.13 g, 5.00 mmol, 1.1 equiv.) and THF (30 mL) as solvent. The crude product was purified by column chromatography (PE/EtOAc 98:2) to yield the product **389f** (0.93 g, 2.8 mmol, 56%) as a colorless solid.

$C_{16}H_{15}BrOS$: 335.26 $\frac{g}{mol}$

R_f: 0.27 (Silica gel, PE/EtOAc 98:2, UV).

Melting point: 83.4–83.9 °C (PE/EtOAc).

^{1}H-NMR (400 MHz, $CDCl_3$): δ [ppm] = 7.52–7.48 (m, 2H), 7.38–7.30 (m, 5H), 7.23–7.19 (m, 2H), 3.74 (t, *J* = 7.4 Hz, 1H), 2.26–2.15 (m, 1H), 1.93–1.82 (m, 1H), 0.93 (t, *J* = 7.4 Hz, 3H).

^{13}C-NMR (101 MHz, $CDCl_3$): δ [ppm] = 198.0, 138.0, 136.0, 132.4, 128.9, 128.5, 127.8, 127.2, 124.1, 62.2, 26.9, 12.2.

GC-MS (EI): t_R = 25.53 min, *m/z* (Int. %) = 334 (1) $[M]^{+\bullet}$, 119 (100) $[M]^{+\bullet}$-$[C_7H_4BrOS]^{\bullet}$, 91 (91) $[M]^{+\bullet}$-$[C_9H_8BrOS]^{\bullet}$.

HR-MS (ESI): *m/z* = $[M+Na]^+$ calc. for $C_{16}H_{15}BrOSNa$ 356.99192, found 356.99178.

IR (ATR): 2963.2 (w, br), 2903.6 (w, sh), 2870.1 (w, sh), 1692.2 (s, sh), 1468.6 (m, sh), 987.7 (s, sh), 805.1 (s, sh).

S-(4-bromophenyl) 2-(6-methoxynaphthalen-2-yl)propanethioate (389g)

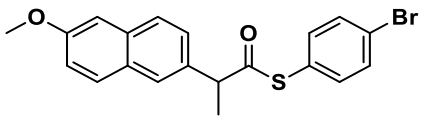

389g

According to GP-B, *S*-(4-bromophenyl) 2-(6-methoxynaphthalen-2-yl)propanethioate (**389g**) was synthesized using 2-(6-methoxynaphthalen-2-yl)propanoic acid (1.3 mL, 5.0 mmol, 1.0 equiv.), 4-bromothiophenol (1.04 g, 5.50 mmol, 1.1 equiv.), DMAP (61.0 mg, 500 µmol, 0.1 equiv.), DCC (1.13 g, 5.50 mmol, 1.1 equiv.) and a mixture of THF (5 mL) and DCM (25 mL) as solvent. Purification by column chromatography (PE/EtOAc 92:8) delivered the product **389g** (0.94 g, 2.3 mmol, 47%) as a colorless, viscous oil.

$C_{20}H_{17}BrO_2S$: 401.32 $\frac{g}{mol}$

R_f: 0.38 (Silica gel, PE/EtOAc 92:8, UV).

Melting point: Ambient temperature (PE/EtOAc).

^{1}H-NMR (400 MHz, $CDCl_3$): δ [ppm] = 7.76–7.73 (m, 3H), 7.51–7.47 (m, 2H), 7.42 (dd, *J* = 8.5, 1.8 Hz, 1H), 7.22–7.14 (m, 4H), 4.12 (q, *J* = 7.1 Hz, 1H), 3.93 (s, 3H), 1.65 (d, *J* = 7.1 Hz, 3H).

^{13}C-NMR (101 MHz, $CDCl_3$): δ [ppm] = 198.7, 158.0, 136.0, 134.5, 134.2, 132.4, 129.5, 129.1, 127.6, 127.2, 127.1, 126.5, 124.0, 119.4, 105.8, 55.5, 54.3, 18.7.

GC-MS (EI): t_R = 33.34 min, *m/z* (Int. %) = 402 (5) $[M]^{+\bullet}$, 185 (100) $[M]^{+\bullet}$-$[C_7H_4BrOS]^{\bullet}$.

HR-MS (ESI): *m/z* = $[M+Na]^+$ calc. for $C_{20}H_{17}BrO_2SNa$ 423.00248, found 423.00269.

IR (ATR): 3056.4 (w, br), 2974.4 (w, br), 2933.4 (w, sh), 1699.7 (s, sh), 1509.6 (s, sh), 1468.6 (s, sh), 1386.6 (s, sh), 1263.6 (s, sh), 931.8 (s, sh), 808.8 (s, sh), 741.7 (m, sh).

S-(4-bromophenyl) 3-phenylpropanethioate (389h)

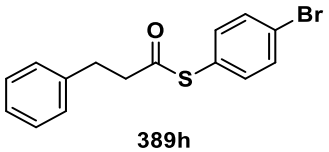

389h

According to GP-B, *S*-(4-bromophenyl) 3-phenylpropanethioate (**389h**) was synthesized using 3-phenylpropanoic acid (0.80 mL, 5.0 mmol, 1.0 equiv.), 4-bromothiophenol (1.13 g, 6.00 mmol, 1.2 equiv.), DMAP (61.0 mg, 500 µmol, 0.1 equiv.), DCC (1.03 g, 5.00 mmol, 1.0 equiv.) and a mixture of THF (5 mL) and DCM (20 mL) as solvent. Purification by column chromatography (PE/EtOAc 95:5) delivered the product **389h** (410 mg, 1.27 mmol, 26%) as a colorless solid.

$C_{15}H_{13}BrOS$: 321.23 $\frac{g}{mol}$

R_f: 0.48 (Silica gel, PE/EtOAc 95:5, UV).

Melting point: 77.8–79.1 °C (PE/EtOAc).

^{1}H-NMR (400 MHz, $CDCl_3$): δ [ppm] = 7.57–7.52 (m, 2H), 7.36–7.19 (m, 7H), 3.07–2.95 (m, 4H).

^{13}C-NMR (101 MHz, $CDCl_3$): δ [ppm] = 196.1, 139.9, 136.0, 132.5, 128.7, 128.5, 126.8, 126.6, 124.2, 77.5, 45.3, 31.4.

GC-MS (EI): t_R = 25.90 min, *m/z* (Int. %) = 321 (7) $[M]^{+\bullet}$, 133 (89) $[M]^{+\bullet}$-$[C_6H_4BrS]^{\bullet}$, 105 (100) $[M]^{+\bullet}$-$[C_7H_4BrOS]^{\bullet}$, 91 (82) $[M]^{+\bullet}$-$[C_8H_6BrOS]^{\bullet}$.

HR-MS (ESI): *m/z* = $[M+Na]^+$ calc. for $C_{15}H_{13}BrOSNa$ 342.97627, found 342.97654.

IR (ATR): 3078.8 (w, br), 3026.6 (w, br), 2955.8 (w, br), 2918.5 (w, br), 1699.7 (s, sh), 1386.6 (m, s), 1028.7 (s, sh), 1006.4 (s, sh), 969.1 (s, sh), 812.6 (s, sh), 738.0 (s, sh), 693.3 (s, sh).

S-(4-bromophenyl) 3-(4-methoxyphenyl)propanethioate (389i)

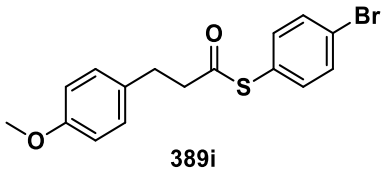

389i

According to GP-B, *S*-(4-bromophenyl) 3-(4-methoxyphenyl)propanethioate (**389i**) was synthesized using 3-(4-methoxyphenyl)propanoic acid (901 mg, 5.00 mmol, 1.0 equiv.), 4-bromothiophenol (1.04 g, 5.50 mmol, 1.1 equiv.), DMAP (61.0 mg, 500 µmol, 0.1 equiv.), DCC (1.13 g, 5.50 mmol, 1.1 equiv.) and a mixture of THF (10 mL) and DCM (20 mL) as solvent. Purification by column chromatography (PE/EtOAc 95:5) delivered the product **389i** (837 mg, 2.38 mmol, 48%) as a colorless solid.

$C_{16}H_{15}BrO_2S$: 351.26 $\frac{g}{mol}$

R_f: 0.17 (Silica gel, PE/EtOAc 95:5, UV).

Melting point: 83.9–84.7 °C (PE/EtOAc).

^{1}H-NMR (400 MHz, $CDCl_3$): δ [ppm] = 7.54–7.52 (m, 2H), 7.25–7.22 (m, 2H), 7.14–7.10 (m, 2H), 6.86–6.83 (m, 2H), 3.79 (s, 3H), 2.98–2.92 (m, 4H).

^{13}C-NMR (101 MHz, $CDCl_3$): δ [ppm] = 196.2, 158.4, 136.0, 132.5, 131.9, 129.5, 126.9, 124.2, 114.1, 55.4, 45.6, 30.7.

GC-MS (EI): t_R = 11.73 min, *m/z* (Int. %) = 352 (4) $[M]^{+\bullet}$, 121 (100) $[M]^{+\bullet}$-$[C_8H_6BrOS]^{\bullet}$.

HR-MS (ESI): *m/z* = $[M+Na]^+$ calc. for $C_{16}H_{15}BrO_2SNa$ 372.98683, found 372.98730.

IR (ATR): 3034.1 (w, br), 2929.7 (w, br), 2832.8 (w, sh), 1699.7 (s, sh), 1509.6 (s, sh), 1241.2 (s, sh), 1177.8 (m, sh), 1036.2 (s, sh), 961.7 (s, sh), 820.0 (s, sh), 786.5 (s, sh).

S-(4-bromophenyl) hexanethioate (389j)

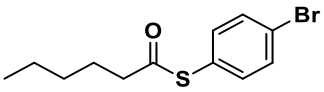

389j

According to GP-B, *S*-(4-bromophenyl) hexanethioate (**389j**) was synthesized using hexanoic acid (0.6 mL, 5.0 mmol, 1.0 equiv.), 4-bromothiophenol (1.13 g, 6.00 mmol, 1.2 equiv.), DMAP (61.0 mg, 500 µmol, 0.1 equiv.), DCC (1.03 g, 5.00 mmol, 1.0 equiv.) and a mixture of THF (5 mL) and DCM (20 mL) as solvent. Purification by column chromatography (PE/EtOAc 95:5) delivered the product **389j** (496 mg, 1.73 mmol, 35%) as colorless crystals. The analytical data are in good agreement with the literature.[247]

$C_{12}H_{15}BrOS$: 287.22 $\frac{g}{mol}$

R_f: 0.32 (Silica gel, PE/EtOAc 95:5, UV).

Melting point: Partly at ambient temperature (PE/EtOAc).

^{1}H-NMR (400 MHz, $CDCl_3$): δ [ppm] = 7.57–7.50 (m, 2H), 7.30–7.23 (m, 2H), 2.64 (t, *J* = 7.5 Hz, 2H), 1.71 (quint, *J* = 7.4 Hz, 2H), 1.41–1.23 (m, 4H), 0.98–0.80 (m, 3H).

^{13}C-NMR (101 MHz, $CDCl_3$): δ [ppm] = 197.0, 136.0, 132.5, 127.2, 124.1, 43.9, 31.2, 25.4, 22.5, 14.0.

GC-MS (EI): t_R = 22.94 min, *m/z* (Int. %) = 287 (11) $[M]^{+\bullet}$, 99 (100) $[M]^{+\bullet}$-$[C_6H_4BrS]^{\bullet}$, 71 (44) $[M]^{+\bullet}$-$[C_7H_4BrOS]^{\bullet}$.

S-(4-bromophenyl) 2-ethylhexanethioate (389k)

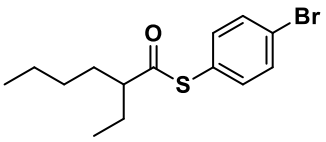

289k

According to GP-B, *S*-(4-bromophenyl) 2-ethylhexanethioate (**389k**) was synthesized using 2-ethylhexanoic acid (799 µL, 5.00 mmol, 1.0 equiv.), 4-bromothiophenol (1.04 g, 5.50 mmol, 1.1 equiv.), DMAP (61.0 mg, 500 µmol, 0.1 equiv.), DCC (1.13 g, 5.00 mmol, 1.1 equiv.) and THF (30 mL) as solvent. The crude product was purified by column chromatography (PE/EtOAc 98:2) to yield the product **389k** (0.77 g, 2.4 mmol, 49%) as a colorless oil.

$C_{14}H_{19}BrOS$: 315.27 $\frac{g}{mol}$

R_f: 0.21 (Silica gel, PE/EtOAc 98:2, UV).

Melting point: Ambient temperature (PE/EtOAc).

^{1}H-NMR (400 MHz, $CDCl_3$): δ [ppm] = 7.55–7.51 (m, 2H), 7.28–7.25 (m, 2H), 2.61–2.54 (m, 1H), 1.78–1.69 (m, 2H), 1.62–1.56 (m, 1H), 1.53–1.49 (m, 1H), 1.39–1.29 (m, 4H), 0.97 (t, *J* = 7.3 Hz, 3H), 0.97–0.88 (m, 3H).

^{13}C-NMR (101 MHz, $CDCl_3$): δ [ppm] = 200.9, 136.0, 132.4, 127.4, 123.9, 56.2, 32.3, 29.6, 26.1, 22.8, 14.1, 11.9.

GC-MS (EI): t_R = 9.14 min, *m/z* (Int. %) = 314 (1) $[M]^{+\bullet}$, 187 (8) $[M]^{+\bullet}$-$[C_8H_{15}O]^{\bullet}$, 127 (33) $[M]^{+\bullet}$-$[C_6H_4BrS]^{\bullet}$, 57 (100) $[M]^{+\bullet}$-$[C_{10}H_{10}BrOS]^{\bullet}$.

HR-MS (ESI): *m/z* = $[M+Na]^+$ calc. for $C_{14}H_{19}BrOSNa$ 337.02322, found 337.02357.

IR (ATR): 2959.5 (m, br), 2929.7 (m, br), 2858.9 (m, br), 1703.4 (s, sh), 1468.6 (m, sh), 1382.8 (m, sh), 976.6 (s, sh), 812.6 (s, sh).

S-(4-bromophenyl) 2-(4-isobutylphenyl)propanethioate (389l)

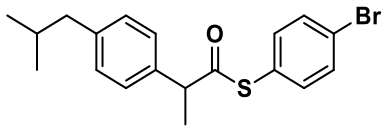

389l

According to GP-B, *S*-(4-bromophenyl) 2-(4-isobutylphenyl)propanethioate (**389l**) was synthesized using 2-(4-isobutylphenyl)propanoic acid (1.24 g, 6.00 mmol, 1.0 equiv.), 4-bromothiophenol (1.36 g, 7.20 mmol, 1.2 equiv.), DMAP (73.3 mg, 600 µmol, 0.1 equiv.), DCC (1.24 g, 6.00 mmol, 1.0 equiv.) and DCM (20 mL) as solvent. Purification by column chromatography (PE/EtOAc 98:2) delivered the product **389l** (730 mg, 1.93 mmol, 32%) as a colorless oil.

$C_{19}H_{21}BrOS$: 377.34 $\frac{g}{mol}$

R_f: 0.32 (Silica gel, PE/EtOAc 98:2, UV).

Melting point: Ambient temperature (PE/EtOAc).

^{1}H-NMR (400 MHz, $CDCl_3$): δ [ppm] = 7.55–7.53 (m, 2H), 7.32–7.23 (m, 4H), 7.20–7.16 (m, 2H), 4.00 (q, *J* = 7.1 Hz, 1H), 2.52 (d, *J* = 7.1 Hz, 2H), 1.91–1.84 (m, 1H), 1.61 (d, *J* = 7.1 Hz, 3H), 0.96 (d, *J* = 7.1 Hz, 6H).

^{13}C-NMR (101 MHz, $CDCl_3$): δ [ppm] = 198.7, 141.3, 136.4, 135.9, 132.3, 129.6, 127.8, 127.2, 123.9, 53.9, 45.1, 30.2, 22.4, 18.6.

GC-MS (EI): t_R = 11.63 min, *m/z* (Int. %) = Molecular peak is not detectable, 189 (6) $[M]^{+\bullet}$-$[C_6H_4BrS]^{\bullet}$, 161 (100) $[M]^{+\bullet}$-$[C_7H_4BrOS]^{\bullet}$.

HR-MS (ESI): *m/z* = $[M+Na]^+$ calc. for $C_{19}H_{21}BrOSNa$ 399.03887, found 399.03835.

IR (ATR): 2952 (w, sh), 2866 (w, sh), 1707 (m, sh), 1469 (m, sh), 1383 (m, sh), 1006 (m, sh), 928 (s, sh), 813 (s, sh), 731 (m, sh).

4.4.2.5 Synthesis of Thiocarbonates
4.4.2.5.1 General Procedure

General Procedure C (GP-C): Synthesis of Thiocarbonates from Thiols and Boc_2O

The thiocarbonates were synthesized according to a procedure described in the literature.[213] A solution of thiol (10 mmol, 1.0 equiv.), DMAP (122 mg, 1.00 mmol, 0.1 equiv.) and triethylamine (2.8 mL, 20 mmol, 2.0 equiv.) in DCM (30 mL) was cooled to 0 °C and treated dropwise with Boc_2O (2.6 mL, 12 mmol, 1.2 equiv.). After warming to room temperature, the reaction mixture was stirred overnight and then diluted with DCM (20 mL). The organic layer was washed with HCl (1 M, 2 × 10 mL), aq. saturated $NaHCO_3$ (2 × 10 mL) and aq. saturated NaCl (2 × 10 mL), dried over anhydrous $MgSO_4$ and concentrated under reduced pressure. The purification methods are described in the individual experiments.

4.4.2.5.2 Experimental Procedure and Analytical Data of Thiocarbonates

O-(*t*-butyl) *S*-phenyl thiocarbonate (391)

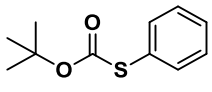

391

According to GP-C, *O*-(*t*-butyl) *S*-phenyl thiocarbonate (**391**) was synthesized using thiophenol (1.0 mL, 10 mmol, 1.0 equiv.), DMAP (122 mg, 1.00 mmol, 0.1 equiv.), triethylamine (2.8 mL, 20 mmol, 2.0 equiv.), Boc_2O (2.6 mL, 12 mmol, 1.2 equiv.) and DCM (30 mL) as solvent. Purification by column chromatography (PE/EtOAc 98:2) delivered the product **391** (509 mg, 2.42 mmol, 24%) as a colorless oil. The analytical data are in good agreement with the literature, however minor amounts of contaminations are obtained.[248]

$C_{11}H_{14}O_2S$: 210.29 $\frac{\mathrm{g}}{\mathrm{mol}}$

R_f: 0.44 (Silica gel, PE/EtOAc 98:2, UV).

Melting point: Ambient temperature (PE/EtOAc).

^{1}H-NMR (400 MHz, $CDCl_3$): δ [ppm] = 7.55–7.50 (m, 2H), 7.44–7.35 (m, 3H), 1.51 (s, 9H).

^{13}C-NMR (101 MHz, $CDCl_3$): δ [ppm] = 168.1, 135.1, 129.5, 129.3, 128.9, 85.8, 28.4.

GC-MS (EI): t_R = 16.52 min, *m/z* (Int. %) = 210 (0.2) $[M]^{+\bullet}$, 137 (11) $[M]^{+\bullet}$-$[C_4H_9O]^{\bullet}$, 109 (29) $[M]^{+\bullet}$-$[C_5H_9O_2]^{\bullet}$, 57 (100) $[M]^{+\bullet}$-$[C_7H_5O_2S]^{\bullet}$.

O-(*t*-butyl) *S*-cyclohexyl thiocarbonate (392)

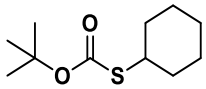

392

According to GP-C, *O*-(*t*-butyl) *S*-cyclohexyl thiocarbonate (**392**) was synthesized using cyclohexanethiol (1.2 mL, 10 mmol, 1.0 equiv.), DMAP (122 mg, 1.00 mmol, 0.1 equiv.), triethylamine (2.8 mL, 20 mmol, 2.0 equiv.), Boc_2O (2.6 mL, 12 mmol, 1.2 equiv.) and DCM (30 mL) as solvent. Purification by column chromatography (PE/EtOAc 98:2) delivered the product **392** (853 mg, 3.94 mmol, 74%) as a colorless oil. The analytical data are in good agreement with the literature, however minor amounts of contaminations are obtained.[213]

$C_{11}H_{20}O_2S$: 216.34 $\frac{g}{mol}$

R_f: 0.28 (Silica gel, PE/EtOAc 98:2, anisaldehyde).

Melting point: Ambient temperature (PE/EtOAc).

^{1}H-NMR (400 MHz, $CDCl_3$): δ [ppm] = 3.27–3.21 (m, 1H), 2.04–1.93 (m, 2H), 1.78–1.66 (m, 2H), 1.64–1.55 (m, 1H), 1.49 (s, 9H), 1.45–1.33 (m, 4H), 1.31–1.18 (m, 1H).

^{13}C-NMR (101 MHz, $CDCl_3$): δ [ppm] = 169.4, 84.4, 44.4, 33.5, 28.4, 26.2, 25.7.

GC-MS (EI): t_R = 16.37 min, *m/z* (Int. %) = 343 (0.3) $[M]^{+\bullet}$, 83 (9) $[M]^{+\bullet}$-$[C_5H_9O_2S]^{\bullet}$, 57 (100) $[M]^{+\bullet}$-$[C_7H_{11}O_2S]^{\bullet}$.

4.4.2.6 Thiocarbamates

Thiocarbamates **393** and **394** were synthesized by R. Richter from the working group of I. Fleischer, University of Tübingen, and kindly provided for the experiments. They were used as received.

4.4.2.7 Synthesis of (By)products
4.4.2.7.1 Synthesis of Standard Ketone

N-methoxy-2-(4-methoxyphenyl)-*N*-methylacetamide (S1)

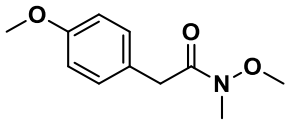

S1

The synthesis of *N*-methoxy-2-(4-methoxyphenyl)-*N*-methylacetamide **S1** followed a literature procedure.[249] To a mixture of *N*,*O*-dimethylhydroxylamine hydrochloride (536 mg, 5.50 mmol, 1.1 equiv.) in DCM (10 mL), 4-methoxyphenylacetyl chloride (0.80 mL, 5.0 mmol, 1.0 equiv.) and anhydrous pyridine (1.00 mL, 12.5 mmol, 2.5 equiv.) were successively added at 0 °C. The reaction was stirred at 0 °C for 30 min, then at rt for additional 30 min. The mixture was diluted with ethyl acetate (50 mL) and the organic layer was washed with HCl (1 M, 3 × 10 mL), aq. saturated $NaHCO_3$ (3 × 10 mL) and aq. saturated NaCl (20 mL), dried over anhydrous Mg_2SO_4 and concentrated under reduced pressure. **S1** was obtained as a yellow oil (856 mg, 4.09 mmol, 82%) and was used as received. The analytical data are in good agreement with the literature.[249]

$C_{11}H_{15}NO_3$: 209.3 $\frac{\mathrm{g}}{\mathrm{mol}}$

R_f: 0.13 (Silica gel, *n*Hex/EtOAc 8:2, UV).

Melting point: Ambient temperature (*n*Hex/EtOAc).

^{1}H-NMR (400 MHz, $CDCl_3$): δ [ppm] = 7.21 (d, *J* = 8.8 Hz, 2H), 6.85 (d, *J* = 8.8 Hz, 2H), 3.78 (s, 3H), 3.71 (s, 2H), 3.61 (s, 3H), 3.18 (s, 3H).

^{13}C-NMR (101 MHz, $CDCl_3$): δ [ppm] = 172.9, 158.6, 130.4, 127.1, 114.0, 61.4, 55.4, 38.6, 32.3.

GC-MS (EI): t_R = 19.83 min, *m/z* (Int. %) = 209 (31) $[M]^{+\bullet}$, 149 (5) $[M]^{+\bullet}$-$[C_2H_6NO]^{\bullet}$, 121 (100) $[M]^{+\bullet}$-$[C_3H_6NO_2]^{\bullet}$.

2-(4-methoxyphenyl)-1-phenylethan-1-one (378a)

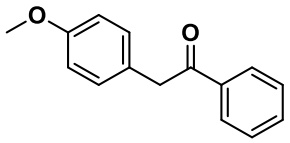

378a

Preparation of Grignard Reagent

Under an inert atmosphere, a three-necked RBF with reflux condenser and dropping funnel was charged with finely ground Mg (437 mg, 18.0 mmol, 1.2 equiv.) and iodine for activation. The compounds were heated for 20 sec with a heat gun, stirred for 10 min and suspended in THF (12 mL). A solution of bromobenzene (1.6 mL, 15 mmol, 1.0 equiv.) in THF (3 mL) was added dropwise. When there was no immediate exothermal reaction after the addition of bromobenzene, the flask was additionally heated. The formation of Grignard compound was accompanied by a color change from yellow to colorless to black. The mixture was refluxed for 30 min, then stirred at rt for additional 30 min.

Addition of Grignard Reagent to Weinreb Amide S1

The ketone synthesis was similar to a published procedure.[238] Phenylmagnesium bromide (1.0 M in THF, 15 mL, 15 mmol, 3.4 equiv.) was added dropwise to a solution of **S1** (0.90 mL, 4.5 mmol, 1.0 equiv.) in THF (100 mL) during cooling from -50 °C– -70 °C. After completion, the solution was stirred at -70 °C for one hour and then warmed to rt. The reaction was quenched with H_2O (30 mL), which was extracted with EtOAc (3 × 20 mL). The combined organic layers were washed with HCl (1 M, 3 × 15 mL), aq. saturated $NaHCO_3$ (2 × 15 mL) and aq. saturated NaCl (2 × 15 mL), dried over anhydrous Mg_2SO_4 and concentrated under reduced pressure. The crude product was purified by column chromatography (*n*Hex/EtOAc 9:1–4:1) to yield **378a** (0.92 g, 4.1 mmol, 91%) as colorless crystals. The analytical data are in good agreement with the literature.[238]

$C_{15}H_{14}O_2$: 226.28 $\frac{\mathrm{g}}{\mathrm{mol}}$

R_f: 0.44 (Silica gel, *n*Hex/EtOAc 4:1, UV).

Melting point: 94.9–95.5 °C (*n*Hex/EtOAc).

^{1}H-NMR (400 MHz, $CDCl_3$): δ [ppm] = 8.01 (d, *J* = 7.3 Hz, 2H), 7.55 (t, *J* = 7.3 Hz, 1H), 7.46 (t, *J* = 7.3 Hz, 2H), 7.19 (d, *J* = 8.7 Hz, 2H), 6.87 (d, *J* = 8.7 Hz, 2H), 4.23 (s, 2H), 3.79 (s, 3H).

^{13}C-NMR (101 MHz, $CDCl_3$): δ [ppm] = 198.1, 158.7, 136.7, 133.2, 130.6, 128.76, 128.73, 126.6, 114.3, 55.4, 44.8.

GC-MS (EI): t_R = 8.86 min, *m/z* (Int. %) = 226 (12) $[M]^{+\bullet}$, 121 (100) $[M]^{+\bullet}$-$[C_7H_5O]^{\bullet}$, 105 (61) $[M]^{+\bullet}$-$[C_8H_9O]^{\bullet}$, 77 (44) $[M]^{+\bullet}$-$[C_9H_9O_2]^{\bullet}$.

4.4.2.8 Synthesis of Standard Thioether

4-methoxybenzyl bromide (396)

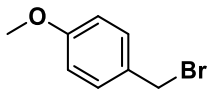

396

The synthesis of **396** followed a literature procedure.[250] PBr_3 (740 µL, 7.80 mmol, 1.3 equiv.) was added dropwise under inert conditions to a stirred solution of 4-methoxybenzyl alcohol (**316b**) (744 µL, 6.00 mmol, 1.0 equiv.) in dry Et_2O (35 mL). After stirring at rt for 25 min (TLC control, *n*Hex/EtOAc 8:2, UV), the reaction was quenched with water (20 mL), which was extracted with EtOAc (2 × 15 mL). The combined organic layers were washed with aq. saturated NaCl (3 × 20 mL), dried over anhydrous Mg_2SO_4, filtered, and concentrated under reduced pressure. No further purification was necessary. The product **396** was obtained as a colorless oil (1.12 g, 5.57 mmol, 93%). The analytical data are in good agreement with the literature.[251]

C_8H_9BrO: 201.06 $\frac{g}{mol}$

R_f: 0.77 (Silica gel, *n*Hex/EtOAc 8:2, UV).

Melting point: Ambient temperature (*n*Hex/EtOAc).

^{1}H-NMR (400 MHz, $CDCl_3$): δ [ppm] = 7.33 (d, *J* = 8.8 Hz, 2H), 6.87 (d, *J* = 8.8 Hz, 2H), 4.51 (s, 2H), 3.81 (s, 3H).

^{13}C-NMR (101 MHz, $CDCl_3$): δ [ppm] = 159.8, 130.6, 130.1, 114.3, 55.5, 34.1.

GC-MS (EI): t_R = 15.50 min, *m/z* (Int. %) = 201 (7) $[M]^{+\bullet}$, 121 (100) $[M]^{+\bullet}$-$[Br]^{\bullet}$.

(4-bromophenyl)(4-methoxybenzyl)sulfane (379b)

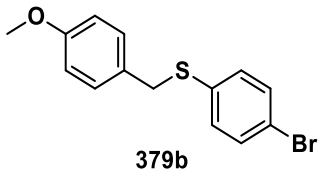

379b

The synthesis of (4-bromophenyl)(4-methoxybenzyl)sulfane (**379b**) followed a literature procedure.[252] In a flame-dried Schlenk-RBF, a mixture of 4-methoxybenzyl bromide **395** (359 µL, 2.50 mmol, 1.0 equiv.), 4-bromothiophenol (520 mg, 2.75 mmol, 1.1 equiv.) and K_2CO_3 (518 mg, 3.75 mmol, 1.5 equiv.) in MeCN (30 mL) was stirred at rt overnight. The reaction was quenched by the addition of water (25 mL), which was extracted with EtOAc (2 × 15 mL). The combined organic layers were washed with aq. saturated $NaHCO_3$ (2 × 10 mL) and aq. saturated NaCl (2 × 10 mL), dried over anhydrous Mg_2SO_4, filtered, and concentrated under reduced pressure. The crude product was purified by column chromatography (PE/EtOAc 95:5) to give thioether **379b** (584 mg, 1.89 mmol, 76%) as a colorless powder. The analytical data are in good agreement with the literature.[253]

$C_{14}H_{13}BrOS$: 309.22 $\frac{g}{mol}$

R_f: 0.44 (Silica gel, PE/EtOAc 95:5, UV).

Melting point: 97.7–98.2°°C (PE/EtOAc).

^{1}H-NMR (400 MHz, $CDCl_3$): δ [ppm] = 7.38–7.34 (m, 2H), 7.20–7.17 (m, 2H), 7.16–7.13 (m, 2H), 6.84–6.80 (m, 2H), 4.04 (s, 2H), 3.79 (s, 3H).

^{13}C-NMR (101 MHz, $CDCl_3$): δ [ppm] = 159.1, 135.8, 132.1, 131.7, 130.2, 129.2, 120.5, 114.2, 55.5, 38.8.

GC-MS (EI): t_R = 25.29 min, *m/z* (Int. %) = 310 (2) $[M]^{+\bullet}$, 121 (100) $[M]^{+\bullet}$-$[C_6H_4BrS]^{\bullet}$.

4.4.2.9 Synthesis of Oxoether

4,4'-(oxybis(methylene))bis(methoxybenzene) (380)

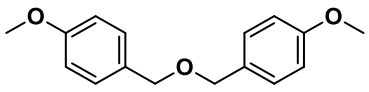

380

The ether synthesis followed a similar procedure as in the literature.[254] To a solution of 4-methoxybenzyl alcohol (**316b**) (622 µL, 5.00 mmol, 1.0 equiv.) in dry THF (10 mL), sodium hydride (144 mg, 6.00 mmol, 1.2 equiv., 60% suspension in mineral oil) was added at 0 °C. After stirring at 0 °C for one hour, 4-methoxybenzyl chloride (**317b**) (817 µL, 6.00 mmol, 1.2 equiv.) was added and the orange mixture was stirred at room temperature overnight. The reaction was quenched with aq. saturated NH_4Cl (10 mL) and the aqueous phase was extracted with EtOAc (3 × 10 mL). The combined organic layers were washed with aq. saturated NH_4Cl (2 × 10 mL), aq. saturated $NaHCO_3$ (2 × 10 mL) and aq. saturated NaCl (2 × 10 mL), dried over anhydrous Mg_2SO_4 and concentrated under reduced pressure. The crude product was purified by column chromatography (PE/EtOAc 95:5) to yield the product **380** (0.64 g, 2.5 mmol, 49%) as colorless crystals. The analytical data are in good agreement with the literature.[255]

$C_{16}H_{18}O_3$: 258.32 $\frac{g}{mol}$

R_f: 0.18 (Silica gel, PE/EtOAc 95:5, UV).

Melting point: 38.1–38.8 °C (PE/EtOAc).

^{1}H-NMR (400 MHz, $CDCl_3$): δ [ppm] = 7.28 (d, *J* = 8.9 Hz, 4H), 6.89 (d, *J* = 8.9 Hz, 4H), 4.46 (s, 4H), 3.81 (s, 6H).

^{13}C-NMR (101 MHz, $CDCl_3$): δ [ppm] = 159.3, 130.6, 129.6, 113.9, 71.6, 55.4.

GC-MS (EI): t_R = 9.89 min, *m/z* (Int. %) = 258 (4) $[M]^{+\bullet}$, 121 (100) $[M]^{+\bullet}$-$[C_7H_5O]^{\bullet}$, 77 (53) $[M]^{+\bullet}$-$[C_9H_9O_2]^{\bullet}$.

4.4.3 Catalytic Procedure
4.4.3.1 General Procedures

General Procedure D (GP-D): Synthesis of Ketones by Nickel-Catalyzed and Lewis Acid-Assisted Cross-Electrophile Coupling of Benzylic Alcohols or Chlorides and Thioesters

In a glovebox, a flame-dried Schlenk tube was charged with Mn powder (54.9 mg, 1.00 mmol, 2.0 equiv.) and titanocene dichloride (3.7 mg, 15 µmol, 3.0 mol%). After removal from the glovebox, $NiCl_2$(Phen) (7.8 mg, 25 µmol, 5.0 mol%), respective thioester, thiocarbonate or thiocarbamate (500 µmol, 1.0 equiv.) and TMSCl (159 µL, 1.25 mmol, 2.5 equiv.) were added successively. 4-Methoxybenzyl alcohol (**316b**) (137 µL, 1.10 mmol, 2.2 equiv.) was added *via* syringe pump over a time range of 5 min (27.4 µL/min), and after stirring for additional 5 min, abs. DMA (2 mL) was also added *via* syringe pump over a time range of 5 min (0.4 mL/min). The reaction was stirred at rt for further 15 h and then quenched by adding two drops of aq. saturated NaCl and Lewatit® TP 207. Yields were determined *via* quantitative GC-FID analysis (see section 4.4.1.3.3) or after isolation of ketones.

For purification, the reactions were worked up as follows: The mixture was filtered through a pad of Celite® 545, activated basic Al_2O_3 and anhydrous $MgSO_4$ with DCM as eluent. The filtrate was washed with HCl (1 M, 3 × 10 mL), aq. saturated $NaHCO_3$ (10 mL) and aq. saturated NaCl (2 × 10 mL). The combined organic layers were dried over anhydrous $MgSO_4$, filtered and concentrated under reduced pressure. Purification by column chromatography is mentioned detailed in individual experiments.

General Procedure E (GP-E): Cross-Electrophile Coupling of Benzylic Chlorides and Thioesters in the Absence of TMSCl

In a glovebox, a flame-dried Schlenk tube was charged with Mn powder (54.9 mg, 1.00 mmol, 2.0 equiv.) and titanocene dichloride (3.7 mg, 15 µmol, 3.0 mol%). After removal from the glovebox, $NiCl_2$(Phen) (7.8 mg, 25 µmol, 5.0 mol%), respective thioester (500 µmol, 1.0 equiv.), respective benzylic chloride (1.3 equiv.–2.2 equiv.) and abs. DMA (2 mL) were added successively. The reaction was stirred at rt for further 15 h and then quenched by adding two drops of aq. saturated NaCl and Lewatit® TP 207. Yields were determined *via* quantitative GC-FID analysis (see section 4.4.1.3.3) or after isolation of ketones.

For purification, the reactions were worked up as follows. The mixture was filtered through a pad of silica gel with DCM as eluent. The filtrate was washed with aq. saturated NaCl (3 × 10 mL). The combined organic layers were dried over anhydrous $MgSO_4$, filtered and concentrated under reduced pressure. Purification by column chromatography is mentioned detailed in individual experiments.

4.4.3.2 Experimental Procedure and Analytical Data of Ketones
4.4.3.2.1 Ketones Synthesized from the Respective Benzylic Alcohols

2-(4-methoxyphenyl)-1-phenylethan-1-one (378a)

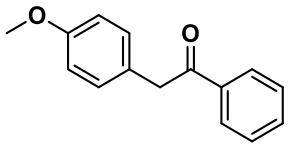

378a

According to GP-D, 2-(4-methoxyphenyl)-1-phenylethan-1-one (**378a**) was synthesized from *S*-phenyl benzothioate (**133**) (107 mg, 500 µmol, 1.0 equiv.). Purification by RP column chromatography (MeOH/H_2O 7:3) delivered the product **378a** (66.0 mg, 258 µmol, 52%) as a colorless solid. The analytical data are in good agreement with the literature; [238] however, no complete separation of ketone **378a** and byproduct **385** could be achieved. The purity of the ketone was determined to be 82% using quantitative ^{1}H-NMR. The corrected yield of ketone is therefore 43%.

$C_{15}H_{14}O_2$: 226.28 $\frac{\mathrm{g}}{\mathrm{mol}}$

R_f: 0.61 (RP-18, MeOH/H_2O 7:3, UV).

Melting point: 94.5–95.5 °C (MeOH/H_2O).

^{1}H-NMR (400 MHz, $CDCl_3$): δ [ppm] = 8.02–8.00 (m, 2H), 7.57–7.53 (m, 1H), 7.48–7.45 (m 2H), 7.20–7.17 (m, 2H), 6.88–6.86 (m, 2H), 4.23 (s, 2H), 3.79 (s, 3H).

^{13}C-NMR (101 MHz, $CDCl_3$): δ [ppm] = 198.8, 158.7, 136.8, 133.2, 130.6, 128.76, 128.73, 126.6, 114.3, 55.4, 44.8.

GC-MS (EI): t_R = 8.86 min, *m/z* (Int. %) = 226 (12) $[M]^{+\bullet}$, 121 (100) $[M]^{+\bullet}$-$[C_7H_5O]^{\bullet}$, 105 (61) $[M]^{+\bullet}$-$[C_8H_9O]^{\bullet}$, 77 (44) $[M]^{+\bullet}$-$[C_9H_9O_2]^{\bullet}$.

2-(4-methoxyphenyl)-1-(*p*-tolyl)ethan-1-one (378b)

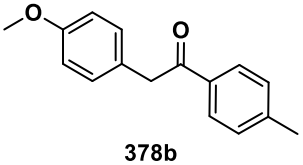

378b

According to GP-D, 2-(4-methoxyphenyl)-1-(*p*-tolyl)ethan-1-one (**378b**) was synthesized from *S*-(4-bromophenyl) 4-methylbenzothioate (**389c**) (154 mg, 500 µmol, 1.0 equiv.). Purification by column chromatography (PE/EtOAc 4:1) delivered the product **378b** (71.6 mg, 298 µmol, 60%) as a colorless solid, but no complete separation of ketone **378b** and oxoether **380** could be achieved. The purity of the ketone was determined to be 88% using quantitative ^{1}H-NMR. The corrected yield of ketone is therefore 53%.The analytical data (disregarding oxoether) are in good agreement with the literature.[256]

$C_{16}H_{16}O_2$: 240.30 $\frac{g}{mol}$

R_f: 0.15 (Silica gel, PE/EtOAc 95:1, UV).

Melting point: Not determined due to contaminations.

^{1}H-NMR (400 MHz, $CDCl_3$): δ [ppm] = 7.91 (d, *J* = 8.2 Hz, 2H), 7.25 (d, *J* = 8.0 Hz, 2H), 7.18 (d, *J* = 8.6 Hz, 2H), 6.88–6.84 (m, 2H), 4.20 (s, 2H), 3.78 (s, 3H), 2.40 (s, 3H).

^{13}C-NMR (101 MHz, $CDCl_3$): δ [ppm] = 197.7, 158.6, 144.0, 134.3, 129.4, 128.9, 126.9, 114.3, 55.4, 44.7, 21.8.

GC-MS (EI): t_R = 24.00 min, *m/z* (Int. %) = 240 (12) $[M]^{+\bullet}$, 121 (100) $[M]^{+\bullet}$-$[C_6H_{11}O]^{\bullet}$, 119 (30) $[M]^{+\bullet}$-$[C_8H_9O]^{\bullet}$, 91 (25) $[M]^{+\bullet}$-$[C_9H_9O_2]^{\bullet}$.

1-(4-fluorophenyl)-2-(4-methoxyphenyl)ethan-1-one (378c)

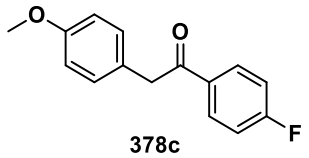

378c

According to GP-D, 1-(4-fluorophenyl)-2-(4-methoxyphenyl)ethan-1-one (**378c**) was synthesized from *S*-(4-bromophenyl) 4-fluorobenzothioate (**420**) (156 mg, 500 µmol, 1.0 equiv.). Purification by column chromatography (PE/EtOAc 95:5) delivered the product **378c** (53.6 mg, 219 µmol, 44%) as a colorless solid, but no complete separation of ketone **378c** and oxoether **380** could be achieved. The purity of the ketone was determined to be 48% using quantitative ^{1}H-NMR. The corrected yield of ketone is therefore 21%. The analytical data (disregarding oxoether) are in good agreement with the literature.[257]

$C_{15}H_{13}FO_2$: 244.27 $\frac{g}{mol}$

R_f: 0.14 (Silica gel, PE/EtOAc 95:5, UV).

Melting point: Not determined due to contaminations.

^{1}H-NMR (400 MHz, $CDCl_3$): δ [ppm] = 8.05–8.01 (m, 2H), 7.18–7.10 (m, 4H), 6.88–6.85 (m, 2H, peak overlap with H_{Ar} from oxoether), 4.19 (s, 2H), 3.79 (s, 3H).

^{13}C-NMR (101 MHz, $CDCl_3$): δ [ppm] = 196.5, doublet at 165.9 ppm not detectable, 158.8, doublet at 133.1 ppm not detectable, 131.4 (d, *J* = 9.3 Hz), 130.5, 126.4, 115.9 (d, *J* = 22.3 Hz), 114.4, 55.4, 44.8.

^{19}F-NMR (377 MHz, $CDCl_3$): δ [ppm] = -105.1 (m).

GC-MS (EI): t_R = 22.190 min, *m/z* (Int. %) = 244 (17) $[M]^{+\bullet}$, 121 (100) $[M]^{+\bullet}$-$[C_7H_4FO]^{\bullet}$.

2-(4-methoxyphenyl)-1-(naphthalen-2-yl)ethan-1-one (378d)

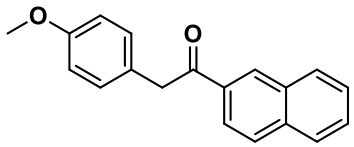

378d

According to GP-D, 2-(4-methoxyphenyl)-1-(naphthalen-2-yl)ethan-1-one (**378d**) was synthesized from *S*-(4-bromophenyl) naphthalene-2-carbothioate (**389d**) (172 mg, 500 µmol, 1.0 equiv.). Purification by column chromatography (PE/EtOAc 95:5) delivered the product **378d** (73.1 mg, 265 µmol, 53%) as a colorless solid, but no complete separation of ketone **378d** and oxoether **380** could be achieved. The purity of the ketone was determined to be 88% using quantitative ^{1}H-NMR. The corrected yield of ketone is therefore 47%.

$C_{19}H_{16}O_2$: 276.34 $\frac{\mathrm{g}}{\mathrm{mol}}$

R_f: 0.20 (Silica gel, PE/EtOAc 95:5, UV).

Melting point: Not determined due to contaminations.

^{1}H-NMR (400 MHz, $CDCl_3$): δ [ppm] = 8.54 (s, 1H), 8.06 (dd, *J* = 8.6, 1.8 Hz, 1H), 7.97 (d, *J* = 8.6 Hz, 1H), 7.92–7.82 (m, 2H), 7.64–7.51 (m, 2H), 7.25–7.20 (m, 2H), 6.90–6.85 (m, 2H), 4.36 (s, 2H), 3.78 (s, 3H).

^{13}C-NMR (101 MHz, $CDCl_3$): δ [ppm] = 198.0, 158.7, 135.7, 134.1, 132.7, 130.5, 129.7, 128.65, 128.63, 127.9, 126.9, 126.8, 124.4, 114.3, 55.4, 44.8.

GC-MS (EI): t_R = 28.03 min, *m/z* (Int. %) = 276 (9) $[M]^{+\bullet}$, 155 (100) $[M]^{+\bullet}$-$[C_8H_9O]^{\bullet}$, 127 (39) $[M]^{+\bullet}$-$[C_9H_9O_2]^{\bullet}$, 121 (18) $[M]^{+\bullet}$-$[C_{11}H_7O]^{\bullet}$.

HR-MS (ESI): *m/z* = $[M+Na]^+$ calc. for $C_{19}H_{16}O_2Na$ 299.10425, found 299.10453.

IR (ATR): 3052.7 (w, br), 3008.0 (w, br), 2952.1 (w, br), 2911.1 (w, br), 2885.0 (w, br), 2836.5 (m, sh), 1677.3 (s, sh), 1606.5 (s, sh), 1509.6 (s, sh), 1461.1 (m, sh), 1356.8 (m, sh), 1241.2 (s, sh), 1032.5 (s, sh), 812.6 (s, sh), 782.7 (s, sh), 745.5 (s, sh).

1-(4-methoxyphenyl)-3-phenylpentan-2-one (378e)

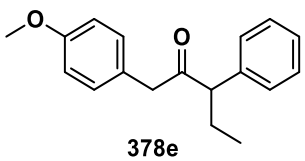

378e

According to GP-D, 1-(4-methoxyphenyl)-3-phenylpentan-2-one (**378e**) was synthesized from *S*-(4-bromophenyl) 2-phenylbutanethioate (**389f**) (168 mg, 500 µmol, 1.0 equiv.). Purification by column chromatography (PE/EtOAc 95:5) delivered the product **378e** (35.0 mg, 130 µmol, 26%) as a light yellow oil. The analytical data are in good agreement with the literature.[6e]

$C_{18}H_{20}O_2$: 268.4 $\frac{g}{mol}$

R_f: 0.31 (Silica gel, PE/EtOAc 95:5, UV).

Melting point: Ambient temperature (PE/EtOAc).

^{1}H-NMR (400 MHz, $CDCl_3$): δ [ppm] = 7.35–7.23 (m, 3H), 7.21–7.16 (m, 2H), 6.99–6.95 (m, 2H), 6.84–6.80 (m, 2H), 3.78 (s, 3H), 3.62 (t, *J* = 7.5 Hz, 1H), 3.56 (s, 2H), 2.09–1.98 (m, 1H), 1.74–1.62 (m, 1H), 0.75 (t, *J* = 7.5 Hz, 3H).

^{13}C-NMR (101 MHz, $CDCl_3$): δ [ppm] = 208.1, 158.7, 138.9, 130.6, 129.0, 128.6, 127.3, 126.4, 114.1, 59.6, 55.4, 48.1, 25.5, 12.1.

GC-MS (EI): t_R = 23.66 min, *m/z* (Int. %) = 268 (16) $[M]^{+\bullet}$, 121 (100) $[M]^{+\bullet}$-$[C_{10}H_{11}O]^{\bullet}$.

3-(6-methoxynaphthalen-2-yl)-1-(4-methoxyphenyl)butan-2-one (378f)

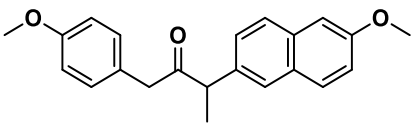

378f

According to GP-D, 3-(6-methoxynaphthalen-2-yl)-1-(4-methoxyphenyl)butan-2-one (**378f**) was synthesized from *S*-(4-bromophenyl) 2-(6-methoxynaphthalen-2-yl)propanethioate (**389g**) (201 mg, 500 µmol, 1.0 equiv.). Purification by column chromatography (PE/EtOAc 95:5) delivered the product **378f** (48.1 mg, 148 µmol, 29%) as a light yellow, viscous oil.

$C_{22}H_{22}O_3$: 334.42 $\frac{g}{mol}$

R_f: 0.14 (Silica gel, PE/EtOAc 95:5, UV).

Melting point: Ambient temperature (PE/EtOAc).

^{1}H-NMR (400 MHz, $CDCl_3$): δ [ppm] = 7.77–7.73 (m, 2H), 7.62–7.61 (m, 1H), 7.32–7.29 (m, 1H), 7.22–7.17 (m, 2H), 7.02–6.98 (m, 2H), 6.86–6.82 (m, 2H), 4.02 (q, *J* = 6.9 Hz, 1H), 3.99 (s, 3H), 3.81 (s, 3H), 3.63 (s, 2H), 1.47 (d, *J* = 6.9 Hz, 3H).

^{13}C-NMR (101 MHz, $CDCl_3$): δ [ppm] = 208.7, 158.6, 157.9, 135.7, 133.8, 130.6, 129.32, 129.5, 127.7, 126.9, 126.60, 126.55, 119.3, 114.1, 105.7, 55.5, 55.4, 51.9, 47.3, 17.8.

GC-MS (EI): t_R = 13.04 min, *m/z* (Int. %) = 334 (16) $[M]^{+\bullet}$, 185 (100) $[M]^{+\bullet}$-$[C_9H_9O_2]^{\bullet}$.

HR-MS (ESI): *m/z* = $[M+Na]^+$ calc. for $C_{22}H_{22}O_3Na$ 357.14612, found 357.14648.

IR (ATR): 2929.7 (w, sh), 2832.8 (w, sh), 1707.1 (m, sh), 1602.8 (s, sh), 1509.6 (s, sh), 1244.9 (s, sh), 1174.1 (m, sh), 1028.7 (s, sh), 853.6 (m, sh), 812.6 (s, sh).

1-(4-methoxyphenyl)-4-phenylbutan-2-one (378g)

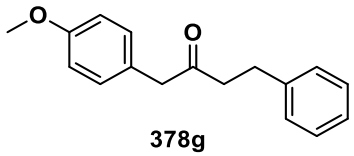

378g

According to GP-D, 1-(4-methoxyphenyl)-4-phenylbutan-2-one (**378g**) was synthesized from *S*-(4-bromophenyl) 3-phenylpropanethioate (**389h**) (161 mg, 500 µmol, 1.0 equiv.). Purification by column chromatography (PE/EtOAc 95:5) delivered the product **378g** (83.7 mg, 329 µmol, 66%) as a colorless solid, but no complete separation of ketone **378g** and oxoether **380** could be achieved. The purity of the ketone was determined to be 95% using quantitative ^{1}H-NMR. The corrected yield of ketone is therefore 63%. The analytical data (disregarding oxoether) are in good agreement with the literature.[258]

$C_{17}H_{18}O_2$: 254.33 $\frac{g}{mol}$

R_f: 0.19 (Silica gel, PE/EtOAc 95:5, UV).

Melting point: Not determined due to contaminations.

^{1}H-NMR (400 MHz, $CDCl_3$): δ [ppm] = 7.27–7.23 (m, 2H), 7.21–7.17 (m, 1H), 7.15–7.11 (m, 2H), 7.10–7.08 (m, 2H), 6.87–6.83 (m, 2H), 3.79 (s, 3H), 3.60 (s, 2H), 2.86 (t, *J* = 7.5 Hz, 2H), 2.75 (t, *J* = 7.5 Hz, 2H).

^{13}C-NMR (101 MHz, $CDCl_3$): δ [ppm] = 208.0, 158.8, 141.1, 130.5, 128.6, 128.5, 126.3, 126.2, 114.3, 49.6, 43.4, 23.0.

GC-MS (EI): t_R = 24.19 min, *m/z* (Int. %) = 254 (20) $[M]^{+\bullet}$, 121 (100) $[M]^{+\bullet}$-$[C_9H_9O]^{\bullet}$, 105 (21) $[M]^{+\bullet}$-$[C_9H_9O_2]^{\bullet}$, 91 (23) $[M]^{+\bullet}$-$[C_{10}H_{11}O_2]^{\bullet}$.

1,4-bis(4-methoxyphenyl)butan-2-one (378h)

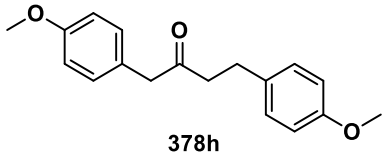

378h

According to GP-D, 1,4-bis(4-methoxyphenyl)butan-2-one (**378h**) was synthesized from *S*-(4-bromophenyl) 3-(4-methoxyphenyl)propanethioate (**389i**) (176 mg, 500 µmol, 1.0 equiv.). Purification by column chromatography (PE/EtOAc 95:5–92:8) delivered the product **378h** (67.9 mg, 239 µmol, 48%) as a colorless solid. The analytical data are in good agreement with the literature.[57]

$C_{18}H_{20}O_3$: 284.14 $\frac{g}{mol}$

R_f: 0.10 (Silica gel, PE/EtOAc 95:5, UV).

Melting point: 81.9–84.1 °C (PE/EtOAc).

^{1}H-NMR (400 MHz, $CDCl_3$): δ [ppm] = 7.10–7.03 (m, 4H), 6.89–6.78 (m, 4H), 3.79 (s, 3H), 3.78 (s, 3H), 3.59 (s, 2H), 2.80 (t, *J* = 7.4 Hz, 2H), 2.72 (t, *J* = 7.4 Hz, 2H).

^{13}C-NMR (101 MHz, $CDCl_3$): δ [ppm] = 208.2, 158.8, 158.1, 133.1, 130.5, 129.4, 126.3, 114.3, 114.0, 55.4, 49.7, 43.7, 29.1.

GC-MS (EI): t_R = 10.92 min, *m/z* (Int. %) = 284 (15) $[M]^{+\bullet}$, 121 (100) $[M]^{+\bullet}$-$[C_{10}H_{11}O_2]^{\bullet}$.

1-(4-methoxyphenyl)heptan-2-one (378i)

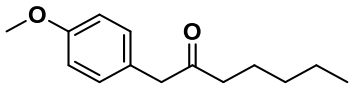

378i

According to GP-D, 1-(4-methoxyphenyl)heptan-2-one (**378i**) was synthesized from *S*-(4-bromophenyl) hexanethioate (**389j**) (144 mg, 500 µmol, 1.0 equiv.). Purification by column chromatography (PE/EtOAc 95:5) delivered the product **378i** (46.3 mg, 210 µmol, 42%) as a colorless oil. The analytical data are in good agreement with the literature.[259]

$C_{14}H_{20}O_2$: 220.31 $\frac{g}{mol}$

R_f: 0.24 (Silica gel, PE/EtOAc 95:5, UV).

Melting point: Ambient temperature (PE/EtOAc).

^{1}H-NMR (400 MHz, $CDCl_3$): δ [ppm] = 7.13–7.10 (m, 2H), 6.88–6.80 (m, 2H), 3.80 (s, 3H), 3.61 (s, 2H), 2.42 (t, *J* = 7.4 Hz, 2H), 1.55 (m, 2H), 1.37–1.13 (m, 4H), 0.86 (t, *J* = 7.0 Hz, 3H).

^{13}C-NMR (101 MHz, $CDCl_3$): δ [ppm] = 209.2, 158.7, 130.5, 126.6, 114.3, 55.4, 49.4, 41.9, 31.4, 23.6, 22.6, 14.0.

GC-MS (EI): t_R = 20.21 min, *m/z* (Int. %) = 220 (13) $[M]^{+\bullet}$, 121 (100) $[M]^{+\bullet}$-$[C_6H_{11}O]^{\bullet}$, 71 (8) $[M]^{+\bullet}$-$[C_9H_9O_2]^{\bullet}$.

3-ethyl-1-(4-methoxyphenyl)heptan-2-one (378j)

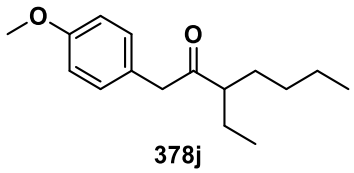

378j

According to GP-D, 3-ethyl-1-(4-methoxyphenyl)heptan-2-one (**378j**) was synthesized from *S*-(4-bromophenyl) 2-ethylhexanethioate (**389k**) (158 mg, 500 µmol, 1.0 equiv.). Purification by column chromatography (PE/EtOAc 98:2–95:5) delivered the product **378j** (56.0 mg, 225 µmol, 45%) as a colorless oil. The analytical data are in good agreement with the literature.[260]

$C_{16}H_{24}O_2$: 248.37 $\frac{g}{mol}$

R_f: 0.33 (Silica gel, PE/EtOAc 95:5, UV).

Melting point: Ambient temperature (PE/EtOAc).

^{1}H-NMR (400 MHz, $CDCl_3$): δ [ppm] = 7.13–7.08 (m, 2H), 6.88–6.80 (m, 2H), 3.79 (s, 3H), 3.63 (s, 2H), 2.54–2.48 (m, 2H), 1.65–1.56 (m, 2H), 1.48–1.35 (m, 2H), 1.27–1.19 (m, 2H), 1.17–1.10 (m, 2H), 0.84 (t, *J* = 7.1 Hz, 3H), 0.79 (t, *J* = 7.3 Hz, 3H).

^{13}C-NMR (101 MHz, $CDCl_3$): δ [ppm] = 212.3, 158.7, 130.8, 126.2, 114.1, 55.4, 52.9, 48.8, 31.1, 29.7, 24.8, 22.9, 14.0, 12.0.

GC-MS (EI): t_R = 8.39 min, *m/z* (Int. %) = 248 (9) $[M]^{+\bullet}$, 121 (100) $[M]^{+\bullet}$-$[C_8H_{15}O]^{\bullet}$, 57 (81) $[M]^{+\bullet}$-$[C_{12}H_{15}O_2]^{\bullet}$.

2-(2-methoxyphenyl)-1-phenylethan-1-one (378l)

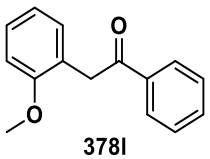

378l

According to GP-D, 2-(2-methoxyphenyl)-1-phenylethan-1-one (**378l**) was synthesized from *S*-(4-bromophenyl) benzothioate (**140**) (146 mg, 500 µmol, 1.0 equiv.) and 2-methoxybenzyl alcohol (146 µL, 1.10 mmol, 2.2 equiv.). Purification by column chromatography (PE/EtOAc 95:5) delivered the product **378l** (31.6 mg, 139 µmol, 28%) as a colorless oil.

$C_{15}H_{14}O_2$: 226.28 $\frac{g}{mol}$

R_f: 0.26 (Silica gel, PE/EtOAc 95:5, UV).

Melting point: 54.5–55.7 °C (PE/EtOAc).

^{1}H-NMR (400 MHz, $CDCl_3$): δ [ppm] = 8.07–8.04 (m, 2H), 7.58–7.53 (m, 1H), 7.50–7.44 (m, 2H), 7.29–7.24 (m, 1H), 7.19 (dd, *J* = 7.6, 1.5 Hz, 1H), 6.97–6.89 (m, 2H), 4.29 (s, 2H), 3.79 (s, 3H).

^{13}C-NMR (101 MHz, $CDCl_3$): δ [ppm] = 198.1, 157.3, 137.1, 133.0, 131.1, 128.62, 128.54, 128.49, 123.8, 120.8, 110.7, 55.5, 40.1.

GC-MS (EI): t_R = 8.76 min, *m/z* (Int. %) = 226 (19) $[M]^{+\bullet}$, 105 (100) $[M]^{+\bullet}$-$[C_8H_9O]^{\bullet}$, 77 (74) $[M]^{+\bullet}$-$[C_9H_9O_2]^{\bullet}$.

HR-MS (ESI): *m/z* = $[M+Na]^+$ calc. for $C_{15}H_{14}O_2Na$ 249.08860, found 249.08894.

IR (ATR): 3056.4 (w, br), 2996.8 (w, sh), 2937.1 (w, sh), 2899.9 (w, sh), 2836.5 (w, sh), 1688.5 (s, sh), 1578.8 (m, sh), 1494.7 (s, sh), 1330.7 (m, sh), 1244.9 (s, sh), 752.9 (s, sh), 689.6 (s, sh).

2-(3,4-dimethoxyphenyl)-1-phenylethan-1-one (378m)

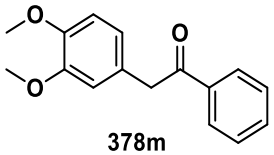

378m

According to GP-D, 2-(3,4-dimethoxyphenyl)-1-phenylethan-1-one (**378m**) was synthesized from *S*-(4-bromophenyl) benzothioate (**140**) (146 mg, 500 µmol, 1.0 equiv.) and (3,4-dimethoxyphenyl)methanol (160 µL, 1.10 mmol, 2.2 equiv.). Purification by column chromatography (PE/EtOAc 92:8–8:2) delivered the product **378m** (66.0 mg, 258 µmol, 52%) as a colorless solid. The analytical data are in good agreement with the literature; [261] however, minor amounts of an uncharacterized compound with an exact mass of 166 *m/z* are present.

$C_{16}H_{16}O_3$: 256.30 $\frac{g}{mol}$

R_f: 0.60 (Silica gel, PE/EtOAc 8:2, UV).

Melting point: Not determined due to contaminations.

^{1}H-NMR (400 MHz, $CDCl_3$): δ [ppm] = 8.02–7.98 (m, 2H), 7.57–7.53 (m, 1H), 7.50–7.40 (m, 2H), 6.84–6.80 (m, 3H), 4.23 (s, 2H), 3.85 (s, 6H).

^{13}C-NMR (101 MHz, $CDCl_3$): δ [ppm] = 197.9, 149.1, 148.1, 136.6, 133.2, 128.67, 128.62, 127.0, 121.7, 112.6, 111.4, 55.9, 55.9, 45.1.

GC-MS (EI): t_R = 9.93 min, *m/z* (Int. %) = 256 (43) $[M]^{+\bullet}$, 151 (100) $[M]^{+\bullet}$-$[C_7H_5O]^{\bullet}$, 105 (68) $[M]^{+\bullet}$-$[C_9H_{11}O_2]^{\bullet}$, 77 (42) $[M]^{+\bullet}$-$[C_{10}H_{11}O_3]^{\bullet}$.

1,3-bis(4-methoxyphenyl)propan-2-one (385)

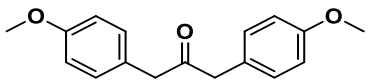

385

According to GP-D, 1,3-bis(4-methoxyphenyl)propan-2-one (**385**) was synthesized from *S*-(4-bromophenyl) 2-(4-methoxyphenyl)ethanethioate (**389e**) (169 mg, 500 µmol, 1.0 equiv.). Purification was achieved by column chromatography (PE/EtOAc 92:8). The product **385** was obtained as a colorless solid (85.5 mg, 316 µmol, 63%). The analytical data are in good agreement with the literature.[262]

$C_{17}H_{18}O_3$: 270.33 $\frac{g}{mol}$

R_f: 0.13 (Silica gel, PE/EtOAc 92:8, UV).

Melting point: 88.9–89.4 °C (PE/EtOAc).

^{1}H-NMR (400 MHz, $CDCl_3$): δ [ppm] = 7.08–7.04 (m, 2H), 6.87–6.83 (m, 2H), 3.80 (s, 6H), 3.64 (s, 4H).

^{13}C-NMR (101 MHz, $CDCl_3$): δ [ppm] = 206.6, 158.8, 130.6, 126.2, 114.3, 55.4, 48.2.

GC-MS (EI): t_R = 25.47 min, *m/z* (Int. %) = 270 (16) $[M]^{+\bullet}$, 121 (100) $[M]^{+\bullet}$-$[C_9H_9O_2]^{\bullet}$.

4.4.3.2.2 Ketones Synthesized from the Respective Benzylic Chlorides

2-(4-methoxyphenyl)-1-phenylethan-1-one (378a)

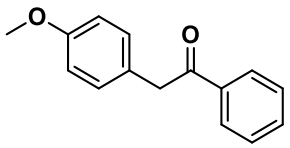

378a

According to GP-E, 2-(4-methoxyphenyl)-1-phenylethan-1-one (**378a**) was synthesized from *S*-(4-bromophenyl) benzothioate (**140**) (146 mg, 500 µmol, 1.0 equiv.) and 4-methoxybenzyl chloride (150 µL, 1.10 mmol, 2.2 equiv.). Purification by column chromatography (PE/EtOAc 95:5) delivered the product **378a** (48.4 mg, 214 µmol, 43%) as a colorless solid. The analytical data are in good agreement with the literature,[238] and correspond to the previously determined data.

1,2-diphenylethan-1-one (378n)

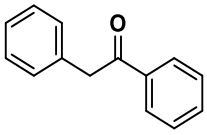

378n

According to GP-D, 1,2-diphenylethan-1-one (**378n**) was synthesized from *S*-(4-bromophenyl) benzothioate (**140**) (146 mg, 500 µmol, 1.0 equiv.) and benzyl chloride (127 µL, 1.10 mmol, 2.2 equiv.). Purification by column chromatography (PE/EtOAc 95:5) delivered the product **378n** (40.2 mg, 205 µmol, 41%) as colorless crystals. The analytical data are in good agreement with the literature.[263]

$C_{14}H_{12}O$: 196.25 $\frac{g}{mol}$

R_f: 0.33 (Silica gel, PE/EtOAc 95:5, UV).

Melting point: 53.5–53.9 °C (PE/EtOAc).

^{1}H-NMR (400 MHz, $CDCl_3$): δ [ppm] = 8.03–7.99 (m, 2H), 7.58–7.54 (m, 1H), 7.48–7.44 (m, 2H), 7.35–7.26 (m, 5H), 4.29 (s, 2H).

^{13}C-NMR (101 MHz, $CDCl_3$): δ [ppm] = 197.8, 136.8, 134.7, 133.3, 129.6, 128.82, 128.79, 128.77, 127.0, 45.7.

GC-MS (EI): t_R = 19.72 min, *m/z* (Int. %) = 196 (3) $[M]^{+\bullet}$, 105 (100) $[M]^{+\bullet}$-$[C_7H_7]^{\bullet}$, 77 (27) $[M]^{+\bullet}$-$[C_8H_7O]^{\bullet}$.

According to GP-E, 1,2-diphenylethan-1-one (**378n**) was synthesized from *S*-(4-bromophenyl) benzothioate (**140**) (146 mg, 500 µmol, 1.0 equiv.) and benzyl chloride (127 µL, 1.10 mmol, 2.2 equiv.). Purification by column chromatography (PE/EtOAc 95:5) delivered the product **378n** (41.2 mg, 210 µmol, 42%) as colorless crystals. The analytical data are in good agreement with the literature,[263] and correspond to the previously determined data, but minor amounts of an uncharacterized impurity are present.

2-(3-methoxyphenyl)-1-phenylethan-1-one (378o)

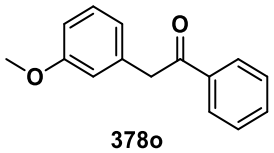

378o

According to GP-D, 2-(3-methoxyphenyl)-1-phenylethan-1-one (**378o**) was synthesized from *S*-(4-bromophenyl) benzothioate (**140**) (146 mg, 500 µmol, 1.0 equiv.) and 3-methoxybenzyl chloride (160 µL, 1.10 mmol, 2.2 equiv.). Purification by column chromatography (PE/EtOAc 95:5) delivered the product **378o** (37.9 mg, 167 µmol, 33%) as a light yellow oil. The analytical data are in good agreement with the literature.[264]

$C_{15}H_{14}O_2$: 226.28 $\frac{g}{mol}$

R_f: 0.23 (Silica gel, PE/EtOAc 95:5, UV).

Melting point: Ambient temperature (PE/EtOAc).

^{1}H-NMR (400 MHz, $CDCl_3$): δ [ppm] = 8.03–8.00 (m, 2H), 7.56–7.53 (m, 1H), 7.48–7.43 (m, 2H), 7.24–7.22 (m, 1H), 6.87–6.85 (m, 1H), 6.83–6.78 (m, 2H), 4.26 (s, 2H), 3.79 (s, 3H).

^{13}C-NMR (101 MHz, $CDCl_3$): δ [ppm] = 197.6, 159.9, 136.7, 136.1, 133.3, 129.8, 128.8, 121.9, 115.2, 112.5, 55.3, 45.7.

GC-MS (EI): t_R = 8.98 min, *m/z* (Int. %) = 226 (13) $[M]^{+\bullet}$, 105 (100) $[M]^{+\bullet}$-$[C_8H_9O]^{\bullet}$, 77 (60) $[M]^{+\bullet}$-$[C_9H_9O_2]^{\bullet}$.

1-phenyl-2-(*p*-tolyl)ethan-1-one (378p)

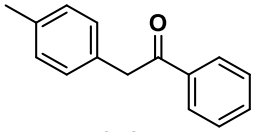

378p

According to GP-D, 1-phenyl-2-(*p*-tolyl)ethan-1-one (**378p**) was synthesized from *S*-(4-bromophenyl) benzothioate (**140**) (146 mg, 500 µmol, 1.0 equiv.) and 4-methylbenzyl chloride (146 µL, 1.10 mmol, 2.2 equiv.). Purification by column chromatography (PE/EtOAc 95:5) delivered the product **378p** (46.6 mg, 222 µmol, 44%) as yellow crystals. The analytical data are in good agreement with the literature.[265]

$C_{15}H_{14}O$: 210.28 $\frac{g}{mol}$

R_f: 0.23 (Silica gel, PE/EtOAc 95:5, UV).

Melting point: 91.6–92.6 °C (PE/EtOAc).

^{1}H-NMR (400 MHz, $CDCl_3$): δ [ppm] = 8.03–8.00 (m, 2H), 7.58–7.52 (m, 1H), 7.48–7.43 (m, 2H), 7.17–7.12 (m, 4H), 4.25 (s, 2H), 2.32 (s, 3H).

^{13}C-NMR (101 MHz, $CDCl_3$): δ [ppm] = 198.0, 136.8, 136.6, 133.2, 131.6, 129.5, 129.4, 128.8, 45.3, 21.2.

GC-MS (EI): t_R = 8.25 min, *m/z* (Int. %) = 210 (7) $[M]^{+\bullet}$, 105 (100) $[M]^{+\bullet}$-$[C_8H_9]^{\bullet}$ or $[M]^{+\bullet}$-$[C_7H_5O]^{\bullet}$, 77 (55) $[M]^{+\bullet}$-$[C_9H_9O]^{\bullet}$.

2-(naphthalen-2-yl)-1-phenylethan-1-one (378q)

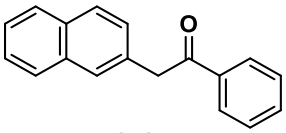

378q

According to GP-E, 2-(naphthalen-2-yl)-1-phenylethan-1-one (**378q**) was synthesized from *S*-(4-bromophenyl) benzothioate (**140**) (293 mg, 1.00 mmol, 1.0 equiv.) and 2-(chloromethyl)naphthalene (217 µL, 1.30 mmol, 1.3 equiv.). Purification by column chromatography (PE/EtOAc 95:5) delivered the product **378q** (34.3 mg, 139 µmol, 14%) as a colorless solid. The analytical data are in good agreement with the literature.[264]

$C_{21}H_{26}O_2$: 246.31 $\frac{g}{mol}$

R_f: 0.28 (Silica gel, PE/EtOAc 95:5, UV).

^{1}H-NMR (400 MHz, $CDCl_3$): δ [ppm] = 8.07–8.04 (m, 2H), 7.82–7.73 (m, 4H), 7.58–7.52 (m,1H), 7.48–7.38 (m, 5H), 4.45 (s, 2H).

^{13}C-NMR (101 MHz, $CDCl_3$): δ [ppm] = *C*(O) not detectable, 136.6, 133.6, 133.2, 132.4, 132.2, 128.7, 128.4, 128.1, 127.81, 127.78, 127.71, 126.1, 125.8, 45.8.

GC-MS (EI): t_R =10.58 min, *m/z* (Int. %) = 246 (13) $[M]^{+\bullet}$, 141 (27) $[M]^{+\bullet}$-$[C_7H_5O]^{\bullet}$, 105 (100) $[M]^{+\bullet}$-$[C_{11}H_9]^{\bullet}$, 77 (38) $[M]^{+\bullet}$-$[C_{12}H_9O]^{\bullet}$.

1-(4-methoxyphenyl)-3-methylbutan-2-one (378r)

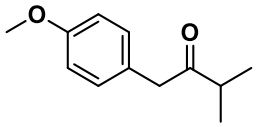

378r

According to GP-E, 1-(4-methoxyphenyl)-3-methylbutan-2-one (**378r**) was synthesized from *S*-(4-bromophenyl) 2-methylpropanethioate (**389b**) (259 mg, 1.00 mmol, 1.0 equiv.) and 4-methoxybenzyl chloride (190 µL, 1.30 mmol, 1.3 equiv.). Purification by column chromatography (PE/EtOAc 95:5) delivered the product **378r** (40.5 mg, 211 µmol, 23%) as a colorless oil. The analytical data are in good agreement with the literature.[266]

$C_{12}H_{16}O_2$: 192.26 $\frac{g}{mol}$

R_f: 0.24 (Silica gel, PE/EtOAc 95:5, UV).

Melting point: Ambient temperature (PE/EtOAc).

^{1}H-NMR (400 MHz, $CDCl_3$): δ [ppm] = 7.13–7.10 (m, 2H), 6.87–6.85 (m, 2H), 3.79 (s, 3H), 3.68 (s, 2H), 2.72 (sept, *J* = 6.9 Hz, 1H), 1.09 (d, *J* = 6.9 Hz, 6H).

^{13}C-NMR (101 MHz, $CDCl_3$): δ [ppm] = 212.4, 158.6, 130.5, 126.5, 114.1, 55.3, 46.8, 39.9,18.4.

GC-MS (EI): t_R = 6.46 min, *m/z* (Int. %) = 192 (12) $[M]^{+\bullet}$, 121 (100) $[M]^{+\bullet}$-$[C_4H_7O]^{\bullet}$.

3-(4-isobutylphenyl)-1-(4-methoxyphenyl)butan-2-one (378s)

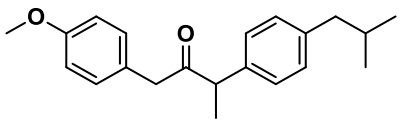

378s

According to GP-E, 3-(4-isobutylphenyl)-1-(4-methoxyphenyl)butan-2-one (**378s**) was synthesized from *S*-(4-bromophenyl) 2-(4-isobutylphenyl)propanethioate (**389l**) (377 mg, 1.00 mmol, 1.0 equiv.) and 4-methoxybenzyl chloride (190 µL, 1.30 mmol, 1.3 equiv.). Purification by column chromatography (PE/EtOAc 95:5) delivered the product **378s** (88.0 mg, 283 µmol, 28%) as a colorless oil.

$C_{21}H_{26}O_2$: 310.44 $\frac{g}{mol}$

R_f: 0.47 (Silica gel, PE/EtOAc 95:5, UV).

Melting point: Ambient temperature (PE/EtOAc).

^{1}H-NMR (400 MHz, $CDCl_3$): δ [ppm] = 7.12–7.07 (m, 4H), 6.97–6.93 (m, 2H), 6.81–6.79 (m, 2H), 3.84–3.81 (m, 1H), 3.78 (s, 3H), 3.56–3.55 (m, 2H), 2.46 (d, *J* = 7.2 Hz, 2H), 1.86 (sept, *J* = 6.6 Hz, 1H), 1.35 (d, *J* = 6.9 Hz, 3H), 0.91 (d, *J* = 6.6 Hz, 6H).

^{13}C-NMR (101 MHz, $CDCl_3$): δ [ppm] = 208.7, 158.5, 140.7, 137.7, 130.6, 129.8, 127.9, 126.7, 114.1, 55.4, 51.8, 47.1, 45.2, 30.3, 22.5, 17.7.

GC-MS (EI): t_R = 10.27 min, *m/z* (Int. %) = 310 (12) $[M]^{+\bullet}$, 161 (72) $[M]^{+\bullet}$-$[C_9H_9O_2]^{\bullet}$, 121 (100) $[M]^{+\bullet}$-$[C_{13}H_{17}O]^{\bullet}$.

HR-MS (ESI): *m/z* = $[M+Na]^+$ calc. for $C_{21}H_{26}O_2Na$ 333.18250, found 333.18282.

IR (ATR): 2952.1 (m, br), 1710.8 (m, sh), 1509.6 (s, sh), 1244.9 (s, sh), 1177.8 (m, sh), 1032.5 (m, sh), 805.1 (m, sh).

4.4.3.3 Cross-Electrophile Coupling at the Bromine Substituent of Thioester

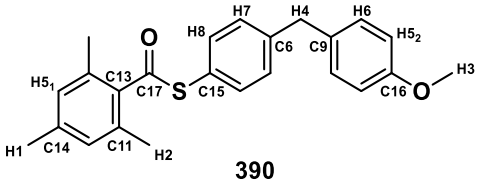

390

According to GP-D, *S*-(4-(4-methoxybenzyl)phenyl) 2,4,6-trimethylbenzothioate (**390**) was synthesized from *S*-(4-bromophenyl) 2,4,6-trimethylbenzothioate (**389a**) (168 mg, 500 µmol, 1.0 equiv.). Purification by column chromatography (PE/EtOAc 95:5) delivered the product **390** (102 mg, 271 µmol, 54%) as a colorless oil.

$C_{24}H_{24}O_2S$: 376.51 $\frac{g}{mol}$

R_f: 0.42 (Silica gel, PE/EtOAc 95:5, UV).

Melting point: Ambient temperature (PE/EtOAc).

^{1}H-NMR (400 MHz, $CDCl_3$): δ [ppm] = 7.45–7.43 (m, 2H, H8), 7.28–7.26 (m, 2H, H7), 7.14–7.11 (m, 2H, H6), 6.88–6.84 (m, 4H, $H5_1$,$H5_2$), 3.98 (s, 2H, H4), 3.81 (s, 3H, H3), 2.38 (s, 6H, H2), 2.31 (s, 3H, H1).

^{13}C-NMR (101 MHz, $CDCl_3$): δ [ppm] = 196.5 (C17), 158.3 (C16), 143.5 (C15), 139.7 (C14), 137.4 (C13), 134.6 (H8), 133.9 (C11), 132.6 (C9), 130.1 (H6), 130.0 (H7), 128.5 ($H5_1$), 125.4 (C6), 114.1 ($H5_2$), 55.4 (H3), 40.9 (H4), 21.3 (H1), 19.2 (H2).

GC-MS (EI): t_R = 33.36 min, *m/z* (Int. %) = Molecular peak is not detectable, 147 (100) $[M]^{+\bullet}$-$[C_{14}H_{13}OS]^{\bullet}$.

HR-MS (ESI): *m/z* = $[M+Na]^+$ calc. for $C_{24}H_{24}O_2SNa$ 399.13892, found 399.13912.

IR (ATR): 2914.8 (w, br), 2832.8 (w, sh), 1681.0 (s, sh), 1509.6 (s, sh), 1244.9 (s, sh), 1032.5 (s, sh), 797.7 (s, sh).

4.4.4 Mechanistic Experiments

4.4.4.1 Investigations in Alcohol Activation

4.4.4.1.1 Implementation of Alcohol under Standard Conditions

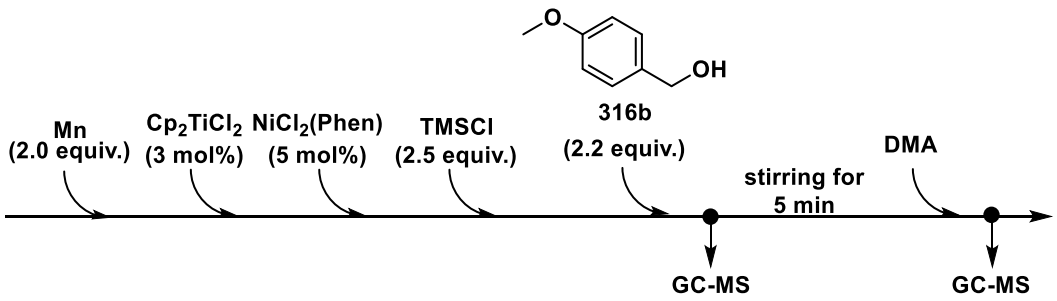

The reaction of alcohol under standard conditions was conducted analogously to GP-D, however in the absence of thioester **140**. After the addition of 4-methoxybenzyl alcohol (**316b**) (137 µL, 1.10 mmol, 2.2 equiv.) *via* syringe pump over a time range of 5 min (27.4 µL/min), a sample was taken and analyzed by GC-MS. The spectra showed conversion to corresponding chloride **317b**, dimeric oxoether **380** and an uncharacterized byproduct with an exact mass of 228 *m/z.* After stirring for 5 min, abs. DMA (2 mL) was added *via* syringe pump over a time range of 5 min (0.4 mL/min) and another sample was prepared. GC-MS analysis showed formation of benzylic dimer **381** as main product, benzyl chloride **317b**, low proportion of oxoether **380** and not transformed alcohol **316b**. The mixture was stirred at rt for further 15 h. GC-MS analysis of the reaction mixture showed no changes in peaks, and benzylic dimer **381** was detected again as main product.

Note: Both samples were measured with GC-MS method A (see section 4.4.1.3.3).

A) Before DMA Addition

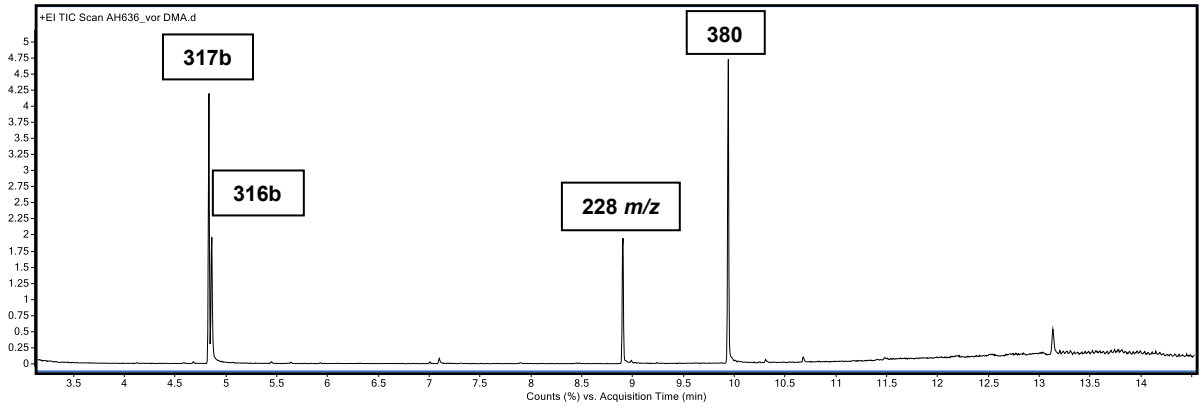

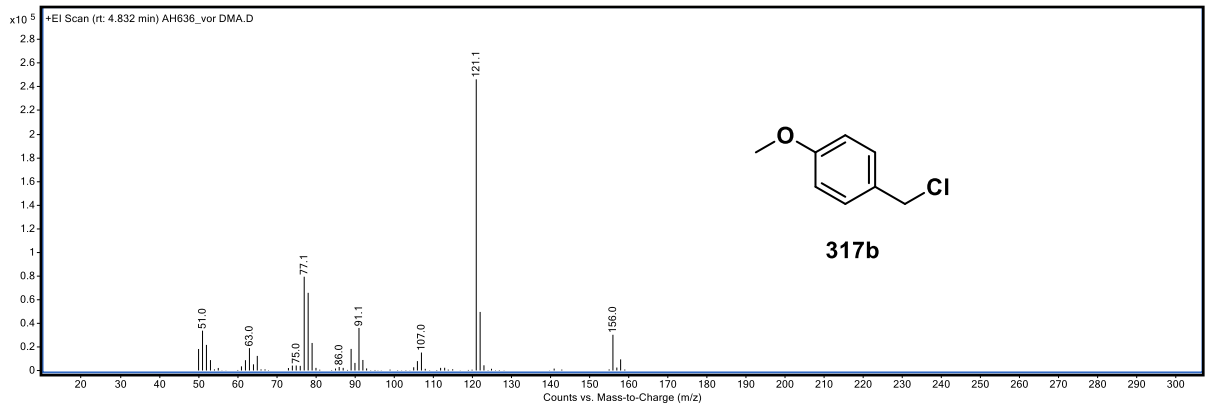
+EI Scan (rt: 4.832 min) AH636_vor DMA.D
x10 5
121.1
77.1
51.0
63.0
91.1
107.0
156.0
75.0
86.0
O
Cl
317b
Counts vs. Mass-to-Charge (m/z)

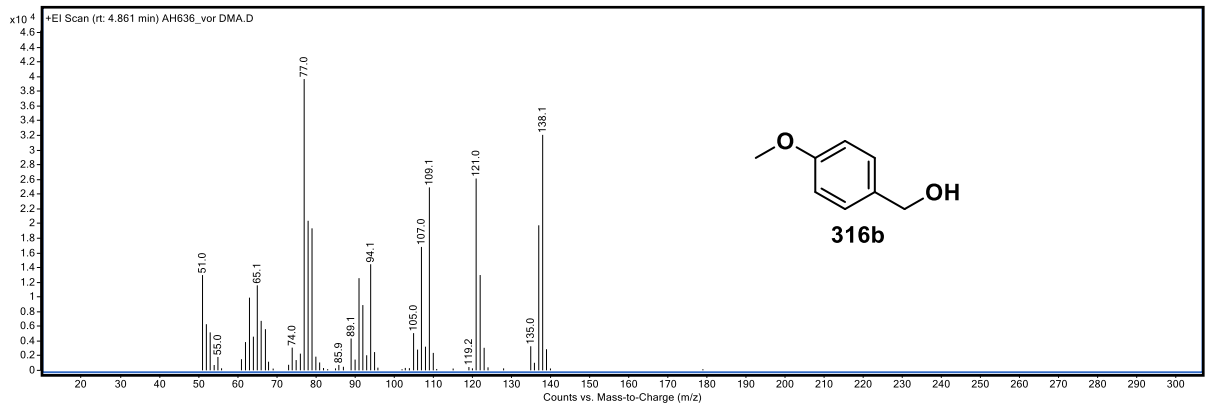
+EI Scan (rt: 4.861 min) AH636_vor DMA.D
x10 4
77.0
138.1
109.1
121.0
107.0
51.0
65.1
94.1
135.0
105.0
74.0
89.1
85.9
119.2
55.0
O
OH
316b
Counts vs. Mass-to-Charge (m/z)

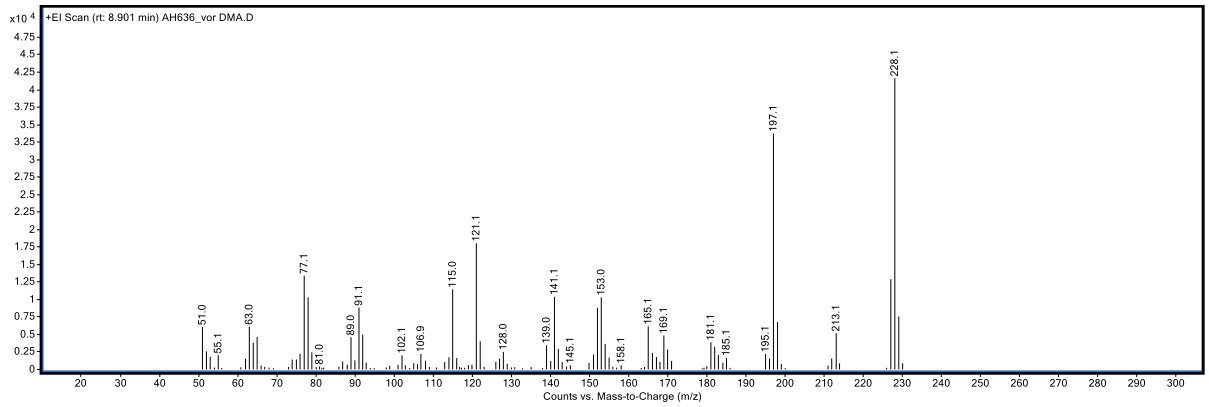
+EI Scan (rt: 8.901 min) AH636_vor DMA.D
x10 4
228.1
197.1
121.1
77.1
115.0
91.1
51.0
63.0
89.0
141.1
153.0
165.1
169.1
213.1
55.1
81.0
102.1
106.9
128.0
139.0
145.1
158.1
181.1
185.1
195.1
Counts vs. Mass-to-Charge (m/z)

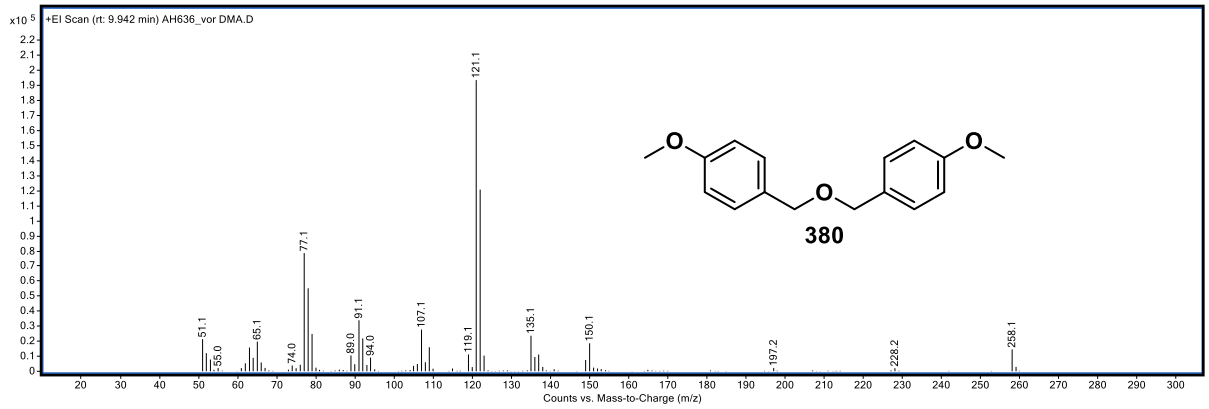
+EI Scan (rt: 9.942 min) AH636_vor DMA.D
x10 5
121.1
77.1
91.1
107.1
51.1
65.1
89.0
135.1
150.1
119.1
94.0
74.0
55.0
197.2
228.2
258.1
O
O
O
380
Counts vs. Mass-to-Charge (m/z)

B) After DMA Addition

Note: The MS spectra of benzylic alcohol **316b**, benzylic chloride **317b** and oxoether **380** correspond to those before DMA addition and are not depicted. However, the compounds are labeled in the total ion chromatogram.

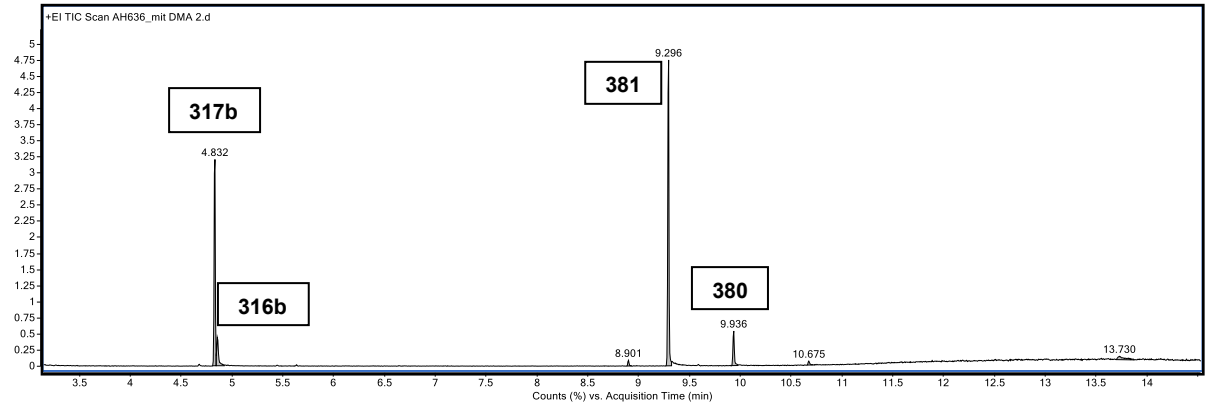

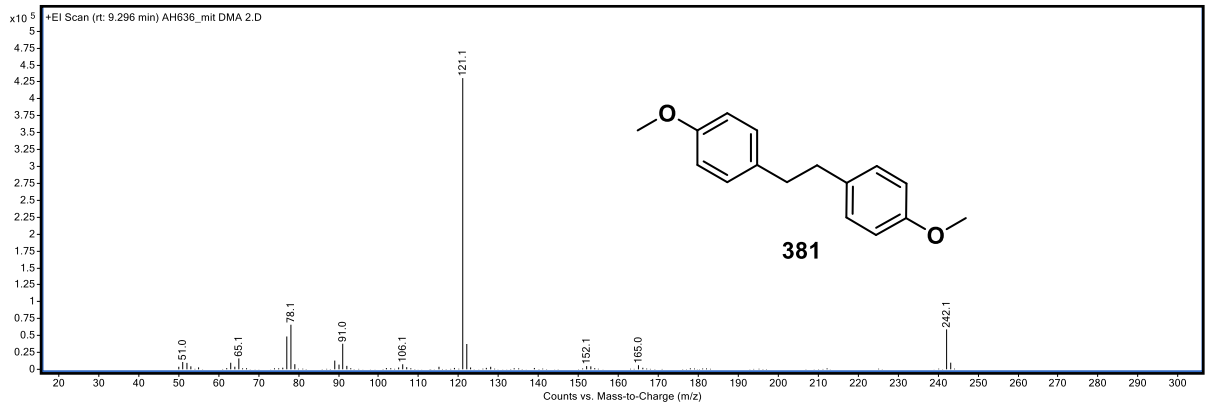

4.4.4.1.2 Implementation of Alcohol under SFRC

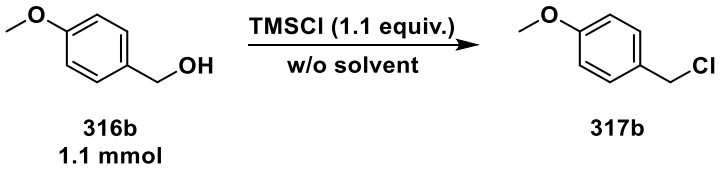

316b
1.1 mmol

317b

For the implementation of alcohol **316b** under SFRC, a Schlenk tube was charged with TMSCl (159 µL, 1.25 mmol, 1.1 equiv.). Then, 4-methoxybenzyl alcohol (**316b**) (137 µL, 1.10 mmol, 2.2 equiv.) was added *via* syringe pump over a time range of 5 min (27.4 µL/min). After stirring for 5 min, a sample was taken and prepared for GC-MS analysis according to the general procedure (see section 4.4.1.3.3.1). GC-MS analysis showed full conversion of alcohol **316b** to benzyl chloride **317b** and only traces of oxoether **380.** This result is in accordance to the report of Ajvazi and Stavber.[214] DMA was then added to the mixture and analyzed again *via* GC-MS. Benzyl chloride **317b** was still present as main product.

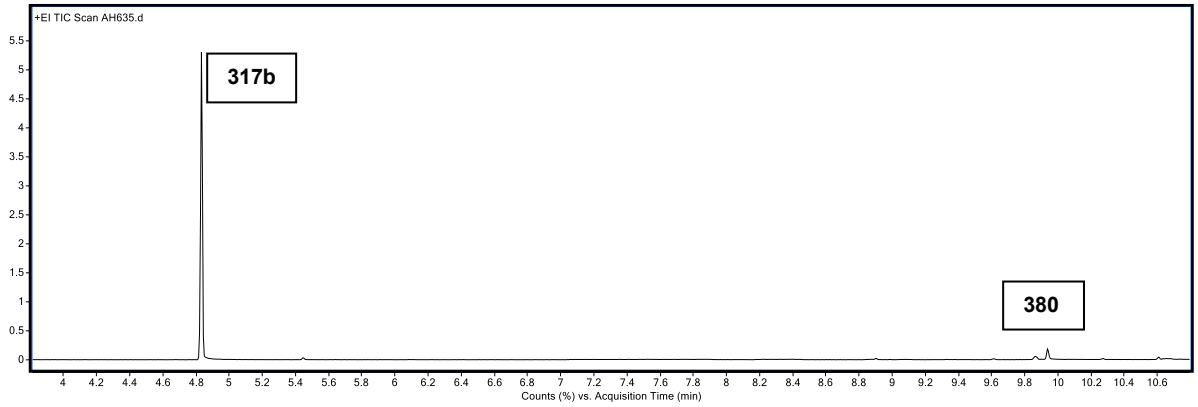

4.4.4.1.3 Implementation of Chloride under Standard Conditions

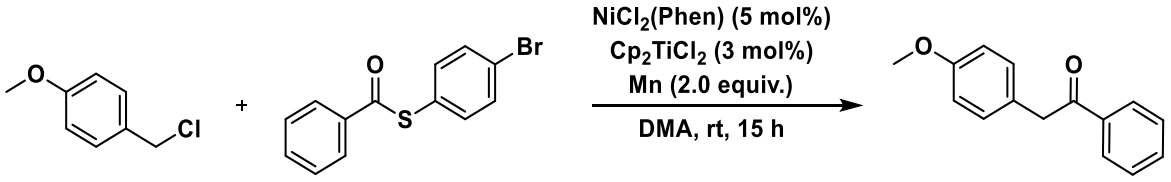

317b
2.2 equiv.

140
0.5 mmol

378a

4-Methoxybenzyl chloride (**317b**) (150 µL, 1.10 mmol, 2.2 equiv.) was reacted under standard conditions using GP-E in the absence of TMSCl, and added *via* a syringe pump over a time range of 5 min (30.0 µL/min). A sample was prepared and analyzed by quantitative GC-FID, yielding ketone **378a** in 73% yield.

4.4.4.1.4 Exclusion of a Silyl Ether as Active Cross Coupling Partner

4.4.4.1.4.1 Synthesis of Silyl-Protected Alcohol

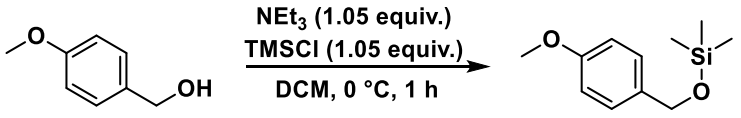

316b
5.0 mmol

397

A solution of 4-methoxybenzyl alcohol (**316b**) (0.60 mL, 5.0 mmol, 1.0 equiv.) in DCM (20 mL) was cooled to 0 °C. At this temperature, triethylamine (0.70 mL, 5.3 mmol, 1.05 equiv.) was added and the solution was stirred for 15 min. Then, TMSCl (0.70 mL. 5.3 mmol, 1.05 equiv.) was added and the reaction was stirred at 0 °C for one hour and then at rt for a further hour. The mixture was quenched by adding water (10 mL). The aqueous layer was extracted with EtOAc (2 × 10 mL). The combined organic layers were washed with aq. saturated NaCl (3 × 15 mL), dried over anhydrous $MgSO_4$, filtered through a pad of silica gel with DCM as eluent and then concentrated under reduced pressure. The product **397** was obtained as a colorless oil (0.75 g, 3.6 mmol, 72%) and used without further purification. The analytical data are in good agreement with the literature.[267]

$C_{11}H_{18}O_2Si$: 210.35 $\frac{g}{mol}$

R_f: 0.44 (Silica gel, PE/EtOAc 95:5, UV).

Melting point: Ambient temperature (PE/EtOAc).

^{1}H-NMR (400 MHz, $CDCl_3$): δ [ppm] = 7.27–7.23 (m, 2H), 6.89–6.85 (m, 2H), 4.63 (s, 2H), 3.80 (s, 3H), 0.14 (s, 9H).

^{13}C-NMR (101 MHz, $CDCl_3$): δ [ppm] = 159.0, 133.3, 128.3, 113.9, 64.5, 55.4, -0.2.

GC-MS (EI): t_R = 5.63 min, *m/z* (Int. %) = 210 (15) $[M]^{+\bullet}$, 195 (24) $[M]^{+\bullet}$-$[CH_3]^{\bullet}$, 121 (100) $[M]^{+\bullet}$-$[C_3H_9OSi]^{\bullet}$.

4.4.4.1.4.2 Application of Silyl-Protected Alcohol in the Catalytic Reaction

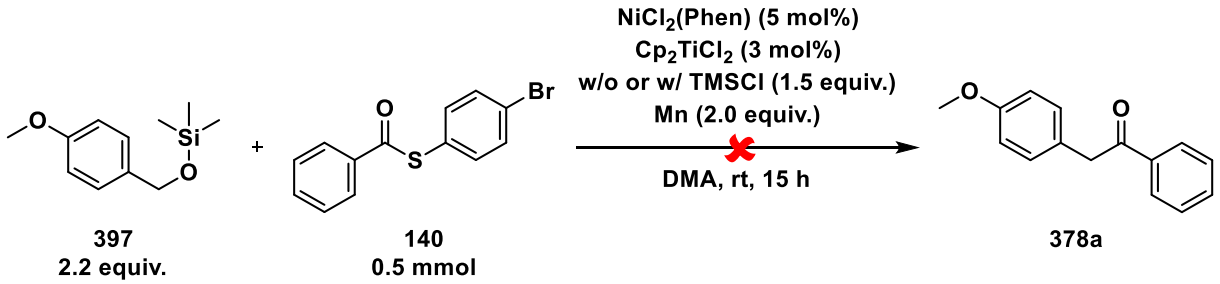

Two different reactions were performed analogously to GP-D with ((4-methoxybenzyl)oxy)trimethylsilane (**397**) (244 µL, 1.10 mmol, 2.2 equiv.) as substrate and in the absence or presence of TMSCl (95.4 µL, 0.75 mmol, 1.5 equiv.). GC-MS analysis of the reaction mixtures showed no ketone formation in either case.

4.4.4.1.4.3 Implementation of other Alcohols under SFRC

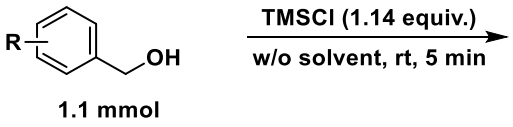

Investigations on chloride formation of other alcohols were conducted by charging a Schlenk tube with TMSCl (159 µL, 1.25 mmol, 1.14 equiv.) and then adding the respective alcohol (1.10 mmol, 1.0 equiv.). Liquids were added *via* syringe pump over a time range of 5 min. The respective samples were prepared for GC-MS measurements analogously to section 4.4.1.3.3.1.

4.4.4.1.4.4 Application of Higher Temperature for Chloride Formation

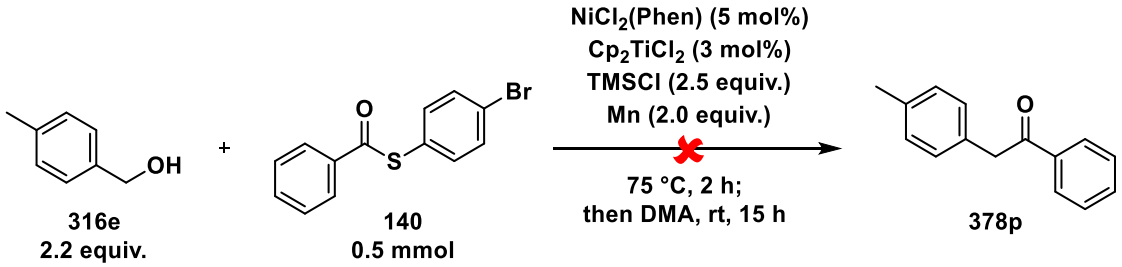

Analogously to GP-D, the compounds were added to a Schlenk tube, the last being *p*-methylbenzyl alcohol (**316e**) (134 mg, 1.10 mmol, 2.2 equiv.). Then, the mixture was stirred at 75 °C for two hours under SFRC. After cooling to rt, DMA was added as in GP-D using a syringe pump. The reaction was stirred for further 15 h. GC-MS analysis showed no product formation.

4.4.4.2 Exclusion of a Traditional Cross Coupling Mechanism
4.4.4.2.1 Quenching Experiments
4.4.4.2.1.1 HCl as Quenching Agent

The catalytic reaction was set up analogously to GP-D on a 1 mmol scale using Mn (110 mg, 2.00 mmol, 2.0 equiv.), titanocene dichloride (7.4 mg, 30 µmol, 3.0 mol%), $NiCl_2$(Phen) (15.5 mg, 50.0 µmol, 5.0 mol%), *S*-(4-bromophenyl) benzothioate (**140**) (292 mg, 1.00 mmol, 1.0 equiv.), TMSCl (318 µL, 2.50 mmol, 2.5 equiv.), 4-methoxybenzyl alcohol (**316b**) (274 uL, 2.20 mmol, 2.2 equiv.) and abs. DMA (4 mL). A respective sample of the reaction mixture (0.1 mL) was taken after 0 min, 5 min, 30 min, 1 h, 2 h, 3 h, 5 h and 19 h, and quenched with Lewatit® TP 207 and HCl (1 M, 0.1 mL). After sample preparation analogously to section 4.4.1.3.3.1, yields of the products **378a** and **404** were determined by quantitative GC-FID and are shown in Figure 4-20. The highest yield (12%) of the quenching product **404** was obtained at the start of the reaction, which then remained constant at around 2%. The yield of ketone **378a** increased over time, with the highest yield of 70% being achieved after 19 h.

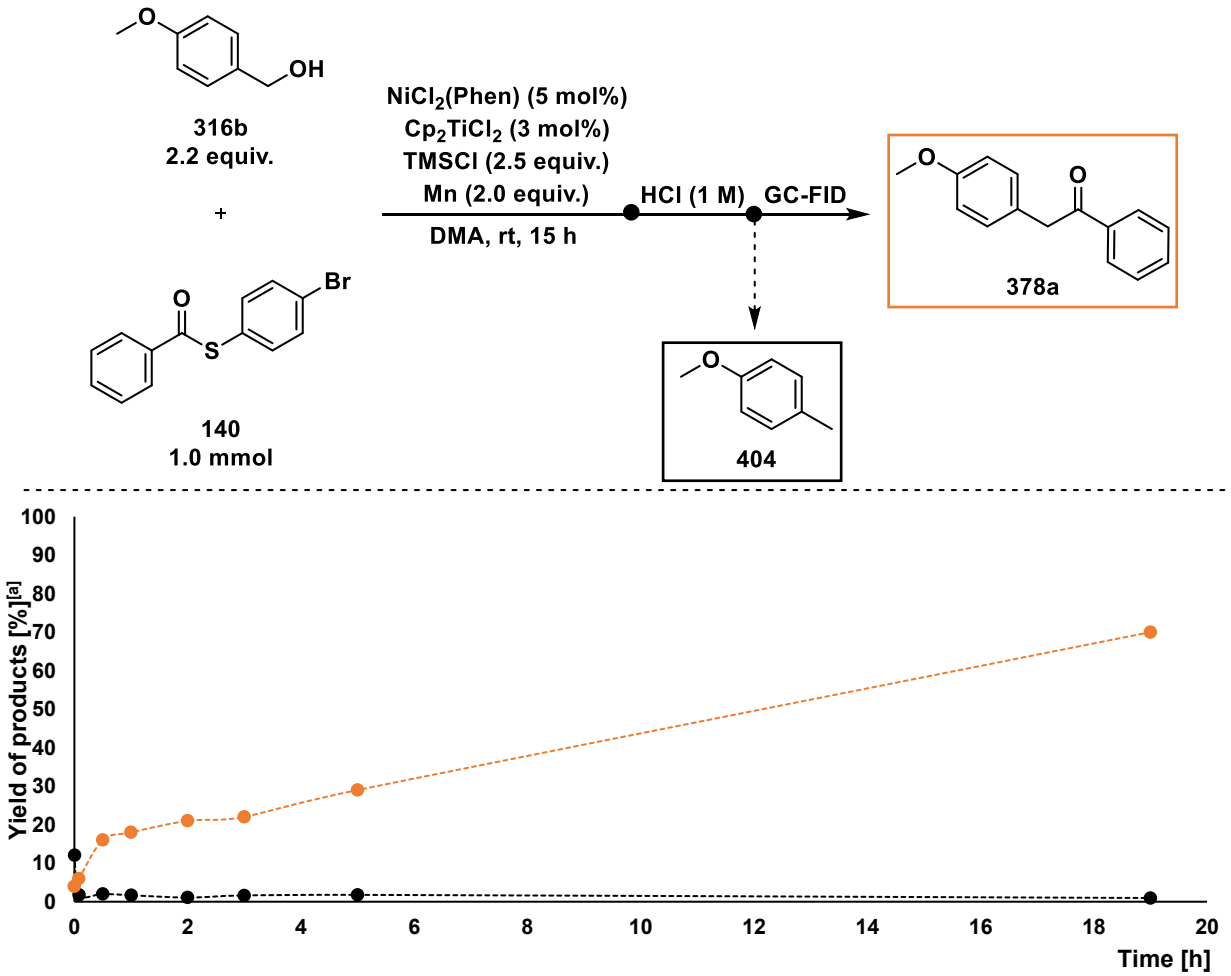

Figure 4-20: Comparison of ketone **378a** and quenching product **404** formation over time. [a]: Determined by GC-FID using *n*-pentadecane as internal standard.

4.4.4.2.1.2 Titration Using I_2

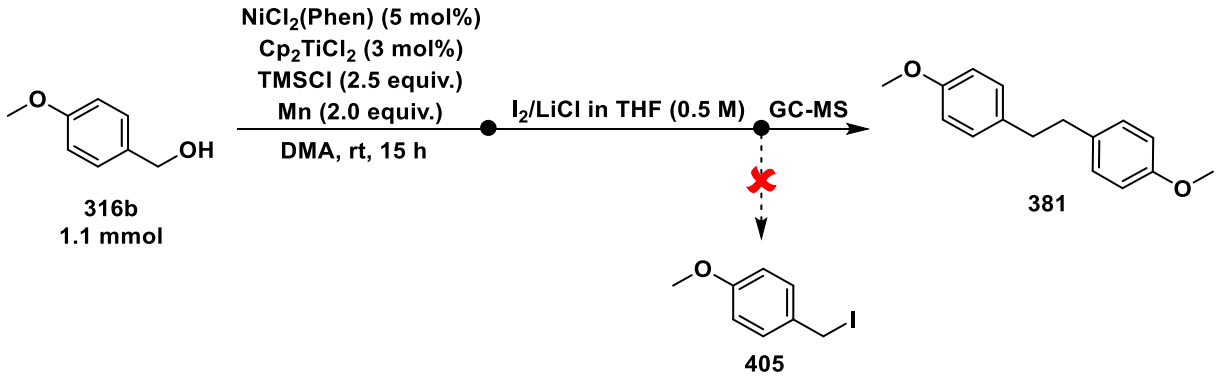

The titration using I_2 was conducted analogously to the procedure developed by Knochel.[218] In a dry Schlenk tube, a LiCl solution in THF (0.5 M) was freshly prepared by dissolving LiCl (84 mg, 2.0 mmol, 4.0 equiv.) in dry THF (4 mL). After stirring the solution for 30 min, the tube was charged with I_2 (254 mg, 1.00 mmol, 2.0 equiv.).

For the catalytic reaction, 4-methoxybenzyl alcohol (**316b**) (137 µL, 1.10 mmol, 1.0 equiv.) was reacted according to GP-D in the absence of thioester. At the beginning of the reaction and after 15 min, 0.1 mL of the reaction mixture was taken, which was quenched with Lewatit® TP 207 and the freshly prepared I_2/LiCl-solution. Then, the mixture was washed with aq. saturated $Na_2S_2O_3$ (1 × 1 mL) and with aq. saturated NaCl (1 × 1 mL). After the general sample preparation analogously to section 4.4.1.3.3.1, the reaction mixture was analyzed by GC-MS, which revealed the absence of the expected quenching product **405**. Instead, bibenzyl **381** was formed as main product.

4.4.4.2.2 Reaction of Alcohol in the Presence of TMSCl and Reductant

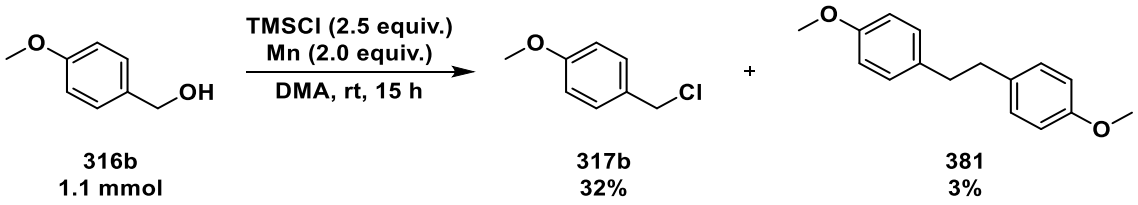

Alcohol **316b** was transformed under standard conditions analogously to GP-D, but in the absence of nickel and titanium catalyst. Quantitative GC-FID analysis gave benzylic chloride **317b** in 32% and benzylic dimer **381** in 3% yield.

4.4.4.3 Evidence of a Radical Intermediate
4.4.4.3.1 Conversion of Alcohol under Different Reaction Conditions

Alcohol **316b** was implemented under different reaction conditions analogously to GP-D (Scheme 4-63). Under standard conditions, alcohol reacted to benzylic dimer **381** as main product and oxoether **380** (Scheme 4-63A). The same main product **381** was obtained after the reaction of alcohol under nickel catalysis and TMSCl as additive (Scheme 4-63B). In the absence of nickel catalyst, benzyl chloride **317b** was generated as main product (Scheme 4-63C). The latter was also observed with TMSCl in DMA (Scheme 4-63D).

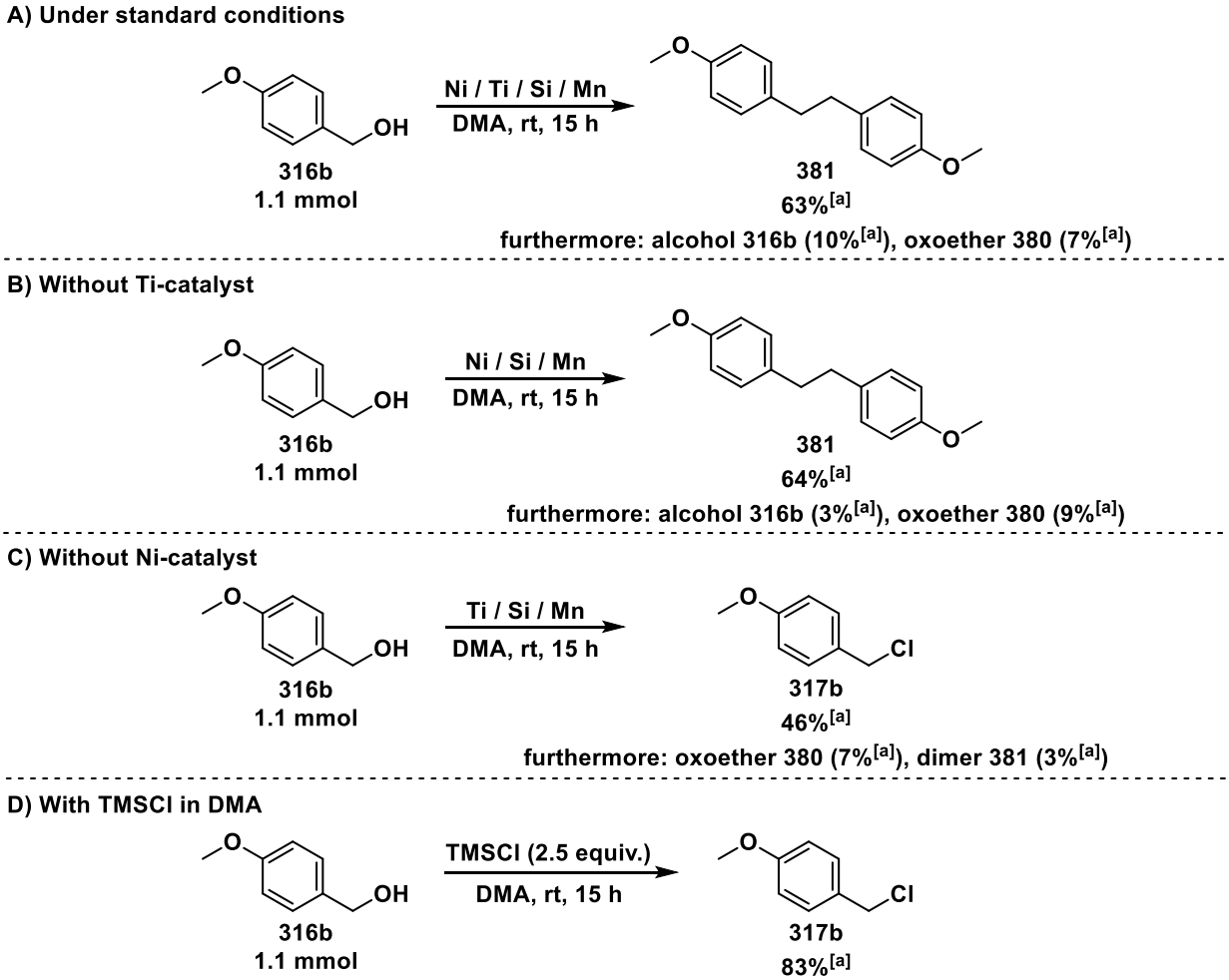

Scheme 4-63: Reaction of alcohol **316b** under different reaction conditions. Reaction conditions for Ni / Ti / Si / Mn: $NiCl_2$(Phen) (5 mol%), Cp_2TiCl_2 (3 mol%), TMSCl (2.5 equiv.), Mn (2.0 equiv.). [a]: Determined by GC-FID using *n*-pentadecane as internal standard.

4.4.4.3.2 Reversibility Experiment

4.4.4.3.2.1 Synthesis of 1,2-Bis(4-methoxyphenyl)ethane (381)

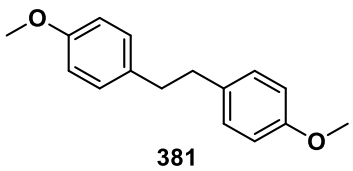

381

Benzylic dimer **381** was synthesized by the homocoupling of 4-methoxybenzyl alcohol (**316b**) (137 µL, 1.10 mmol, 1.0 equiv.) analogously to GP-D, but in the absence of thioester **140**. Purification by column chromatography (PE/EtOAc 95:5) delivered 1,2-bis(4-methoxyphenyl) ethane (**381**) (60.0 mg, 250 µmol, 50%) as colorless crystals.

$C_{16}H_{18}O_2$: 242.32 $\frac{g}{mol}$

R_f: 0.35 (Silica gel, PE/EtOAc 95:5, UV).

Melting point: 74–76 °C (PE/EtOAc).

^{1}H-NMR (400 MHz, $CDCl_3$): δ [ppm] = 7.06–7.00 (m, 4H), 6.80–6.74 (m, 4H), 3.74 (s, 6H), 2.78 (s, 4H).

^{13}C-NMR (101 MHz, $CDCl_3$): δ [ppm] = 157.9, 134.1, 129.5, 113.8, 55.4, 37.4.

GC-MS (EI): t_R = 9.30 min, *m/z* (Int. %) = 242 (29) $[M]^{+\bullet}$, 121 (100) $[M]^{+\bullet}$-$[C_8H_9O]^{\bullet}$.

HR-MS (APCI): *m/z* = $[M+H]^+$ calc. for $C_{16}H_{19}O_2$ 243.13796, found 243.13801.

IR (ATR): 2929.7 (w, sh), 2959.5 (w, sh), 2851.4 (w, sh), 1610.2 (m, sh), 1505.8 (s, sh), 1241.2 (s, sh), 1174.1 (s, sh), 1028.7 (m, sh), 827.5 (s, sh), 723.1 (m, sh).

4.4.4.3.2.2 Reaction of Benzylic Dimer under Standard Conditions

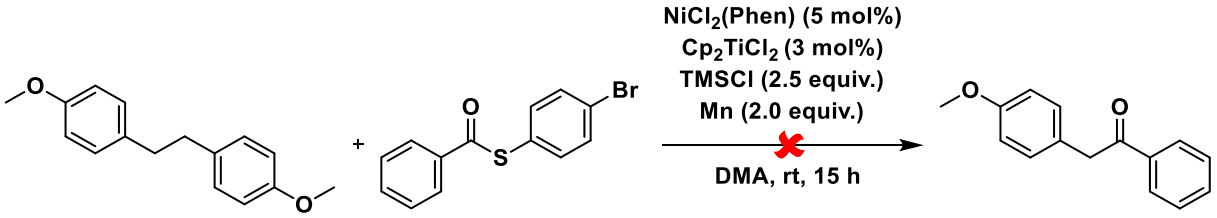

381
1.1 equiv.

140
0.19 mmol

378a

The experiment was set up according to GP-D using Mn (20.6 mg, 380 µmol, 2.0 equiv.), titanocene dichloride (1.4 mg, 5.6 µmol, 3.0 mol%), $NiCl_2$(Phen) (2.9 mg, 9.3 µmol, 5.0 mol%), thioester **140** (55.0 mg, 190 µmol, 1.0 equiv.), TMSCl (59.7 µL, 470 µmol, 2.5 equiv.) and benzylic dimer **381** (50.0 mg, 210 µmol, 1.1 equiv.). Ketone **378a** was not detected by GC-MS analysis.

4.4.4.3.3 Radical Scavenger Screening

In a glovebox, a flame-dried Schlenk tube was charged with Mn powder (54.9 mg, 1.00 mmol, 2.0 equiv.) and titanocene dichloride (3.7 mg, 15 µmol, 3.0 mol%). After removal from the glovebox, $NiCl_2$(Phen) (7.8 mg, 25 µmol, 5.0 mol%), *S*-(4-bromophenyl) benzothioate (**140**) (146 mg, 500 µmol, 1.0 equiv.) and TMSCl (159 µL, 1.25 mmol, 2.5 equiv.) were added successively. 4-Methoxybenzyl alcohol (**316b**) (137 µL, 1.10 mmol, 2.2 equiv.) was added *via* syringe pump over a time range of 5 min (27.4 µL/min). Then, the corresponding radical scavenger (1.0 mmol, 2.0 equiv.) was added all at once. After stirring for 5 min, abs. DMA (2 mL) was added *via* syringe pump over a time range of 5 min (0.4 mL/min). The mixture was stirred at rt for further 15 h. After sample preparation analogously to section 4.4.1.3.3.1, ketone yields were determined *via* quantitative GC-FID analysis.

4.4.4.3.4 Trapping with TEMPO

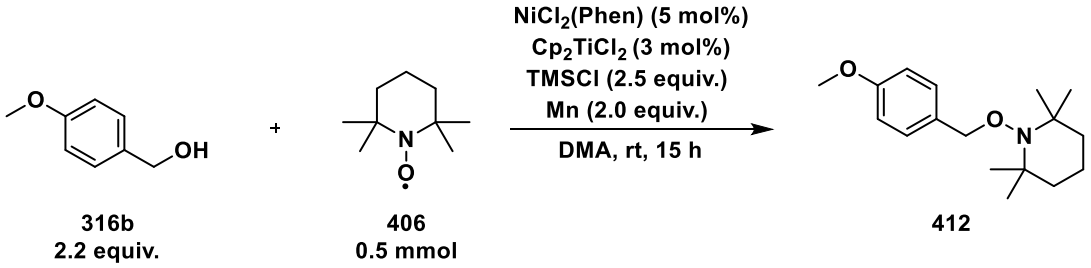

The radical trapping experiment was set up according to GP-D, but thioester **140** was substituted by TEMPO **406** (78.1 mg, 500 µmol, 1.0 equiv.). After stirring at rt for 15 h, the reaction was filtered through a pad of Celite® 545, activated basic Al_2O_3 and anhydrous $MgSO_4$ with DCM as eluent. The combined organic layers were washed with aq. saturated NaCl (2 × 20 mL), dried over anhydrous Mg_2SO_4, and concentrated under reduced pressure. The TEMPO adduct **412** was detected by HPLC-HR-MS.

$C_{17}H_{27}NO_2$: 277.41 $\frac{\mathrm{g}}{\mathrm{mol}}$

HPLC-HR-MS (ESI): *m/z* = $[M+H]^+$ calc. for $C_{17}H_{28}NO_2$ 278.21146, found 278.21130.

4.4.4.3.5 Trapping with *t*-Butyl Acrylate

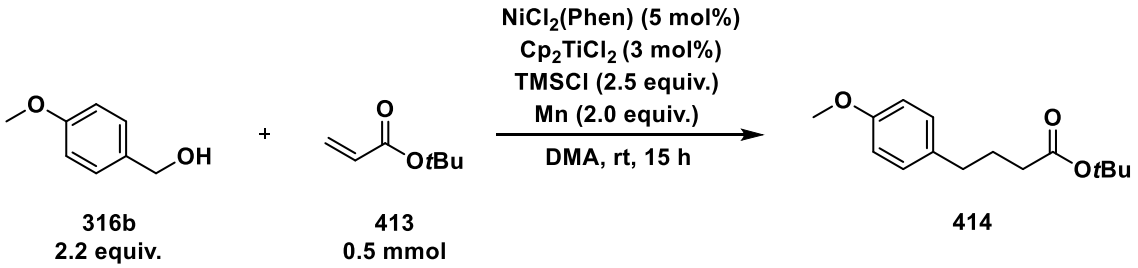

316b
2.2 equiv.

413
0.5 mmol

414

The radical trapping experiment was set up according to GP-D, but thioester **140** was substituted by *t*-butyl acrylate **413** (72.8 µL, 500 µmol, 1.0 equiv.). After stirring at rt for 15 h, the reaction was filtered through a pad of silica gel using DCM as eluent. The reaction mixture was poured into a separatory funnel containing water (15 mL), which was extracted with a solution of DCM and ethyl acetate (2 × 30 mL, 3/1 v/v). The combined organic layers were washed with water (2 × 20 mL) and aq. saturated NaCl (2 × 20 mL), dried over anhydrous Mg_2SO_4 and concentrated under reduced pressure. The crude product was purified by column chromatography (PE/EtOAc 95:5) and the radical adduct **414** was isolated as an inseparable mixture with benzylic dimer **381**. The mass ratio between dimer **381** and adduct **414** was determined to be 97:3 by quantitative ^{1}H-NMR spectroscopy.

Note: The radical adduct could not be fully proved by ^{1}H-NMR analysis because the peaks of the respective aromatic protons and the protons of the OMe substituents of benzylic dimer **381** and radical adduct **414** overlapped (Figure 4-21A). However, the proton signals of the aliphatic moieties of adduct **414** are consistent with the literature data (Figure 4-21B).[268] The proportion of adduct **414** was too low to obtain a meaningful ^{13}C-NMR spectrum. Complete proof of **414** was provided by GC-MS and HR-MS analysis.

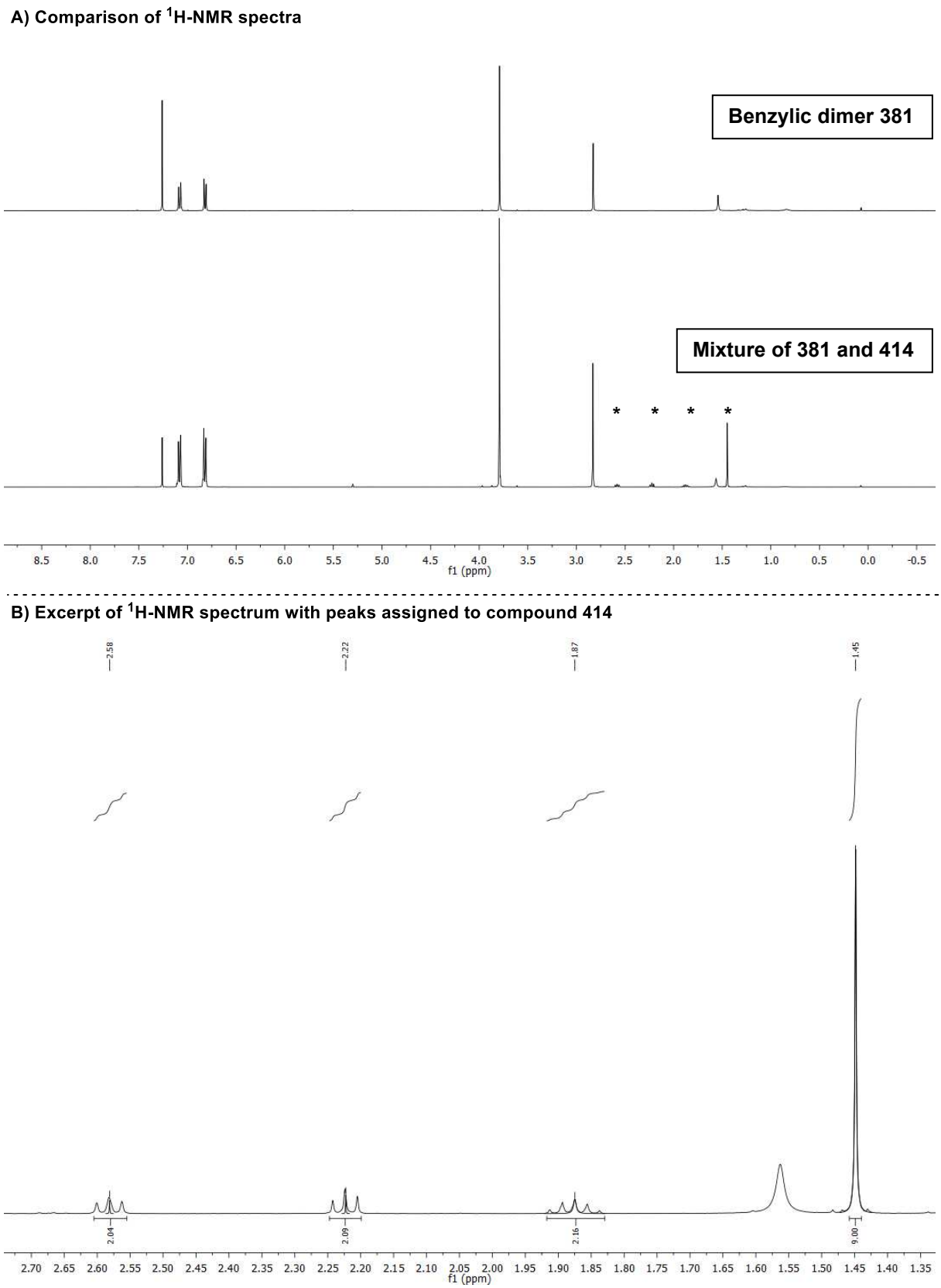

Figure 4-21: A) Comparison of ^{1}H-NMR spectra of **381** and the mixture of **381** and **414**. The peaks marked with an asterisk are assigned to the alkyl moiety of **414**.[268] B) Excerpt of the ^{1}H-NMR spectrum with peaks assigned to compound **414**.

$C_{15}H_{22}O_3$: 250.34 $\frac{g}{mol}$

^{1}H-NMR (400 MHz, $CDCl_3$): δ [ppm] = 2.58 (t, *J* = 7.8 Hz, 2H), 2.22 (t, *J* = 7.6 Hz, 2H), 1.87 (quint, *J* = 7.6 Hz, 2H), 1.45 (s, 9H).

GC-MS (EI): t_R = 7.89 min, *m/z* (Int. %) = 250 (11) $[M]^{+\bullet}$, 193 (44) $[M]^{+\bullet}$-$[C_4H_9O]^{\bullet}$, 177 (49) $[M]^{+\bullet}$-$[C_4H_9O]^{\bullet}$**,** 121 (100) $[M]^{+\bullet}$-$[C_7H_{13}O_2]^{\bullet}$.

HR-MS (ESI): *m/z* = $[M+Na]^+$ calc. for $C_{15}H_{22}O_3Na$ 273.14612, found 273.14629.

4.4.4.3.6 Radical Clock Experiments

4.4.4.3.6.1 Synthesis of Cyclopropyl(4-methoxyphenyl)methanol (316o)

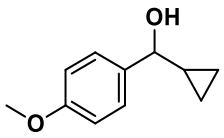

316o

Preparation of Cyclopropylmagnesium Bromide

Under an inert atmosphere, a three-necked RBF with reflux condenser and dropping funnel was charged with finely ground Mg (0.73 g, 30 mmol, 2.0 equiv.) and iodine for activation. The compounds were heated for 20 sec with a heat gun, stirred overnight and then suspended in THF (12 mL). A solution of cyclopropyl bromide (1.2 mL, 15 mmol, 1.0 equiv.) in THF (3 mL) was added dropwise over 45 min. When there was no immediate exothermal reaction after the addition of the bromide, the flask was additionally heated with a heat gun. The formation of Grignard compound was accompanied by a color change from yellow to grey-greenish and the formation of a cloudy mixture, which was stirred at rt for additional 30 min.

Addition of Cyclopropylmagnesium Bromide to 4-Methoxybenzaldehyde

The synthesis of cyclopropyl(4-methoxyphenyl)methanol (**316o**) followed a literature procedure.[269] The cyclopropyl magnesium bromide reagent (1.0 M in THF, 15 mL, 15 mmol, 2.1 equiv.) was cooled to 0 °C and a solution of 4-methoxybenzaldehyde (0.85 mL, 7.0 mmol, 1.0 equiv.) in THF (20 mL) was added dropwise over 30 min. The green-brownish suspension was warmed to rt and stirred for further 2 h. Unreacted Mg flakes were filtered off and the reaction mixture was quenched with MeOH (5 mL) and aq. saturated NH_4Cl (15 mL). The aqueous phase was extracted with Et_2O (3 × 30 mL), and the combined organic layers were washed with aq. saturated NaCl (40 mL), dried over anhydrous $MgSO_4$ and concentrated under reduced pressure. The crude product was purified by column chromatography (PE/EtOAc 4:1) to afford the product **316o** (0.96 g, 5.4 mmol, 77%) as a yellow oil. The analytical data are in good agreement with the literature.[269]

$C_{11}H_{14}O_2$: 178.23 $\frac{g}{mol}$

R_f: 0.30 (Silica gel, PE/EtOAc 4:1, UV).

^{1}H-NMR (400 MHz, $CDCl_3$): δ [ppm] = 7.38–7.32 (m, 2H), 6.92–6.86 (m, 2H), 3.97 (d, *J* = 8.2 Hz, 1H), 3.81 (s, 3H), 1.97 (s, 1H), 1.26–1.17 (m, 1H), 0.66–0.60 (m, 1H), 0.57–0.50 (m, 1H), 0.48–0.42 (m, 1H), 0.36–0.30 (m, 1H).

^{13}C-NMR (101 MHz, $CDCl_3$): δ [ppm] = 159.0, 136.1, 127.2, 113.7, 78.1, 55.3, 19.1, 3.6, 2.7.

GC-MS (EI): t_R = 6.61 min, *m/z* (Int. %) = 178 (18) $[M]^{+\bullet}$, 150 (100) $[M]^{+\bullet}$-$[C_9H_{10}O_2]^{2\bullet}$.

4.4.4.3.6.2 Application of Cyclopropyl(4-methoxyphenyl)methanol in the Catalytic Reaction

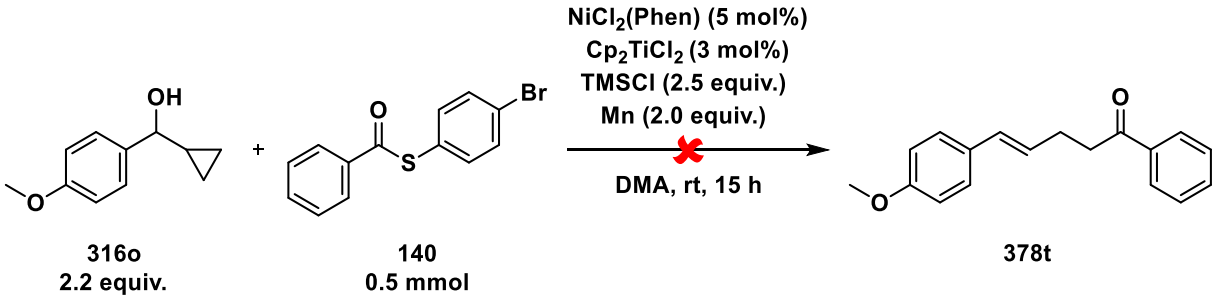

The radical clock reaction was conducted analogously to GP-D, but 4-methoxybenzyl alcohol (**316b**) was substituted by cyclopropyl(4-methoxyphenyl) methanol (**316o**) (170 µL, 1.10 mmol, 2.2 equiv.). GC-MS analysis of the mixture showed no formation of the desired ketone **378t**. Instead, unreacted thioester **140** and the formation of (*E*)-1-(4-chlorobut-1-en-1-yl)-4-methoxybenzene (**317e**) was observed.

4.4.4.3.6.3 Chlorination of Cyclopropyl(4-methoxyphenyl)methanol

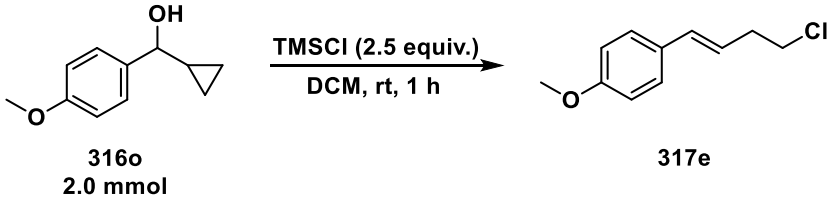

A solution of cyclopropyl(4-methoxyphenyl)methanol (**316o**) (310 µL, 2.00 mmol, 1.0 equiv.) in DCM was treated dropwise with TMSCl (1.3 mL, 10 mmol, 5.0 equiv.) at 0 °C. The mixture was warmed to rt and stirred for 1 h. Then, the reaction was quenched by adding water (5 mL) and the aqueous phase was extracted with DCM (3 × 5 mL). The combined organic layers were washed with aq. saturated NaCl (5 mL), dried over anhydrous $MgSO_4$ and concentrated under reduced pressure. The residue was filtered through a pad of silica gel with PE/EtOAc 9:1 as eluent. Ring-opened chloride **317e** was isolated as light yellow crystals (286 mg, 1.46 mmol, 73%). The analytical data are in good agreement with the literature.[270]

$C_{11}H_{13}ClO$: 196.67 $\frac{g}{mol}$

R_f: 0.57 (Silica gel, PE/EtOAc 9:1, UV).

^{1}H-NMR (400 MHz, $CDCl_3$): δ [ppm] = 7.32–7.28 (m, 2H), 6.87–6.84 (m, 2H), 6.46 (dt, *J* = 15.8, 1.4 Hz, 1H), 6.07 (dt, *J* = 15.8, 7.0 Hz, 1H), 3.81 (s, 3H), 3.61 (t, *J* = 7.0 Hz, 2H), 2.66 (ddt, *J* = 7.0, 7.0, 1.4 Hz, 2H).

^{13}C-NMR (101 MHz, $CDCl_3$): δ [ppm] = 159.1, 132.2, 129.9, 127.3, 123.6, 114.0, 55.3, 44.3, 36.3.

GC-MS (EI): t_R = 7.26 min, *m/z* (Int. %) = 196 (29) $[M]^{+\bullet}$, 147 (100) $[M]^{+\bullet}$-$[CH_2Cl]^{\bullet}$.

4.4.4.3.6.4 Cyclopropyl(phenyl)methanol as Radical Clock

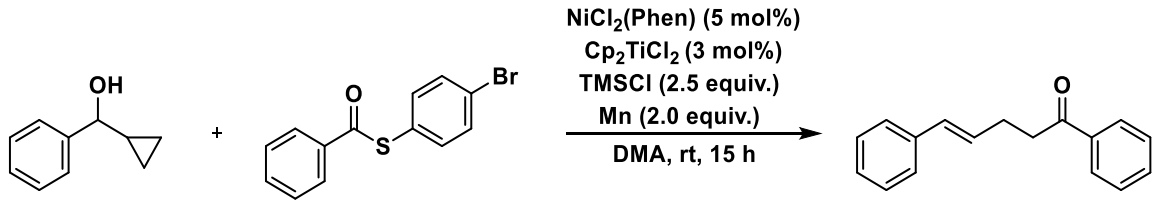

316p
2.2 equiv.

140
0.5 mmol

378u

The reaction was carried out analogously to GP-D, but 4-methoxybenzyl alcohol (**316b**) was substituted by cyclopropyl(phenyl)methanol (**316p**) (143 µL, 1.10 mmol, 2.2 equiv.). After stirring at rt for 15 h, the reaction mixture was filtered through a pad of Celite® 545, activated basic Al_2O_3 and anhydrous $MgSO_4$ with DCM as eluent. The mixture was poured into a separatory funnel containing water (15 mL) and the aqueous phase was extracted with a solution of DCM and EtOAc (2 × 30 mL, 3/1 v/v). The combined organic layers were washed with water (2 × 20 mL) and aq. saturated NaCl (2 × 20 mL), dried over anhydrous Mg_2SO_4 and concentrated under reduced pressure. The crude product was purified by column chromatography (PE/EtOAc 95:5) to afford the product **378u** as a yellowish solid (28.2 mg, 119 µmol, 24%). The analytical data are in good agreement with the literature,[271] but small amounts of an uncharacterized impurity are present.

$C_{17}H_{16}O$: 236.31 $\frac{g}{mol}$

R_f : 0.35 (Silica gel, PE/EtOAc 95:5,UV).

^{1}H-NMR (400 MHz, $CDCl_3$): δ [ppm] = 7.94 (d, *J* = 7.0 Hz, 2H), 7.47–7.35 (m, 1H), 7.34–7.22 (m, 2H), 7.16 (d, *J* = 7.2 Hz, 2H), 6.42 (d, *J* = 15.8 Hz, 1H), 6.30–6.20 (m, 1H), 3.12 (t, *J* = 6.9 Hz, 2H), 2.67–2.56 (m, 2H).

^{13}C-NMR (101 MHz, $CDCl_3$): δ [ppm] = 199.3, 136.9, 135.3, 133.1, 130.8, 129.1, 128.6, 128.5, 128.0, 127.1, 126.0, 38.3, 27.5.

GC-MS (EI): t_R = 38.35 min, *m/z* (Int. %) = 236 (28) $[M]^{+\bullet}$, 117 (13) $[M]^{+\bullet}$-$[C_8H_7O]^{\bullet}$, 105 (100) $[M]^{+\bullet}$-$[C_{10}H_{11}]^{\bullet}$.

HR-MS (ESI): *m/z* = $[M+Na]^+$ calc. for $C_{17}H_{16}ONa$ 259.10934, found 259.10943.

4.4.4.3.6.5 Experiments with Chlorinated Radical Clocks

4.4.4.3.6.5.1 Synthesis of (*E*)-(4-Chlorobut-1-en-1-yl)benzene (317g)

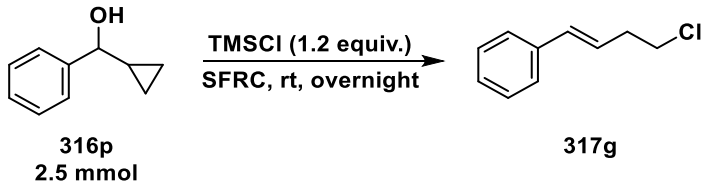

Under an inert atmosphere, cyclopropyl(phenyl)methanol (**316p**) (325 µL, 2.50 mmol, 1.0 equiv.) was treated with trimethylsilyl chloride (387 µL, 3.00 mmol, 1.2 equiv.) and stirred overnight. The reaction was quenched by adding water (5 mL) and diluted with EtOAc (5 mL). The aqueous phase was extracted with EtOAc (3 × 5 mL). The combined organic layers were washed with aq. saturated NaCl (3 × 5 mL), dried over anhydrous Mg_2SO_4 and concentrated under reduced pressure. GC-MS analysis of the crude product showed a mixture of chlorinated radical clock **317f** and ring-opened chloride **317g**. After purification by column chromatography (PE/EtOAc 95:5), only ring-opened chloride **317g** was isolated as a colorless oil (212 mg, 1.27 mmol, 51%) showing the instability of **317f** on silica gel. The analytical data are in good agreement with the literature.[272]

$C_{10}H_{11}Cl$: 166.65 $\frac{g}{mol}$

R_f: 0.57 (Silica gel, PE/EtOAc 95:5, UV).

Melting point: Ambient temperature (PE/EtOAc).

^{1}H-NMR (400 MHz, $CDCl_3$): δ [ppm] = 7.40–7.23 (m, 5H), 6.54–6.50 (m, 1H), 6.27–6.20 (m, 1H), 3.65 (t, *J* = 6.9 Hz, 2H), 2.71 (ddt, *J* = 6.9, 6.9, 1.4 Hz, 2H).

^{13}C-NMR (101 MHz, $CDCl_3$): δ [ppm] = 137.2, 132.9, 128.7, 127.6, 126.3, 125.9, 44.2, 36.3.

GC-MS (EI): t_R = 5.61 min, *m/z* (Int. %) = 166 (18) $[M]^{+\bullet}$, 117 (100) $[M]^{+\bullet}$-$[CH_2Cl]^{\bullet}$.

4.4.4.3.6.5.2 Synthesis of (Chloro(cyclopropyl)methyl)benzene (317f)

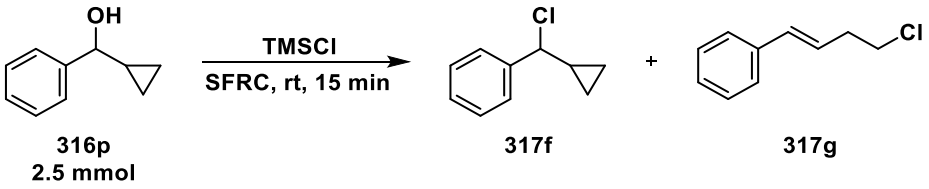

Under an inert atmosphere, cyclopropyl(phenyl)methanol (**316p**) (325 µL, 2.50 mmol, 1.0 equiv.) was treated with trimethylsilyl chloride (477 µL, 3.80 mmol, 1.5 equiv.) and stirred for 15 min. The reaction was quenched by adding water (2 mL) and diluted with EtOAc (2 mL). The organic layer was washed with H_2O (3 × 5 mL), dried over anhydrous Mg_2SO_4 and concentrated under reduced pressure. GC-MS and NMR analysis of the crude product showed a mixture of chlorinated radical clock **317f**, ring-opened chloride **317g** and traces of not

transformed alcohol **316p** (Figure 4-22). Determination of the mass fraction by quantitative ^{1}H-NMR spectroscopy showed the presence of **317f** as the main compound in the mixture with a purity of 64% (197 mg, 1.10 mmol, 47%).

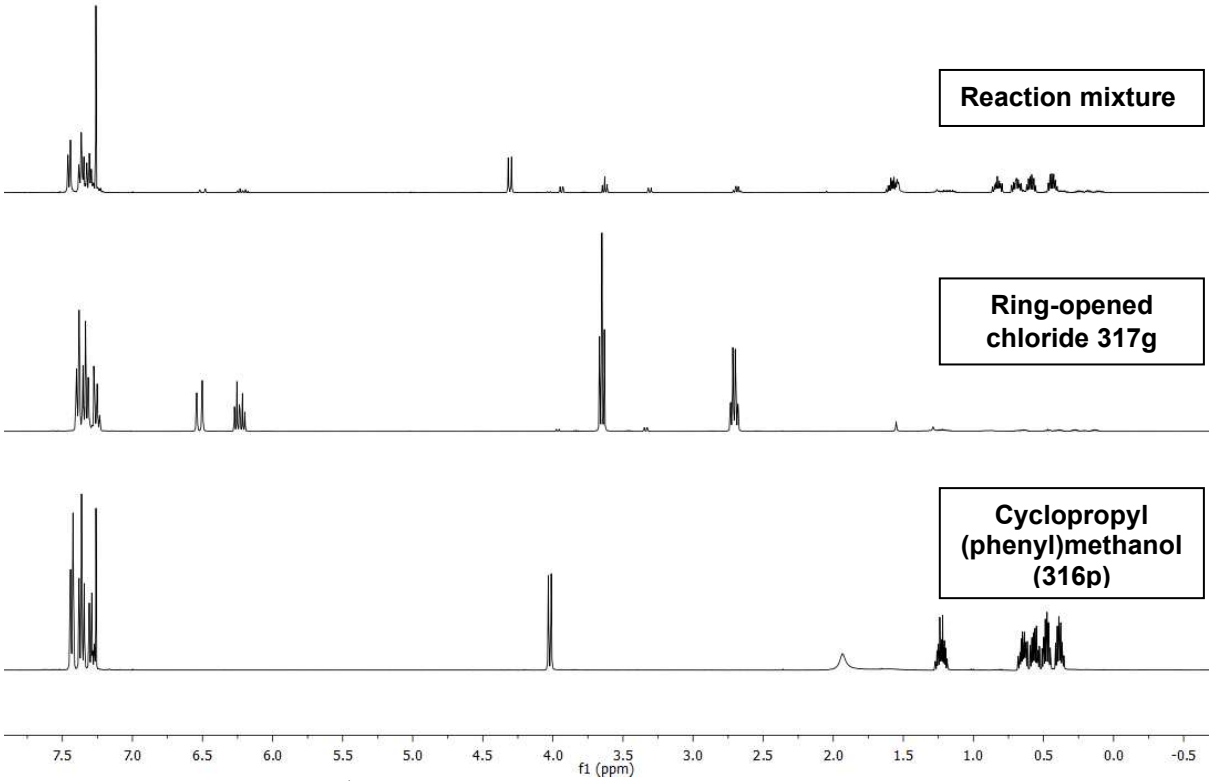

Figure 4-22: Comparison of ^{1}H-NMRs in $CDCl_3$ after the reaction of radical clock **316p** with TMSCl.

4.4.4.3.6.5.3 Application of Ring-Opened Chloride in the Catalytic Reaction

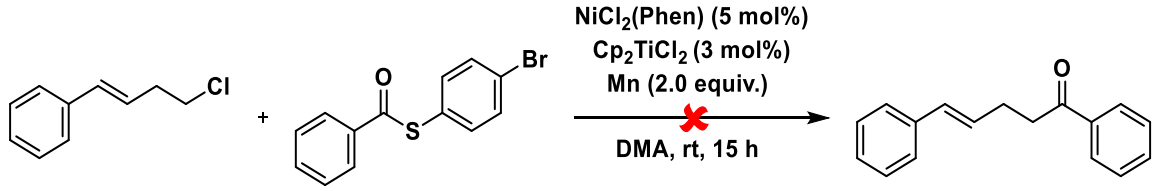

317g
0.38 mmol

140
1.3 equiv.

378u

The catalytic reaction was conducted analogously to GP-D, but using (*E*)-(4-chlorobut-1-en-1-yl)benzene (**317g**) (60.0 µL, 378 µmol, 1.2 equiv.) and thioester **140** (95.3 mg, 325 µmol, 1.0 equiv.) as substrates in the absence of TMSCl. GC-MS analysis of the reaction mixture revealed no formation of ketone **378u** and only unreacted substrates.

4.4.4.3.6.5.4 Application of (Chloro(cyclopropyl)methyl)benzene in the Catalytic Reaction

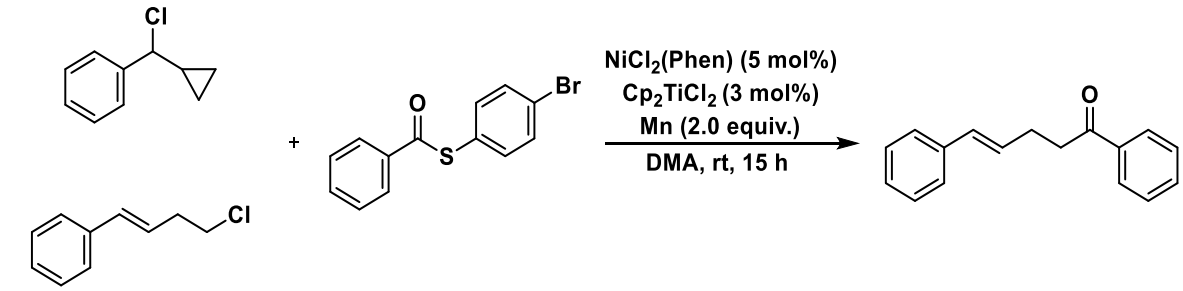

mixture of 317f and 317g
2.2 equiv.

140
0.5 mmol

378u
detected *via* GC-MS

The catalytic reaction was conducted analogously to GP-D, but in the absence of TMSCl. The mixture of **317f** and **317g** (174 µL, 1.10 mmol, 2.2 equiv.) was added *via* syringe pump over a time range of 5 min (34.8 µL/min). GC-MS analysis of the reaction mixture showed full conversion of chlorinated radical clock **317f**, not transformed ring-opened chloride **317g** and the formation of ketone **378u**.

4.4.4.4 Role of Manganese

4.4.4.4.1 Dependence of Ketone Yield on the Amount of Manganese

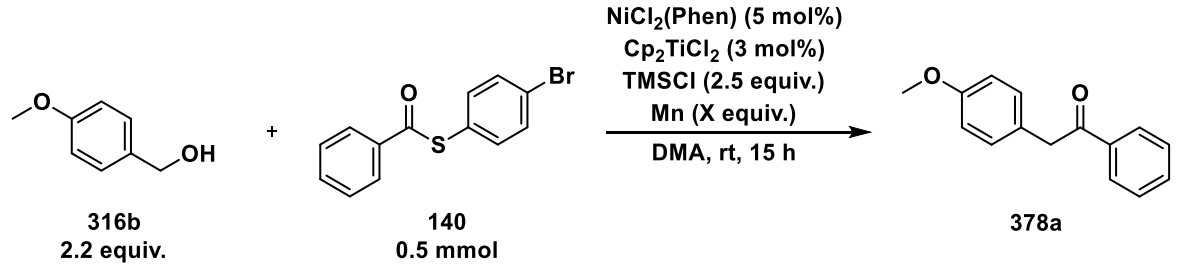

316b
2.2 equiv.

140
0.5 mmol

378a

The dependence of the ketone yield on the amount of manganese was investigated by reactions conducted analogously to GP-D, whereby the amount of manganese was varied. After sample preparation as described in section 4.4.1.3.3.1, the yields were determined by quantitative GC-FID analysis. Product formation was completely inhibited in the absence of reductant. With one equivalent of manganese (27.5 mg, 500 µmol, 1.0 equiv.), the yield of ketone **378a** was halved to 35%. Under standard conditions, ketone was obtained in 73% yield. With a significant excess of Mn powder (82.4 mg, 1.50 mmol, 3.0 equiv.), *S*-phenyl benzothioate (**133**) (107 mg, 500 µmol, 1.0 equiv.) was used instead of bromine-substituted thioester **140**. Under these conditions, ketone **378a** was detected in 71% yield.

4.4.4.4.2 Experiments with Ni(0) Source

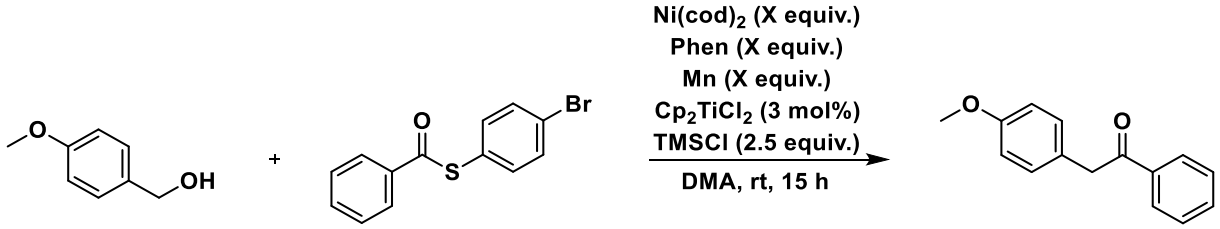

316b
2.2 equiv.

140
0.5 mmol

378a

Different experiments were performed with $Ni(cod)_2$ to establish nickel(0) as a possible oxidation state. For this purpose, the reactions were set up analogously to GP-D, but the respective amounts of $Ni(cod)_2$, Phen and Mn were modified. After the general sample preparation as described in section 4.4.1.3.3.1, the reaction mixtures were analyzed by GC-MS and quantitative GC-FID analysis.

In the absence of manganese but with $Ni(cod)_2$ (6.9 mg, 25 µmol, 5.0 mol%) and 1,10-phenanthroline (9.0 mg, 50 µmol, 10 mol%), no ketone formation was observed. With stoichiometric amount of $Ni(cod)_2$ (138 mg, 500 µmol, 1.0 equiv.) and 1,10-phenanthroline (99.1 mg, 550 µmol, 1.1 equiv.), GC-MS analysis again showed the inhibition of product formation. Product generation was accessible when using catalytic amount of $Ni(cod)_2$ (13.8 mg, 50.0 µmol, 10 mol%), catalytic amount of 1,10-phenanthroline (9.0 mg, 50 µmol,

10 mol%) and Mn powder (54.9 mg, 1.00 mmol, 2.0 equiv.). Ketone **378a** was obtained in 39% yield. With a catalytic amount of $Ni(cod)_2$ (13.8 mg, 50.0 µmol, 10 mol%), a stoichiometric amount of 1,10-phenanthroline (99.1 mg, 550 µmol, 1.1 equiv.) and Mn powder (54.9 mg, 1.00 mmol, 2.0 equiv.), the yield of ketone was decreased to 17%.

4.4.4.4.3 Experiments with TEMPO

4.4.4.4.3.1 Reaction of Alcohol, TEMPO, TMSCl and Manganese

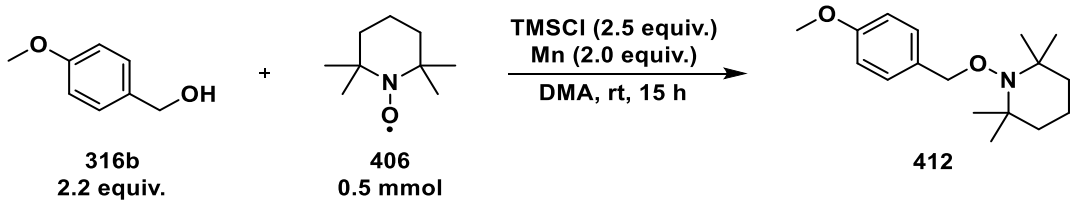

In a glovebox, a flame-dried Schlenk tube was charged with Mn powder (54.9 mg, 1.00 mmol, 2.0 equiv.). After removal from the glovebox, TEMPO (78.1 mg, 500 µmol, 1.0 equiv.) and TMSCl (160 µL, 1.25 mmol, 2.5 equiv.) were added first, followed by the addition of 4-methoxybenzyl alcohol (**316b**) (137 µL, 1.10 mmol, 2.2 equiv.) *via* syringe pump over a time range of 5 min (27.4 µL/min). After stirring for 5 min, abs. DMA (2 mL) was added *via* syringe pump over a time range of 5 min (0.4 mL/min) and the reaction was stirred at rt for 15 h. Then, the mixture was filtered through a pad of silica gel with DCM as eluent. The filtrate was washed with aq. saturated NaCl (3 × 10 mL), dried over anhydrous $MgSO_4$, filtered and concentrated under reduced pressure. A sample of the crude product was analyzed by HPLC-HR-MS, which revealed the expected TEMPO adduct **412**.

$C_{17}H_{27}NO_2$: 277.41 $\frac{g}{mol}$

HPLC-HR-MS (ESI): *m/z* = $[M+H]^+$ calc. for $C_{17}H_{28}NO_2$ 278.21146, found 278.21196.

4.4.4.4.3.2 Reaction of Chloride, TEMPO and Manganese

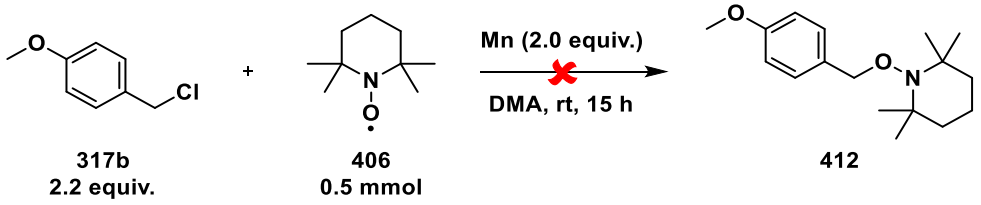

In a glovebox, a flame-dried Schlenk tube was charged with Mn powder (54.9 mg, 1.00 mmol, 2.0 equiv.). After removal from the box, TEMPO **406** (78.1 mg, 500 µmol, 1.0 equiv.) was added first, followed by the addition of 4-methoxybenzyl chloride (**317b**) (149 µL, 1.10 mmol, 2.2 equiv.) *via* syringe pump over a time range of 5 min (29.8 µL/min). After stirring for 5 min, abs. DMA (2 mL) was added *via* syringe pump over a time range of 5 min (0.4 mL/min). The reaction was stirred at rt for 15 h. Then, the mixture was filtered through a pad of silica gel with DCM as eluent. The filtrate was washed with aq. saturated $NaHCO_3$ (3 × 10 mL) and

aq. saturated NaCl (2 × 10 mL), dried over anhydrous $MgSO_4$ and concentrated under reduced pressure. A sample of the crude product was analyzed by GC-MS and HPLC-HR-MS, but the expected trapping adduct **412** was not detected.

4.4.4.4.3.3 Reaction of Chloride, TEMPO, TMSCl and Manganese

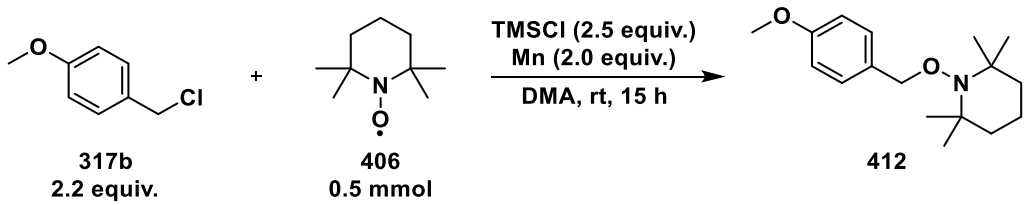

317b **2.2 equiv.** | **406** **0.5 mmol** | **412**

In a glovebox, a flame-dried Schlenk tube was charged with Mn powder (54.9 mg, 1.00 mmol, 2.0 equiv.). After removal from the box, TEMPO (78.1 mg, 500 µmol, 1.0 equiv.) and TMSCl (160 µL, 1.25 mmol, 2.5 equiv.) were added successively, followed by the addition of 4-methoxybenzyl chloride (**317b**) (149 µL, 1.10 mmol, 2.2 equiv.) *via* syringe pump over a time range of 5 min (29.8 µL/min). After stirring for 5 min, abs. DMA (2 mL) was added *via* syringe pump over a time range of 5 min (0.4 mL/min) and the reaction was stirred at rt for 15 h. Then, the mixture was filtered through a pad of silica gel with DCM as eluent. The filtrate was washed with aq. saturated NaCl (2 × 10 mL), dried over anhydrous $MgSO_4$, filtered and concentrated under reduced pressure. A sample of the crude product was analyzed by HPLC-LR-MS, which revealed the expected trapping adduct **412**.

$C_{17}H_{27}NO_2$: 277.41 $\frac{g}{mol}$

HPLC-LR-MS (ESI): *m/z* = $[M+H]^+$ calc. for $C_{17}H_{28}NO_2$ 278.2115, found 278.2118.

4.4.4.5 Oxidation States of Nickel Catalyst

4.4.4.5.1 Synthesis of Ni(cod)(Phen) 421

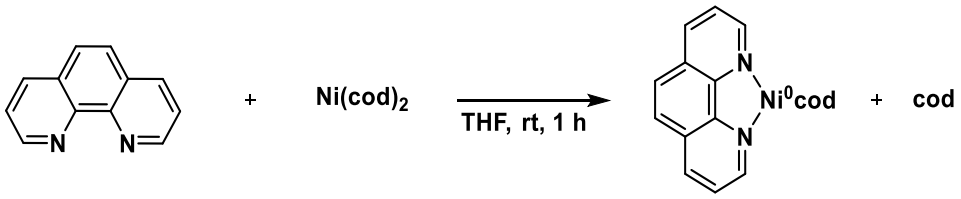

L12 **1.0 equiv.** | **422** **150 µmol** | **421**

The synthesis was conducted based on a literature report.[273] The mixture of 1,10-phenanthroline (27.0 mg, 150 µmol, 1.0 equiv.) and $Ni(cod)_2$ (41.3 mg, 150 µmol, 1.0 equiv.) in THF (1.0 mL) was stirred at rt for one hour. Then, the solvent was removed *in vacuo.* The dark blue solid was dried for 6 hours. Analysis of the complex was conducted by comparing the ^{1}H-NMR spectra of the substrates with the product mixture, which shows complete conversion of $Ni(cod)_2$ and 1,10-phenanthroline as well as released cod

(Figure 4-23). All other signals were assigned to Ni(cod)(Phen) **421**, which was stored in a glovebox in a freezer or freshly prepared before use.

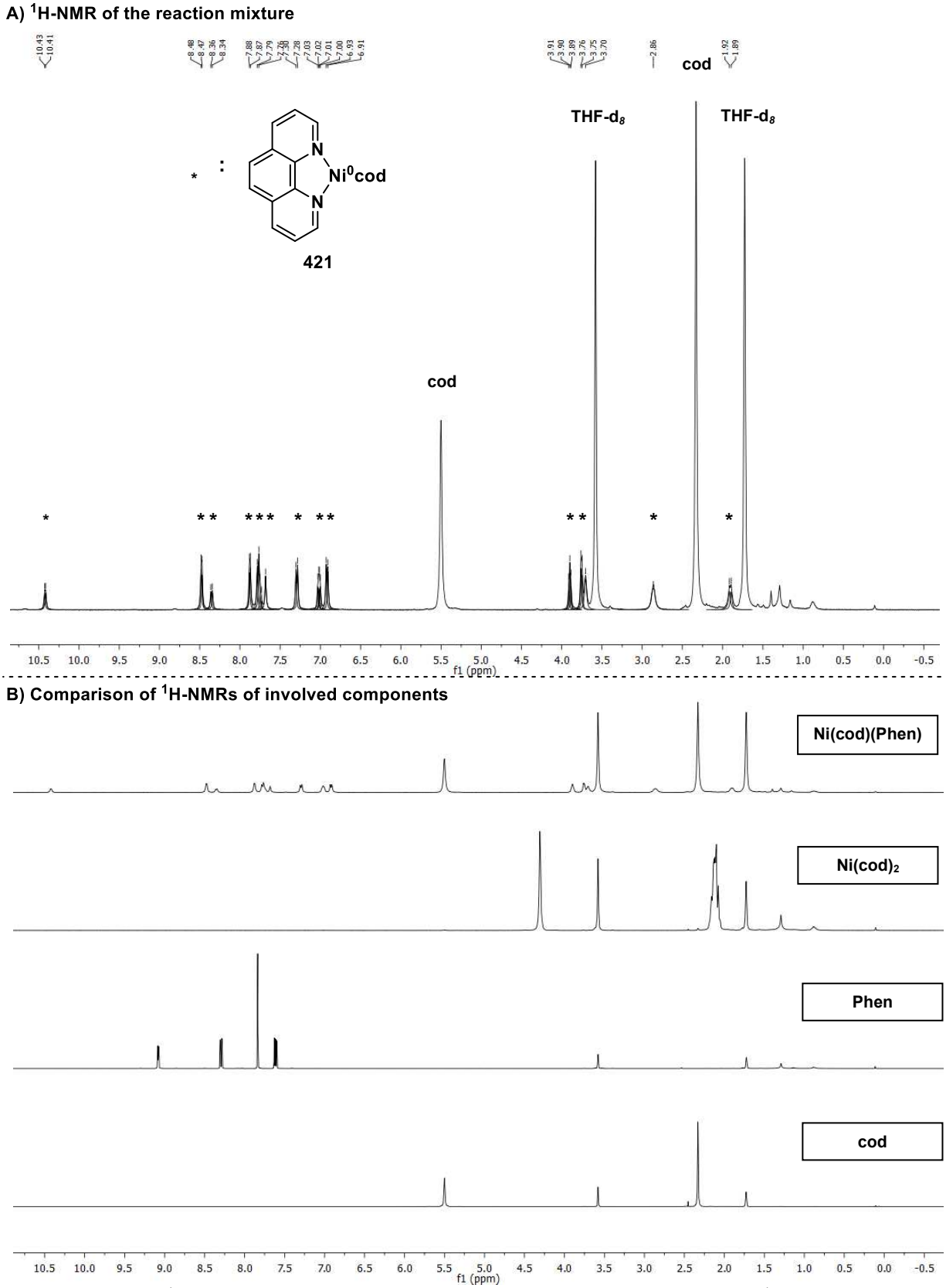

Figure 4-23: A) ^{1}H-NMR of Ni(cod)(Phen) **421** in THF-d_8 and B) comparison of ^{1}H-NMR spectra of involved compounds.

4.4.4.5.2 ^{19}F-NMR studies of Standard Reaction

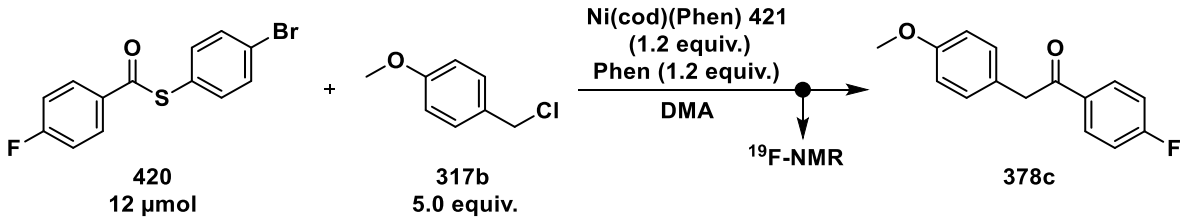

Ni(cod)(Phen) was synthesized as described in section 4.4.4.5.1. Then, a screw cap NMR tube was charged with Ni(cod)(Phen) **421** (5.0 mg, 14 µmol, 1.2 equiv.), 1,10-phenanthroline (2.6 mg, 14 µmol, 1.2 equiv.) and thioester **420** (3.9 mg, 12 µmol, 1.0 equiv.). The NMR tube was removed from the glovebox in a Schlenk tube holder. Benzyl chloride **317b** (8.8 µL, 60 µmol, 5.0 equiv.) and DMA (0.7 mL) were added successively, and the mixture was immediately frozen in a Dewar vessel filled with acetone/liq. N_2 (temperature: -45 °C– -55 °C). The NMR tube was taken to the NMR instrument in the Dewar vessel and ^{19}F-NMR spectra were recorded at 658.85 MHz and 298 K. After completion of the measurements, the mixture was analyzed by GC-MS, which revealed the formation of ketone **378c** and thioether **379b**.

4.4.4.5.3 ^{19}F-NMR studies of Oxidative Addition

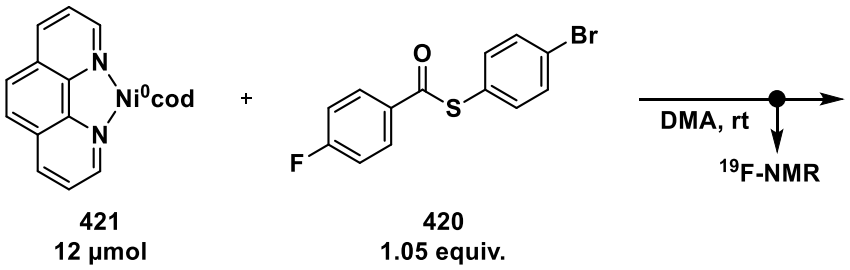

Ni(cod)(Phen) was synthesized as described in section 4.4.4.5.1. Then, a J. Young® NMR tube was charged with Ni(cod)(Phen) **421** (4.2 mg, 12 µmol, 1.0 equiv.) and thioester **420** (3.9 mg, 12.5 µmol, 1.05 equiv.). The filled NMR tube was removed from the glovebox in a Schlenk tube holder and cooled in a Dewar vessel filled with acetone/liq. N_2 (temperature: -45 °C– -55 °C). DMA (0.7 mL) was added to the NMR tube, which was immediately frozen. The NMR tube was brought to the NMR device in the Dewar vessel and ^{19}F-NMR spectra were acquired at 758.93 MHz and 286 K in a time interval of 28 s over 7 min.

4.4.4.5.4 Synthesis of Oxidative Addition Product 423-A/B

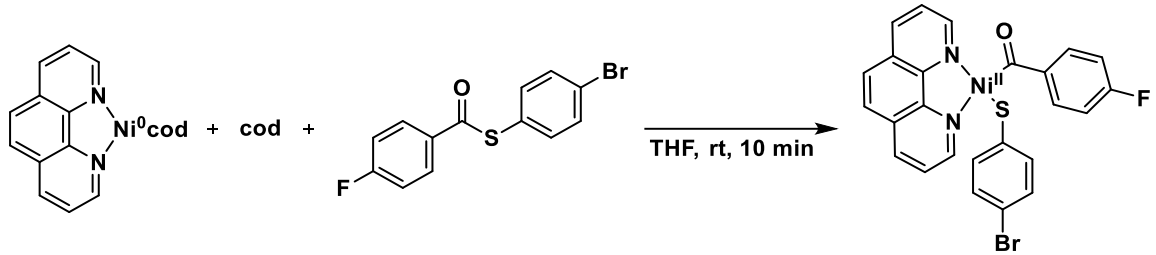

Ni(cod)(Phen) was freshly synthesized analogously to section 4.4.4.5.1 using 1,10-phenanthroline (21.6 mg, 120 µmol, 1.0 equiv.) and $Ni(cod)_2$ (33.0 mg, 120 µmol, 1.0 equiv.) in THF (1.0 mL), and the mixture was stirred at rt for one hour. Thioester **420** (37.3 mg, 120 µmol, 1.0 equiv.) was then added and the mixture was stirred for further 10 min.

Work-up process **423-A**: The resulting dark violet solution was triturated with *n*-pentane (0.3 mL) and the precipitate was immediately collected on a frit. The dark grey residue was washed with *n*-pentane (2 × 0.4 mL) and dried under vacuum for 4 h. The complex **423-A** (25.0 mg, 45.8 µmol, 38%) was isolated as a dark blue solid and stored in a glovebox in a freezer.

^{19}F-NMR (376 MHz, DMA): δ [ppm] = -111.4 (s), -126.1 (s).

Work-up process **423-B**: The resulting dark violet solution was triturated with *n*-pentane (0.1 mL) and *n*-hexane (0.2 mL), and the precipitate was immediately collected on a frit. The dark grey residue was washed with *n*-hexane (2 × 0.4 mL) and dried under vacuum for 4 h. The complex **423-B** (42.8 mg, 77.8 µmol, 65%) was isolated as a dark blue solid and stored in a glovebox in a freezer. The ^{19}F-NMR spectrum of **423-B** showed traces of not converted thioester **420** at -105.3 ppm.

^{19}F-NMR (376 MHz, DMA): δ [ppm] = -111.2 (s), -125.8 (s).

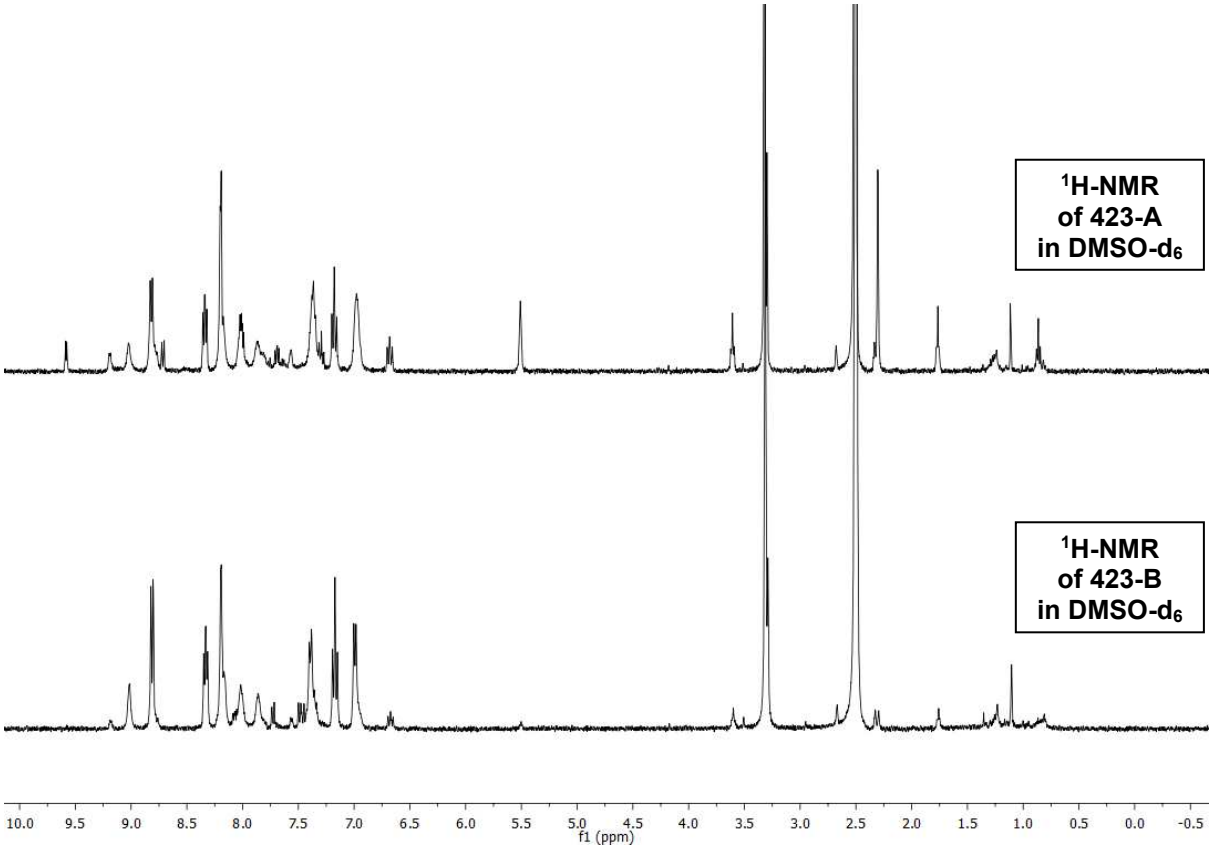

Figure 4-24: Comparison of ^{1}H-NMR spectra of **423-A** and **423-B** in DMSO-d$_6$.

4.4.4.5.5 ^{19}F-NMR Studies of Reactions between 423-A/B and Benzylic Chloride

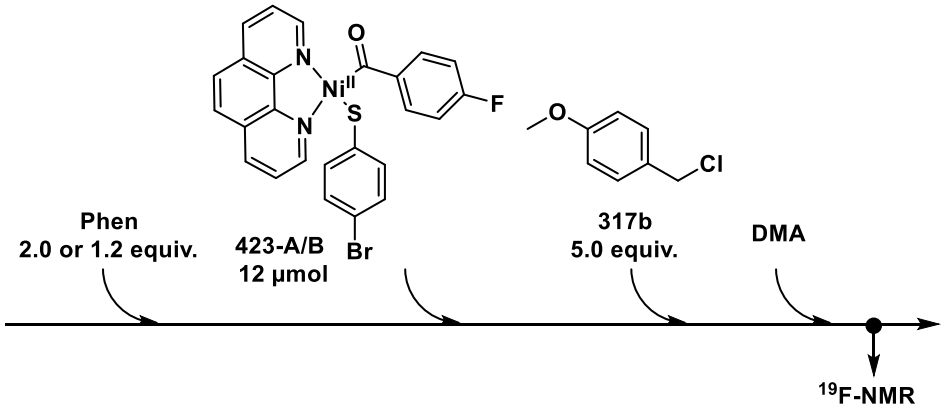

The ^{19}F-NMR spectrum of the reaction between nickel(II) complex **423-A** (6.6 mg, 12 µmol, 1.0 equiv.), 1,10-phenanthroline (4.3 mg, 24 µmol, 2.0 equiv.) and 4-methoxybenzyl chloride (**317b**) (8.8 µL, 60 µmol, 5.0 equiv.) in DMA (0.5 mL) was recorded without deuterated solvent at 282.40 MHz, 296 K and after 3 h. In a subsequent spike experiment, ketone **378c** was added to the NMR tube to identify it as formed product.

The ^{19}F-NMR spectrum of the reaction between nickel(II) complex **423-B** (6.6 mg, 12 µmol, 1.0 equiv.), 1,10-phenanthroline (2.6 mg, 14 µmol, 1.2 equiv.) and 4-methoxybenzyl chloride (**317c**) (8.8 µL, 60 µmol, 5.0 equiv.) in DMA (0.7 mL) was recorded without

deuterated solvent at 658.79 MHz, 296 K and after 1 h 38 min. Product analysis was conducted using GC-MS and showed the formation of ketone **378c** as main product.

4.4.4.5.6 Synthesis of Oxidative Addition Product 401

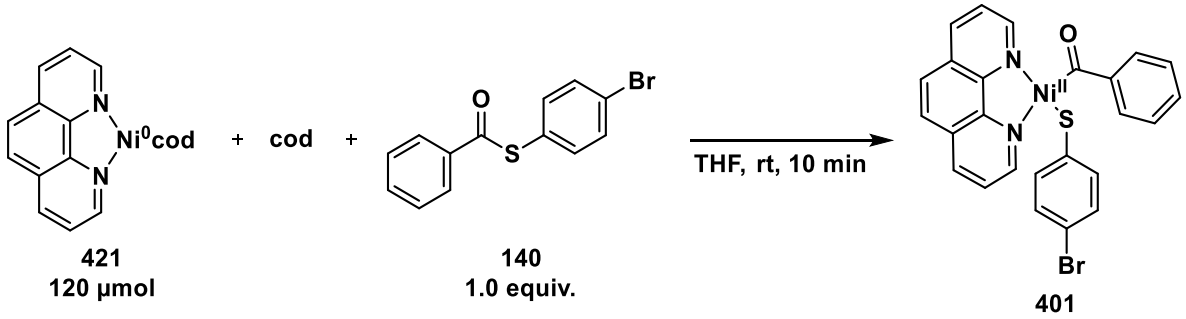

421
120 µmol

140
1.0 equiv.

401

Ni(cod)(Phen) was generated *in situ* analogously to the procedure in section 4.4.4.5.1 using 1,10-phenanthroline (33.0 mg, 120 µmol, 1.0 equiv.) and $Ni(cod)_2$ (21.6 mg, 120 µmol, 1.0 equiv.) in THF (0.3 mL). After stirring for one hour, thioester **140** (35.2 mg, 120 µmol, 1.0 equiv.) was added and the mixture was stirred for further 10 min. The resulting dark violet solution was triturated with *n*-pentane (0.3 mL) and the precipitate was immediately collected on a frit. The dark brown residue was washed with *n*-pentane (2 × 0.4 mL) and dried under vacuum for 4 h. The complex **401** (34.0 mg, 63.6 µmol, 53%) was isolated as a brown solid with minor impurities and stored in a glovebox in a freezer.

Note:
The amount of solvent is crucial for the reaction. In previous attempts to synthesize complex **401**, 1 mL of solvent (THF or DMA) was used, which led to decomposition of the complex. In addition, the complex must be filtered immediately after the addition of pentane to avoid decomposition.

$C_{25}H_{17}BrN_2NiOS$: 532.08 $\frac{g}{mol}$

^{1}H-NMR (400 MHz, DMSO-d_6): δ [ppm] = 9.02 (s, 1H), 8.81 (d, *J* = 8.3 Hz, 2H), 8.29–8.27 (m, 2H), 8.20–8.19 (m, 3H), 8.02–7.98 (m, 1H), 7.88–7.85 (m, 1H), 7.46–7.34 (m, 5H), 6.99 (d, *J* = 8.3 Hz, 2H).

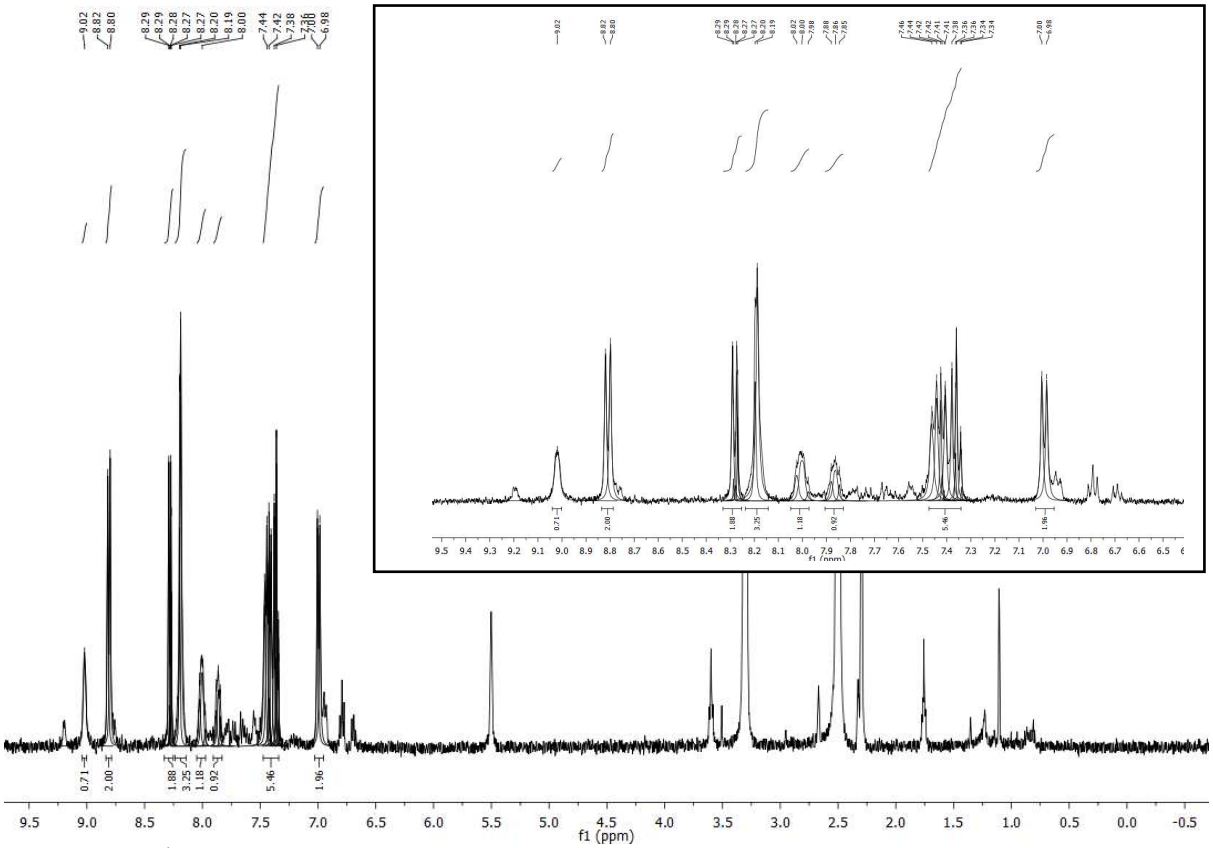

Figure 4-25: ^{1}H-NMR of nickel(II) complex **401** in DMSO-d_6.

4.4.4.5.7 Reactions of Oxidative Addition Product 401 with Benzyl Chloride

In general, the reactions of oxidative addition product **401** with chloride **317b** were conducted as follows: In a glovebox, a screw cap glass vial was charged with the oxidative addition complex **401**, either without or with Mn powder, either without or with 1,10-phenanthroline, 4-methoxybenzyl chloride (**317b**) (5.0 equiv.) and DMA (0.3 mL). Exact amounts for each experiment are listed in Table 4-20. The respective reaction mixture was stirred at rt for 3 h. Then, a sample was taken (0.1 mL), which was quenched with Lewatit® TP 207. After dilution with DCM and general sample preparation, the mixtures were analyzed by GC-MS.

Table 4-20: Amounts of involved components in reactions with oxidative addition product **401**.

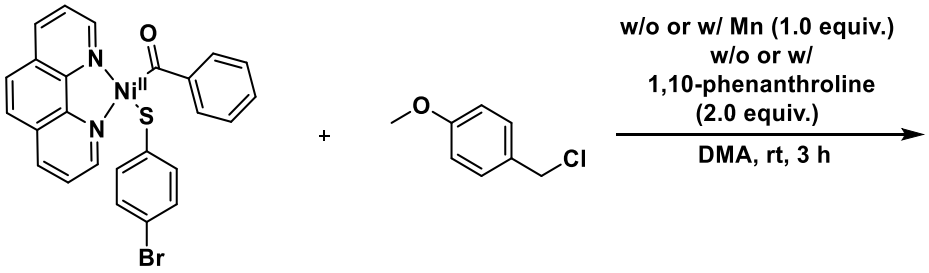

401
1.0 equiv.

317b
5.0 equiv.

Entry	Amount of complex 401 [mg µmol equiv.]	Amount of Mn [mg µmol equiv.]	Amount of 1,10-phenanthroline [mg µmol equiv.]	Amount of chloride 317b [µL µmol equiv.]
A	8.0 15 1.0	✘	✘	11 75 5.0
B	16.0 30.0 1.0	1.7 30 1.0	✘	22 150 5.0
C	8.0 15 1.0	✘	5.4 30 2.0	11.0 75 5.0
D	6.0 11 1.0	0.6 11 1.0	4.1 23 2.0	8.2 56 5.0

4.4.4.5.8 Catalytic Reaction with Krossing's Ni(I) Complex

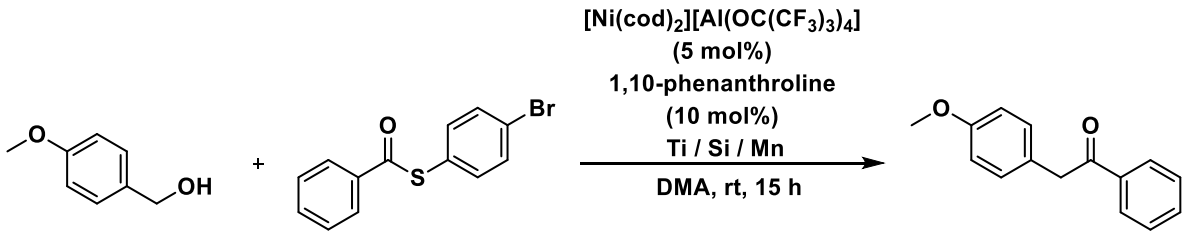

316b
2.2 equiv.

140
0.5 mmol

378a

The nickel(I) complex was synthesized analogously to Krossing's procedure [229] by R. Richter from the working group of I. Fleischer, University of Tübingen, and kindly provided for the experiment. The reaction was conducted as described in GP-D with Krossing's Ni(I) complex (31.0 mg, 25.0 µmol, 5.0 mol%), Cp_2TiCl_2 (3.7 mg, 15 µmol, 3.0 mol%), 1,10-phenanthroline (9.0 mg, 50 µmol, 10 mol%), Mn powder (54.9 mg, 1.00 mmol, 2.0 equiv.), thioester **140** (146 mg, 500 µmol, 1.0 equiv.), TMSCl (159 µL, 1.25 mmol, 2.5 equiv.), 4-methoxybenzyl alcohol (**316b**) (137 µL, 1.10 mmol, 2.2 equiv.) and abs. DMA (2 mL). After the general sample preparation as described in section 4.4.4.5.1, the reaction mixture was analyzed by GC-MS and quantitative GC-FID, yielding the ketone **378a** in 74%.

4.4.4.5.9 Stoichiometric Reaction with Krossing's Ni(I) Complex

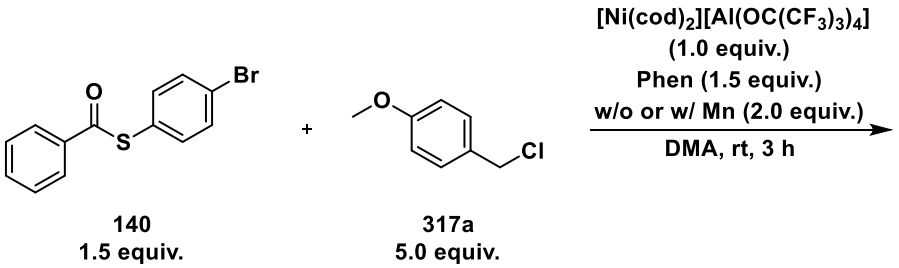

The nickel(I) complex was synthesized analogously to Krossing's procedure [229] by R. Richter of the working group of I. Fleischer, University of Tübingen, and kindly provided for the experiment.

In general, the reactions of nickel(I) complex with thioester **140** and chloride **317a** in the presence or absence of manganese were conducted as follows: In a glovebox, a screw cap glass vial was charged with the Ni(I) complex (9.3 mg, 7.5 µmol, 1.0 equiv.), either without or with Mn powder (0.8 µg, 15 µmol, 2.0 equiv.), 1,10-phenanthroline (2.3 mg, 7.9 µmol, 1.05 equiv.), *S*-(4-bromophenyl) benzothioate (**140**) (2.3 mg, 7.9 µmol, 1.05 equiv.), 4-methoxybenzyl chloride (**317a**) (5.5 µL, 38 µmol, 5.0 equiv.) and abs. DMA (0.2 mL). After stirring at rt for 3 h, a sample was taken (0.1 mL), which was quenched by Lewatit® TP 207. After dilution with DCM and the general sample preparation, the mixtures were analyzed *via* GC-MS.

4.4.4.5.10 Synthesis of Oxidative Addition Product 425

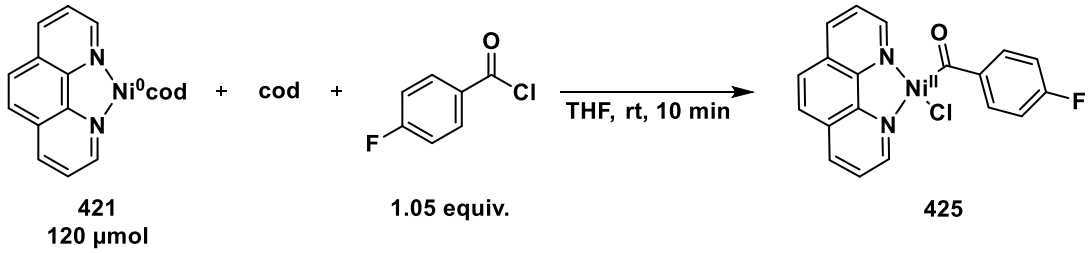

The synthesis was conducted analogously to a literature report.[274] Ni(cod)(Phen) **421** was generated *in situ* as described in section 4.4.4.5.1 using $Ni(cod)_2$ (33.0 mg, 120 µmol, 1.0 equiv.) and 1,10-phenanthroline (21.6 mg, 120 µmol, 1.0 equiv.) in THF (0.3 mL), and the mixture was stirred at rt for one hour. Then, 4-fluorobenzoyl chloride (14.9 µL, 126 µmol, 1.05 equiv.) was added and the red mixture was stirred for further 10 min. The solution was triturated with *n*-pentane (0.3 mL) and the precipitate was immediately collected on a frit. The red residue was washed with *n*-pentane (2 × 0.4 mL) and dried under vacuum for 4 h. The complex **425** (31.6 mg, 63.6 µmol, 66%) was isolated as a red solid. The analytical data are in good agreement with the literature.[274]

$C_{19}H_{12}ClFN_2NiO$: 397.46 $\frac{g}{mol}$

^{1}H-NMR (400 MHz, CD_2Cl_2): δ [ppm] = 9.22 (d, *J* = 4.6 Hz, 1H), 8.69 (dd, *J* = 8.4, 5.9 Hz, 2H), 8.47–8.42 (m, 2H), 8.15 (d, *J* = 5.0 Hz, 1H), 7.96–7.83 (m, 3H), 7.53 (dd, *J* = 7.8, 5.4 Hz, 1H), 7.11 (t, *J* = 8.6 Hz, 2H).

^{19}F-NMR (377 MHz, CD_2Cl_2): δ [ppm] = -108.9 (m).

4.4.4.5.11 Reactions of Oxidative Addition Product 425 with Chloride

In general, the reactions of oxidative addition product **425** with chloride **317b** were conducted as follows: In a glovebox, a screw cap glass vial was charged with complex **425**, either without or with Mn powder, 4-methoxybenzyl chloride (**317b**) (5.0 equiv.) and DMA (0.3 mL). Exact amounts for each experiment are listed in Table 4-21. The respective reaction mixture was stirred at rt overnight. Then, a sample was taken (0.1 mL), which was quenched by Lewatit® TP 207. After dilution with DCM and the general sample preparation, the mixtures were analyzed *via* GC-MS.

Table 4-21: Amounts of involved components in reactions with oxidative addition product **425**.

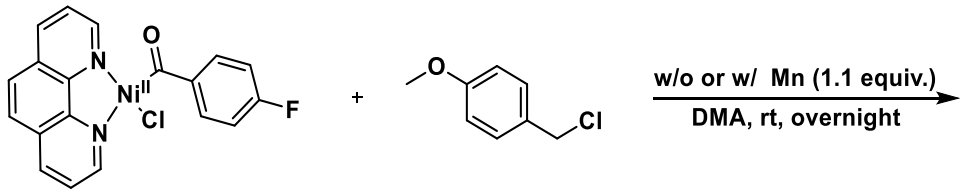

425
1.0 equiv.

317b
5.0 equiv.

Entry	Amount of complex 425 [mg µmol equiv.]	Amount of Mn [mg µmol equiv.]	Amount of chloride 317b [µL µmol equiv.]
A	**11.9 30.0 1.0**	**✘**	**22.0 150 5.0**
B	**6.0 15 1.0**	**0.9 17 1.1**	**11 75 5.0**

4.4.4.5.12 EPR Experiments

The general sample set-up for EPR experiments was as follows: In a glovebox, flame-dried Schlenk tubes were charged with different combinations of Mn powder (54.9 mg, 1.00 mmol, 2.0 equiv.), titanocene dichloride (3.7 mg, 15 µmol, 3.0 mol%), $NiCl_2$(Phen) (7.8 mg, 25 µmol, 5.0 mol%) and *S*-(4-bromophenyl) benzothioate (**140**) (146 mg, 500 µmol, 1.0 equiv.). After removal from the glovebox, TMSCl (159 µL, 1.25 mmol, 2.5 equiv.), 4-methoxybenzyl alcohol (**316b**) (137 µL, 1.10 mmol, 2.2 equiv.) or 4-methoxybenzyl chloride (**317b**) (161 µL, 1.10 mmol, 2.2 equiv.) and abs. DMA (2 mL) were added. After stirring for 5 min, a sample (0.5 mL) was taken and given into an EPR tube (3 mm outer diameter), which was precooled in a NaCl/ice bath. The sample was then immediately frozen in a Dewar vessel filled with acetone/liq. N_2 (temperature: -45 °C– -55 °C). The EPR spectra were recorded with the aid of the NMR department of the University of Tübingen and measured at 180 K.

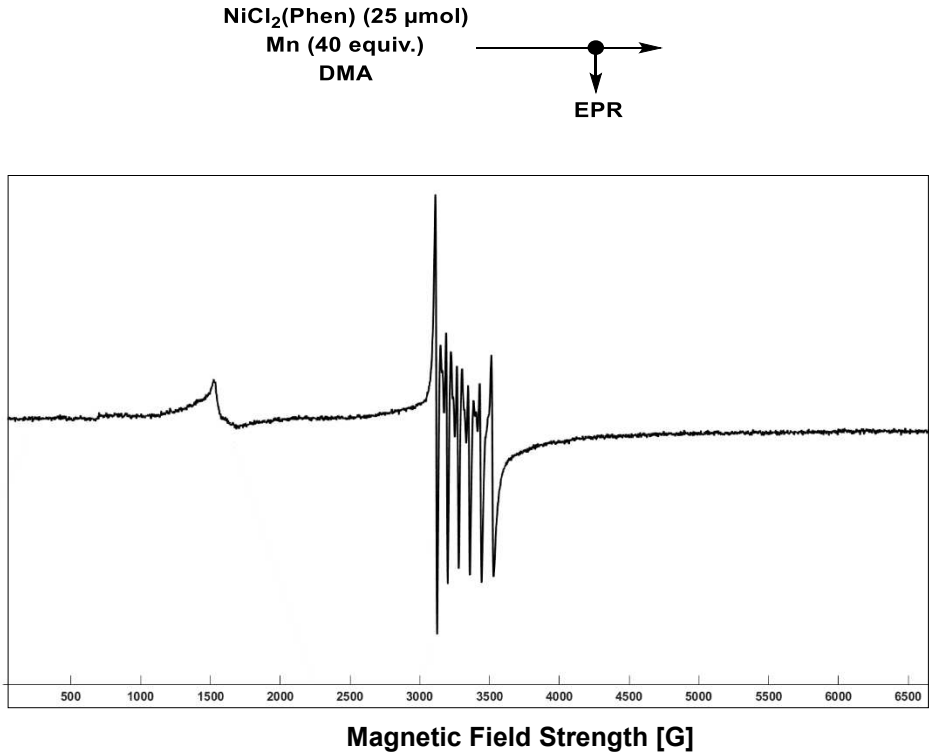

Figure 4-26: EPR spectrum (X-band, 9.299 GHz, DMA, 180 K) of Ni precatalyst and Mn in DMA.

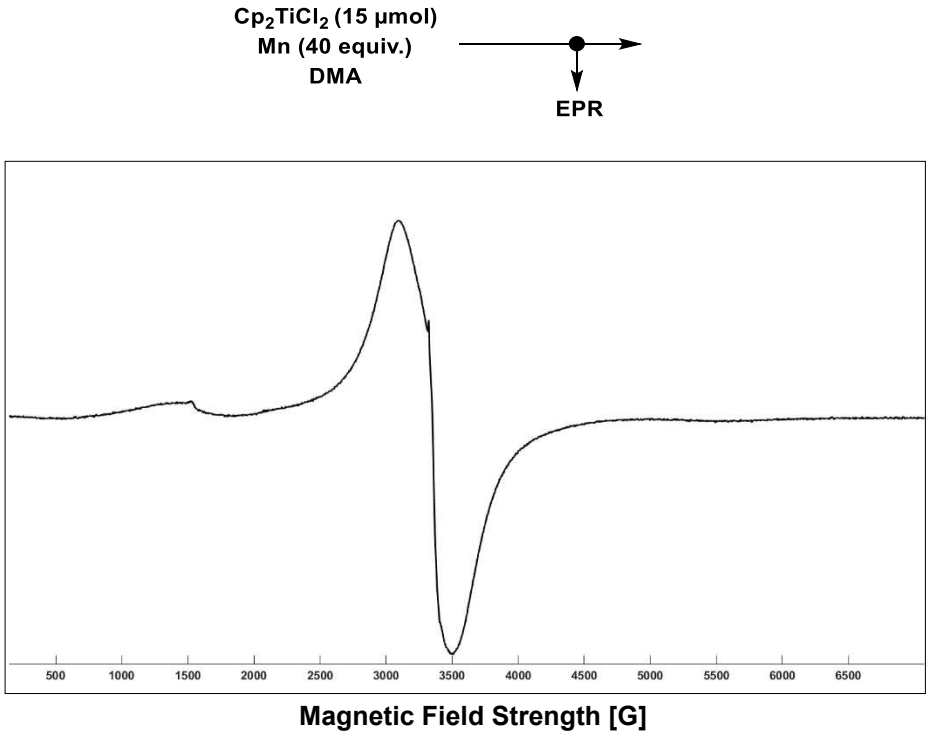

Figure 4-27: EPR spectrum (X-band, 9.299 GHz, DMA, 180 K) of Ti catalyst and Mn in DMA.

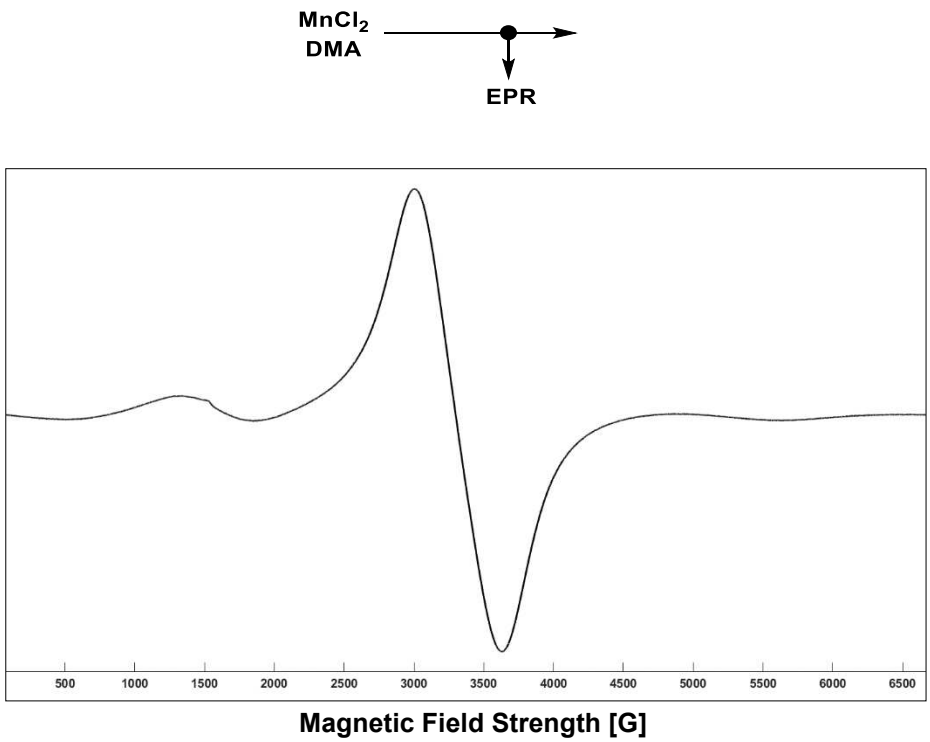

Figure 4-28: EPR spectrum (X-band, 9.301 GHz, DMA, 180 K) of $MnCl_2$ in DMA.

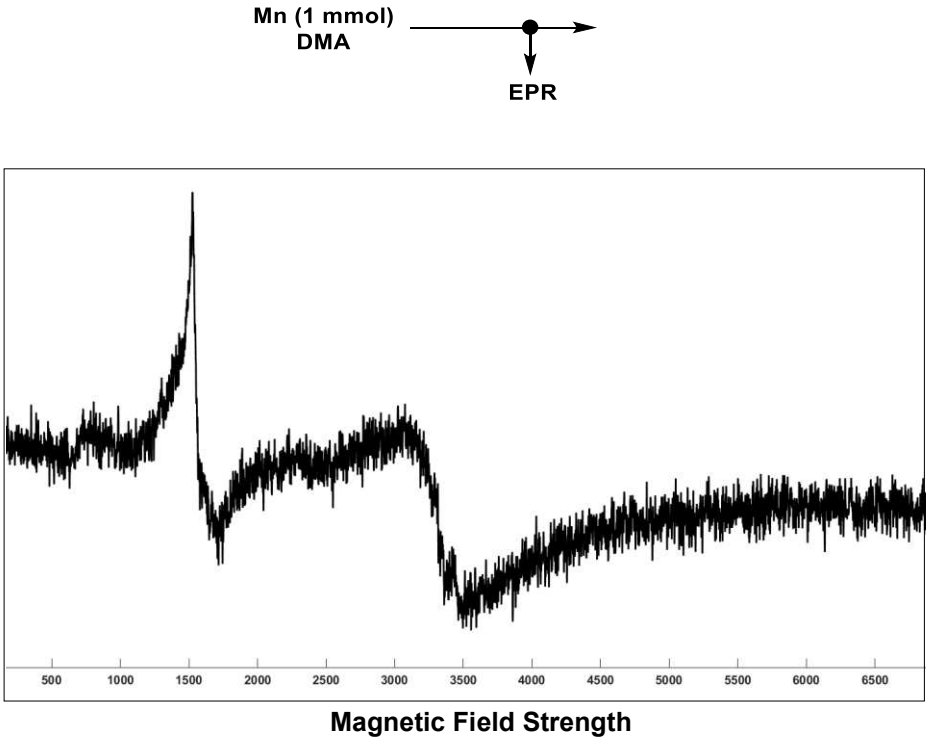

Figure 4-29: EPR spectrum (X-band, 9.299 GHz, DMA, 180 K) of Mn in DMA.

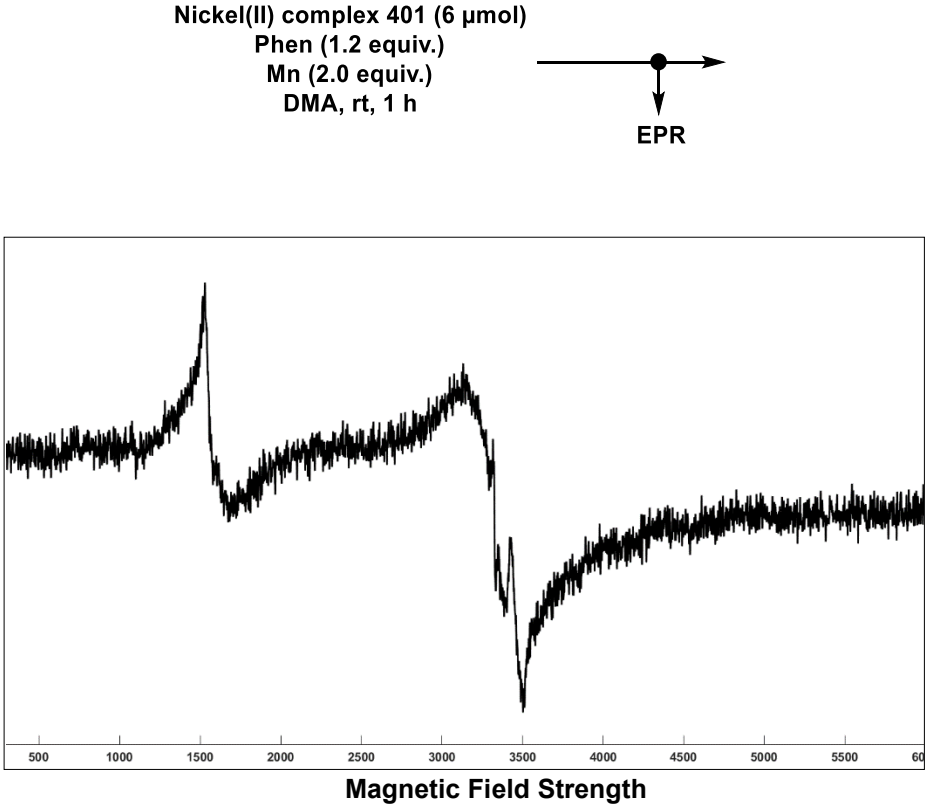

Figure 4-30: EPR spectrum after the reaction of nickel(II) complex **401** and Mn in DMA (X-band, 9.319 GHz, DMA, 180 K).

4.4.4.6 Role of Titanium Catalyst

4.4.4.6.1 Cross-Electrophile Coupling in the Absence of Titanium Catalyst

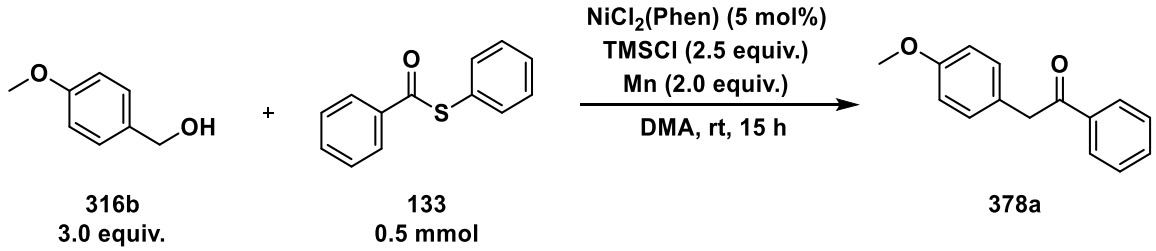

In a glovebox, a flame-dried Schlenk tube was charged with Mn powder (54.9 mg, 1.00 mmol, 2.0 equiv.). After removal from the glovebox, $NiCl_2$(Phen) (7.8 mg, 25 µmol, 5.0 mol%), *S*-phenyl benzothioate (**133**) (107 mg, 500 µmol, 1.0 equiv.), 4-methoxybenzyl alcohol (**316b**) (186 µL, 1.50 mmol, 3.0 equiv.) and TMSCl (159 µL, 1.25 mmol, 2.5 equiv.) were added successively. The mixture was stirred for 5 min and then abs. DMA (2 mL) was added. The reaction was stirred at rt for further 15 h. After the general sample preparation, quantitative GC-FID analysis gave the ketone **378a** in 27% yield.

4.4.4.6.2 Dependence of Thioester Conversion on Titanium Catalyst Loading

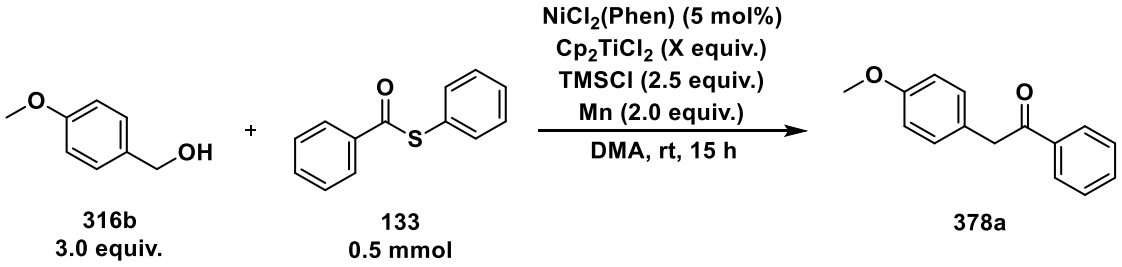

In a glovebox, a flame-dried Schlenk tube was charged with Mn powder (54.9 mg, 1.00 mmol, 2.0 equiv.) and the respective amount of titanocene dichloride (5.0 µmol–500 µmol, 0.01 equiv.–1.0 equiv., see Table 4-22). After removal from the glovebox, $NiCl_2$(Phen) (7.8 mg, 25 µmol, 5.0 mol%), *S*-phenyl benzothioate (**133**) (107 mg, 500 µmol, 1.0 equiv.), 4-methoxybenzyl alcohol (**316b**) (186 µL, 1.50 mmol, 3.0 equiv.) and TMSCl (159 µL, 1.25 mmol, 2.5 equiv.) were added successively. The mixture was stirred for 5 min and then abs. DMA (2 mL) was added. The reaction was stirred at rt for further 15 h. After the general sample preparation, the yields of ketone **378a** were determined by quantitative GC-FID analysis and are listed in Table 4-22.

Table 4-22: Amounts of titanocene dichloride. [a]: Determined by GC-FID using *n*-pentadecane as internal standard.

Amount of Cp_2TiCl_2			Yield of Ketone [%][a]
[mg]	[µmol]	[equiv.]	
0	0	0	31
1.2	5.0	0.01	79
2.5	10	0.02	79
3.7	15	0.03	83
6.2	25	0.05	78
8.7	35	0.07	64
12.5	50.0	0.1	64
24.9	100	0.2	42
49.8	200	0.4	38
87.1	350	0.7	35
124.5	500.0	1.0	9

4.4.4.6.3 Reaction of Alcohol or Chloride under Titanium Catalysis and Reductive Conditions

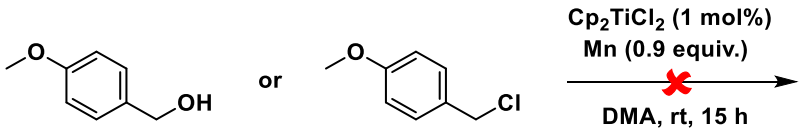

316b
1.1 mmol

317b
1.1 mmol

In a glovebox, a flame-dried Schlenk tube was charged with Mn powder (54.9 mg, 1.00 mmol, 0.9 equiv.) and titanocene dichloride (3.7 mg, 15 µmol, 1.0 mol%). After removal from the glovebox, 4-methoxybenzyl alcohol (**316b**) (137 µL, 1.10 mmol, 1.0 equiv.) or 4-methoxybenzyl chloride (**317b**) (161 µL, 1.10 mmol, 1.0 equiv.) were added *via* syringe pump over a time range of 5 min (27.4 µL/min resp. 32.1 µL/min). After stirring for 5 min and the addition of abs. DMA (2 mL) *via* syringe pump over a time range of 5 min (0.4 mL/min), the reaction was stirred at rt for further 15 h. GC-MS analysis revealed unreacted substrates in both reactions.

4.4.4.6.4 Conversion of Thioesters under Different Reaction Conditions

The subsequent sections describe experiments, in which thioester **140** was reacted under different reaction conditions. After the general sample preparation, the reaction mixtures were analyzed using GC-FID with *n*-pentadecane (PD) as internal standard and GC-MS, for which two different methods A and B were used (see section 4.4.1.3.3).

4.4.4.6.4.1 Conversion under Standard Conditions

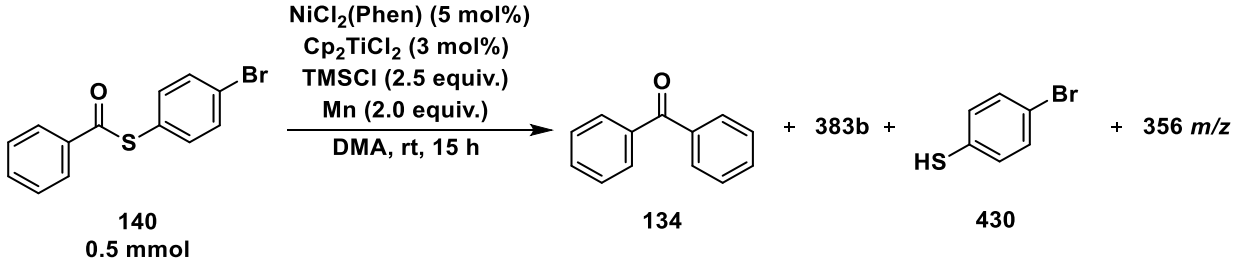

140
0.5 mmol

134

430

The reaction of thioester **140** under standard conditions was conducted analogously to GP-D. GC-MS analysis (method B, see section 4.4.1.3.3) showed complete conversion of thioester **140** to several products, including traces of benzophenone **134**, thioether **383b** and thiol **430**. Additionally, an uncharacterized compound with an exact mass of 356 *m/z* was detected.

Note: For both peaks at 20.898 and 21.108 min, the exact mass of 356 *m/z* was reported.

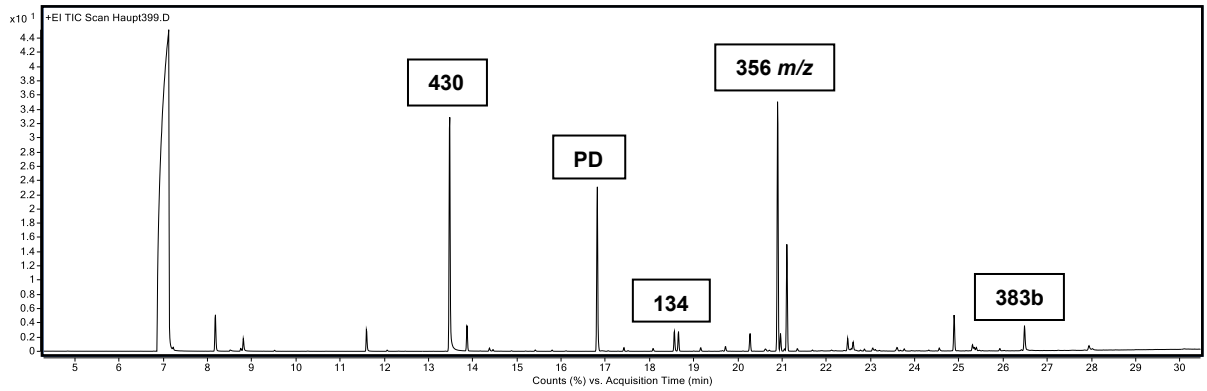

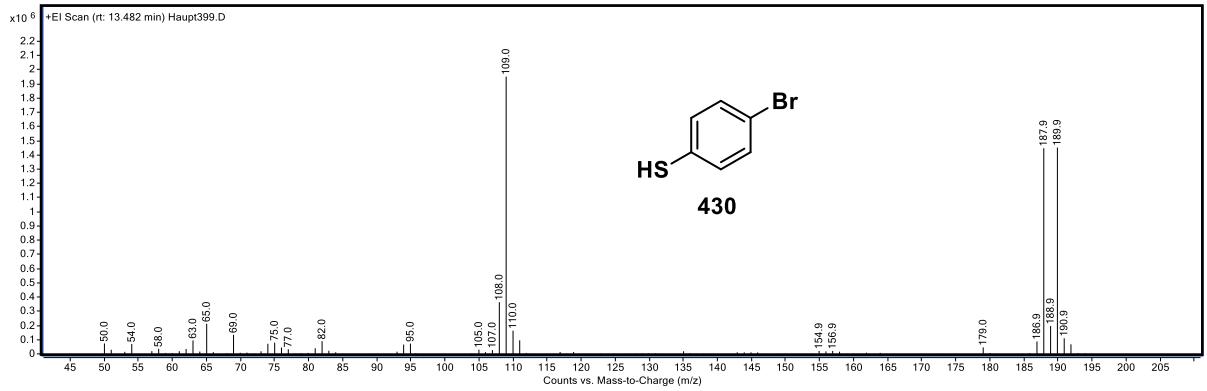

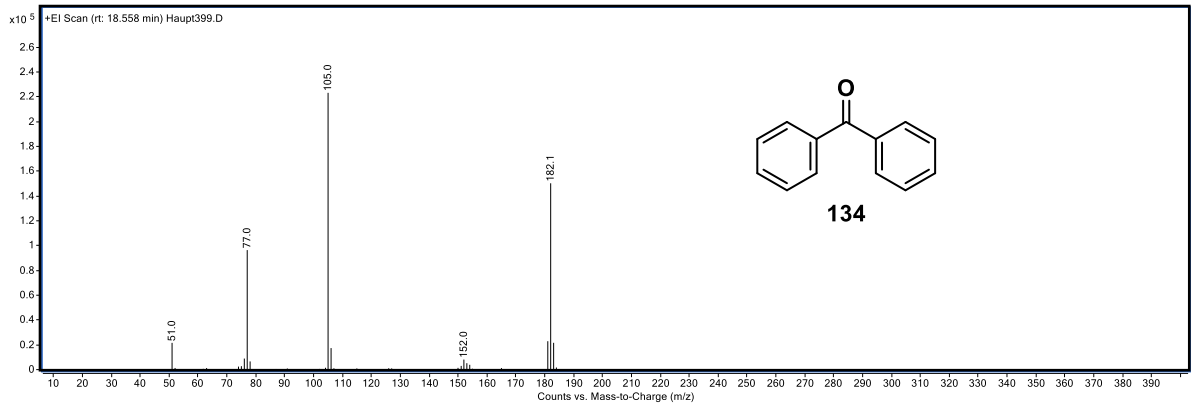
x10 5
+EI Scan (rt: 18.558 min) Haupt399.D
105.0
182.1
77.0
51.0
152.0
O
134
Counts vs. Mass-to-Charge (m/z)

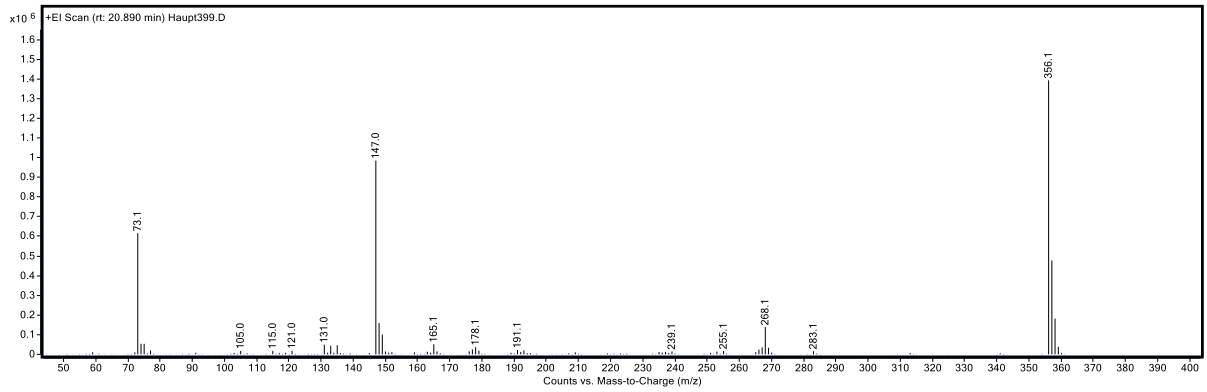
x10 6
+EI Scan (rt: 20.890 min) Haupt399.D
356.1
147.0
73.1
105.0
115.0
121.0
131.0
165.1
178.1
191.1
239.1
255.1
268.1
283.1
Counts vs. Mass-to-Charge (m/z)

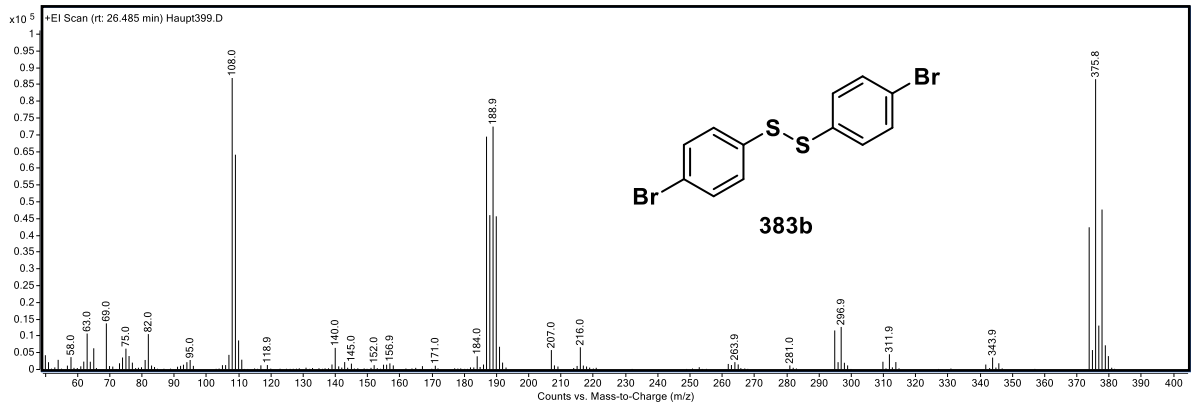
x10 5
+EI Scan (rt: 26.485 min) Haupt399.D
108.0
188.9
375.8
Br
S
S
Br
383b
Counts vs. Mass-to-Charge (m/z)

4.4.4.6.4.2 Synthesis of 1,2-Bis(4-bromophenyl)disulfane (383b)

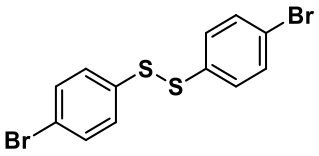

383b

The synthesis of 1,2-bis(4-bromophenyl)disulfane (**383b**) was performed by implementing thioester **140** with TMSCl and manganese under standard conditions as described in GP-D. After reaction completion, the mixture was filtered through a pad of silica gel with DCM as eluent. The filtrate was washed with aq. saturated NaCl (3 × 10 mL), dried over anhydrous $MgSO_4$ and concentrated under reduced pressure. Purification by column chromatography (PE/EtOAc 95:5) delivered the disulfide **383b** (23.7 mg, 63.0 µmol, 13%) as colorless crystals. The analytical data are in good agreement with the literature.[275]

$C_{12}H_8Br_2S_2$: 376.16 $\frac{g}{mol}$

R_f: 0.76 (Silica gel, PE/EtOAc 95:5, UV).

Melting point: 89.3–90.4 °C (PE/EtOAc).

^{1}H-NMR (400 MHz, $CDCl_3$): δ [ppm] = 7.45–7.41 (m, 4H), 7.35–7.32 (m, 4H).

^{13}C-NMR (101 MHz, $CDCl_3$): δ [ppm] = 135.9, 132.4, 129.6, 121.7.

GC-MS (EI): t_R = 11.01 min, *m/z* (Int. %) = 376 (14) $[M]^{+\bullet}$, 190 (49) $[M]^{+\bullet}$-$[C_6H_4BrS]^{\bullet}$, 109 (100) $[M]^{+\bullet}$-$[C_6H_4Br_2S]^{\bullet}$.

4.4.4.6.4.3 Conversion of Thioester under Ni/Ti Catalysis and Reductive Conditions

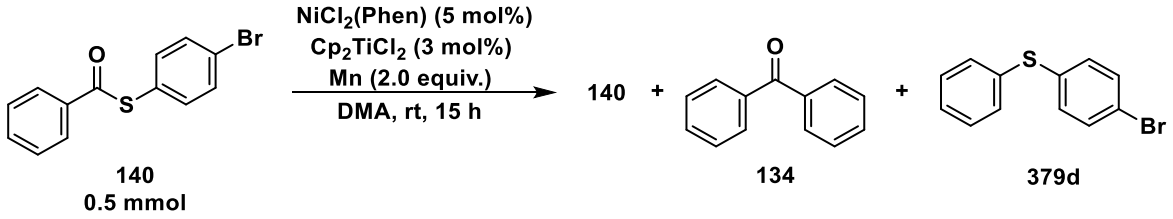

The reaction of thioester **140** in the absence of TMSCl was conducted analogously to GP-D. GC-MS analysis (method B, see section 4.4.1.3.3) showed not transformed thioester **140** (32% recovered starting material), benzophenone **134** (5% yield) and thioether **379d**.

In contrast, the reaction with *S*-phenyl benzothioate (**133**) as substrate was completely suppressed under these reaction conditions and no benzophenone (**134**) was formed.

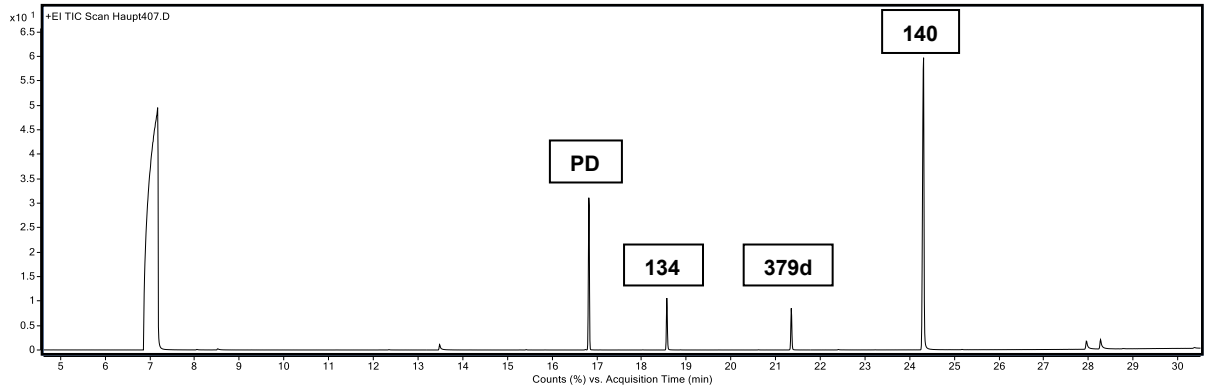

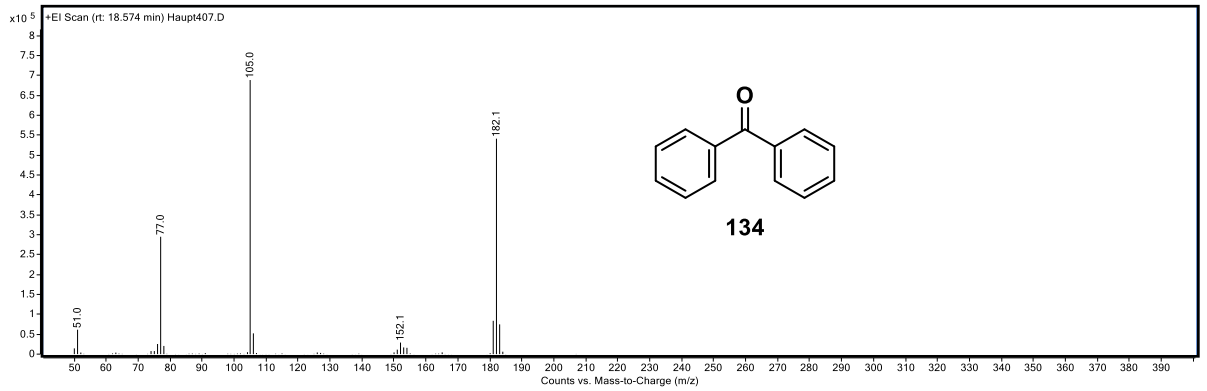

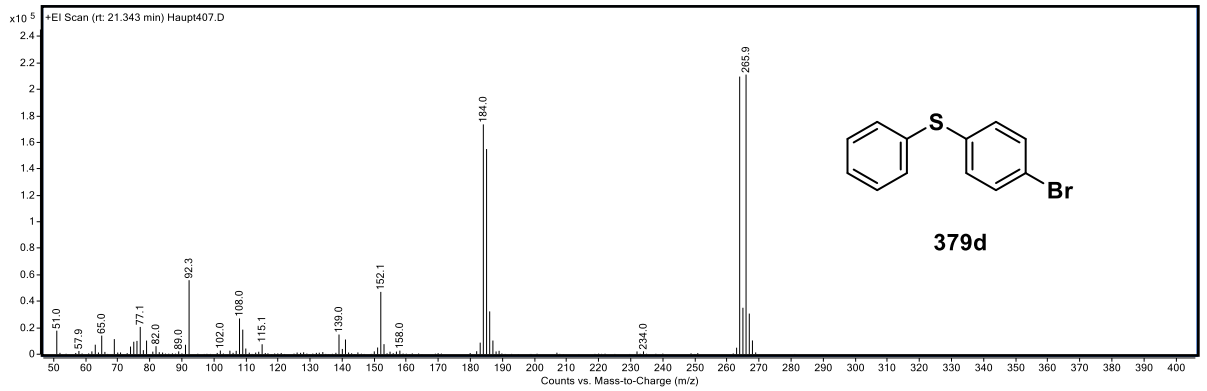

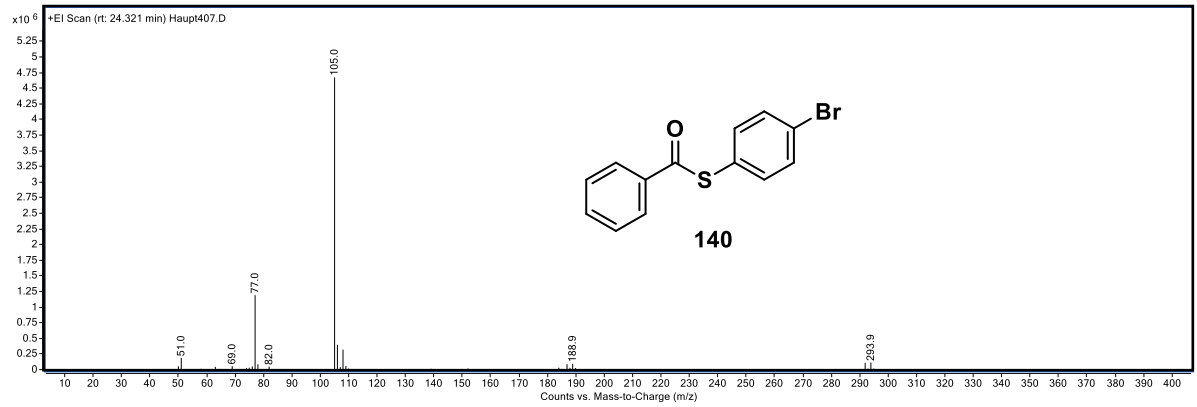

4.4.4.6.4.4 Synthesis of 1,2-Diphenylethane-1,2-dione (426)

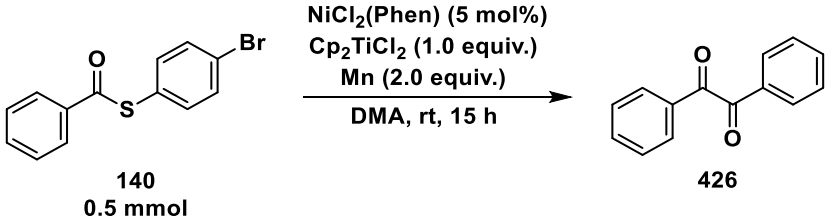

The synthesis of benzil **426** was conducted analogously to GP-D using Mn powder (54.9 mg, 1.00 mmol, 2.0 equiv.), Cp_2TiCl_2 (124 mg, 500 µmol, 1.0 equiv.), $NiCl_2$(Phen) (7.8 mg, 25 µmol, 5.0 mol%) and *S*-(4-bromophenyl) benzothioate (**140**) (146 mg, 500 µmol, 1.0 equiv.). After stirring at rt overnight, the mixture was filtered through a pad of silica gel with DCM as eluent. The filtrate was washed with aq. saturated NaCl (3 × 15 mL), dried over anhydrous $MgSO_4$ and concentrated under reduced pressure. Purification by column chromatography (PE/EtOAc 95:5) delivered the product **426** (20.0 mg, 100 µmol, 20%) as a yellow solid. The analytical data are in good agreement with the literature.[276]

$C_{14}H_{10}O_2Si$: 210.23 $\frac{g}{mol}$

R_f: 0.51(Silica gel, PE/EtOAc 95:5, UV).

Melting point: 86.6–86.9 °C (DCM).

^{1}H-NMR (400 MHz, $CDCl_3$): δ [ppm] = 8.03–7.97 (m, 4H), 7.68–7.64 (m, 2H), 7.54–7.47 (m, 4H).

^{13}C-NMR (101 MHz, $CDCl_3$): δ [ppm] = 194.7, 135.0, 133.1, 130.1, 129.2.

GC-MS (EI): t_R = 8.09 min, *m/z* (Int. %) = 210 (35) $[M]^{+\bullet}$, 105 (100) $[M]^{+\bullet}$-$[C_7H_5O]^{\bullet}$, 77 (46) $[M]^{+\bullet}$-$[C_8H_5O_2]^{\bullet}$.

Note: In this reaction, GC-MS method A was used (see section 4.4.1.3.3).

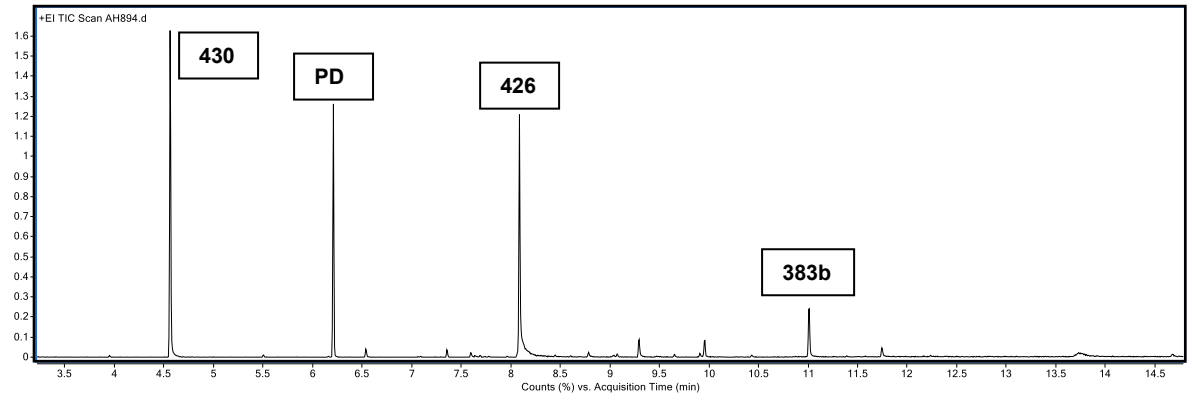

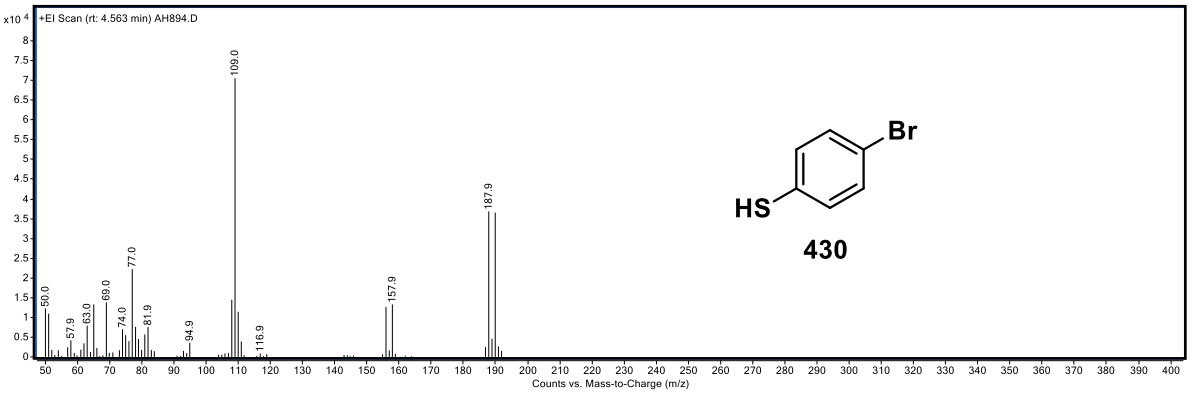

430

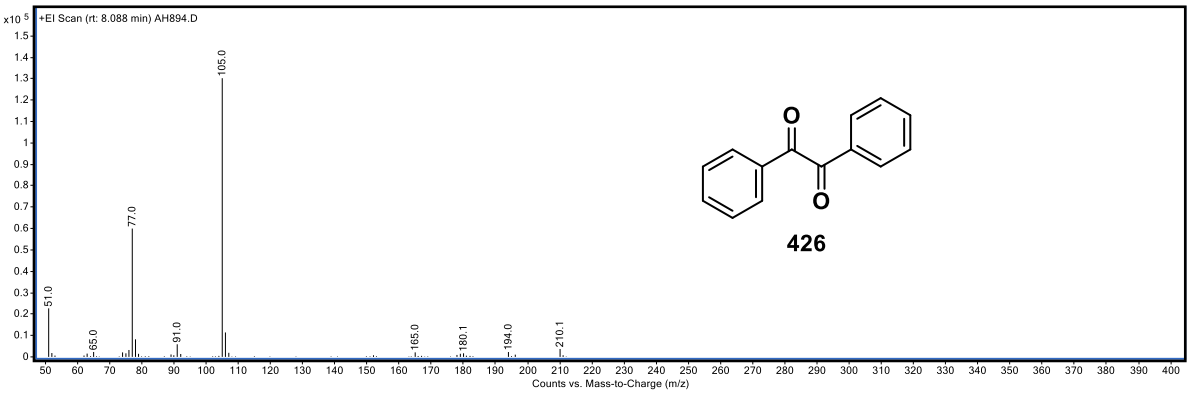

426

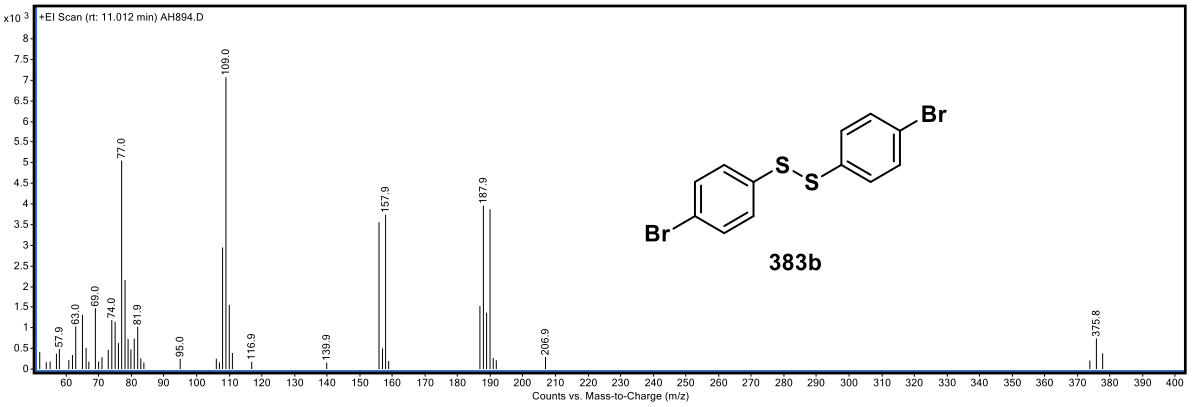

383b

4.4.4.6.4.5 Acyl Radical Trapping

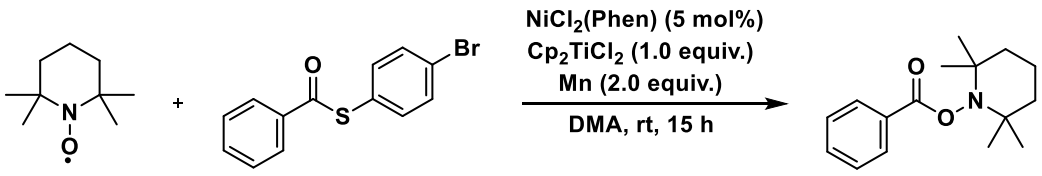

406
0.5 mmol

140
1.1 equiv.

427

In a glovebox, a flame-dried Schlenk tube was charged with Mn powder (54.9 mg, 1.00 mmol, 2.0 equiv.) and titanocene dichloride (124 mg, 500 µmol, 1.0 equiv.). After removal from the glovebox, $NiCl_2$(Phen) (7.8 mg, 25 µmol, 5.0 mol%), *S*-(4-bromophenyl) benzothioate (**140**) (161 mg, 550 µmol, 1.1 equiv.) and TEMPO (78.1 mg, 500 µmol, 1.0 equiv.) were added successively. After stirring for 5 min and the addition of abs. DMA (2 mL) *via* syringe pump over a time range of 5 min (0.4 mL/min), the reaction was stirred at rt for further 15 h. Then, the mixture was filtered through a pad of silica gel with DCM as eluent. The filtrate was washed with aq. saturated NaCl (3 × 15 mL), dried over anhydrous $MgSO_4$ and concentrated under reduced pressure. HPLC-HR-MS of the crude product revealed the formation of TEMPO adduct **427**.

$C_{16}H_{23}NO_2$: 261.37 $\frac{\mathrm{g}}{\mathrm{mol}}$

HPLC-HR-MS (ESI): *m/z* = $[M+H]^+$ calc. for $C_{16}H_{24}NO_2$ 262.18016, found 262.17990.

4.4.4.6.4.6 Further Combinations of Reaction Conditions

Thioester **140** is completely stable in the presence of TMSCl under SFRC or in DMA (Scheme 4-64A, B), and was almost completely recovered under nickel catalysis and reductive conditions (Scheme 4-64C).

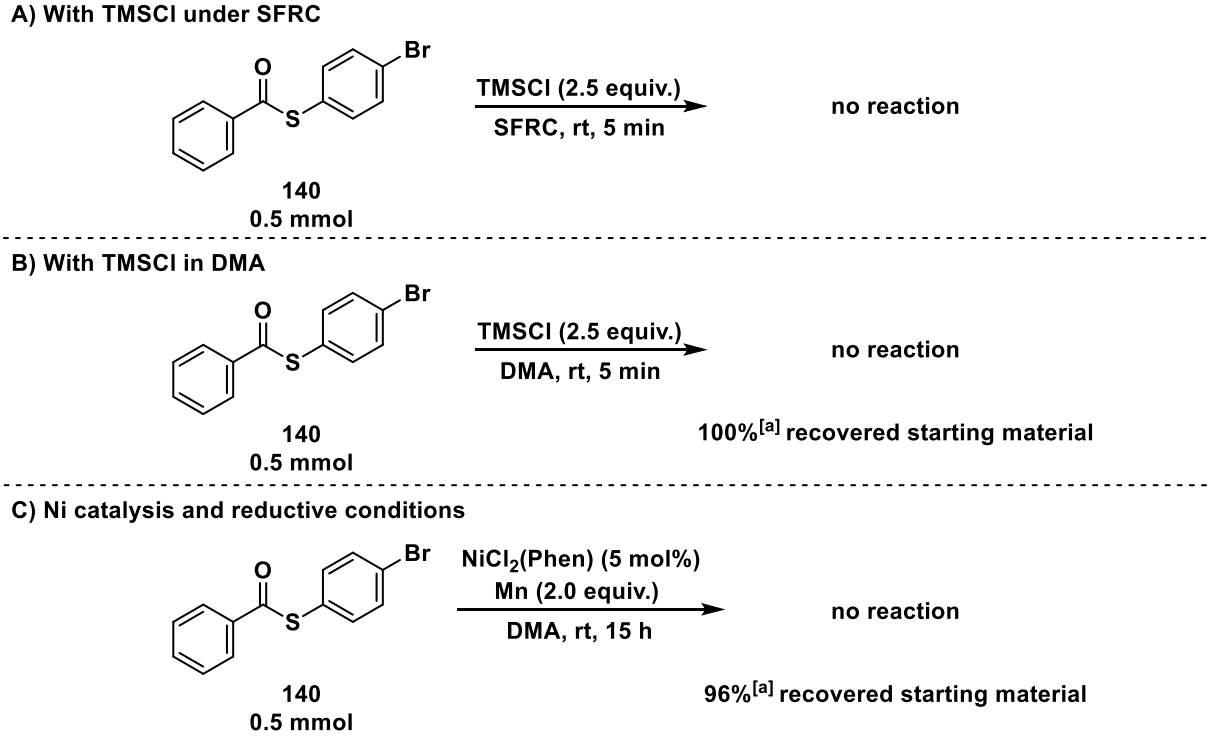

Scheme 4-64: Stability tests of thioester **140** under Lewis acidic conditions. [a]: Determined by GC-FID using *n*-pentadecane as internal standard.

Further reactions of thioester **140** under different reaction conditions are shown in Scheme 4-65. With nickel catalyst, TMSCl as additive and reductive conditions, thioester **140** reacted completely to form several products, including disulfide **383b** as main product and benzophenone (**134**) in traces (Scheme 4-65A). Additionally, a compound with an exact mass of 356 *m/z* was detected. Using titanium catalyst, TMSCl as an additive and reductive conditions, 59% of thioester **140** was recovered and disulfide **383b** as well as an uncharacterized byproduct with an exact mass of 390 *m/z* were generated (Scheme 4-65B). The same products, but in lower proportions, were already observed with titanium catalyst and reductive conditions, illustrating the additional activation of the manganese surface by TMSCl (Scheme 4-65C). With Cp_2TiCl_2 as additive and manganese as reducing agent, a complete conversion of thioester **140** to several products was observed, amongst others thiol **430** and disulfide **383b** as the main products (Scheme 4-65D). An uncharacterized compound with an exat mass of 167 *m/z* was also found. With TMSCl as an additive and manganese, 24% of thioester **140** were recovered and several products were formed, including disulfide **383b** as well as two uncharacterized compounds with an exact mass of 207 *m/z* and 353 *m/z* (Scheme 4-65E).

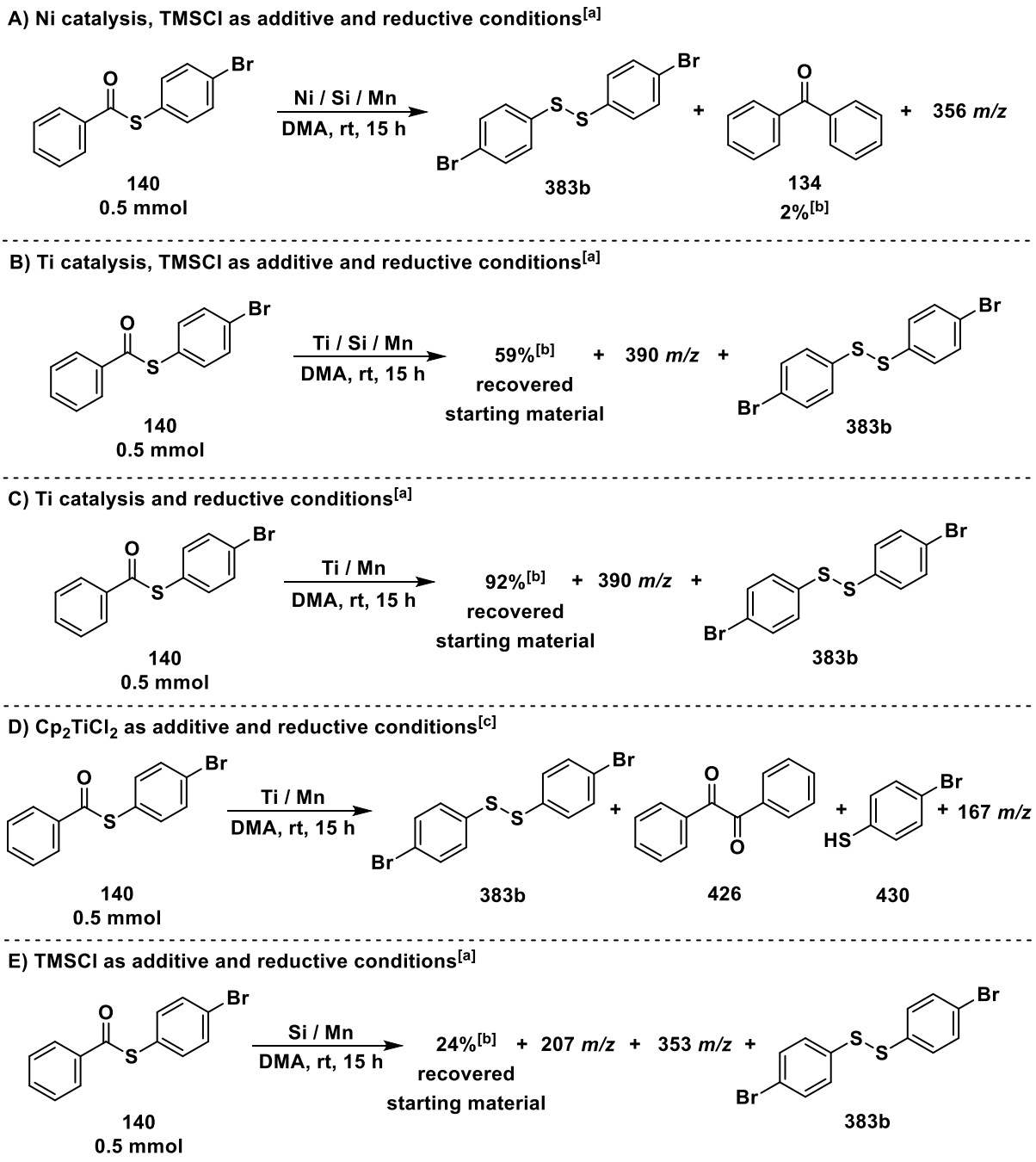

Scheme 4-65: Implementation of thioester **140** under different reaction conditions. [a]: Reaction conditions for Ni / Ti / Si / Mn: $NiCl_2$(Phen) (5 mol%), Cp_2TiCl_2 (3 mol%), TMSCl (2.5 equiv.), Mn (2.0 equiv.); [b]: Determined by GC-FID using *n*-pentadecane as internal standard; [c]: Reaction conditions: Cp_2TiCl_2 (1.0 equiv.), Mn (2.0 equiv.).

Note: The subsequent reactions were measured with GC-MS method B (see section 4.4.1.3.3). The MS spectra of thioester **140**, thioether **383b** and thiol **430** correspond to those in section 4.4.11.4.1 and are not depicted. However, the compounds are labeled in the total ion chromatogram.

A) Ni catalysis, TMSCl as additive and reductive conditions

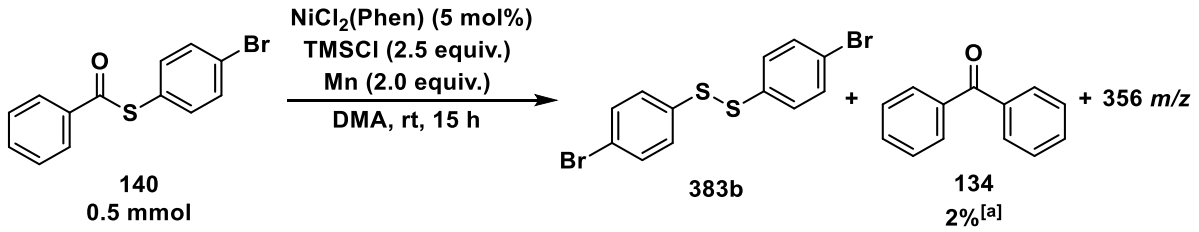

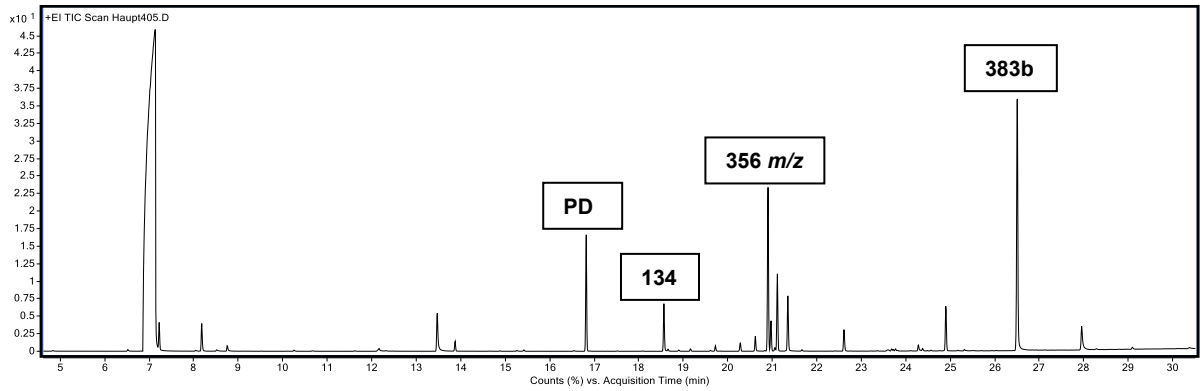

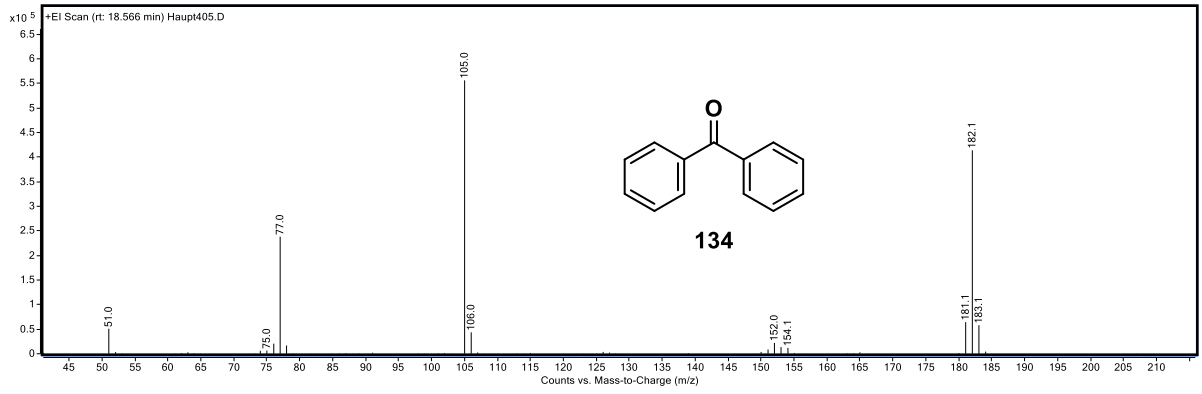

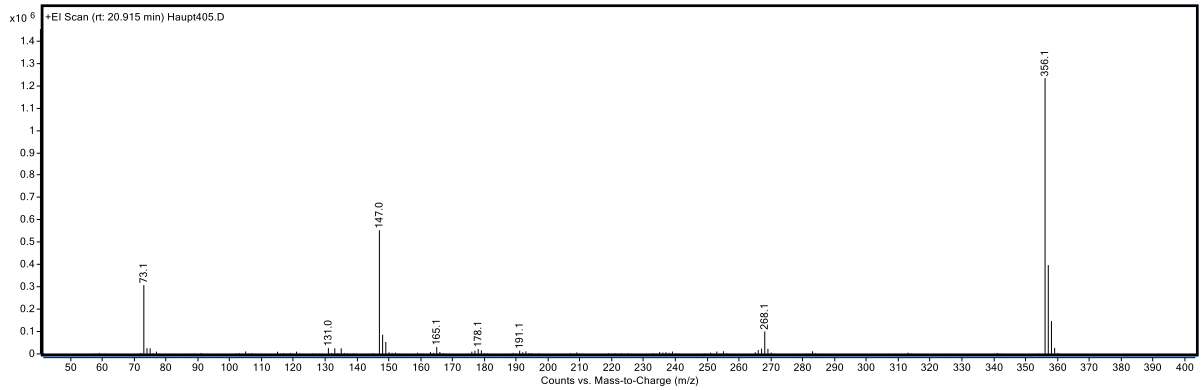

B) Ti catalysis, TMSCl as additive and reductive conditions

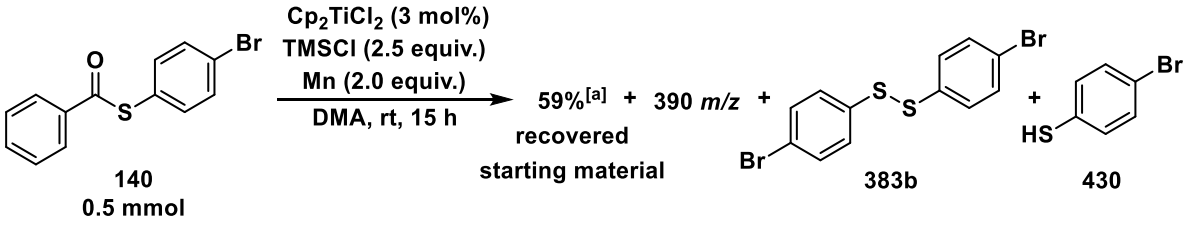

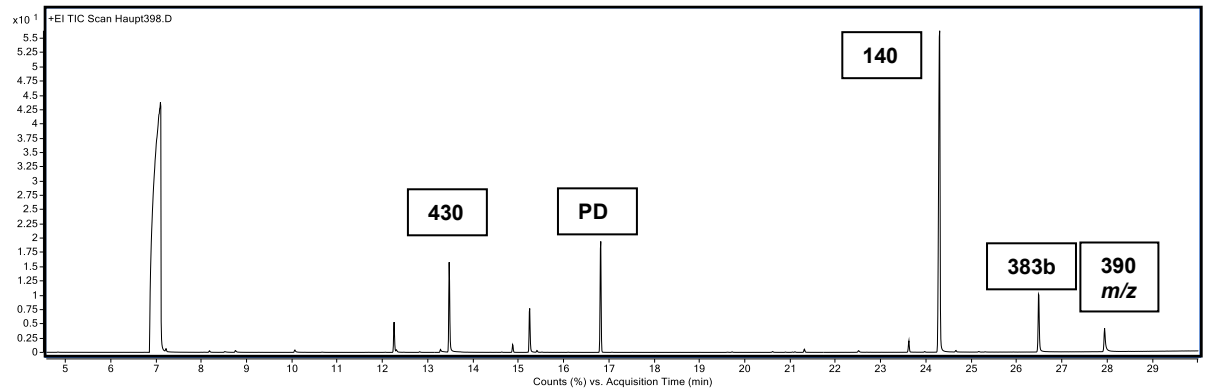

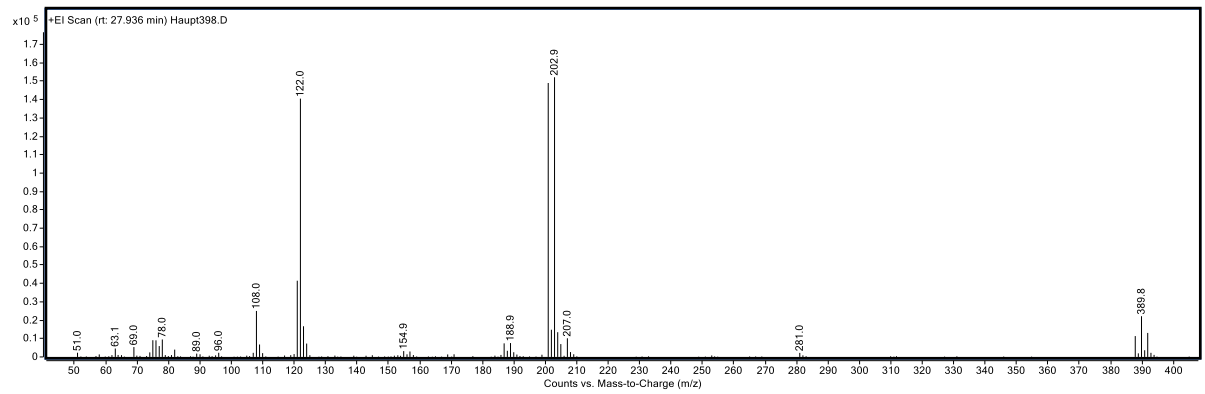

C) Ti catalysis and reductive conditions

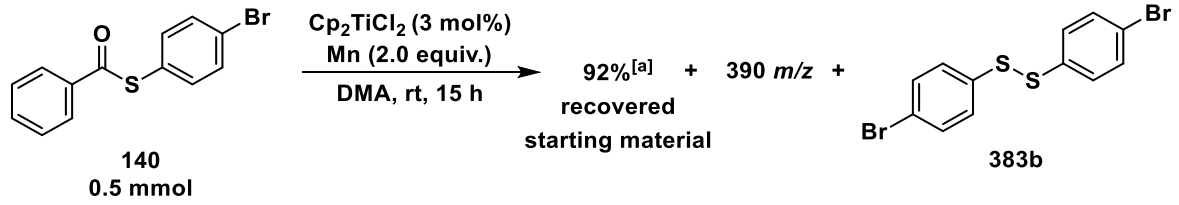

140
0.5 mmol

383b

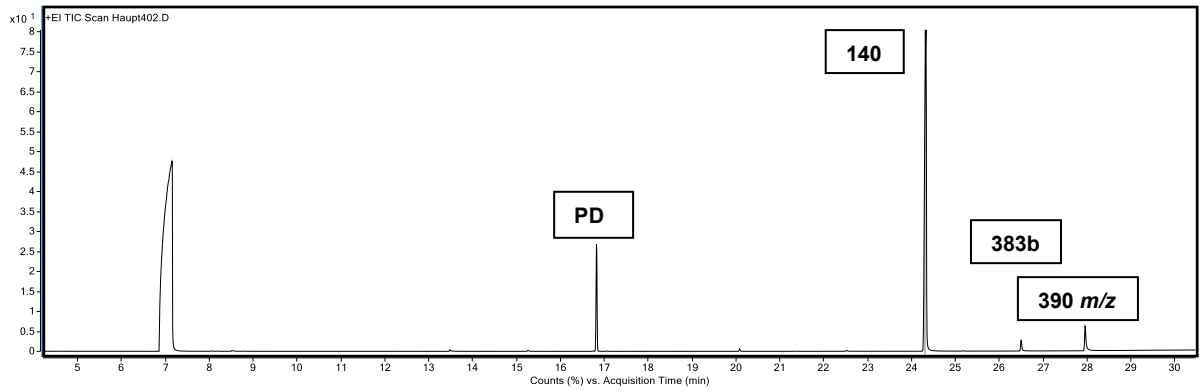

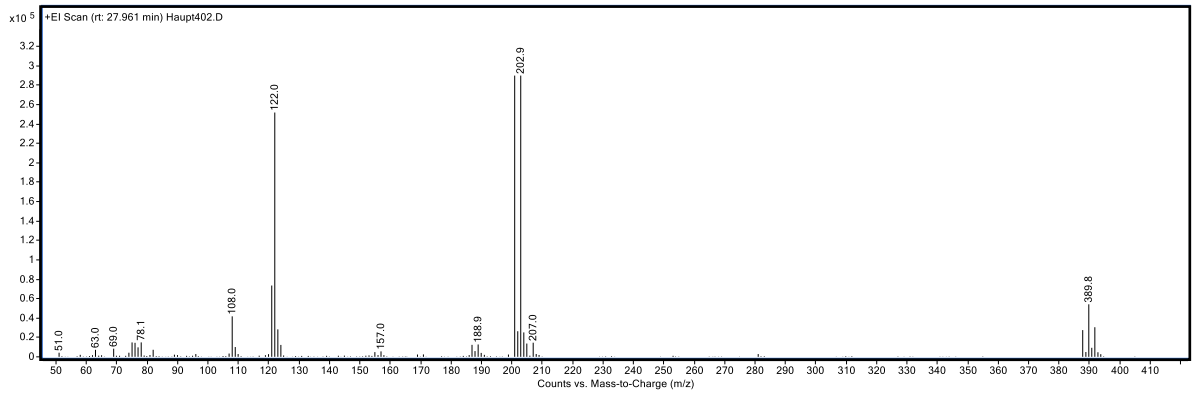

D) Cp_2TiCl_2 as additive and reductive conditions

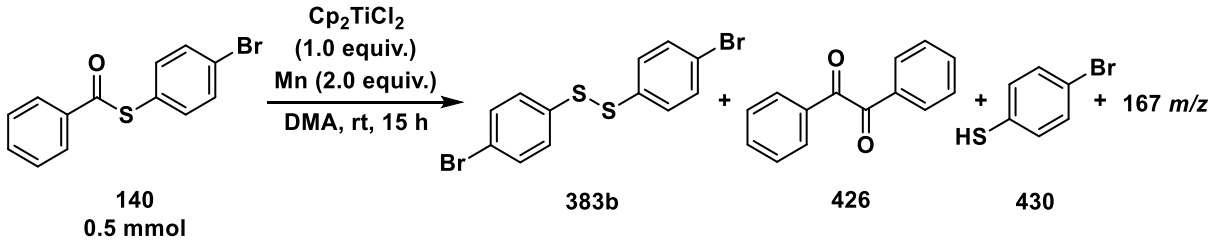

140
0.5 mmol

383b

426

430

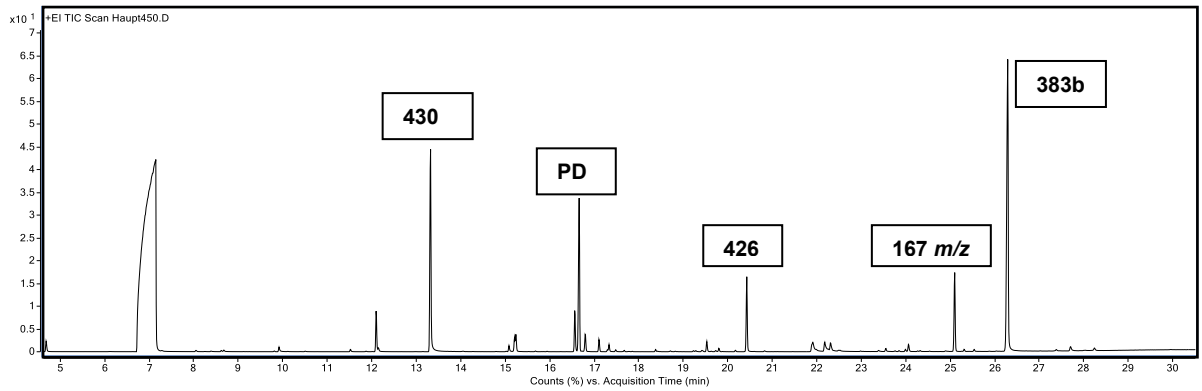

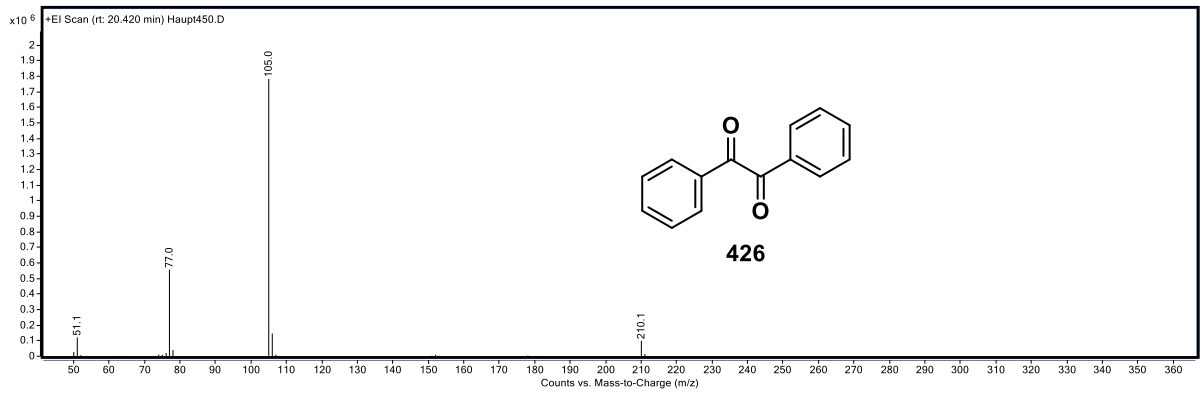

426

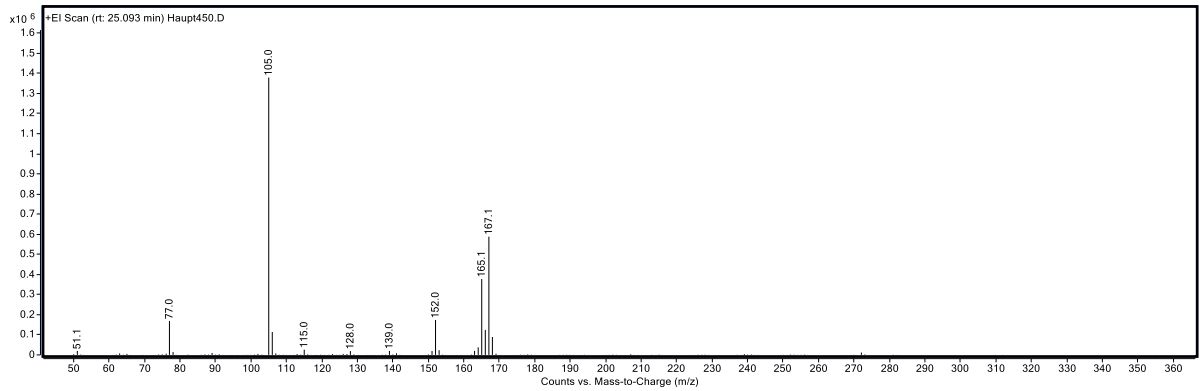

E) TMSCl as additive and reductive conditions

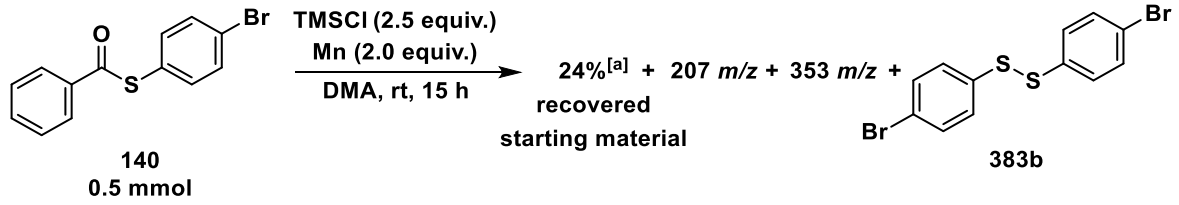

140
0.5 mmol

383b

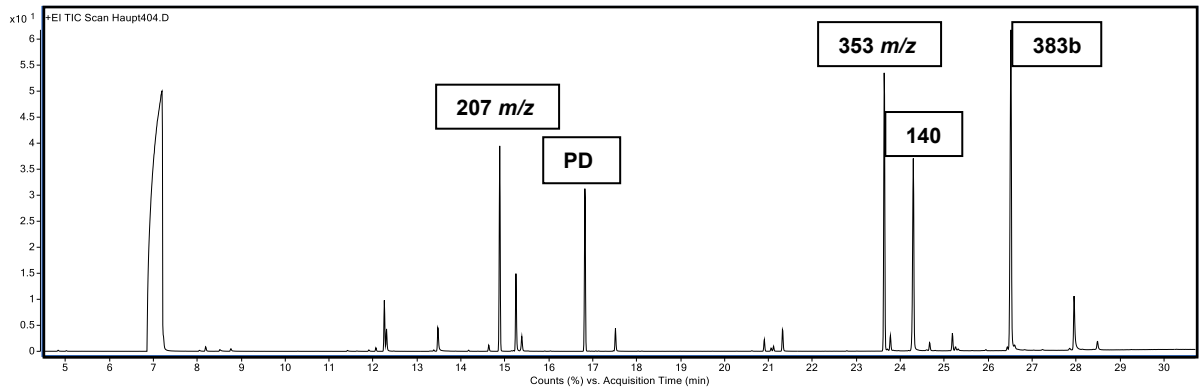

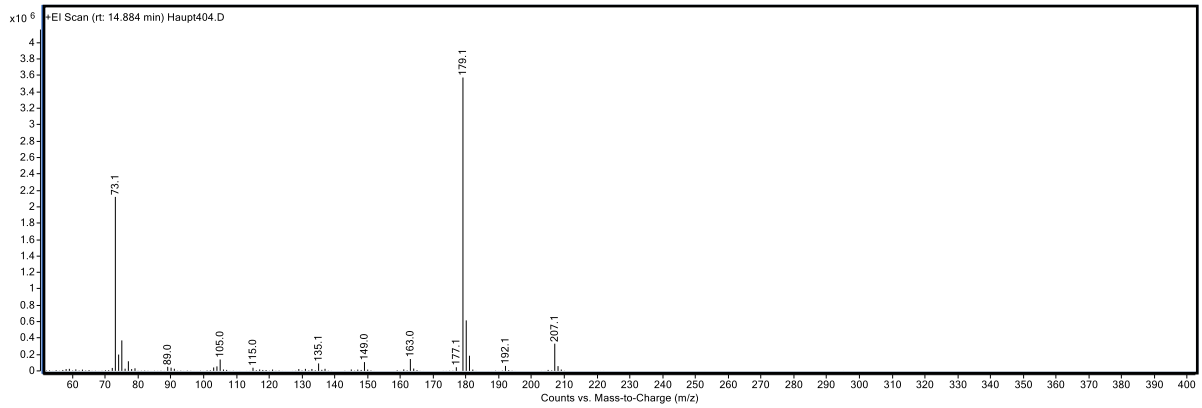

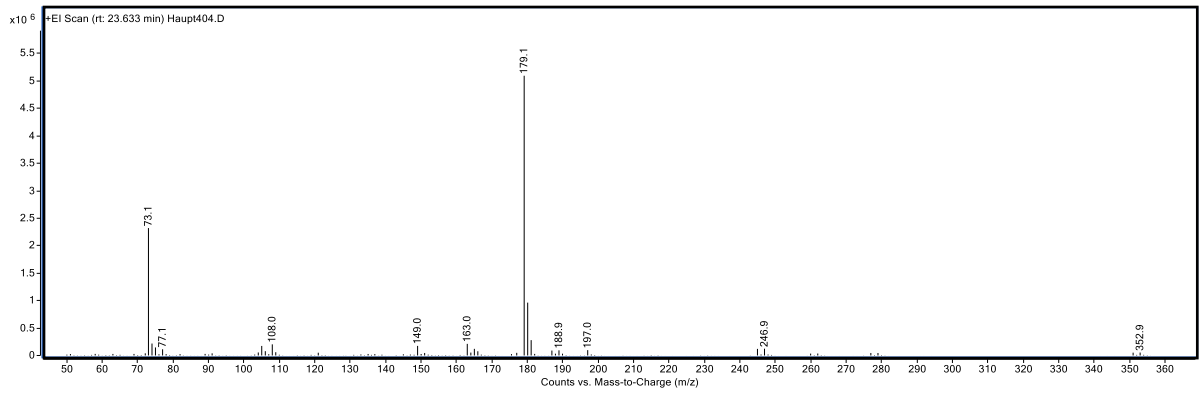

4.4.4.6.4.7 Activation of *S*-Phenyl Benzothioate (133) by Titanium Catalyst

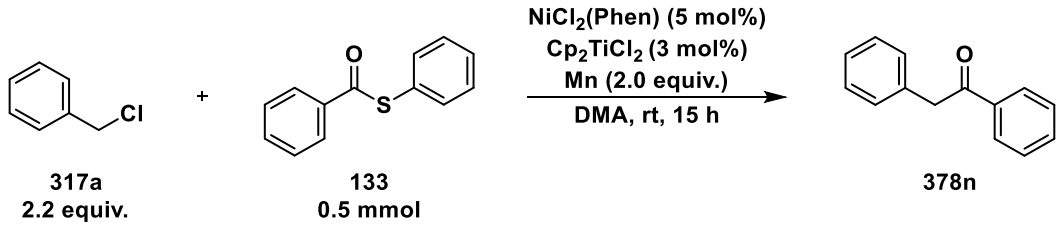

In a glovebox, a flame-dried Schlenk tube was charged with Mn powder (54.9 mg, 1.00 mmol, 0.9 equiv.) and titanocene dichloride (3.7 mg, 15 µmol, 3.0 mol%). After removal from the glovebox, $NiCl_2$(Phen) (7.8 mg, 25 µmol, 5.0 mol%), *S*-phenyl benzothioate (**133**) (107 mg, 500 µmol, 1.0 equiv.) and TMSCl (159 µL, 1.25 mmol, 2.5 equiv.) were added successively. Benzyl chloride (**317a**) (127 µL, 1.10 mmol, 1.0 equiv.) was added *via* syringe pump over a time range of 5 min (25.4 µL/min). The mixture was stirred for 5 min and then abs. DMA (2 mL) was added *via* syringe pump over a time range of 5 min (0.4 mL/min). The reaction was stirred at rt for further 15 h and then filtered through a pad of silica gel with DCM as eluent. The filtrate was washed with aq. saturated $NaHCO_3$ (2 × 10 mL) and aq. saturated NaCl (2 × 10 mL), dried over anhydrous $MgSO_4$ and concentrated under reduced pressure. Purification by column chromatography (PE/EtOAc 95:5) delivered the product **378n** (22.9 mg, 120 µmol, 23%) as colorless crystals. The analytical data are in good accordance with the literature and to the analytical data listed in section 4.4.3.2.2.[263]

$C_{14}H_{12}O$: 196.25 $\frac{\mathrm{g}}{\mathrm{mol}}$

^{1}H-NMR (400 MHz, $CDCl_3$): δ [ppm] = 8.03–7.99 (m, 2H), 7.58–7.53 (m, 1H), 7.48–7.44 (m, 2H), 7.35–7.23 (m, 5H), 4.29 (s, 2H).

^{13}C-NMR (101 MHz, $CDCl_3$): δ [ppm] = 197.7, 136.8, 134.7, 133.3, 129.6, 128.82, 128.79, 128.77, 127.0, 45.6.

4.4.5 Calibration Data for GC-FID
S-(phenyl) benzothioate (133)

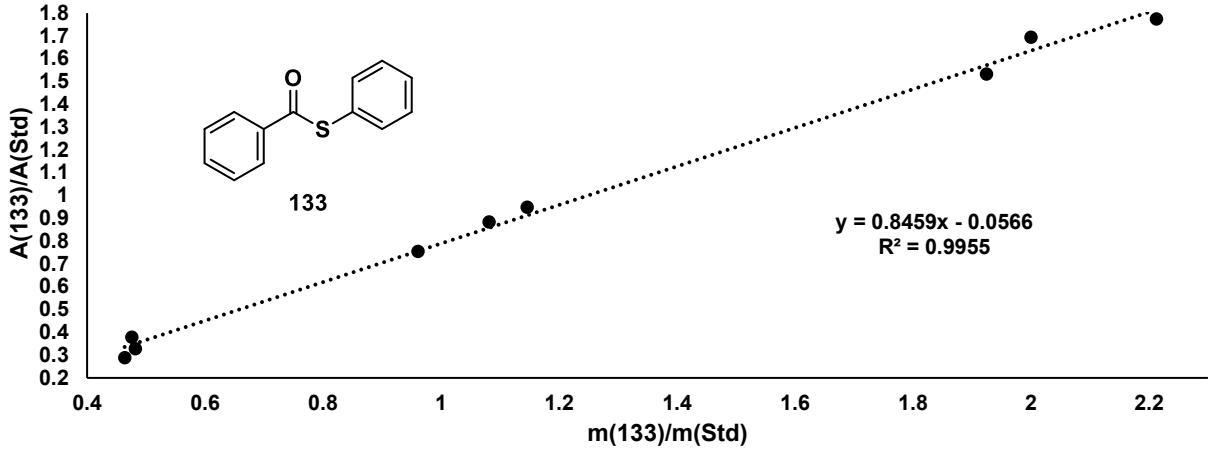

Mass ratio [mg(133)/mg(Std)]	A(133)	A(Std)	Area ratio [A(133)/A(Std)]
1.1	11462	12088	0.9482
1.1	10831	12263	0.8833
1.0	11816	15658	0.7546
2.0	20626	12173	1.6944
2.2	22873	12895	1.7738
1.9	22566	14730	1.5320
0.5	9399.0	28731	0.3271
0.5	8004.1	27695	0.2890
0.5	11797	31149	0.3787

S-(4-bromophenyl) benzothioate (140)

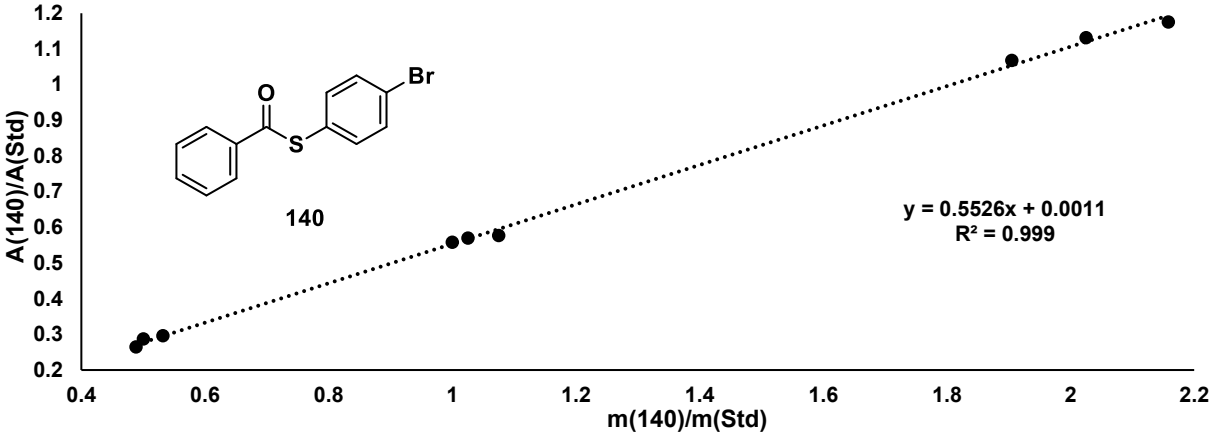

Mass ratio [mg(140)/mg(Std)]	A(140)	A(Std)	Area ratio [A(140)/A(Std)]
1.1	6672.4	11576	0.5764
1.0	5776.6	10349	0.5582
1.0	6283.7	11030	0.5697
1.9	12355	11571	1.0678
2.2	13237	11262	1.1754
2.0	12439	10995	1.1314
0.5	6332.3	22099	0.2865
0.5	6469.8	21834	0.2963
0.5	6148.6	23234	0.2646

4-methoxybenzyl alcohol (316b)

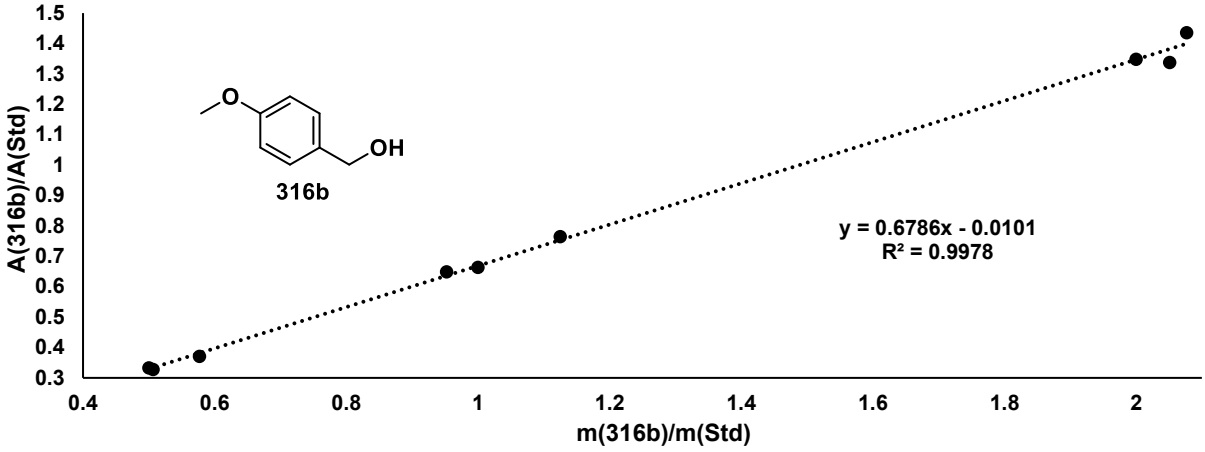

Mass ratio [mg(316b)/mg(Std)]	A(316b)	A(Std)	Area ratio [A(316b)/A(Std)]
1.0	7400.9	11416	0.6483
1.1	7948.5	10394	0.7647
1.0	7768.1	11705	0.6637
2.1	13945	10426	1.3376
2.0	14135	10481	1.3486
2.1	14936	10404	1.4355
0.5	7937.0	24229	0.3276
0.5	7353.7	22057	0.3334
0.6	9266.9	24974	0.3711

4-methoxybenzyl chloride (317b)

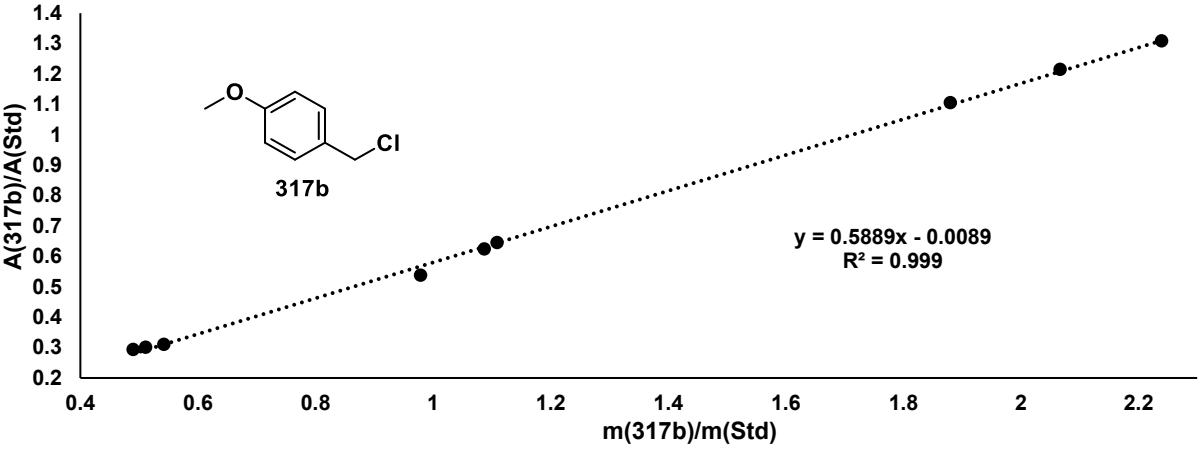

Mass ratio [mg(317b)/mg(Std)]	A(317b)	A(Std)	Area ratio [A(317b)/A(Std)]
1.1	11880	19042	0.6239
1.0	10370	19277	0.5379
1.1	12082	18729	0.6451
2.1	22817	18786	1.2146
1.9	23173	20969	1.1051
2.2	25380	19393	1.3088
0.5	12282	39523	0.3108
0.5	11362	38764	0.2931
0.5	11495	38208	0.3009

2-(4-methoxyphenyl)-1-phenylethan-1-one (378a)

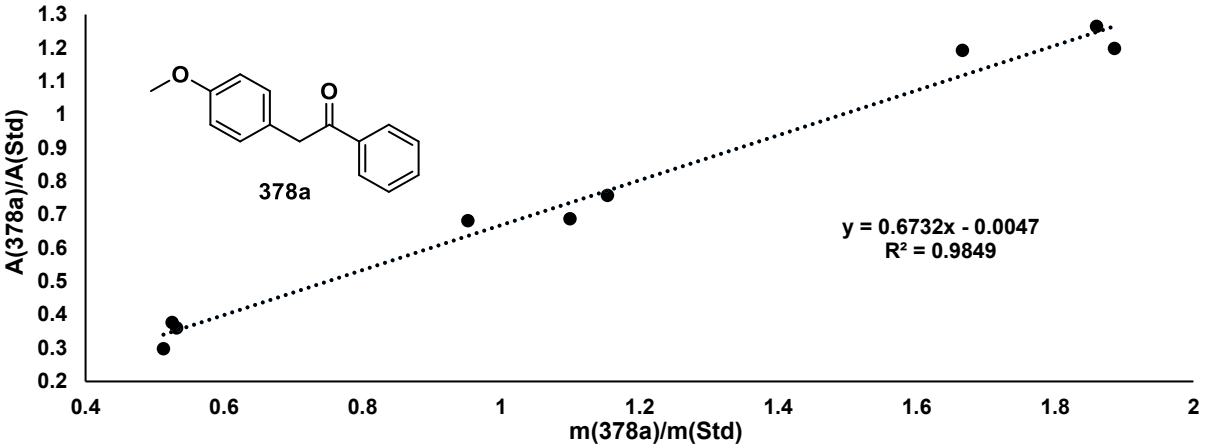

Mass ratio [mg(378a)/mg(Std)]	A(378a)	A(Std)	Area ratio [A(378a)/A(Std)]
1.1	8552.2	12433	0.6879
1.2	7954.3	10497	0.7577
1.0	8225.6	12074	0.6813
1.9	17703	14773	1.1984
1.7	14579	12229	1.1922
1.9	14344	11346	1.2642
0.5	9322.9	24738	0.3769
0.5	7236.1	20073	0.3605
0.6	6580.3	22122	0.2975

1,2-diphenylethan-1-one (378n)

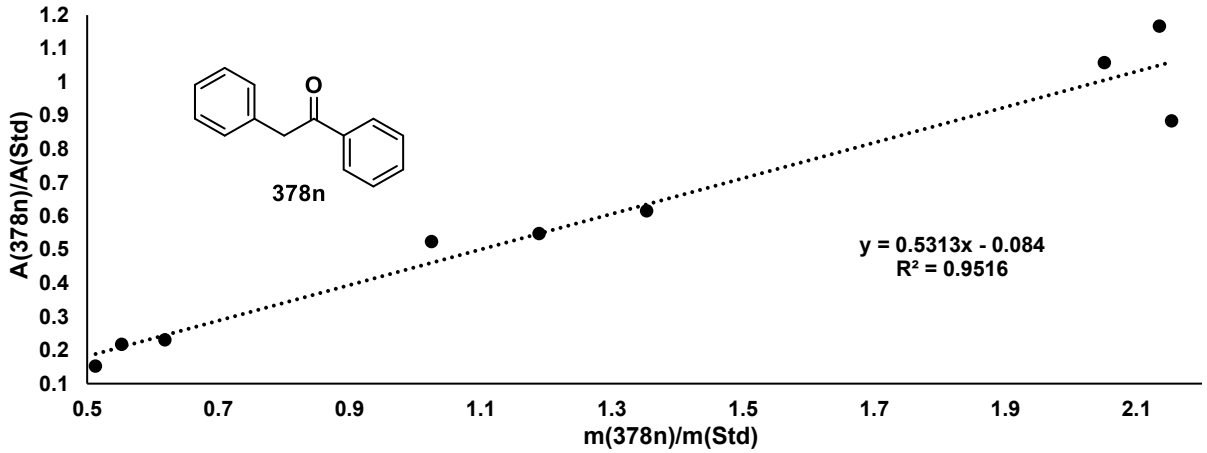

Mass ratio [mg(378n)/mg(Std)]	A(378n)	A(Std)	Area ratio [A(378n)/A(Std)]
1.0	5915.5	11287	0.5241
1.4	5799.0	9415.1	0.6159
1.2	5875.6	10706	0.5488
2.1	11941	10226	1.1677
2.1	9587.8	10841	0.8844
2.0	11346	10714	1.0589
0.6	4556.9	20893	0.2181
0.6	4822.9	20863	0.2312
0.5	3449.1	22552	0.1529

(4-methoxybenzyl)(phenyl)sulfane (379a)

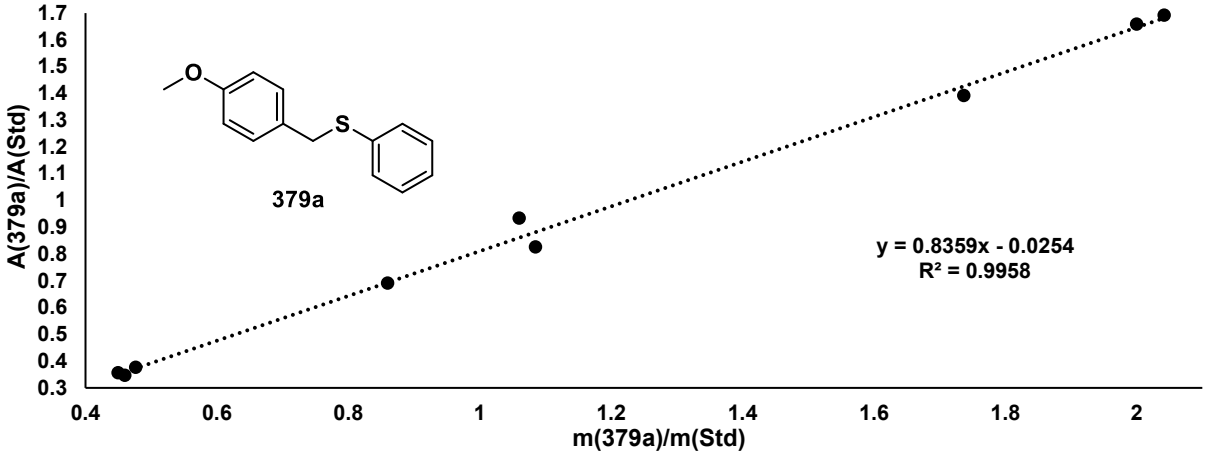

Mass ratio [mg(379a)/mg(Std)]	A(379a)	A(Std)	Area ratio [A(379a)/A(Std)]
1.1	12948	15664	0.8266
1.0	11184	11978	0.9337
0.9	10354	14995	0.6905
2.0	20790	12534	1.6587
1.7	20267	14562	1.3918
2.0	20851	12323	1.6921
0.5	9946.6	28711	0.3464
0.5	10479	29434	0.3560
0.5	10583	28146	0.3759

(4-bromophenyl)(4-methoxybenzyl)sulfane (379b)

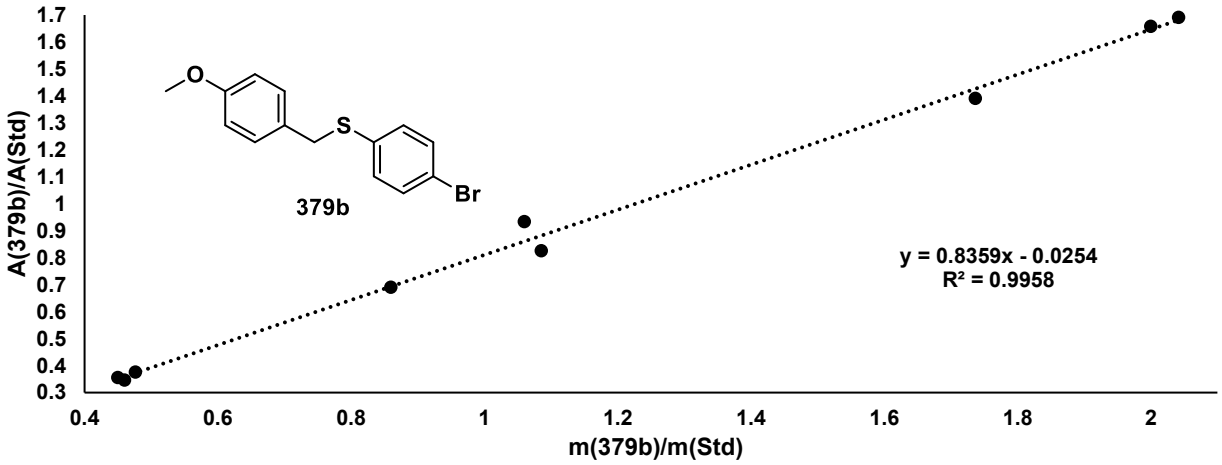

Mass ratio [mg(379b)/mg(Std)]	A(379b)	A(Std)	Area ratio [A(379b)/A(Std)]
1.0	6325.2	11413	0.5542
1.0	6266.7	11430	0.5483
1.0	6500.4	11433	0.5686
2.0	12737	11062	1.1515
2.0	15020	13419	1.1194
2.1	12977	11139	1.1649
0.5	6288.6	22138	0.2841
0.5	6246.7	22442	0.2783
0.6	6176.2	22788	0.2710

4,4'-(oxybis(methylene))bis(methoxybenzene) (380)

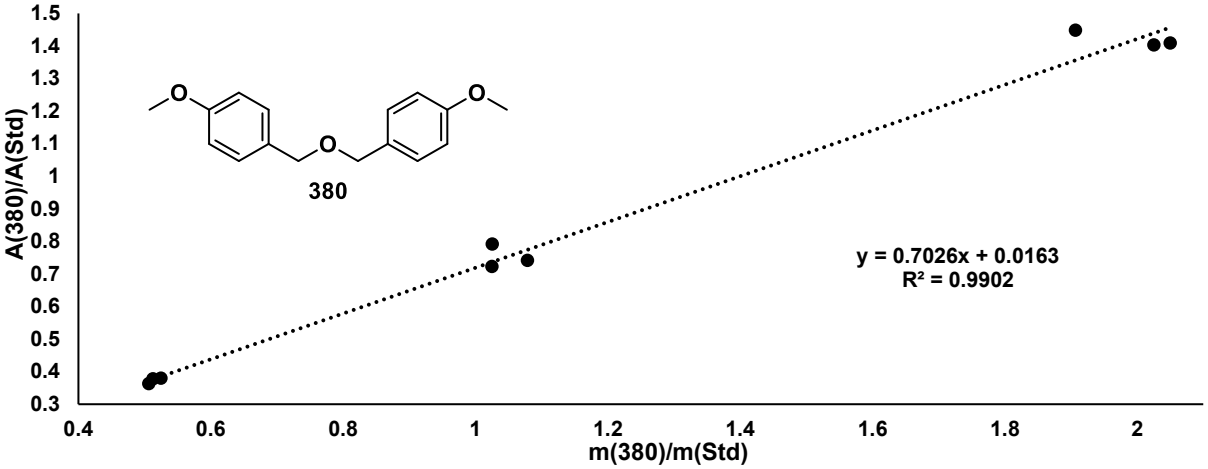

Mass ratio [mg(380)/mg(Std)]	A(380)	A(Std)	Area ratio [A(380)/A(Std)]
1.0	8333.0	11529	0.7228
1.1	7437.7	10038	0.7409
1.0	9257.4	11704	0.7910
2.0	14429	10289	1.4024
2.0	14574	10346	1.4087
1.9	16719	11544	1.4484
0.5	7694.3	20373	0.3777
0.5	7646.9	21069	0.3630
0.6	7911.8	20854	0.3794

1,2-bis(4-methoxyphenyl)ethane (381)

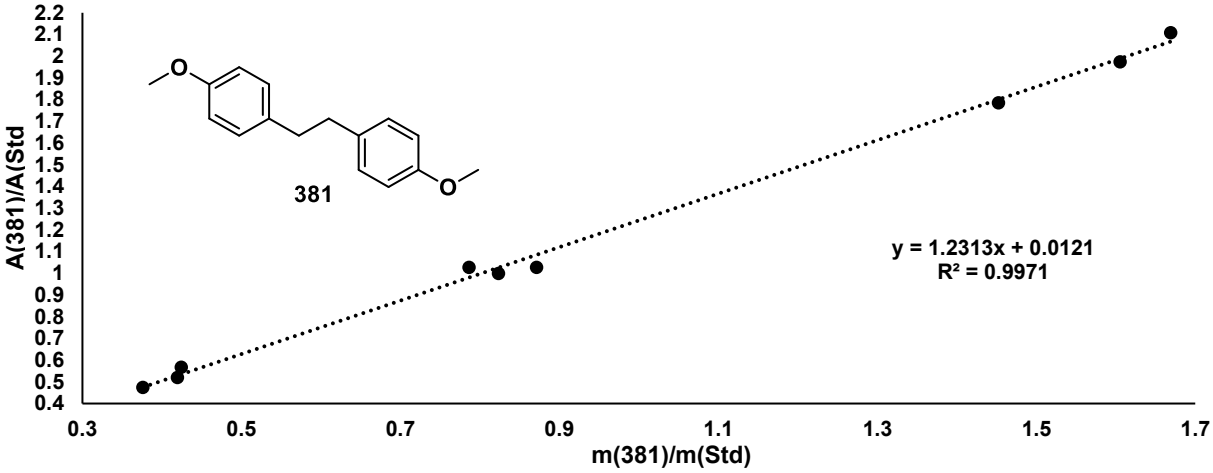

Mass ratio [mg(381)/mg(Std)]	A(381)	A(Std)	Area ratio [A(381)/A(Std)]
1.0	8333.0	11529	0.7228
1.1	7437.7	10038	0.7409
1.0	9257.4	11704	0.7910
2.0	14429	10289	1.4024
2.0	14574	10346	1.4087
1.9	16719	11544	1.4484
0.5	7694.3	20373	0.3777
0.5	7646.9	21069	0.3630
0.6	7911.8	20854	0.3794

4.4.6 NMR Spectra of Thioesters

S-(3-bromophenyl) benzothioate (384d)

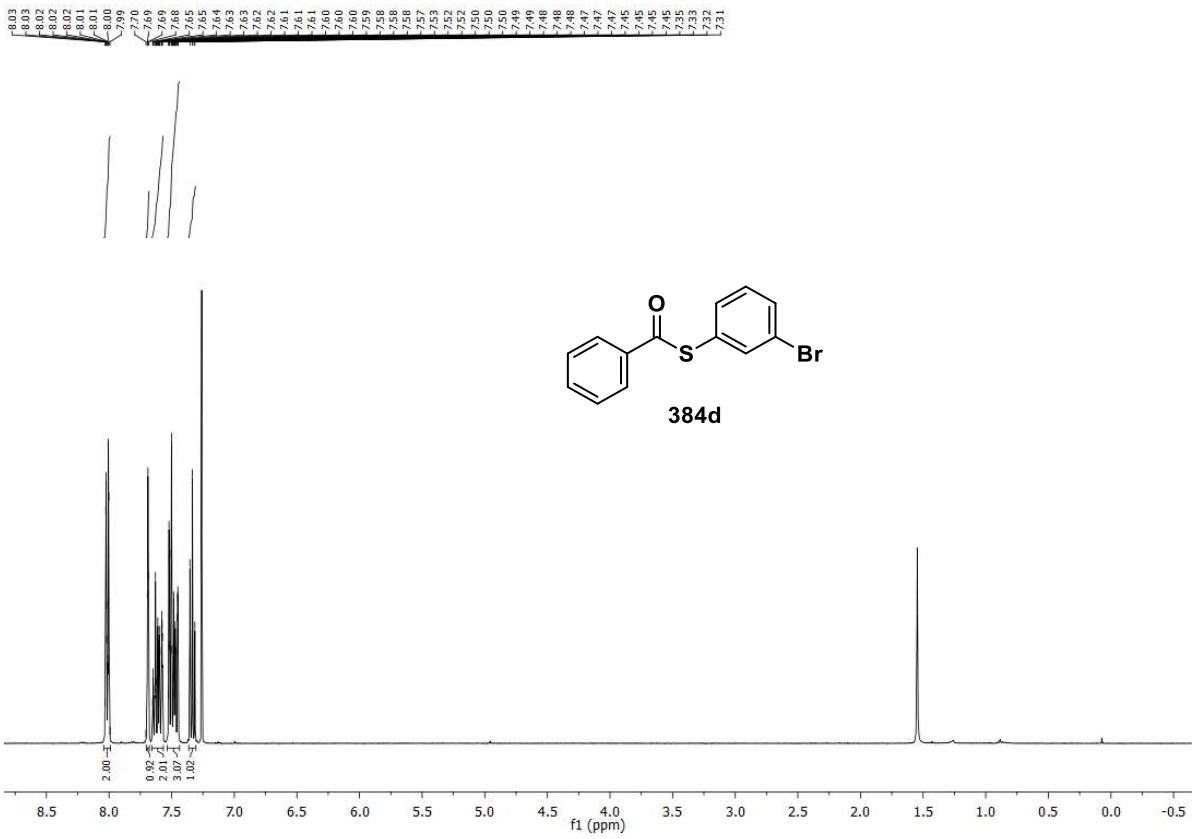

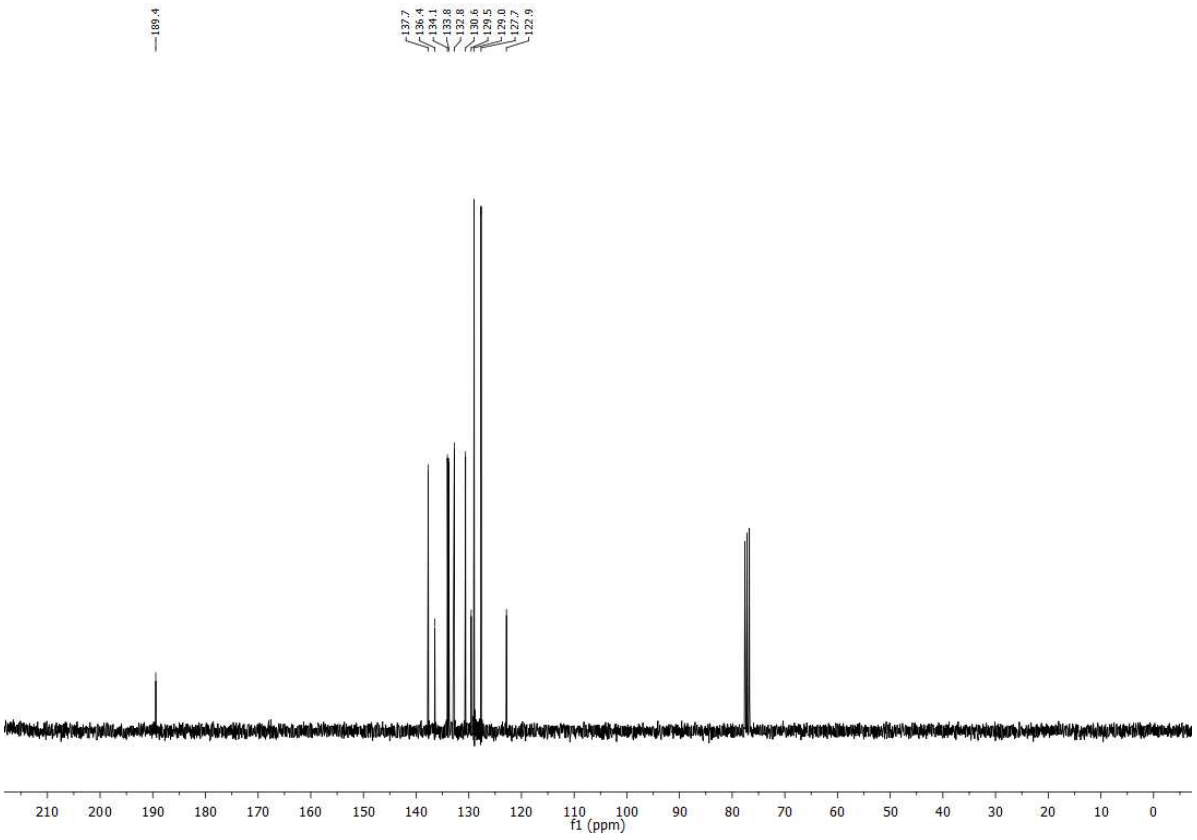

S-(4-bromophenyl) 2,4,6-trimethylbenzothioate (389a)

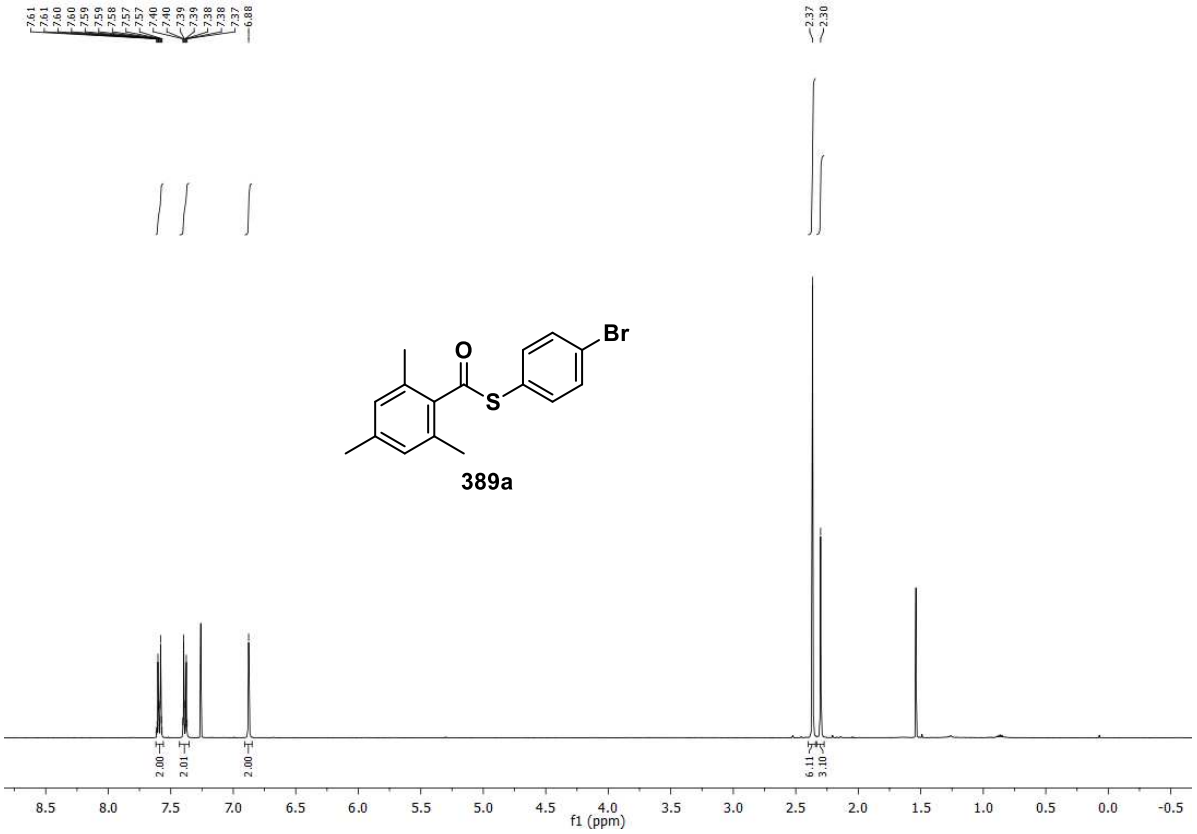

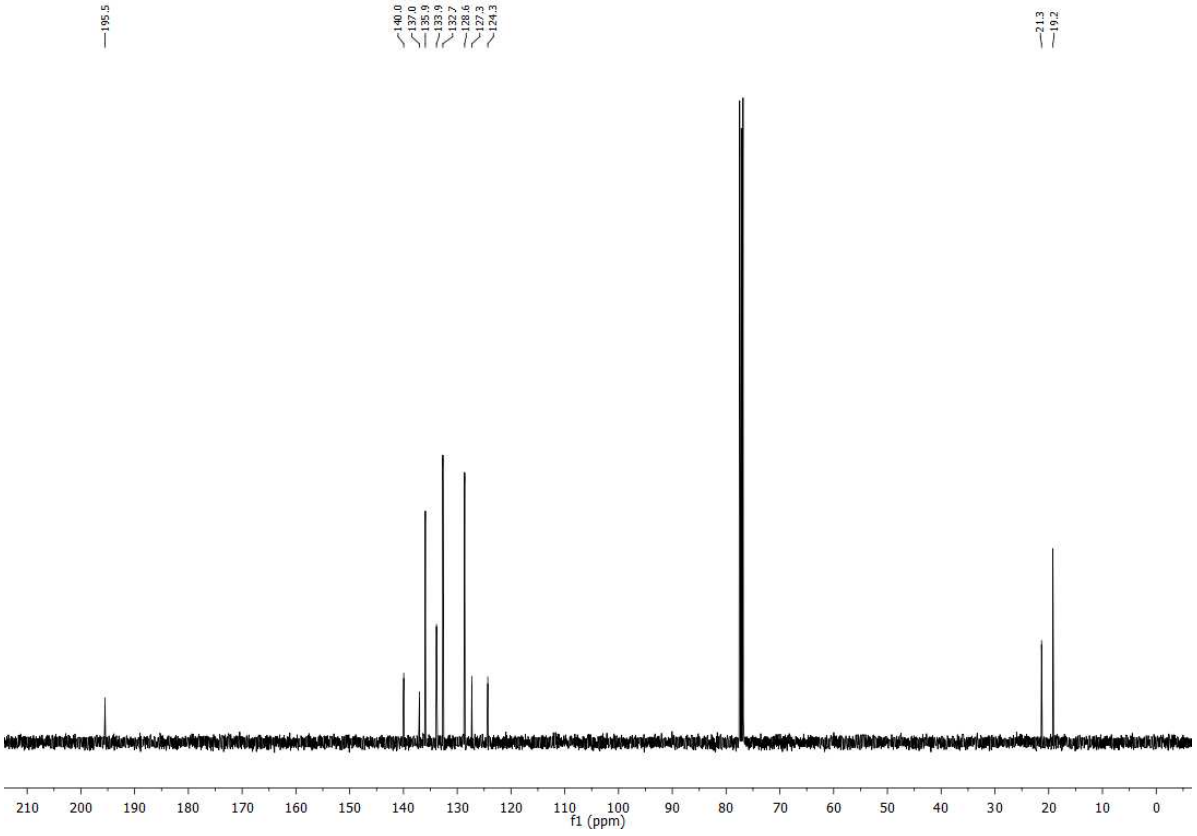

S-(4-bromophenyl) naphthalene-2-carbothioate (389d)

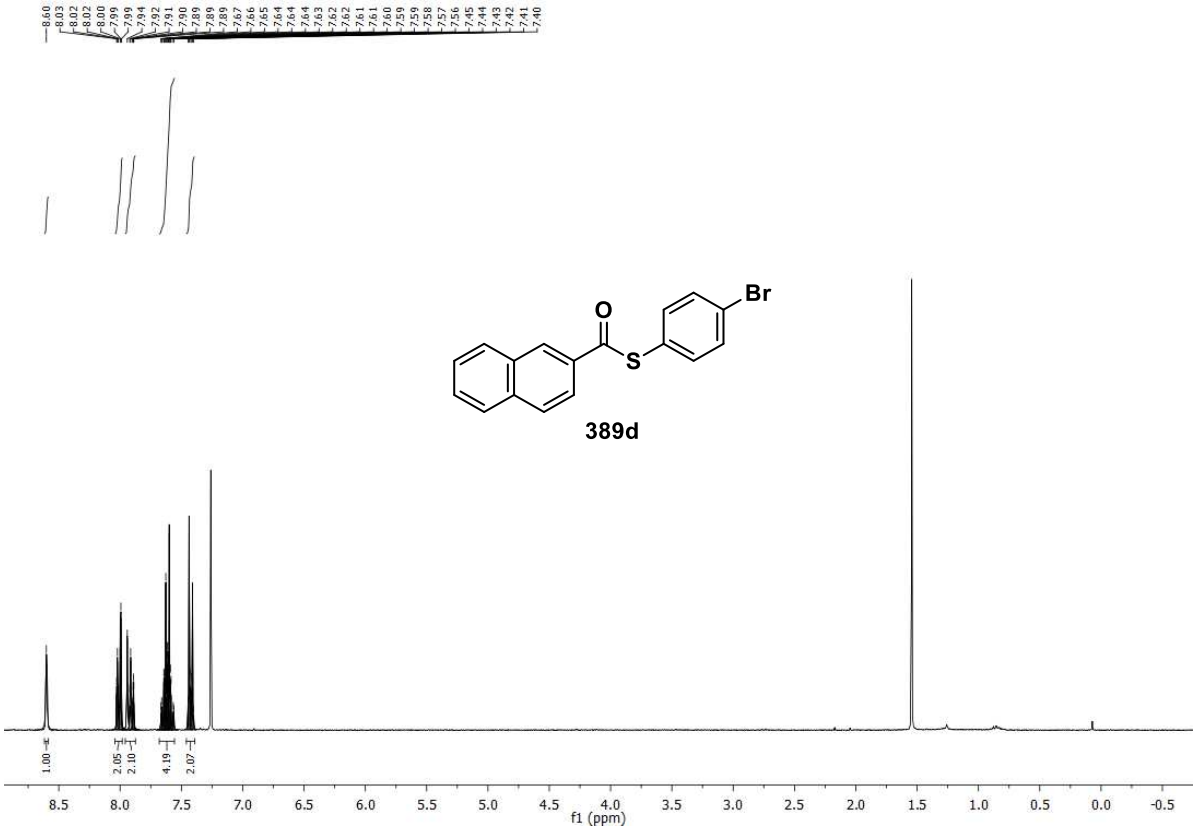

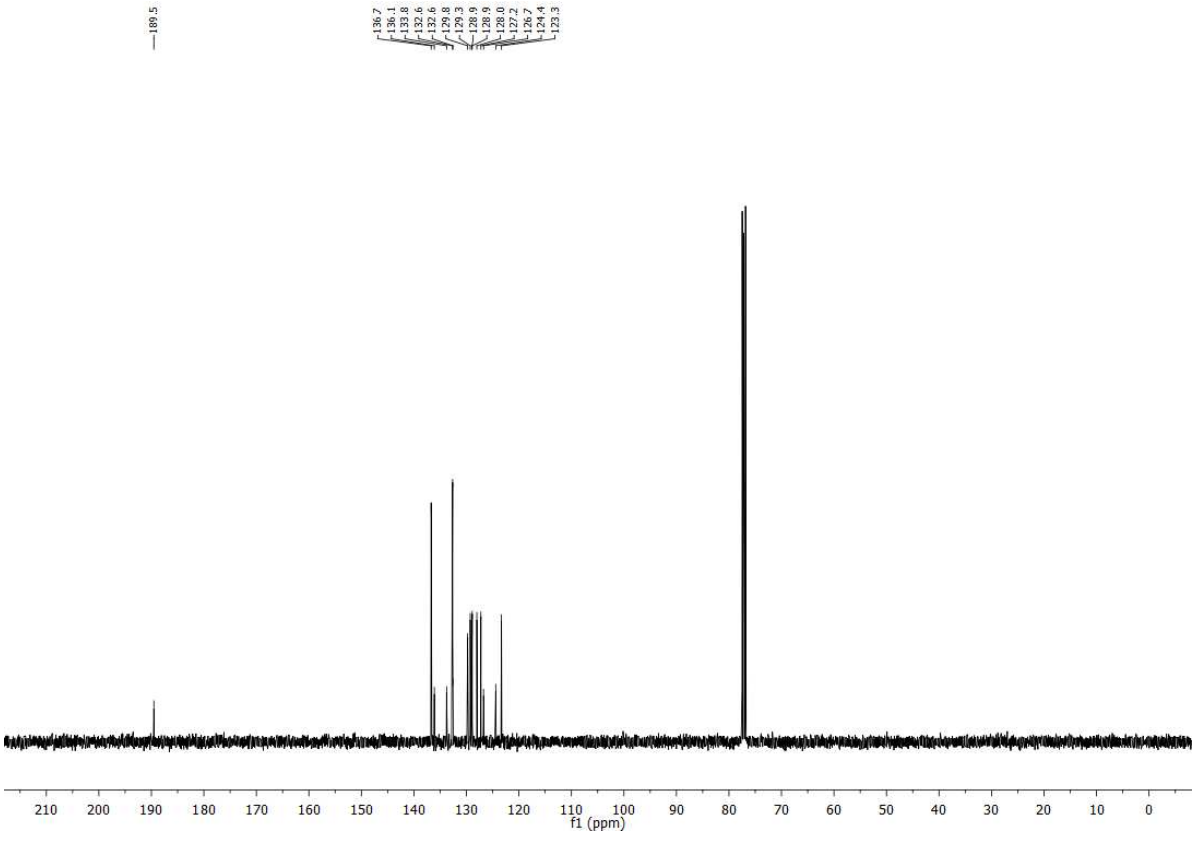

S-(4-bromophenyl) 2-(4-methoxyphenyl)ethanethioate (389e)

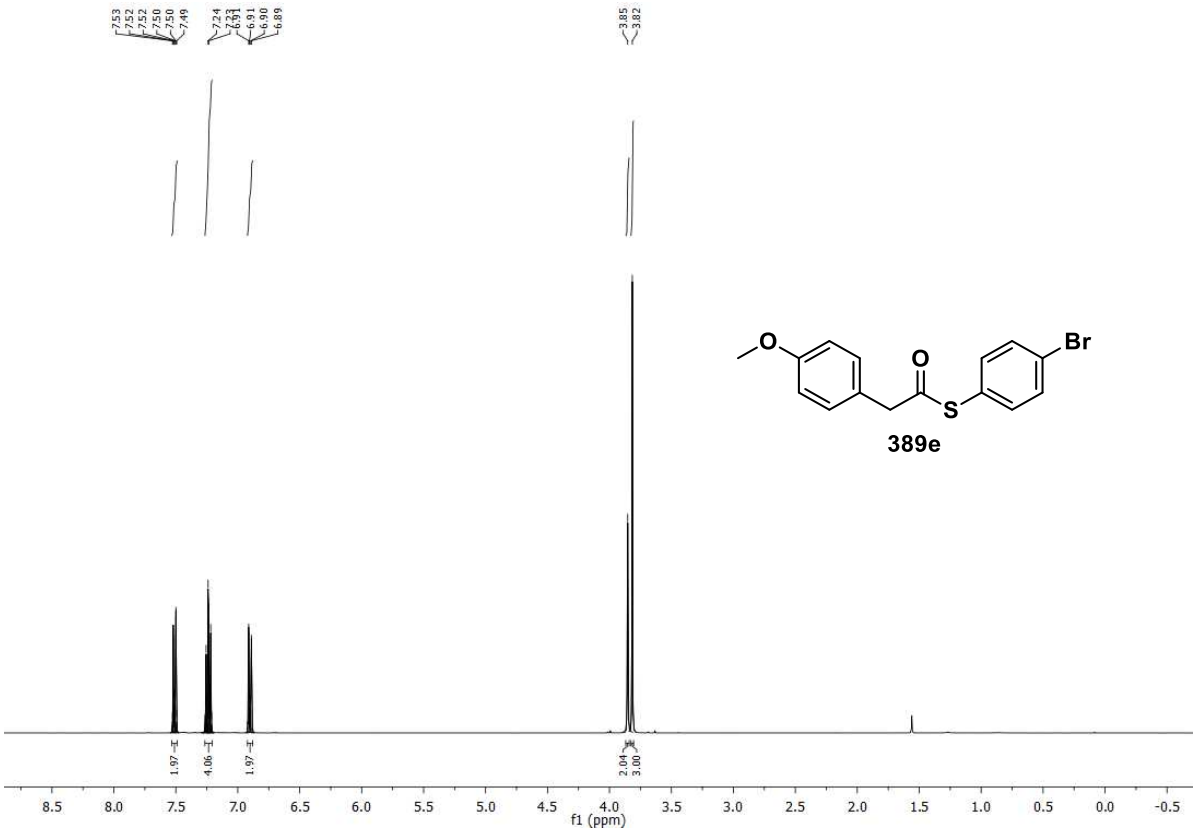

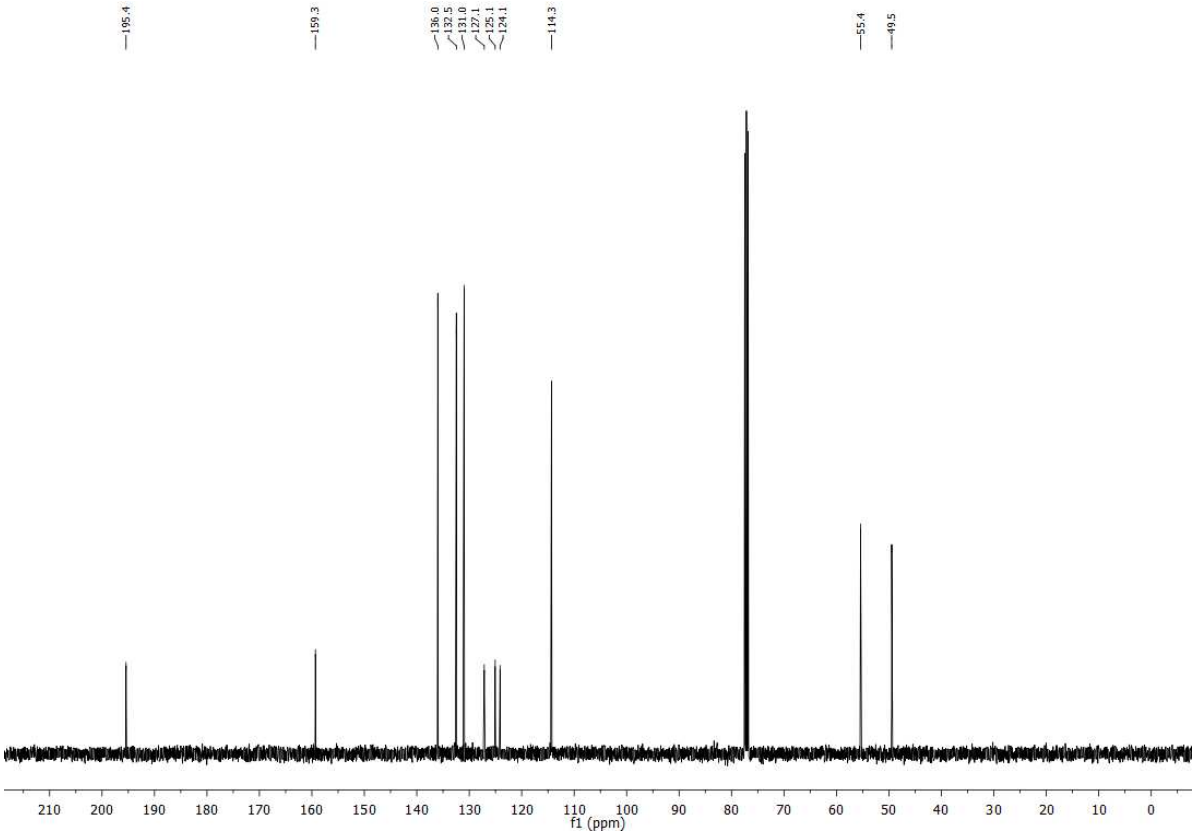

S-(4-bromophenyl) 2-phenylbutanethioate (389f)

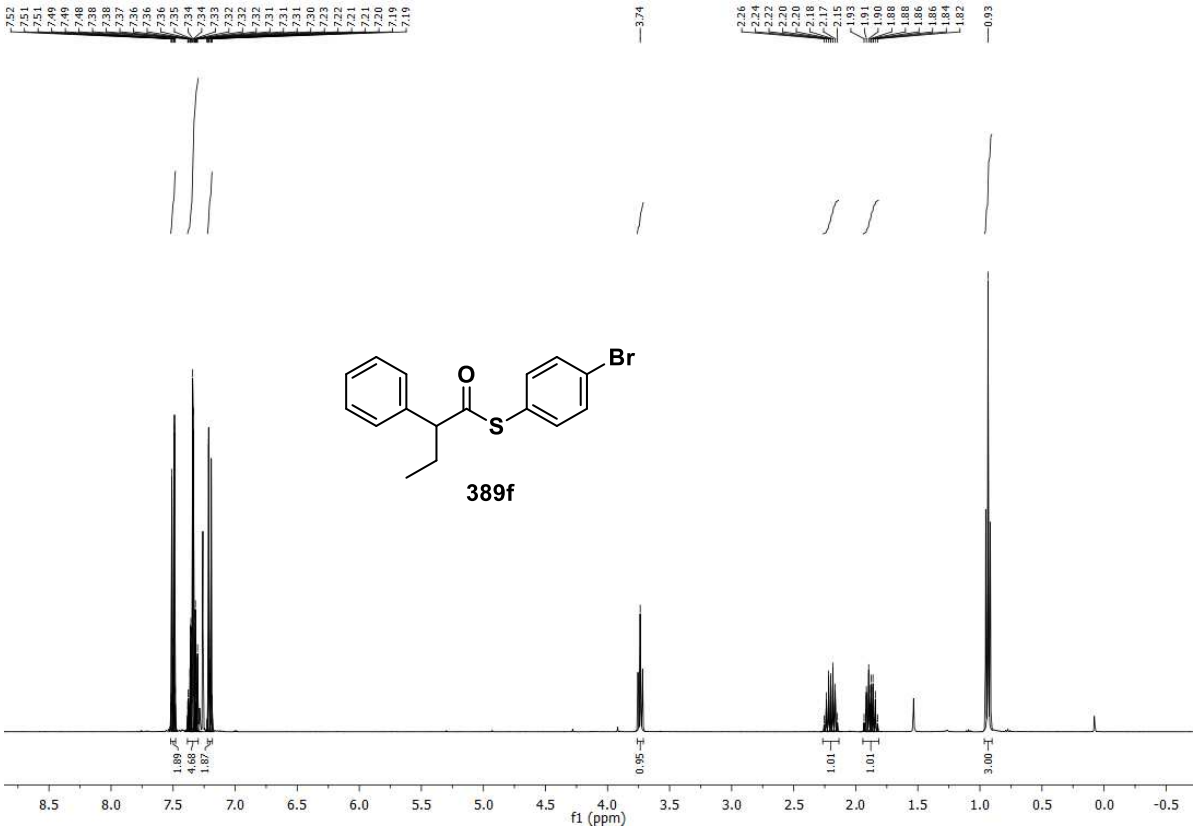

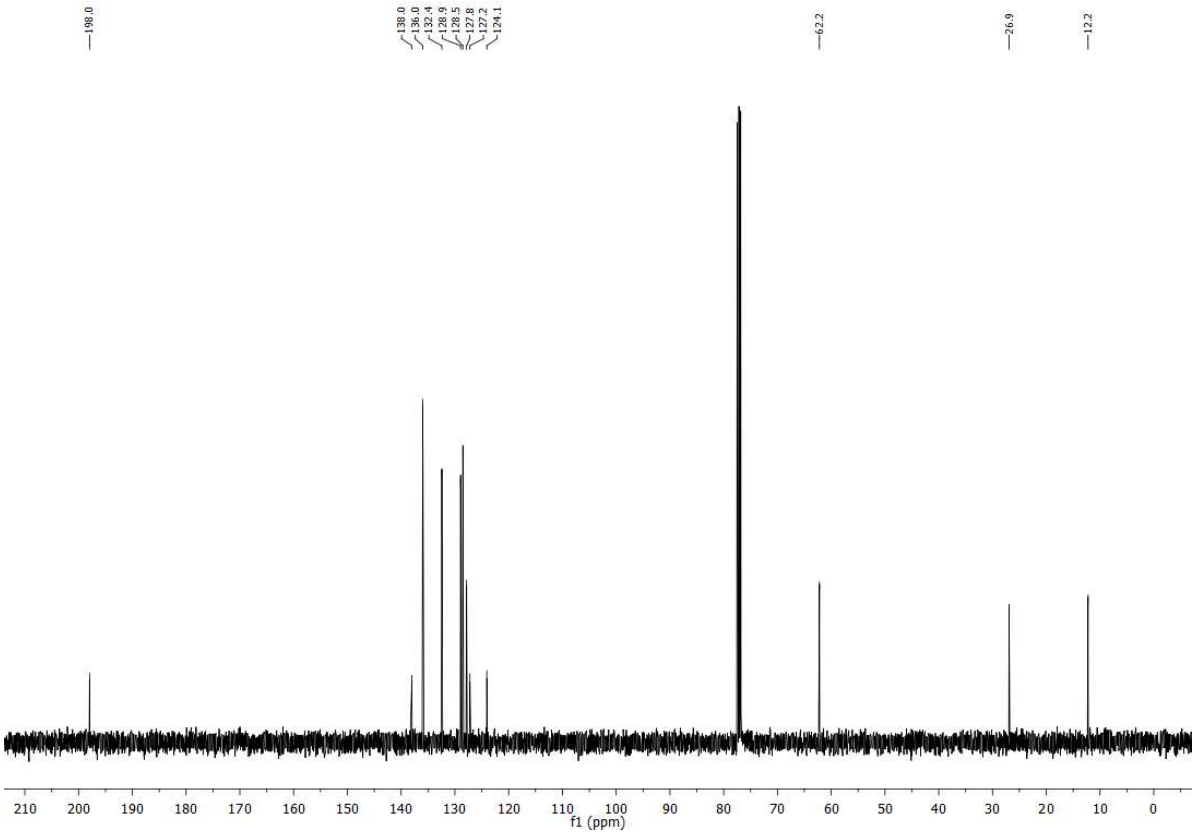

S-(4-bromophenyl) 2-(6-methoxynaphthalen-2-yl)propanethioate (389g)

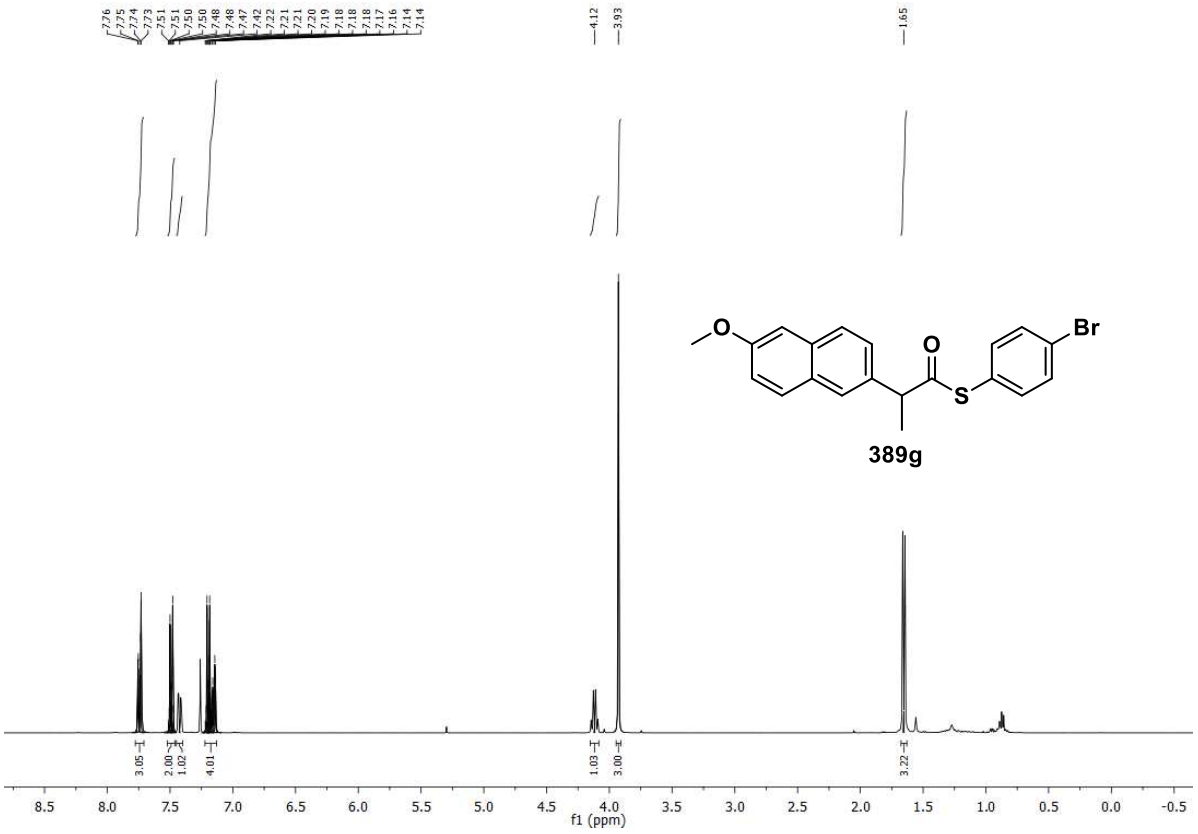

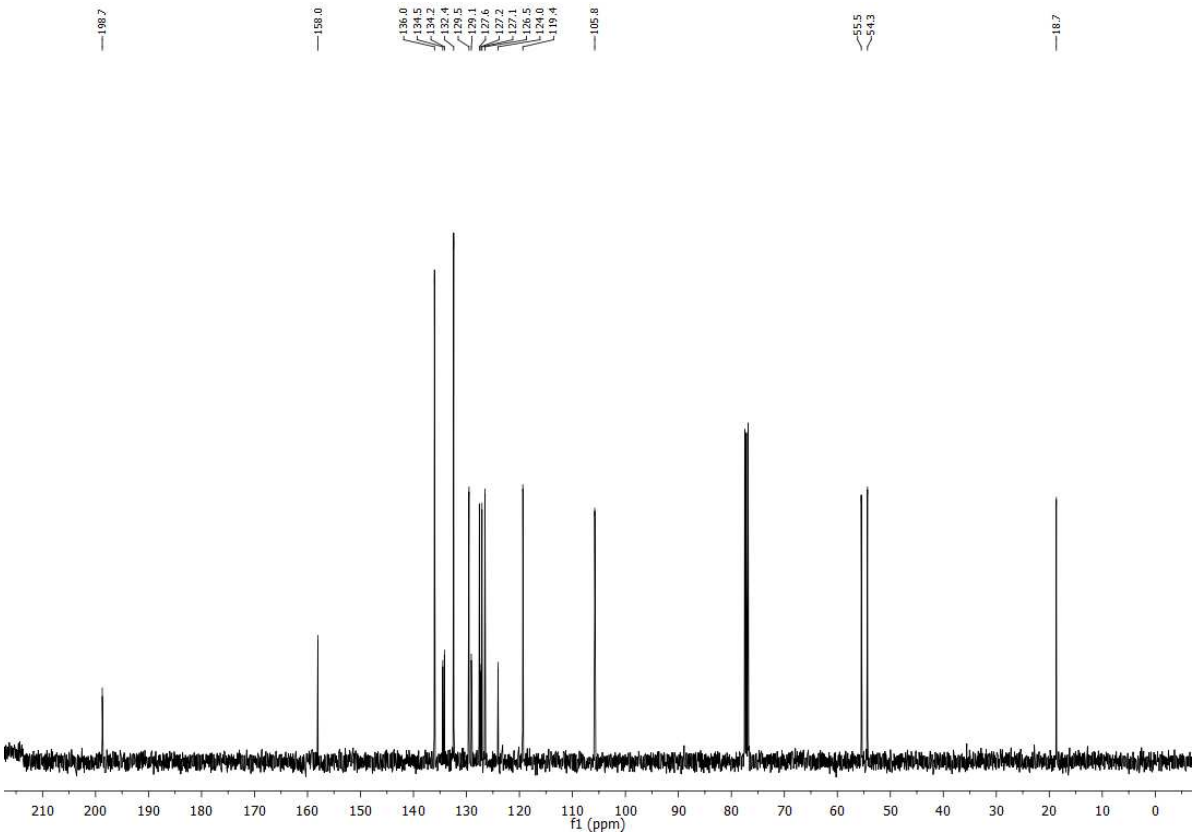

S-(4-bromophenyl) 3-phenylpropanethioate (389h)

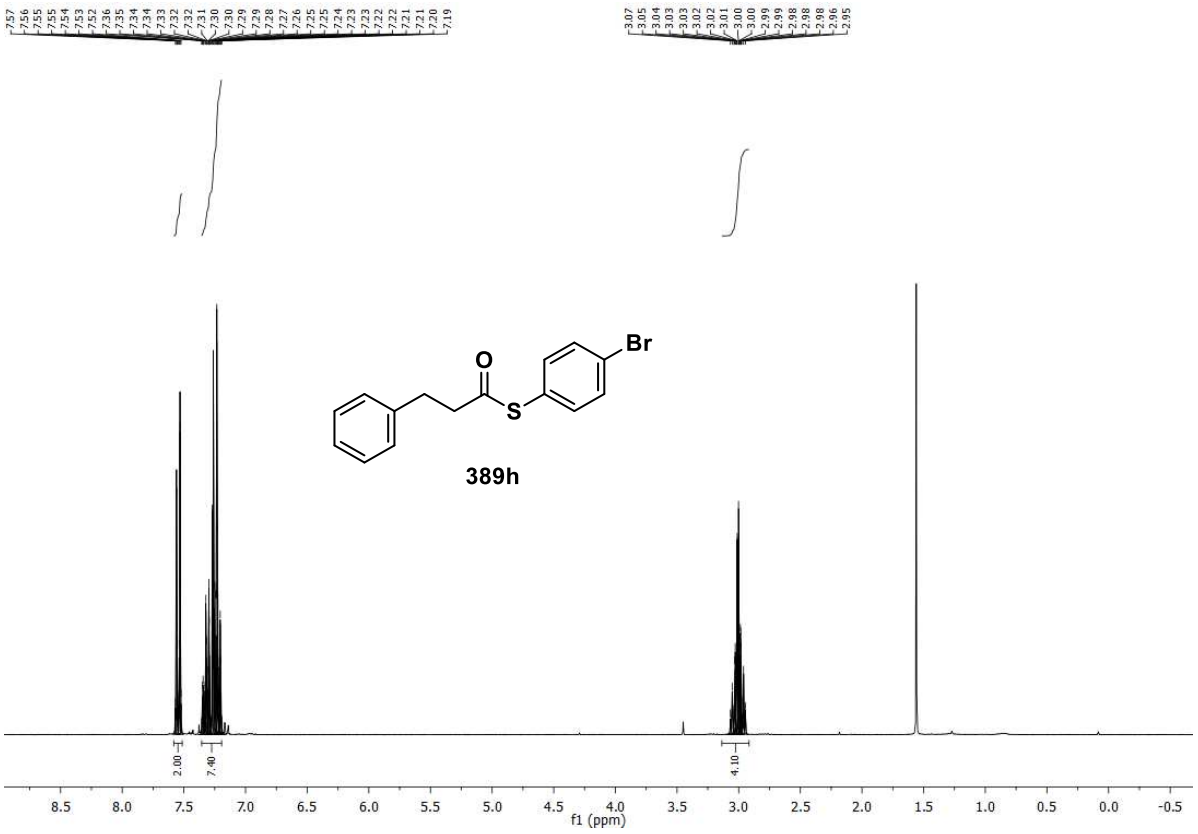

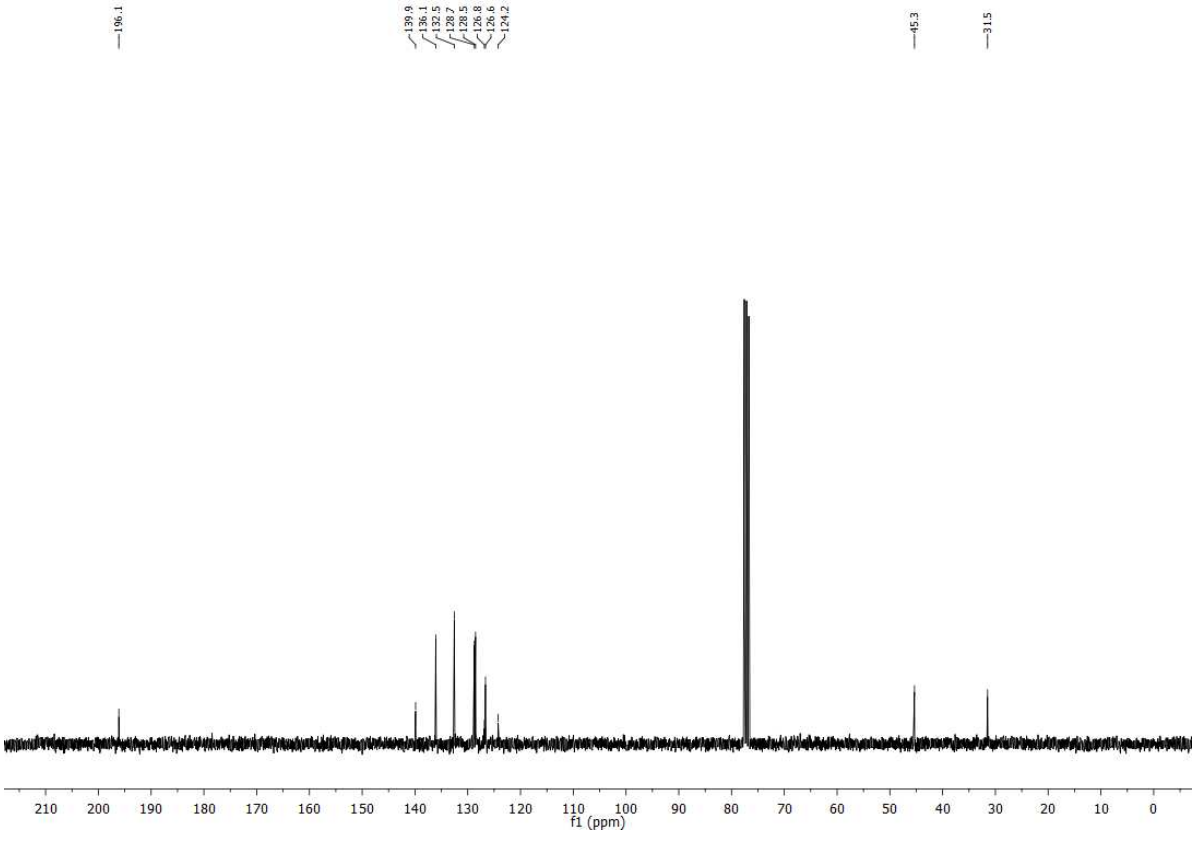

S-(4-bromophenyl) 3-(4-methoxyphenyl)propanethioate (389i)

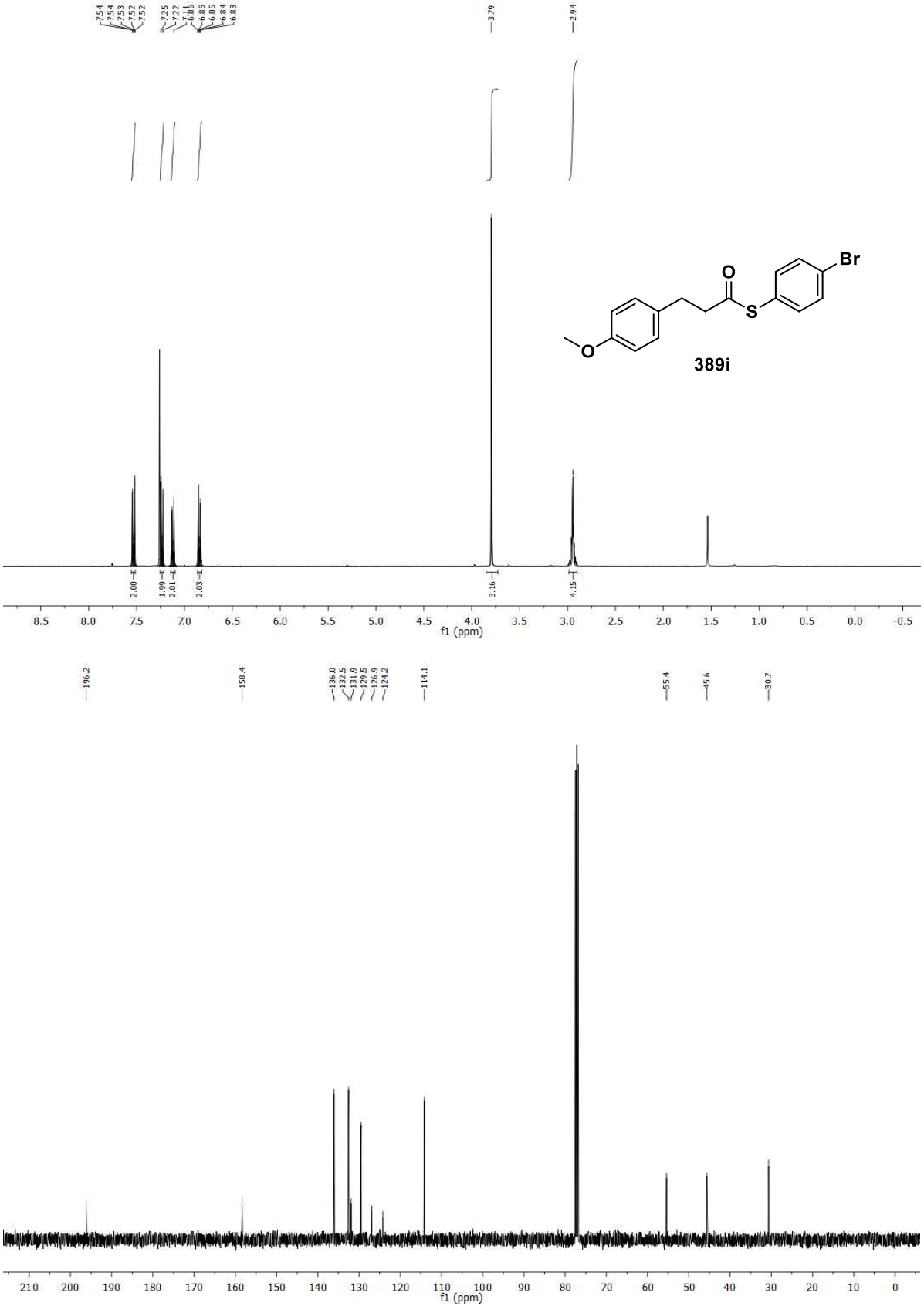

S-(4-bromophenyl) 2-ethylhexanethioate (389k)

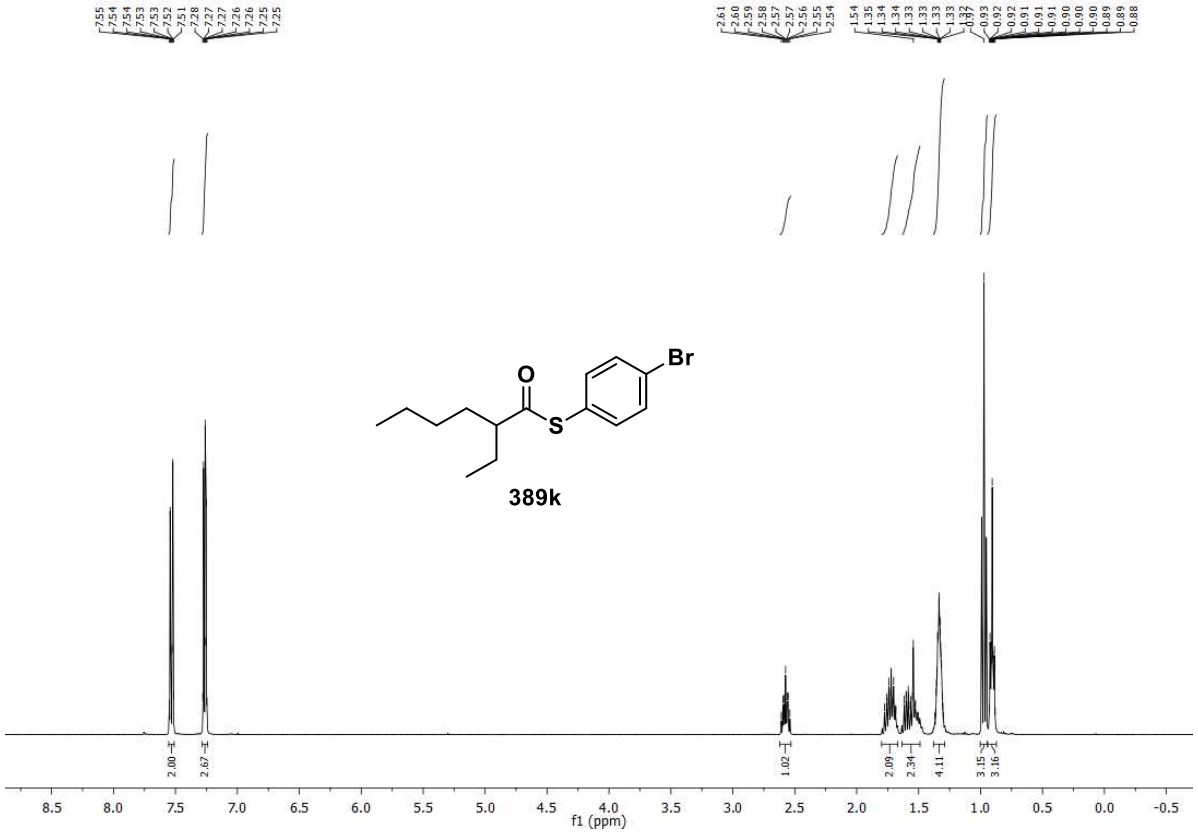

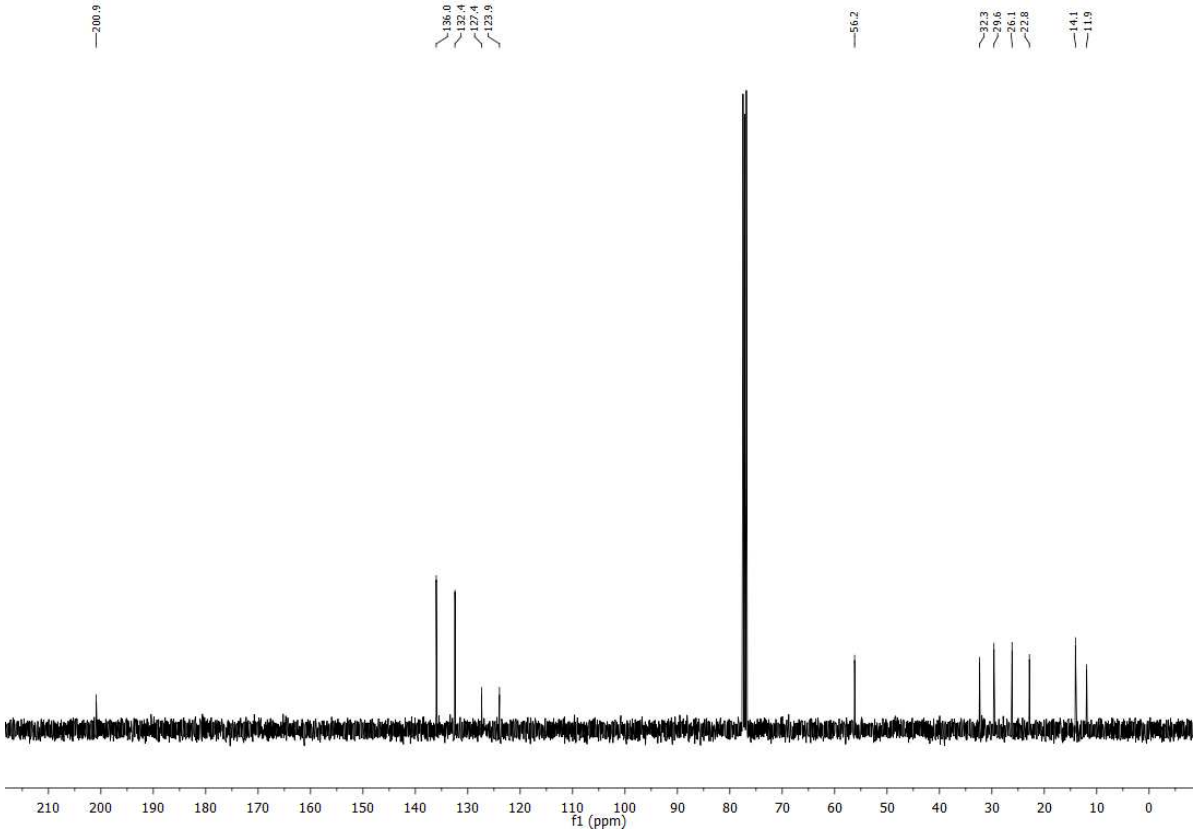

S-(4-bromophenyl) 2-(4-isobutylphenyl)propanethioate (389l)

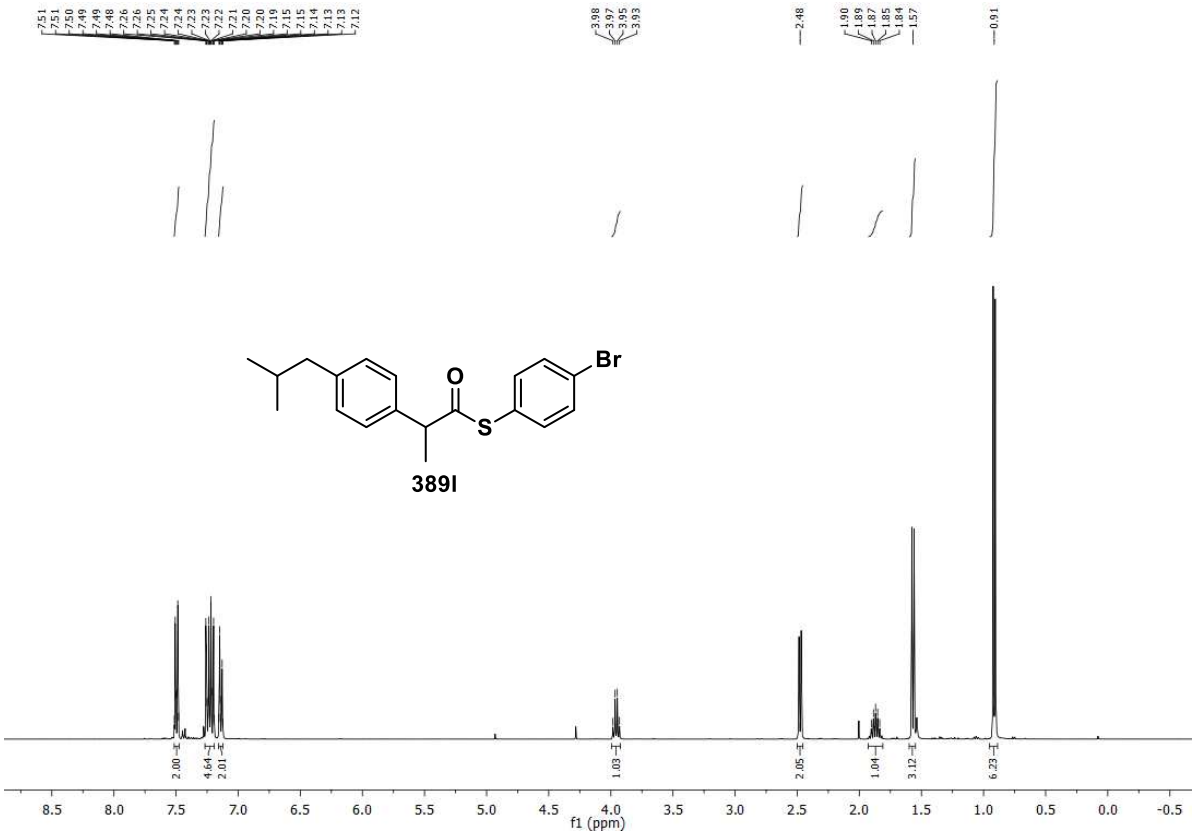

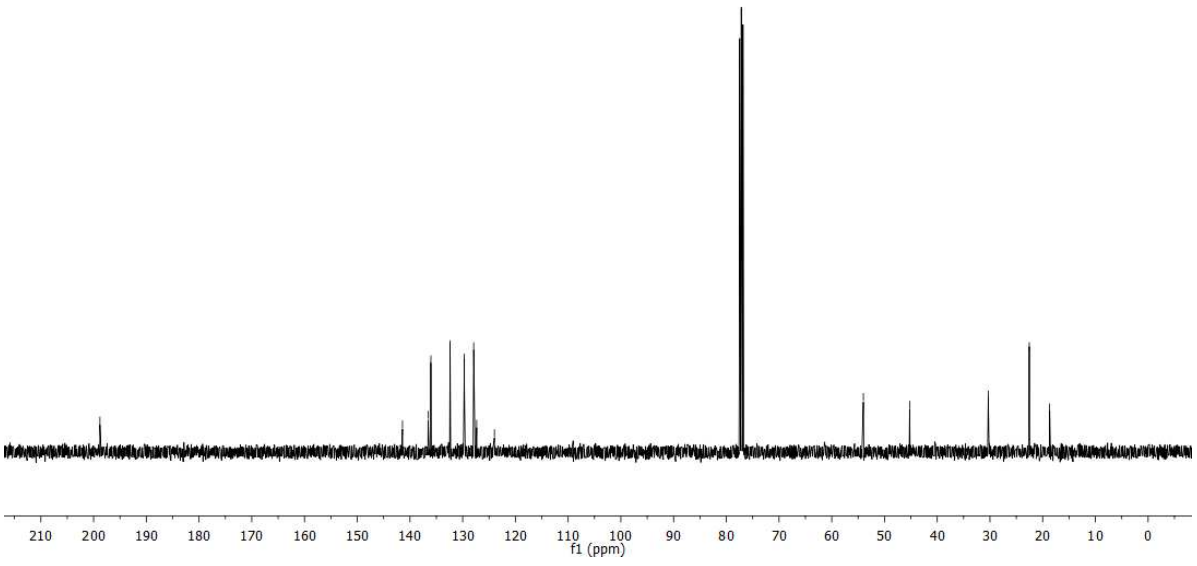

S-(4-bromophenyl) 4-fluorobenzothioate (420)

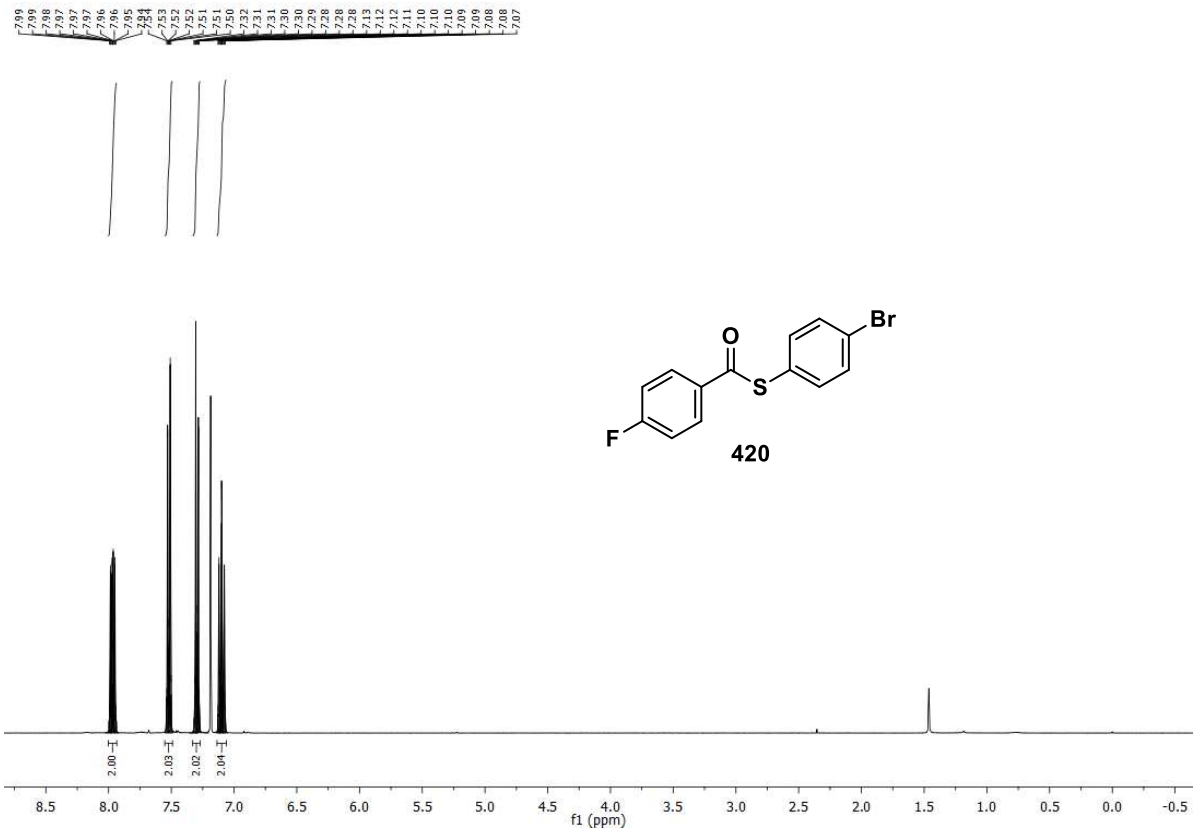

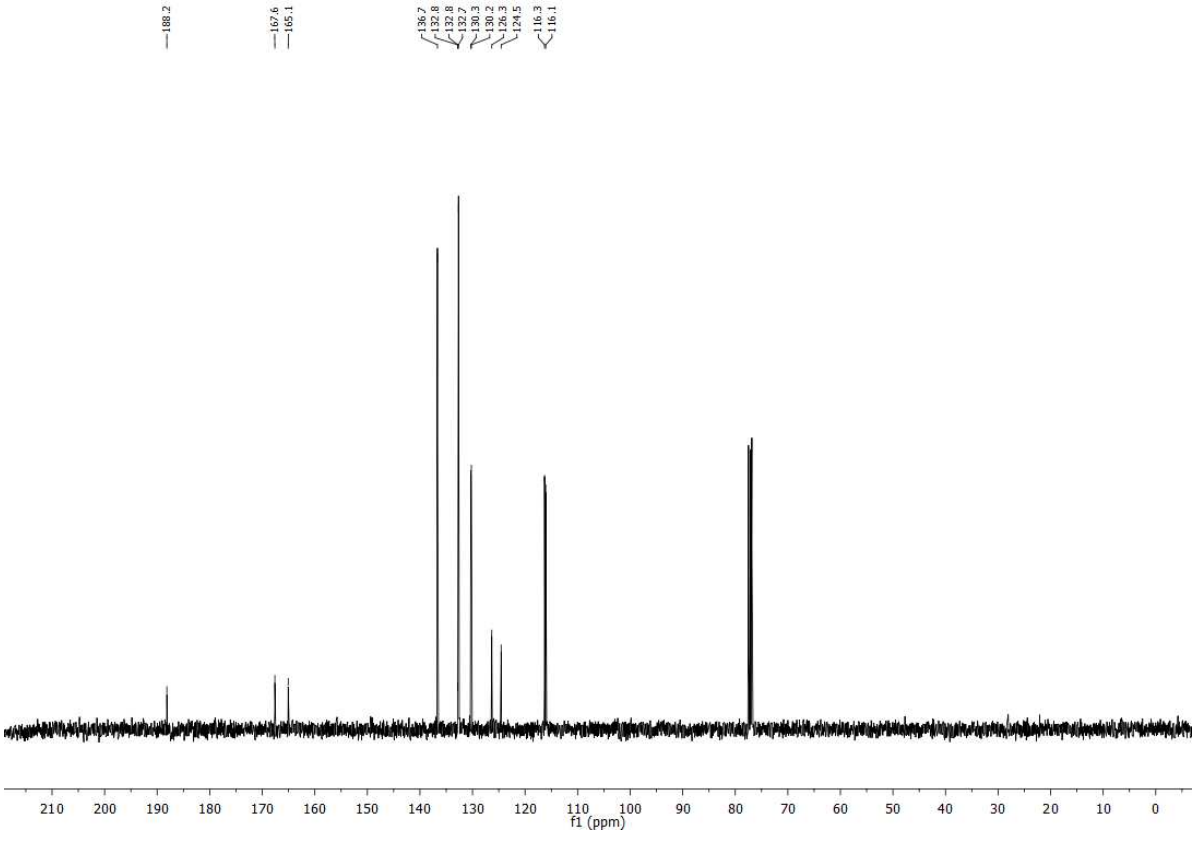

4.4.7 NMR Spectra of Ketones Synthesized from Alcohols

2-(4-methoxyphenyl)-1-phenylethan-1-one (378a) analogously to GP-D

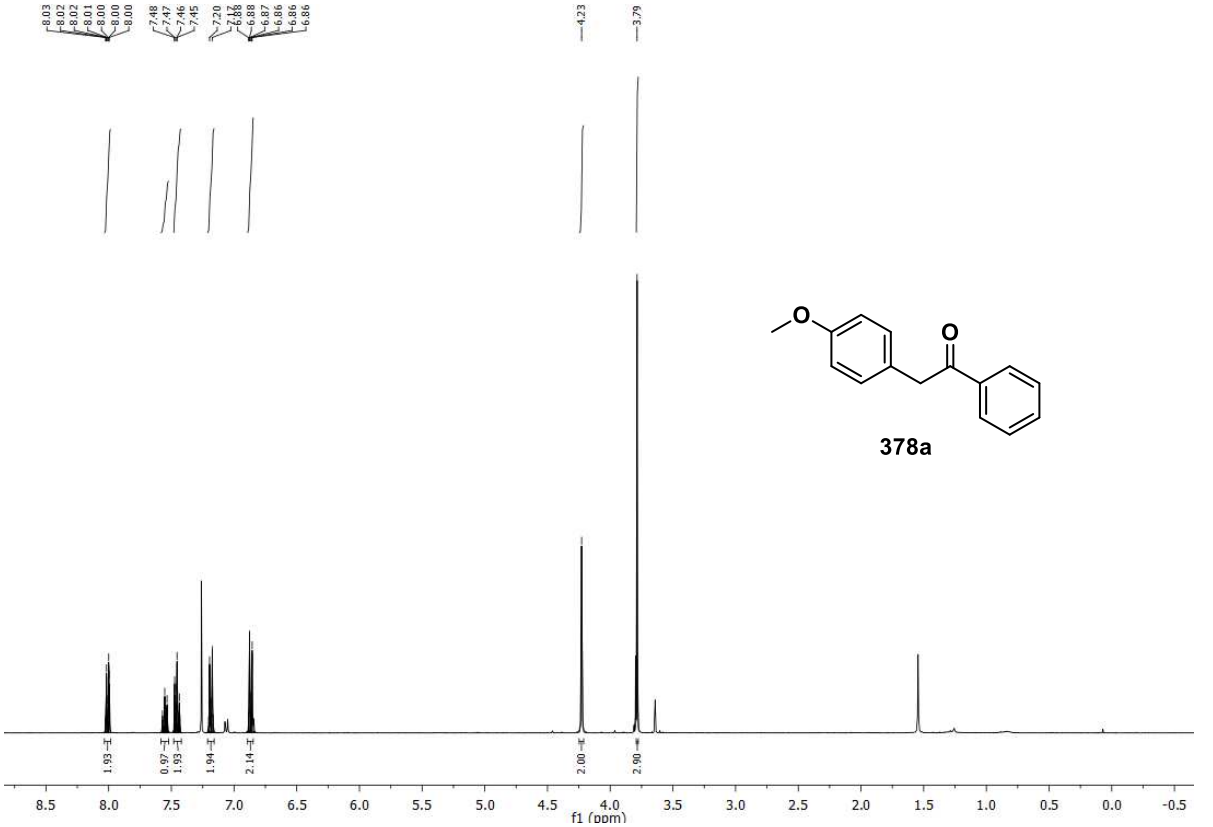

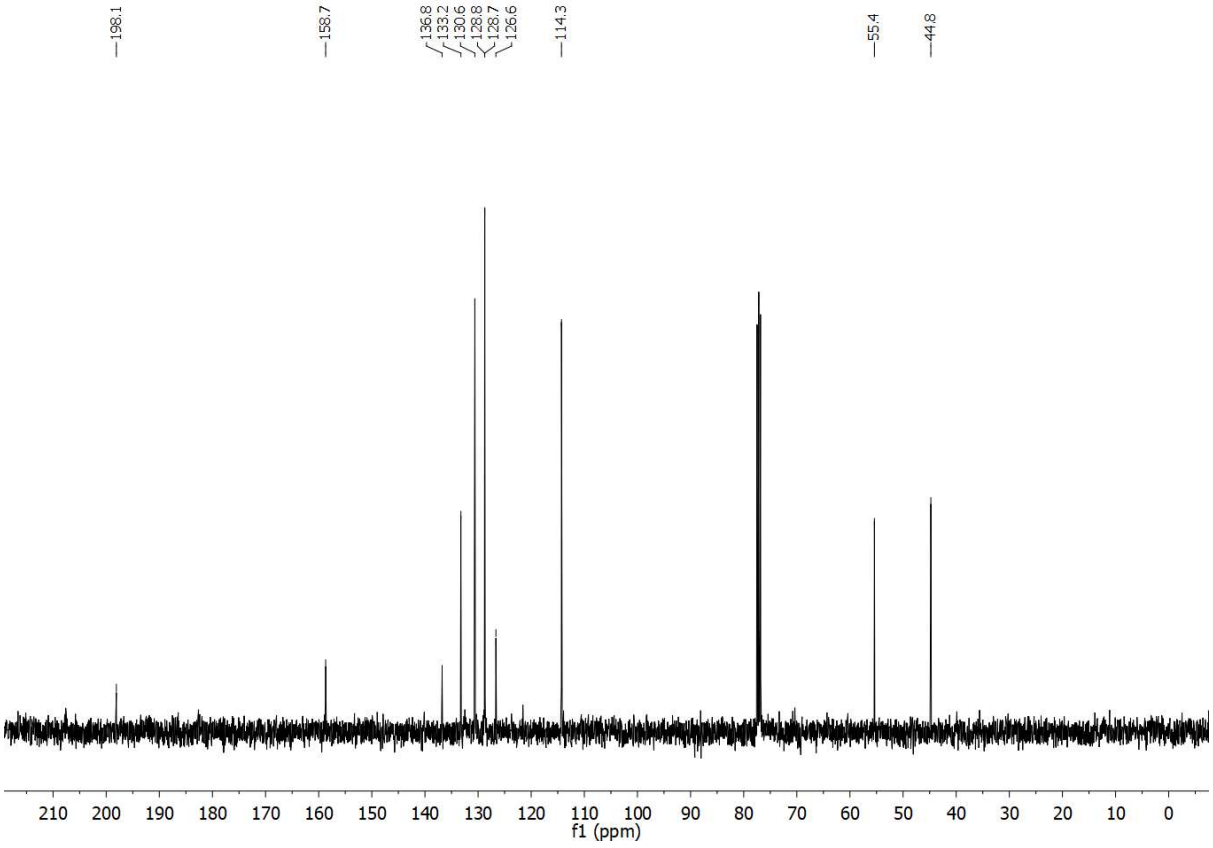

2-(4-methoxyphenyl)-1-(*p*-tolyl)ethan-1-one (378b)

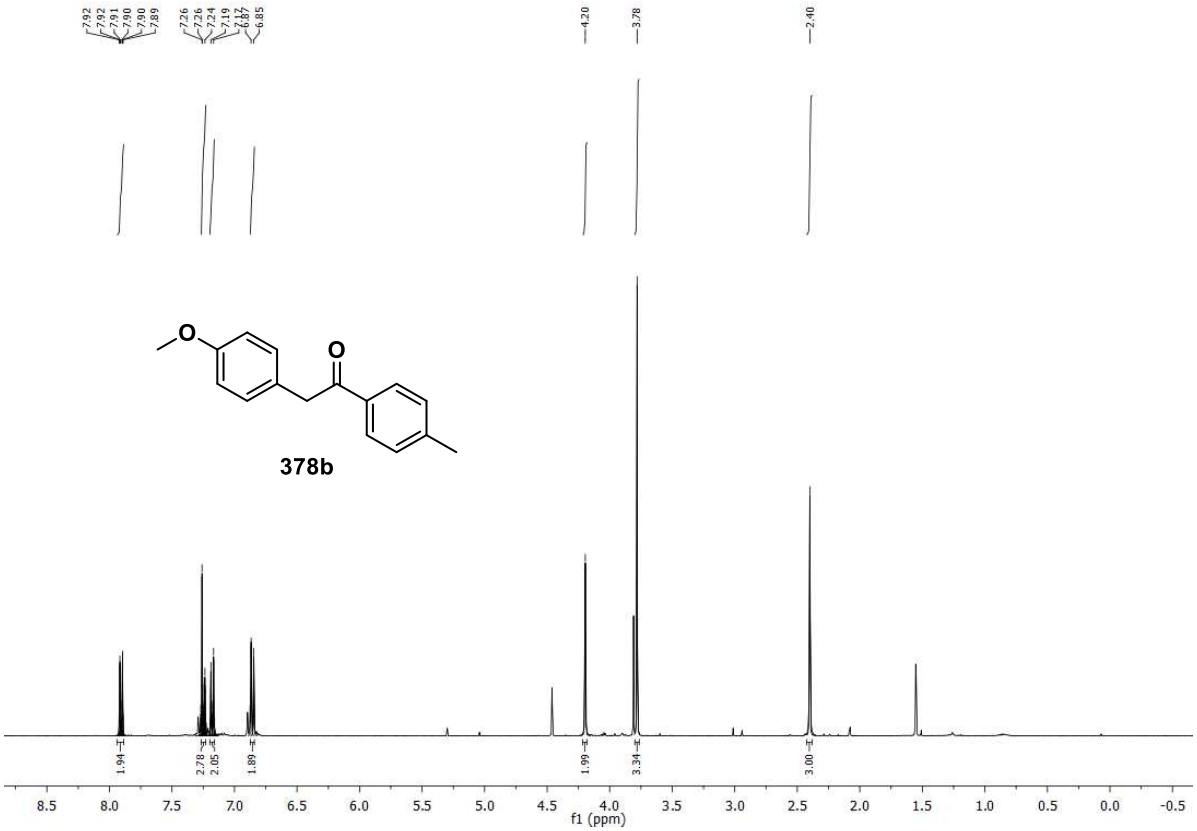

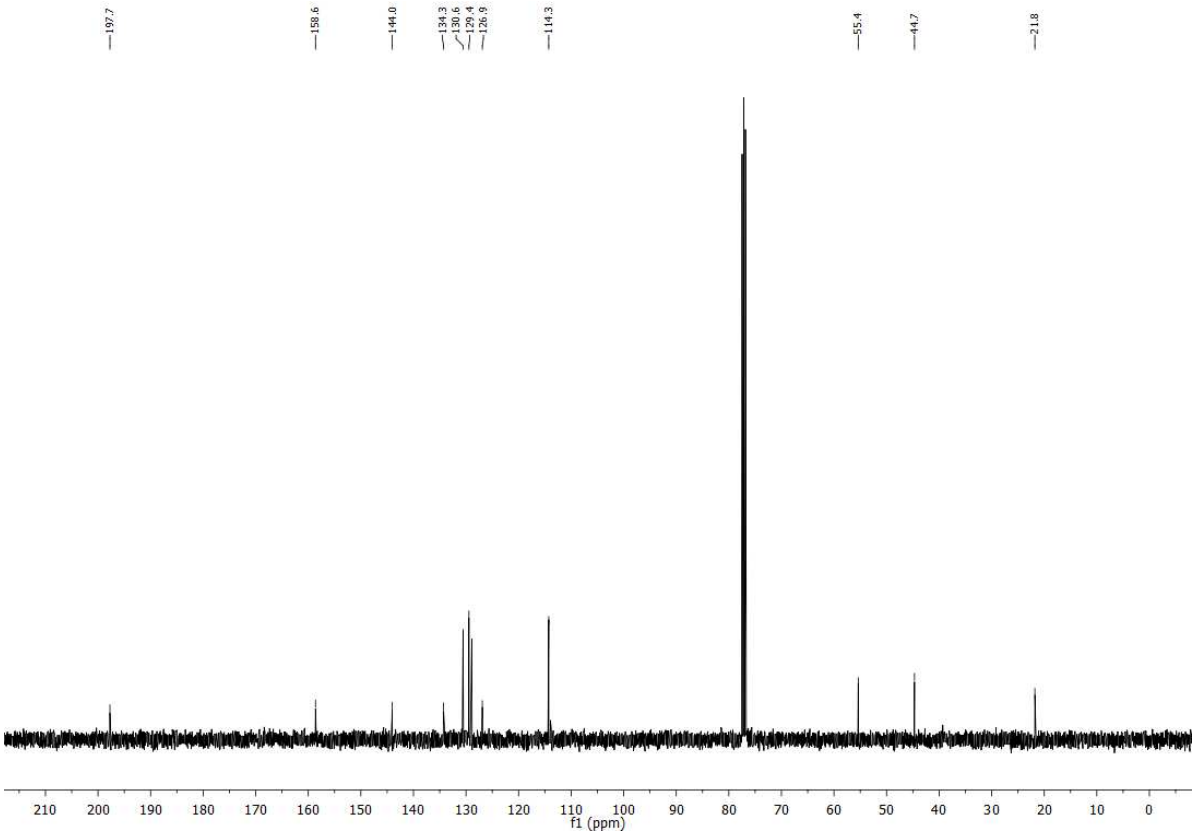

1-(4-fluorophenyl)-2-(4-methoxyphenyl)ethan-1-one (378c)

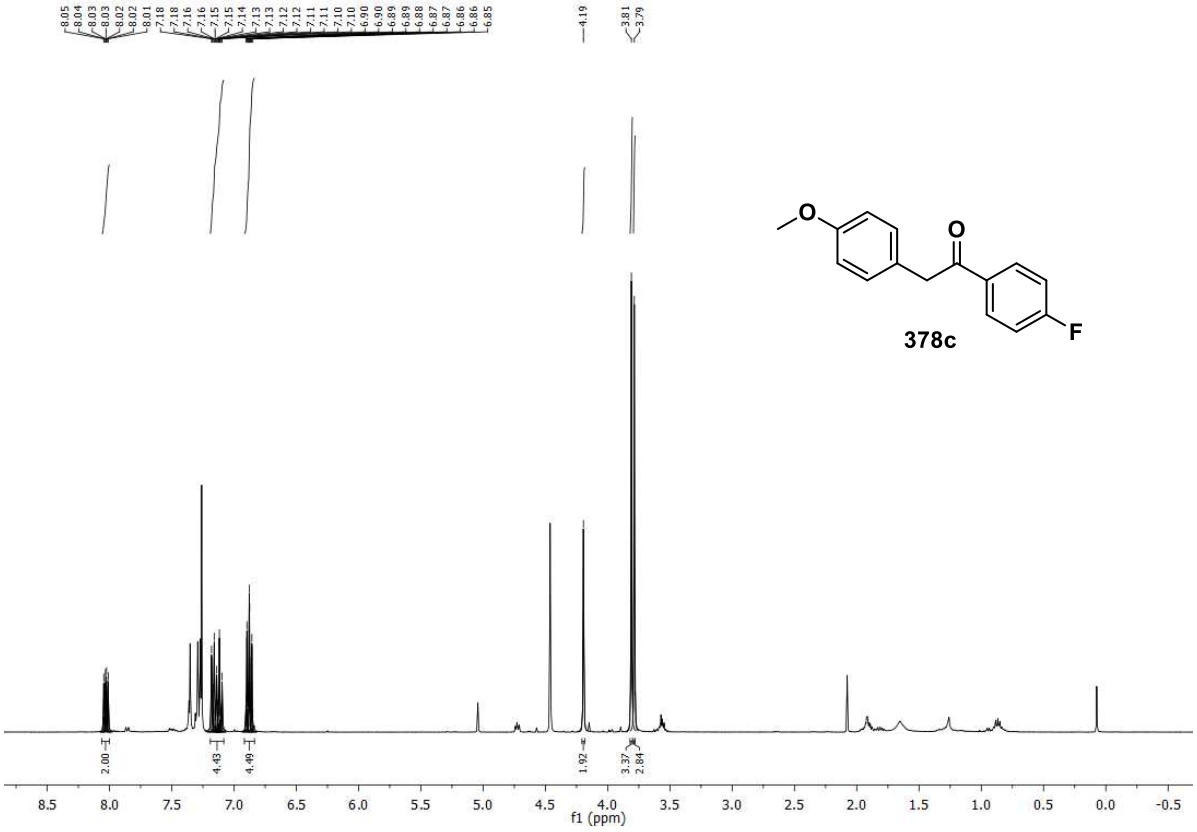

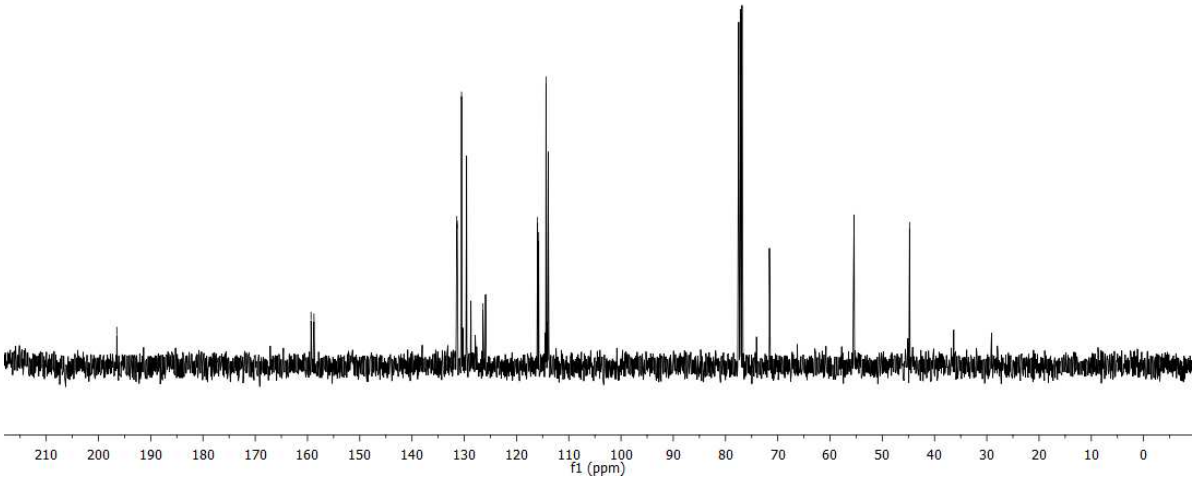

2-(4-methoxyphenyl)-1-(naphthalen-2-yl)ethan-1-one (378d)

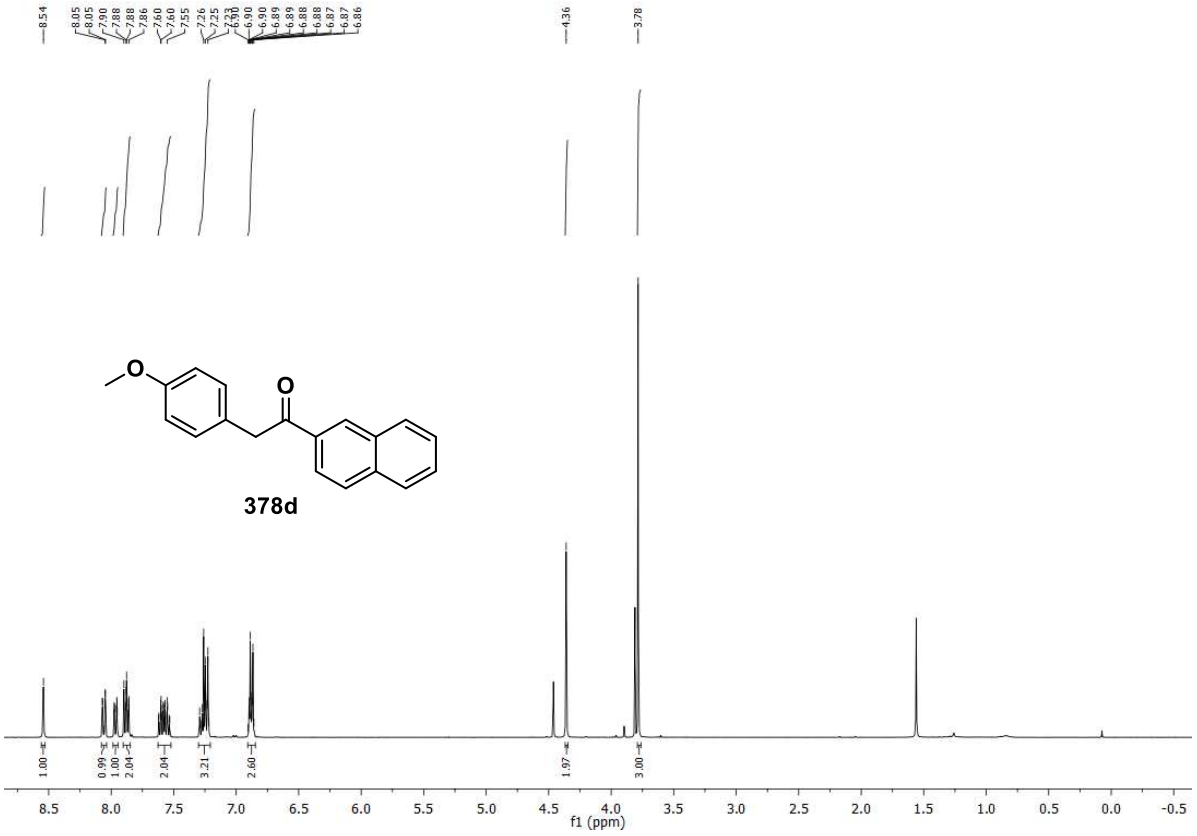

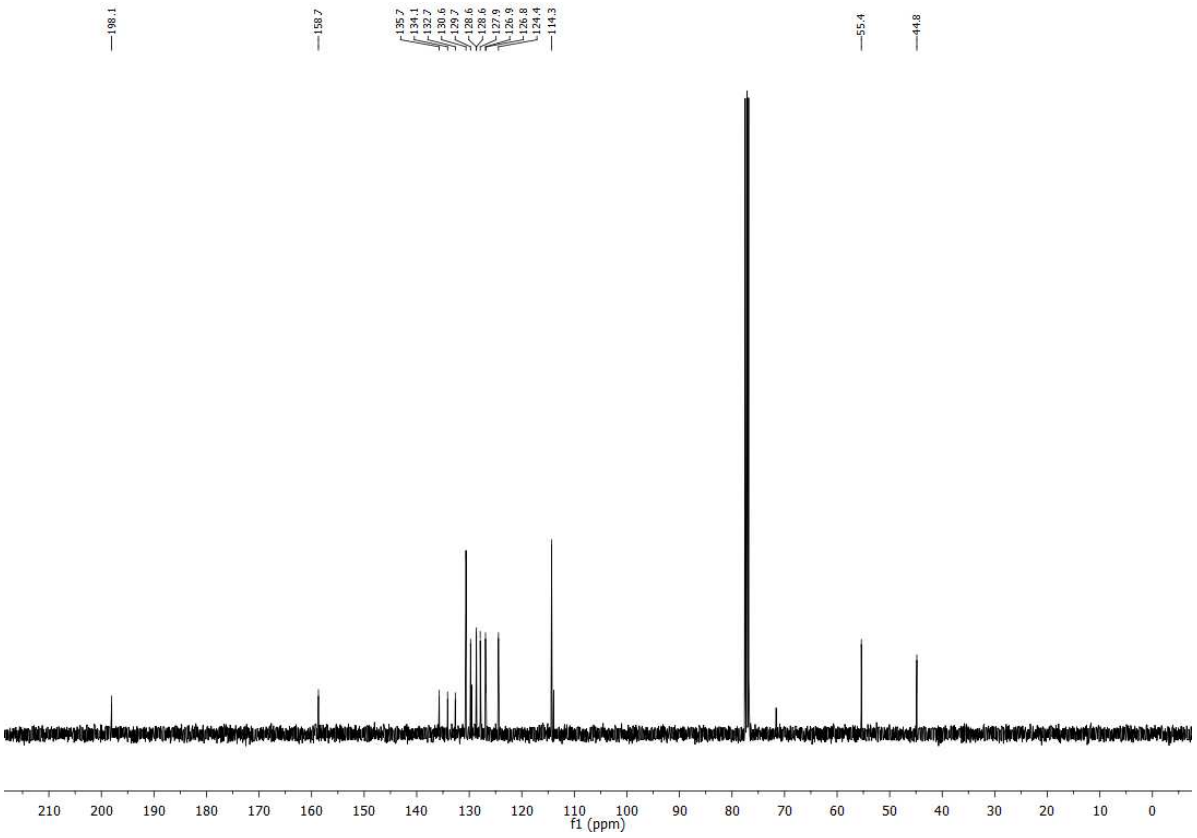

1-(4-methoxyphenyl)-3-phenylpentan-2-one (378e)

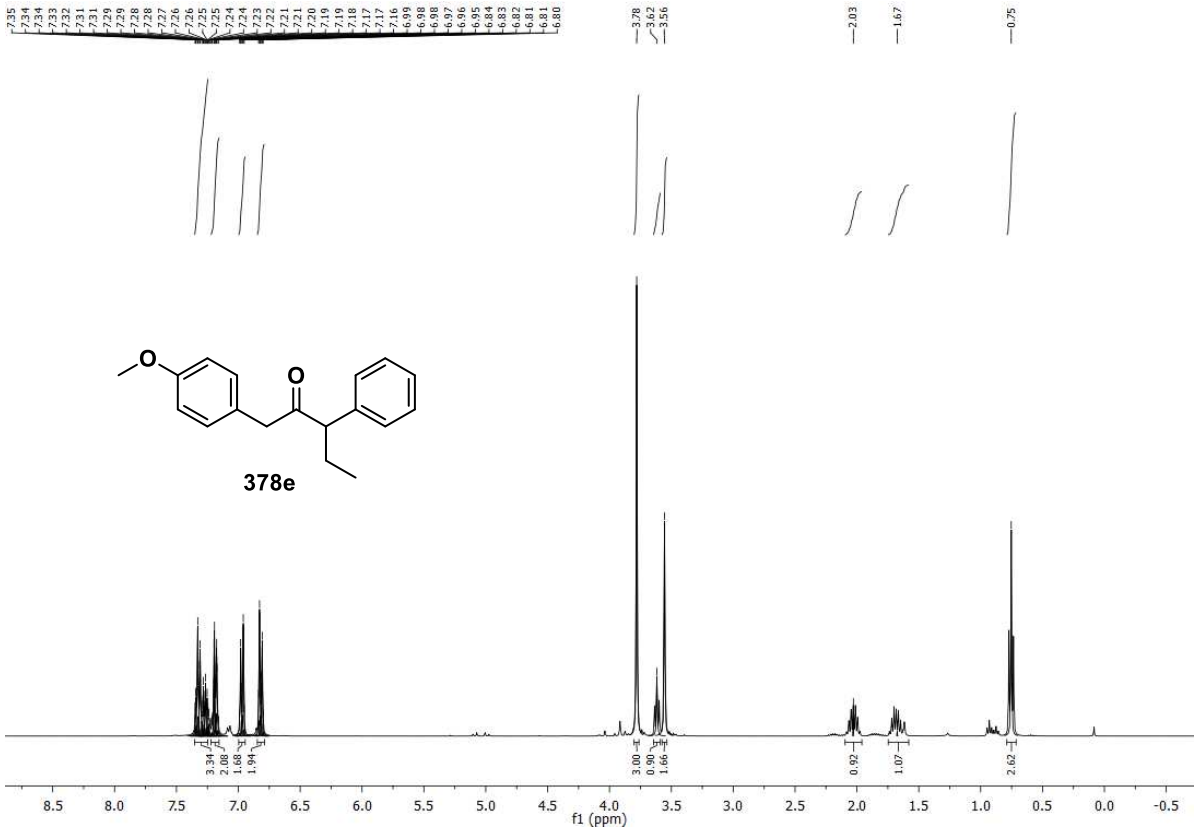

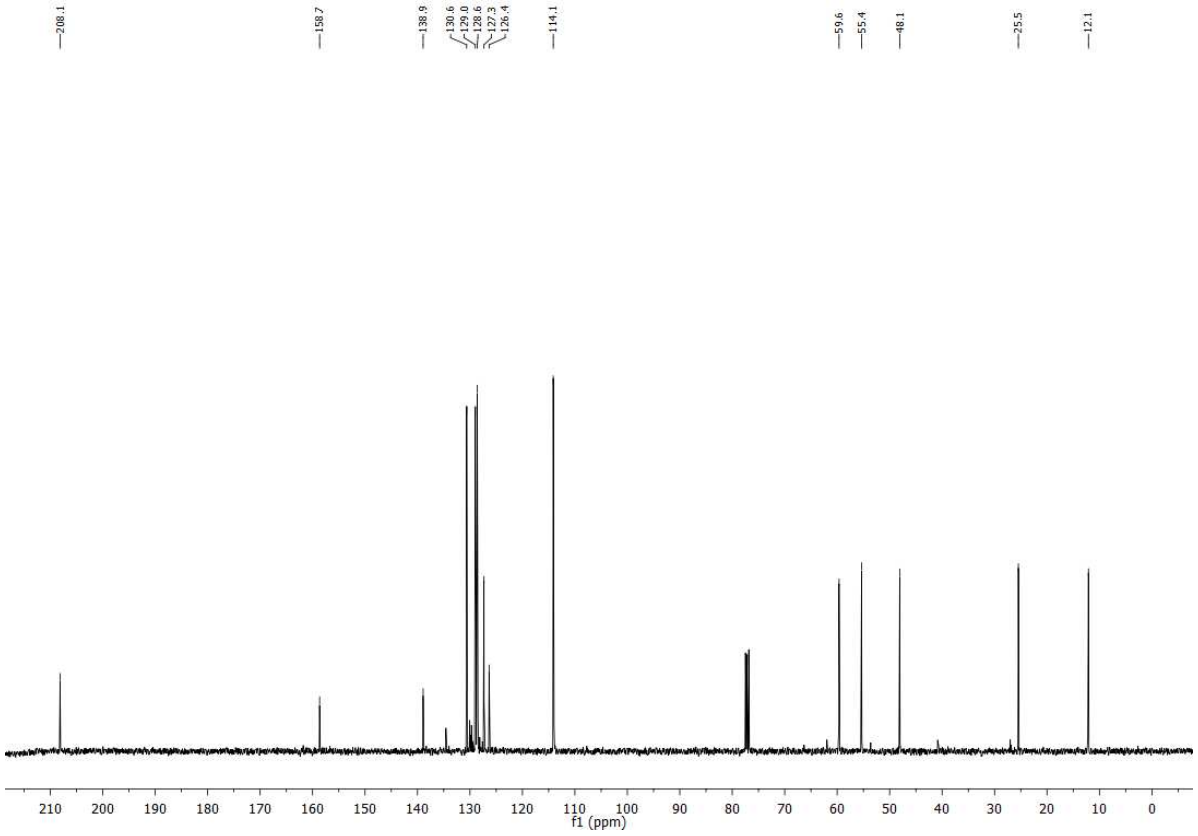

3-(6-methoxynaphthalen-2-yl)-1-(4-methoxyphenyl)butan-2-one (378f)

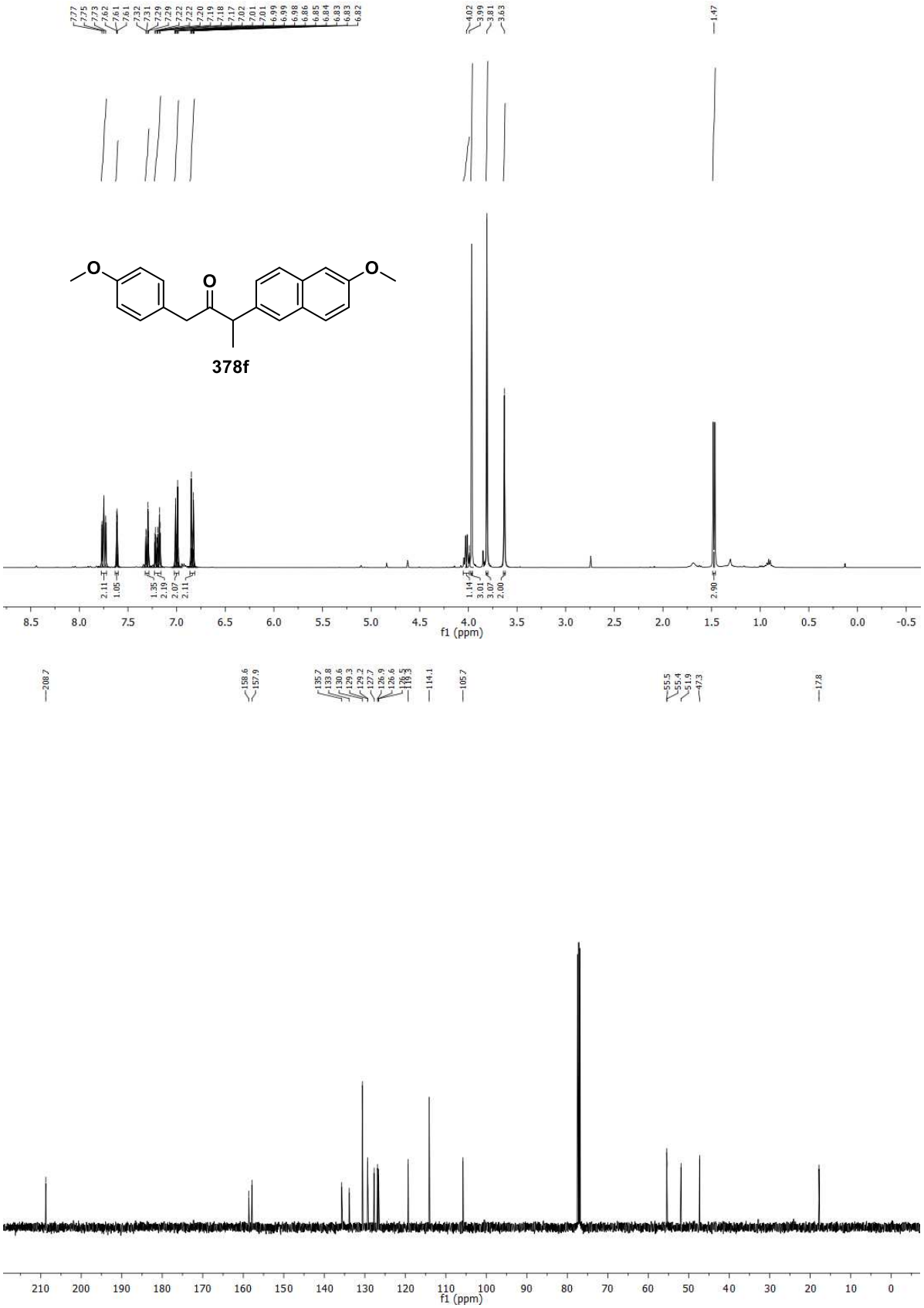

1-(4-methoxyphenyl)-4-phenylbutan-2-one (378g)

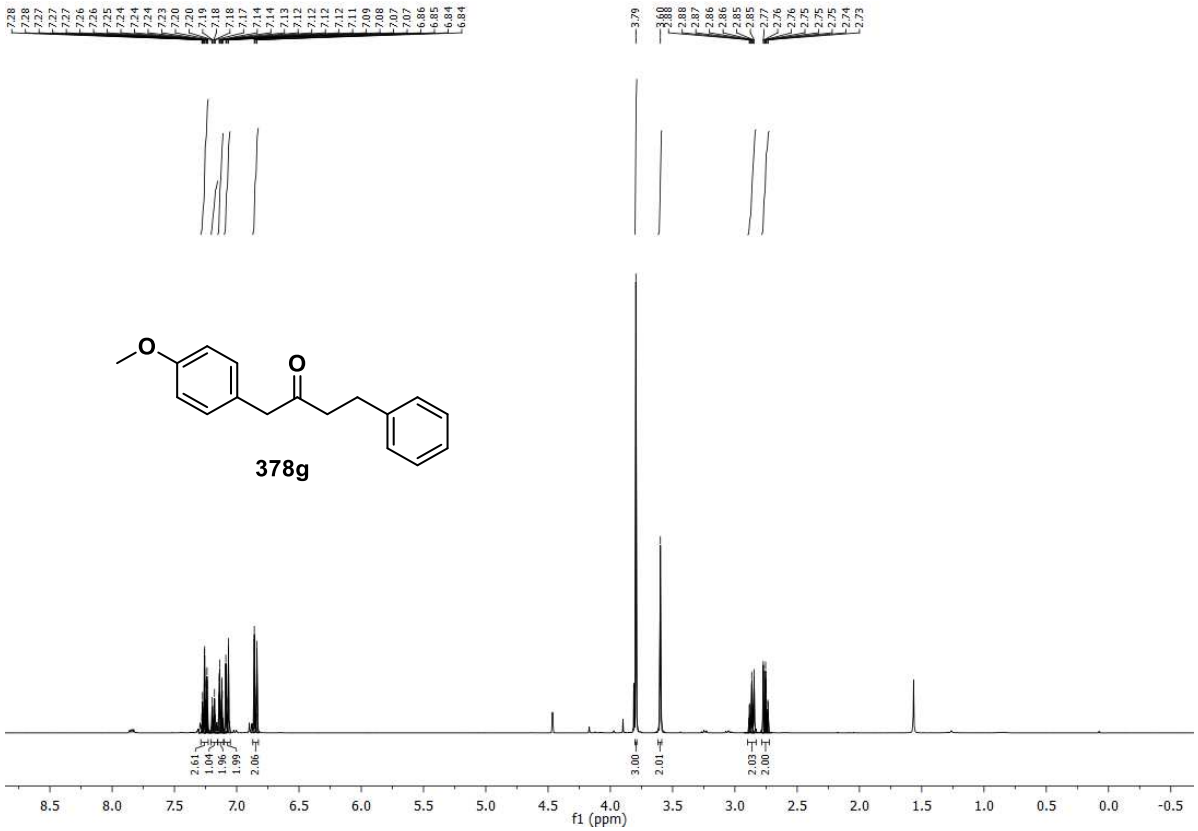

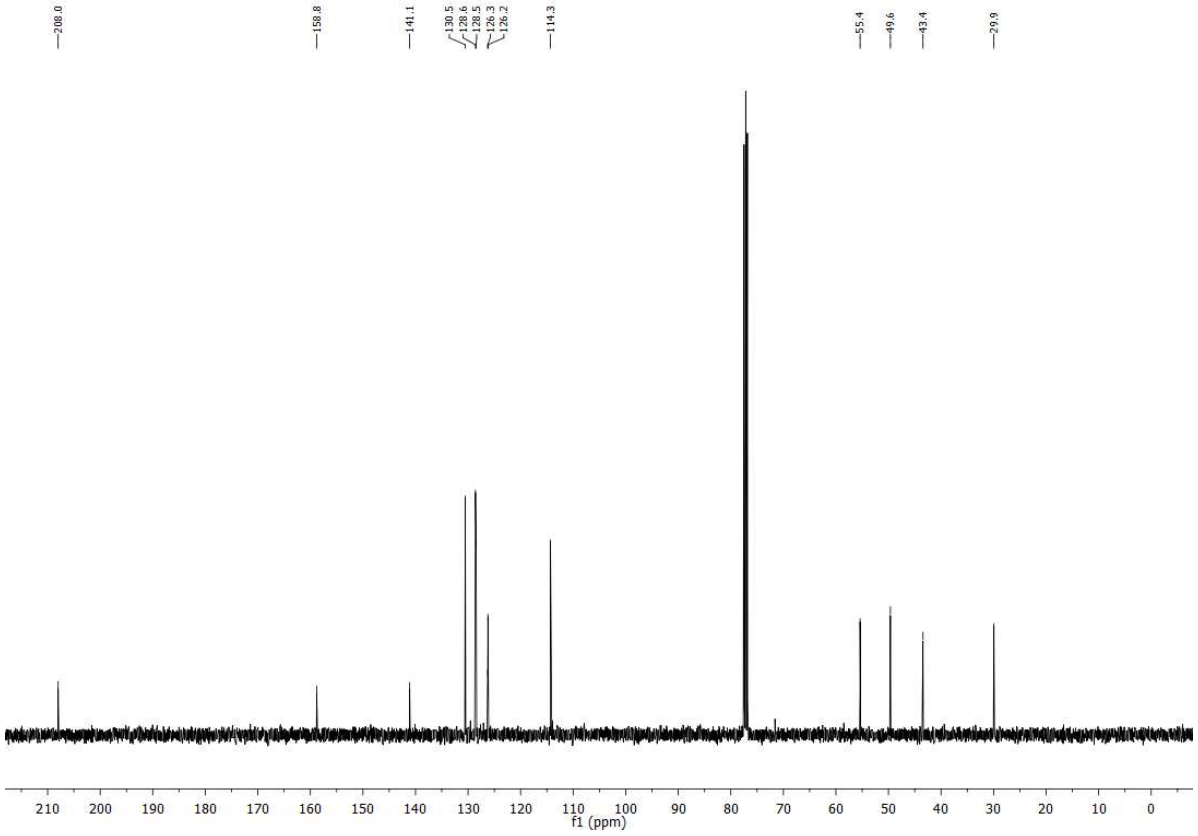

1,4-bis(4-methoxyphenyl)butan-2-one (378h)

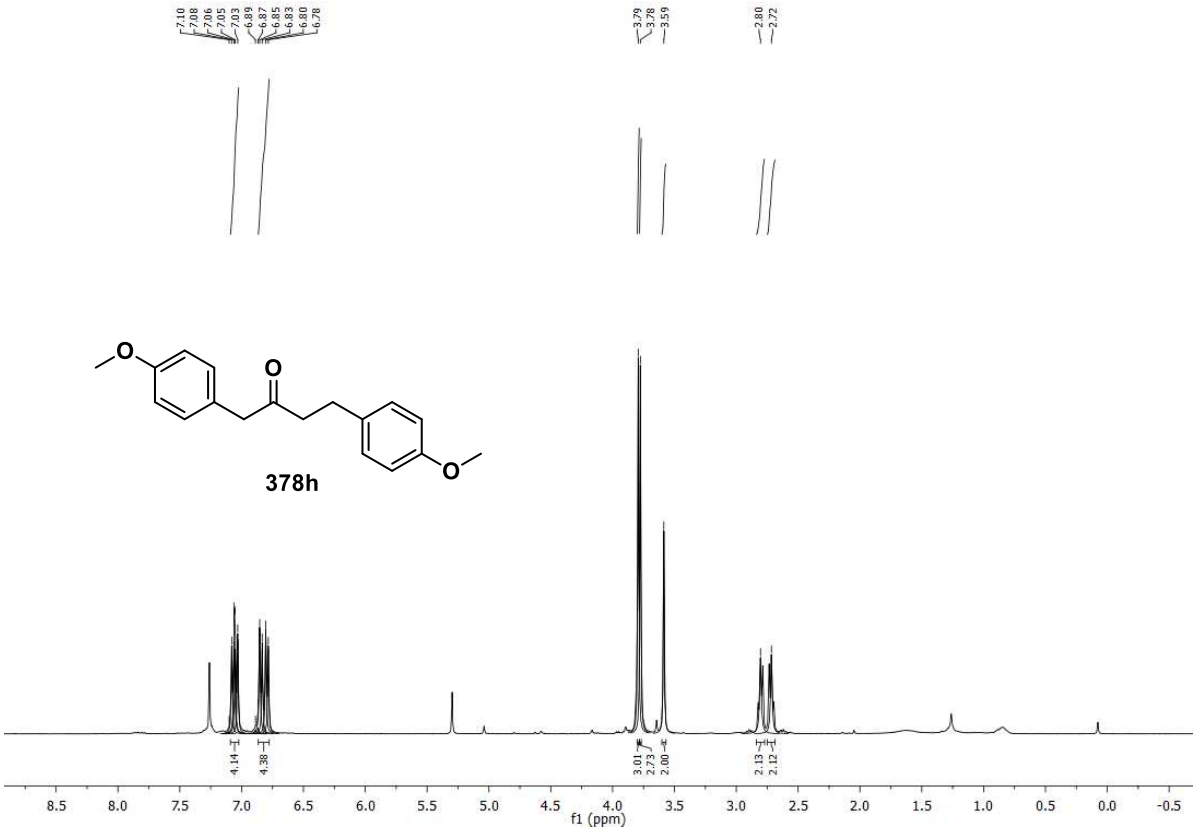

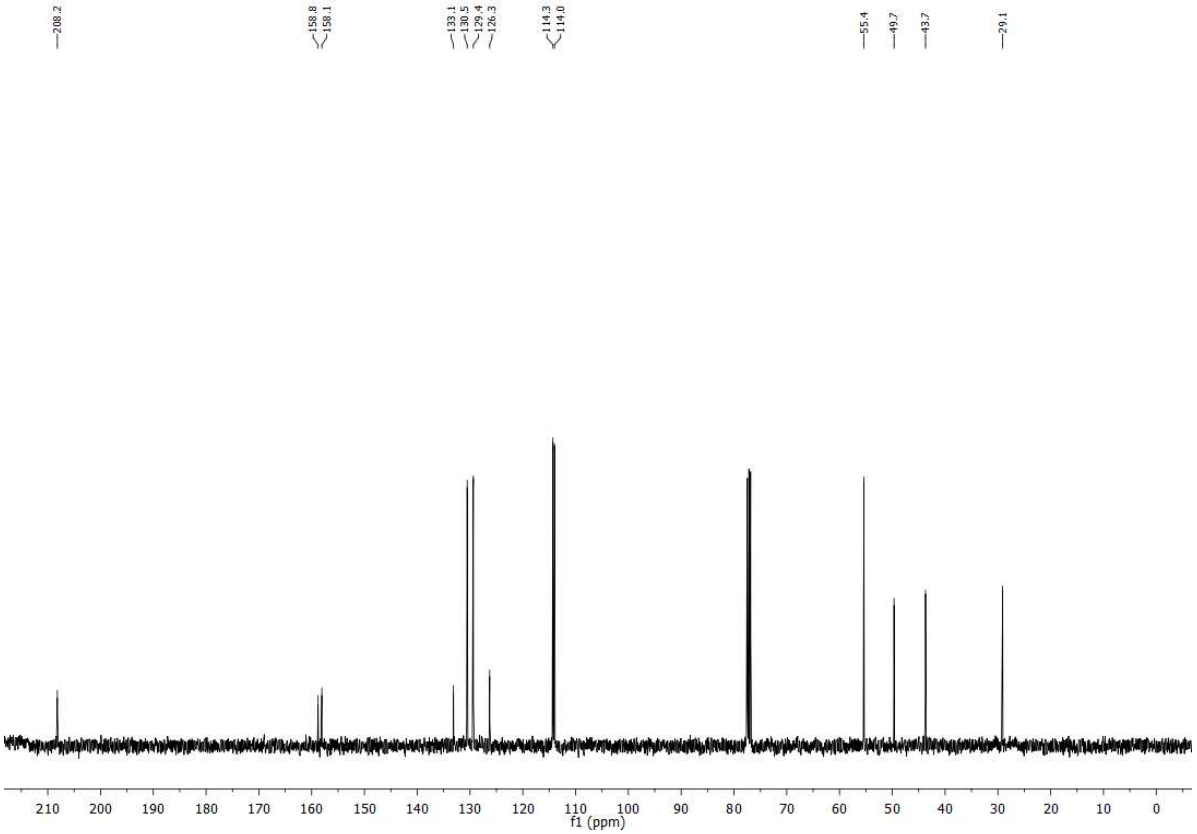

1-(4-methoxyphenyl)heptan-2-one (378i)

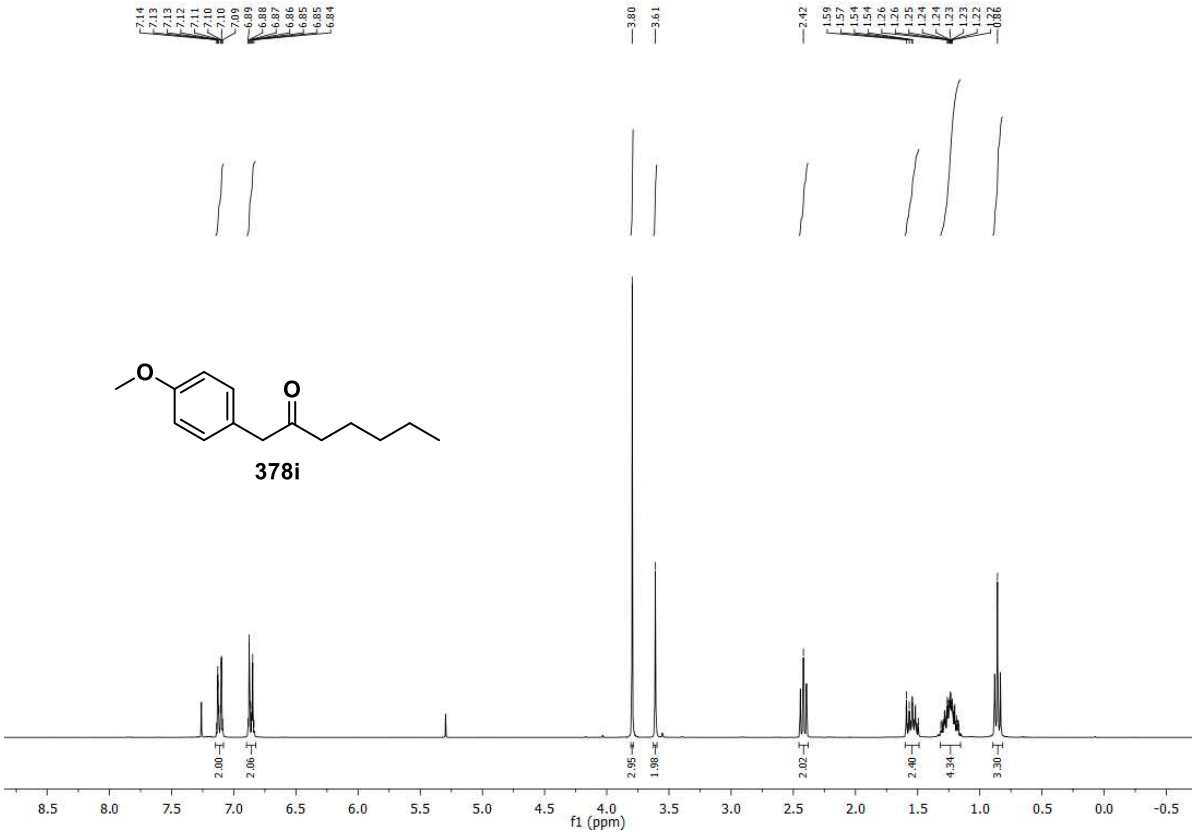

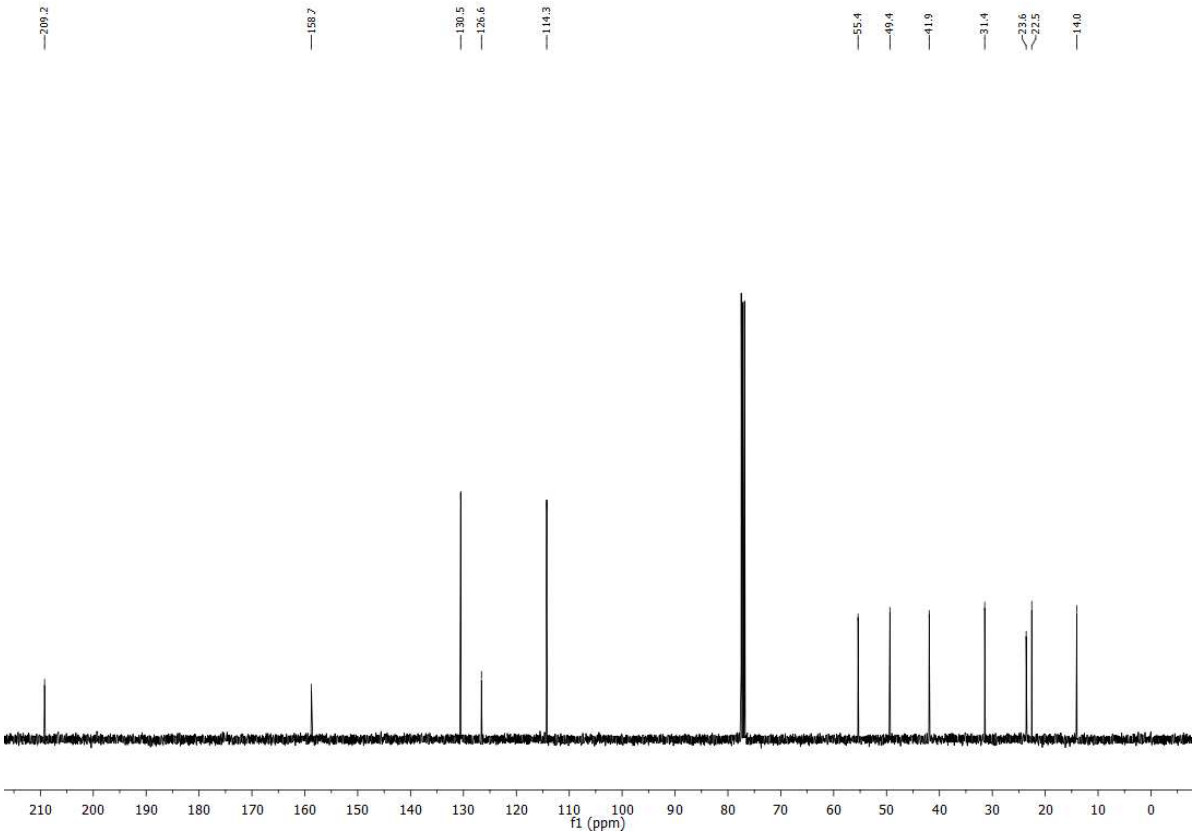

3-ethyl-1-(4-methoxyphenyl)heptan-2-one (378j)

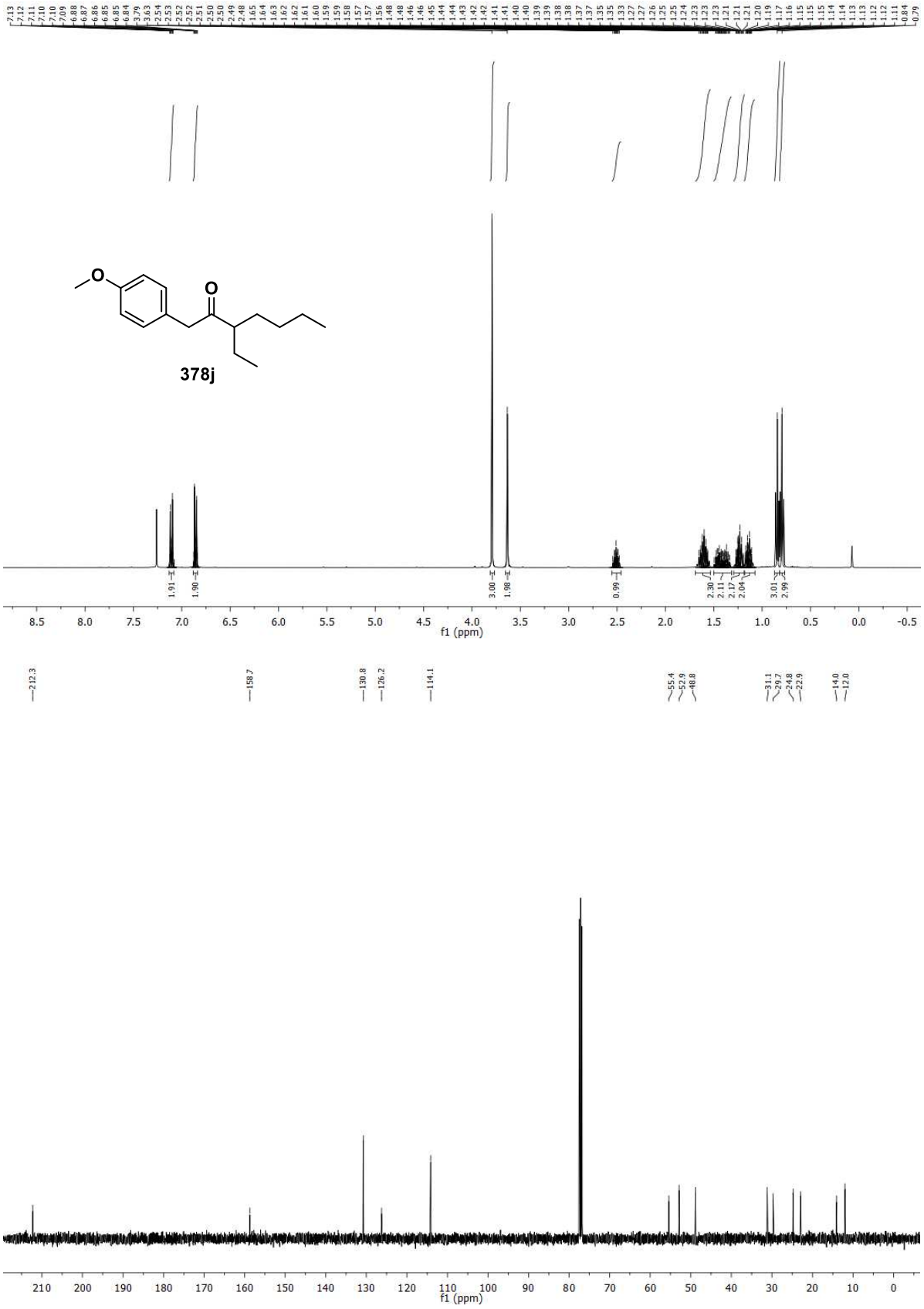

2-(2-methoxyphenyl)-1-phenylethan-1-one (378l)

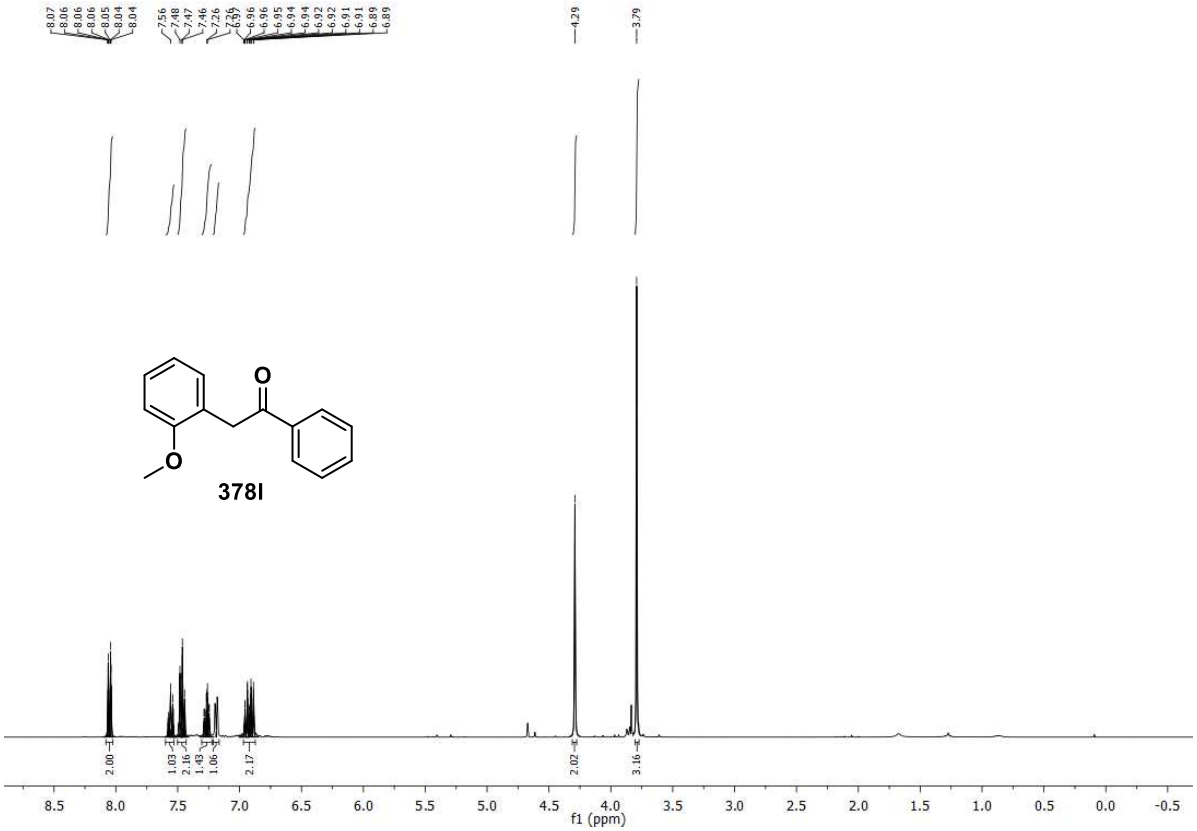

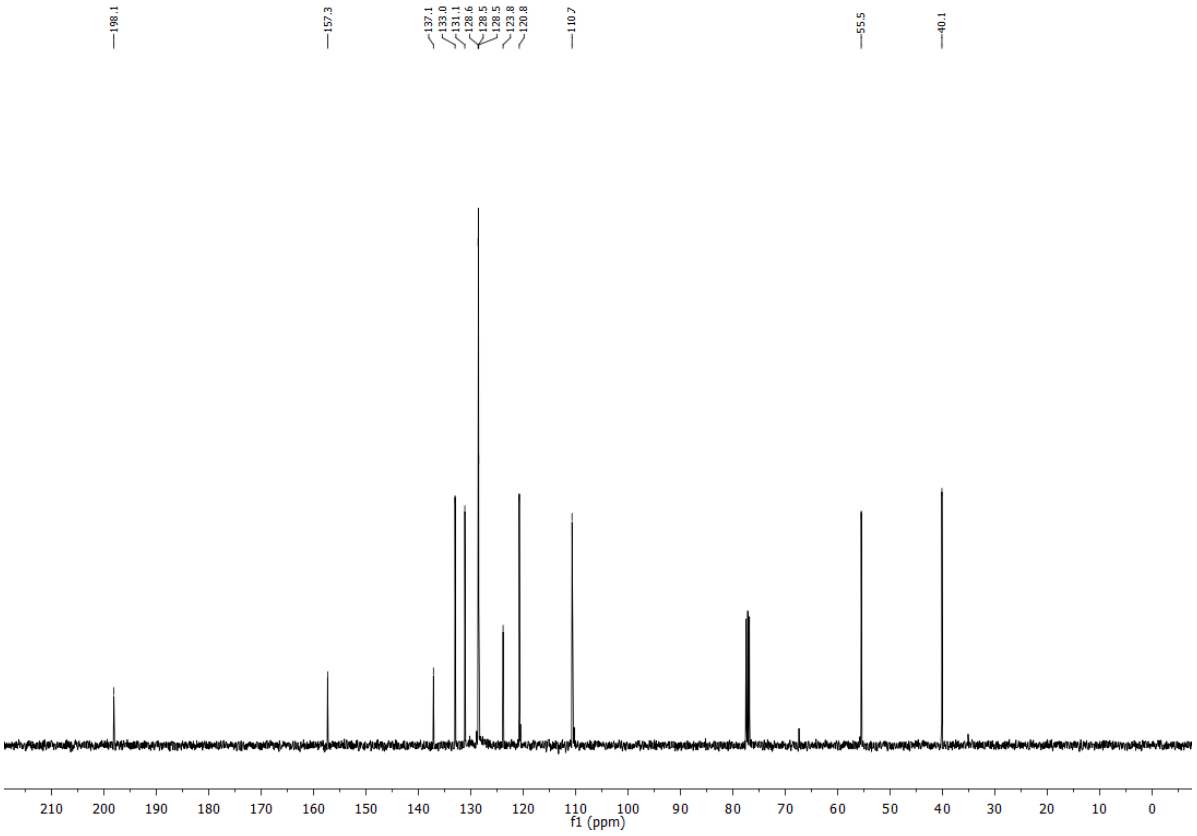

2-(3,4-dimethoxyphenyl)-1-phenylethan-1-one (378m)

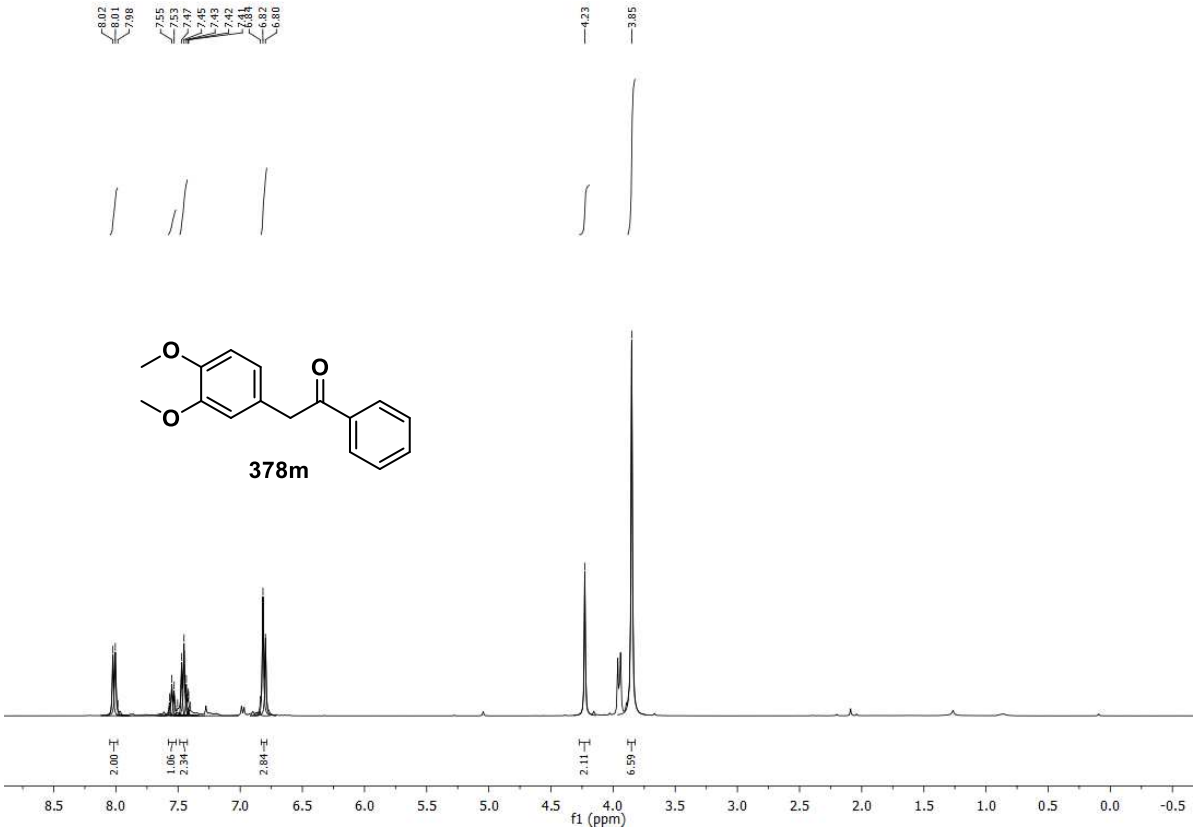

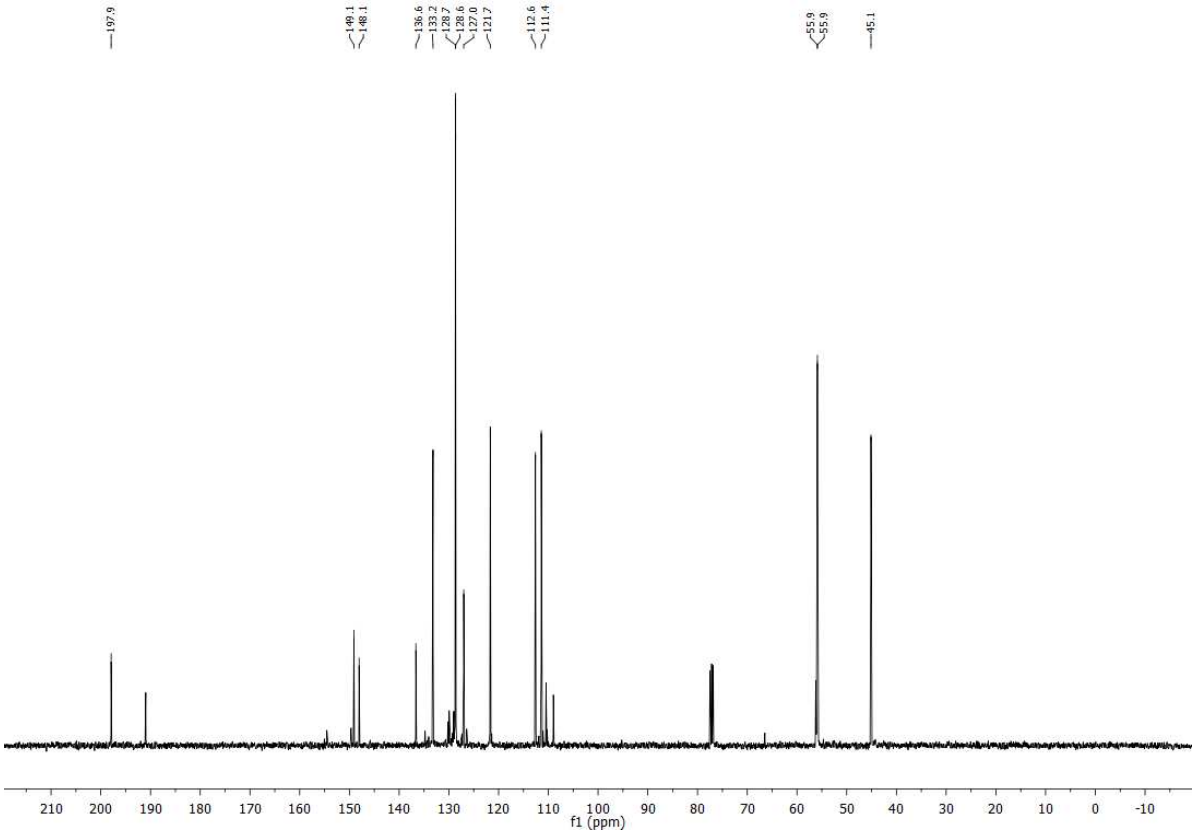

1,3-bis(4-methoxyphenyl)propan-2-one (385)

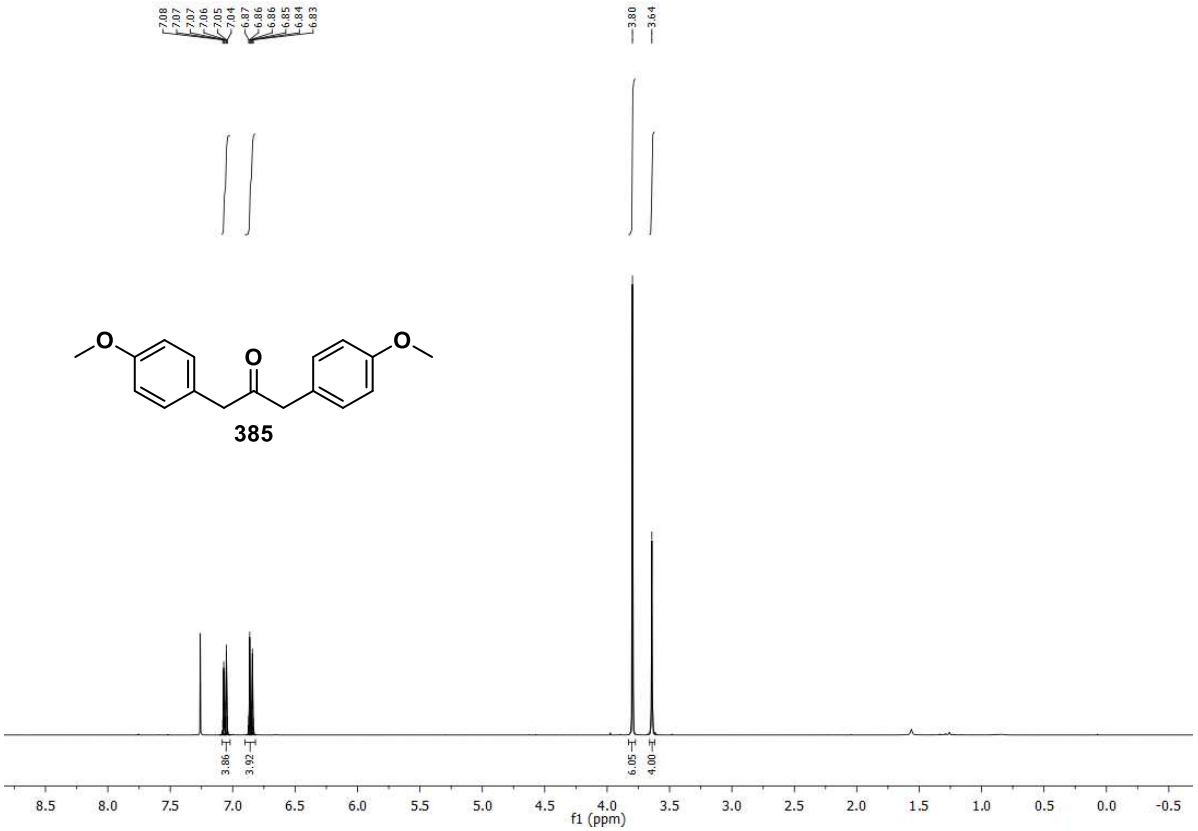

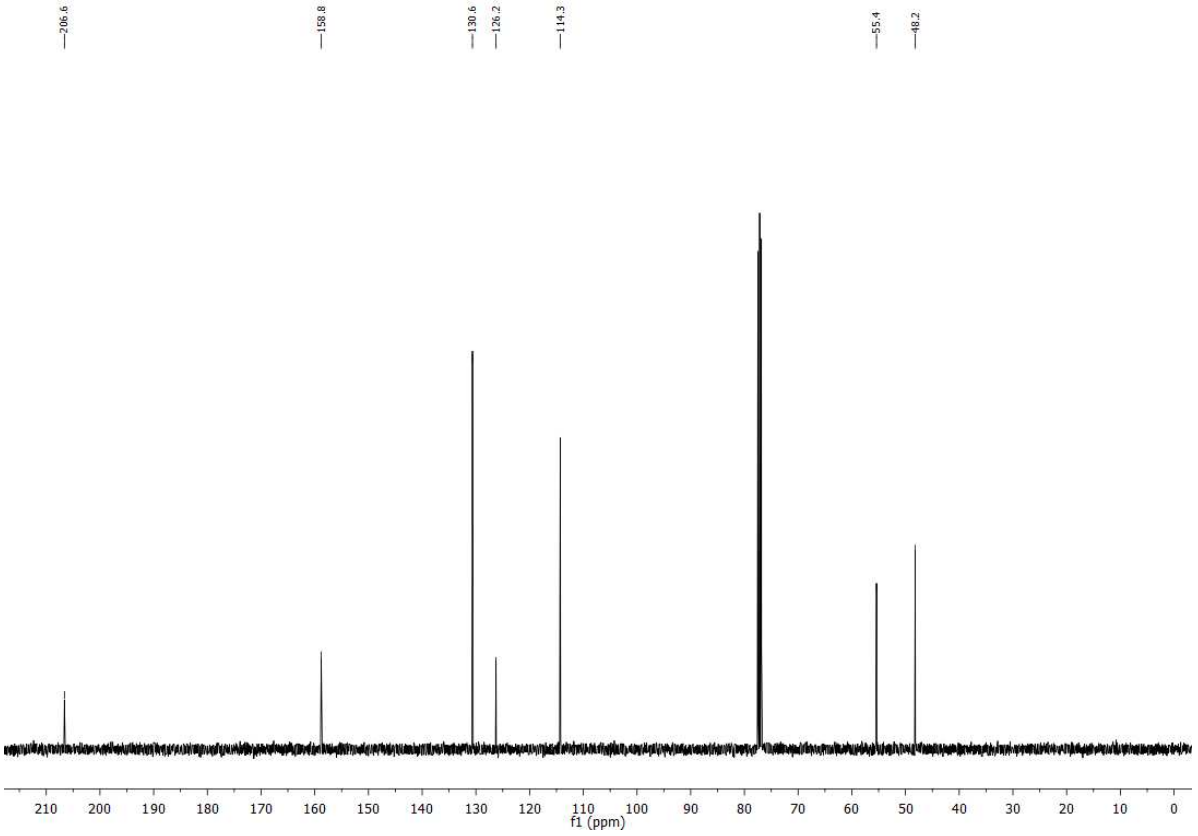

4.4.8 NMR Spectra of Ketones Synthesized from Chlorides

2-(4-methoxyphenyl)-1-phenylethan-1-one (378a) analogously to GP-E

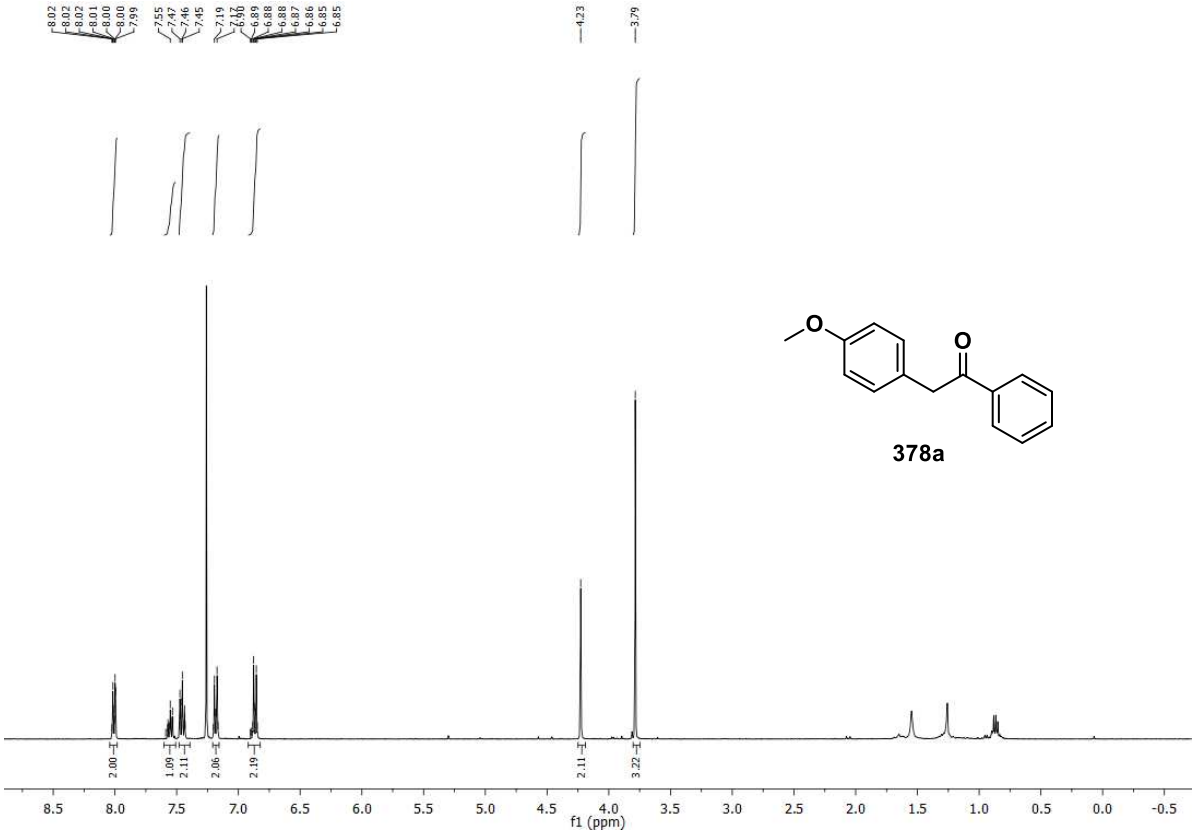

378a

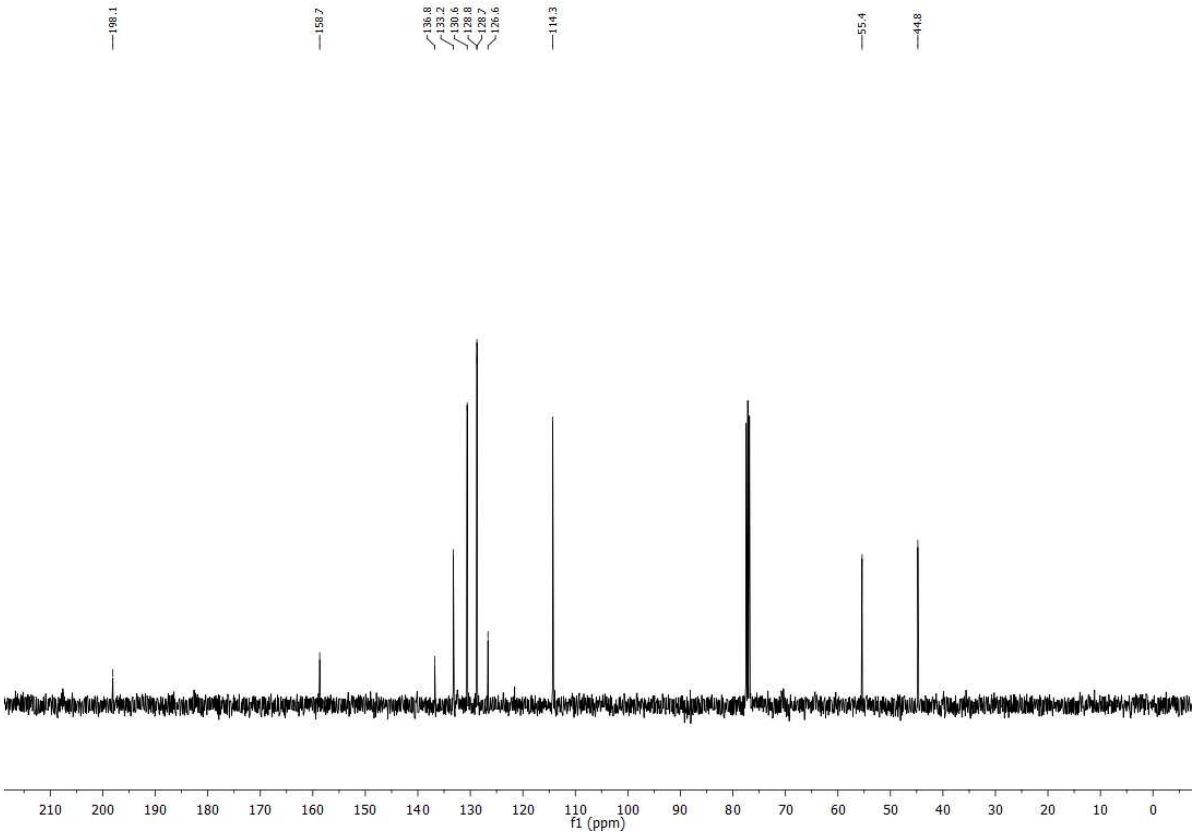

1,2-diphenylethan-1-one (378n) analogously to GP-D

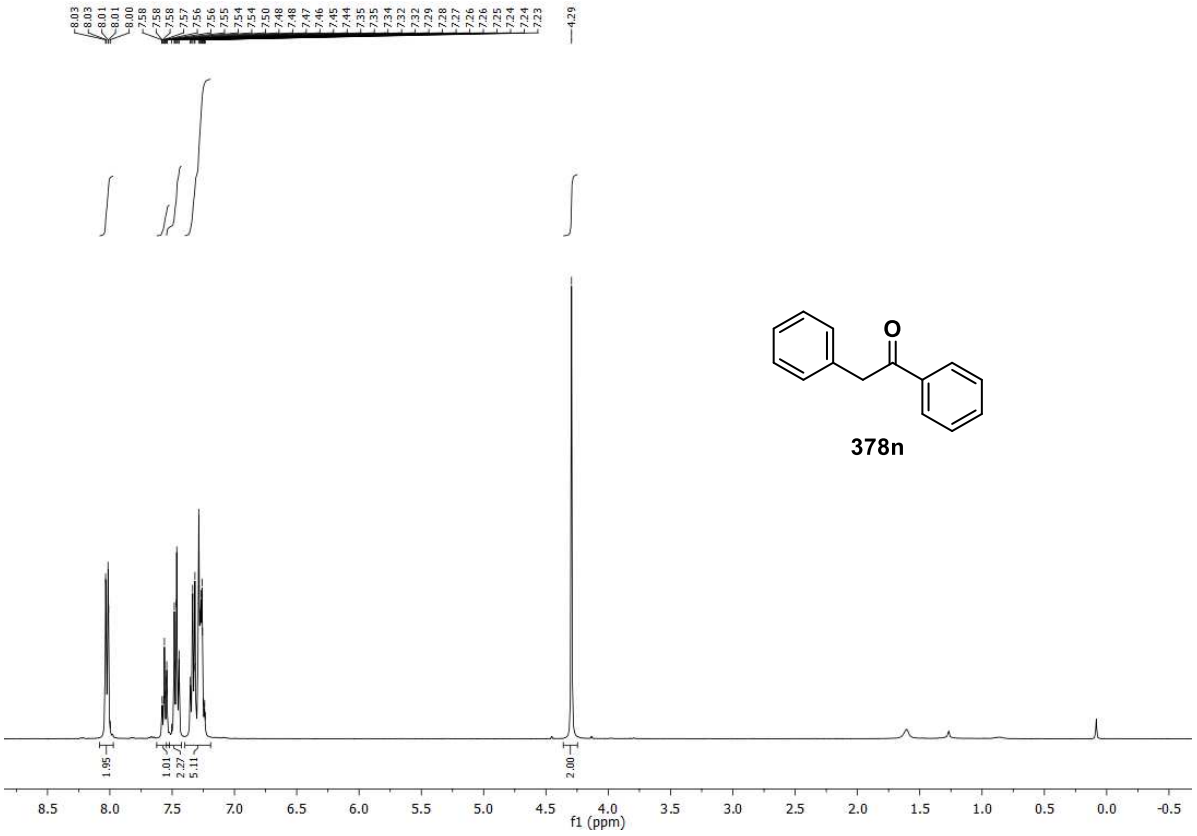

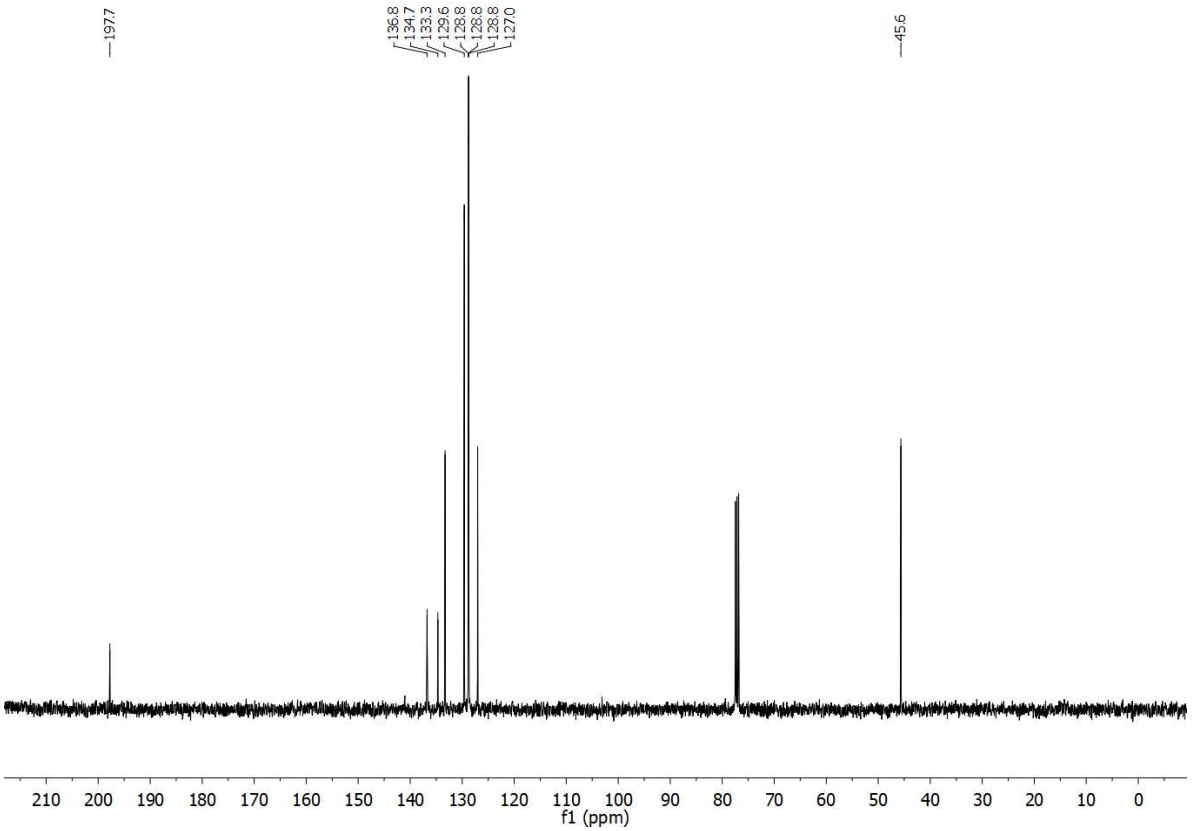

1,2-diphenylethan-1-one (378n) analogously to GP-E

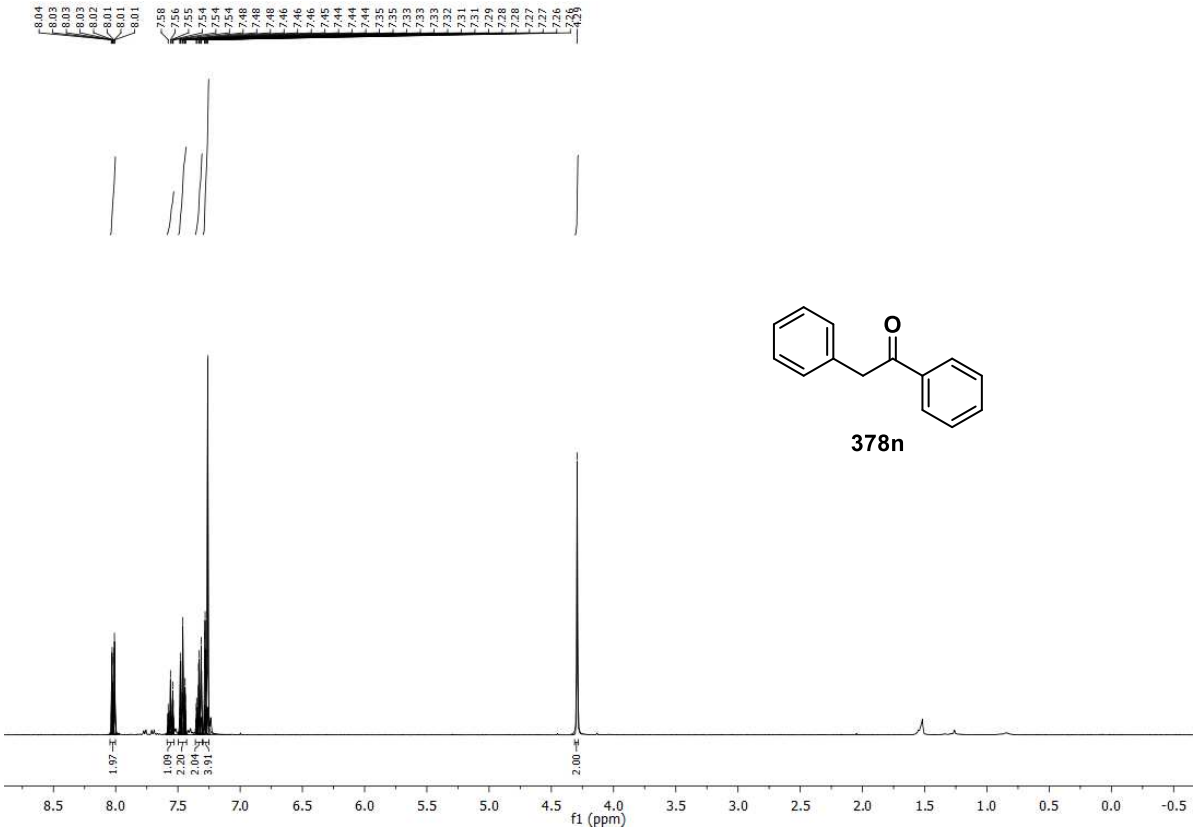

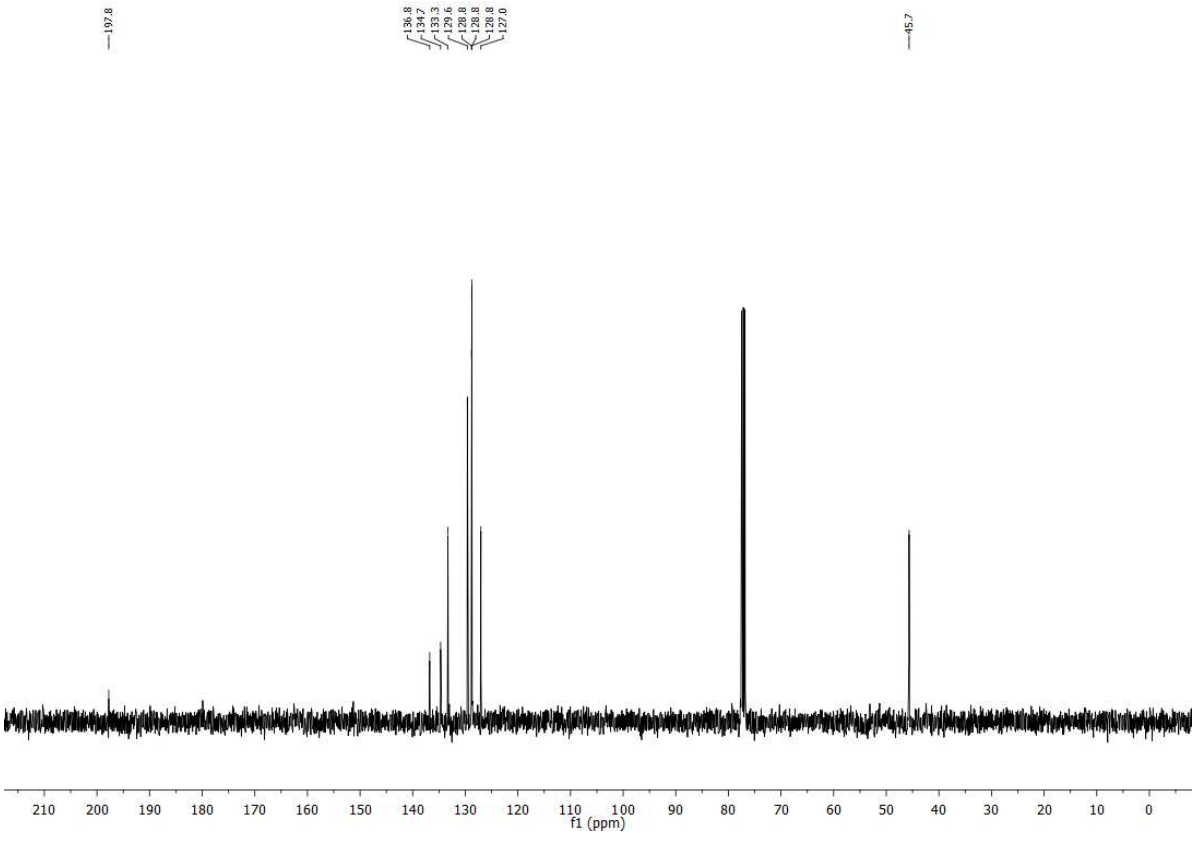

2-(3-methoxyphenyl)-1-phenylethan-1-one (378o)

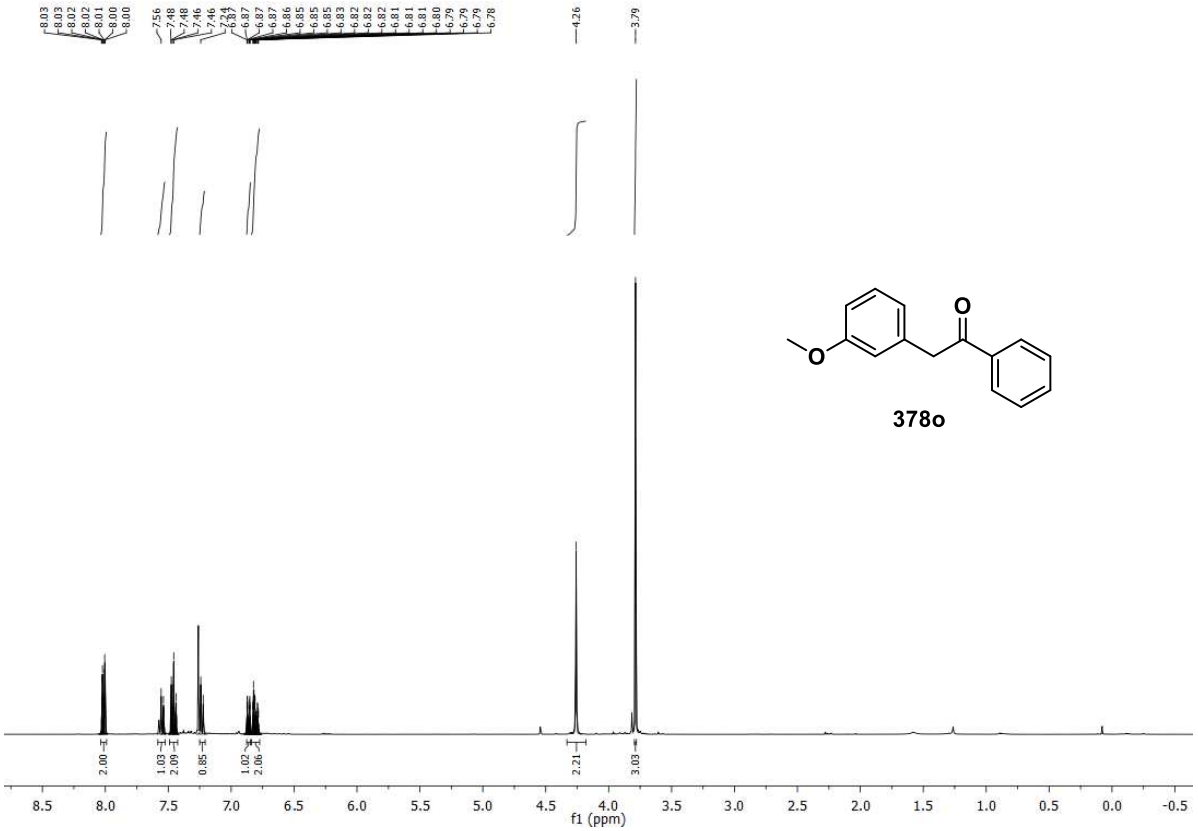

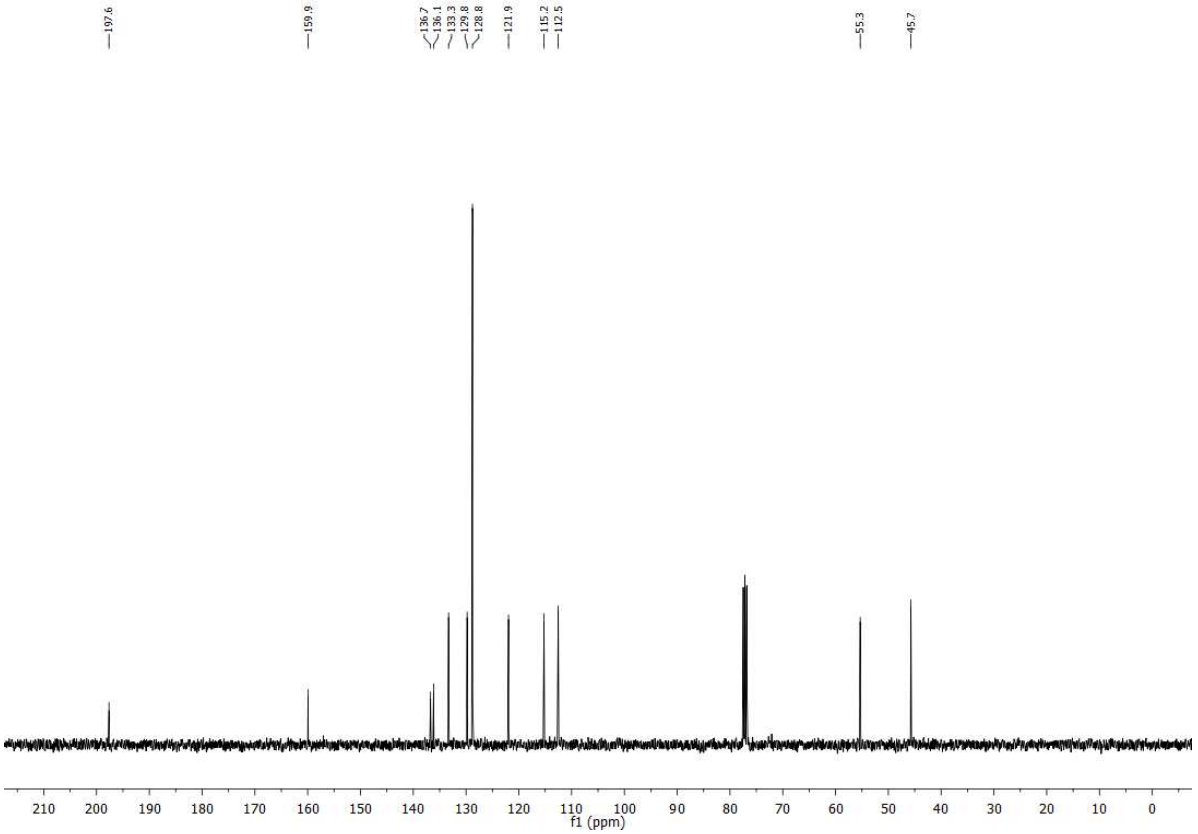

1-phenyl-2-(*p*-tolyl)ethan-1-one (378p)

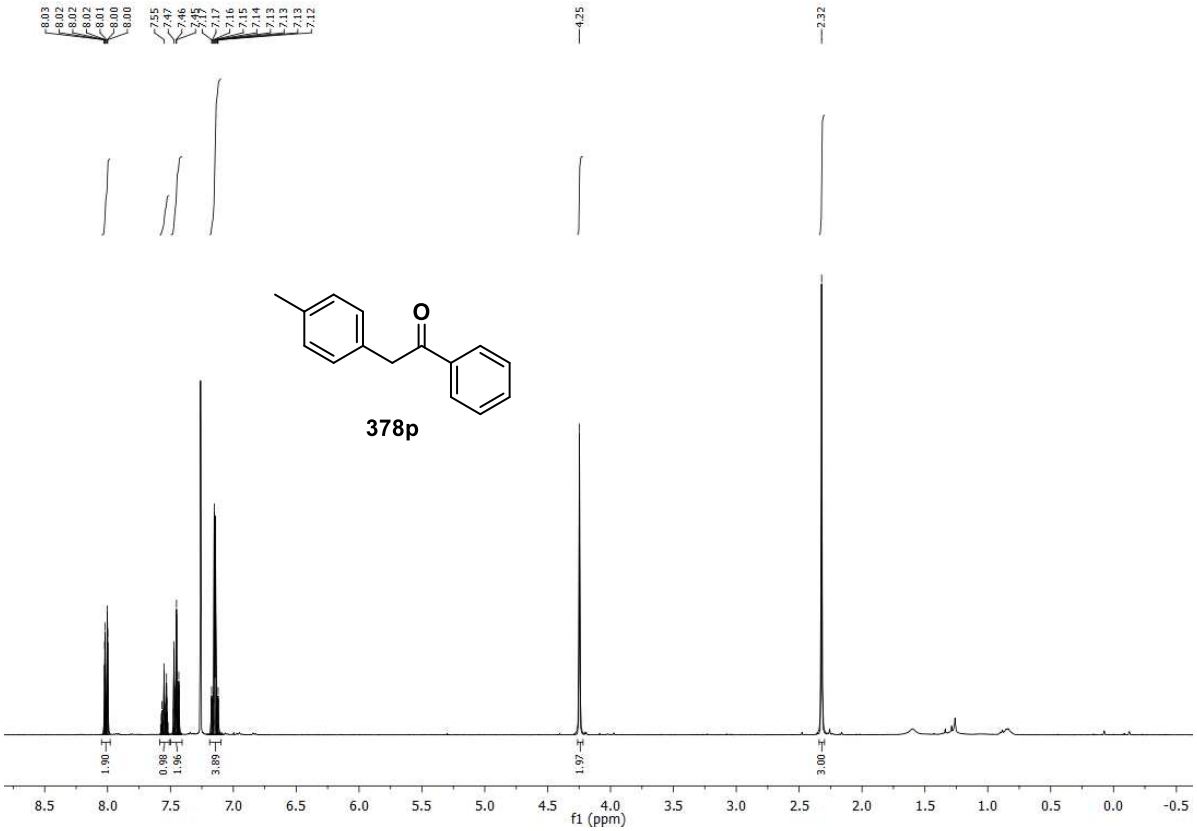

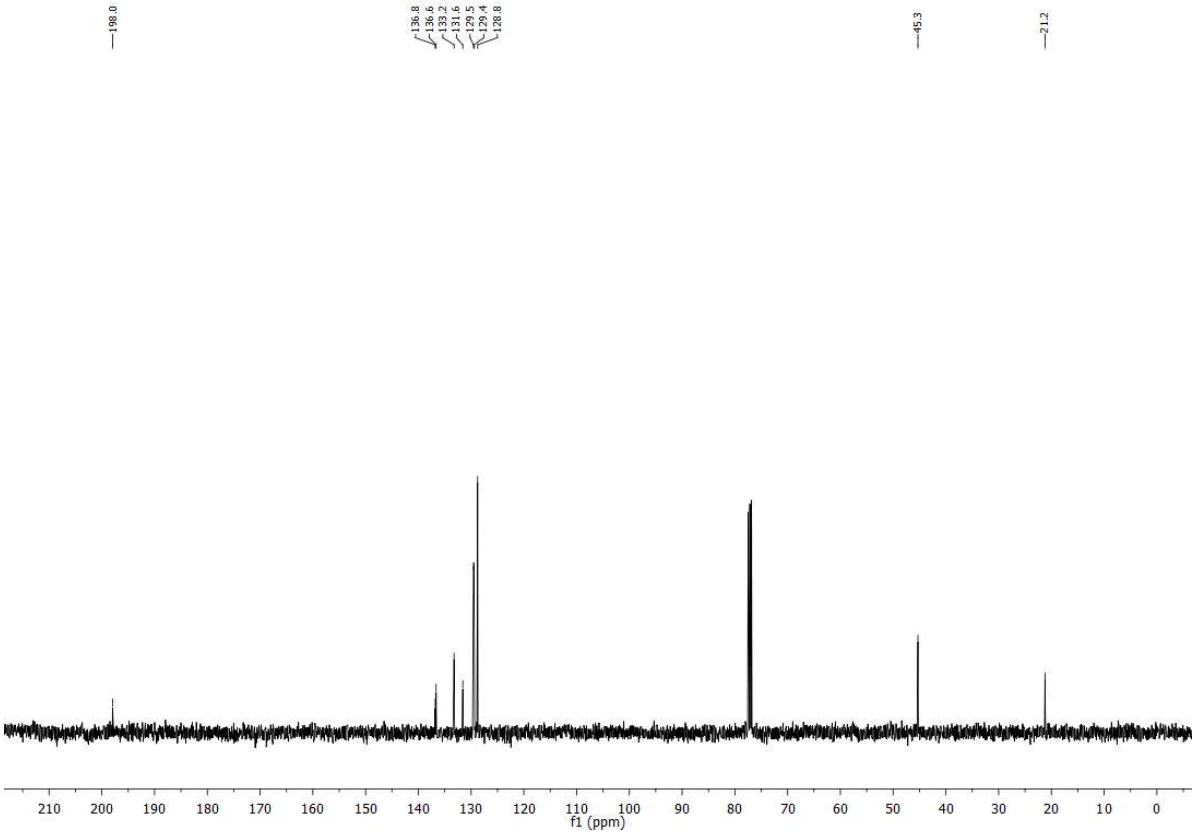

2-(naphthalen-2-yl)-1-phenylethan-1-one (378q)

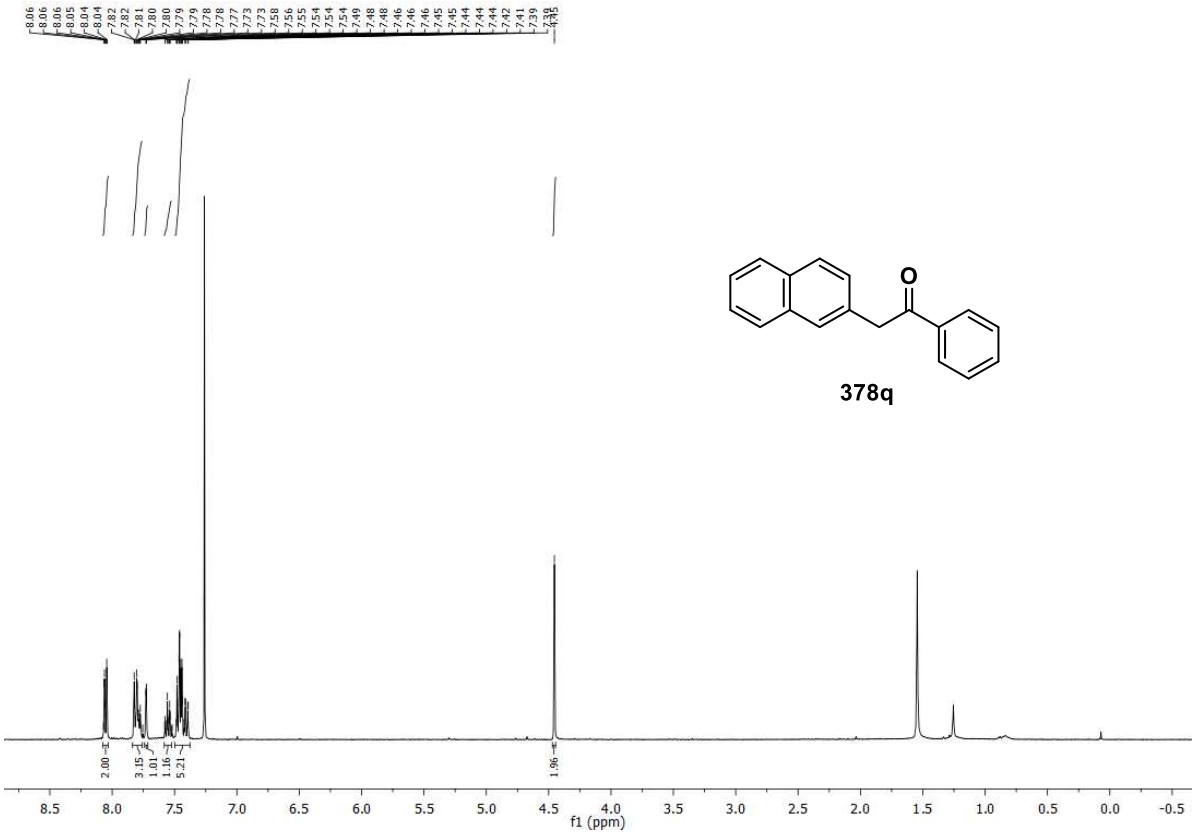

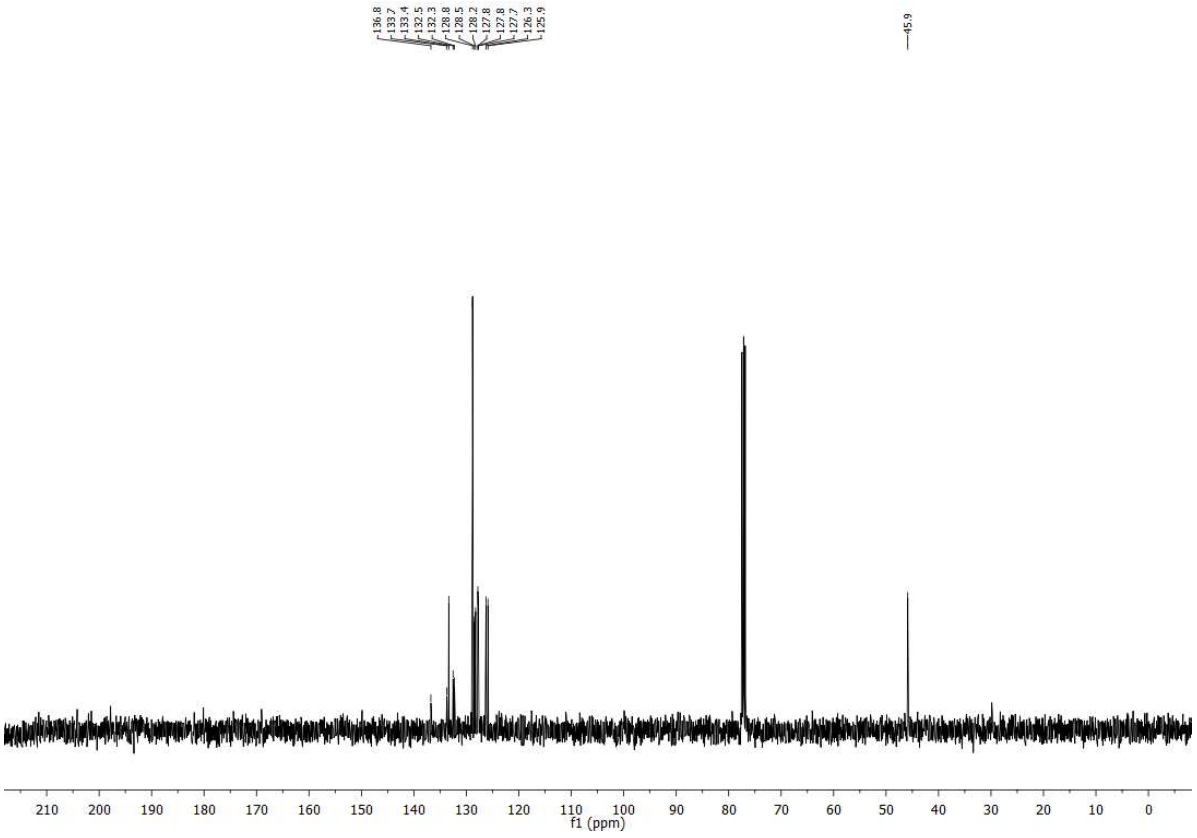

1-(4-methoxyphenyl)-3-methylbutan-2-one (378r)

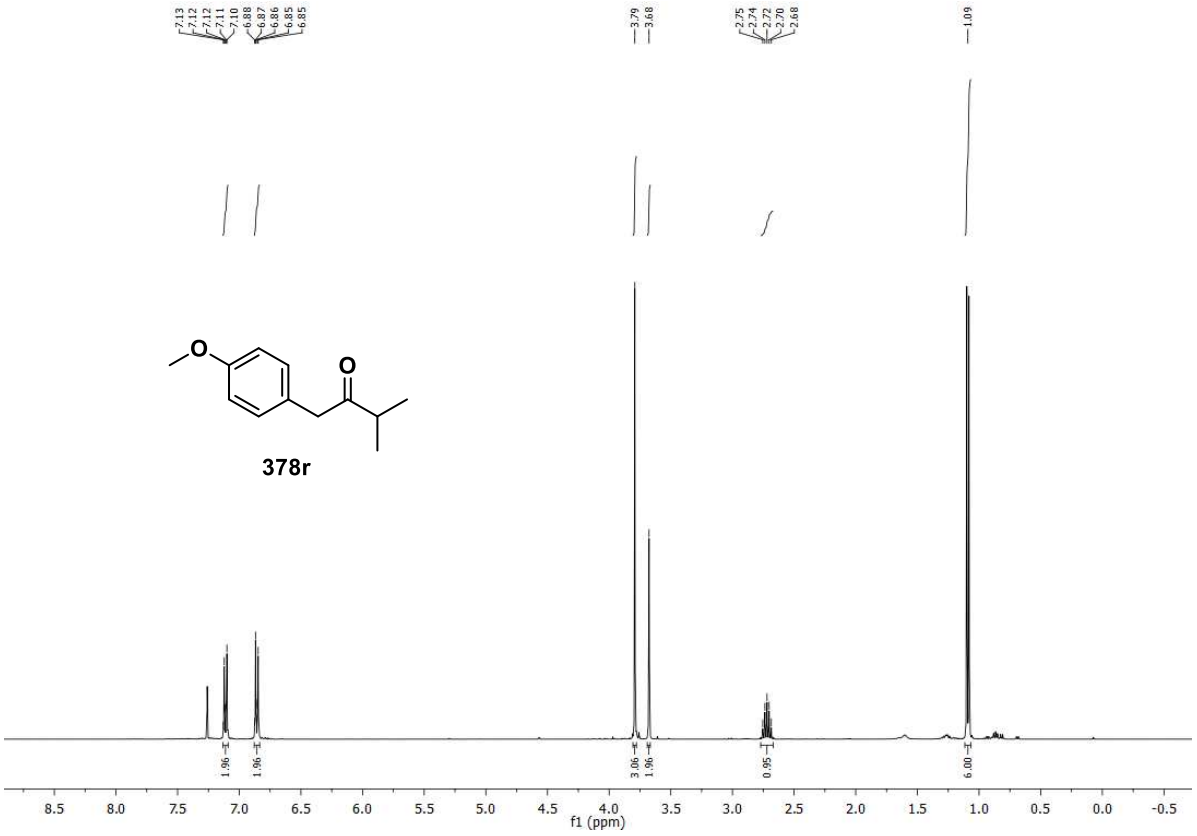

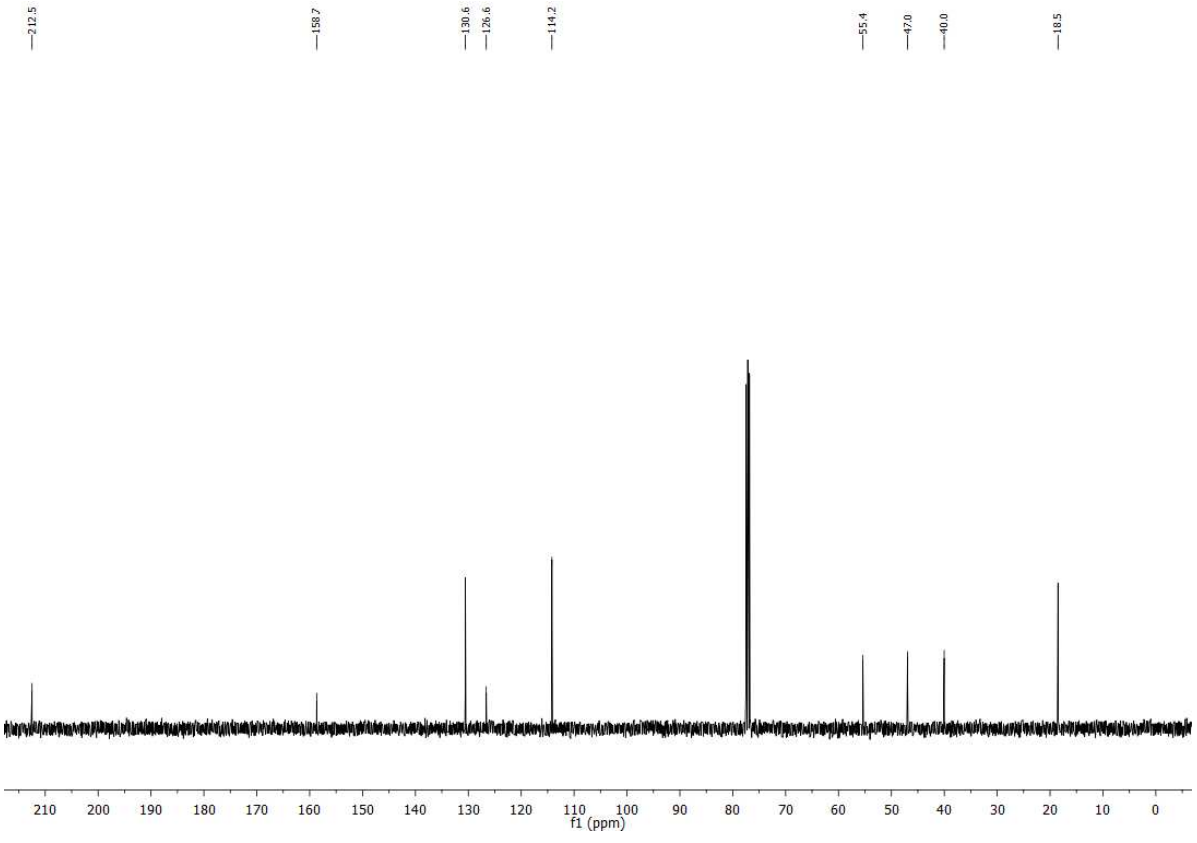

3-(4-isobutylphenyl)-1-(4-methoxyphenyl)butan-2-one (378s)

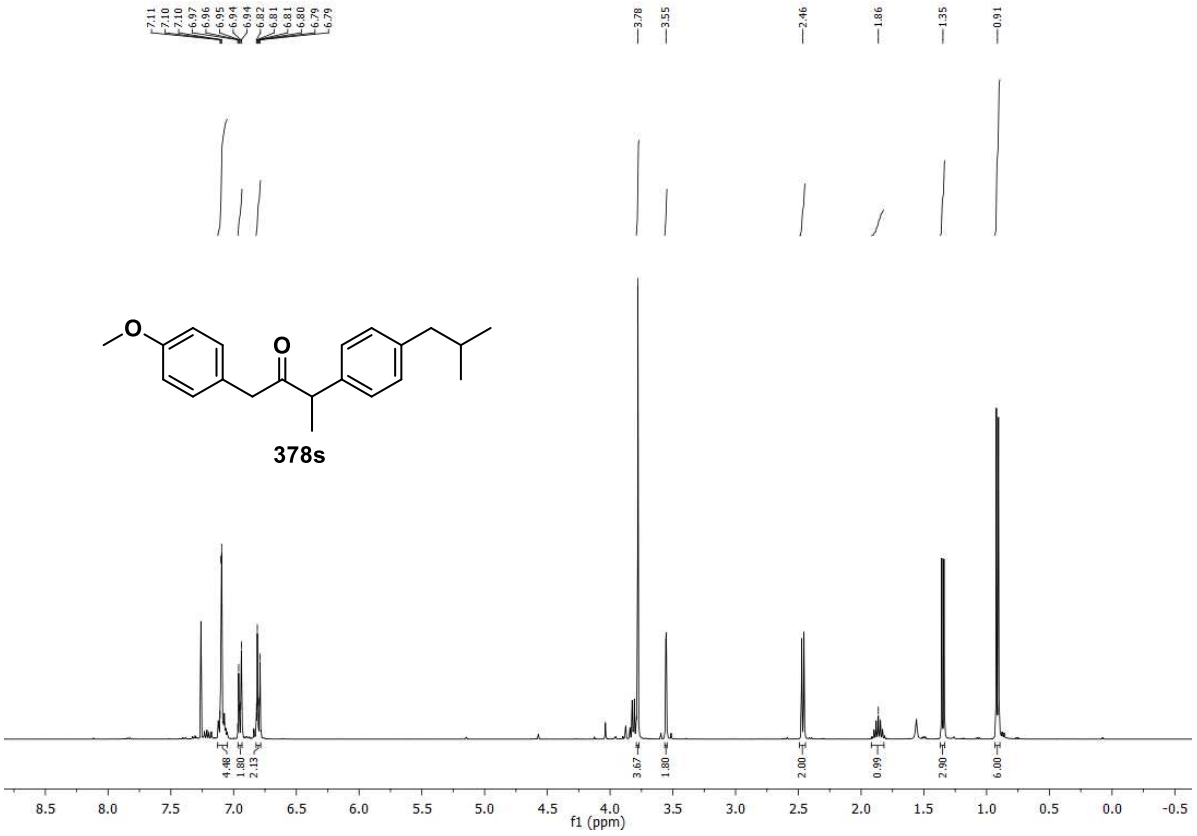

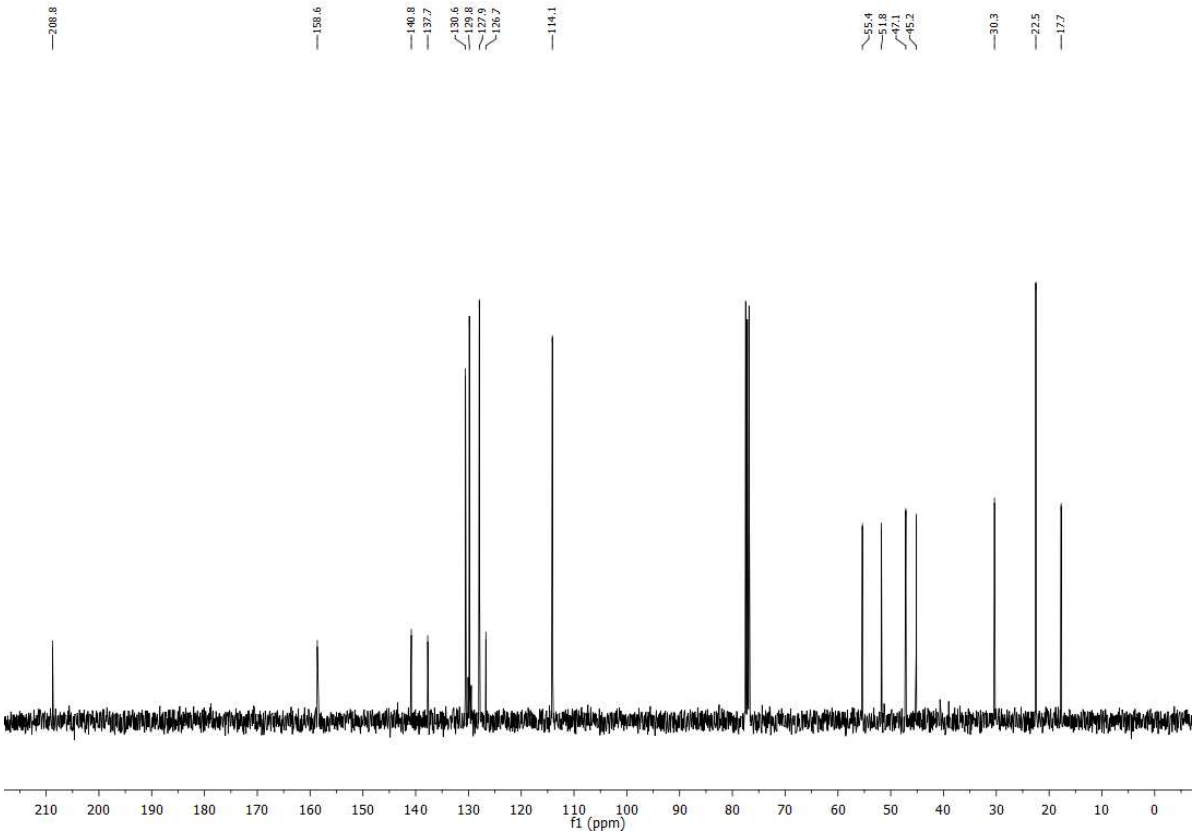

4.4.9 NMR Spectra of Miscellaneous Compounds

cyclopropyl(4-methoxyphenyl)methanol (316o)

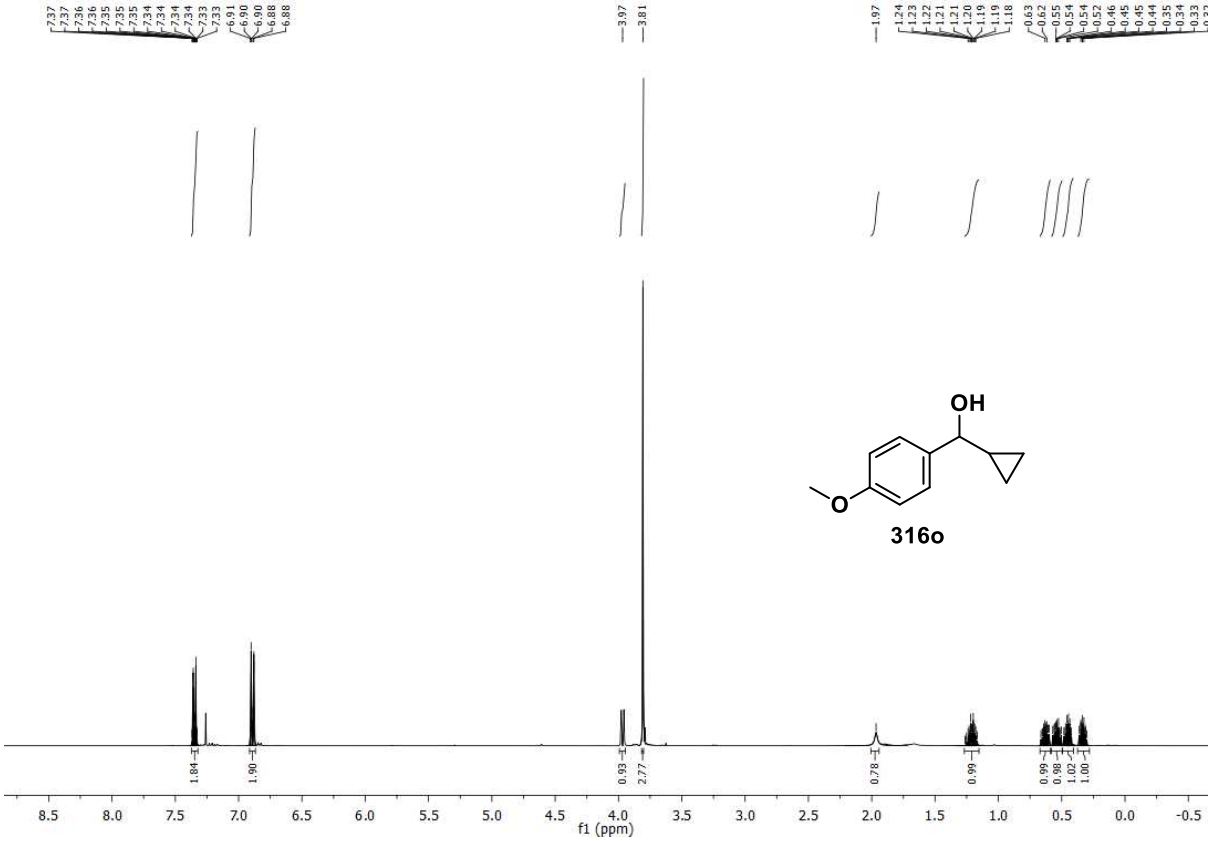

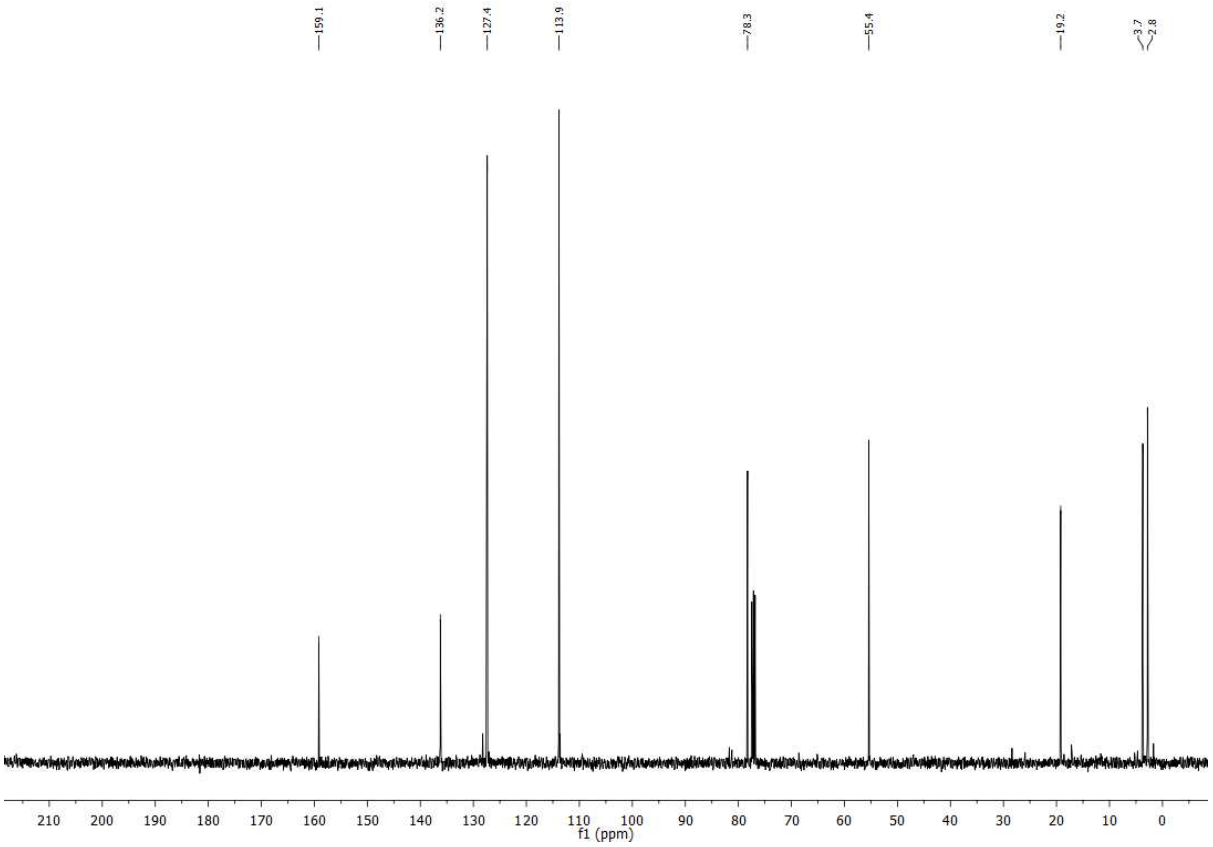

(*E*)-1-(4-chlorobut-1-en-1-yl)-4-methoxybenzene (317e)

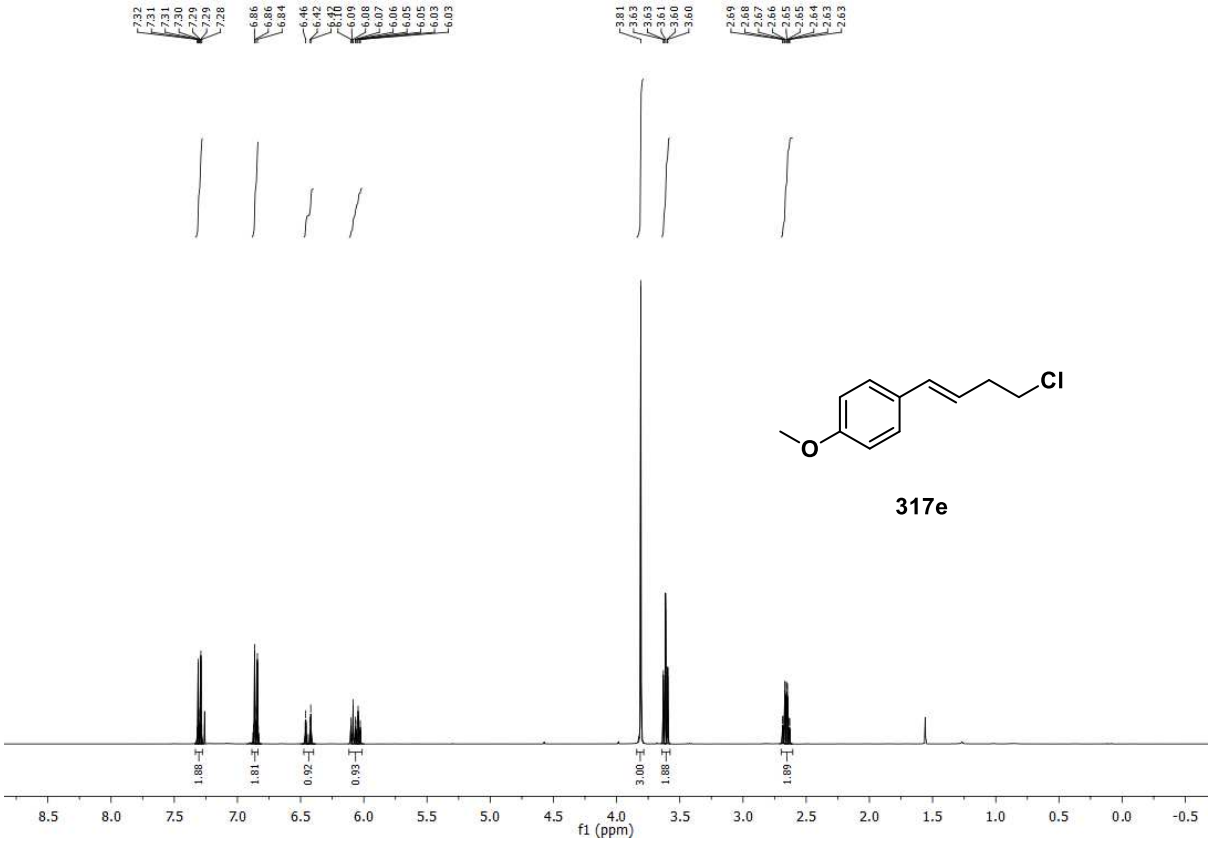

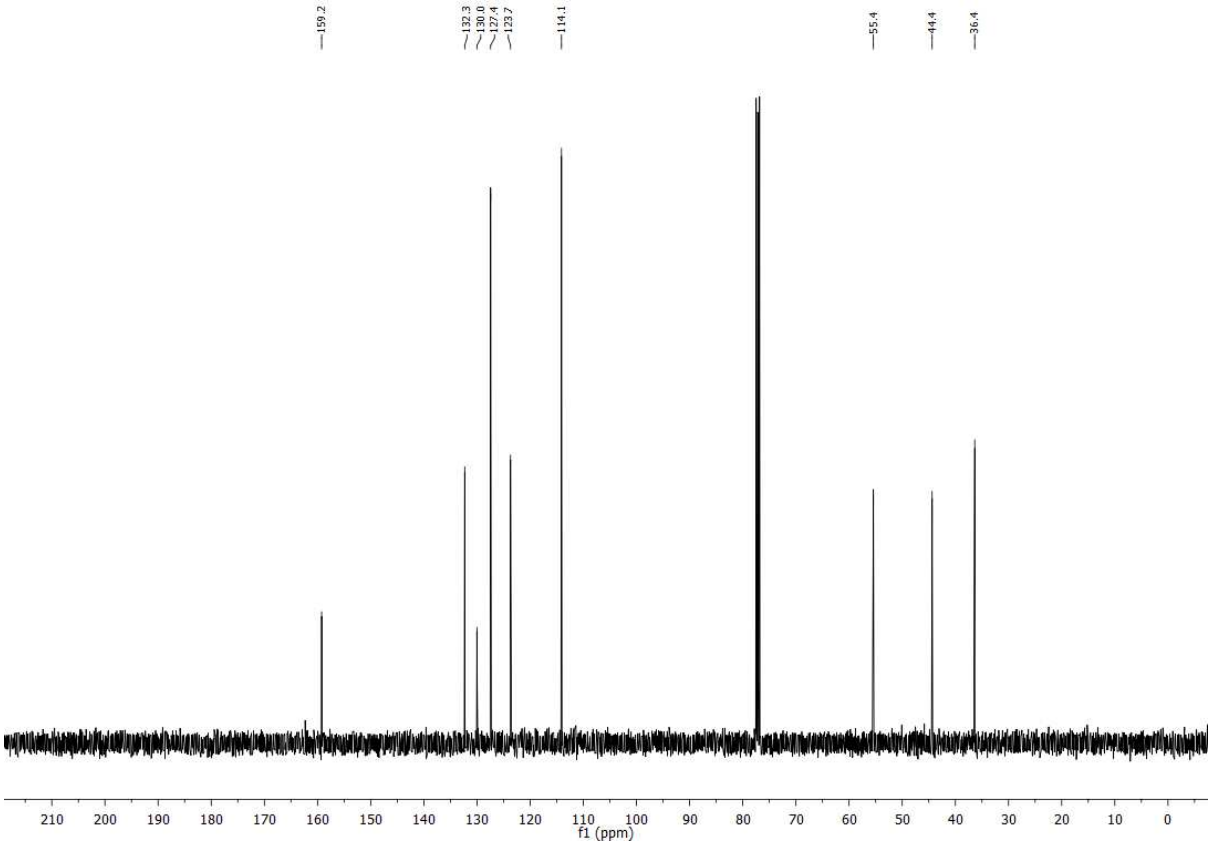

(*E*)-(4-chlorobut-1-en-1-yl)benzene (317g)

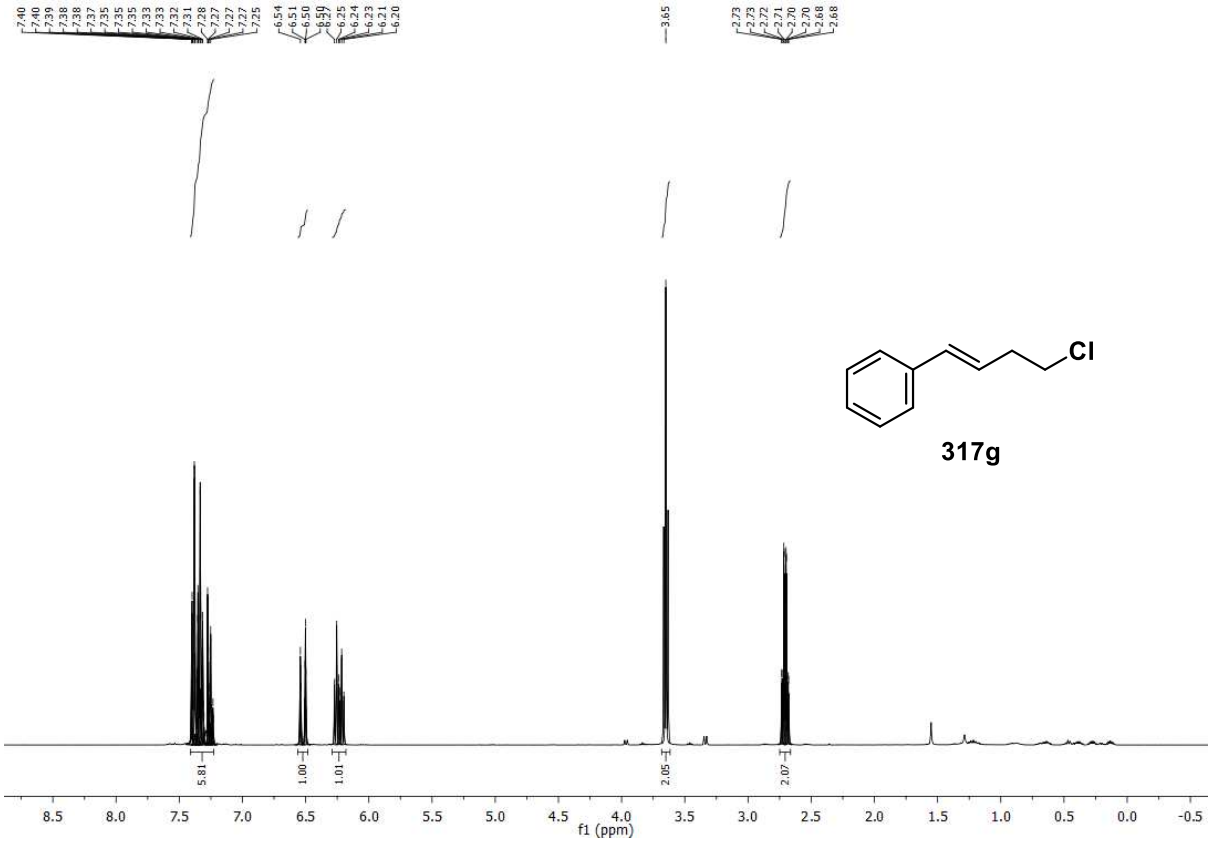

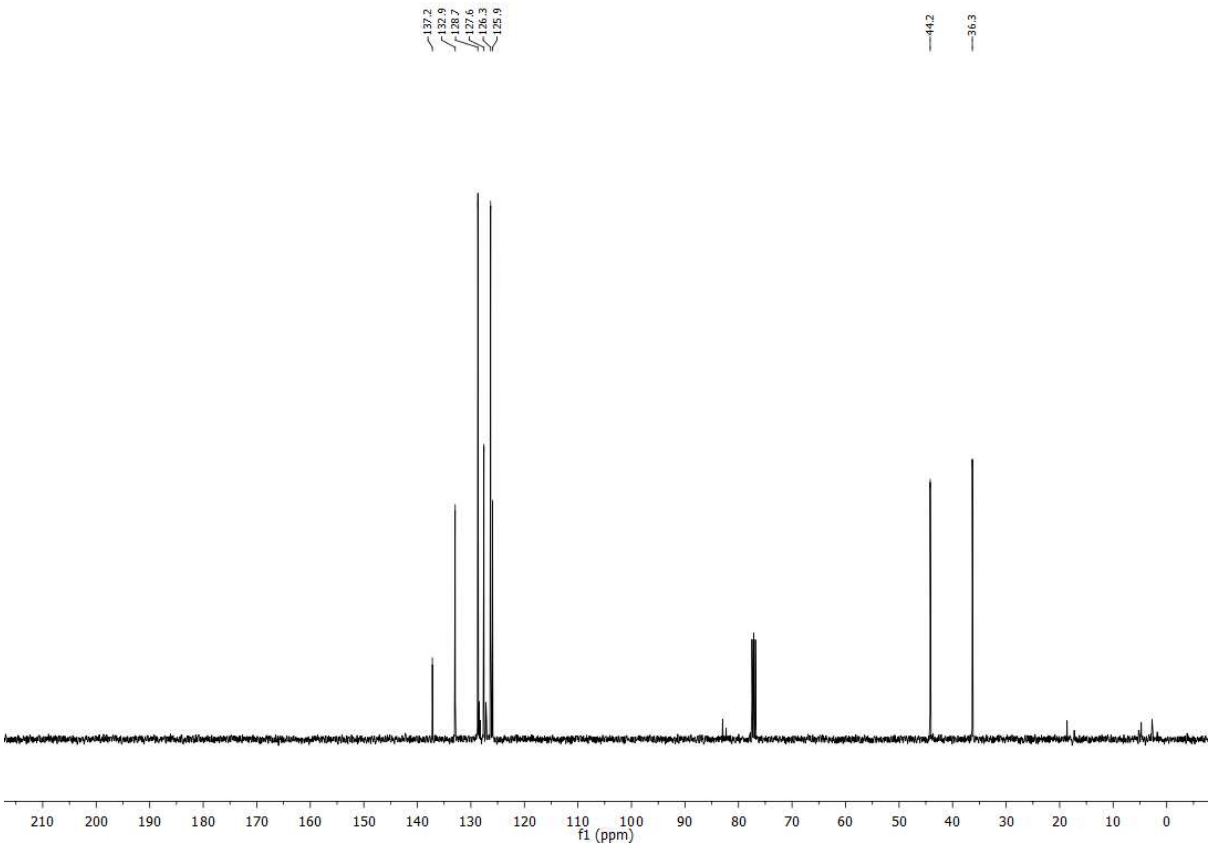

(*E*)-1,5-diphenylpent-4-en-1-one (378u)

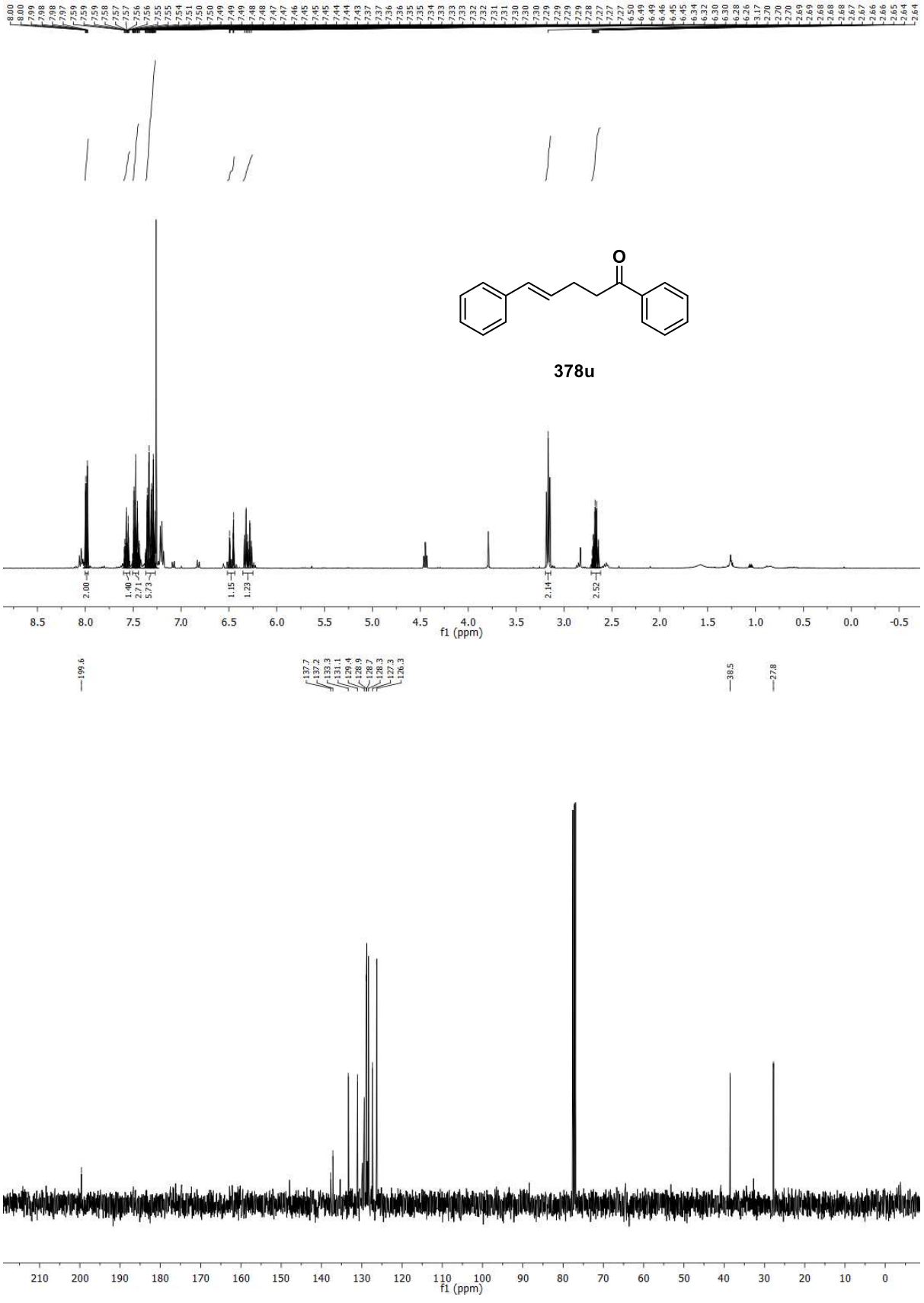

1,2-bis(4-methoxyphenyl)ethane (381)

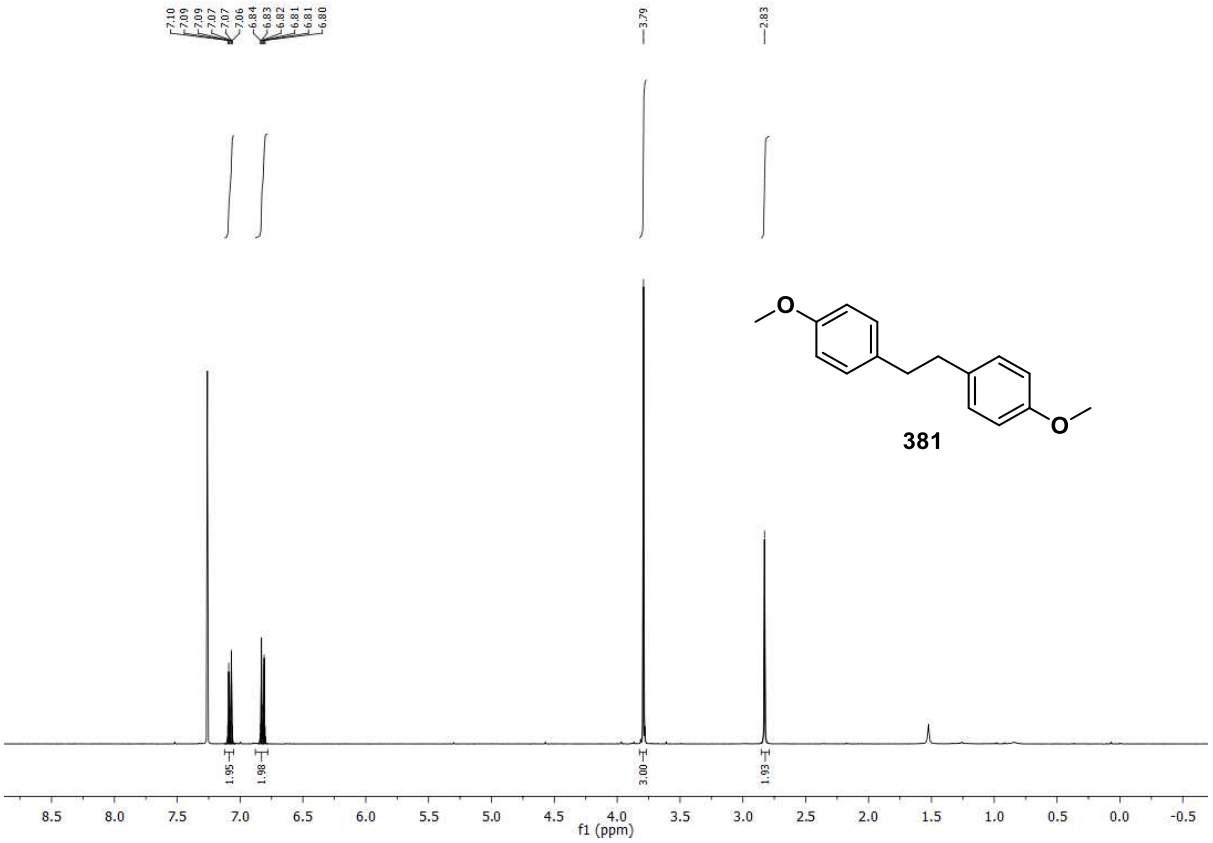

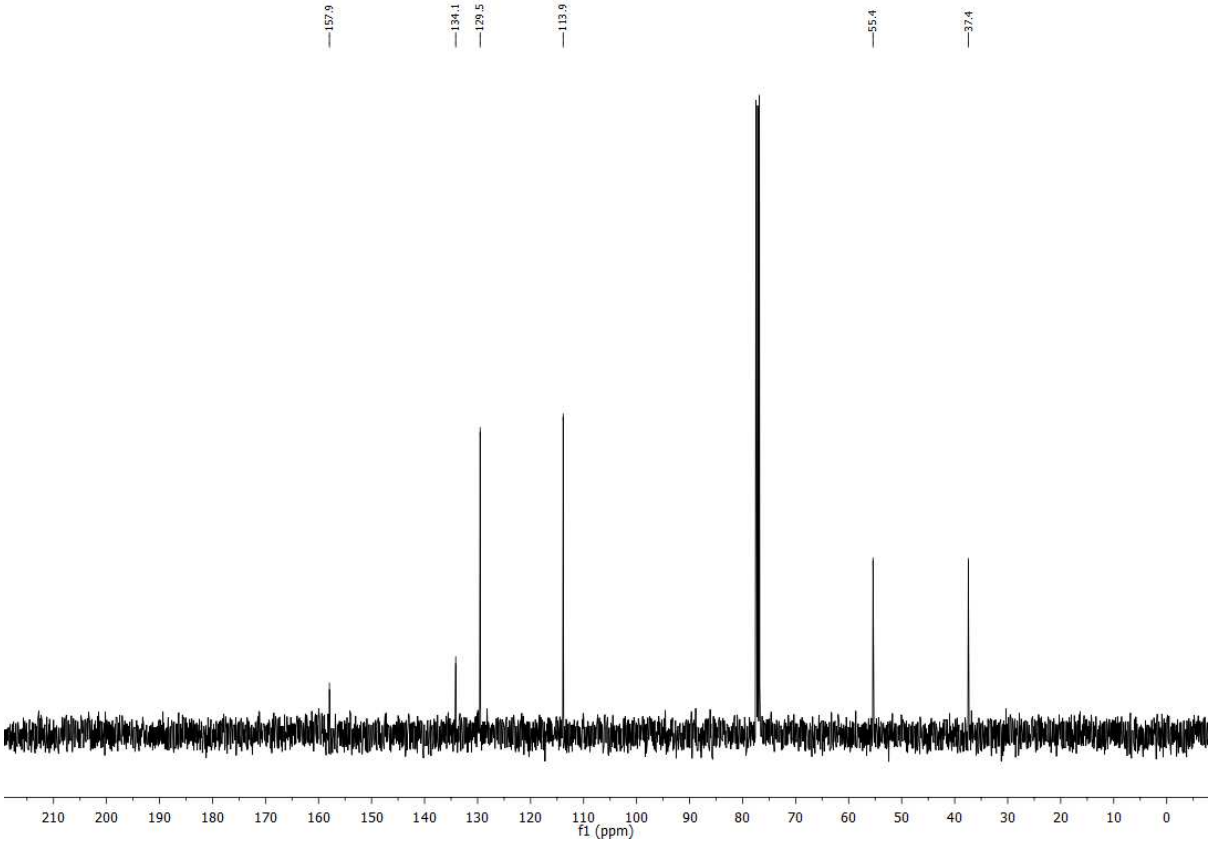

1,2-bis(4-bromophenyl)disulfane (383b)

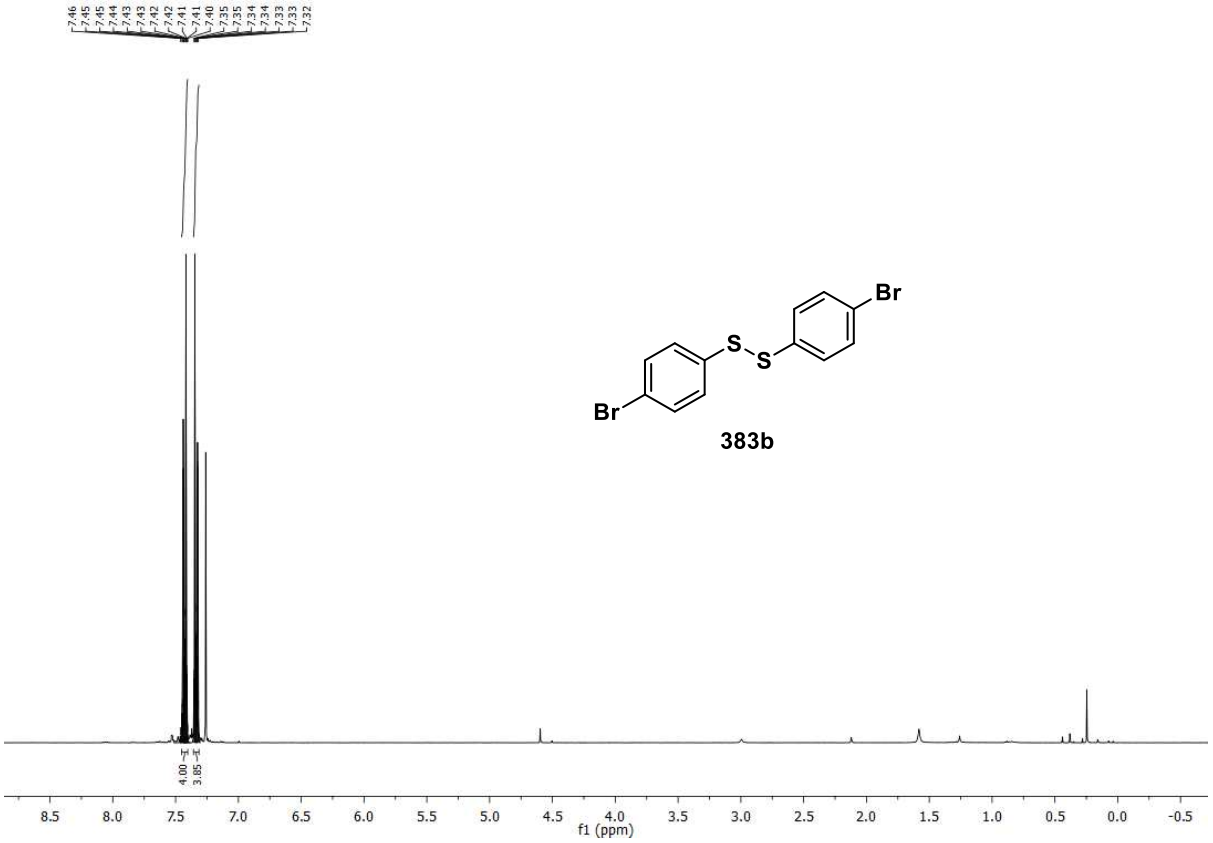

383b

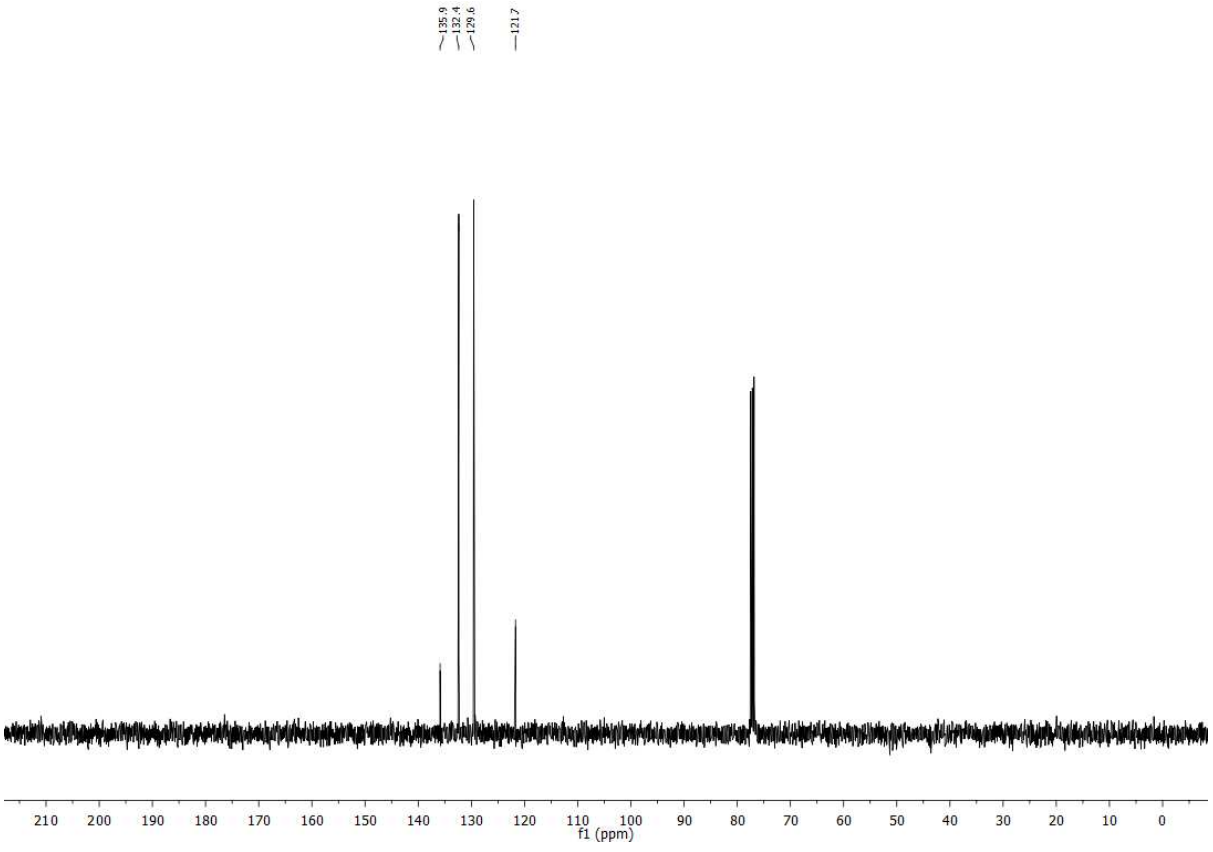

S-(4-(4-methoxybenzyl)phenyl) 2,4,6-trimethylbenzothioate (390)

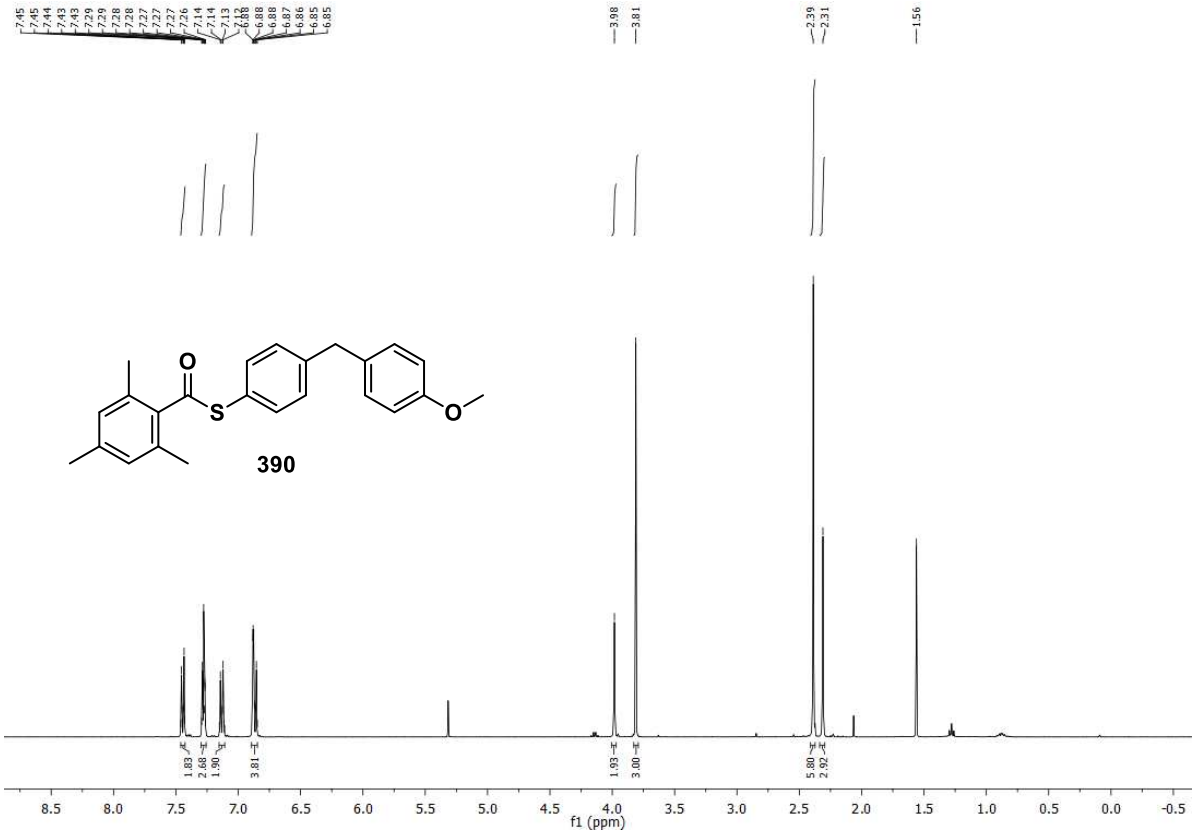

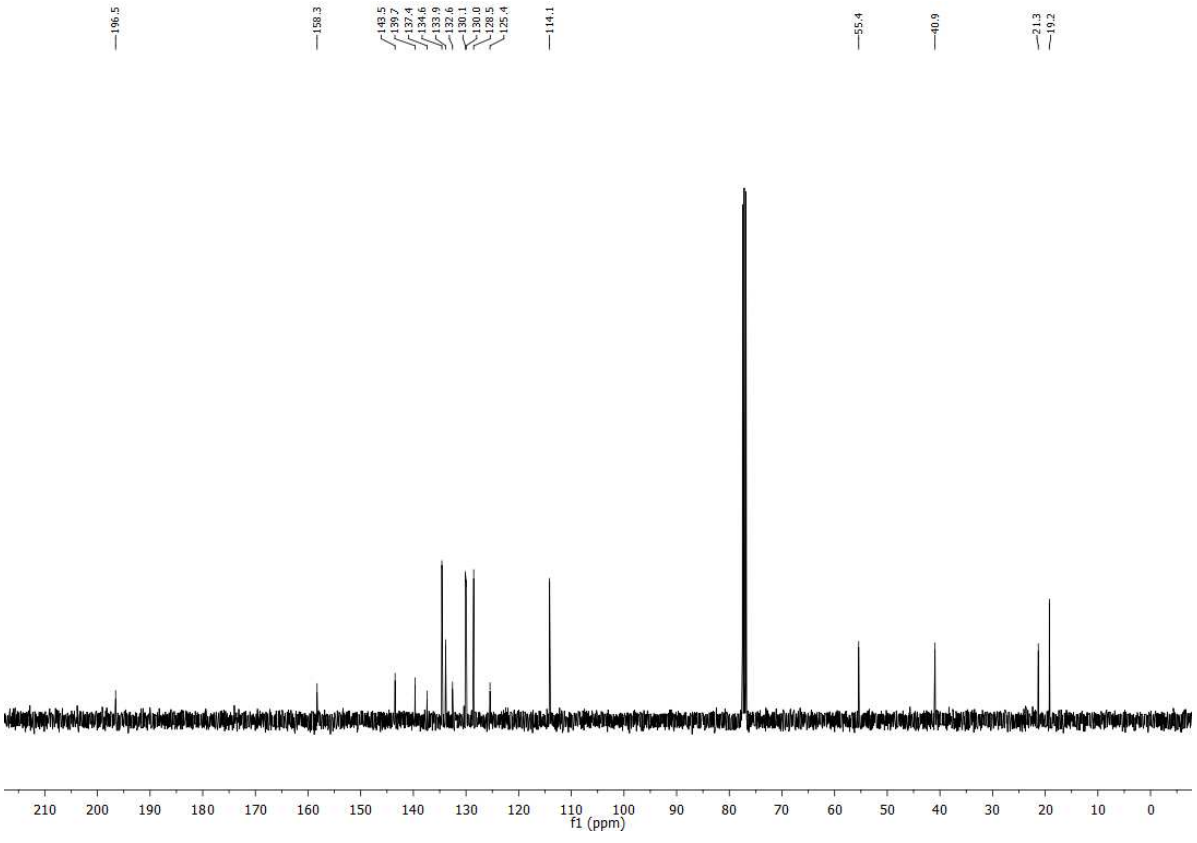

((4-methoxybenzyl)oxy)trimethylsilane (397)

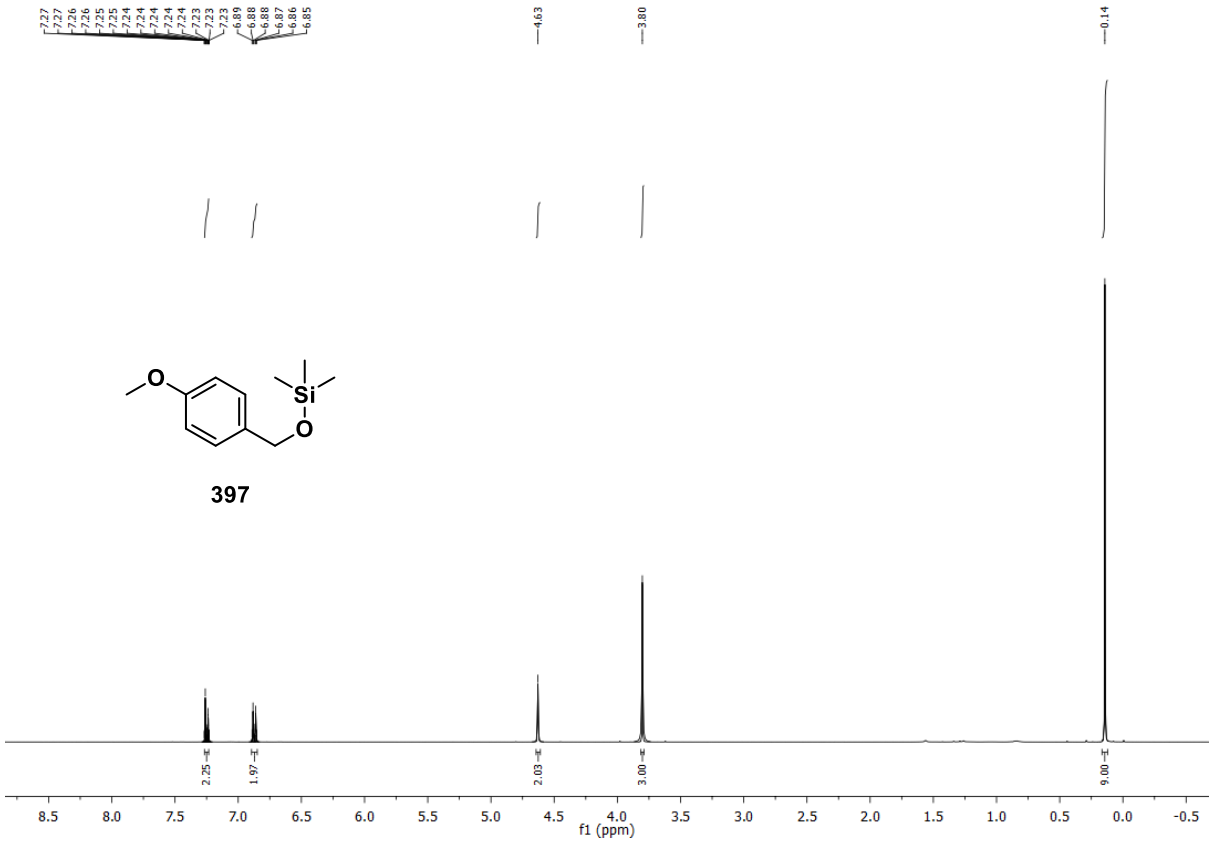

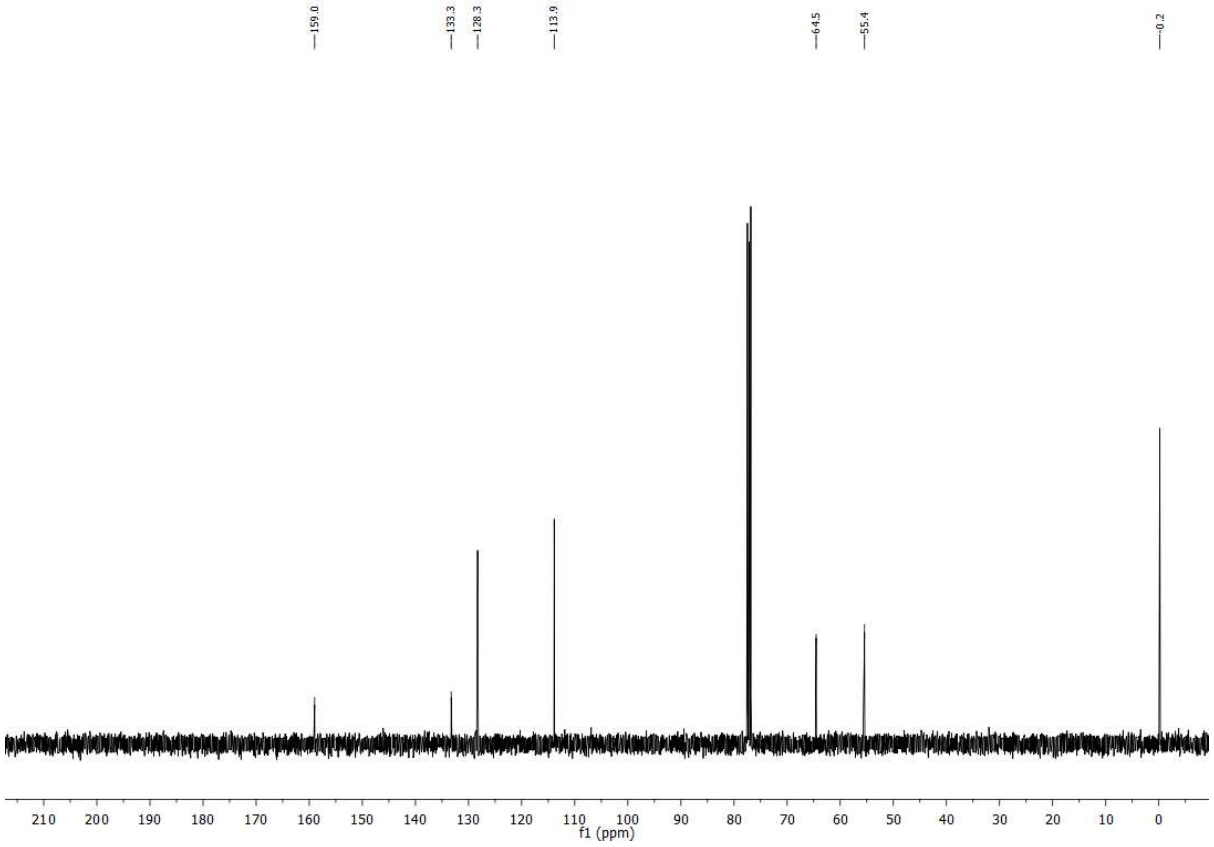

biphenylethane-1,2-dione (426)

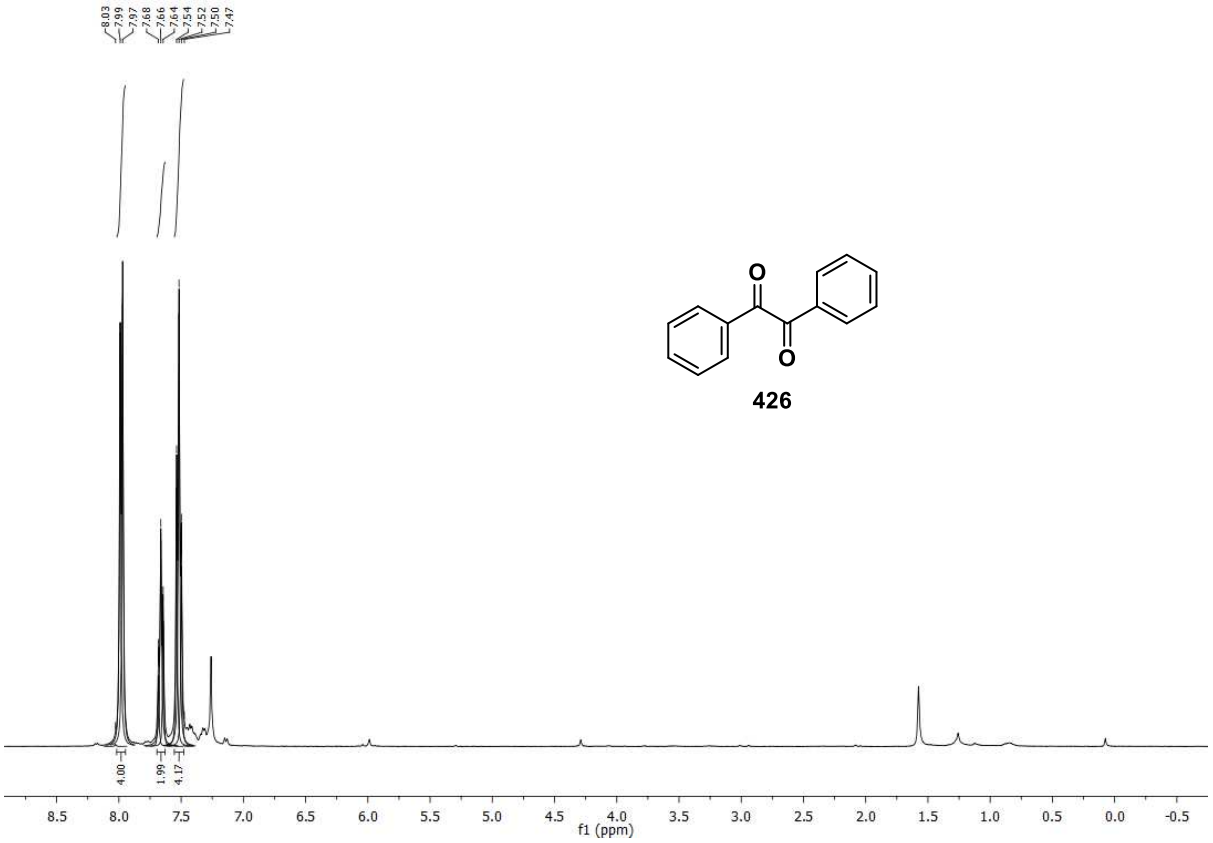

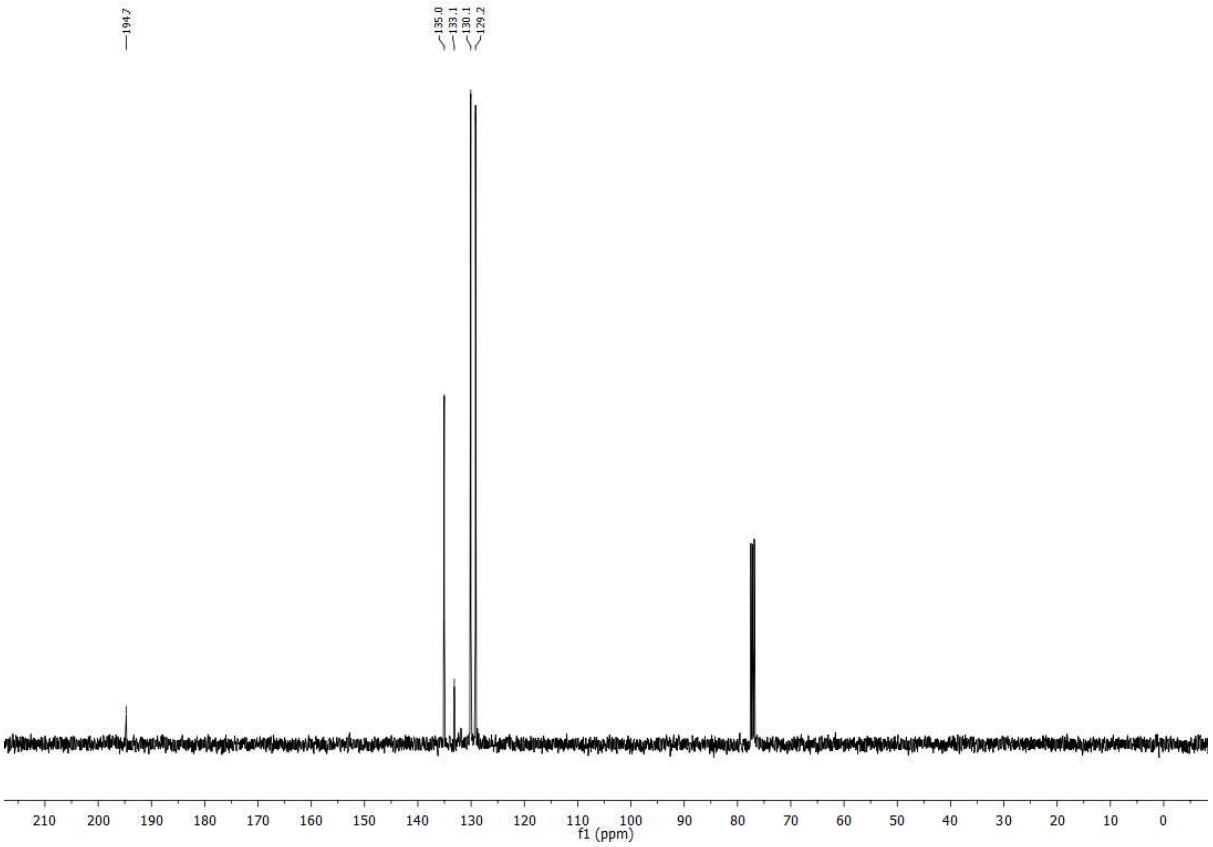

4.5 References

[1] A. Haupt, Master Thesis, *Nickel/Titanium Dual Catalytic Cross-Electrophile Coupling of Benzylic Alcohols and Thioesters* (University of Tübingen), **2020**.
[2] a) C. Liu, H. Zhang, W. Shi, A. Lei, *Chem. Rev.* **2011**, *111*, 1780–1824; b) W. Shi, C. Liu, A. Lei, *Chem. Soc. Rev.* **2011**, *40*, 2761–2776.
[3] C.-J. Li, *Acc. Chem. Res.* **2009**, *42*, 335–344.
[4] D. A. Everson, R. Shrestha, D. J. Weix, *J. Am. Chem. Soc.* **2010**, *132*, 920–921.
[5] a) C. E. I. Knappke, S. Grupe, D. Gärtner, M. Corpet, C. Gosmini, A. Jacobi von Wangelin, *Chem. Eur. J.* **2014**, *20*, 6828–6842; b) D. A. Everson, D. J. Weix, *J. Org. Chem.* **2014**, *79*, 4793–4798; c) T. Moragas, A. Correa, R. Martin, *Chem. Eur. J.* **2014**, *20*, 8242–8258; d) D. J. Weix, *Acc. Chem. Res.* **2015**, *48*, 1767–1775; e) J. Gu, X. Wang, W. Xue, H. Gong, *Org. Chem. Front.* **2015**, *2*, 1411–1421; f) X. Wang, Y. Dai, H. Gong, *Top. Curr. Chem.* **2016**, *374*, 43; g) E. L. Lucas, E. R. Jarvo, *Nat. Rev. Chem.* **2017**, *1*, 1–7; h) E. Richmond, J. Moran, *Synthesis* **2018**, *50*, 499–513; i) L.-C. Campeau, N. Hazari, *Organometallics* **2019**, *38*, 3–35; j) M. J. Goldfogel, L. Huang, D. J. Weix in *Cross-Electrophile Coupling: Principles and New Reactions*, (Ed. S. Ogoshi), Wiley-VCH, **2020**, pp. 183–222; k) K. E. Poremba, S. E. Dibrell, S. E. Reisman, *ACS Catal.* **2020**, *10*, 8237–8246; l) X. Pang, X. Peng, X.-Z. Shu, *Synthesis* **2020**, *52*, 3751–3763.
[6] a) L. Yi, T. Ji, K.-Q. Chen, X.-Y. Chen, M. Rueping, *CCS Chem.* **2022**, *4*, 9–30; b) K. P. Shing Cheung, S. Sarkar, V. Gevorgyan, *Chem. Rev.* **2021**, *122*, 1543–1625; c) A. Y. Chan, I. B. Perry, N. B. Bissonnette, B. F. Buksh, G. A. Edwards, L. I. Frye, O. L. Garry, M. N. Lavagnino, B. X. Li, Y. Liang, E. Mao, A. Millet, J. V. Oakley, N. L. Reed, H. A. Sakai, C. P. Seath, D. W. C. MacMillan, *Chem. Rev.* **2022**, *122*, 1485–1542; d) J. Twilton, P. Zhang, M. H. Shaw, R. W. Evans, D. W. MacMillan, *Nat. Rev. Chem.* **2017**, *1*, 1–19; e) X. Wu, J. Han, S. Xia, W. Li, C. Zhu, J. Xie, *CCS Chem.* **2022**, *4*, 2469–2480.
[7] a) P. Villo, A. Shatskiy, M. D. Kärkäs, H. Lundberg, *Angew. Chem.* **2023**, *135*, e202211952; b) C. A. Malapit, M. B. Prater, J. R. Cabrera-Pardo, M. Li, T. D. Pham, T. P. McFadden, S. Blank, S. D. Minteer, *Chem. Rev.* **2022**, *122*, 3180–3218.
[8] a) K. Kubota, H. Ito, *Trends Chem.* **2020**, *2*, 1066–1081; b) F. Effaty, X. Ottenwaelder, T. Friščić, *Curr. Opin. Green Sustain. Chem.* **2021**, *32*, 100524; c) A. Porcheddu, E. Colacino, L. De Luca, F. Delogu, *ACS Catal.* **2020**, *10*, 8344–8394; d) A. C. Jones, M. T. J. Williams, L. C. Morrill, D. L. Browne, *ACS Catal.* **2022**, *12*, 13681–13689.
[9] a) L. Fakhouri, C. D. Cook, M. H. Al-Huniti, L. M. Console-Bram, D. P. Hurst, M. B. Spano, D. J. Nasrallah, M. G. Caron, L. S. Barak, P. H. Reggio, *Bioorg. Med. Chem.* **2017**, *25*, 4355–4367; b) J. M. E. Hughes, P. S. Fier, *Org. Lett.* **2019**, *21*, 5650–5654; c) A. Dumas, J.-B. Garsi, G. Poissonnet, S. Hanessian, *ACS Omega* **2020**, *5*, 27591–27606; d) K. M. Mennie, B. A. Vara, S. M. Levi, *Org. Lett.* **2020**, *22*, 556–559.
[10] a) Y. Fegheh-Hassanpour, T. Arif, H. O. Sintim, H. H. Al Mamari, D. M. Hodgson, *Org. Lett.* **2017**, *19*, 3540–3543; b) R. K. Boeckman Jr, J. M. Niziol, K. F. Biegasiewicz, *Org. Lett.* **2018**, *20*, 5062–5065; c) M. Menger, D. Lentz, M. Christmann, *J. Org. Chem.* **2018**, *83*, 6793–6797; d) Z. C. Girvin, M. K. Andrews, X. Liu, S. H. Gellman, *Science* **2019**, *366*, 1528–1531; e) H. G. Cheng, Z. Yang, R. Chen, L. Cao, W. Y. Tong, Q. Wei, Q. Wang, C. Wu, S. Qu, Q. Zhou, *Angew. Chem. Int. Ed.* **2021**, *60*, 5141–5146; f) Y. Watanabe, K. Sakata, D. Urabe, K. Hagiwara, M. Inoue, *J. Org. Chem.* **2023**, *88*, 17479–17484.
[11] a) B. Tollens, R. Fittig, *Liebigs Ann. Chem.* **1864**, *131*, 303–323; b) A. Wurtz, *Liebigs Ann. Chem.* **1855**, *96*, 364–375.

[12] a) A. S. Kende, L. S. Liebeskind, D. M. Braitsch, *Tetrahedron Lett.* **1975**, *16*, 3375–3378; b) I. Colon, D. R. Kelsey, *J. Org. Chem.* **1986**, *51*, 2627–2637.
[13] a) M. Semmelhack, P. Helquist, L. Jones, *J. Am. Chem. Soc.* **1971**, *93*, 5908–5910; b) M. F. Semmelhack, L. S. Ryono, *J. Am. Chem. Soc.* **1975**, *97*, 3873–3875; c) M. Semmelhack, P. Helquist, L. Jones, L. Keller, L. Mendelson, L. S. Ryono, J. Gorzynski Smith, R. Stauffer, *J. Am. Chem. Soc.* **1981**, *103*, 6460–6471.
[14] M. Zembayashi, K. Tamao, J.-I. Yoshida, M. Kumada, *Tetrahedron Lett.* **1977**, *18*, 4089–4091.
[15] M. Onaka, Y. Matsuoka, T. Mukaiyama, *Chem. Lett.* **1981**, *10*, 531–534.
[16] Y. Rollin, M. Troupel, D. G. Tuck, J. Perichon, *J. Organomet. Chem.* **1986**, *303*, 131–137.
[17] G. Meyer, Y. Rollin, J. Perichon, *J. Organomet. Chem.* **1987**, *333*, 263–267.
[18] J. Folest, J. Périchon, J. Fauvarque, A. Jutand, *J. Organomet. Chem.* **1988**, *342*, 259–261.
[19] H. Marzouk, Y. Rollin, J. Folest, J. Nédélec, J. Périchon, *J. Organomet. Chem.* **1989**, *369*, C47-C50.
[20] a) Q. Lin, T. Diao, *J. Am. Chem. Soc.* **2019**, *141*, 17937–17948; b) J. B. Diccianni, T. Diao, *Trends Chem.* **2019**, *1*, 830–844.
[21] S. Biswas, D. J. Weix, *J. Am. Chem. Soc.* **2013**, *135*, 16192–16197.
[22] S. Ni, N. M. Padial, C. Kingston, J. C. Vantourout, D. C. Schmitt, J. T. Edwards, M. M. Kruszyk, R. R. Merchant, P. K. Mykhailiuk, B. B. Sanchez, S. Yang, M. A. Perry, G. M. Gallego, J. J. Mousseau, M. R. Collins, R. J. Cherney, P. S. Lebed, J. S. Chen, T. Qin, P. S. Baran, *J. Am. Chem. Soc.* **2019**, *141*, 6726–6739.
[23] C. S. Day, R. Martin, *Chem. Soc. Rev.* **2023**, *52*, 6601–6616.
[24] S. L. Shevick, C. Obradors, R. A. Shenvi, *J. Am. Chem. Soc.* **2018**, *140*, 12056–12068.
[25] a) A. Studer, *Chem. Eur. J.* **2001**, *7*, 1159–1164; b) H. Fischer, *Chem. Rev.* **2001**, *101*, 3581–3610.
[26] L. K. G. Ackerman-Biegasiewicz, S. K. Kariofillis, D. J. Weix, *J. Am. Chem. Soc.* **2023**, *145*, 6596–6614.
[27] R. Pilli, B. Chindan, R. Rasappan, *Eur. J. Org. Chem.* **2022**, e202200985.
[28] G. A. Dawson, E. H. Spielvogel, T. Diao, *Acc. Chem. Res.* **2023**, *56*, 3640–3653.
[29] Q. Lin, Y. Fu, P. Liu, T. Diao, *J. Am. Chem. Soc.* **2021**, *143*, 14196–14206.
[30] Q. Lin, E. H. Spielvogel, T. Diao, *Chem.* **2023**, *9*, 1295–1308.
[31] a) L. Huang, L. K. G. Ackerman, K. Kang, A. M. Parsons, D. J. Weix, *J. Am. Chem. Soc.* **2019**, *141*, 10978–10983; b) X. Wang, G. Ma, Y. Peng, C. E. Pitsch, B. J. Moll, T. D. Ly, X. Wang, H. Gong, *J. Am. Chem. Soc.* **2018**, *140*, 14490–14497.
[32] G. A. Dawson, Q. Lin, M. C. Neary, T. Diao, *J. Am. Chem. Soc.* **2023**, *145*, 20551–20561.
[33] A. Umehara, Y. Kishi, *Chem. Lett.* **2019**, *48*, 947–950.
[34] a) L. K. G. Ackerman, M. M. Lovell, D. J. Weix, *Nature* **2015**, *524*, 454–457; b) K. Kang, N. L. Loud, T. A. DiBenedetto, D. J. Weix, *J. Am. Chem. Soc.* **2021**, *143*, 21484–21491; c) A. M. Olivares, D. J. Weix, *J. Am. Chem. Soc.* **2018**, *140*, 2446–2449; d) K. Kang, L. Huang, D. J. Weix, *J. Am. Chem. Soc.* **2020**, *142*, 10634–10640; e) B. Xiong, Y. Li, J. Zhang, J. Liu, X. Zhang, Z. Lian, *Adv. Synth. Catal.* **2022**, *364*, 1009–1015.
[35] a) L. K. G. Ackerman, L. L. Anka-Lufford, M. Naodovic, D. J. Weix, *Chem. Sci.* **2015**, *6*, 1115–1119; b) D. J. Charboneau, E. L. Barth, N. Hazari, M. R. Uehling, S. L. Zultanski, *ACS Catal.* **2020**, *10*, 12642–12656; c) A. Potrząsaj, M. Musiejuk, W. Chaładaj, M. Giedyk, D. Gryko, *J. Am. Chem. Soc.* **2021**.
[36] D. J. Charboneau, N. Hazari, H. Huang, M. R. Uehling, S. L. Zultanski, *J. Org. Chem.* **2022**, *87*, 7589–7609.

[37] D. J. Charboneau, H. Huang, E. L. Barth, C. C. Germe, N. Hazari, B. Q. Mercado, M. R. Uehling, S. L. Zultanski, *J. Am. Chem. Soc.* **2021**, *143*, 21024–21036.
[38] S. Geng, C. Shi, B. Guo, H. Hou, Z. Liu, Z. Feng, *ACS Catal.* **2023**, *13*, 15469–15480.
[39] H. Xu, C. Zhao, Q. Qian, W. Deng, H. Gong, *Chem. Sci.* **2013**, *4*, 4022–4029.
[40] V. V. Pavlishchuk, A. W. Addison, *Inorg. Chim. Acta* **2000**, *298*, 97–102.
[41] a) C. C. Le, D. W. C. MacMillan, *J. Am. Chem. Soc.* **2015**, *137*, 11938–11941; b) J. Amani, E. Sodagar, G. A. Molander, *Org. Lett.* **2016**, *18*, 732–735; c) C. L. Joe, A. G. Doyle, *Angew. Chem. Int. Ed.* **2016**, *55*, 4040–4043; d) J. Amani, R. Alam, S. Badir, G. A. Molander, *Org. Lett.* **2017**, *19*, 2426–2429; e) L. Buzzetti, A. Prieto, S. R. Roy, P. Melchiorre, *Angew. Chem.* **2017**, *129*, 15235–15239; f) Z. Sun, N. Kumagai, M. Shibasaki, *Org. Lett.* **2017**, *19*, 3727–3730; g) L. K. G. Ackerman, J. I. Martinez Alvarado, A. G. Doyle, *J. Am. Chem. Soc.* **2018**, *140*, 14059–14063; h) S. O. Badir, A. Dumoulin, J. K. Matsui, G. A. Molander, *Angew. Chem. Int. Ed.* **2018**, *57*, 6610–6613; i) E. Gandolfo, X. Tang, S. Raha Roy, P. Melchiorre, *Angew. Chem.* **2019**, *131*, 17010–17014; j) E. Levernier, V. Corcé, L.-M. Rakotoarison, A. Smith, M. Zhang, S. Ognier, M. Tatoulian, C. Ollivier, L. Fensterbank, *Org. Chem. Front.* **2019**, *6*, 1378–1382; k) T. Kerackian, A. Reina, D. Bouyssi, N. Monteiro, A. Amgoune, *Org. Lett.* **2020**, *22*, 2240–2245; l) G. S. Lee, J. Won, S. Choi, M. H. Baik, S. H. Hong, *Angew. Chem. Int. Ed.* **2020**, *59*, 16933–16942; m) R. Ruzi, K. Liu, C. Zhu, J. Xie, *Nat. Commun.* **2020**, *11*, 1–9; n) Y. Wei, B. Ben-zvi, T. Diao, *Angew. Chem.* **2021**, *133*, 9519–9524; o) X. Xi, Y. Luo, W. Li, M. Xu, H. Zhao, Y. Chen, S. Zheng, X. Qi, W. Yuan, *Angew. Chem. Int. Ed.* **2022**, *61*, e202114731; p) J. Brauer, E. Quraishi, L. Kammer, T. Opatz, *Chem. Eur. J.* **2021**, *27*, 18168–18174; q) Y. Wei, J. Lam, T. Diao, *Chem. Sci.* **2021**, *12*, 11414–11419.
[42] J. J. Habeeb, D. G. Tuck, *J. Chem. Soc., Chem. Commun.* **1976**, 696–697.
[43] C. Amatore, A. Jutand, J. Périchon, Y. Rollin, *Monatsh. Chem.* **2000**, *131*, 1293–1304.
[44] B. Corain, G. Favero, *J. Chem. Soc., Dalton Trans.* **1975**, 283–285.
[45] a) S.-i. Inaba, R. D. Rieke, *Tetrahedron Lett.* **1983**, *24*; b) S. Inaba, R. D. Rieke, *J. Org. Chem.* **1985**, *50*, 1373–1381.
[46] A. C. Wotal, D. J. Weix, *Org. Lett.* **2012**, *14*, 1476–1479.
[47] W. Lu, Z. Liang, Y. Zhang, F. Wu, Q. Qian, H. Gong, *Synthesis* **2013**, *45*, 2234–2240.
[48] F. Wu, W. Lu, Q. Qian, Q. Ren, H. Gong, *Org. Lett.* **2012**, *14*, 3044–3047.
[49] A. H. Cherney, N. T. Kadunce, S. E. Reisman, *J. Am. Chem. Soc.* **2013**, *135*, 7442–7445.
[50] H. Ji, D. Lin, L. Tai, X. Li, Y. Shi, Q. Han, L.-A. Chen, *J. Am. Chem. Soc.* **2022**, *144*, 23019–23029.
[51] J. Wu, H. Wu, X. Liu, Y. Zhang, G. Huang, C. Zhang, *Org. Lett.* **2022**, *24*, 4322–4327.
[52] A. C. Wotal, R. D. Ribson, D. J. Weix, *Organometallics* **2014**, *33*, 5874–5881.
[53] Z. Liang, W. Xue, K. Lin, H. Gong, *Org. Lett.* **2014**, *16*, 5620–5623.
[54] A. C. Wotal, D. C. Batesky, D. J. Weix, *Org. Synth.* **2016**, *93*, 50–62.
[55] K. M. M. Huihui, J. A. Caputo, Z. Melchor, A. M. Olivares, A. M. Spiewak, K. A. Johnson, T. A. DiBenedetto, S. Kim, L. K. G. Ackerman, D. J. Weix, *J. Am. Chem. Soc.* **2016**, *138*, 5016–5019.
[56] F.-F. Pan, P. Guo, C.-L. Li, P. Su, X.-Z. Shu, *Org. Lett.* **2019**, *21*, 3701–3705.
[57] F. T. Pulikottil, R. Pilli, R. V. Suku, R. Rasappan, *Org. Lett.* **2020**, *22*, 2902–2907.
[58] D. Ding, C. Wang, *ACS Catal.* **2018**, *8*, 11324–11329.
[59] L. Wang, C. Wang, *Org. Chem. Front.* **2018**, *5*, 3476–3482.
[60] X. Zhao, H.-Y. Tu, L. Guo, S. Zhu, F.-L. Qing, L. Chu, *Nat. Commun.* **2018**, *9*, 3488.
[61] L. J. Gooßen, N. Rodríguez, K. Gooßen, *Angew. Chem. Int. Ed.* **2008**, *47*, 3100–3120.
[62] a) E. Dincan, S. Sibille, J. Perichon, M.-O. Moingeon, J. Chaussard, *Tetrahedron Lett.* **1986**, *27*, 4175–4176; b) J.-P. Gisselbrecht, H. Lund, *Acta Chem. Scand.* **1985**, *39*, 823–827.

[63] H. Yin, C. Zhao, H. You, K. Lin, H. Gong, *Chem. Commun.* **2012**, *48*, 7034–7036.
[64] a) C. Zhao, X. Jia, X. Wang, H. Gong, *J. Am. Chem. Soc.* **2014**, *136*, 17645–17651; b) X. Jia, X. Zhang, Q. Qian, H. Gong, *Chem. Commun.* **2015**, *51*, 10302–10305.
[65] J. He, P. Song, X. Xu, S. Zhu, Y. Wang, *ACS Catal.* **2019**, *9*, 3253–3259.
[66] K.-J. Jiao, C. Ma, D. Liu, H. Qiu, B. Cheng, T.-S. Mei, *Org. Chem. Front.* **2021**, *8*, 6603–6608.
[67] T. Lin, J. Mi, L. Song, J. Gan, P. Luo, J. Mao, P. J. Walsh, *Org. Lett.* **2018**, *20*, 1191–1194.
[68] T. Lin, Y. Gu, P. Qian, H. Guan, P. J. Walsh, J. Mao, *Nat. Commun.* **2020**, *11*, 5638.
[69] J. Wang, M. Hoerrner, M. P. Watson, D. J. Weix, *Angew. Chem. Int. Ed.* **2020**, *59*, 13484–13489.
[70] a) J. Ishizu, T. Yamamoto, A. Yamamoto, *Chem. Lett.* **1976**, *5*, 1091–1094; b) T. Yamamoto, J. Ishizu, T. Kohara, S. Komiya, A. Yamamoto, *J. Am. Chem. Soc.* **1980**, *102*, 3758–3764.
[71] H. Yu, Z.-X. Wang, *Org. Biomol. Chem.* **2023**, *21*, 3423–3431.
[72] F. Yang, D. Ding, C. Wang, *Org. Lett.* **2020**, *22*, 9203–9209.
[73] F. Yang, C. Wang, *J. Org. Chem.* **2023**, https://doi.org/10.1021/acs.joc.1023c00425.
[74] T. Goto, M. Onaka, T. Mukaiyama, *Chem. Lett.* **1980**, *9*, 51–52.
[75] J. Wang, B. P. Cary, P. D. Beyer, S. H. Gellman, D. J. Weix, *Angew. Chem. Int. Ed.* **2019**, *58*, 12081–12085.
[76] Y. Ai, N. Ye, Q. Wang, K. Yahata, Y. Kishi, *Angew. Chem. Int. Ed.* **2017**, *56*, 10791–10795.
[77] I. N. C. Kiran, R. Kranthikumar, *Org. Lett.* **2023**, *25*, 3623–3627.
[78] Y.-C. Huang, K. K. Majumdar, C.-H. Cheng, *J. Org. Chem.* **2002**, *67*, 1682–1684.
[79] Y. Sun, L. Su, W. Tong, K. Yao, H. Gong, *Synlett* **2021**, *32*, 1762–1766.
[80] J. Wang, Y. Yin, X. He, Q.-L. Duan, R. Bai, H.-W. Shi, R. Shi, *ACS Catal.* **2023**, *13*, 8161–8168.
[81] M. Zheng, W. Xue, T. Xue, H. Gong, *Org. Lett.* **2016**, *18*, 6152–6155.
[82] R. Shi, X. Hu, *Angew. Chem. Int. Ed.* **2019**, *58*, 7454–7458.
[83] H. Chen, H. Yue, C. Zhu, M. Rueping, *Angew. Chem.* **2022**, *134*, e202204144.
[84] J. Chen, S. Zhu, *J. Am. Chem. Soc.* **2021**, *143*, 14089–14096.
[85] B. Yuan, D. Ding, C. Wang, *ACS Catal.* **2022**, *12*, 4261–4267.
[86] a) M. Gao, D. Sun, H. Gong, *Org. Lett.* **2019**, *21*, 1645–1648; b) X. Tao, K. Yao, W. Xue, *Tetrahedron Lett.* **2021**, *73*, 153129; c) C. Ye, W. Tong, F. Wu, *Synthesis* **2022**, *54*, A-G.
[87] J.-C. Hsieh, Y.-C. Chen, A.-Y. Cheng, H.-C. Tseng, *Org. Lett.* **2012**, *14*, 1282–1285.
[88] V. K. Chenniappan, S. Silwal, R. J. Rahaim, *ACS Catal.* **2018**, *8*, 4539–4544.
[89] J. Gao, X.-C. He, Y.-L. Liu, K.-R. Li, J.-P. Guan, H.-B. Chen, H.-Y. Xiang, K. Chen, H. Yang, *Org. Lett.* **2023**, *25*, 8824–8828.
[90] S. Ni, W. Zhang, H. Mei, J. Han, Y. Pan, *Org. Lett.* **2017**, *19*, 2536–2539.
[91] T. Kerackian, D. Bouyssi, G. Pilet, M. Médebielle, N. Monteiro, J. Vantourout, A. Amgoune, *ACS Catal.* **2022**, *12*, 12315–12325.
[92] C.-G. Yu, Y. Matsuo, *Org. Lett.* **2020**, *22*, 950–955.
[93] J. Zhuo, Y. Zhang, Z. Li, C. Li, *ACS Catal.* **2020**, *10*, 3895–3903.
[94] V. K. Chenniappan, S. Silwal, R. J. Rahaim, *ACS Catal.* **2018**, *8*, 4539–4544.
[95] J. Cornella, C. Zarate, R. Martin, *Chem. Soc. Rev.* **2014**, *43*, 8081–8097.
[96] P. Ertl, T. Schuhmann, *J. Nat. Prod.* **2019**, *82*, 1258–1263.
[97] a) D.-G. Yu, B.-J. Li, Z.-J. Shi, *Acc. Chem. Res.* **2010**, *43*, 1486–1495; b) B.-J. Li, D.-G. Yu, C.-L. Sun, Z.-J. Shi, *Chem. Eur. J.* **2011**, *17*, 1728–1759; c) B. M. Rosen, K. W. Quasdorf,

D. A. Wilson, N. Zhang, A.-M. Resmerita, N. K. Garg, V. Percec, *Chem. Rev.* **2011**, *111*, 1346–1416; d) A. Correa, J. Cornella, R. Martin, *Angew. Chem. Int. Ed.* **2013**, *52*, 1878–1880; e) J. Yamaguchi, K. Muto, K. Itami, *Eur. J. Org. Chem.* **2013**, *2013*, 19–30; f) T. Mesganaw, N. K. Garg, *Org. Process Res. Dev.* **2013**, *17*, 29–39.
[98] a) R.-D. He, C.-L. Li, Q.-Q. Pan, P. Guo, X.-Y. Liu, X.-Z. Shu, *J. Am. Chem. Soc.* **2019**, *141*, 12481–12486; b) J. Liu, Y. Ye, J. L. Sessler, H. Gong, *Acc. Chem. Res.* **2020**, *53*, 1833–1845; c) L. Cheng, Q. Lin, Y. Chen, H. Gong, *Synthesis* **2022**, *54*, 4426–4446; d) X. Pang, P.-F. Su, X.-Z. Shu, *Acc. Chem. Res.* **2022**, *55*, 2491–2509.
[99] E. Bisz, M. Szostak, *ChemSusChem* **2017**, *10*, 3964–3981.
[100] C. A. Herbert, E. R. Jarvo, *Acc. Chem. Res.* **2023**, *56*, 3313–3324.
[101] a) A. B. Sanford, T. A. Thane, T. M. McGinnis, P.-P. Chen, X. Hong, E. R. Jarvo, *J. Am. Chem. Soc.* **2020**, *142*, 5017–5023; b) P.-P. Chen, T. M. McGinnis, P. C. Lin, X. Hong, E. R. Jarvo, *ACS Catal.* **2023**, *13*, 5472–5481.
[102] a) K. A. Hewitt, C. A. Herbert, E. R. Jarvo, *Org. Lett.* **2022**, *24*, 6093–6098; b) T. M. McGinnis, T. A. Thane, E. R. Jarvo, *Org. Lett.* **2022**, *24*, 5619–5623.
[103] G. A. Molander, K. M. Traister, B. T. O'Neill, *J. Org. Chem.* **2015**, *80*, 2907–2911.
[104] K. Komeyama, R. Ohata, S. Kiguchi, I. Osaka, *Chem. Commun.* **2017**, *53*, 6401–6404.
[105] J. Wang, J. Zhao, H. Gong, *Chem. Commun.* **2017**, *53*, 10180–10183.
[106] M. Y. S. Ibrahim, G. R. Cumming, R. Gonzalez de Vega, P. Garcia-Losada, O. de Frutos, C. O. Kappe, D. Cantillo, *J. Am. Chem. Soc.* **2023**, *145*, 17023–17028.
[107] X. Li, Y.-X. Li, W. Shan, Z. Wang, R. Liu, Z. Zhang, X. Li, D. Shi, *Chem. Commun.* **2023**, *59*, 6893–6896.
[108] J. Duan, Y.-F. Du, X. Pang, X.-Z. Shu, *Chem. Sci.* **2019**, *10*, 8706–8712.
[109] X.-B. Yan, C.-L. Li, W.-J. Jin, P. Guo, X.-Z. Shu, *Chem. Sci.* **2018**, *9*, 4529–4534.
[110] Y. Ye, H. Chen, J. L. Sessler, H. Gong, *J. Am. Chem. Soc.* **2019**, *141*, 820–824.
[111] H. Xiang, Z. Yu, T. Xie, X.-Y. Ye, Y. Ye, *Eur. J. Org. Chem.* **2022**, *2022*, e202200937.
[112] Y. Pan, Y. Gong, Y. Song, W. Tong, H. Gong, *Org. Biomol. Chem.* **2019**, *17*, 4230–4233.
[113] A. Correa, T. León, R. Martin, *J. Am. Chem. Soc.* **2014**, *136*, 1062–1069.
[114] M. O. Konev, L. E. Hanna, E. R. Jarvo, *Angew. Chem. Int. Ed.* **2016**, *55*, 6730–6733.
[115] X. Tao, Y. Chen, J. Guo, X. Wang, H. Gong, *Chem. Sci.* **2021**, *12*, 220–226.
[116] L. Huang, A. M. Olivares, D. J. Weix, *Angew. Chem. Int. Ed.* **2017**, *129*, 12063–12067.
[117] A. L. Gabbey, N. W. M. Michel, J. M. E. Hughes, L.-C. Campeau, S. A. L. Rousseaux, *Org. Lett.* **2022**, *24*, 3173–3178.
[118] K. Kang, D. J. Weix, *Org. Lett.* **2022**, *24*, 2853–2857.
[119] X.-G. Liu, Q. Yang, D.-Y. Liu, J. Liu, D.-H. Tan, Y.-J. Ruan, P.-F. Wang, X.-L. Wang, H. Wang, *Org. Lett.* **2023**, *25*, 5022–5026.
[120] S. Wang, Q. Qian, H. Gong, *Org. Lett.* **2012**, *14*, 3352–3355.
[121] R.-D. He, Y. Bai, G.-Y. Han, Z.-Z. Zhao, X. Pang, X. Pan, X.-Y. Liu, X.-Z. Shu, *Angew. Chem.* **2021**, *61*, e202114556.
[122] Y. Li, Z. Wang, L. Li, X. Tian, F. Shao, C. Li, *Angew. Chem. Int. Ed.* **2021**, *61*, e202110391.
[123] M. Su, X. Huang, C. Lei, J. Jin, *Org. Lett.* **2021**, *24*, 354–358.
[124] X. He, J. Liu, G. Chen, B. Xiong, X. Xiao, L. Chen, X. Zhang, L. Dong, X. Ma, Z. Lian, *Org. Lett.* **2022**, *24*, 3538–3543.
[125] Z.-C. Cao, Q.-Y. Luo, Z.-J. Shi, *Org. Lett.* **2016**, *18*, 5978–5981.
[126] E. L. Lucas, T. M. McGinnis, A. J. Castro, E. R. Jarvo, *Synlett* **2021**, *32*, 1525–1530.
[127] E. J. Tollefson, L. W. Erickson, E. R. Jarvo, *J. Am. Chem. Soc.* **2015**, *137*, 9760–9763.

[128] L. Lombardi, A. Cerveri, R. Giovanelli, M. Castiñeira Reis, C. Silva-Lopez, G. Beertuzzi, M. Bandini, *Angew. Chem. Int. Ed.* **2022**, *134*, e202211732.
[129] K. M. Arendt, A. G. Doyle, *Angew. Chem.* **2015**, *127*, 10014–10018.
[130] S. K. Kariofillis, S. Jiang, A. M. Żurański, S. S. Gandhi, J. I. Martinez Alvarado, A. G. Doyle, *J. Am. Chem. Soc.* **2022**, *144*, 1045–1055.
[131] T. Suga, Y. Takahashi, C. Miki, Y. Ukaji, *Angew. Chem. Int. Ed.* **2022**, *61*, e202112533.
[132] X. Pang, X. Z. Shu, *Chin. J. Chem.* **2023**, *41*, 1637–1652.
[133] D.-G. Yu, X. Wang, R.-Y. Zhu, S. Luo, X.-B. Zhang, B.-Q. Wang, L. Wang, Z.-J. Shi, *J. Am. Chem. Soc.* **2012**, *134*, 14638–14641.
[134] S. P. Verevkin, E. L. Krasnykh, J. S. Wright, *Phys. Chem. Chem. Phys.* **2003**, *5*, 2605–2611.
[135] a) M. Bandini, M. Tragni, *Org. Biomol. Chem.* **2009**, *7*, 1501–1507; b) E. Emer, R. Sinisi, M. G. Capdevila, D. Petruzziello, F. De Vincentiis, P. G. Cozzi, *Eur. J. Org. Chem.* **2011**, *2011*, 647–666; c) R. Kumar, E. Van der Eycken, *Chem. Soc. Rev.* **2013**, *42*, 1121–1146; d) A. Chaskar, K. Murugan, *Catal. Sci. Technol.* **2014**, *4*, 1852–1868; e) L. Chen, X.-P. Yin, C.-H. Wang, J. Zhou, *Org. Biomol. Chem.* **2014**, *12*, 6033–6048.
[136] a) G. Guillena, D. J. Ramón, M. Yus, *Angew. Chem. Int. Ed.* **2007**, *46*, 2358–2364; b) F. Huang, Z. Liu, Z. Yu, *Angew. Chem. Int. Ed.* **2016**, *55*, 862–875; c) A. Corma, J. Navas, M. J. Sabater, *Chem. Rev.* **2018**, *118*, 1410–1459; d) T. Irrgang, R. Kempe, *Chem. Rev.* **2018**, *119*, 2524–2549; e) B. G. Reed-Berendt, D. E. Latham, M. B. Dambatta, L. C. Morrill, *ACS Cent. Sci.* **2021**, *7*, 570–585.
[137] a) Z. C. Cao, D. G. Yu, R. Y. Zhu, J. B. Wei, Z. J. Shi, *Chem Commun (Camb)* **2015**, *51*, 2683–2686; b) S. Akkarasamiyo, J. Margalef, J. S. M. Samec, *Org. Lett.* **2019**, *21*, 4782–4787; c) S. Akkarasamiyo, S. Ruchirawat, P. Ploypradith, J. S. Samec, *Synthesis* **2020**, *52*, 645–659.
[138] Z. Li, W. Sun, X. Wang, L. Li, Y. Zhang, C. Li, *J. Am. Chem. Soc.* **2021**, *143*, 3536–3543.
[139] Z. Dong, D. W. MacMillan, *Nature* **2021**, *598*, 451–456.
[140] Z. Zuo, D. T. Ahneman, L. Chu, J. A. Terrett, A. G. Doyle, D. W. C. MacMillan, *Science* **2014**, *345*, 437–440.
[141] C. A. Gould, A. L. Pace, D. W. C. MacMillan, *J. Am. Chem. Soc.* **2023**, *145*, 16330–16336.
[142] H. A. Sakai, D. W. C. MacMillan, *J. Am. Chem. Soc.* **2022**, *144*, 6185–6192.
[143] J. Z. Wang, H. A. Sakai, D. W. C. MacMillan, *Angew. Chem. Int. Ed.* **2022**, *61*, e2022071.
[144] Q. Cai, I. McWhinnie, N. Dow, A. Chan, D. MacMillan, *ChemRxiv* **2023**.
[145] E. E. Stache, A. B. Ertel, T. Rovis, A. G. Doyle, *ACS Catal.* **2018**, *8*, 11134–11139.
[146] W.-D. Li, Y. Wu, S.-J. Li, Y.-Q. Jiang, Y.-L. Li, Y. Lan, J.-B. Xia, *J. Am. Chem. Soc.* **2022**, *144*, 8551–8559.
[147] K. Anwar, K. Merkens, F. J. A. Troyano, A. Gómez-Suárez, *Eur. J. Org. Chem.* **2022**, *2022*, e202200330.
[148] a) H. G. Roth, N. A. Romero, D. A. Nicewicz, *Synlett* **2016**, *27*, 714–723; b) Q. Lin, G. Dawson, T. Diao, *Synlett* **2021**, *32*, 1606–1620.
[149] P. Guo, K. Wang, W.-J. Jin, H. Xie, L. Qi, X.-Y. Liu, X.-Z. Shu, *J. Am. Chem. Soc.* **2020**, *143*, 513–523.
[150] X. Peng, J. Huang, G.-Y. Han, X.-Z. Shu, *Org. Chem. Front.* **2024**, *11*, 94–99.
[151] Q. Lin, G. Ma, H. Gong, *ACS Catal.* **2021**, *11*, 14102–14109.
[152] a) B. K. Chi, J. K. Widness, M. M. Gilbert, D. C. Salgueiro, K. J. Garcia, D. J. Weix, *ACS Catal.* **2022**, *12*, 580–586; b) J. B. Hendrickson, S. M. Schwartzman, *Tetrahedron Lett.* **1975**, *16*, 277–280.

[153] A. Corma, H. García, *Chem. Rev.* **2003**, *103*, 4307–4366.
[154] R. G. Pearson, *J. Am. Chem. Soc.* **1963**, *85*, 3533–3539.
[155] C. Wang, Z. Xi, *Chem. Soc. Rev.* **2007**, *36*, 1395–1406.
[156] a) Y. Nakao, S. Ebata, A. Yada, T. Hiyama, M. Ikawa, S. Ogoshi, *J. Am. Chem. Soc.* **2008**, *130*, 12874–12875; b) M. Tobisu, T. Xu, T. Shimasaki, N. Chatani, *J. Am. Chem. Soc.* **2011**, *133*, 19505–19511; c) Y.-X. Li, Q.-Q. Xuan, L. Liu, D. Wang, Y.-J. Chen, C.-J. Li, *J. Am. Chem. Soc.* **2013**, *135*, 12536–12539; d) Y. Minami, H. Yoshiyasu, Y. Nakao, T. Hiyama, *Angew. Chem.* **2013**, *125*, 917–921; e) Y. Miyazaki, N. Ohta, K. Semba, Y. Nakao, *J. Am. Chem. Soc.* **2014**, *136*, 3732–3735; f) W. Guan, S. Sakaki, T. Kurahashi, S. Matsubara, *ACS Catal.* **2015**, *5*, 1–10; g) L. K. Dil'mukhametova, M. G. Shaibakova, I. R. Ramazanov, *J. Organomet. Chem.* **2023**, *1006*, 122978; h) M. Oestreich, H. F. Klare, A. J. Rahman, *Synfacts* **2023**, *19*, 1214.
[157] X. Pang, X.-Z. Shu, *Synlett* **2021**, *32*, 1269–1274.
[158] G. Wilkinson, J. Birmingham, *J. Am. Chem. Soc.* **1954**, *76*, 4281–4284.
[159] J. Birmingham, A. Fischer, G. Wilkinson, *Sci. Nat.* **1955**, *42*, 96–96.
[160] R. J. Enemaerke, J. Larsen, T. Skrydstrup, K. Daasbjerg, *Organometallics* **2004**, *23*, 1866–1874.
[161] a) M. Paradas, A. G. Campaña, R. E. Estévez, L. Álvarez de Cienfuegos, T. Jiménez, R. Robles, J. M. Cuerva, J. E. Oltra, *J. Org. Chem.* **2009**, *74*, 3616–3619; b) M. Paradas, A. G. Campana, M. L. Marcos, J. Justicia, A. Haidour, R. Robles, D. J. Cárdenas, J. E. Oltra, J. M. Cuerva, *Dalton Trans.* **2010**, *39*, 8796–8800.
[162] K. P. Kepp, *Inorg. Chem.* **2016**, *55*, 9461–9470.
[163] P. J. Davidson, M. F. Lappert, R. Pearce, *Chem. Rev.* **1976**, *76*, 219–242.
[164] a) W. A. Nugent, T. V. RajanBabu, *J. Am. Chem. Soc.* **1988**, *110*, 8561–8562; b) T. V. RajanBabu, W. A. Nugent, *J. Am. Chem. Soc.* **1989**, *111*, 4525–4527; c) A. Rosales, I. Rodríguez-García, J. Muñoz-Bascón, E. Roldan-Molina, N. M. Padial, L. P. Morales, M. García-Ocaña, J. E. Oltra, *Eur. J. Org. Chem.* **2015**, *2015*, 4567–4591.
[165] a) A. Gansäuer, M. Pierobon, H. Bluhm, *Angew. Chem. Int. Ed.* **1998**, *37*, 101–103; b) A. Gansäuer, *J. Org. Chem.* **1998**, *63*, 2070–2071; c) A. Gansäuer, *Chem. Commun.* **1997**, 457–458.
[166] a) B. Rossi, S. Prosperini, N. Pastori, A. Clerici, C. Punta, *Molecules* **2012**, *7*, 14700–14732; b) T. Hilche, S. L. Younas, A. Gansäuer, J. Streuff, *ChemCatChem* **2022**, *14*, e202200530.
[167] J. M. Cuerva, J. Justicia, J. L. Oller-López, J. E. Oltra, *Radicals in Synthesis II* **2006**, 63–91.
[168] E. E. van Tamelen, M. A. Schwartz, *J. Am. Chem. Soc.* **1965**, *87*, 3277–3278.
[169] H. R. Diéguez, A. López, V. Domingo, J. F. Arteaga, J. A. Dobado, M. M. Herrador, J. F. Quílez del Moral, A. F. Barrero, *J. Am. Chem. Soc.* **2010**, *132*, 254–259.
[170] X. Zheng, X. J. Dai, H. Q. Yuan, C. X. Ye, J. Ma, P. Q. Huang, *Angew. Chem.* **2013**, *125*, 3578–3582.
[171] T. Suga, S. Shimazu, Y. Ukaji, *Org. Lett.* **2018**, *20*, 5389–5392.
[172] T. Suga, R. Takada, S. Shimazu, M. Sakata, Y. Ukaji, *J. Org. Chem.* **2022**, *87*, 7487–7493.
[173] T. Suga, M. Nakamura, R. Takada, Y. Ukaji, *Bull. Chem. Soc. Jpn.* **2021**, *94*, 1258–1260.
[174] H. Xie, J. Guo, Y.-Q. Wang, K. Wang, P. Guo, P.-F. Su, X. Wang, X.-Z. Shu, *J. Am. Chem. Soc.* **2020**, *142*, 16787–16794.
[175] H. Xie, S. Wang, Y. Wang, P. Guo, X.-Z. Shu, *ACS Catal.* **2022**, *12*, 1018–1023.

[176] Q. Lin, W. Tong, X.-Z. Shu, Y. Chen, *Org. Lett.* **2022**, *24*, 8459–8464.
[177] K. Sumiyama, N. Toriumi, N. Iwasawa, *Eur. J. Org. Chem.* **2021**, *2021*, 2474–2478.
[178] A. G. Campaña, B. Bazdi, N. Fuentes, R. Robles, J. M. Cuerva, J. E. Oltra, S. Porcel, A. M. Echavarren, *Angew. Chem. Int. Ed.* **2008**, *47*, 7515–7519.
[179] Á. Martínez-Peragón, A. Millán, A. G. Campaña, I. Rodríguez-Márquez, S. Resa, D. Miguel, L. Á. de Cienfuegos, J. M. Cuerva, *Eur. J. Org. Chem.* **2012**, *2012*, 1499–1503.
[180] A. Millan, L. Alvarez de Cienfuegos, D. Miguel, A. G. Campana, J. M. Cuerva, *Org. Lett.* **2012**, *14*, 5984–5987.
[181] I. R. Márquez, D. Miguel, A. Millán, M. L. Marcos, L. Á. de Cienfuegos, A. G. Campaña, J. M. Cuerva, *J. Org. Chem.* **2014**, *79*, 1529–1541.
[182] Y. Zhao, D. J. Weix, *J. Am. Chem. Soc.* **2014**, *136*, 48–51.
[183] Y. Zhao, D. J. Weix, *J. Am. Chem. Soc.* **2015**, *137*, 3237–3240.
[184] M. Parasram, B. J. Shields, O. Ahmad, T. Knauber, A. G. Doyle, *ACS Catal.* **2020**, *10*, 5821–5827.
[185] T. Suga, Y. Ukaji, *Org. Lett.* **2018**, *20*, 7846–7850.
[186] T. Suga, Y. Takahashi, Y. Ukaji, *Adv. Synth. Catal.* **2020**, *362*, 5622–5626.
[187] T. Suga, M. Kondo, Y. Takahashi, Y. Ukaji, *Bull. Chem. Soc. Jpn.* **2023**, uoad003.
[188] X.-G. Jia, P. Guo, J. Duan, X.-Z. Shu, *Chem. Sci.* **2018**, *9*, 640–645.
[189] H. Yu, Z.-X. Wang, *Org. Biomol. Chem.* **2021**, *19*, 9723–9731.
[190] V. Kumar Chenniappan, D. Peck, R. Rahaim, *Tetrahedron Lett.* **2020**, *61*, 151729.
[191] a) T. V. RajanBabu, W. A. Nugent, M. S. Beattie, *J. Am. Chem. Soc.* **1990**, *112*, 6408–6409; b) T. V. RajanBabu, W. A. Nugent, *J. Am. Chem. Soc.* **1994**, *116*, 986–997.
[192] G. A. Dawson, E. H. Spielvogel, T. Diao, *Acc. Chem. Res.* **2023**, *56*, 3640–3653.
[193] D. G. Yakhvarov, A. Petr, V. Kataev, B. Büchner, S. Gómez-Ruiz, E. Hey-Hawkins, S. V. Kvashennikova, Y. S. Ganushevich, V. I. Morozov, O. G. Sinyashin, *J. Organomet. Chem.* **2014**, *750*, 59–64.
[194] A. Klein, A. Kaiser, B. Sarkar, M. Wanner, J. Fiedler, *Eur. J. Inorg. Chem.* **2007**, *2007*, 965–976.
[195] a) C. Hamacher, N. Hurkes, A. Kaiser, A. Klein, A. Schüren, *Inorg. Chem.* **2009**, *48*, 9947–9951; b) J. T. Ciszewski, D. Y. Mikhaylov, K. V. Holin, M. K. Kadirov, Y. H. Budnikova, O. Sinyashin, D. A. Vicic, *Inorg. Chem.* **2011**, *50*, 8630–8635.
[196] a) O. R. Luca, R. H. Crabtree, *Chem. Soc. Rev.* **2013**, *42*, 1440–1459; b) G. D. Jones, J. L. Martin, C. McFarland, O. R. Allen, R. E. Hall, A. D. Haley, R. J. Brandon, T. Konovalova, P. J. Desrochers, P. Pulay, D. A. Vicic, *J. Am. Chem. Soc.* **2006**, *128*, 13175–13183.
[197] S. Otsuka, A. Nakamura, T. Yoshida, M. Naruto, K. Ataka, *J. Am. Chem. Soc.* **1973**, *95*, 3180–3188.
[198] a) A. Moncomble, P. L. Floch, A. Lledos, C. Gosmini, *J. Org. Chem.* **2012**, *77*, 5056–5062; b) M. Amatore, C. Gosmini, *Chem. Eur. J.* **2010**, *16*, 5848–5852; c) M. R. Friedfeld, M. Shevlin, J. M. Hoyt, S. W. Krska, M. T. Tudge, P. J. Chirik, *Science* **2013**, *342*, 1076–1080.
[199] Prices were adapted from: https://www.sigmaaldrich.com/DE/en?gclid=CjwKCAjw7oeqBhBwEiwALyHLM9MrUctlpPwCTs6aEHTdiLii0Gi14TSeqNdulDP6em-KEXZ4CnycyxoC_yQQAvD_BwE (accessed 01.11.2023).
[200] C. Feng, D. W. Cunningham, Q. T. Easter, S. A. Blum, *J. Am. Chem. Soc.* **2016**, *138*, 11156–11159.
[201] a) S. Kim, M. J. Goldfogel, M. M. Gilbert, D. J. Weix, *J. Am. Chem. Soc.* **2020**, *142*, 9902–9907; b) I. Nohira, N. Chatani, *ACS Catal.* **2021**, 4644–4649; c) X. Wang, G. Ma, Y.

Peng, C. E. Pitsch, B. J. Moll, T. D. Ly, X. Wang, H. Gong, *J. Am. Chem. Soc.* **2018**, *140*, 14490–14497.
[202] a) J. Liao, C. H. Basch, M. E. Hoerrner, M. R. Talley, B. P. Boscoe, J. W. Tucker, M. R. Garnsey, M. P. Watson, *Org. Lett.* **2019**, *21*, 2941–2946; b) B. Mirabi, A. D. Marchese, M. Lautens, *ACS Catal.* **2021**, 12785–12793.
[203] a) K. A. Johnson, S. Biswas, D. J. Weix, *Chem. Eur. J.* **2016**, *22*, 7399–7402; b) D. A. Everson, B. A. Jones, D. J. Weix, *J. Am. Chem. Soc.* **2012**, *134*, 6146–6159.
[204] a) Y. Li, Y. Li, L. Peng, D. Wu, L. Zhu, G. Yin, *Chem. Sci.* **2020**, *11*, 10461–10464; b) F.-F. Pan, P. Guo, X. Huang, X.-Z. Shu, *Synthesis* **2021**, *53*, A-G.
[205] Y.-L. Zheng, P.-P. Xie, O. Daneshfar, K. N. Houk, X. Hong, S. G. Newman, *Angew. Chem. Int. Ed.* **2021**, *60*, 13476–13483.
[206] S. L. Younas, J. Streuff, *ACS Catal.* **2021**, *11*, 11451–11458.
[207] S. Okamoto, *Chem. Rec.* **2016**, *16*, 857–872.
[208] D. P. Nair, M. Podgorski, S. Chatani, T. Gong, W. Xi, C. R. Fenoli, C. N. Bowman, *Chem. Mater.* **2014**, *26*, 724–744.
[209] L. S. Liebeskind, J. Srogl, *J. Am. Chem. Soc.* **2000**, *122*, 11260–11261.
[210] a) N. A. Till, S. Oh, D. W. C. MacMillan, M. J. Bird, *J. Am. Chem. Soc.* **2021**, *143*, 9332–9337; b) S. Ting, W. Williams, A. Doyle, **2022**, *144*, 5575–5582; c) S. Bajo, G. Laidlaw, A. R. Kennedy, S. Sproules, D. J. Nelson, *Organometallics* **2017**, *36*, 1662–1672.
[211] a) C. Dayakar, B. S. Kumar, G. Sneha, G. Sagarika, K. Meghana, S. Ramakrishna, R. S. Prakasham, B. C. Raju, *Bioorg. Med. Chem.* **2017**, *25*, 5678–5691; b) X. Xu, P. Zavalij, M. Doyle, *Angew. Chem. Int. Ed* **2012**, *51*, 9829–9833.
[212] a) N. T. Akinchan, *Glob. J. Pure Appl. Sci.* **2004**, *10*, 81–85; b) R. A. Daignault, E. L. Eliel, *Org. Synth.* **1973**, *5*, 303–304.
[213] Z. Zhu, Y. Gong, W. Tong, W. Xue, H. Gong, *Org. Lett.* **2021**, *23*, 2158–2163.
[214] N. Ajvazi, S. Stavber, *Tetrahedron Lett.* **2016**, *57*, 2430–2433.
[215] R. F. Turro, J. L. H. Wahlman, Z. J. Tong, X. Chen, M. Yang, E. P. Chen, X. Hong, R. G. Hadt, K. N. Houk, Y.-F. Yang, S. E. Reisman, *J. Am. Chem. Soc.* **2023**, *145*, 14705–14715.
[216] a) M. Tobisu, A. Yasutome, H. Kinuta, K. Nakamura, N. Chatani, *Org. Lett.* **2014**, *16*, 5572–5575; b) E. J. Tollefson, L. E. Hanna, E. R. Jarvo, *Acc. Chem. Res.* **2015**, *48*, 2344–2353.
[217] a) P. Politzer, J. S. Murray, T. Clark, *Phys. Chem. Chem. Phys.* **2010**, *12*, 7748–7757; b) P. Politzer, J. S. Murray, T. Clark, *Phys. Chem. Chem. Phys.* **2013**, *15*, 11178–11189.
[218] A. Krasovskiy, P. Knochel, *Synthesis* **2006**, *2006*, 0890–0891.
[219] M. E. Greaves, T. O. Ronson, G. C. Lloyd-Jones, F. Maseras, S. Sproules, D. J. Nelson, *ACS Catal.* **2020**, *10*, 10717–10725.
[220] a) J. P. McCormick, D. L. Barton, *J. Org. Chem.* **1980**, *45*, 2566–2570; b) J. P. McCormick, A. S. Fitterman, D. L. Barton, *J. Org. Chem.* **1981**, *46*, 4708–4712.
[221] A. Duan, F. Xiao, Y. Lan, L. Niu, *Chem. Soc. Rev.* **2022**, *51*, 9986–10015.
[222] G. Yin, I. Kalvet, U. Englert, F. Schoenebeck, *J. Am. Chem. Soc.* **2015**, *137*, 4164–4172.
[223] L. Nattmann, J. Cornella, *Organometallics* **2020**, *39*, 3295–3300.
[224] A. Egorov, S. Matyukhova, E. Dashkova, *Russ. J. Gen. Chem.* **2012**, *82*, 1686–1699.
[225] R. Langer, L. Wünsche, D. Fenske, O. Fuhr, *Z. Anorg. Allg. Chem.* **2009**.
[226] A. K. Vitek, A. K. Leone, A. J. McNeil, P. M. Zimmerman, *ACS Catal.* **2018**, *8*, 3655–3666.
[227] I. R. Márquez, D. Miguel, A. Millán, M. L. Marcos, L. Á. de Cienfuegos, A. G. Campaña, J. M. Cuerva, *J. Org. Chem.* **2014**, *79*, 1529–1541.
[228] H. Zipse in *Radical stability—a theoretical perspective*, **2006**, pp. 163–189.

[229] M. M. Schwab, D. Himmel, S. Kacprzak, D. Kratzert, V. Radtke, P. Weis, K. Ray, E. W. Scheidt, W. Scherer, B. de Bruin, S. Weber, I. Krossing, *Angew. Chem. Int. Ed.* **2015**, *54*, 14706–14709.
[230] B. J. McNicholas, Z. J. Tong, D. Bím, R. F. Turro, N. P. Kazmierczak, J. Chalupský, S. E. Reisman, R. G. Hadt, *Inorg. Chem.* **2023**, *62*, 14010–14027.
[231] R. Cheng, H.-Y. Zhao, S. Zhang, X. Zhang, *ACS Catal.* **2020**, *10*, 36–42.
[232] H. R. Diéguez, A. López, V. Domingo, J. F. Arteaga, J. A. Dobado, M. M. Herrador, J. F. Quílez del Moral, A. F. Barrero, *J. Am. Chem. Soc.* **2010**, *132*, 254–259.
[233] a) H. Urabe, F. Sato, *Lewis Acids in Organic Synthesis* **2000**, 653–798; b) K. Mikami, M. Terada, *Lewis Acids in Organic Synthesis* **2000**, 799–847; c) H. Yamamoto, K. Ishihara, *Acid catalysis in modern organic synthesis*, Wiley-VCH Weinheim, **2008**; d) D. J. Ramón, M. Yus, *Chem. Rev.* **2006**, *106*, 2126–2208.
[234] D. Jian-Guo, P. Yu-Xing, *Chin. J. Chem.* **1998**, *16*, 452–457.
[235] P. H. Gehrtz, P. Kathe, I. Fleischer, *Chem. Eur. J.* **2018**, *24*, 8774–8778.
[236] G. R. Fulmer, A. J. Miller, N. H. Sherden, H. E. Gottlieb, A. Nudelman, B. M. Stoltz, J. E. Bercaw, K. I. Goldberg, *Organometallics* **2010**, *29*, 2176–2179.
[237] Y. Yamashita, H. Suzuki, I. Sato, T. Hirata, S. Kobayashi, *Angew. Chem. Int. Ed.* **2018**, *57*, 6896–6900.
[238] Y. Zhang, T. Sugai, T. Yamamoto, N. Yamamoto, N. Kutsumura, Y. Einaga, S. Nishiyama, T. Saitoh, H. Nagase, *ChemElectroChem* **2019**, *6*, 4194–4198.
[239] D. F. Fischer, A. Barakat, Z. q. Xin, M. E. Weiss, R. Peters, *Chem. Eur. J.* **2009**, *15*, 8722–8741.
[240] R. A. Fernandes, P. Kattanguru, *Helv. Chim. Acta* **2015**, *98*, 92–107.
[241] D. S. Sharada, A. Z. Muresan, K. Muthukumaran, J. S. Lindsey, *J. Org. Chem.* **2005**, *70*, 3500–3510.
[242] B. Neises, W. Steglich, *Angew. Chem. Int. Ed. Eng.* **1978**, *17*, 522–524.
[243] Y. Sato, S.-i. Kawaguchi, A. Nomoto, A. Ogawa, *Synthesis* **2017**, *49*, 3558–3567.
[244] J.-X. Xu, L.-C. Wang, X.-F. Wu, *Org. Lett.* **2022**, *24*, 4820–4824.
[245] F. Wang, H. Liu, H. Fu, Y. Jiang, Y. Zhao, *Adv. Synth. Catal.* **2009**, *351*, 246–252.
[246] Y.-J. Lin, Y.-P. Wu, M. Thul, M.-W. Hung, S.-H. Chou, W.-T. Chen, W. Lin, M. Lin, D. M. Reddy, H.-R. Wu, *Molecules* **2020**, *25*, 352.
[247] Y.-T. Huang, S.-Y. Lu, C.-L. Yi, C.-F. Lee, *J. Org. Chem.* **2014**, *79*, 4561–4568.
[248] Y. Saito, H. Ouchi, H. Takahata, *Tetrahedron* **2006**, *62*, 11599–11607.
[249] H. Huo, X. Shen, C. Wang, L. Zhang, P. Röse, L.-A. Chen, K. Harms, M. Marsch, G. Hilt, E. Meggers, *Nature* **2014**, *515*, 100–103.
[250] M. A. Romero, J. A. González-Delgado, J. F. Arteaga, *Nat. Prod. Commun.* **2015**, *10*, 1258–1262.
[251] F. Louafi, J.-P. Hurvois, A. Chibani, T. Roisnel, *J. Org. Chem.* **2010**, *75*, 5721–5724.
[252] A. M. Romine, K. S. Yang, M. K. Karunananda, J. S. Chen, K. M. Engle, *ACS Catal.* **2019**, *9*, 7626–7640.
[253] F. M. Piller, A. Metzger, M. A. Schade, B. A. Haag, A. Gavryushin, P. Knochel, *Chem. Eur. J.* **2009**, *15*, 7192–7202.
[254] V. Valerio, D. Petkova, C. Madelaine, N. Maulide, *Chem. Eur. J.* **2013**, *19*, 2606–2610.
[255] X. X. Zhao, P. Zhang, Z. X. Guo, *ChemistrySelect* **2017**, *2*, 7670–7677.
[256] C. O. Kangani, B. W. Day, *Org. Lett.* **2008**, *10*, 2645–2648.
[257] L.-Z. Yuan, D. Renko, I. Khelifi, O. Provot, J.-D. Brion, A. Hamze, M. Alami, *Org. Lett.* **2016**, *18*, 3238–3241.
[258] T. Kawasaki, N. Ishida, M. Murakami, *J. Am. Chem. Soc.* **2020**, *142*, 3366–3370.

[259] L. Ackermann, V. P. Mehta, *Chem. Eur. J.* **2012**, *18*, 10230–10233.
[260] O. M. Griffiths, H. A. Esteves, Y. Chen, K. Sowa, O. S. May, P. Morse, D. C. Blakemore, S. V. Ley, *J. Org. Chem.* **2021**, *86*, 13559–13571.
[261] S. Maksymenko, K. N. Parida, G. K. Pathe, A. A. More, Y. B. Lipisa, A. M. Szpilman, *Org. Lett.* **2017**, *19*, 6312–6315.
[262] N. Meitinger, A. K. Mengele, K. Witas, S. Kupfer, S. Rau, D. Nauroozi, *Eur. J. Org. Chem.* **2020**, *2020*, 6555–6562.
[263] J.-F. Chen, C. Li, *Org. Lett.* **2018**, *20*, 6719–6724.
[264] W. C. Fu, C. M. So, O. Y. Yuen, I. T. C. Lee, F. Y. Kwong, *Org. Lett.* **2016**, *18*, 1872–1875.
[265] X.-X. Nie, Y.-H. Huang, P. Wang, *Org. Lett.* **2020**, *22*, 7716–7720.
[266] V. Murugesan, A. Ganguly, A. Karthika, R. Rasappan, *Org. Lett.* **2021**, *23*, 5389–5393.
[267] G. Rajagopal, H. Lee, S. S. Kim, *Tetrahedron* **2009**, *65*, 4735–4741.
[268] X.-J. Dai, H. Wang, C.-J. Li, *Angew. Chem. Int. Ed.* **2017**, *56*, 6302–6306.
[269] T. Fukuyama, T. Kippo, K. Hamaoka, I. Ryu, *Sci. China Chem.* **2019**, *62*, 1525–1528.
[270] D. Polyak, B. Xu, I. J. Krauss, *Org. Lett.* **2022**, *24*, 4656–4659.
[271] D. J. Fox, D. S. Pedersen, S. Warren, *Org. Biomol. Chem.* **2006**, *4*, 3102–3107.
[272] D. Parmar, L. A. Duffy, D. V. Sadasivam, H. Matsubara, P. A. Bradley, R. A. Flowers, D. J. Procter, *J. Am. Chem. Soc.* **2009**, *131*, 15467–15473.
[273] H. Li, F. Wang, S. Zhu, L. Chu, *Angew. Chem. Int. Ed.* **2022**, *61*, e202116725.
[274] R. Cheng, H.-Y. Zhao, S. Zhang, X. Zhang, *ACS Catal.* **2019**, *10*, 36–42.
[275] a) J. Huang, Y.-X. Luo, L. Wang, X.-Y. Tang, *Org. Lett.* **2023**, *25*, 5613–5618; b) A. Talla, B. Driessen, N. J. W. Straathof, L.-G. Milroy, L. Brunsveld, V. Hessel, T. Noël, *Adv. Synth. Catal.* **2015**, *357*, 2180–2186.
[276] T. Song, Z. Ma, P. Ren, Y. Yuan, J. Xiao, Y. Yang, *ACS Catal.* **2020**, *10*, 4617–4629.

5 Summary/Zusammenfassung

Ketones constitute an important structural motif in organic chemistry and the search for new methods to synthesize them is still in high demand. Thioesters as derivatives of carboxylic acids serve as fundamental building blocks in biochemistry and represent a highly attractive acyl source. Selective activation of the relatively weak C(O)–S bond can be achieved by cross couplings, which are a valuable option to traditional synthetic methods. Advantageously, functionalized substrates as well as low-cost and environmentally friendly reagents can be used with high atom-economy under mild reaction conditions. While palladium dominates in the choice of metal catalyst for such transformations, the replacement of this precious metal by nickel is incentivized by its favorable cost-efficiency, abundance and versatile chemical properties, which are presented in chapter 1. Both aspects, thioesters as acyl sources and nickel catalysis, were combined in this thesis with the overall aim of developing new approaches for ketone syntheses.

Chapter 3 was targeted on ketone synthesis by the so-called Liebeskind–Srogl coupling, in which thioesters and organoboron compounds react under palladium catalysis and stoichiometric amounts of a copper(I) reagent. To date, Liebeskind–Srogl couplings are limited to palladium catalysis, wherefore preliminary studies on a nickel-catalyzed Liebeskind–Srogl coupling were performed. It was found that the cross coupling of aryl thioesters and organoboroxines enables the formation of benzophenone, although the mediator of the reaction is not nickel but solely copper(I).

In chapter 4, the focus shifted from traditional cross couplings to cross-electrophile couplings. Benzylic alcohols were coupled with thioesters under Lewis acids assistance and nickel catalysis, yielding ketones instead of the expected transesterification products. The reaction depends strongly on the substituents of the two substrates. Thioesters with different acyl moieties can be used to give the desired ketones, while the formation of thioether byproduct is minimized with an electron-withdrawing substituent on the thiol moiety. Contrariwise, electron-rich benzylic alcohols with a methoxy substituent in *para*-position are required for ketone formation, but benzylic chlorides are also suitable substrates, being more tolerant to changes in substituents. Mechanistically, a classical cross coupling mechanism was excluded. Instead, the alcohol is converted *in situ* to benzyl chloride by TMSCl, leading to a more facile formation of a benzyl radical. The latter seems to be involved in a radical-chain mechanism as the main catalytic cycle. Thioesters are presumably activated by interaction with Lewis acid Cp_2TiCl_2, producing acyl radicals as the active intermediate.

Ketone stellen ein wichtiges Strukturmotiv in der organischen Chemie dar und die Suche nach neuen Methoden zu ihrer Synthese ist nach wie vor sehr gefragt. Thioester als Derivate von Carbonsäuren dienen als grundlegende Bausteine in der Biochemie und sind äußerst attraktive Acylgruppen-Donatoren. Die selektive Aktivierung der relativ schwachen C(O)–S Bindung kann durch Kreuzkupplung erreicht werden, was eine wertvolle Alternative zu herkömmlichen Synthesemethoden darstellt. Ein Vorteil besteht darin, dass sowohl funktionalisierte Substrate als auch preiswerte und umweltfreundliche Reagenzien mit hoher Atomökonomie unter milden Reaktionsbedingungen verwendet werden können. Palladium ist zwar nach wie vor ein wichtiges Katalysatormetall für solche Umwandlungen, jedoch wird der Ersatz dieses Edelmetalls durch Nickel wegen dessen Kosteneffizienz, Vorkommen und der vielseitigen chemischen Eigenschaften anvisiert. Eine Übersicht über diese Thematik findet sich in Kapitel 1. Beide Aspekte, Thioester als Acylgruppen-Donatoren und Nickelkatalyse, wurden in dieser Arbeit mit dem übergeordneten Ziel kombiniert, neue Ansätze für Ketonsynthesen zu entwickeln.

Kapitel 3 befasste sich mit der Ketonsynthese durch die sogenannte Liebeskind–Srogl Kupplung, bei der Thioester und bororganische Verbindungen unter Palladiumkatalyse und stöchiometrischen Mengen eines Kupfer(I)-Reagenzes umgesetzt werden. Bislang waren Liebeskind–Srogl-Kupplungen auf die Palladium-Katalyse beschränkt, weshalb erste Untersuchungen zu einer nickelkatalysierten Liebeskind–Srogl Kupplung durchgeführt wurden. Es konnte gezeigt werden, dass die Kreuzkupplung von Arylthioestern und Organoboroxinen die Bildung von Benzophenon ermöglicht, obwohl der Mediator nicht Nickel, sondern Kupfer(I) ist.

In Kapitel 4 verlagerte sich der Schwerpunkt von traditionellen Kreuzkupplungen auf Kreuz-Elektrophil Kupplungen. Benzylalkohole wurden unter Verwendung von Lewis Säuren und Nickelkatalyse mit Thioestern umgesetzt, wobei anstelle der erwarteten Umesterungsprodukte Ketone entstanden. Die Reaktion hängt stark von den Substituenten der beiden Substrate ab. Thioester mit verschiedenen Acylgruppen können umgesetzt werden und die unerwünschte Thioetherbildung kann durch einen elektronenziehenden Substituenten an der Thiolkomponente minimiert werden. Im Gegensatz dazu sind elektronenreiche Benzylalkohole mit einem Methoxysubstituenten in *para*-Position erforderlich. Aber auch Benzylchloride sind geeignete Substrate, die toleranter gegenüber den Substituenten sind. Mechanistisch wurde ein klassischer Kreuzkupplungsmechanismus ausgeschlossen. Stattdessen wird der Alkohol durch die *in situ* Generierung des Benzylchlorides aktiviert, was die Bildung eines Benzylradikals erleichtert. Letzteres scheint an einem Radikalkettenmechanismus als dem wichtigsten katalytischen Zyklus beteiligt zu sein. Der Thioester wird vermutlich durch Lewis-Säure-Base-Wechselwirkung mit Cp_2TiCl_2 aktiviert, wobei Acylradikale als aktive Zwischenprodukte entstehen.

6 Appendix

6.1 List of Abbreviations

Ac	Acetyl
Acac	Acetylacetonate
Ad	Adamantyl
APCI	Atmospheric pressure chemical ionization
aq.	Aqueous
Alk	Alkyl
Approx	Approximately
Ar	Aryl
ATR	Attenuated total reflection
BBN	9-Borabicyclo[3.3.1]nonane
BDE	Bond dissociation energy
BHT	2,6-Di-*tert*-butyl-4-methylphenol
BINAP	2,2'-Bis(diphenylphosphino)-1,1'-binaphthyl
Bn	Benzyl
BnOH	Benzyl alcohol
Boc	*tert*-Butyloxycarbonyl
BPhen	Bathophenanthroline
bpy	2,2'-Bipyridine
BzBr	Benzyl bromide
cod	Cycloocta-1,5-diene
CuTC	Copper 2-thiophenecarboxylate
CuDPP	Copper diphenylphosphinate
CuMeSal	Copper 3-methylsalicylate
CEBO	2-Chloro-3-ethylbenzoxazolium tetrafluoroborate
Cp	Cyclopentadiene
d	Doublet (NMR)
δ	Chemical shift (NMR)
dba	Dibenzylideneacetone
DCC	*N*,*N'*-Dicyclohexylcarbodiimide
DCM	Dichloromethane
dcype	1,2-Bis(dicyclohexylphosphino)ethane
DFT	Density functional theory
DIPEA	*N*,*N*-Diisopropylethylamine
diglyme	2-Methoxyethyl ether
DMA	*N*,*N*-Dimethylacetamide
DMAP	4-Dimethylaminopyridine
dmbpy	Dimethyl-2,2'-dipyridyl
DME	1,2-Dimethoxyethane
DMF	*N*,*N*-Dimethylformamide
DMI	1,3-Dimethyl-2-imidazlidinone
DMO	Dimethyl oxalate
DMPE	1-(4-(Dimethylamino)phenyl)ethanol
DMPU	*N*,*N'*-Dimethylpropyleneurea
dPhbpy	4,4'-Diphenyl-2,2'-bipyridine

dppb	1,2-Bis(diphenylphosphino)butane
dppe	1,2-Bis(diphenylphosphino)ethane
dppf	1,1'-Bis(diphenylphosphino)ferrocene
dppp	1,2-Bis(diphenylphosphino)propane
dpppe	1,5-Bis(diphenylphosphino)pentane
dtbbpy	4,4'-Di-*tert*-butyl-2,2'-dipyridyl
EI	Electron ionization
EPR	Electron paramagnetic resonance
equiv.	Equivalent
ESI	Electrospray ionization
EtOAc	Ethylacetate
FG	Functional group
FID	Flame ionization detection
Galvinoxyl	4-[3,5-Di-*tert*-butyl-4-oxocyclohexa-2,5-dien-1-ylidene)methyl] -2,6-di-*tert*-butylphenoxyl
GC	Gas chromatography
GP	General procedure
HAT	Hydrogen atom transfer
HE	Hantzsch ester
het	Heteroatom
Hex	*n*-Hexane
HSAB	Hard and soft acids and bases
Hz	Hertz
ICP	Inductively coupled plasma
i.e.	*id est*, that is
I^{t}Bu	1,3-Di-*tert*-butylimidazol-2-ylidene
J	Coupling constant (NMR)
KOAc	Potassium acetate
liq.	Liquid
LSC	Liebeskind–Srogl coupling
m	Multiplet (NMR)
M	Molar
MeCN	Acetonitrile
Mes	Mesityl
MeOH	Methanol
MP	Melting point
MS	Mass spectrometry
Ms	Mesylate
Ms_2O	Methanesulfonic anhydride
MOM	Methoxymethyl ether
MTBE	Methyl *tert*-butyl ether
nep	Neopentyl glycolate
NHC	*N*-Heterocyclic carbenes
NHP	*N*-Hydroxyphthalimide esters
NMP	*N*-Methyl-2-pyrrolidone
NMR	Nuclear magnetic resonance
OA	Oxidative addition

PBI	2-(2-Pyridyl)benzimidazole
PD	*n*-Pentadecane
Pd_2dba_3	Tris(dibenzylidenaceton)dipalladium(0)
PE	Petrolether
PG	Protecting group
Ph	Phenyl
Piv	Pivaloyl
pin	Pinacolato
Phbpy	6-Phenyl-2,2‘-bipyridine
Phen	1,10-Phenanthroline
PhMe	Toluene
PMP	*p*-Methoxyphenyl ether
POP	Triphenyl phosphine ditriflate
ppm	Parts per million
prim	Primary
***p*Tol**	*p*-Toluoyl
***p*TsOH**	*p*-Toluenesulfonic acid
py	Pyridyl
pyphos	2-[2-(Diphenylphosphanyl)ethyl]pyridine
RBF	Round-bottom flask
RDS	Rate-determining step
Resp.	Respectively
RE	Reductive elimination
R_f	Retardation factor
rt	Room temperature
s	Singlet (NMR)
sat.	Saturated
SCE	Saturated calomel electrode
SEM	Trimethylsilylethoxymethyl
SFRC	Solvent-free reaction conditions
sec	Secondary
SET	Single-electron transfer
stb	*trans*-Stilbene
SP	Syringe pump
t	Triplet (NMR)
TADDOL	α,α,α’,α’-Tetraaryl-1,3-dioxolane-4,5-dimethanol
TBAB	Tetrabutylammonium bromide
TBAC	Tetrabutylammonium chloride
TBAI	Tetrabutylammonium iodide
tpy	Terpyridine
TEMPO	(2,2,6,6-Tetramethylpiperidin-1-yl)oxyl
TESCl	Chlorotriethylsilane
TFP	Tri(2-furyl)phosphine
THF	Tetrahydrofuran
THP	Tetrahydropyranyl
TLC	Thin-layer chromatography
TMEDA	*N*,*N*,*N*‘,*N*‘-Tetramethylethylenediamine

TMSCl	Trimethylsilyl chloride
Tol	Toluene
tpy	Terpyridine
Ts	Tosylate
UV	Ultraviolet
quint	Quintett (NMR)
µw	Microwave

6.2 Acknowledgements

Es war ein langer Lebensweg von einer Realschülerin über eine ausgebildete Chemielaborantin und den zweiten Bildungsweg hin zu einer (hoffentlich bald auch promovierten) Chemikerin. All das wäre nicht in diesem Ausmaß möglich gewesen ohne die folgenden Personen an meiner Seite:

Ich danke Frau Prof. Dr. Ivana Fleischer für die Betreuung, die Diskussionen und die Unterstützung in den letzten Jahren. Ganz besonders möchte ich mich dafür bedanken, dass ich mich auch in einem nicht-akademischen Sinne weiterentwickeln konnte, sei es bei einer Agilent Fortbildung oder bei einem Bildungsurlaub.

Ich bedanke mich recht herzlich bei Herrn Senior-Prof. Dr. Martin E. Maier für die Übernahme des Zweitgutachtens.

Allen ehemaligen Kolleg:innen – Valentin Geiger und Regina Oechsner – und der derzeitigen Besetzung des AK Fleischers – Alexandru Caciuleanu, Savva Ponomarev, Robert Richter, Ivo Lindenmaier, Felix Vöhringer, Dhananjay Nair, Sandra Papińska und Maria Mikova – danke ich für die Unterstützung und den Austausch im Labor, sowie für all die unterhaltsame gemeinsame Zeit. Alexandru Caciuleanu danke ich für all die Gespräche, in denen die Chemie auch mal in den Hintergrund rücken konnte. Deine Art hat die Zeit im Labor sehr bereichert. Ich bin froh, Robert Richter und Ivo Lindenmaier als Kollegen gehabt zu haben, zwei smarte Chemiker, die die Arbeitsgruppe maßgeblich prägen und den Teamspirit wieder aufleben lassen. Ich danke euch besonders für das unermüdliche und detailreiche Lesen meiner Arbeit. Ich weiß, das ist nicht selbstverständlich und ihr habt viel eurer kostbaren Zeit geopfert. Robert Richter danke ich zudem für die Aufnahme von hochauflösenden NMR Spektren und für das Bereitstellen von Krossing's Nickel(I) Komplex.

Dem AK Grond danke ich für all die schönen Stunden im Seminarraum und auf dem Stockwerk.

Norbert Grzegorzek danke ich für all die Hilfe und Diskussion bezüglich des GC-MS. Eine solche helfende Hand hat vieles leichter gemacht.

Dominik Brzecki danke ich für die Aufnahme der EPR Spektren.

Außerdem möchte ich mich bei meinen Praktikant:innen Xian Xiao, Pascal Stopper, Niklas Thiess und Elisa Travers für die Mitarbeit an meinem nicht immer einfachen Projekt bedanken.

Rudolf Neugebauer soll auch erwähnt werden. Er prägte die Jahre meiner Ausbildung als Chemielaborantin und zeigte mir die ersten Schritte in einem Chemielabor. Ich denke oft an

die Zeit als Auszubildende zurück und hoffe, dass ich wieder einmal in einem solchen Arbeitsumfeld arbeiten kann, wie ich es zu der damaligen Zeit erlebt habe.

Den Kletterschlümpfen des DAV Tübingen danke ich für all die schönen Stunden am Freitagnachmittag, die mich herausgeholt haben aus der akademischen Blase und mir gezeigt haben, was wirklich wichtig ist: ein respektvolles Miteinander.

Meinen Tübingern Freunden Ophelia und Frederick möchte ich für all die gemeinsamen (Siedler-) Abende danken. Besonders während der Corona Pandemie war das ein Rettungsanker.

Meinen langjährigen Freundinnen Anna und Franziska möchte ich danken, dass unsere Freundschaft seit all den Jahren besteht. Wir haben schon so viel gemeinsam erlebt und durchgestanden. Ich freue mich auf die weiteren Jahre mit euch.

Meiner lieben Freundin Anna Bäuerle danke ich für die zahlreichen Gespräche, Kletterrouten, Wanderungen und Fahrradtouren. Ich bin froh, dich an meiner Seite zu haben.

Erica Schmitt begleitet mich nun schon seit dem ersten Semester und es ist ein echtes Privileg, eine solche wertvolle Freundin gefunden zu haben. Danke dafür, dass du Teile meiner Arbeit korrekturgelesen hast.

Eva Maria und Leonard Goll möchte ich für all die emotionale und finanzielle Unterstützung in den letzten Jahren danken. Danke, dass ihr Korbinian und mir ein solches Leben in Tübingen ermöglicht habt.

Meiner Oma Ernelies und Opa Heinz möchte ich danken, dass ich immer vorbeikommen kann und so aufgenommen werde, als wäre ich nie weggewesen.

Meinen Eltern Roland und Elke, sowie meinen Schwestern Nina und Lena danke ich für ihren unermüdlichen Rückhalt. Die nie endende Unterstützung und Fürsorge, die ich während meines gesamten Studiums erfahren durfte, haben mich weitermachen lassen. Elena und Emil danke ich für ihren Blick auf die Welt durch Kinderaugen. Ich bin froh, eine so wundervolle Familie zu haben.

Der größte Dank geht an meinen Lebensgefährten Korbinian Goll. Vor mehr als acht Jahren kamen wir zusammen nach Tübingen. Seitdem haben wir viel erlebt, geschafft und sind erwachsen geworden. Ich danke dir für deine Liebe, Offenheit, Geduld und deinen Rückhalt, den du mir ausnahmslos entgegenbringst. Ich weiß, es war nicht immer einfach und ich denke, dass ich ohne dich diesen Weg nicht so weit gegangen wäre. Ich freue mich auf unsere gemeinsame Zukunft.